PNWD-3699
WTP-RPT-141, Rev. 0

Waste, Process, and Product Variations and Uncertainties for Waste Treatment Plant IHLW and ILAW

G. F. Piepel
B. G. Amidan
A. Heredia-Langner

February 2006

Prepared for Bechtel National, Inc.
under Contract Number 24590-101-TSA-W000-00004

LEGAL NOTICE

This report was prepared by Battelle Memorial Institute (Battelle) as an account of sponsored research activities. Neither Client nor Battelle nor any person acting on behalf of either:

MAKES ANY WARRANTY OR REPRESENTATION, EXPRESS OR IMPLIED, with respect to the accuracy, completeness, or usefulness of the information contained in this report, or that the use of any information, apparatus, process, or composition disclosed in this report may not infringe privately owned rights; or

Assumes any liabilities with respect to the use of, or for damages resulting from the use of any information, apparatus, process, or composition disclosed in this report.

Reference herein to any specific commercial product, process, or service by trade name, trademark, manufacturer, or otherwise, does not necessarily constitute or imply its endorsement, recommendation, or favoring Battelle. The views and opinions of authors expressed herein do not necessarily state or reflect those of Battelle.

Waste, Process, and Product Variations and Uncertainties for Waste Treatment Plant IHLW and ILAW

G. F. Piepel
B. G. Amidan
A. Heredia-Langner

2/27/06
for W. Tamosaitis
ACCEPTED FOR
WTP PROJECT USE

February 2006

Test Specification: 24590-WTP-TSP-RT-02-007
Test Plan: TP-RPP-WTP-193, Rev. 1
and ICN-TP-RPP-WTP-193.1
Test Exceptions: 24590-WTP-TEF-RT-03-041
24590-WTP-TEF-RT-04-00017
R&T Focus Area: Waste Form Qualification
Test Scoping Statements: B-61 and B-65

Battelle—Pacific Northwest Division
Richland, Washington 99352

Completeness of Testing

This report describes the results of work and testing specified by Test Specification 24590-WTP-TSP-RT-02-007, Test Exception 24590-WTP-TEF-RT-03-041, Test Exception 24590-WTP-TEF-RT-04-00017, Test Plan TP-RPP-WTP-193, Rev. 1, and Interim Change Notice ICN-TP-RPP-WTP-193.1 on the test plan. The work and any associated testing followed the quality assurance requirements outlined in the Test Specification and Test Plan. The descriptions provided in this test report are an accurate account of both the conduct of the work and the data collected. Test plan results are reported. Also reported are any unusual or anomalous occurrences that are different from expected results. The test results and this report have been reviewed and verified.

Approved:

Gordon H. Beeman, Manager
BNI Support Program

Date

Summary

The high-level waste (HLW) and low-activity waste (LAW) vitrification processes of the Waste Treatment and Immobilization Plant (WTP) will be subject to variation and several uncertainties. The variation and uncertainties at various process steps will translate into variation and uncertainty in immobilized HLW (IHLW) and immobilized LAW (ILAW) compositions and properties. The compositions, compliance properties (e.g., Product Consistency Test [PCT] for IHLW and ILAW and Vapor Hydration Test [VHT] for ILAW), and process control properties (e.g., viscosity and electrical conductivity for IHLW and ILAW, and temperature at one-percent crystallinity [$T_{1\%}$] for IHLW) of the IHLW and ILAW melts and products will be subject to variation because the compositions of waste feeds will vary over time. The state of knowledge at any step of the IHLW or ILAW processes will be subject to sampling, chemical analysis, volume measurement, mixing, weighing, transfer, and other uncertainties.

WTP strategies for operating the IHLW and ILAW facilities account for uncertainties in making process decisions such as volume transfers and addition of glass forming chemicals (GFCs) to waste. WTP strategies also use statistically based estimates of variations and uncertainties in demonstrating compliance with applicable specifications. Magnitudes of uncertainties impact the number of samples, analyses per sample, and measurements that are needed to make process decisions and demonstrate compliance in the WTP IHLW and ILAW facilities. WTP strategies also account for variations and uncertainties in demonstrating compliance with applicable specifications. Hence, it is vitally important to the successful operation of the WTP IHLW and ILAW facilities to have well-supported estimates of variations and uncertainties for various stages of the vitrification processes as well as in the waste glass compositions and glass properties.

There were two main objectives for the work documented in this report. The first main objective was to gather and summarize the best, currently available WTP Project estimates of variations and uncertainties that will affect various stages of the WTP IHLW and ILAW vitrification processes. The estimates included in this report are updates of those included in a previous interim report (Heredia-Langner et al. 2003). There are still some parts of the WTP IHLW and ILAW processes where experimental work to quantify biases and uncertainties in mixing, sampling, and transfer of wastes and melter feeds (waste with added GFCs) is planned for the future. In such cases, the best current estimates of the WTP Project were used for this work. The second main objective was to quantify variations and uncertainties expected in WTP IHLW and ILAW glass compositions, compliance properties, and processing properties. Quantifying uncertainties in glass compositions and properties involved propagating the applicable uncertainties using a Monte Carlo simulation approach. Estimates of variations in pretreated waste over an HLW or LAW waste type were also included in the Monte Carlo simulations to quantify variations in WTP IHLW and ILAW compositions and properties corresponding to HLW and LAW waste types.

Section 4 presents and discusses the estimates of variations and uncertainties in steps of the HLW and LAW vitrification processes. Section 7 (IHLW) and Section 8 (ILAW) present and discuss estimates of variations and uncertainties in product compositions and properties. Section 9 summarizes these results and discusses variations and uncertainties for which additional work may be needed to confirm the estimates in this report or to obtain final estimates. Section 10 discusses the needs of the WTP Project that are satisfied by the results in this report.

Objectives

The test objectives from the Test Specification (Swanberg 2002) and the Test Plan (Piepel and Heredia-Langner 2003) are listed (in italics) and then discussed (in normal text).

1. *Quantify expected variations and uncertainties in the compositions of pretreated waste feeds to the WTP HLW and LAW vitrification facilities.*

   This objective was not completely met because the WTP Project does not have any actual operating data to quantify variations in pretreated waste feeds over an HLW or an LAW waste type. Further, the waste form qualification testing that will produce data to quantify various uncertainties associated with pretreated HLW and LAW has not yet occurred (Sundar 2005a, 2005b). However, Section 4.1 discusses estimates of expected variations in HLW and LAW over waste types. Section 4.2 discusses estimates of expected uncertainties for HLW and LAW.

2. *Analyze variations and uncertainties from DWPF[(a)] and WVDP[(b)] operating data to determine applicability to WTP vitrification processes and serve as baselines for comparison.*

   This objective was met in the previous phase of the B-61 and B-65 work, which was documented in an interim report: A Heredia-Langner, GF Piepel, and SA Hartley. 2003. *Interim Report: Initial Assessment of Waste, Process, and Product Variations and Uncertainties for Waste Treatment Plant IHLW and ILAW*, WTP-RPT-073 Rev. 0, Battelle—Pacific Northwest Division, Richland, WA. Per direction from the WTP Project, those results were not included in this report.

3. *Apply statistical experimental design methods, as necessary,[(c)] for input to other experimental studies that will generate data needed to quantify sampling, analytical, measurement, and other uncertainties applicable to the HLW and LAW vitrification processes. Interface with these other efforts so that resulting data are suitable for estimating variations and uncertainties.*

   This objective was deleted from the scope as part of Test Exception 24590-WTP-TEF-RT-03-041 and addressed via Interim Change Notice ICN-TP-RPP-WTP-193.1 to Test Plan TP-RPP-WTP-193 Rev. 1. The rationale was that experimental studies generating data for quantifying variations and uncertainties should have their own statistical support for experimental design and data analyses.

4. *Quantify expected variations and uncertainties at each step of the HLW and LAW vitrification processes.*

   These variations and uncertainties are presented in Section 4, Appendix C, and Appendix D.

(a) DWPF = Defense Waste Processing Facility.
(b) WVDP = West Valley Demonstration Project.
(c) Where applicable for the WTP, existing data or studies of variations and uncertainties should be used so that new studies are only performed where necessary. Also, related testing (e.g., mixing and sampling studies) should incorporate statistical planning to provide for obtaining adequate data to quantify variations and uncertainties in the HLW and LAW vitrification processes.

5. *Project the expected variations in IHLW and ILAW chemical and radionuclide compositions resulting from variations and uncertainties in HLW and LAW waste feeds and the HLW and LAW vitrification processes.*

   Sections 5 and 6 discuss the methods used. Section 7 and Appendix E present the resulting estimates of variation and uncertainty in IHLW ILAW compositions (mass fractions of oxide or halogen components). Section 8 and Appendix E present the ILAW results. Section 9 summarizes the IHLW and ILAW results.

6. *Develop methods to relate IHLW and ILAW composition variations to variations in glass properties (e.g., durability tests such as the PCT, VHT, and TCLP[(a)]) through the use of property-composition models. These methods will be used to evaluate the sensitivity of PCT, VHT, and TCLP properties to variations in glass composition*.

   This objective was met. The properties for IHLW are PCT (B, Li, and Na releases), TCLP Cd release, $T_{1\%}$, viscosity at temperatures of 1373.15 K (1100ºC) and 1423.15 K (1150ºC), and electrical conductivity at temperatures of 1373.15 K (1100ºC) and 1473.15 K (1200ºC). The properties for ILAW are PCT (B and Na releases),[(b)] VHT, viscosity at temperatures of 1373.15 K (1100ºC) and 1423.15 K (1150ºC), and electrical conductivity at temperatures of 1373.15 K (1100ºC) and 1473.15 K (1200ºC). Sections 5 and 6 discuss the methods used. Section 7 and Appendix E present the resulting estimates of variation and uncertainty for IHLW properties. Section 8 and Appendix F present the results for ILAW properties. Section 9 summarizes the IHLW and ILAW results.

7. *Develop methods to demonstrate that projected IHLW and ILAW composition variations for each HLW or LAW waste type will remain within composition specification limits (e.g., waste loading and radionuclide composition limits). This work will make use of compliance methods developed as part of the B-62/70 and B-60/69 (Statistics for IHLW and ILAW Compliance) work scope*.

   This objective was met by work in the B-62/70 and B-60/69 scope, which was documented in the report by Piepel et al. (2005). That work and report are scheduled to be updated in the future.

8. *Establish acceptance limits for waste feeds to the HLW and LAW vitrification facilities, to provide high confidence of compliance over the course of processing a waste type*.

   Establishing acceptance limits for waste feeds is a WTP Project activity. This objective was intended to provide some of the necessary inputs for the WTP Project to establish such limits. The estimates of variations and uncertainties of IHLW and ILAW compositions and properties provided in this report, and also information on the sensitivity of these variations and uncertainties to variations and uncertainties in the HLW and LAW vitrification processes, provide some of the inputs the WTP Project needs to establish such acceptance limits. The remaining inputs are the relevant statistically-based compliance methods presented and illustrated by Piepel et al. (2005).

(a) TCLP = toxicity characteristic leach procedure.
(b) PCT Si release was not investigated per agreement with the WTP Project because for ILAW, the Si release was always less than the B and Na releases for all test glasses used to develop property-composition models. Hence, PCT Si release from LAW glasses was not modeled.

Test Exceptions

Two test exceptions are listed (in italics) and then discussed (in normal text).

1. *24590-WTP-TEF-RT-03-041*: This test exception (1) reduced three phases of work and reports to two phases, (2) removed the scope to determine the extent of variation that should correspond to the definition of a new waste type, and (3) deleted the scope to develop test matrices for related research and technology (R&T) work that will generate data on expected variations and uncertainties in the WTP process. This report documents the results of the revised second phase of work.

2. *24590-WTP-TEF-RT-04-00017*: The portion of this test exception relevant to B-61 and B-65 work added scope to quantify the variations and uncertainties in viscosity (IHLW and ILAW), electrical conductivity (IHLW and ILAW), and percent crystallinity temperature, denoted $T_{1\%}$ (IHLW).

Results and Performance against Success Criteria

The success criteria in the Test Plan (Piepel and Heredia-Langner 2003) are listed (in italics) and then discussed (in normal text).

1. *Obtain, for each HLW and LAW waste type, quantitative estimates of expected variations and uncertainties in waste feeds and processing steps that lead to variations and uncertainties in IHLW and ILAW (glass) compositions and properties. These estimates are required inputs for some objectives of this work, and objectives of statistics activities associated with TSSs B-6270, B-6069, B-68, and B-73.*

   This report documents (1) current estimates of variations and uncertainties affecting the HLW and LAW vitrification processes and (2) variations and uncertainties in IHLW and ILAW compositions and properties corresponding to Melter Feed Preparation Vessel (MFPV) batches. The estimated variations and uncertainties in (1) were used to quantify the variations and uncertainties in (2). This is the final report scheduled for work associated with test scoping statement (TSS) B-61 and B-65. In certain cases, no test or operational data were yet available to quantify variations and uncertainties affecting the HLW and LAW vitrification processes. In other cases, only preliminary data or information was available regarding variations and uncertainties. Hence, in this report, ranges of variations and uncertainties affecting the HLW and LAW vitrification processes were used. This in turn led to estimates of variations and uncertainties in IHLW and ILAW compositions and properties dependent on combinations of the process variations and uncertainties considered. It will likely be necessary to review and update as required the estimates of variations and uncertainties in this report after the remaining IHLW and ILAW waste form qualification testing, cold commissioning, and hot commissioning are completed.

2. *Demonstrate that IHLW and ILAW expected to be produced from each HLW and LAW waste type will meet all compliance requirements with high confidence, after accounting for variations and uncertainties.*

   The report by Piepel et al. (2005) documents the initial iteration of the work to develop methods for satisfying this success criterion. A future revision of that report will address the compliance

requirements not addressed in the initial iteration. The results in this report will be used as inputs for the future compliance demonstration work that will be documented in the future revision of Piepel et al. (2005).

3. *Develop acceptance criteria for waste feed or any vitrification process step needed to ensure that the IHLW or ILAW product will be acceptable.*

   Establishing acceptance criteria for waste feeds and vitrification process steps are WTP Project activities. This report provides some of the necessary inputs for the WTP Project to establish acceptance criteria, namely (1) the estimates of variations and uncertainties of IHLW and ILAW compositions and properties and (2) information on the sensitivity of these variations and uncertainties to variations and uncertainties in the HLW and LAW vitrification processes. The remaining inputs the WTP Project requires to establish acceptance criteria are the relevant statistically-based compliance methods presented and illustrated by Piepel et al. (2005).

4. *Complete work in accordance with QA requirements as described in Section 5 of the Test Plan (Piepel and Heredia-Langner 2003).*

   All work was completed in accordance with quality assurance (QA) requirements, as described in the subsequent "Quality Requirements" section of the Summary.

5. *Document the results in technical reports as described in Section 7 of the Test Plan (Piepel and Heredia-Langner 2003).*

   This technical report is the second of two required reports. The first was an interim report: A Heredia-Langner, GF Piepel, and SA Hartley. 2003. *Interim Report: Initial Assessment of Waste, Process, and Product Variations and Uncertainties for Waste Treatment Plant IHLW and ILAW*, WTP-RPT-073 Rev. 0, Battelle—Pacific Northwest Division, Richland, WA.

R&T Test Conditions

The test conditions applicable to this work from the Test Specification (Swanberg 2002), and clarified in the Test Plan (Piepel and Heredia-Langner 2003), are listed (in italics) and then discussed (in normal text). These conditions were adapted from Section 5 of the Test Plan, with minor revisions made to match current terminology and strategies. The discussions address whether the test condition was followed and if any deviations were necessary.

1. *Use available data on waste compositions and pretreatment processing to assess the expected extent of variation and uncertainties in pretreated HLW and LAW compositions and radionuclide contents over the course of an HLW or LAW waste type. The assessment of variation in pretreated waste feed will include analysis of variation in tank farm or staging tank samples, analysis of variation in blending schemes, impact of LAW staging and blending, and uncertainties in flowsheets or models used. Such detailed work will be performed primarily by the WTP Project, with input from PNWD statistics as needed. The results of that work will serve as inputs for any additional statistical assessment needed under this Test Plan. This activity will interface with the WTP Project so that the data developed are suitable for estimating variations and uncertainties.*

   Input from the WTP Project of the type envisioned was not available. In consultation with the WTP Project technical contacts for this work, it was decided to assume a range of values for the

variation of HLW and LAW compositions over a waste type as a way of assessing the sensitivity of the results to that variation.

2. *Use existing data or data from new tests to quantify expected variations and uncertainties in the HLW and LAW vitrification processes. The variations and uncertainties to be quantified include:*

   (a) Variation in pretreated waste feed from the HBV or ILAW Concentrate Storage Vessel (CSV) in the pretreatment facility to the HLW MFPV or LAW CRV in the HLW or LAW vitrification facility. This activity will provide input to aid the WTP Project in developing acceptance specifications for pretreated HLW or LAW feed from pretreatment.

   (b) Mixing/sampling and chemical analysis uncertainties for an HLW MFPV or LAW CRV

   (c) Mixing/sampling and chemical analysis uncertainties for a Melter Feed Preparation Vessel (MFPV) and a Melter Feed Vessel (MFV).

   (d) GFC composition, weighing, and transfer/addition uncertainties. This activity will help the WTP Project define the envisioned process specification for accepting GFCs from the GFC facility.

   (e) Uncertainties in material transfers between process vessels

   (f) Uncertainties in process calculations (e.g. algorithms used to calculate batch composition and account for process heels)

   (g) Variations or trends in target IHLW or ILAW composition over a waste type

   (h) Any other variations or uncertainties that might significantly impact the ultimate variation in IHLW or ILAW composition over a waste type.

   Data for Item 2(a) were not available, so this issue was addressed as discussed in Item 1. Data from a planned melter feed study (Sundar 2005a, 2005b) were also not available to address Items 2(b) and 2(c). Hence, reasonable ranges of values for mixing/sampling and chemical analysis uncertainties were investigated to assess the sensitivity of results to these values. Limited vendor data and WTP design specifications were available related to Items 2(d) and 2(e). Hence, in this work, a reasonable range of uncertainty values were assumed and the sensitivity to results investigated. Regarding Item 2(f), the mass balance equations for calculating masses and eventually mass fractions of IHLW and ILAW components are not subject to calculational uncertainties beyond the uncertainties associated with the input variables. Item 2(g) was addressed for IHLW by investigating three pure waste types (AY-102, AZ-102, and C-104) and one transition waste type (AY-102 to AZ-102). For ILAW, five waste types with varying severity of trends based on output of the WTP Project's G2 dynamic simulation software (Deng 2005) were investigated. Regarding Item 2(h), the known sources of variation and uncertainty were addressed in the work.

3. *Project the expected variations in IHLW and ILAW chemical compositions and radionuclide contents resulting from variations and uncertainties in the HLW and LAW waste feed and the HLW and LAW vitrification processes.*

   Batch-to-batch variation, within-batch uncertainty, and total variation plus uncertainty percent relative standard deviations (%RSDs) for chemical and radionuclide compositions of IHLW are presented in Sections 7.1 and 7.2 and of ILAW in Sections 8.1 and 8.2.

4. *Translate IHLW and ILAW composition variations to glass property variations using property-composition models (e.g., durability tests such as PCT, VHT, and TCLP). These results will be used to determine the sensitivities of glass properties to variations in glass composition.*

   Batch-to-batch variation, within-batch uncertainty, and total variation plus uncertainty %RSDs are presented for IHLW properties in Section 7.3 and for ILAW properties in Section 8.3.

5. *Demonstrate that IHLW and ILAW composition and radionuclide variations over a waste type will remain within specification limits on composition (e.g., waste loading limits; radionuclide limits). Statistical approaches appropriate for each specification will be used to demonstrate expected compliance over a waste type as part of qualification work.*

   The methods to address this scope item were presented by Piepel et al. (2005).

6. *Provide an analysis of the ability to detect variations in the HLW or LAW feed received from the pretreatment facility, and to mitigate the variations by varying GFC additions or other process control activities.*

   This condition was not addressed because it was beyond the scope of work performed. The scope of the work in this report did not involve developing glass formulation or GFC addition algorithms, which would be needed to address this criterion. The development of glass formulation and GFC addition algorithms is being performed by the WTP Project. The initial work for ILAW has been completed (Vienna 2005) and is in progress for IHLW.

7. *Assist the WTP Project in developing criteria for accepting HLW and LAW feed from the pretreatment facility.*

   The WTP Project has not started work to address this condition, and so no PNWD support was provided.

Simulant Use

The work involved in this report was of a paper-study nature. No physical testing was performed, and thus no simulants were used.

Discrepancies and Follow-on Tests

The known discrepancies that remain unresolved or partially resolved are discussed below.

1. This report contains currently available data and results on the magnitudes of all relevant sources of variation and uncertainty affecting estimates of composition and properties of ILAW and IHLW to be produced by the WTP. However, certain specific WTP data for estimating variations and uncertainties affecting the HLW and LAW vitrification processes were not yet available. The first main example of this is the data for quantifying mixing, sampling, analytical, vessel level, and vessel volume uncertainties. The second main example is that no WTP-relevant data were available with which to quantify the variation in pretreated HLW feed over the course of an HLW waste type (which corresponds to the contents of an HBV). Section 9 provides a complete assessment of the bases for current estimates of variations and uncertainties affecting the WTP HLW and LAW vitrification processes as well as the needs for additional data.

2. One of the objectives and success criteria called for developing acceptance criteria for (1) HLW and LAW feeds and (2) any vitrification process step needed to verify that the IHLW or ILAW product will be acceptable. Establishing acceptance criteria for waste feeds and vitrification process steps is a

WTP Project activity. This report provides some of the necessary inputs for the WTP Project to establish acceptance criteria, namely (1) the estimates of variations and uncertainties of IHLW and ILAW compositions and properties and (2) information on the sensitivity of these variations and uncertainties to variations and uncertainties in the HLW and LAW vitrification processes. The remaining inputs the WTP Project requires to establish acceptance criteria are the relevant statistically-based compliance methods presented and illustrated by Piepel et al. (2005).

No follow-on work is currently planned under TSSs B-61 and B-65. However, in the future after the WTP Project has finished waste form qualification (WFQ) testing or possibly after cold commissioning, the final, pre-production estimates of variations and uncertainties need to be established. These include the (1) variations and uncertainties affecting the HLW and LAW vitrification processes and (2) variations and uncertainties of IHLW and ILAW compositions and properties.

Quality Assurance

The work and results in this report were performed according to the Waste Treatment Plant Support Project (WTPSP) QA plan (PNWD 2005a) and QA manual and procedures (PNWD 2005b). The Battelle—Pacific Northwest Division (PNWD) QA plan and procedures have been approved by the WTP Project and are in conformance with NQA-1 (1989), NQA-2a, Part 2.7 (1990), and the *Quality Assurance Requirements and Description* (QARD) (DOE-RW 2003) as appropriate per the Test Plan (Piepel and Heredia-Langner 2003).

The data and inputs used in this report to develop estimates of variations and uncertainties are from a variety of sources and QA pedigrees. Data obtained from potential vendors are of commercial quality. Data obtained from testing work by PNWD, Savannah River National Laboratory (SRNL), or other WTP subcontractors are, at a minimum, compliant with requirements of NQA-1 (1989) and NQA-2a, Part 2.7 (1990). Quality-affecting data involving HLW are compliant with QARD (DOE-RW 2003). Values obtained from WTP Project design documents and other requirements documents are compliant with NQA-1 (1989) and NQA-2a, Part 2.7 (1990) as applicable.

Various kinds of data and results are summarized in tables of this report, and a comment arose during the review cycle regarding the number of significant figures used in some tables. In tables that summarize inputs provided by the WTP Project or from other reports, we included the same number of significant figures as in the original source. Also, the work in this report required the use of computer software to generate simulated data and perform statistical analyses of the simulated data. Sufficient numbers of significant figures (or decimal places) were retained in the input values to avoid round-off error in calculated values. Finally, variations and uncertainties in this report are generally reported as %RSDs, which are presented to one decimal place in tables.

Acknowledgments

The authors acknowledge the support of cognizant Waste Treatment and Immobilization Plant (WTP) Project staff in the Research and Technology organization, including Keith Abel and John Vienna (the technical contacts for this work) and Joe Perez (the lead for Waste Form Qualification). We also acknowledge Joe Westsik (a previous technical contact for this work) and Chris Musick (the previous Waste Form Qualification lead). John Vienna, Keith Abel, and Joe Westsik gathered key information and inputs for quantifying variations and uncertainties in the high-level waste and low-activity waste vitrification processes. David Dodd and Bruce Kaiser of the WTP analytical organization are also gratefully acknowledged for providing estimates of analytical uncertainties.

The authors also acknowledge and thank other Battelle—Pacific Northwest Division contributors to this report: Scott Cooley for statistical technical review, Kirsten Meier for quality assurance review, Gordon Beeman for project review, Wayne Cosby for editorial review and formatting, and Chrissy Charron for other preparations and transmittal of the report.

Acronyms, Terms, Abbreviations, and Notations

Please note that the list of Acronyms, Terms, and Abbreviations and the list of Notations are located in Appendices G and H, respectively.

Contents

Figures

Tables

1.0 Introduction

Process samples, chemical analyses of composition, and measurements (e.g., volume, weight, and density) will be required to control Waste Treatment and Immobilization Plant (WTP) vitrification facilities that will produce immobilized high-level waste (IHLW) and immobilized low-activity waste (ILAW). In addition, process and/or product samples, chemical analyses, and measurements will be required to satisfy applicable compliance requirements. For example, the Waste Acceptance System Requirements Document (WASRD) describes the compliance requirements of the national geological repository for IHLW (DOE-RW 2002). Also, the contract between the U.S. Department of Energy (DOE) Office of River Protection (ORP) and Bechtel National, Inc. (BNI) specifies compliance requirements for ILAW as well as additional compliance requirements for IHLW (DOE-ORP 2005).

Although the process-product control and compliance strategies for the WTP IHLW and ILAW facilities have not been finalized, many aspects have been determined. The current compliance strategies for the WTP IHLW and ILAW facilities are described, respectively, in the IHLW Product Compliance Plan (IHLW PCP) by Nelson (2005) and the ILAW Product Compliance Plan (ILAW PCP) by Westsik et al. (2004). Many of the compliance strategies outlined in the IHLW PCP and ILAW PCP are statistical in nature. That is, the strategies involve quantifying and accounting for variations and uncertainties in controlling the IHLW and ILAW vitrification processes and in satisfying compliance requirements. Statistically based strategies are being developed for pre-production activities (i.e., waste form qualification activities), production activities (i.e., batch-by-batch process-product control and compliance activities), and post-production activities (i.e., compliance and acceptance activities for product resulting from specified quantities of waste or periods of production). Strategies for environmental regulatory compliance (e.g., plant emissions or complying with Land Disposal Restriction [LDR] and delisting criteria) are described in the delisting/LDR data quality objectives document (Cook and Blumenkranz 2003). These strategies are also statistically based in that they account for applicable variations and uncertainties.

Several aspects of the WTP IHLW and ILAW qualification, process-product control, and compliance strategies require estimates of variations and uncertainties of (1) incoming waste feed, (2) process materials and vessel contents at individual steps of the IHLW and ILAW processes, and (3) the compositions and properties of IHLW and ILAW products. A report by Heredia-Langner et al. (2003) summarizes the initial work in quantifying variations and uncertainties that may affect the WTP IHLW and ILAW processes and the ability to demonstrate compliance with various specifications. That report also summarized variation and uncertainty estimates extracted from initial operations data at the Defense Waste Processing Facility (DWPF) and the West Valley Demonstration Project (WVDP). This report provides updated estimates of variations and uncertainties expected by the WTP IHLW and ILAW processes and the resulting products. This report is the final iteration of the Statistical Analysis task's B-61 and B-65 work. When the WTP Project completes additional testing and waste form qualification (WFQ) work (e.g., the Melter Feed Testing work scheduled for 2006-2007 to quantify mixing, sampling, transfer, vessel level measurement, and other uncertainties), any impact to the assumptions, inputs, or results in this report should be assessed.

Before continuing, it is important to clarify the use of the terms *variation* and *uncertainty* in this report. *Variation* refers to real changes in a variable over time or space (for example, variation in glass

composition because of variation in waste feed composition). *Uncertainty* refers to a lack of knowledge about a true, fixed state of affairs (for example, analytical uncertainty in the chemical analysis of a glass sample). Hence, WTP IHLW and ILAW slurry and glass compositions will be subject to *variation* over time, whereas samples, chemical analyses, volume measurements, weight measurements, density measurements, and other measurements at specific times will be subject to *uncertainty*.

WTP strategies for operating the IHLW and ILAW facilities account for uncertainties in making process decisions such as volume transfers and the addition of glass forming chemicals (GFCs) to waste. Magnitudes of uncertainties impact the number of samples, analyses per sample, and measurements that are needed to make process decisions and demonstrate compliance in the WTP IHLW and ILAW facilities. WTP strategies also account for variations and uncertainties in demonstrating compliance with applicable specifications. Hence, it is important to the successful operation of the WTP IHLW and ILAW facilities to have well-supported estimates of variations and uncertainties for individual stages of the vitrification processes as well as in the waste glass compositions and glass properties.

There were two main objectives for the work documented in this report. The first main objective was to gather and summarize the best, currently available WTP Project estimates of variations and uncertainties that will affect stages of the WTP IHLW and ILAW vitrification processes. The estimates included in this report are updates of those included in a previous interim report (Heredia-Langner et al. 2003). There are still some parts of the WTP IHLW and ILAW processes where experimental work to quantify biases and uncertainties in mixing, sampling, and transfer of wastes and melter feeds (waste with added GFCs) is planned for the future. In such cases, the best current estimates of the WTP Project were used for this work. The second main objective was to quantify variations and uncertainties expected in WTP IHLW and ILAW glass compositions, compliance properties, and processing properties. Quantifying uncertainties in glass compositions and properties involved propagating the applicable uncertainties using a Monte Carlo simulation approach. Estimates of variations in pretreated waste over a high-level waste (HLW) or low-activity waste (LAW) waste type (see Section 2.4) were also included in the Monte Carlo simulations to quantify variations in WTP IHLW and ILAW compositions and properties corresponding to HLW and LAW waste types.

The estimates of IHLW and ILAW process variations and uncertainties contained in this report will serve as inputs to other WTP Project work, including:

- Developing statistical methods to implement WTP IHLW and ILAW processing constraints as well as to meet compliance specifications. A substantial portion of this work has been completed and documented by Piepel et al. (2005) with a final iteration of the work and report scheduled for the future.

- Determining the required numbers of samples, analyses, and process measurements needed in the WTP HLW and LAW vitrification facilities to demonstrate compliance with applicable WASRD (DOE-RW 2002) and Contract (DOE-ORP 2005) specifications. The first iteration of this work is documented in the Piepel et al. (2005) report, with a final iteration scheduled for the future.

- Developing and implementing algorithms that will be used in operating the WTP HLW and LAW vitrification facilities and demonstrating that the IHLW and ILAW products meet all acceptance requirements. During WTP operations, these algorithms will be used to calculate volume

transfers, glass formulations (i.e., melter feed batch compositions), and GFC additions to achieve these compositions. The algorithms will use the statistical methods and results discussed in the first two bullets, along with the estimated variations and uncertainties in this report, to make these calculations so that all processing and compliance requirements are met with sufficient confidence. The first iteration of the development portion of this work has been completed for ILAW (Vienna 2005; Vienna et al. 2006) and is in progress for IHLW. The WTP Project also has planned final iterations of the algorithm work for each of the ILAW and IHLW waste types. The PNWD Statistical Support Task is supporting this WTP work so that the statistical methods, variations, and uncertainties are appropriately factored into the algorithms.

Work in these areas will be documented in separate future reports issued by PNWD for the work in the first two bullets and the WTP Project for the work in the last bullet.

The remainder of this document is organized as follows. Section 2 provides a general overview of the IHLW and ILAW vitrification processes, discusses the steps of the IHLW and ILAW process control and compliance strategies, describes the concept of a *waste type* for HLW and LAW, and identifies the basis for quantifying variations and uncertainties. Section 3 discusses the IHLW and ILAW compositions and properties for which variations and uncertainties are quantified in this report as well as the sources of variation and uncertainties in the HLW and LAW vitrification processes that affect IHLW and ILAW compositions and properties. Section 4 summarizes current estimates of variations and uncertainties associated with several steps of the WTP HLW and LAW vitrification processes. Section 5 describes the computer experiment and Monte Carlo simulation methods used to study the effects of process variation and uncertainties on IHLW and ILAW compositions and properties. Section 6 presents the equations for calculating IHLW and ILAW compositions, and the property-composition models for calculating properties of HLW and LAW melts and glasses as a function of composition (and where applicable, melt temperature). Sections 7 and 8 present the results of the computer experiment and Monte Carlo investigations to quantify variations and uncertainties in IHLW (Section 7) and ILAW (Section 8) compositions and properties. Section 9 summarizes the work and results, and makes recommendations for data needed to support future efforts to better quantify WTP IHLW and ILAW variations and uncertainties. Section 10 discusses how the results in this report meet, or can be used to meet, WTP needs. Section 11 lists the references cited in the text of the report. Appendices provide equations and other information too detailed to include in the main body of the report.

2.0 The WTP IHLW and ILAW Vitrification Processes and Bases for the Process Control and Compliance Strategies

Section 2.1 provides a general overview of the IHLW and ILAW vitrification processes and introduces the generic terms used to refer to IHLW and ILAW process vessels and other process steps. Sections 2.2 and 2.3 discuss the steps of the IHLW and ILAW process control and compliance strategies, respectively. Section 2.4 describes the concept of a *waste type*, over which variations are quantified in this report. Section 2.5 describes the single-batch basis for quantifying uncertainties and the batch-to-batch basis for quantifying variations. Readers familiar with the WTP processes and strategies could skip over Sections 2.1 to 2.3 and quickly read the short Sections 2.4 and 2.5.

2.1 IHLW and ILAW Vitrification Processes

This report focuses on estimating variations and uncertainties associated with the WTP IHLW and ILAW vitrification processes and products. Figure 2.1 and Figure 2.2, which were supplied by the WTP Project, display simplified overviews of the IHLW and ILAW vitrification processes. The figures illustrate the key process vessels, the glass former chemicals (GFCs) system, the melter, and possible sampling and measurement points. Symbols in the figures denote sampling points (S in a circle), non-routine sampling points (S_n in a circle), weight determinations (W in a diamond), and level measurements of vessels (L in a diamond).

In the IHLW vitrification facility (Figure 2.1), only the Melter Feed Preparation Vessel (MFPV) will be routinely sampled and analyzed. Each MFPV batch will be sampled and analyzed after transfer of pretreated HLW from the HLW Blend Vessel (HBV)[(a)] but before GFCs are added. Each HLW MFPV batch will be sampled and analyzed again after GFCs are added to establish the composition of IHLW that would be produced from that batch. In the ILAW vitrification facility (Figure 2.2), only the Concentrate Receipt Vessel (CRV) will be routinely sampled and analyzed. Each CRV batch will be sampled and analyzed after transfer of pretreated LAW from the LAW Concentrate Storage Vessel (CSV). The composition of ILAW that would be produced from each MFPV batch will be calculated using the (1) analyses of CRV samples, (2) weights of GFCs added to the MFPV batch, and (3) composition of the heel from the previous MFPV batch. Non-routine samples may be taken during commissioning testing of the HLW and LAW vitrification facilities or during production operations as determined by the WTP compliance strategies.

Weight determinations will be used to quantify the amounts of individual GFCs added to waste feed concentrates in the IHLW and ILAW MFPVs. Weights of individual GFCs will be determined as well as weights of combined GFCs in the GFC batch makeup hopper and the GFC feed hopper. Multiple weighing points provide for verifying transfers of individual and combined GFCs. Note that Figure 2.1 and Figure 2.2 only show GFC silos and not the hoppers, but it will be in the hoppers that GFC weight determinations are made.

(a) The HLW Blend Vessel (HBV) is located in the pretreatment facility and will contain mixtures of all HLW waste streams. The HBV will not be refilled until emptied and will nominally supply HLW for 18 IHLW MFPV batches.

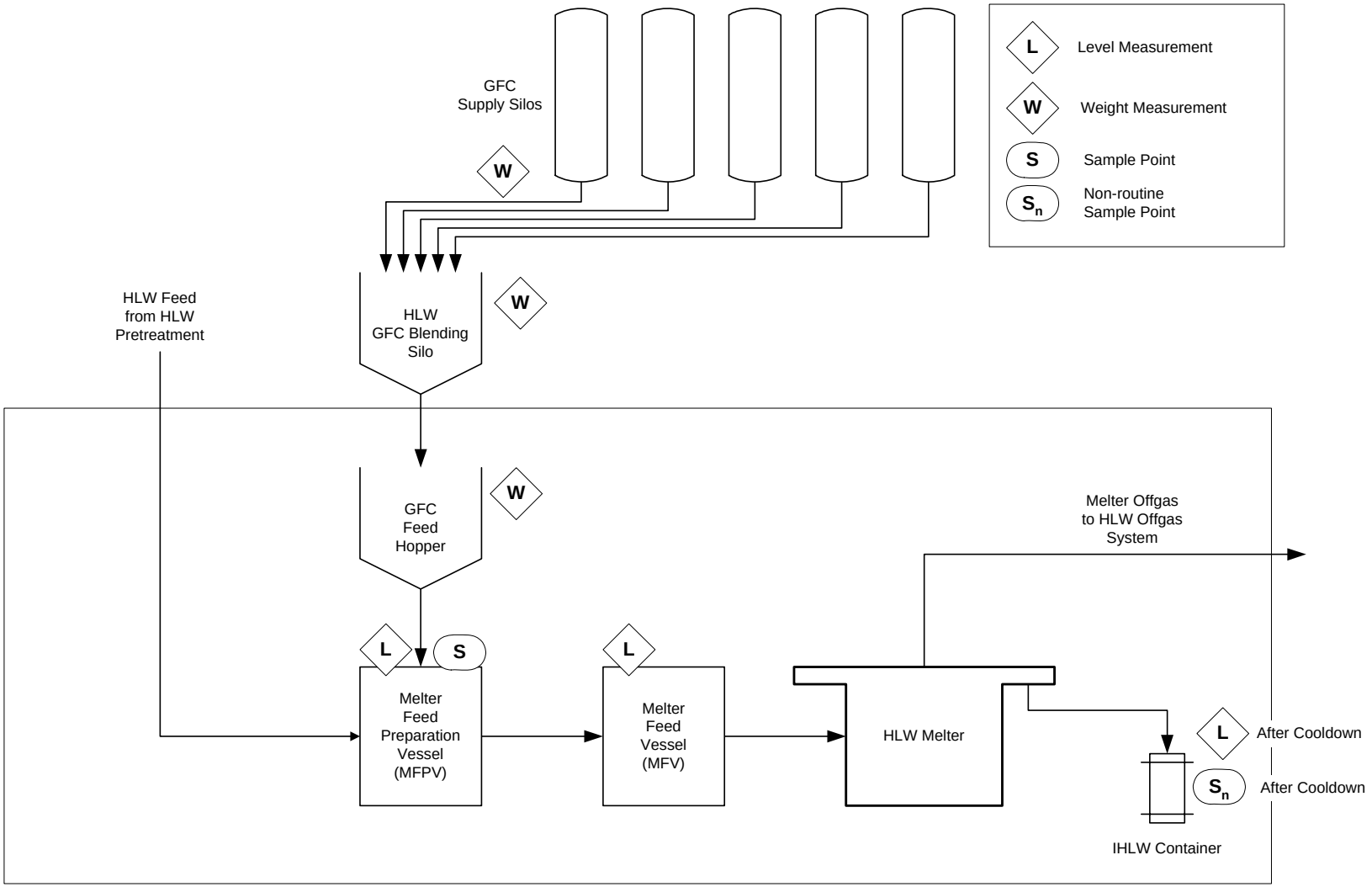

Figure 2.1. Overview of the HLW Vitrification Process

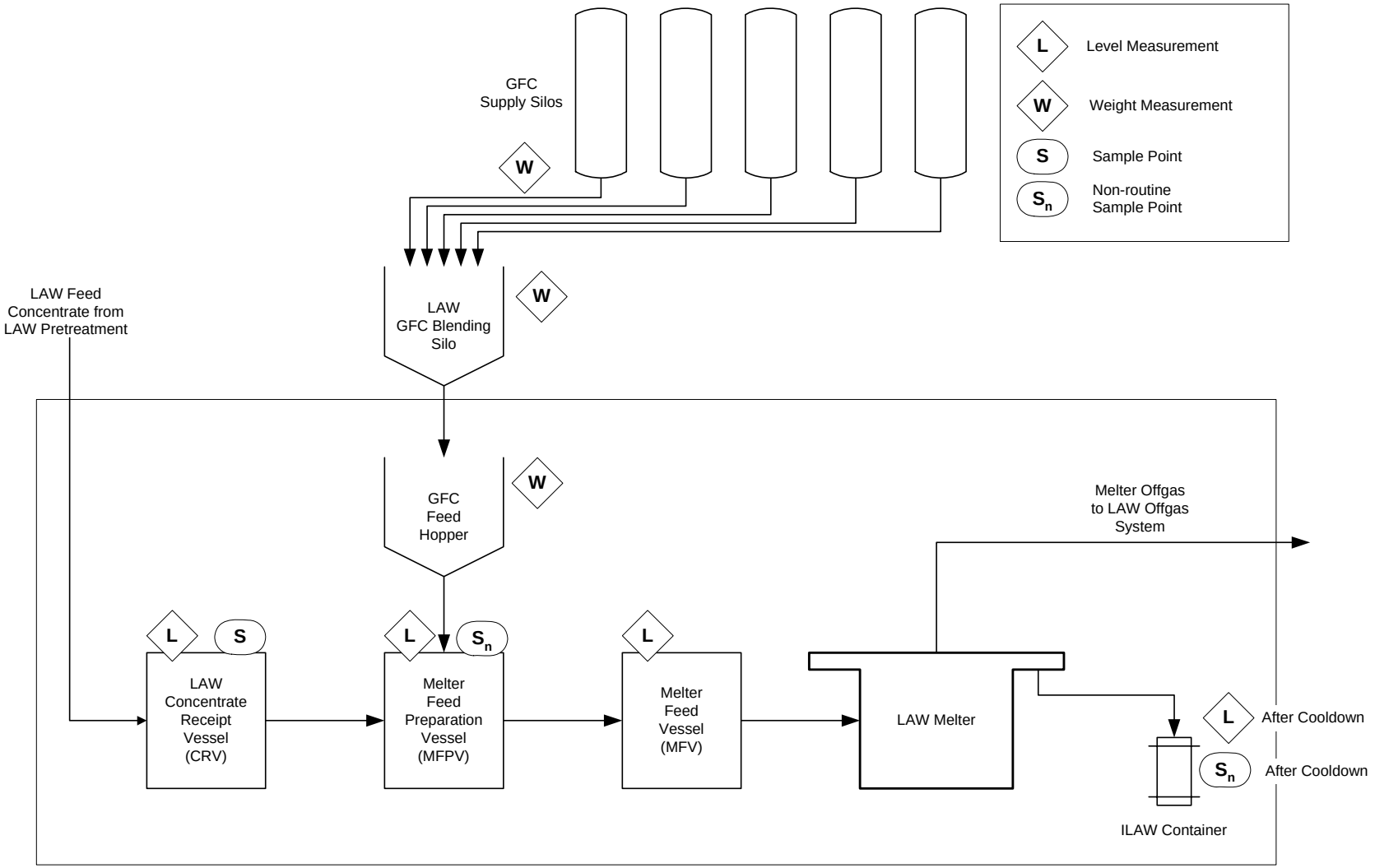

Figure 2.2. Overview of the LAW Vitrification Process

Level measurements will be made in the CRV (ILAW only), MFPV (IHLW and ILAW), and Melter Feed Vessel (MFV) (IHLW and ILAW). A level-to-volume calibration equation for each vessel will then be used to calculate the vessel volume corresponding to a measured vessel level. Such measurements are important for estimating compositions and verifying transfers to and from the CRV (ILAW only), MFPV (IHLW and ILAW), and MFV (IHLW and ILAW). Fill levels of IHLW canisters and ILAW containers will also be measured, as shown in Figure 2.1 and Figure 2.2.

Although not indicated by symbols in Figure 2.1 and Figure 2.2, sampling and chemical analyses are planned in the pretreatment facility to verify that pretreated waste is acceptable for transfer to the IHLW vitrification facility. Similarly, individual GFCs may be sampled and chemically analyzed to verify their compositions before being introduced to the GFC batch makeup facility. The density of material in the CRV (ILAW only) and MFPV (ILAW and IHLW) will be determined and used for process control purposes as well as compliance purposes in some cases.

2.2 Steps of the WTP IHLW Process Control and Compliance Strategies

The current WTP IHLW process control and compliance strategies are discussed in detail by Nelson (2005). According to these strategies, the process samples, analyses, and measurements that will be used during production to control the process and demonstrate compliance with IHLW specifications are outlined in the following steps.

1. For each HLW MFPV batch, transfer a portion of the current HBV to the HLW MFPV. Measure n_V^{MFPV} times the level of the HLW MFPV contents before and after the HBV-to-MFPV transfer and average each set of measurements to obtain the level determinations of the MFPV batch before and after the HBV transfer. Apply level-to-volume calibration equations for the HLW MFPV to convert the average vessel levels (before and after HBV transfers) to volumes. Use the before and after determinations of the HLW MFPV volumes to calculate the HBV-to-MFPV transfer volume (L).

2. After the transfer from the HBV to the HLW MFPV, collect n_{S1}^{MFPV} samples from each HLW MFPV and analyze each sample n_{A1}^{MFPV} times. Based on work in Piepel et al. (2005), it is expected that each sample will only be analyzed once.

3. For each HLW MFPV batch,[(a)] obtain and/or calculate the oxide mass-fraction compositions of each GFC from vendor certification sheets. The oxide mass fractions for a given GFC should be relative to the total GFC mass, including absorbed water or other volatiles that will not persist in the HLW melter.

4. Calculate the masses of GFCs to be added to each HLW MFPV batch so that when combined with the volume of waste transferred from the HBV and the HLW MFPV heel, the resulting HLW MFPV slurry will make HLW glass satisfying all processing constraints and compliance requirements. Add the calculated amounts of GFCs to the HLW MFPV.

(a) Presumably, the nominal oxide mass fraction compositions of GFCs and uncertainties thereof will change infrequently, but the WTP Project must have the capability to change this information for any MFPV batch when appropriate.

5. For each HLW MFPV batch, measure n_V^{MFPV} times the level of the HLW MFPV contents after adding the GFCs. Average the resulting measurements to obtain the level determination. Apply the level-to-volume calibration equation for the HLW MFPV to convert the MFPV level determination to a volume (L).

6. For each completed HLW MFPV batch, collect n_{S2}^{MFPV} samples.

7. For each completed HLW MFPV batch, analyze n_{A2}^{MFPV} times the chemical composition (element concentrations in µg/mL = mg/L) of each sample. Based on work in Piepel et al. (2005), it is expected that each sample will only be analyzed once.

8. For the first HLW MFPV batch from each HBV, analyze the concentrations of the radionuclides listed in the second column of Table 2.1. These radionuclides are more difficult to measure and thus will only be measured in the first MFPV batch of an HLW waste type (see Section 2.4). In subsequent MFPV batches of an HLW waste type, these radionuclide concentrations will be assigned values equal to those measured in the first MFPV batch.

9. For the remaining HLW MFPV batches from each HBV, analyze the radionuclides listed in the third column of Table 2.1. These radionuclides are more easily measured and hence will be measured in each MFPV batch corresponding to an HLW waste type.

10. For each IHLW canister produced, determine the mass of glass in the canister.

In Steps 7 and 8, it is important that all detectable chemical and radionuclide composition components be quantified in chemical and radionuclide analyses. Only some of the detectable IHLW components are deemed important[(a)] as shown in Table 2.1 and Table 2.2. However, failing to analyze for and quantify detectable components can lead to underestimating the mass of all IHLW components and thus result in biased estimates of IHLW composition (i.e., mass fractions of IHLW components).

Steps 1 to 5 are relevant to process control whereas Steps 6 to 10 are relevant to demonstrating compliance with IHLW specifications during production. The quantities of interest in this report for which variations and uncertainties are quantified (e.g., IHLW chemical and radionuclide composition and processing and product quality properties) can be calculated using the information in Steps 6 to 10. Section 6 discusses the equations for calculating IHLW composition and properties of interest in this report. Because only n_{S2}^{MFPV} and n_{A2}^{MFPV} are relevant to the work in this report, for simplicity of notation, they are henceforth denoted n_S^{MFPV} and n_A^{MFPV}, respectively.

2.3 Steps of the WTP ILAW Process Control and Compliance Strategies

The WTP ILAW process control and compliance strategies are discussed in detail by Westsik et al. (2004). According to these strategies, the process samples, analyses, and measurements that will be used to comply with ILAW specifications are outlined in the following steps.

(a) A chemical or radionuclide composition component of IHLW is considered "reportable" if it must be used to satisfy one or more IHLW specifications, either directly or indirectly, through a property-composition model.

1. For each LAW CRV batch, collect n_S^{CRV} samples.

2. For each LAW CRV batch, analyze n_A^{CRV} times the chemical composition (element concentrations in μg/mL = mg/L) of each sample. Based on work in Piepel et al. (2005), it is expected that each sample will only be analyzed once.

3. For each LAW CRV batch, analyze the concentrations of the radionuclides listed in the "LAW from Each CRV" column of Table 2.1.

4. For each LAW MFPV batch, transfer a portion of the current LAW CRV batch to the LAW MFPV. Measure n_V^{CRV} times the levels of LAW CRV and LAW MFPV contents before and after the CRV-to-MFPV transfer. Average the resulting measurements in each set to obtain the level determinations before and after transfer. Apply level-to-volume calibration equations for the LAW CRV and MFPV to convert the vessel level determinations (before and after transfer) to volumes. Use the before and after determinations of the LAW CRV and MFPV volumes to calculate the CRV-to-MFPV transfer volume.

5. For each LAW MFPV batch,[(a)] obtain and/or calculate the oxide mass-fraction compositions of each GFC from vendor certification sheets. The oxide mass fractions for a given GFC should be relative to the total GFC mass, including absorbed water or other volatiles that will not persist in the LAW melter.

6. Calculate the masses of GFCs to be added to each LAW MFPV batch so that when combined with the volume of waste transferred from the LAW CRV and the LAW MFPV heel, the resulting LAW MFPV slurry will make LAW glass satisfying all processing constraints and compliance requirements.

7. For each LAW MFPV batch, weigh the amounts of GFCs to be added to the LAW MFPV. Add the GFCs to the LAW MFPV.

8. For each ILAW container produced, calculate the mass of glass in the container based on volume and fill height of the container as well as the density of the glass.

In Steps 2 and 3, it is important that all detectable chemical and radionuclide composition components be quantified in chemical and radionuclide analyses. Only some of the detectable ILAW components are deemed important[(b)] as shown in Table 2.1 and Table 2.2. However, failing to analyze for detectable components can lead to underestimating the mass of all ILAW components and thus result in biased estimates of ILAW composition (i.e., mass fractions of ILAW components).

(a) Presumably, the nominal oxide mass fraction compositions of GFCs and uncertainties thereof will change infrequently, but the WTP Project must have the capability to change this information for any MFPV batch when appropriate.

(b) A chemical or radionuclide composition component of ILAW is considered "reportable" if it must be used to satisfy one or more ILAW specifications, either directly or indirectly, through a property-composition model.

Table 2.1. Important Isotopes to be Analyzed in the WTP IHLW MFPV and ILAW CRV

Isotope[a]	First HLW MFPV from Each HBV	Remaining HLW MFPVs from Each HBV	LAW from Each CRV
^{59}Ni	Y[b]	-	-
^{60}Co	-[b]	-	Y
^{63}Ni	Y	-	Y
^{90}Sr	Y	Y	Y
^{93}Zr	Y	-	-
^{93}Nb	Y	-	-
^{99}Tc	Y	-	Y
^{125}Sb	-	-	Y
^{126}Sn	Y	-	-
^{129}I	-	-	Y
^{135}Cs	Y	-	-
^{137}Cs	Y	Y	Y
^{151}Sm	Y	-	Y
^{152}Eu	Y	-	-
^{154}Eu	-	-	Y
^{155}Eu	-	-	Y
^{233}U	Y	-	Y
^{234}U	Y	-	-
^{235}U	Y	-	Y
^{236}U	Y	-	-
^{237}Np	Y	-	Y
^{238}U	Y	-	Y
^{238}Pu	Y	Y	Y
^{239}Pu	Y	^{239}Pu + ^{240}Pu	Y
^{240}Pu	Y	^{239}Pu + ^{240}Pu	Y
^{241}Pu	Y	-	Y
^{241}Am	Y	-	Y
^{242}Pu	Y	-	-
^{242}Cm	Y	-	-
^{243}Cm	-	-	Y[b]
^{244}Cm	Y[c]	-	Y[b]
^{243}Am	Y	-	-

(a) A chemical or radionuclide composition component of immobilized waste is considered "important" if it must be used to satisfy one or more applicable specifications, either directly or indirectly, through a property-composition model. The list of important radionuclides was provided by John Vienna and Keith Abel of the WTP Project and is based primarily on Kaiser et al. (2003, 2004).

(b) A dash (-) indicates that the isotope is not important for that particular location. Y indicates that it is.

(c) The analytical methods typically used report only ^{243}Cm + ^{244}Cm.

Table 2.2. Important Chemical Composition Oxides for IHLW and ILAW

Oxide or Halogen Component	IHLW[(a)] Important?	ILAW[(b)] Important?
Al_2O_3	Y[(c)]	Y
B_2O_3	Y	Y
CaO	Y	Y
CdO	Y	-
Cl	-[(c)]	Y
Cr_2O_3	Y	-
Fe_2O_3	Y	Y
K_2O	-	Y
Li_2O	Y	Y
MgO	Y	Y
MnO	Y	-
Na_2O	Y	Y
NiO	Y	-
P_2O_5	Y	Y
PdO	Y	-
Rh_2O_3	Y	-
RuO_2	Y	-
SO_3	Y	Y
Sb_2O_3	Y	-
SeO_2	Y	-
SiO_2	Y	Y
SrO	Y	-
ThO_2	Y	-
UO_3	Y	-
ZnO	Y	Y
ZrO_2	Y	Y
Others[(d)]	-	Y

(a) The list of important IHLW chemical composition components was provided by John Vienna and Keith Abel of the WTP Project, and is based primarily on Kaiser et al. (2003, 2004). It includes not only components that must be reportable according to one or more specifications, but also components expected to be present in one or more glass product or processing property-composition models.

(b) The list of important ILAW chemical composition components was provided by the WTP Project. It includes not only components that must be reportable according to one or more specifications, but also components expected to be present in one or more glass product or processing property-composition models. The list was developed and provided by the WTP Project.

(c) A dash (-) indicates that the component is not important in the sense described. Y indicates that it is.

(d) Others is the sum of all other oxides or halogens not specifically listed.

Steps 1 to 6 provide data for both process control and compliance aspects of the WTP strategy for ILAW. The quantities of interest in this report for which variations and uncertainties are quantified (e.g., ILAW chemical and radionuclide composition, and processing and product quality properties) can be calculated using the information in Steps 1 to 6. Section 6 discusses the equations for calculating ILAW composition and properties of interest in this report.

2.4 Variation over an HLW or LAW Waste Type

In this report, the term *waste type* is used to refer to a specified quantity of HLW or LAW yielding a given number of MFPV batches (and the HLW or LAW glass that will be produced from those MFPV batches). One of the objectives of the work in this report is to quantify the variation in HLW and LAW glass compositions and properties over an HLW or LAW waste type. Such variations will impact the reporting and compliance demonstration strategies and methods for WTP IHLW and ILAW (Piepel et al. 2005).

The WTP compliance strategy for IHLW (Nelson 2005) specifies an HLW waste type as corresponding to the contents of a pretreatment HBV. An HBV is the last vessel in the pretreatment facility that sends HLW to the MFPV in the IHLW facility. An HBV will be filled and then emptied with successive transfers to the HLW MFPV before being refilled. In this sense, an HBV is "capped" and serves as an appropriate basis for defining an HLW waste type. An HBV will yield roughly 18 MFPV batches, with an MFPV batch roughly equivalent to 2 to 5 canisters of HLW glass, depending on the HLW and waste loading. Hence, an HBV (and thus an HLW waste type) will yield 18 MFPV batches and roughly from 36 to 90 canisters of HLW glass.

The WTP ILAW compliance strategy (Westsik et al. 2004) envisions different definitions of an LAW waste type, depending on the compliance specification. For some specifications, an LAW waste type corresponds to the LAW from a given waste tank. This definition of a waste type is different for LAW than for HLW because of two main reasons. First, the composition of LAW is dominated by sodium with the next most important component being sulfate—hence, the composition of LAW from a waste tank will not vary as significantly as that of HLW. Second, the LAW CSV in the pretreatment facility that feeds the LAW CRV will not be "capped" as will the similar HBV for HLW. That is, more LAW will be added to the CSV after every transfer from the CSV to the LAW CRV. Because the composition of the LAW CSV will be continuously (albeit slowly) changing over a waste tank, an LAW tank was chosen by the WTP Project as defining an LAW waste type. Depending on the LAW waste tank, an LAW waste type is expected to yield varying numbers of MFPV batches and containers of LAW glass. For other specifications, an LAW waste type corresponds to a specified small number of LAW MFPV batches over which ILAW results will be reported or compliance demonstrated. It is this latter definition that is the focus of work in this report.

2.5 Quantifying Variations and Uncertainties on an MFPV Basis

As described in Sections 2.2 and 2.3, the focus of the WTP process control and compliance strategies during IHLW and ILAW production is the MFPV batch. During WTP operations, process control and compliance quantities (e.g., chemical composition, radionuclide composition, product durability, and processing properties) and their uncertainties will be calculated for each MFPV batch. Uncertainties will

be accounted for in the algorithms to formulate IHLW and ILAW compositions for each MFPV batch. For compliance specifications with limits, compliance will be demonstrated during WTP operations for each MFPV batch before it is transferred to the MFV. Also, the WTP Project will account for variations of the calculated compliance quantities and their uncertainties for MFPV batches corresponding to a waste type to demonstrate compliance over a waste type. Hence, in this report, uncertainties are quantified on an MFPV-batch basis, and variations are quantified on a waste-type basis, where a waste type corresponds to some number of IHLW or ILAW MFPV batches.

3.0 Sources of Variation and Uncertainties Affecting WTP IHLW and ILAW Compositions and Properties

This section summarizes the sources of variation and uncertainties in the WTP HLW and LAW vitrification processes that affect IHLW and ILAW compositions and properties. Recall from Section 1.0 the meanings of the terms variation and uncertainty. *Variation* refers to real changes in a variable over time or space (for example, variation in glass composition because of variation in waste feed composition). *Uncertainty* refers to a lack of knowledge about a true, fixed state of affairs (for example, analytical uncertainty in the chemical analysis of a glass sample).

Section 3.1 discusses the IHLW and ILAW compositions and properties for which variations and uncertainties are quantified in this report. Section 3.2 discusses the general categories of variation and uncertainties that affect the IHLW and ILAW compositions and properties. Section 3.3 discusses the sources of variation and uncertainties in the HLW and LAW vitrification processes that affect IHLW and ILAW compositions and properties.

3.1 WTP IHLW and ILAW Compositions and Properties for which Variations and Uncertainties are Quantified

In this report, variations and uncertainties are quantified for several aspects of the IHLW and ILAW products that must be (1) controlled to verify processability, (2) reported in production records, and (3) demonstrated to meet specification limits. These aspects include:

- Chemical and radionuclide compositions, which are expressed in mass fractions of glass components (typically oxides) that sum to one over all chemical and radionuclide composition components in IHLW or ILAW
- Processability properties, including viscosity and electrical conductivity (IHLW and ILAW) and temperature at which crystallinity in the melt is 1% by volume (IHLW, denoted $T_{1\%}$)
- Compliance properties involving chemical durability of glass, which include
    - Product Consistency Test (PCT) B, Li, and Na releases (IHLW)
    - PCT B and Na releases (ILAW)
    - Toxicity Characteristic Leach Procedure (TCLP) Cd release (IHLW)
    - Vapor Hydration Test (VHT) (ILAW).

The sources of variation and uncertainty that affect these aspects of IHLW and ILAW are discussed in the following section.

3.2 Categories of Variation and Uncertainty Affecting IHLW and ILAW Composition and Properties

This section defines and discusses the general categories of variation and uncertainty in the HLW and LAW vitrification processes addressed in this report. These general categories apply to both HLW and LAW vitrification processes, with any specific cases noted.

Batch-to-Batch Random Variation: This refers to the random differences in true average compositions or property values of IHLW or ILAW corresponding to MFPV batches associated with an HLW or LAW waste type. Such differences occur as a result of random changes over time in the composition of the waste type being processed and the random effects associated with making each MFPV batch.

Batch-to-Batch Systematic Variation: This refers to systematic (i.e., non-random) differences in true average compositions of IHLW or ILAW corresponding to MFPV batches associated with an HLW or LAW waste type. Systematic changes occur as a result of systematic changes in the composition of the waste type being processed. These changes are somewhat dampened as a result of each new MFPV batch containing a mixture of newly added waste and GFCs and the heel of the previous MFPV batch. Thus, systematic variations in waste composition along with "heel mixing" result in the effective systematic batch-to-batch variation experienced over a waste type.

Random Mixing Uncertainty: This refers to random differences, because of mixing, in IHLW or ILAW composition or properties throughout a given MFPV batch compared to the true or average values for that MFPV batch. Similarly, random mixing uncertainty can occur for waste in an LAW CRV.

Systematic Mixing Uncertainty: This refers to systematic differences in the IHLW or ILAW composition or properties of material at different locations in an MFPV batch that are greater than the differences expected based on random mixing uncertainty. For example, systematic mixing uncertainty would occur in cases where the solids content of an MFPV batch increases from the top to bottom. Another example might be a zone in the MFPV that is not mixed well compared to the rest of the MFPV. Similarly, systematic mixing uncertainty can occur in an LAW CRV. However, in this report, systematic mixing uncertainty was assumed to be nonexistent or negligible. The consequences of non-negligible systematic mixing/sampling uncertainty were investigated in the report by Amidan et al. (2004).

Random Sampling Uncertainty: This refers to random differences in the composition (or associated properties) of samples collected by a sampling system from the LAW CRV or HLW MFPV compared to the true average composition (or associated properties) of the vessel's contents.

Systematic Sampling Uncertainty (Bias): This refers to a difference in the average composition of samples taken by a sampling system compared to the true or average composition of the material being sampled. For the work in this report, sampling bias was assumed to be nonexistent or negligible. The WTP Project is planning tests to assess whether the automated sampling system (ASX) planned for use in the WTP IHLW and ILAW facilities is subject to sampling bias. If so, it was assumed for this work that the cause of the sampling system bias would be isolated and resolved. For both DWPF and WVDP, initial tests identified sampling system biases. However, modifications were made to eliminate these biases. Hence, the assumption of no sampling system bias made for this work was deemed to be

reasonable. However, note that the Engineering Specification for the Autosampling System (24590-WTP-3PS-MHSS-T0002, Section 3.3.1) requires sampling representativeness between source and sample of ± 1%. It is likely that an estimated bias in that range would be statistically non-significant, in which case the assumption in this work of no bias would be appropriate. However, if the WTP qualification testing of the ASX ultimately detects a statistically significant bias within ± 1%, then that bias would have to be accounted for in waste form qualification and compliance activities. A report by Amidan et al. (2004) investigated the consequences of various levels of mixing/sampling bias.

Random Analytical or Measurement Uncertainty: This refers to random differences in measurements or chemical analyses of a quantity (e.g., concentration, mass, density) compared to the true or average value of that quantity. These random differences include those resulting from sample preparation as well as the actual analytical or measurement procedure.

Systematic Analytical or Measurement Uncertainty (Bias): This refers to the systematic differences in measurements or chemical analyses of a quantity compared to the true or average value of that quantity. For example, chemical analysis processes that do not properly dissolve all of the silica in waste glass can result in a biased (underestimated) amount of silica in the glass. For the work in this report, we assumed analytical or measurement bias would be nonexistent or negligible. This assumption is reasonable if analytical and measurement systems are properly tested and qualified. Also, it was assumed the WTP analytical laboratory will have certified standards and bias detection and correction procedures in place so that any unexpected biases in analytical and measurement results can be detected and corrected. Weier and Piepel (2003) discuss and illustrate methods that can be used to identify and correct biases and reduce uncertainties in analyzed slurry and glass compositions.

Random Volume Determination Uncertainty: This refers to random differences in volume or volume transfer determinations compared to the true volume or volume transfer. In the HLW and LAW vitrification facilities, volume transfers can be calculated by using before-transfer and after-transfer volumes of the receiving vessel (or a weighted average of the transfer volumes calculated from sending and receiving vessel volumes to reduce uncertainty). However, vessel volumes will not be measured directly. Rather, the levels of contents in vessels will be measured and then translated to volumes using the level-to-volume calibration equation appropriate for each vessel. Hence, volume and volume transfer determinations will be affected by uncertainties in level measurements as well as uncertainties in the level-to-volume calibration equation. For the work in this report, it was assumed that volume determinations will not be subject to systematic uncertainties (biases). Presumably, if any such biases are found in the level measurement system, they would be adjusted or corrected. Also, it was assumed that unbiased level-to-volume calibration equations can be developed.

Random GFC Composition Uncertainty: This refers to the random differences in composition in a large batch of a given GFC compared to the average composition of the batch. GFCs used in the HLW and LAW vitrification facilities are expected to be delivered by vendors with certified compositions that give the average composition and the uncertainty or variability for each component in a given batch of a GFC. The certification of GFC compositions, possibly along with some independent sampling and chemical analysis of GFCs as part of acceptance protocols, should rule out the likelihood of systematic uncertainties (biases) in GFC compositions.

Random GFC Addition Uncertainty: This refers to random differences in the amounts of GFCs actually added to an IHLW or ILAW MFPV batch compared to the intended amounts. Such random differences could occur because of random uncertainties in weighing individual GFCs, random uncertainties in transferring individual GFCs to the combined GFC weigh hopper, random uncertainties in mixing the individual GFCs, and random uncertainties in transferring the combined GFCs to the HLW or LAW MFPV. For the work in this report, systematic uncertainties in GFC addition were assumed to be negligible and thus were not addressed.

Systematic and Random Property Model Uncertainties: IHLW and ILAW glass properties, such as those identified in Section 3.1, are predicted using property-composition models developed from property-composition databases. If a model form chosen to represent the true property-composition relationship yields significantly different predicted response values than true response values for one or more subregions of composition space, the model has systematic uncertainty (bias) in those subregions. In the statistical literature, this is referred to as model lack-of-fit. Even if a model form adequately approximates the true property-composition relationship and does not have any systematic uncertainty, the model will have random uncertainty in its predictions because it was developed from a property-composition database subject to random uncertainty. The property-composition models used in this work are discussed for IHLW in Section 6.1.4 and for ILAW in Section 6.2.3.

Total Variation and Random Uncertainty: This is the total variability (inclusive of batch-to-batch random and systematic variations and all sources of random uncertainty) across the composition or property values corresponding to a specified number of IHLW or ILAW MFPV batches. The specified number of batches may correspond to an HLW or LAW waste type, as discussed in Section 2.4.

Section 3.3 discusses specific sources of uncertainty in the HLW and LAW vitrification processes within these categories for IHLW and ILAW. Before continuing to that section, certain aspects of the preceding categories of uncertainties are discussed.

During operation of the WTP HLW and LAW vitrification facilities, it will not be possible to separately estimate mixing and sampling random uncertainties. That is, samples taken by the ASX from a given vessel will be subject to both mixing and sampling random uncertainties. Hence, for the purposes of work in this document, combined estimates of mixing and sampling random uncertainties were used. However, we note that the WTP Project is planning testing work that will provide separate estimates of mixing and sampling systematic and random uncertainties. That work will provide useful information about the contributions of these two sources of uncertainty, which can be used to reduce one or both if necessary.

Model random uncertainties were not addressed in the work of this report because they are addressed separately in waste form qualification activities as well as in process control and compliance activities for the WTP HLW and LAW vitrification facilities. In this report, the focus is on quantifying random variations and uncertainties in IHLW and ILAW compositions and properties associated with composition-related uncertainties. Random variations and uncertainties are expressed either as a standard deviation (SD) or percent relative standard deviation (%RSD).[(a)]

(a) %RSD = 100(SD/Mean).

3.3 Sources of Variation and Uncertainty Affecting the HLW and LAW Vitrification Processes

Table 3.1 identifies the specific sources of variation and uncertainty that affect the estimation of IHLW and ILAW compositions and properties associated with MFPV batches corresponding to an HLW or LAW waste type (see Section 3.1). Because the WTP process control and compliance strategies involve estimating compositions and properties of IHLW and ILAW corresponding to MFPV batches, only variations and uncertainties through the MFPV are of interest.

Table 3.1. Variations and Uncertainties in the HLW and LAW Vitrification Processes

Source of Variation or Uncertainty	HLW	LAW
1. Waste Variation within a Waste Type		
▪ Random	X[(a)]	X
▪ Systematic (waste)	X	X
▪ Systematic (heel mixing)	X	X
2. Random Uncertainties After Initial Waste Transfers[(b)]		
▪ Mixing	MFPV[(c)]	CRV
▪ Sampling	MFPV[(c)]	CRV
▪ Chemical Composition Analysis	MFPV[(c)]	CRV
▪ Radionuclide Analysis	MFPV[(c)]	CRV
▪ Density	MFPV[(c)]	CRV
▪ Receipt and Transfer	MFPV[(c)]	CRV
3. Vessel Level, Volume, and Volume Transfer Uncertainties		
▪ Level/Volume	MFPV[(c)]	CRV, MFPV
▪ Volume Transfer (waste)	HBV to MFPV[(c)]	CRV to MFPV
▪ Volume Transfer (waste + GFCs)	MFPV to MFV[(c)]	MFPV to MFV
4. GFC Uncertainties		
▪ Individual GFC Composition	X[(c)]	X
▪ Weighing GFCs (separate hoppers)	X[(c)]	X[(d)]
▪ Weighing GFCs (combined hopper)	X[(c)]	X[(d)]
▪ Transfer of GFCs to MFPV	X[(c)]	X[(d)]
5. MFPV Random Uncertainties After Addition of GFCs		
▪ Mixing	X	N/A[(a)]
▪ Sampling	X	N/A
▪ Chemical Composition Analysis	X	N/A
▪ Radionuclide Analysis	X	N/A
▪ Density	X[(c)]	N/A
▪ Receipt and Transfer	X[(c)]	N/A

(a) X = the variation or uncertainty applies in this case. N/A = not applicable, because under the ILAW process control and compliance strategies, no samples, analyses, or measurements are made in the ILAW MFPV.
(b) HLW waste is transferred from the HBV to the MFPV. LAW is transferred from the CSV to the CRV.
(c) For the work in this report, variations and uncertainties in IHLW compositions and properties are considered from the compliance strategy perspective of sampling and analyzing the IHLW MFPV after GFCs are added. Hence, these sources of uncertainty do not directly affect the results in this report. Only the mixing, sampling, and analytical uncertainties affect the uncertainties of IHLW composition and properties.
(d) The GFC weighing and transfer uncertainties are represented by a single uncertainty later in this report.

4.0 Preliminary Estimates of Variations and Uncertainties Affecting the WTP HLW and LAW Vitrification Processes

This section summarizes preliminary estimates of variations and uncertainties associated with several aspects of the WTP HLW and LAW vitrification processes, as listed in Table 3.1 of Section 3.3. The results in this section are based on WTP testing data and information in reports published by the WTP Project or subcontractors, vendor literature, and information provided by knowledgeable personnel associated with these processes. Previously, variations and uncertainties in operations data from the DWPF and WVDP facilities were summarized (Heredia-Langner et al. 2003).

The available information on variations and uncertainties in the WTP IHLW and ILAW processes was limited in many cases because the work to quantify the variations and uncertainties has not yet taken place. The available data and information, however limited, were collected to provide needed inputs for (1) the work in this report, (2) WFQ activities, (3) initial efforts to develop algorithms to operate and control the WTP HLW and LAW vitrification processes, and (4) efforts to develop and illustrate statistical and other approaches for demonstrating compliance with applicable IHLW and ILAW specifications. The available data and information on variations and uncertainties affecting the HLW and LAW vitrification processes also provide a basis for planning future data-collection and data-analysis efforts to improve the current estimates of variations and uncertainties presented.

The following subsections provide brief explanations of the available information and how it contributes to the preliminary estimates of variation and uncertainty for the sources of variation and uncertainties listed in Table 3.1. Section 4.1 discusses variation in waste composition (including radionuclides), density, and percent solids for a given waste type.[(a)] Section 4.2 addresses sources of uncertainty applicable to HLW MFPVs (before GFCs are added) and LAW CRVs. Section 4.3 discusses uncertainties associated with determining levels, volumes, and volume transfers between various vessels associated with the HLW and LAW vitrification facilities. Section 4.4 discusses uncertainties in (1) GFC compositions, (2) weighing GFCs, and (3) transferring GFCs. Section 4.5 addresses uncertainties associated with MFPVs (after GFCs have been added) in the IHLW and ILAW facilities.

4.1 Variation in IHLW and ILAW Associated with HLW and LAW Waste Types

Work by the WTP Project so far indicates that the compositions of HLW and LAW feed to the IHLW and ILAW vitrification facilities may vary over relatively short time frames, especially during transitions from one source tank to another in the delivery sequence. Hence, the current WTP compliance strategies for IHLW (Nelson 2005) and ILAW (Westsik et al. 2004) envision waste types (see Section 2.4) as corresponding to smaller quantities of waste and thus smaller quantities of IHLW and ILAW. For example, the WTP Project currently envisions an HLW as corresponding to the contents of one HBV, which is expected to make 18 IHLW MFPV batches.

(a) The concept of a waste type is discussed in Section 2.4.

Information on the variation in waste composition, density, and percent solids is of interest, as is the variation in IHLW and ILAW compositions that results from waste variations. Output from the WTP Project's G2 dynamic simulation software (Vora 2004; Lee 2004) was considered as a possible source for such information. The G2 software (Deng 2005) takes as input a "feed vector" specifying the retrieval order and compositions of HLW and LAW tanks and then simulates the processing steps and production of IHLW and ILAW. However, at the time of the work summarized in this report, the G2 software assumed no variation within an HLW or LAW waste type. However, in calculating IHLW and ILAW compositions associated with IHLW batches and ILAW MFPV batches, G2 does reflect the systematic variation that results from transitioning from one HLW or LAW waste type to the next. Data on the actual variation within waste types were not available to be included in the work documented in this report.

For the IHLW work in this report, batch-to-batch random variation over a waste type is quantified in terms of %RSD values on IHLW MFPV compositions (i.e., after GFCs are added). Based on inputs from the WTP Project and previous analyses of DWPF and WVDP operating data (Heredia-Langner et al. 2003), %RSDs of 1, 5, and 10% were used for the low, medium, and high values of batch-to-batch random variation. These values were used for all components. Four HLW waste types were considered, associated with waste tanks AY-102, AZ-102, C-104, and the transition from AY-102 to AZ-102. For this last waste type, batch-to-batch systematic variation was accounted for in the work discussed later in the report.

For the ILAW work in this report, within-waste-type (batch-to-batch) variation was represented in five separate sets of G2 batches used in the investigations. These five sets of G2 batches represent LAW waste types corresponding to waste tanks AP-101/AY-102 (Envelope A), AZ-102 (Envelope B), AN-102 (Envelope C), an unknown tank with a Na/S ratio on the border between Envelopes B and C, and a transition from AP-101/AY-102 (Envelope A) to AZ-101 (Envelope B). The compositions of the main oxides for these five sets of G2 batches are further discussed and plotted in Section 5.3. However, only systematic batch-to-batch variation is included in the G2 results, as noted previously. Thus, batch-to-batch random variation values of either 1 or 5% RSD were assumed for elemental concentrations of analytes in the LAW CRV.

4.2 Uncertainties Associated with the HLW MFPV and LAW CRV

Knowledge regarding the contents of a specific HLW MFPV batch (after pretreated HLW is transferred from an HBV, but before GFCs are added) or the LAW CRV batch is subject to several possible sources of uncertainty, including systematic mixing (i.e., inhomogeneity), random mixing, systematic sampling (i.e., biased samples), random sampling, systematic chemical analysis (i.e., biased chemical analyses), random chemical analysis, systematic radionuclide analysis (i.e., biased radionuclide analyses), random radionuclide analysis, systematic density measurement (i.e., biased density measurements), and random density measurement. Also, there could be systematic or random uncertainty in (1) the receipt of HLW into a MFPV or LAW into a CRV from the pretreatment facility and (2) the transfer of material from an LAW CRV to an LAW MFPV. These sources of uncertainty are discussed in the following subsections.

4.2.1 HLW MFPV and LAW CRV Mixing Uncertainties

During WTP operations, the contents of HLW MFPVs and LAW CRVs will be mixed by mechanical mixers (MMs). Ideally, MMs will mix IHLW MFPVs and ILAW CRVs without any systematic uncertainty (i.e., inhomogeneity). However, mixing will always be subject to some amount of random mixing uncertainty. See Section 3.2 for definitions and examples of systematic and random mixing uncertainties.

Experimental work is being planned by the WTP to assess the performance of (1) HLW MFPV and LAW CRV mixing systems with pretreated waste simulants and (2) HLW MFPV and LAW MFPV melter feed simulants. Test specifications have been issued for the HLW work (Sundar 2005a) and the LAW work (Sundar 2005b), with the testing and data analyses anticipated to be conducted in 2006 and 2007. After the planned HLW MFPV and LAW CRV mixing work (Sundar 2005a, 2005b) is completed, the data will be used to quantify any systematic and random uncertainties in solids content, density, and chemical composition.

For the work discussed later in this report, combined mixing/sampling random uncertainties were used. The magnitudes of these combined uncertainties used for the work are discussed at the end of Section 4.2.2 for ILAW and at the end of Section 4.5.2 for IHLW.

4.2.2 HLW MFPV and LAW CRV Sampling Uncertainties

During WTP operations, the contents of HLW MFPVs and LAW CRVs each will be sampled using an ASX connected to a recirculation line fed by a vertical turbine pump. HLW MFPV and LAW CRV samples will have their density measured and will be analyzed for composition (including radionuclides) with the results used for process control and compliance purposes. Ideally, samples will be subject only to random uncertainty and not systematic uncertainty. An example of a systematic sampling uncertainty would be obtaining too much liquid and too little solids in samples collected with the sampling system.[(a)] Any systematic sampling uncertainty discovered in the WTP HLW MFPV or LAW CRV sampling systems during qualification testing will require modifications to the sampling systems and additional qualification work to show that unbiased (representative) samples are being obtained. Random sampling uncertainty refers to random variations in samples obtained that, on average, have the true (but unknown) average composition, solids content, and density for a given HLW MFPV or LAW CRV batch.

During WTP operations, it will not be possible to separately quantify random mixing uncertainty from random sampling uncertainty in an HLW MFPV or an LAW CRV.[(b)] Assuming adequate mixing

(a) During qualification testing, initial sampling systems at both the DWPF and WVDP were determined to yield biased samples. However, the sampling systems were modified and subsequently shown statistically to obtain representative, unbiased samples.

(b) Similarly, it would not be possible during WTP operations to separately identify systematic sampling uncertainty from systematic mixing uncertainty. However, the presumption for this work was that the final HLW MFPV and ILAW CRV mixing and sampling systems will be demonstrated via qualification testing to not have statistically significant systematic mixing and sampling uncertainties. If this turns out not to be the case and the systematic uncertainties cannot be resolved, the systematic uncertainties would need to be accounted for in waste form qualification and compliance activities.

and unbiased sampling, differences in compositions, solids contents, and densities of multiple samples taken from an HLW MFPV or LAW CRV will include random mixing and sampling uncertainties. The assumption of no systematic uncertainty in the composition (including radionuclides), solids content, or density of HLW MFPV or LAW CRV samples, either because of inadequate mixing or biased sampling, has to be demonstrated via testing. Such testing is being planned by the WTP Project for the HLW MFPV (Sundar 2005a) and the ILAW CRV (Sundar 2005b).

For the work quantifying variation and uncertainties in ILAW composition and properties associated with ILAW MFPV batches (discussed later in this report), %RSD values of 1 and 5% were used to represent the possible range of combined mixing and sampling uncertainties in the LAW CRV. These values were chosen based on inputs from the WTP Project. The work to quantify variation and uncertainties in IHLW composition and properties associated with IHLW MFPV batches is based on the compliance strategy of sampling and analyzing the IHLW MFPV after GFCs are added. Hence, sampling and other uncertainties in the HLW MFPV before addition of GFCs are not relevant to the work in this report. Mixing, sampling, and analytical uncertainties for IHLW MFPV batches after the addition of GFCs are discussed subsequently in Sections 4.5.1 to 4.5.3.

4.2.3 HLW MFPV and LAW CRV Chemical and Radionuclide Composition Analytical Uncertainties

During WTP operations, slurry samples from the HLW MFPVs and LAW CRVs will be prepared for chemical and radiochemical composition analyses by mechanically homogenizing them to reduce solids particle size, and then drying, weighing, and dissolving them using a mixture of mineral acids or by fusion dissolution. Samples will then be diluted (if necessary) to reduce radiological dose rates. The prepared samples will be analyzed for chemical composition by inductively coupled plasma-atomic emission spectrometry (ICP-AES). Radionuclides will be analyzed with alpha spectrometers and gas proportional counters for alpha-emitting nuclides or liquid scintillation counters for nuclides with low-energy beta emissions. Gamma spectroscopy will be used to quantitate the gamma-emitting radionuclides. In some cases, inductively coupled plasma-mass spectrometry (ICP-MS) will be used to quantify radionuclide concentrations, especially for isotopic analyses of plutonium and uranium.

Analytical uncertainty[(a)] for chemical and radionuclide composition includes all short-term, within-laboratory random sources of uncertainty (e.g., sample aliquot extraction, sample preparation, instrument and its calibration, analyst, and time-of-day effects) associated with obtaining a reported determination. If typical procedures involve averaging replicate measurements (e.g., three ICP-AES "burns") or counts to obtain a determination, then the uncertainty in a determination obtained in that way is needed.

Systematic chemical or radionuclide composition analytical uncertainties occur when one or more aspects of an analytical procedure (examples of which are given in the preceding paragraph) yield analyzed compositions that are different from their true (but unknown) values by more than random analytical or measurement uncertainty. Experience over many years indicates that systematic uncertainties (biases) in analyzed glass or slurry compositions occur for several reasons. For example, aliquot extraction problems can lead to a non-representative aliquot. As another example, it can be

(a) The term "analytical uncertainty" is used to refer to uncertainty from chemical analyses or counting methods employed to estimate chemical or radionuclide composition.

difficult to completely dissolve into solution the SiO_2 in a glass or slurry sample, which leads to biased, under-estimates of SiO_2 composition. Problems with instrument calibration standards can also cause biased results. As a final example, if the technetium-99 is not in the pertechnetate oxidation state, the technetium will not be adsorbed on the ion exchange resin during the purification analytical process. The measured concentration will then be biased low. Quality control measures employed may not detect this deficiency if equilibrium between the tracer and sample matrix is not established before initiating separations.

It is desirable that certified slurry standards representative of HLW MFPV and LAW CRV chemical and radionuclide composition be prepared and analyzed with samples from these vessels so that analyzed compositions can be bias corrected if needed. Bias correction often eliminates most of what can appear as long-term within-lab or lab-to-lab random variations. (See Weier and Piepel [2003] for additional discussion of methods for bias correction and weighted normalization of analyzed glass compositions.) The WTP Project is also considering periodic inter-laboratory comparison of analyte results from actual samples to assess the accuracy of results. If certified representative slurry standards, inter-laboratory comparisons, or some other method will not be available for bias assessment and correction, it may be necessary to use estimates of analytical uncertainty for HLW MFPV and LAW compositions that include long-term within-lab random uncertainties. Typically, long-term within-lab uncertainties are much larger than short-term within-lab uncertainties.

Regulatory data quality objectives (DQO) work described in a test plan by Patello et al. (2001) was performed to determine minimum detection limits (MDL) for various analytes with some level of confidence. This work used seven replicated samples at a specified spike level, determined by estimating the MDL and multiplying it by 3 to 5 times. After the analytical measurement uncertainty was determined, it was used to establish a confidence interval around the MDL. A convention was also proposed for determining the minimum reportable quantity (MRQ) from the estimated MDL. The uncertainty estimates from that work were not used in this report because the material that was being measured was spiked non-waste, and the estimates would not reflect the situations involving waste in the HLW MFPV[(a)] and LAW CRV. Also, the report summarizing the work was never approved for publication and thus cannot be referenced.

The report by Arakali et al. (2004) summarizes the methods evaluation and development work performed in accordance with the Regulatory Data Quality Objectives. This report lists in various tables the MDL, estimated Quantitation limit (EQL), and MRQ values for regulatory constituents of concern. It also lists in Appendix B the means and standard deviations of analyte concentrations from three laboratories' chemical analyses of AN-102 supernate, AN-107 supernate, and AY-102 solids.

(a) Note that an HLW MFPV after waste addition from the HBV will contain not only HLW, but also some GFCs remaining in the MFPV from the heel of the previous MFPV batch.

David Dodd of the WTP analytical laboratory group compiled information on random analytical uncertainties (expressed as %RSDs) applicable to the chemical and radionuclide composition contents of HLW MFPVs[(a)] and LAW CRVs[(b)]. This information was based on data from Geeting et al. (2002), Brooks et al. (2000), Urie et al. (1999), Hay et al. (2003), Martin et al. (2003), and Goheen et al. (2002), as well as experience of the WTP analytical laboratory group. Note that analytical uncertainties include not only uncertainties associated with an instrument, but also uncertainties associated with any preparatory steps (including taking aliquots or subsamples) in the analytical process. The %RSD values are summarized in Tables C.1, C.2, and C.3 of Appendix C for HLW and in Table D.6 in Appendix D for LAW. These tables contain the %RSD values for each of the analytes and radionuclides, depending on their concentrations in the HLW MFPV or LAW CRV. If a concentration is larger than the decision point, then the low %RSD applies; if the concentration is smaller than the decision point, then the high %RSD applies. The %RSDs are larger below the decision point because relative uncertainties increase for smaller analyte concentrations.

It should be noted that analytical uncertainties associated with material in an HLW MFPV batch before GFCs are added is relevant only to process control and not compliance activities. This is the case because the WTP IHLW compliance strategy involves using information from sampling and analyzing the IHLW MFPV after GFCs are added. Mixing, sampling, and analytical sources of uncertainty relevant to the IHLW MFPV after GFC addition are discussed subsequently in Sections 4.5.1 to 4.5.3.

4.2.4 HLW MFPV and LAW CRV Density Measurement Uncertainties

During WTP operations, HLW MFPV and LAW CRV samples will have density and specific gravity measured by commercially available density instrumentation. The commercial density instrument draws a known volume of sample into a temperature-regulated enclosure and measures the weight internal to the instrument. The instrument that will be used in the WTP analytical laboratory is accurate to 0.0001 g/mL under ideal operating conditions and to 0.001 g/mL under normal operating conditions. Uncertainties will arise when transferring a representative aliquot of slurry and may also be caused by the temperature of the sample from decay heat. In addition to this method, an apparent density (or, more appropriately, specific gravity) measurement will be made in-line for process control purposes by measuring the pressure generated in a dip tube by a measured volume[(c)] of material in the vessel.

For the laboratory measurement of density, measurement uncertainty includes all short-term, within-lab random sources of uncertainty (e.g., preparation, instrument and its calibration, analyst, and time-of-day effects) associated with obtaining a reported density determination. For the in-line measurement of density, measurement uncertainty includes all uncertainties associated with measuring the level of vessel contents as well as all uncertainties associated with the volume-level calibration equation. If typical procedures for either the laboratory or in-line methods involve averaging replicate density measurements

(a) "Estimated Analytical Measurement Uncertainties of Selected HLW Analytes," CCN 132102, February 7, 2006, memorandum from David Dodd and Bruce Kaiser to John Vienna, Waste Treatment and Immobilization Plant, Richland, WA.

(b) "Estimated Analytical Measurement Uncertainties for Selected Analytes," CCN 111456, June 13, 2005, memorandum from David Dodd and Bruce Kaiser to John Vienna, Waste Treatment and Immobilization Plant, Richland, WA.

(c) Volume will not be measured directly, but calculated using a volume-level calibration equation with a measured level of the vessel contents.

(e.g., three measurements of a given sample) to obtain a density determination, the uncertainty in a determination obtained in that way is needed.

Systematic density measurement uncertainties occur when one or more aspects of the measurement procedure yield measured densities that are different from their true (but unknown) values by more than random measurement uncertainty. Density measurements usually are not subject to systematic uncertainties (biases) because they involve measuring the volume and mass of samples (for which biases are rare). However, an incorrectly calibrated pipette or analytical balance, or an incorrect sample extraction, can produce biased density measurements.

It is desirable that certified, representative slurry standards be prepared and densities measured with HLW MFPV and LAW CRV samples so that bias corrections to density determinations can be made if needed. Bias correction often eliminates most of what can appear as long-term within-lab or lab-to-lab random variations. If certified, representative slurry standards will not be available for bias correction, it may be necessary to use estimates of analytical uncertainty for densities of HLW MFPV and LAW CRV slurries that include long-term within-lab random uncertainties.

The Hanford HLW samples available to estimate density measurement uncertainties are centrifuged solids. When solids are separated, it is extremely difficult to obtain a good measurement of volume, which is needed in the calculation of density (= mass/volume). Hence, density measurements were not made for the HLW separated solids samples by Geeting et al. (2002), Brooks et al. (2000), Urie et al. (1999), and Hay et al. (2003). However, it should be noted that samples from the WTP HLW MFPVs will be slurries, and densities will be determined using the in-line and laboratory methods previously described. Future work with actual or simulated HLW slurries representative of MFPV contents in the HLW vitrification facility will be needed to quantify uncertainties in measuring density using the in-line and laboratory methods.

Table 4.1 summarizes the LAW density measurements and their associated measurement uncertainties obtained from Geeting et al. (2002), Brooks et al. (2000), Urie et al. (1999), Hay et al. (2003), Martin et al. (2003), and Goheen et al. (2002). The first column identifies the envelope and tank from which the waste was taken, the second column is the density measurement, the third column is the measurement %RSD, and the fourth column provides the standard deviation for convenience. The uncertainty results are from laboratory measurements. Future work with actual or simulated LAW slurries representative of CRV contents in the LAW vitrification facility will be needed to quantify uncertainties in measuring density by the in-line and laboratory methods.

The LAW density uncertainty results in Table 4.1 were not used in the work reported subsequently in this report. Density of waste in the HLW MFPV and LAW CRV is not required to calculate HLW and LAW glass compositions or properties, and hence density uncertainties were not needed to quantify uncertainties in HLW and LAW glass compositions or properties. However, densities and their uncertainties are relevant to process control and some compliance requirements for the WTP, and thus the available information is reported.

Table 4.1. LAW (Envelopes A, B, and C) Density Means and Measurement Uncertainties

Waste	Mean (g/mL)	%RSD (%)	SD (g/mL)
AP-101 PNWD[(a)] Envelope A	1.256	0.00[(d)]	0.00[(d)]
AW-101 PNWD Envelope A	1.23	0.00	0.00[(d)]
AW-101 SRTC[(b)] Envelope A	1.25	0.50	0.00625
AZ-101 PNWD Envelope B	---	---	---
AZ-102 PNWD Envelope B	1.016	0.0707	0.00072
AN-107 PNWD Envelope C	1.2	---	---
AN-107 SRTC Envelope C[(c)]	1.18	0.41	0.004838

(a) PNWD = Battelle−Pacific Northwest Division
(b) SRTC = Savannah River Technology Center
(c) The density of diluted AN-107 from SRTC was estimated from the reported density of undiluted waste by dividing by 1.2. This dilution factor was necessary for the data to represent what the WTP expects to process.
(d) If density measurements had the same value, then their resulting %RSD or SD was reported as zero. However, analytical uncertainties are not expected to be zero.

4.2.5 HLW MFPV and LAW CRV Composition Uncertainties for Transfers

In addition to composition uncertainties associated with the contents of an HLW MFPV or LAW CRV, there may be composition uncertainties (systematic or random) associated with transferring waste from pretreatment to an HLW MFPV or LAW CRV. Specifically, the process of transferring waste in or out of an LAW CRV may introduce systematic or random differences in composition at (1) the receipt point of the LAW CRV compared to the transfer point of the LAW CSV in pretreatment or (2) the transfer point of the LAW CRV compared to the receipt point of the LAW MFPV. The process of transferring waste from an HBV to an HLW MFPV may also introduce systematic or random differences in composition. No experimental data on these sources of uncertainty were available.

In this report, the focus is on quantifying variation and uncertainties as experienced within the HLW and LAW vitrification facilities. The initial focus of uncertainties for IHLW begins with sampling of the IHLW MFPV after GFCs are added because that is the basis for the IHLW compliance strategy. Hence, receipt and transfer uncertainties for the IHLW MFPV are not relevant to the work in this report. The initial focus of uncertainties for ILAW begins with sampling of the LAW CRV because that is the initial aspect of the ILAW compliance strategy. Hence, transfer uncertainties from the HBV to the HLW MFPV, and from the LAW CSV to the LAW CRV, were not relevant to the work documented in this report. Transfer uncertainties from the LAW CRV to the LAW MFPV are relevant. It was assumed that such transfers do not involve any systematic transfer uncertainty in waste compositions. Also, it was assumed that random transfer uncertainty in composition is negligible compared to random mixing uncertainties in the LAW CRV and LAW MFPV.

4.3 Uncertainties for LAW CRV Volumes, HLW and CRV MFPV Volumes, and Associated Volume Transfers

The WTP IHLW and ILAW process control and compliance strategies require determining the volume of LAW CRV, LAW MFPV, and HLW MFPV[(a)] contents at various stages of the vitrification process. A vessel volume will not be measured directly. Rather, the level of material in a vessel will be determined, and then a volume-level calibration equation will be used to calculate the vessel volume given the measured vessel level.

The WTP ILAW and IHLW process control and compliance strategies also require determining the volume of LAW added to an LAW CRV and the volume transfers from (1) an LAW CRV to an LAW MFPV and (2) the HLW HBV to an HLW MFPV. The volumes or volume transfers could be calculated by subtracting the volume of the receiving vessel before the transfer from the volume of the receiving vessel after the transfer. However, as discussed by Piepel et al. (2005), volume transfers could be determined as weighted averages of volume transfer estimates from the sending and receiving vessels. The volume estimate for a sending or receiving vessel would be obtained by subtracting volumes of the vessels before and after transfer. Weighted averages account for the uncertainties of the two volume transfer estimates and yield an average estimate with less uncertainty than either of the sending and receiving vessel estimates. Because the method for calculating volume transfers has not yet been decided by the WTP Project, the focus in the remainder of this section is on the uncertainties in volume measurements.

As noted previously, during WTP operations, it will be necessary to determine the levels/volumes of the LAW CRVs, LAW MFPVs, and HLW MFPVs at various states during the vitrification processes.

- The level/volume of an HLW MFPV must be measured before a transfer from the HBV (i.e., the MFPV heel), after a transfer from the HBV, and after adding GFCs to the MFPV.

- For ILAW, a CRV will nominally supply four MFPV batches for Envelope A and C wastes. An ILAW CRV will nominally supply more than four batches for Envelope B wastes to which water must be added in the MFPV. Hence, it will be necessary to measure the level/volume of an LAW CRV (1) before an LAW CSV transfer (i.e., the CRV heel), (2) after an LAW CSV transfer when the CRV is full, and (3) after each transfer to an LAW MFPV. It will be necessary to measure the level/volume of an LAW MFPV (1) before a CRV transfer (i.e., the MFPV heel), (2) after a CRV transfer, (3) after a water addition in the case of Envelope B wastes, and (4) after adding GFCs to the MFPV.

If volume flow meters are used to measure volume transfers, it may be possible to reduce the preceding number of stages at which LAW CRV, LAW MFPV, and HLW MFPV levels/volumes are determined.

(a) The WTP IHLW and ILAW compliance strategies do not call for measuring MFV level/volume because the IHLW and ILAW MFVs continuously feed the IHLW and ILAW melters. However, the level/volume of the IHLW and ILAW MFVs will be determined during operations for process control purposes.

Uncertainties in determining vessel levels and volumes should reflect the differences in results in measuring level/volume multiple times with intervening times for each stage of the process involving an LAW CRV, LAW MFPV, or HLW MFPV. Estimates of these uncertainties must reflect differences in level/volume caused by movement of vessel contents if measurements will be made while vessels are being mixed. The WTP Project is considering a radar level detection method that would use a tube to remove or damp variations in level caused by agitation. This method is capable of continuous level measurements so that measurements over a period of time could be averaged if necessary to reduce uncertainty caused by agitation. As discussed previously, vessel levels will be measured and vessel volumes calculated from a volume-level calibration equation for each vessel. However, because the volume-level calibration equations will not be developed for some time, estimates of uncertainties in volume determinations are needed now in addition to estimates of uncertainties in level determinations.

Knowledgeable personnel estimate that level measurement systems operating during mixing of LAW CRVs, HLW and LAW MFPVs, and HLW and LAW MFVs will likely have accuracies (systematic and random uncertainties combined) from ± 0.5 to ± 1.5 inches. The engineering specification for radar level measurement (Fielding 2003) is ± 0.5 inches. Also, EchoTouch, a potential vendor, claims that their non-contact level measurements have an accuracy of ± 0.75 inches. It was decided to treat 0.5 inch as the estimated level measurement SD because it is not clear at this time whether level accuracies of ± 0.5 or ± 0.75 inches will be achievable during vessel mixing. With an SD of 0.5 inches, plus or minus three SDs yields ± 1.5 inches (which corresponds to the upper estimate for uncertainty by knowledgeable personnel).

Because level-volume calibration equations are not yet available for LAW CRVs, HLW and LAW MFPVs, and HLW and LAW MFVs, a stand-in approach was needed to convert the 0.5-inch level SD to a volume SD for each vessel and status (e.g., full, half-full, heel). Information in the IHLW and ILAW vessel design specifications and calculation sheets was used to convert the 0.5-inch level SD to an equivalent volume SD for each vessel and status.

Table C.4 in Appendix C summarizes the level and volume uncertainties, expressed as SDs and %RSDs, for the IHLW MFPV and MFV. Vessel levels, volumes, and diameters to convert the 0.5-inch level SD to calculated volume SDs were obtained from Cross (2005). Table D.11 in Appendix D summarizes the level and volume uncertainties, expressed as SDs and %RSDs, for the ILAW CRV, MFPV, and MFV. Vessel levels, volumes, and diameters to convert the 0.5-inch level SD to a calculated volume SD were obtained from Holgado (2001), Holgado (2003), and Wilson (2002). For both IHLW and ILAW, the "Full" volume of a given vessel represents the "heel" volume plus the "batch" volume. The fractional (e.g., ½ and ¼) levels and volumes were obtained by taking the relevant fraction of the batch level or volume and adding it to the heel level or volume. Table D.12 summarizes all the nominal ILAW MFPV volumes used in the work documented subsequently in the report.

The estimate of 0.5-inch SD for level detection measurement systems is preliminary and will need to be updated after tests of level detection measurement systems under representative conditions are conducted for ILAW CRVs, IHLW and ILAW MFPVs, and IHLW and ILAW MFVs. Such work is planned as discussed in test specifications by Sundar (2005a, 2005b). The uncertainties in volumes calculated with level-volume calibration equations will also need to be addressed in the future. These volume uncertainties will need to include the uncertainty in level measurement as well as the uncertainty in the level-volume calibration equation for each IHLW or ILAW vessel.

4.4 Glass Forming Chemical Uncertainties

Section 4.4.1 addresses variations in compositions of GFCs and Section 4.4.2 discusses uncertainties in weighing GFCs. Section 4.4.3 discusses uncertainties in transferring GFCs from the GFC facility to a MFPV.

4.4.1 GFC Nominal Compositions and Variations

Table D.9 of Appendix D lists the nominal compositions of 13 GFCs that will be used during WTP operations to make IHLW and/or ILAW. Tentative WTP plans call for using the following specific GFCs: (1) for IHLW, silica, zincite, borax, sodium carbonate, lithium carbonate, and alumina and (2) for ILAW, kyanite, boric acid, wollastonite, hematite, olivine, silica, rutile, zincite, zircon, and lithium carbonate. However, not every GFC listed will necessarily be used with every HLW or LAW batch.

The nominal compositions in Table D.9 are the result of calculations for the WTP Project by John Vienna, based on GFC composition information from vendors, as documented by Schumacher (2003). Additional calculations using vendor information were necessary to express the GFC compositions as mass fractions of glass oxide or halide components. GFC compositions expressed in this way will be used during production in WTP compliance equations to calculate glass compositions based on IHLW and ILAW process data.

Table D.9 also displays the expected variation range for the mass fraction of each oxide or halide component for each GFC. These ranges are based on vendor information where available. Component range information was obtained from Schumacher (2003) for kyanite, alumina, boric acid, sodium carbonate, lithium carbonate, olivine, rutile, zinc oxide, and zircon. GFC range information was obtained for: kyanite from Kyanite Mining Corporation (2001), alumina from Alcoa World Chemicals (2003), borax from U.S. Borax, Inc. (2001), wollastonite from NYCO Minerals, Inc. (1998), and iron oxide from Prince Manufacturing Company (1999). It has not yet been decided from which of four locations of U.S. Silica Company (1997a,b,c,d) the WTP will purchase silica. Because no silica ranges were provided by the company, the variation of nominal values from location to location was used as a conservative estimate of possible ranges in silica composition for the one intended location for purchase. When vendor information on component ranges was not available, ranges were estimated based on similar ranges for major and minor components of GFCs for which information was available.

The GFC component nominal values and ranges were used to convert the ranges to SDs, which are listed in Table D.10 of Appendix D. The conversion was performed assuming a triangular probability distribution to represent uncertainties in GFC component mass fractions. A triangular probability distribution for a GFC component mass fraction is defined by its mode (most frequent value) and range. The nominal values were taken to be the modes for the triangular distributions. The equation for converting a nominal value and range to a standard deviation is given in Appendix D. A triangular distribution was assumed because (1) it is consistent with the inputs of a nominal value and range for a given component, (2) it allows for a non-symmetric distribution when the nominal value is not in the middle of the range, and (3) restricts values to be within the specified range.

4.4.2 Uncertainties in Weighing GFCs

During WTP IHLW and ILAW operations, required amounts of GFCs for a given IHLW or ILAW MFPV batch will be determined based on samples and analyses of an HLW MFPV batch (before GFCs) or LAW CRV batch. The WTP GFC facility will contain hoppers of various sizes into which the required amounts of individual GFCs will be transferred. Then, the contents of individual hoppers will be transferred to the HLW or LAW GFC Blending Hopper. Weights of GFCs in individual hoppers or the blending hoppers will be determined by load cells incorporated with each hopper.

Information on various kinds of uncertainty associated with the precision (not ultra-precision) load cells planned for use with the WTP GFC weigh hoppers was obtained from literature of potential vendors (e.g., Cooper 2002; Sensotec 2003; Futek 2003; Amcells 2003). Table 4.2 summarizes the load cell uncertainty information from these four vendors. The vendors expressed uncertainties as percentages of different terms ("full scale," "rated output," "rated load," and "rated capacity") where these terms refer to the rated capacity (i.e., upper load or weight limit of a load cell within its specification). Vendors were not consistent with terminology within their own literature, and so telephone calls were made to clarify terms and their meanings both within and across vendors. For consistency, the term "rated capacity" was adopted for use in Table 4.2 and subsequent discussion.

Table 4.2. Vendor Information on Uncertainties for Precision Load Cells

Load Cell Vendor	Source of Uncertainty		
	Non-Linearity [(b)]	**Hysteresis [(c)]**	**Non-repeatability [(d)]**
Cooper (2002)	± 0.1% of R.C.[(a)]	± 0.08% of R.C.	± 0.03% of R.C.
Sensotec (2003)	± 0.1% of R.C.	± 0.08% of R.C.	± 0.03% of R.C.
Futek (2003)	± 0.1% of R.C.	± 0.2% of R.C.	± 0.02% of R.C.
Amcells (2003)	± 0.03% of R.C.	± 0.02% of R.C.	± 0.05% of R.C.
Range over Vendors	± 0.03 – 0.1% of R.C.	± 0.02 – 0.2% of R.C.	± 0.02 – 0.05% of R.C.

(a) *Rated Capacity* (R.C.) is defined as the maximum load (in lb) that a load-cell is designed to measure within its specification.
(b) *Non-linearity* is defined as the maximum deviation of a load cell calibration curve from a straight line drawn between load cell transducer readings for no-load and the R.C. Non-linearity is expressed as a percentage of the R.C. and is measured on increasing load only.
(c) *Hysteresis* is defined as the maximum difference between load cell readings for the same applied load, with one reading obtained by increasing the load from zero and the other reading obtained by decreasing the load from the R.C. Hysteresis is usually measured at one-half the R.C. and expressed as a percentage of the R.C. Measurements should be taken as rapidly as possible to minimize Creep. *Creep* is defined as the change in load cell output occurring with time while under load and with all environmental conditions and other variables remaining constant. Creep is usually measured with the R.C. load applied and expressed as a percentage of the R.C. over a specific period of time.
(d) *Non-repeatability* is defined as the inability of a load cell to reproduce output readings when the same load is applied to it consecutively, under the same conditions and in the same direction. Non-repeatability is expressed as the maximum difference between output readings as a percentage of the R.C.

Based on the definitions given in the footnotes of Table 4.2, the imprecision of a load cell is described by its non-repeatability. Because non-repeatability is expressed by the vendors as the maximum percentage difference in results from repeated load measurements, those values may be considered to equal three times the percent relative standard deviations (%RSDs). Hence, the non-repeatability values given in Table 4.2 would be divided by three if %RSD estimates of uncertainty are desired. Reproduc-

ibility[(a)] is also an important component of imprecision, often being considerably larger than repeatability (non-repeatability). The combination of repeatability and reproducibility is the statistic of importance for WTP operations. However, none of the vendors' literature contained information on reproducibility uncertainty. Non-linearity and hysteresis uncertainty information may be considered measures of (in)accuracy, although they could conceivably also be considered as other components of imprecision.

Table 4.3 lists the working volume of each GFC weigh hopper, the relevant GFCs, the estimated density of each GFC, the estimated maximum weights of GFCs for each hopper, and the likely load cell capacity needed. The last three columns of Table 4.3 give estimates of non-linearity, hysteresis, and non-repeatability uncertainties in pounds (lb), obtained by multiplying the % of R.C. ranges in the last row of Table 4.2 by the "Suggested Load Cell Capacity" for each GFC weigh hopper.

Table 4.3. Estimated Uncertainties in Weighing GFCs Associated with WTP Weigh Hoppers

GFCs Associated with Each GFC Weigh Hopper	GFC Weigh Hopper Volume (ft^3)	Estimated Density[(a)] (lb/ft^3)	Mass (lb)	Suggested Load Cell Capacity (lb)	Non-Linearity[(b)] (lb)	Hysteresis[(b)] (lb)	Non-Repeatability[(b)] (lb)
Silica	190	49.6	9424	15,000	4.5–15	3.0–30	3.0–7.5
Olivine	20	89.3	1786	3,000	0.9–3.0	0.6–6.0	0.6–1.5
Zircon	20	96	1920				
Ferric Oxide	20	88.9	1778				
Rutile	20	91	1820				
Zinc Oxide	80	33.8	2704	5,000	1.5–5.0	1.0–10.0	1.0–2.5
Lithium Carbonate	80	53.1	4248				
Boric Acid	120	54.6	6552	10,000	3.0–10	2.0–20.0	2.0–5.0
Kyanite	120	56.1	6732				
Wollastonite	120	46.4	5568				
Borax	90	48	4320	10,000	3.0–10	2.0–20.0	2.0–5.0
Sodium Carbonate	90	64.2	5778				
Sucrose	50	52.6	2630	5,000	1.5–5.0	1.0–10.0	1.0–2.5

(a) Densities from Reutell (2005).
(b) Non-linearity, hysteresis, and non-repeatability are defined in the footnotes of Table 4.2. The table entries are uncertainty ranges in pounds, corresponding to the range of maximum deviations expressed as percentages of R.C. in the last row of Table 4.2.

Reutell (2005) documents requirements for the glass former weighing system, which are discussed in Section 4.4.3.

4.4.3 Uncertainty in Transfer of GFCs from GFC Facility to MFPV

During WTP operations, the GFCs to be added to a given IHLW or ILAW MFPV batch will be combined and weighed in a GFC Blending Silo in the GFC facility. Then, a batch of GFCs will be transported to the GFC Feed Hopper in the respective IHLW or ILAW facility. After receipt at the GFC Feed Hopper, a GFC batch will be weighed. A discrepancy in weights of the GFC batch in a GFC

(a) Repeatability and reproducibility are defined in the list of "Acronyms, Terms, and Abbreviations" in Appendix G.

Blending Silo and a GFC Feed Hopper that is larger than the estimated uncertainties in the two weights could indicate a transfer error or hold-up. During transfers, portions of GFC materials can be held-up in the transfer lines, or previously held-up material can be released and be transferred with the current GFC batch. Hence, it is possible that the weight of a GFC batch in a GFC Feed Hopper may be statistically larger or smaller than the weight of the GFC batch in a GFC Blending Silo (after accounting for weighing uncertainties in both).

It is assumed that uncertainties in transfer of GFCs from the GFC Blending Silos to the GFC Feed Hoppers are caused by hold-up or release of hold-up in transfer lines and not to hold-up in the GFC Blending Silo or GFC Feed Hopper. Both of these containers have load cells that would indicate any hold-up in the container, thus enabling it to be cleared for transfer (in the case of the GFC Blending Silo) or added to the HLW or LAW MFPV (in the case of a GFC Feed Hopper).

At the time of this work, WTP Project testing or other data on the magnitudes of GFC transfer uncertainties were not available. However, Reutell (2005) provides the following requirements for the GFC system, where the numbers listed are subsection numbers from that document.

3.1.2.6 Confirm the total GFC batch weight after all the bulk solids have been transferred to a Blending Silo. The total GFC batch weight shall be reconfirmed after all the bulk solids have been transferred to the Mixer. After that weight is verified, and if in agreement with requested batch weight (± 2%), the batch will be transferred to MFPV.

3.1.2.7 Insure that the weight of any individual GFC shall not vary more than 0.5% from the weight required by the recipe. If the variation in weight of a GFC exceeds 0.5%, the system shall alarm and pause operation until an Operator determines the cause of the error. At that point, the Operator must choose to trim the batch to bring it into compliance, reject the batch and send it to the Reject Station, or accept as is.

3.1.2.8 Insure that the total weight of any complete batch of GFCs does not vary more than 2% from the required weight. If a batch total weight differs from the recipe target weight by more than ± 2%, the system shall alarm and pause operation until an Operator determines the cause of the error. At that point, the Operator must choose to trim the batch to bring it into compliance, reject the batch and send it to the Reject Station, or accept as is.

Note that these requirements address transfers of individual GFCs from weigh hoppers to a Blending Silo, as well as transfers of the combined GFC batch in a Blending Silo to the HLW or LAW GFC Mixer in the HLW or LAW vitrification facility.

It is clear from Section 4.4.2 that uncertainties in weighing GFCs are expected to be much less than the ± 0.5% allowable deviation requirement for individual GFCs and the ± 2% allowable deviation requirement for the combined GFCs. However, in the absence of data or information on GFC transfer uncertainties (e.g., holdup, periodic release of holdup), it is unclear whether the overall ± 2% allowable deviation for GFC addition will be achievable. It is the combination of weighing uncertainties and transfer uncertainties that must be assessed to judge the likelihood of meeting the ± 2% requirement.

GFC uncertainties were not explicitly considered in the work to quantify IHLW uncertainties. Under the IHLW compliance strategy, sampling from the IHLW MFPV occurs after the GFCs have been added. Therefore, random uncertainties in the measurement and addition of GFCs are incorporated into the other sources of random uncertainties for the IHLW MFPV.

For the work in this report to quantify ILAW uncertainties, Table D.7 of Appendix D lists the masses of individual GFCs calculated for addition to the selected G2 ILAW batches from a G2 run (Vora 2004). How the G2 batches were selected is discussed subsequently in Section 5.3. The GFC masses corresponding to the selected G2 batches were obtained from John Vienna of the WTP Project. Table D.8 lists the %RSDs that quantify the uncertainties of the GFC masses added to LAW MFPV batches. The %RSDs in Table D.8 are taken to include GFC batching, weighing, and transfer uncertainties.

4.5 IHLW and ILAW MFPV Uncertainties

Knowledge about the contents of a specific IHLW or ILAW MFPV batch is subject to several possible sources of uncertainty, including systematic mixing (i.e., inhomogeneity), random mixing, systematic sampling (i.e., biased samples), random sampling, systematic chemical analysis (i.e., biased chemical analyses), random chemical analysis, systematic density measurement (i.e., biased density measurements), and random density measurement.

Note that there could be systematic or random uncertainties in the transfer of material from an HLW or LAW MFPV to an HLW or LAW MFV. However, the WTP IHLW and ILAW process control and compliance strategies are based on IHLW and ILAW that would be made from MFPV batches. Hence, MFPV-to-MFV transfer uncertainties are not relevant to the work in this report.

The relevant sources of uncertainty mentioned above are discussed in the following subsections.

4.5.1 IHLW and ILAW MFPV Mixing Uncertainties

During WTP operations, the IHLW and ILAW MFPVs will be mixed by mechanical mixers (MMs). Ideally, MMs will mix IHLW and ILAW MFPVs without any systematic mixing uncertainty (i.e., inhomogeneity), which can be defined as differences in composition (including radionuclides) or density at different positions in the MFPV that are beyond the differences expected based on random mixing uncertainty. Random mixing uncertainty refers to the random differences in composition or density that would occur within a well-mixed vessel having a true (but unknown) average composition.

Experimental work to assess the performance of the IHLW and ILAW MFPV mixing systems with representative melter feed simulants (i.e., including GFCs) is being planned. Test specifications have been issued (Sundar 2005a, 2005b), and the experimental work will follow. After the planned IHLW and ILAW MFPV mixing work is completed, the data will be used to quantify any systematic and random uncertainties in density and chemical composition.

Variations and uncertainties in compositions and properties of IHLW corresponding to MFPV batches are based on the compliance strategy of sampling and analyzing an IHLW MFPV after adding

GFCs. The magnitudes of combined mixing and sampling uncertainties assumed for the IHLW work are discussed at the end of Section 4.5.2. In the WTP ILAW process control and compliance strategies, the ILAW MFPV is not sampled and analyzed after GFC addition, so mixing, sampling, and analytical uncertainties are not relevant.

4.5.2 IHLW MFPV Sampling Uncertainty

The WTP process control and compliance strategies call for sampling the IHLW MFPVs using an ASX during WTP operations. IHLW MFPV samples will be collected, analyzed for chemical composition (i.e., non-radionuclide), and measured for density. The results will be used for process control and compliance purposes. Ideally, samples will be subject only to random uncertainty and not systematic uncertainty. An example of a systematic sampling uncertainty would be obtaining too much liquid and too little solids in samples collected with the sampling system.[(a)]

The WTP ILAW process control and compliance strategies do not call for routine sampling of the ILAW MFPVs during WTP operation. However, qualification testing will assess systematic and random sampling uncertainties for using an ASX to sample ILAW as well as IHLW MFPV simulants (Sundar 2005a, 2005b). Any systematic sampling uncertainty discovered in the WTP IHLW or ILAW MFPV sampling systems during qualification testing will require modifications to the sampling systems and additional qualification work to show that unbiased (representative) samples are being obtained. Random sampling uncertainty refers to random differences in samples obtained that on average have the true (but unknown) average composition and density for a given MFPV batch.

During WTP IHLW operations, it will not be possible to separately quantify random mixing uncertainty from random sampling uncertainty in an IHLW MFPV. Assuming adequate mixing and unbiased sampling, differences in compositions of multiple samples taken from an IHLW MFPV will include the differences caused by random mixing uncertainty within an IHLW MFPV batch as well as random uncertainty caused by the sampling system. The assumption made for this work of no statistically significant systematic uncertainty in the composition (including radionuclides) or density of IHLW MFPV samples, either because of inadequate mixing or biased sampling, has to be demonstrated via testing.[(b)] Such testing is being planned (Sundar 2005a).

For the work quantifying variation and uncertainties in IHLW composition and properties associated with IHLW MFPV batches (discussed later in this report), %RSD values ranging from 1 to 15% were used to represent the possible range of combined mixing and sampling uncertainties in the IHLW MFPV. These values were chosen based on inputs from the WTP Project.

(a) During qualification testing, initial sampling systems at both the DWPF and WVDP were determined to yield biased samples. However, the sampling systems were modified and subsequently shown statistically to obtain representative, unbiased samples.

(b) The Engineering Specification for the Autosampling System (24590-WTP-3PS-MHSS-T0002, Section 3.3.1) requires sampling representativeness between source and sample of ± 1%. See the discussion under the Systematic Sampling Uncertainty (Bias) heading of Section 3.2.

4.5.3 IHLW MFPV Chemical and Radionuclide Composition Analytical Uncertainties

During WTP operations, slurry samples from the IHLW MFPV will be analyzed for chemical and radiochemical composition by first mechanically homogenizing a sample to reduce particle size of the solids for optimum suspension in the liquid fraction. The aliquot sample for elemental analyses will then be dried, weighed, and dissolved using a mixture of mineral acids or by fusion dissolution. Samples will then be diluted (if necessary) to reduce radiological dose rates. The prepared samples will be analyzed for chemical composition by ICP-AES. Radionuclides will be analyzed with alpha spectrometers and gas proportional counters for alpha-emitting nuclides or liquid scintillation counters for nuclides emitting low energy beta emissions. Gamma spectroscopy will be used to quantitate the gamma-emitting radionuclides. In some cases, ICP-MS will be used to quantify radionuclide concentrations, especially for isotopic analyses of plutonium and uranium.

Analytical uncertainty[(a)] for chemical and radionuclide composition includes all short-term, within-lab random sources of uncertainty (e.g., sample aliquot extraction, sample preparation, instrument and its calibration, analyst, and time-of-day effects) associated with obtaining a reported determination. If typical procedures involve averaging replicate measurements (e.g., three ICP-AES "burns") or counts to obtain a determination, the uncertainty in a determination obtained in that way is needed.

Systematic chemical or radionuclide composition analytical uncertainties occur when one or more aspects of an analytical procedure (examples of which are given in the preceding paragraph) yield analyzed compositions that are different from their true (but unknown) values by more than random analytical or measurement uncertainty. Experience over many years indicates that systematic uncertainties (biases) in analyzed glass or slurry compositions occur for several reasons. Section 4.2.3 discusses examples of such biases.

It is desirable that certified slurry standards representative of IHLW MFPV chemical and radionuclide composition be prepared and analyzed with IHLW MFPV samples so that analyzed compositions can be bias corrected if needed. Bias correction often eliminates most of what can appear as long-term within-lab or lab-to-lab random variations. (See Weier and Piepel [2003] for additional discussion of methods for bias correction and weighted normalization of analyzed glass compositions.) The WTP Project is also considering periodic inter-laboratory comparison of analyte results from actual samples to assess the accuracy of results. If certified representative slurry standards, inter-laboratory comparisons, or some other method will not be available for bias assessment and correction, it may be necessary to use estimates of analytical uncertainty for HLW MFPV and LAW compositions that include long-term within-lab random uncertainties.

Currently, there are no data-based estimates of analytical uncertainty for IHLW MFPV samples. However, David Dodd of the WTP analytical laboratory group compiled information on random analytical uncertainties (expressed as %RSDs) applicable to the chemical and radionuclide composition contents of IHLW MFPVs after GFC addition. These estimates are based on experience of the WTP

(a) The term "analytical uncertainty" is used to refer to uncertainty from chemical analyses or counting methods employed to estimate chemical or radionuclide composition.

analytical laboratory group.[(a)] Note that analytical uncertainties include not only uncertainties associated with an instrument, but also uncertainties associated with any preparatory steps (including taking aliquots or subsamples) in the analytical process. The %RSD values are summarized in Tables C.1, C.2, and C.3 of Appendix C for IHLW. These tables contain the %RSD values for each of the analytes and radionuclides, depending on their concentrations in an IHLW MFPV.

4.5.4 IHLW and ILAW MFPV Density Measurement Uncertainty

During WTP operations, in the IHLW facility, MFPV samples (after GFC addition) will have density and specific gravity measured by commercially available instrumentation. The first four paragraphs of Section 4.2.4, which address the uncertainty of density and specific gravity measurements of HLW MFPV samples (before GFC addition) and LAW CRV samples, also apply to the IHLW MFPV samples discussed in this section.

No WTP Project data on density measurement uncertainties for IHLW or ILAW MFPV-type samples were available. Hence, there are no separate quantitative density uncertainty estimates for MFPV samples presented at this time. The results presented in Section 4.2.5 for IHLW and ILAW CRV samples could be used as estimates until results applicable to MFPV contents become available. MFPV samples will have larger densities than CRV samples because of the addition of GFCs, but the measurement uncertainties may be of similar magnitudes. When data on IHLW and ILAW MFPV density measurement uncertainties (using both the in-line and laboratory methods) become available, they should be compared with the estimates in this report.

4.5.5 IHLW and ILAW MFPV Composition Uncertainties for Transfers

In addition to composition uncertainties associated with the contents of an IHLW or ILAW MFPV, there may be composition uncertainties (systematic or random) associated with transferring slurries from an IHLW or ILAW MFPV to an IHLW or ILAW MFV during WTP operations. Specifically, the process of transferring slurries out of an MFPV may introduce systematic or random differences in composition at the transfer point of the IHLW or ILAW MFPV compared to the receipt point of the IHLW or ILAW MFV. No experimental data on these sources of uncertainty were available at the time of the work documented in this report. However, such uncertainties were not needed for the work to quantify variations and uncertainties discussed in subsequent sections of the report. The reason for this is that variations and uncertainties are quantified for IHLW and ILAW compositions that would result from MFPV batches, which are the basis for the WTP IHLW and ILAW process control and compliance strategies. Hence, MFPV-to-MFV transfers and their uncertainties were not relevant for the work in this report. However, note that IHLW and ILAW MFV vessels can be sampled via the ASX system, so during cold commissioning, it may be possible to determine if there is any change between the MFPV and MFV.

(a) "Estimated Analytical Measurement Uncertainties of Selected HLW Analytes," CCN 132102, February 7, 2006, memorandum from David Dodd and Bruce Kaiser to John Vienna, Waste Treatment and Immobilization Plant, Richland, WA.

5.0 Methods Used to Study the Effects of Variation and Uncertainties on IHLW and ILAW Composition and Properties

To study the effects that variation and uncertainties during WTP operations will have on IHLW and ILAW compositions and properties, a combination of Monte Carlo simulations and statistically designed computer experiments was used. Section 5.1 discusses the computer experiment and Monte Carlo methods. The factors and their values that varied in the computer experiments are discussed in Section 5.2 for IHLW and in Section 5.3 for ILAW.

5.1 Computer Experiment and Monte Carlo Simulation Approach

Monte Carlo simulation involves assuming statistical distributions for random (i.e., uncertain) variables, generating random realizations from these distributions, and calculating quantities of interest using the random realizations of the random variables. In this report, the quantities of interest are IHLW and ILAW chemical and radionuclide compositions and various IHLW and ILAW glass properties. Random variables of interest involve any process steps or measurements subject to uncertainty (e.g., mixing/sampling, or analytical).

A systematic approach to study the effects of sources of variation and uncertainty involves computer simulation of data that realistically reflect the effect of these sources on the quantities of interest. A designed computer experiment starts with the selection of a few values that cover the range of magnitudes that can be expected to occur in practice for all sources of variation and uncertainty. After these values have been selected (usually a low and high magnitude value for every source under consideration), a design is built by creating all combinations of variables and their values (or a fraction of this design, if it is too large), and simulated values for the response of interest are generated using the magnitudes prescribed by the design. These simulated values can then be analyzed with traditional statistical methodologies to assess the effects that the selected sources of variation and uncertainty (within the magnitudes chosen) have on the responses of interest.

Sections 5.2 and 5.3 discuss the factors and values of those factors that were varied in the Monte Carlo computer experiments for IHLW and ILAW, respectively. We note that only those sources of variation and uncertainty affecting IHLW and ILAW compositions were varied. Property-composition models to predict properties of IHLW and ILAW are also subject to uncertainty, as discussed in Section 3.2. However, property model uncertainties are independent of IHLW and ILAW composition uncertainties, and are dealt with as part of applicable WTP operations and compliance strategies. Hence, for the work in this report, model uncertainties were not addressed.

5.2 Factors and Values Used in the Monte Carlo Computer Experiment to Study Effects of Variation and Uncertainties on IHLW Composition and Properties

The experimental design discussed in this section was used to determine the effects of the following factors on the batch-to-batch variation and within-batch uncertainty in IHLW MFPV compositions and glass properties:

- batch-to-batch variation in the concentration of the j^{th} element in an IHLW MFPV batch [$\%RSD_B(c_j^{MFPV})$]
- %RSD of random mixing/sampling uncertainty in the concentration of the j^{th} element in an IHLW MFPV batch [$\%RSD_S(c_j^{MFPV})$]
- %RSD of random analytical uncertainty in the concentration of the j^{th} element in an IHLW MFPV batch [$\%RSD_A(c_j^{MFPV})$].

Only these sources of variation and uncertainty affect the calculation of IHLW compositions that correspond to an IHLW MFPV batch because the calculations are based on chemical and radiochemical analyses of MFPV samples after the GFCs are added to the HLW in the MFPV. Thus, uncertainties in GFC compositions, masses of GFCs added to the IHLW MFPV, and various volume determinations are not relevant for the WTP approach to calculating IHLW compositions for MFPV batches.

In addition to investigating the effects of the three factors above for each of three single waste types (AY-102, AZ-102, and C-104), a transition between two waste types (AY-102 to AZ-102) was also investigated. This transition occurs when material from an HLW waste type in an IHLW MFPV (with a relatively well-defined chemical and radionuclide composition) is being depleted and material from a new waste type is brought in. The transition between two HLW waste types (from AY-102 to AZ-102) was incorporated into the computer simulations via mass-balance equations. Note that such transitions are waste types in their own right, and hence the AY-102 to AZ-102 transition is subsequently referred to as the fourth HLW waste type investigated.

A factorial computer experiment was used to investigate the effects that the preceding factors have on the variations and uncertainties of IHLW compositions and properties. Table 5.1 summarizes the factors and values used. Note that the number of samples per IHLW MFPV batch was held constant at 8, and the number of chemical and radiochemical analyses per sample was held fixed at 1. These values were specified by the WTP Project based on prior WTP planning and the results of investigations discussed by Piepel et al. (2005).

The effects of variation and uncertainties in the HLW vitrification process on the IHLW MFPV composition and properties were investigated for four HLW waste types representing material from tanks AY-102, AZ-102, C-104, and the transition from AY-102 to AZ-102. Table C.1 (chemical composition analytes) and Table C.2 (radionuclides) of Appendix C list the nominal concentration data for IHLW compositions corresponding to each of these HLW tanks. Table C.1 (chemical composition analyte

Table 5.1. Factors and Levels Used in IHLW Monte Carlo Simulations

HLW Waste Type[a]	IHLW MFPV Mixing/Sampling %RSD[b]	IHLW MFPV Analytical %RSD[c]	IHLW MFPV Batch-to-Batch %RSD Variation[d]	Number of Samples per IHLW MFPV Batch	Number of Analyses per IHLW MFPV Sample
AY-102 AZ-102 C-104 AY-102 to AZ-102	Low High	Low High	Low Medium High	8	1

(a) Waste types associated with AY-102, AZ-102, and C-104 are considered as "pure" waste types not affected by transitional effects from a previous waste type. The AY-102 to AZ-102 waste type addresses transitional effects.

(b) Low and high values for IHLW MFPV mixing/sampling uncertainty are listed in Table C.1 for chemical composition analyte concentrations and in Table C.2 for radionuclide concentrations.

(c) Low and high values for IHLW MFPV analytical uncertainty are given in Table C.1 for chemical composition analyte concentrations and in Table C.2 (based on Table C.3) for radionuclide concentrations.

(d) Low, medium, and high values for IHLW batch-to-batch variation are given by %RSDs of 1, 5, and 10%, respectively.

concentrations) and Table C.2 (radionuclide concentrations) list IHLW MFPV mixing/sampling uncertainties (low and high %RSD values). Table C.1 (chemical composition analyte concentrations) and Table C.2 (radionuclide concentrations) list MFPV analytical uncertainties (low and high %RSD values).

The computer experiment followed a full-factorial structure where all combinations of the factors shown in Table 5.1 were used. Table 5.2 shows the combinations of the factors studied. For each combination of HLW waste type (waste tank), batch-to-batch variation, mixing/sampling uncertainty, and analytical uncertainty, one thousand simulated samples (each of size eight) were created.

All IHLW Monte Carlo simulations were performed using MATLAB 7.0.4 (The MathWorks, Inc., 2005) and summarizations of the simulation results were performed using S-Plus 6.2 software (Insightful Corp. 2003).

Table 5.2. Test Cases Used in the Experimental Design for the Factors Studied in the Monte Carlo Investigation for IHLW Corresponding to each of the Four HLW Waste Types[(a)]

Run	IHLW MFPV Random Batch-to-Batch %RSD	IHLW MFPV Mixing/ Sampling %RSD [(b)]	IHLW MFPV Analytical %RSD [(b)]
1	Low	Low	Low
2	Low	Low	High
3	Low	High	Low
4	Low	High	High
5	Medium	Low	Low
6	Medium	Low	High
7	Medium	High	Low
8	Medium	High	High
9	High	Low	Low
10	High	Low	High
11	High	High	Low
12	High	High	High

(a) The 12 runs in the experiment defined in the table were run for each of the four HLW waste types.
(b) See the footnotes of Table 5.1 for the table references where the low, medium, and high values for the factors may be found.

5.3 Factors and Values Used in the Monte Carlo Computer Experiment to Study Effects of Variation and Uncertainties on ILAW Composition and Properties

The experimental design discussed in this section was used to determine the effects of the following factors on the batch-to-batch variation and within-batch uncertainty in ILAW MFPV compositions and glass properties:

- five different sections of batches from the G2 run data (as discussed later in this section)
- %RSD of random batch-to-batch variation in the concentration of the j^{th} element in an LAW CRV batch [$\%RSD_B(c_j^{CRV})$]
- %RSD of random mixing/sampling uncertainty in the concentration of the j^{th} element in an LAW CRV batch [$\%RSD_S(c_j^{CRV})$]

- %RSD of random analytical uncertainty in the concentration of the j^{th} element in an LAW CRV batch [$\%RSD_A(c_j^{CRV})$]
- random GFC composition uncertainty, represented by the standard deviation in the mass fraction of the j^{th} component (oxide or halogen) in the k^{th} GFC [$SD(G_{jk}^{GFC})$]
- random GFC mass uncertainty, represented by the standard deviation of the mass of the k^{th} GFC added to an ILAW MFPV batch. This uncertainty includes uncertainties caused by batching, weighing, and transfers of GFCs [$SD(a_k^{GFC})$]
- random volume uncertainties in the LAW CRV and MFPV. The magnitudes of these uncertainties (represented as SDs) will depend on the level of contents in a vessel, but a generic notation is used for now (SD_V^{CRV} and SD_V^{MFPV}).

Table 5.3 shows the values used for each of these factors. The values of three other factors were held constant for each of the simulation runs. These other factors were as follows: three samples per LAW CRV batch ($n_S^{CRV} = 3$), one analysis per CRV sample ($n_A^{MFPV} = 1$), and one volume determination of the CRV and MFPV before and after transfers ($n_V^{CRV} = 1$ and $n_V^{MFPV} = 1$). These values were specified by the WTP Project based on prior WTP planning and the results of investigations discussed by Piepel et al. (2005).

Data from a G2 run (Vora 2004) consisted of approximately 1400 runs that represent multiple streams of LAW tank waste that will go through the vitrification process. Five sections of the G2 runs were identified that represented five different compositions of glasses or waste streams, including a transition between waste streams (from AP-101/AY-102 to AZ-101). Figure 5.1 shows plots of the glass mass fractions across the first half of the G2 runs for 18 different analytes or radionuclides. Within each section, 10 continuous runs were selected in which the CRV concentrations and GFC amounts were used as inputs for the simulation calculations. These 10 runs were used to quantify the batch-to-batch variation over 10 batches. Red Xs in Figure 5.1 denote the five sets of 10 batches each that were chosen from the G2 output.

Tables D.1 to D.5 of Appendix D list the nominal CRV concentration data (μg/L) on chemical and radionuclide composition components for the five selected G2 runs. CRV mixing/sampling uncertainties were set to 1% RSD for low cases and 5% RSD for high cases for all of the analytes. Table D.6 lists CRV analytical uncertainties (%RSD values for low case). If the CRV concentration value is above the decision point, then the "Low %RSD" is used whereas if the CRV concentration value is below the decision point, the "Hi %RSD" is used. High uncertainties in the Monte Carlo simulations used %RSD values two times the low values. Table D.7 contains the nominal masses of the GFCs added to the LAW MFPV for each LAW tank. Table D.8 contains the low and high uncertainties associated with the masses of GFCs added to the ILAW MFPV. GFC composition data and corresponding low and high uncertainties are found in Tables D.9 and D.10. Table D.11 contains the low and high values for the volume uncertainties (SDs) for both the CRV and MFPV tanks. Table D.12 lists all of the nominal value amounts and number of MFPV batches for each CRV batch in the selected G2 runs.

Table 5.3. Factors and Levels Used in ILAW Monte Carlo Simulations

G2 Run Sections[a]	LAW CRV Random Batch-to-Batch %RSD	LAW CRV Mixing/Sampling %RSD	LAW CRV Analytical %RSD[b]	GFC Composition Uncertainty[c]	GFC Batching and Transfer Uncertainty (%RSD)[d]	Volume Uncertainty[e]
Set 1 Set 2 Set 3 Set 4 Set 5	Low (1%) High (5%)	Low (1%) High (5%)	Low High	Low High	Low High	Low High

(a) The sections of G2 runs selected to represent various patterns of batch-to-batch variation are discussed in following text.

(b) Low values for LAW CRV analytical uncertainties are given in Table D.6. If the CRV concentration value is below the decision point, then the "Hi %RSD" is used; if the CRV concentration value is above the decision point, then the "Low %RSD" is used. The high values are two times the low values.

(c) Low and high values for GFC composition uncertainties are given in Table D.9. Specifically, the nominal values and ranges in Table D.9 were used to define triangular distributions from which samples were taken in the Monte Carlo simulation.

(d) Low and high values for GFC batching and transfer uncertainties are given in Table D.8. These values are determined based upon the amounts of the GFCs added to the waste as listed in Table D.7.

(e) Low and high values for volume uncertainties are given in Table D.11.

Table 5.4 shows the 2^6 full-factorial design that was performed using the Monte Carlo simulation code for each of the five sets of G2 runs. This resulted in 64 scenarios for each of the five sets, or 320 total scenarios. Because it was a full-factorial design, all interactions can be isolated and tested for individual significance as well as interactions involving the factor representing the five sets. Each of the 320 scenarios consisted of 10 consecutive ILAW MFPV batches being simulated 200 different times.

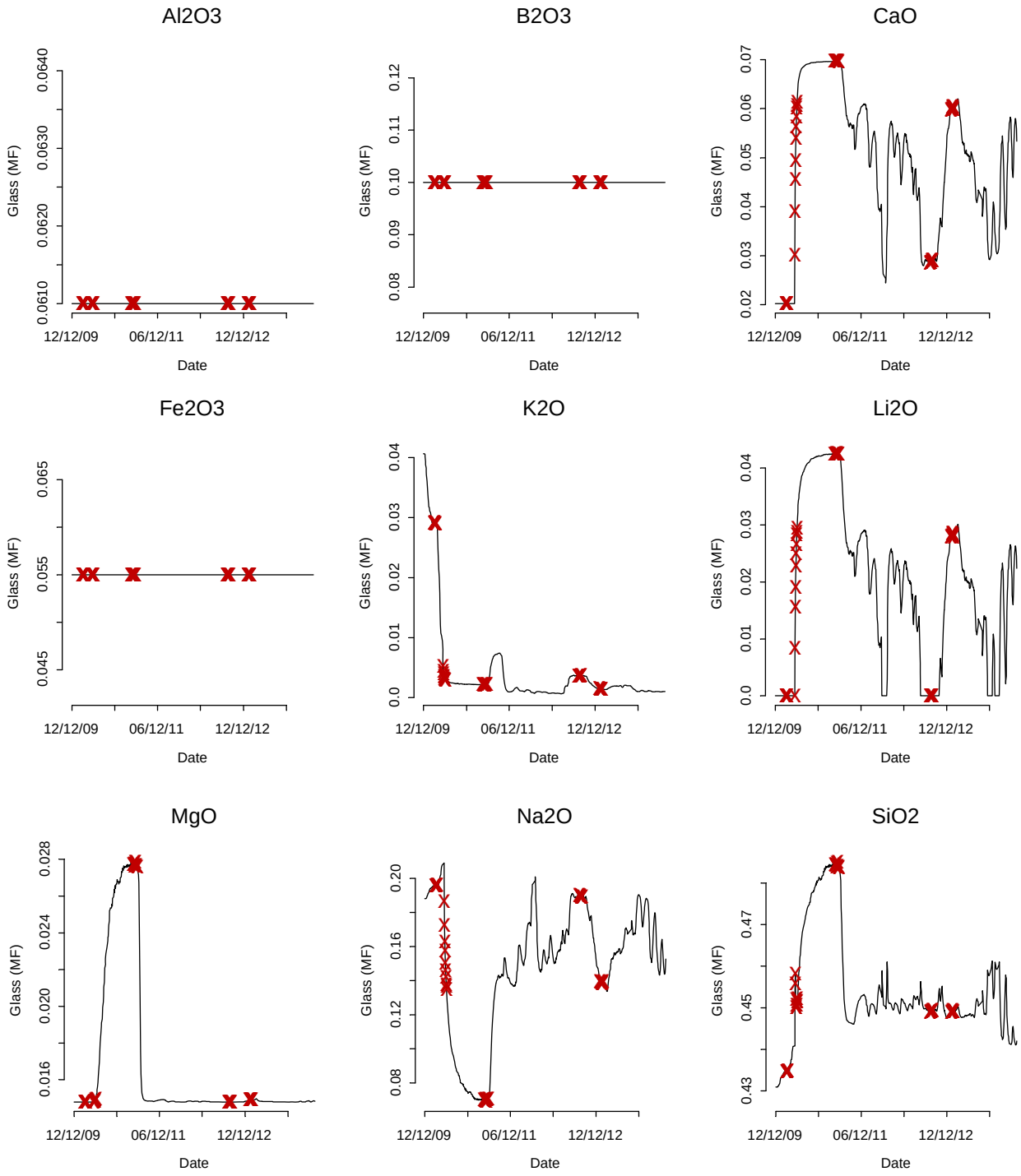

Figure 5.1. Glass Mass Fractions (MF) from G2 Runs with Red X's Representing Sets of MFPV Batches Used in the ILAW Simulation

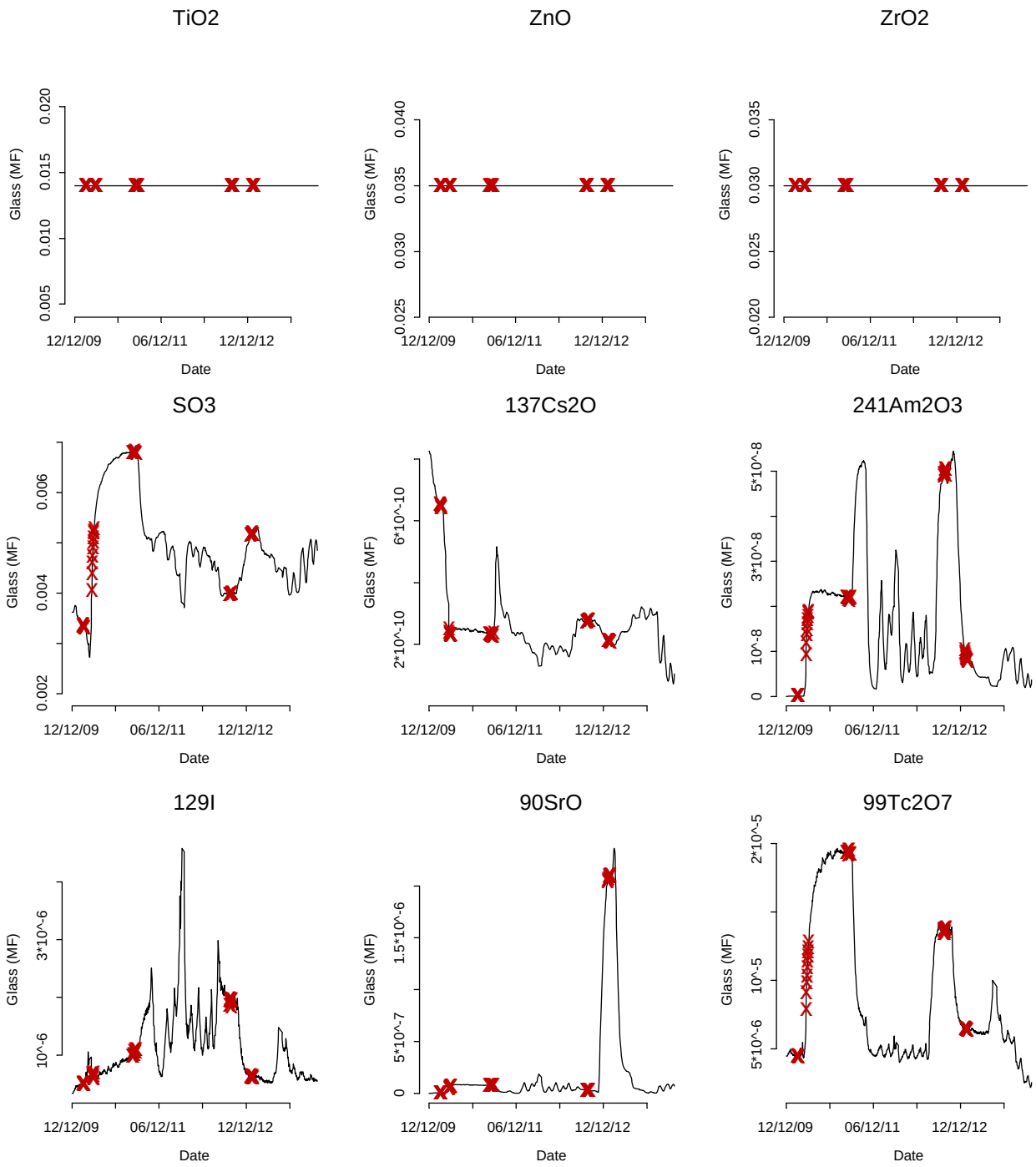

Figure 5.1. Glass Mass Fractions (MF) from G2 Runs with Red X's Representing Sets of MFPV Batches Used in the ILAW Simulation (cont'd)

Table 5.4. Scenarios Used in the ILAW Experimental Design for the Six Two-Level Factors Studied in the ILAW Monte Carlo Investigation for each of the Five Sets of MFPV Batches[(a)]

Scenario	LAW CRV Random Batch-to-Batch %RSD	LAW CRV Mixing/ Sampling %RSD [(b)]	LAW CRV Analytical %RSD [(b)]	LAW GFC Composition Uncertainty [(b)]	LAW GFC Batching Uncertainty [(b)]	Volume Uncertainty [(b)]
1	Low	Low	Low	Low	Low	Low
2	Low	Low	Low	Low	Low	High
3	Low	Low	Low	Low	High	Low
4	Low	Low	Low	Low	High	High
5	Low	Low	Low	High	Low	Low
6	Low	Low	Low	High	Low	High
7	Low	Low	Low	High	High	Low
8	Low	Low	Low	High	High	High
9	Low	Low	High	Low	Low	Low
10	Low	Low	High	Low	Low	High
11	Low	Low	High	Low	High	Low
12	Low	Low	High	Low	High	High
13	Low	Low	High	High	Low	Low
14	Low	Low	High	High	Low	High
15	Low	Low	High	High	High	Low
16	Low	Low	High	High	High	High
17	Low	High	Low	Low	Low	Low
18	Low	High	Low	Low	Low	High
19	Low	High	Low	Low	High	Low
20	Low	High	Low	Low	High	High
21	Low	High	Low	High	Low	Low
22	Low	High	Low	High	Low	High
23	Low	High	Low	High	High	Low
24	Low	High	Low	High	High	High
25	Low	High	High	Low	Low	Low
26	Low	High	High	Low	Low	High
27	Low	High	High	Low	High	Low
28	Low	High	High	Low	High	High
29	Low	High	High	High	Low	Low
30	Low	High	High	High	Low	High
31	Low	High	High	High	High	Low
32	Low	High	High	High	High	High

(a) The 64 scenarios in the experiment defined in the table were run for each of the five sets of MFPV batches from the G2 runs. This resulted in 320 (5 × 64) total scenarios.

(b) See the footnotes of Table 5.3 for the table references where the low and high values for each factor may be found.

Table 5.4. Scenarios Used in the ILAW Experimental Design for the Six Two-Level Factors Studied in the ILAW Monte Carlo Investigation for each of the Five Sets of MFPV Batches[a] (cont'd)

Scenario	LAW CRV Random Batch-to-Batch %RSD	LAW CRV Mixing/ Sampling %RSD [b]	LAW CRV Analytical %RSD [b]	GFC Composition Uncertainty [b]	GFC Batching Uncertainty [b]	Volume Uncertainty [b]
33	High	Low	Low	Low	Low	Low
34	High	Low	Low	Low	Low	High
35	High	Low	Low	Low	High	Low
36	High	Low	Low	Low	High	High
37	High	Low	Low	High	Low	Low
38	High	Low	Low	High	Low	High
39	High	Low	Low	High	High	Low
40	High	Low	Low	High	High	High
41	High	Low	High	Low	Low	Low
42	High	Low	High	Low	Low	High
43	High	Low	High	Low	High	Low
44	High	Low	High	Low	High	High
45	High	Low	High	High	Low	Low
46	High	Low	High	High	Low	High
47	High	Low	High	High	High	Low
48	High	Low	High	High	High	High
49	High	High	Low	Low	Low	Low
50	High	High	Low	Low	Low	High
51	High	High	Low	Low	High	Low
52	High	High	Low	Low	High	High
53	High	High	Low	High	Low	Low
54	High	High	Low	High	Low	High
55	High	High	Low	High	High	Low
56	High	High	Low	High	High	High
57	High	High	High	Low	Low	Low
58	High	High	High	Low	Low	High
59	High	High	High	Low	High	Low
60	High	High	High	Low	High	High
61	High	High	High	High	Low	Low
62	High	High	High	High	Low	High
63	High	High	High	High	High	Low
64	High	High	High	High	High	High

(a) The 64 scenarios in the experiment defined in the table were run for each of the five sets of batches from the G2 runs. This resulted in 320 (5 × 64) total scenarios.

(b) See the footnotes of Table 5.3 for the table references where the low and high values for each factor may be found.

In addition to the Monte Carlo simulation scenarios in Table 5.4, a smaller set of simulation scenarios was then performed, which are referred to as *control scenarios*. These scenarios were necessary to isolate batch-to-batch variations from combined estimates of batch-to-batch variation and within-batch uncertainties. The control scenarios set to zero all uncertainties associated with the LAW CRV concentrations ($\%RSD_S(c_j^{CRV})$ and $\%RSD_A(c_j^{CRV})$), the tank volumes (SD_V^{CRV} and SD_V^{MFPV}), and GFC additions ($SD(G_{jk}^{GFC})$ and $SD(a_k^{GFC})$). Hence, the control scenarios varied only the five different sets of batches from the G2 run data (five data sets) and the random batch-to-batch variation in the concentration of the j^{th} element in the LAW CRV batch [$\%RSD_B(c_j^{CRV})$]. Thus, the control scenario simulations provide for separately estimating batch-to-batch variation for each scenario. Table 5.5 shows the 10 control scenarios that were used in a Monte Carlo simulation. The batch-to-batch variations for the 10 control scenarios are directly linked to the within-batch uncertainties of the 64 scenarios for each data set in Table 5.4. For example, the batch-to-batch variations for the first control scenario for data set # 1 (Table 5.5) are associated with the within-batch uncertainty of the first 32 scenarios in Table 5.4 for data set # 1. The batch-to-batch variations for the second control scenario for data set # 1 (Table 5.5) are associated with the within-batch uncertainty of the last 32 scenarios in Table 5.4 for data set # 1. This same logic is followed for each of the remaining control scenarios and data sets.

All ILAW Monte Carlo simulations and summarizations of the simulation results were performed using S-Plus 6.2 software (Insightful Corp. 2003).

Table 5.5. Control Scenarios Used in the ILAW Monte Carlo Investigation Isolating the Batch-to-Batch Variation

Control Scenario	G2 Run Set[(a)]	Random LAW CRV Batch-to-Batch %RSD
1	Set 1	Low (1%)
2	Set 1	High (5%)
3	Set 2	Low (1%)
4	Set 2	High (5%)
5	Set 3	Low (1%)
6	Set 3	High (5%)
7	Set 4	Low (1%)
8	Set 4	High (5%)
9	Set 5	Low (1%)
10	Set 5	High (5%)

(a) Section 5.3 discusses the sets of G2 runs selected to represent various patterns of batch-to-batch variation.

6.0 Equations Used to Simulate IHLW and ILAW Compositions and Properties to Assess the Effects of Variation and Uncertainties

This section presents the mass-balance and statistical equations used to simulate IHLW and ILAW composition and properties using as inputs the sources of variation and uncertainty described in Section 4. Also presented are the property-composition models used to predict glass properties of interest for compliance and process control purposes. Finally, the equations for summarizing the results of the data are presented. Section 6.1 presents the equations for IHLW whereas Section 6.2 presents the equations for ILAW.

6.1 Equations Used to Assess the Effects of Variation and Uncertainties on IHLW Composition and Properties

To assess the effects of variation and uncertainties on IHLW compositions and properties using the Monte Carlo simulation approach described in Section 5, equations are needed to calculate IHLW compositions (expressed in mass fractions of glass components) corresponding to MFPV batches. Then these mass fractions are used as inputs in calculating the IHLW properties of interest, which include PCT (B, Li, and Na releases), TCLP Cd release, spinel $T_{1\%}$ (temperature at which spinel crystals make up 1 vol% of a glass melt), viscosity, and electrical conductivity.

Changes in IHLW composition during WTP operations will be caused not only by the variation over batches within a given waste type and uncertainties introduced by the factors described in Section 5.2, but also the variation that occurs when transitioning from one waste type to the next. It is assumed that IHLW produced from a particular waste type will have relatively constant composition and that deviations from it will occur only as a result of the sources of variation and uncertainties described in Section 5.2. However, when the last material from an HLW waste type has been completely introduced into an HLW MFPV and a new waste type with a different average composition is started to be brought in, the composition of waste and the resulting melter feed in the MFPV also changes.

Section 6.1.1 discusses the mass-balance equations used to calculate the IHLW MFPV mass fractions of components (including radionuclides). Section 6.1.2 discusses the equation used to calculate the transition from one waste type to another. Section 6.1.3 discusses how Monte Carlo simulation methods were applied with the mass-balance equations to simulate the variations and uncertainties associated with IHLW compositions of MFPV batches. Section 6.1.4 discusses the models used to calculate the IHLW properties relevant for process control and compliance. Section 6.1.5 discusses equations used to summarize the resulting variations and uncertainties in the ILAW MFPV compositions (mass fractions) and property values from the Monte Carlo simulations.

6.1.1 Mass-Balance Equations Used to Calculate IHLW MFPV Mass-Fraction Compositions

Piepel et al. (2005) present the mass-balance equations for calculating the mass-fraction compositions of IHLW (both chemical and radionuclide composition components) corresponding to single analyses of single samples from MFPV batches. Section A.1.1 and A.1.2 of Appendix A in Piepel et al. (2005) provide equations and the derivations of those equations. Per the WTP's tentative sampling and analysis plan and the results from Piepel et al. (2005), it was decided for the work in this report to simulate eight samples in the IHLW MFPV ($n_S^{MFPV} = 8$) and one chemical and radiochemical analysis per sample ($n_A^{MFPV} = 1$). Hence, the mass-balance equation for calculating IHLW mass-fraction compositons for single analyses from multiple samples per MFPV batch is now presented.

For single chemical and radionuclide analyses of the j^{th} analyte in the l^{th} sample from the i^{th} IHLW MFPV batch, the mass-balance equation to calculate IHLW composition is given by

$$g_{ijl}^{MFPV} = \frac{c_{ijl}^{MFPV} f_j}{\sum_{j=1}^{J} c_{ijl}^{MFPV} f_j} \tag{6.1.1}$$

where

g_{ijl}^{MFPV} = mass fraction of the j^{th} glass component (oxide or halogen) resulting from single chemical and radionuclide analyses of the l^{th} sample from the i^{th} IHLW MFPV batch (g_{oxide}/g_{oxides})

c_{ijl}^{MFPV} = analyzed concentration of the j^{th} analyte from a single analysis of the l^{th} sample from the i^{th} IHLW MFPV batch (μg/mL = mg/L)

f_j = $\frac{MW_j^{oxide}}{MW_j^{analyte}} R_j$ where MW_j^{oxide} and $MW_j^{analyte}$ are the molecular weights of oxide j and analyte j, respectively, and R_j is the ratio of moles of oxide per mole of analyte for oxide j. Hence, f_j is the factor for converting the concentration of analyte j (μg analyte j/mL = mg analyte j/L) to the concentration of oxide j (μg oxide j/mL = mg oxide/L). The quantity f_i is called the oxide factor for oxide j.

J = number of chemical and radionuclide composition components (oxides and halogens) for the IHLW composition.

Equation (6.1.1) is a reduced version of Eq. (A.1) in Appendix A for the case of single chemical and radionuclide analyses per sample (i.e., when $n_A^{MFPV} = 1$).

6.1.2 The Transition between High-Level Waste Types

When transitioning from one HLW waste type to another, the resulting compositions in successive IHLW MFPV batches will undergo systematic changes as a result of blending the current and previous waste types. These systematic changes can be described using mass-balance equations to calculate the new compositions during this transition period.

Let the nominal IHLW composition corresponding to an MFPV batch produced from the first waste type (denoted Material *A*) be described by a vector of nominal mass fractions $\boldsymbol{x}_A^{MFPV}$, made up of entries x_{Aj}^{MFPV}, so that $\sum_{j=1}^{N_A} x_{Aj}^{MFPV} = 1$ (where N_A is the total number of components making up Material *A*). Also, let the total mass of glass that would be produced from an IHLW MFPV batch be represented by M^{MFPV}. Similarly, let the nominal composition of IHLW corresponding to a second waste type (denoted Material *B*) be described by a vector of nominal mass fractions $\boldsymbol{x}_B^{MFPV}$, made up of entries x_{Bj}^{MFPV}, so that $\sum_{j=1}^{N_B} x_{Bj}^{MFPV} = 1$ (where N_B is the total number of components making up Material *B*). Under these conditions, the mass of the j^{th} IHLW component in an IHLW MFPV batch containing only Material *A* is given by

$$m_{Aj}^{MFPV} = x_{Aj}^{MFPV} M^{MFPV} \tag{6.1.2}$$

where

m_{Aj}^{MFPV} = mass of the j^{th} IHLW component in an IHLW MFPV batch containing only Material *A* (kg)

x_{Aj}^{MFPV} = mass fraction of the j^{th} IHLW component in an IHLW MFPV batch containing only Material *A* ($kg_{component\ i}$/kg IHLW)

M^{MFPV} = total mass of IHLW that would be made from an MFPV batch (kg).

If a mass *m* (in kg) is withdrawn from an MFPV batch containing only Material *A* and replaced with the same mass *m* of Material *B*, then the mass (in kg) of the j^{th} IHLW component present in the first MFPV transition batch is given by

$$m_{1j}^{MFPV} = x_{Aj}^{MFPV} (M^{MFPV} - m) + x_{Bj}^{MFPV} m \tag{6.1.3}$$

where the subscript 1 denotes the first transition batch. The mass fraction of the j^{th} component in this first transition batch is given by

$$x_{1j} = \frac{m_{1j}^{MFPV}}{M^{MFPV}} = x_{Aj}^{MFPV}\left(1 - \frac{m}{M^{MFPV}}\right) + x_{Bj}^{MFPV}\left(\frac{m}{M^{MFPV}}\right) \tag{6.1.4}$$

If this process of withdrawing and adding m kg from each MFPV batch continues, then the mass fraction of the j^{th} component after p additions (i.e., in the p^{th} MFPV transition batch) is given by

$$x_{pj}^{MFPV} = x_{(p-1)j}^{MFPV}\left(1 - \frac{m}{M^{MFPV}}\right) + x_{Bj}^{MFPV}\left(\frac{m}{M^{MFPV}}\right), \text{ where } p = 2, 3, \ldots \quad (6.1.5)$$

Equation (6.1.5) can be applied recursively after the initial use of Eq. (6.1.4) to obtain the mass-fraction compositions of all IHLW components for any given MFPV batch during the transition period. Values of the nominal chemical and radionuclide compositions for the first 10 batches of the transition period are shown in Tables C.6 and C.7, respectively, of Appendix C. Note that batches 11 to 18 of this transition waste type have essentially the same composition as AZ-102 and thus are not listed separately in Tables C.6 and C.7. Equation (6.1.5) can also be used to obtain nominal values for variation and uncertainty %RSDs for the transition batches. Mixing/sampling %RSDs for the chemical composition components of the first 10 transition batches are shown in Table C.8. Mixing/sampling %RSD values are the same for the reported radionuclides in AY-102 and AZ-102, and hence the values in Table C.2 apply. Analytical %RSD values for the first 10 transition batches are shown in Table C.9 for the chemical composition components and Table C.10 for radionuclides.

6.1.3 Equations for Simulating Mass-Fraction Compositions of IHLW Associated with MFPV Batches

This section describes how IHLW compositions associated with each IHLW MFPV batch were simulated for the investigations discussed in this report. Equation (6.1.1) provides for calculating mass fractions of IHLW components given analyte concentrations c_{ijl}^{MFPV}. During operation of the WTP IHLW facility, such concentrations will be obtained from chemical and radiochemical analyses of IHLW MFPV samples. In the Monte Carlo simulation work, these concentrations were simulated.

The general equation chosen to describe the relationship between the analyzed concentration of an analyte in an IHLW MFPV batch and the sources of variation and uncertainty mentioned in Section 4.1 is given by

$$c_{ijlm}^{MFPV} = \mu_j^{MFPV} + \varepsilon_{B,ij}^{MFPV} + \varepsilon_{MS,ijl}^{MFPV} + \varepsilon_{A,ijlm}^{MFPV}, \quad (6.1.6)$$

where

c_{ijlm}^{MFPV} = simulated value of an analyzed concentration of the j^{th} analyte from the m^{th} analysis of the l^{th} sample from the i^{th} IHLW MFPV batch (μg/mL = mg/L)

μ_j^{MFPV} = nominal concentration of the j^{th} analyte over the IHLW MFPV batches associated with an HLW waste type (μg/mL = mg/L)

$\varepsilon_{B,ij}^{MFPV}$ = random effect caused by batch-to-batch variation on the concentration of the j^{th} analyte in the i^{th} IHLW MFPV batch (μg/mL = mg/L)

$\varepsilon_{MS,ijl}^{MFPV}$ = random effect caused by mixing and sampling uncertainties on the concentration of the j^{th} analyte in the l^{th} sample from the i^{th} IHLW MFPV batch (μg/mL = mg/L)

$\varepsilon_{A,ijlm}^{MFPV}$ = random effect caused by analytical uncertainty in the analyzed concentration of the j^{th} analyte from the m^{th} analysis of the l^{th} sample from the i^{th} IHLW MFPV batch (μg/mL = mg/L).

The preceding are given in general terms, although we note that the WTP plans to analyze each IHLW MFPV sample only once, so the "*m*" subscript is not needed in that case.

By starting with nominal analyte concentrations and simulating the various random effects according to statistical normal (Gaussian) distributions with zero means and selected standard deviations, Eq. (6.1.6) can be used to simulate analyte concentrations in an IHLW MFPV (after GFC addition). For the work in this report, analyte concentrations were simulated in this way according to the Monte Carlo approach described in Section 5.2. The simulated concentrations were then substituted into Eq. (6.1.1) to calculate mass-fraction compositions for IHLW corresponding to each MFPV batch. The resulting IHLW compositions were then used to assess the effects of the selected sources of variation and uncertainty on IHLW MFPV compositions and properties.

6.1.4 Glass Property-Composition Models Used to Calculate IHLW Properties

This section discusses and presents the glass property-composition models used to calculate the property values for estimated IHLW compositions corresponding to MFPV batches. The modeled properties include PCT normalized B, Li, and Na releases ($r^{PCT\ h}$, h = B, Li, or Na in g/L), TCLP Cd release ($c^{TCLP\ Cd}$ in mg/L), spinel $T_{1\%}$ ($T_{1\%}$ in ºC), viscosity (η in poise), and electrical conductivity (ε in S/cm, where S denotes Siemens). As discussed in the following subsections, mathematical transformations of properties were modeled in some cases.

6.1.4.1 Property-Composition Models for PCT Normalized Releases of B, Li, and Na from HLW Glasses

Linear mixture experiment models were developed by PNWD and the Vitreous State Laboratory (VSL) (Kot et al. 2005) for predicting PCT normalized releases of B, Li, and Na for IHLW compositions. These models, as applied in this work, are of the general form

$$\hat{y}_{il}^{PCT\ h} = \hat{\ln}(r_{il}^{PCT\ h}) = \sum_{k=1}^{n_{nmc}^{PCT\ h}} b_k^{PCT\ h}\, x_{ikl}^{MFPV} \qquad (6.1.7)$$

where

$\hat{y}_{il}^{PCT\ h}$ = $\hat{\ln}(r_{il}^{PCT\ h})$ = predicted natural logarithm of the PCT normalized release of h = B, Li, or Na for IHLW corresponding to the l^{th} sample from the i^{th} MFPV batch [ln(g/L)]

$n_{nmc}^{PCT\ h}$ = number of normalized IHLW components used in the model for PCT normalized release of h = B, Li, or Na

$b_k^{PCT\ h}$ = coefficients for the linear mixture model form involving normalized components (k) of IHLW in the model for PCT normalized release of h = B, Li, or Na. The coefficients are obtained by fitting the linear model form to a property-composition data set using least squares regression.

x_{ikl}^{MFPV} = normalized mass fraction of the k^{th} IHLW component from a single analysis of the l^{th} sample from the i^{th} MFPV batch, where k is one of the IHLW components in a property-composition model, such that $\sum_{k=1}^{n_{nmc}^{PCT\ h}} x_{ikl}^{MFPV} = 1$ (g_{oxide}/g_{oxides}).

The normalized mass-fraction compositions of IHLW in Eq. (6.1.7) are obtained from the ordinary (unnormalized) mass-fraction compositions by

$$x_{ikl}^{MFPV} = \frac{g_{ikl}^{MFPV}}{\sum_{j}^{n_{nmc}\ of\ J} g_{ijl}^{MFPV}} \quad k = 1,2,\cdots,n_{nmc} \tag{6.1.8}$$

where g_{ijl}^{MFPV} is calculated using Eq. (6.1.1). Note that Eq. (6.1.8) uses the general notation n_{nmc} in place of the specific $n_{nmc}^{PCT\ h}$ because Eq. (6.1.8) is referred to subsequently for use with other property-composition models. Finally, note that $\bar{x}_{ik}^{MFPV}$ for the k^{th} IHLW component generally will not be the same for different IHLW property-composition models because the number of components in the model used to calculate the normalized composition can differ from property to property.

Table 6.1 lists the linear mixture model terms and the coefficients for IHLW PCT B, PCT Li, and PCT Na used for the work in this report. These models and coefficients are documented in the report by Kot et al. (2005).

Table 6.1. IHLW PCT Model Terms and Coefficients

Model Term[(a)]	ln(PCT B)[(b)] Coefficient	ln(PCT Li)[(b)] Coefficient	ln(PCT Na)[(b)] Coefficient
Al_2O_3	-16.0111	-11.5792	-13.7309
B_2O_3	6.0139	3.0320	1.7213
Li_2O	20.5142	15.7575	19.9566
MnO	3.7888	1.4622	3.6828
Na_2O	12.2908	7.4435	13.2619
SiO_2	-3.9574	-2.3693	-3.8031
ThO_2	6.1476	2.5351	3.1327
ZrO_2	-9.6868	-6.0292	-8.9994

(a) Model terms use normalized mass fractions of the IHLW oxide components.
(b) PCT normalized elemental releases are modeled in ln(g/L).

6.1.4.2 TCLP Cd Release Model for HLW Glasses

A linear regression model was developed by PNWD and VSL (Kot et al. 2004) for predicting TCLP Cd releases for IHLW compositions. This model, as applied in this work, is of the general form

$$\hat{y}_{il}^{TCLP\ Cd} = \hat{\ln}(c_{il}^{TCLP\ Cd}) = \sum_{k=1}^{n_{nmc}^{TCLP\ Cd}} b_k^{TCLP\ Cd}\, x_{ikl}^{MFPV} + b_{CdO}^{TCLP\ Cd}\, \ln(g_{il,CdO}^{MFPV}) \qquad (6.1.9)$$

where

$\hat{y}_{il}^{TCLP\ Cd}$ = $\hat{\ln}(c_{il}^{TCLP\ Cd})$ = predicted natural logarithm of TCLP Cd release, for IHLW corresponding to the l^{th} sample from the i^{th} MFPV batch [ln(mg/L)]

$n_{nmc}^{TCLP\ Cd}$ = number of normalized IHLW components used in the model for TCLP Cd release

$b_k^{TCLP\ Cd}$ = coefficients for the linear mixture portion of the model form for TCLP Cd release, which involves normalized components (k) of IHLW. The coefficients are obtained by fitting the model form to a property-composition data set using least squares regression.

x_{ikl}^{MFPV} = normalized mass fraction of the k^{th} IHLW component from a single analysis of the l^{th} sample from the i^{th} MFPV batch, where k is one of the IHLW components in the property-composition model, such that $\sum_{k=1}^{n_{nmc}^{TCLP\ Cd}} x_{ikl}^{MFPV} = 1$ (g_{oxide}/g_{oxides})

$b_{CdO}^{TCLP\ Cd}$ = coefficient for the term of the TCLP Cd release model involving the unnormalized mass fraction of CdO. This coefficient was obtained in the same regression analysis as the $b_k^{TCLP\ Cd}$ coefficients.

$g_{il,CdO}^{MFPV}$ = original, unnormalized mass fraction of CdO for the l^{th} sample from the i^{th} IHLW MFPV batch.

The normalized mass-fraction compositions of IHLW in Eq. (6.1.9) are obtained from the ordinary (unnormalized) mass-fraction compositions using Eq. (6.1.8) presented in Section 6.1.4.1, where in that notation $n_{nmc} = n_{nmc}^{TCLP\ Cd}$. That is, Eq. (6.1.8) is applied using the components involved in the TCLP Cd model.

Table 6.2 lists the terms and the coefficients for the IHLW TCLP Cd model used for the work in this report. This model and coefficients are documented in Kot et al. (2004).

Table 6.2. IHLW TCLP Cd Model Terms and Coefficients

Model Term[(a)]	ln(TCLP Cd)[(b)] Coefficient
Al_2O_3	0.3257
B_2O_3	8.0665
Fe_2O_3	1.5677
Li_2O	11.3541
MnO	10.7633
Na_2O	9.3328
SiO_2	0.1617
ZrO_2	2.0438
ZnO	15.4324
$\ln(\bar{g}_{i,CdO}^{MFPV})$	0.9859

(a) All model terms except the last use normalized mass fractions of the IHLW oxide components.
(b) TCLP normalized elemental releases are modeled in ln(mg/L).

6.1.4.3 $T_{1\%}$ Spinel Crystallinity Models for HLW Glasses

Two linear mixture experiment models were developed for predicting the temperature at which one volume percent of a glass melt is spinel crystals (spinel $T_{1\%}$) for IHLW compositions. PNWD and VSL (Kot et al. 2005) developed one of these models, denoted the IHLW Phase 1 model. This model was subsequently updated for use in planning the IHLW Phase 2 test matrices. PNWD developed[(a)] the updated model, referred to as the IHLW Phase 1a model. These models, as applied in this work, are of the general form

(a) The updated model was only documented in informal summaries provided to the WTP Project and other participants in the work. These informal summaries cannot be referenced.

$$\hat{y}_{il}^{T1\%\,h} = \sum_{k=1}^{n_{nmc}^{T1\%\,h}} b_k^{T1\%\,h}\, x_{ikl}^{MFPV} \qquad (6.1.10)$$

where

$\hat{y}_{il}^{T1\%\,h}$ = predicted spinel $T_{1\%}$ for IHLW corresponding to the l^{th} sample from the i^{th} MFPV batch, where $h = 1$ denotes the IHLW Phase 1 model and $h = 1a$ denotes the updated IHLW Phase 1a model (^oC)

$n_{nmc}^{T1\%\,h}$ = number of normalized IHLW components used in the spinel $T_{1\%}$ model, where $h = 1$ denotes the IHLW Phase 1 model and $h = 1a$ denotes the updated IHLW Phase 1a model

$b_k^{T1\%\,h}$ = coefficients for the $T_{1\%}$ model form involving normalized components (k) of IHLW, where $h = 1$ denotes the IHLW Phase 1 model and $h = 1a$ denotes the updated IHLW Phase 1a model. The coefficients are obtained by fitting the model form to a property-composition data set using least squares regression.

x_{ikl}^{MFPV} = normalized mass fraction of the k^{th} IHLW component from a single chemical analysis of the l^{th} sample from the i^{th} MFPV batch, where k is one of the IHLW components in the property-composition model, such that $\sum_{k=1}^{n_{nmc}^{T1\%\,h}} x_{ikl}^{MFPV} = 1$ (g_{oxide}/g_{oxides}).

The normalized mass-fraction compositions of IHLW in Eq. (6.1.10) are obtained from the ordinary (unnormalized) mass-fraction compositions using Eq. (6.1.8) presented in Section 6.1.4.1, where in that notation $n_{nmc} = n_{nmc}^{T1\%\,h}$. That is, Eq. (6.1.8) is applied using the components involved in the $T_{1\%}$ (Phase 1 or 1a) model.

Table 6.3 lists the linear mixture model terms and the coefficients for IHLW spinel $T_{1\%}$ used for the work in this report. The IHLW Phase 1 model and its coefficients are documented in the report by Kot et al. (2005). The IHLW Phase 1a model and its coefficients are documented only in informal summaries that cannot be referenced. However, they are available for use within the WTP Project.

Table 6.3. IHLW $T_{1\%}$ Spinel Crystallinity Model Terms and Coefficients

Model Term[(a)]	$T_{1\%}$ Phase 1[(b)] Coefficient	$T_{1\%}$ Phase 1a[(b)] Coefficient
Al_2O_3	3139.3911	2976.0468
B_2O_3	16.8471	73.3956
Cr_2O_3	17827.9333	16850.0307
Fe_2O_3	3616.2420	3511.7682
Li_2O	-1982.3832	-1463.5620
MnO	2182.6998	2559.2867
Na_2O	-1177.8694	-1014.1423
NiO	11230.9464	12586.4914
SiO_2	573.8247	513.0767
SrO	-164.6976	-138.8209
ThO_2	1659.3672	1587.3524
ZnO	3948.6108	3909.4625
ZrO_2	2029.1022	1634.7205

(a) Model terms use normalized mass fractions of the IHLW oxide components.
(b) Spinel T1% values are modeled in ^{o}C.

6.1.4.4 Property-Composition Model for Viscosity of HLW Glasses

VSL[(a)] developed the property-composition model form for viscosity used in this work for predicting the natural logarithm of viscosity (poise) as a function of the IHLW composition and melt temperature. This model, as applied in this work, is in the general form

$$\hat{y}_{il}^{\eta} = \hat{\ln}(\eta_{il}) = b_0^{\eta 0} + \sum_{t=1}^{n_{umc}^{\eta 2}} b_s^{\eta 2} \frac{w_{isl}^{MFPV}}{T^2} \qquad (6.1.11)$$

where

$\hat{y}_{il}^{\eta}$ = $\hat{\ln}(\eta_{il})$ = predicted natural logarithm of the viscosity for IHLW corresponding to the l^{th} sample from the i^{th} MFPV batch [$\hat{\ln}$(poise)]

$n_{umc}^{\eta 2}$ = number of unnormalized IHLW components used in the "linear component divided by temperature squared" terms of the viscosity model. Note that the number of unnormalized IHLW components used in the model may be less than the total number of unnormalized components varied in the data set used to develop the model.

(a) H Gan, Z Feng, and IL Pegg. 2004. *Summary and Recommendations on Viscosity and Electrical Conductivity Model Forms to Support HLW Vitrification*. Letter Report VSL-04L4780-1 Rev. 0, Vitreous State Laboratory, The Catholic University of America, Washington DC.

$b_0^{\eta 0}$, $b_s^{\eta 2}$ = IHLW viscosity model coefficients, including the intercept ($b_0^{\eta 0}$) and the coefficients ($b_s^{\eta 2}$) for terms involving IHLW components divided by temperature squared (T^2). The coefficients were obtained by fitting the model form to a property-composition data set using least squares regression.(a)

w_{isl}^{MFPV} = wt% of the s^{th} IHLW component in the "linear component divided by temperature squared" portion of a property-composition model, where the composition is for the l^{th} sample from the i^{th} IHLW MFPV batch. These wt% values are not normalized to sum to 100% over the components in the model. Note that $w_{isl}^{MFPV} = 100\, g_{isl}^{MFPV}$.

T = temperature measured in Kelvin.

Table 6.4 lists the IHLW viscosity model terms and the coefficients used for the work in this report. This model and its coefficients are documented in the report by Gan et al.(a) The model contains 16 terms involving an intercept and 15 of the oxide components (which have not been normalized to sum to 100%). Predictions were made at temperatures of 1373.15 K (1100ºC) and 1423.15 K (1150ºC) using the model information from Table 6.4.

(a) H Gan, Z Feng, and IL Pegg. 2004. *Summary and Recommendations on Viscosity and Electrical Conductivity Model Forms to Support HLW Vitrification*. Letter Report VSL-04L4780-1 Rev. 0, Vitreous State Laboratory, The Catholic University of America, Washington DC.

Table 6.4. IHLW Viscosity Model Terms and Coefficients

Model Term[(a)]	Coefficient[(b)]
Intercept[(c)]	-2.37916
Al_2O_3/T^2 [(d)]	309980.228
B_2O_3/T^2	-25524.485
CdO/T^2	101859.606
Cr_2O_3/T^2	1054196.628
Fe_2O_3/T^2	45087.363
Li_2O/T^2	-603322.997
MnO/T^2	-1862.382
Na_2O/T^2	-128973.946
NiO/T^2	-34606.026
Sb_2O_3/T^2	-80395.215
SeO_2/T^2	423261.260
SiO_2/T^2	287011.241
SrO/T^2	3437.917
Tl_2O/T^2	-145158.299
ZrO_2/T^2	228749.388

(a) Model terms use unnormalized wt% values of the IHLW oxide components.
(b) Viscosity is modeled in ln(poise).
(c) An intercept term is present in this model.
(d) T^2 is temperature squared, with temperature measured in Kelvin.

6.1.4.5 Property-Composition Model for Electrical Conductivity of HLW Glasses

VSL[(a)] developed the property-composition model form for electrical conductivity used in this work for predicting the natural logarithm of electrical conductivity (S/cm) as a function of the IHLW composition and melt temperature. This model, as applied in this work, is in the general form

$$\hat{y}_{il}^{\varepsilon} = \hat{\ln}(\varepsilon_{il}) = \sum_{k=1}^{n_{umc}^{\varepsilon 0}} b_k^{\varepsilon 0}\, w_{ikl}^{MFPV} + \sum_{t=1}^{n_{umc}^{\varepsilon 1}} b_t^{\varepsilon 1}\, \frac{w_{itl}^{MFPV}}{T} + \sum_{s=1}^{n_{umc}^{\varepsilon 2}} b_s^{\varepsilon 2}\, \frac{w_{isl}^{MFPV}}{T^2} \qquad (6.1.12)$$

where

$\hat{y}_{il}^{\varepsilon}$ = $\hat{\ln}(\varepsilon_{il})$ = predicted natural logarithm of the electrical conductivity for IHLW corresponding to the l^{th} sample from the i^{th} MFPV batch [$\hat{\ln}$(S/cm), where S denotes Siemens]

(a) H Gan, Z Feng, and IL Pegg. 2004. *Summary and Recommendations on Viscosity and Electrical Conductivity Model Forms to Support HLW Vitrification*. Letter Report VSL-04L4780-1 Rev. 0, Vitreous State Laboratory, The Catholic University of America, Washington DC.

$n_{umc}^{\varepsilon 0}$ = number of unnormalized IHLW components used in the "linear component" terms of the electrical conductivity model. Note that the number of unnormalized IHLW components used in the model is less than the total number of unnormalized components varied in the data set used to develop the model per Gan et al.[(a)]

$n_{umc}^{\varepsilon 1}$ = number of unnormalized IHLW components used in the "linear component divided by temperature" terms of the electrical conductivity model

$n_{umc}^{\varepsilon 2}$ = number of unnormalized IHLW components used in the "linear component divided by temperature squared" terms of the electrical conductivity model

$b_k^{\varepsilon 0}$, $b_t^{\varepsilon 1}$, $b_s^{\varepsilon 2}$ = IHLW electrical conductivity model coefficients for terms involving IHLW components (indexed by k), components divided by temperature (indexed by t), and components divided by temperature squared (indexed by s). The coefficients were obtained by fitting the model form to a property-composition data set using least squares regression (see Gan et al.[(a)]).

w_{ikl}^{MFPV} = wt% of the k^{th} IHLW component in the "linear component" portion of a property-composition model, where the composition is for the l^{th} sample from the i^{th} IHLW MFPV batch. These wt% values are not normalized to sum to 100% over the components in the model. Note that $w_{ikl}^{MFPV} = 100\ g_{ikl}^{MFPV}$.

w_{itl}^{MFPV} = wt% of the t^{th} IHLW component in the "linear component divided by temperature" portion of a property-composition model, where the composition is for the l^{th} sample from the i^{th} IHLW MFPV batch. These wt% values are not normalized to sum to 100% over the components in the model. Note that $w_{itl}^{MFPV} = 100\ g_{itl}^{MFPV}$.

w_{isl}^{MFPV} = wt% of the s^{th} IHLW component in the "component divided by temperature squared" portion of the property-composition model, where the composition is for the l^{th} sample from the i^{th} IHLW MFPV batch. These wt% values are not normalized to sum to 100% over the components in the model. Note that $w_{isl}^{MFPV} = 100\ g_{isl}^{MFPV}$.

T = temperature measured in Kelvin.

Table 6.5 lists the IHLW electrical conductivity model terms and the coefficients used for the work in this report. The report by Gan et al.[(a)] documents this model and its coefficients. The model contains 14 terms involving 9 of the oxide components (which have not been normalized to sum to 100%). Predictions were made at temperatures of 1373.15 K (1100ºC) and 1473.15 K (1200ºC) using the model information from Table 6.5.

Table 6.5. IHLW Electrical Conductivity Model Terms and Coefficients

Model Term[(a)]	Coefficient[(b)]
Al_2O_3	-0.035719
B_2O_3	0.014964
Fe_2O_3	-0.023870
Li_2O	0.177034
MnO	0.017739
Na_2O	0.053575
SiO_2	0.001441
SrO	0.045768
ZrO_2	0.041137
ZrO_2/T[(c)]	-82.81435
B_2O_3/T^2	-87316.319
MnO/T^2	-121107.017
SiO_2/T^2	-70295.405
SrO/T^2	-120757.126

(a) Model terms use unnormalized wt% values of the IHLW oxide components.
(b) Electrical conductivity is modeled in ln(S/cm) where S denotes Siemens.
(c) T is temperature measured in Kelvin.

6.1.5 Equations Used to Summarize IHLW Monte Carlo Simulation Results

Monte Carlo simulations for IHLW produced results for 12 different scenarios (consisting of combinations of variation and uncertainty values) for each of the four waste types investigated (AY-102, AZ-102, C-104, and the transition from AY-102 to AZ-102) described in Section 6.1.2. The 12 scenarios for each of the four waste types correspond to the 12 rows of Table 5.2. For each of the scenarios, data for 18 IHLW MFPV batches (the number corresponding to an HLW waste type), 8 samples per batch, and 1 chemical and radiochemical analysis per sample were simulated a total of 200 times.

The simulated data must be summarized so that insight can be provided. Summarizations are necessary for the resulting IHLW mass-fraction compositions as well as the property values. The following discussion explains how a statistical data analysis method known as *variance component analysis* was applied to simulated data to estimate the %RSDs associated with batch-to-batch variation and within-batch uncertainty for each of the 200 simulations of each of the 12 scenarios for each of the four HLW waste types. Then, means and 90% empirical confidence intervals (90% ECIs) were calculated to summarize the %RSD values for batch-to-batch variation, within-batch uncertainty, and total

(a) H Gan, Z Feng, and IL Pegg. 2004. *Summary and Recommendations on Viscosity and Electrical Conductivity Model Forms to Support HLW Vitrification*. Letter Report VSL-04L4780-1 Rev. 0, Vitreous State Laboratory, The Catholic University of America, Washington DC.

(batch-to-batch variation plus within-batch uncertainty) of %RSD for each scenario and waste type combination. A 90% ECI is expected (on average) to capture 90% of the %RSD values that might be obtained with the WTP HLW vitrification facility operating at the conditions of a given scenario for a given HLW waste type. How 90% ECIs were calculated is discussed subsequently.

Simulated data for an IHLW component (mass fraction) or property for a set of 18 IHLW MFPV batches associated with an HLW waste type can be represented by the following equation

$$y_{pqr} = \mu_{pq} + \varepsilon_{B,pq} + \varepsilon_{W,pq} \tag{6.1.13}$$

where

y_{pqr} = IHLW component (mass fraction) or property value calculated for the p^{th} scenario, the q^{th} simulation, and the r^{th} IHLW MFPV batch associated with an HLW waste type

μ_{pq} = nominal value of the IHLW component or property for the q^{th} simulation of the p^{th} scenario over the IHLW MFPV batches associated with an HLW waste type

$\varepsilon_{B,pq}$ = effect on an IHLW component or property value because of batch-to-batch variation over the $r = 1, 2, \ldots, 18$ batches for the q^{th} simulation of the p^{th} scenario for a given HLW waste type, where the effect has mean 0 and standard deviation $\sigma_{B,pq}$

$\varepsilon_{W,pq}$ = effect on an IHLW component or property value because of within-batch uncertainty over the $r = 1, 2, \ldots, 18$ batches for the q^{th} simulation of the p^{th} scenario for a given HLW waste type, where the effect has mean 0 and standard deviation $\sigma_{W,pq}$.

Note that μ_{pq}, $\sigma_{B,pq}$, and $\sigma_{W,pq}$ are assumed to be constant over a given waste type, and that $\sigma_{W,pq}$ is assumed to be constant over batches of a waste type.

Given this structure of the simulated data, *variance component analysis* software can be used to obtain estimates of the two "variance components," denoted here by the standard deviations $SD_{B,pq} = \hat{\sigma}_{B,pq}$ and $SD_{W,pq} = \hat{\sigma}_{W,pq}$. The standard deviation for batch-to-batch variation in the q^{th} simulation of the p^{th} scenario ($SD_{B,pq}$) quantifies all of the differences from batch-to-batch over the 18 batches associated with a given HLW waste type. The standard deviation for within-batch uncertainty in the q^{th} simulation of the p^{th} scenario ($SD_{W,pq}$) quantifies (in component mass fraction or property units) all of the uncertainties affecting each IHLW MFPV batch associated with a given HLW waste type. These uncertainties include mixing and sampling of the HLW MFPV as well as analyzing the samples.

Note that $SD_{W,pq}$ is an estimate of the within-batch uncertainty for an IHLW component (mass fraction) or property that represents the uncertainty associated with mixing the IHLW MFPV, taking a single sample, and analyzing the sample once. However, the WTP plans to take eight samples from each IHLW MFPV batch and analyze each one once. Thus, the interest is in the within-batch uncertainty in IHLW components or properties corresponding to averaging the results of the 8 samples. This is represented by

$$\overline{SD}_{W,pq} = \frac{SD_{W,pq}}{\sqrt{8}} \approx 0.354\, SD_{W,pq} \tag{6.1.14}$$

where $\overline{SD}_{W,pq}$ denotes the within-batch uncertainty (standard deviation) for an IHLW component or property based on averaging the results from the 8 samples per IHLW MFPV batch. In what follows, $\overline{SD}_{W,pq}$ is reported and used rather than $SD_{W,pq}$. This is consistent with what is reported and used for IHLW compositions and properties where there is no choice because of the mass-balance equations for the IHLW compliance strategy.[(a)]

The batch-to-batch and within-batch standard deviations ($SD_{B,pq}$ and $\overline{SD}_{W,pq}$, respectively) can then be converted into %RSDs by applying the following equations

$$\%RSD_{B,pq} = 100\frac{SD_{B,pq}}{\text{Mean}} = \frac{100\, SD_{B,pq}}{\frac{\sum_{r=1}^{n} y_{pqr}}{n}} \tag{6.1.15}$$

$$\%RSD_{W,pq} = 100\frac{\overline{SD}_{W,pq}}{\text{Mean}} = \frac{100\, \overline{SD}_{W,pq}}{\frac{\sum_{r=1}^{n} y_{pqr}}{n}} \tag{6.1.16}$$

where

$\%RSD_{B,pq}$ = batch-to-batch variation %RSD (for an IHLW component or property) associated with the q^{th} simulation of the p^{th} scenario for a given HLW waste type

$\%RSD_{W,pq}$ = within-batch uncertainty %RSD (for an IHLW component or property) associated with the q^{th} simulation of the p^{th} scenario when averaging results over the 8 samples per IHLW MFPV batch from a given HLW waste type

(a) The mass-balance equations for estimating ILAW composition in the ILAW MFPV do not provide for producing separate estimates of ILAW composition for each LAW CRV sample and then averaging them. Rather, results from analyses of replicate sample, replicate volume determinations, etc. are all averaged first before use in the mass-balance equations.

n = the number of IHLW MFPV batches per HLW waste type (n = 18 according to the current WTP IHLW compliance strategy).

and y_{pqr}, $SD_{B,pq}$, and $\overline{SD}_{W,pq}$ are as previously defined. Note that to avoid confusion in subsequent notation, $\%RSD_{W,pq}$ does not have a bar over it to denote it is a measure of uncertainty based on averages over 8 samples per IHLW MFPV.

Equations (6.1.15) and (6.1.16), respectively, result in the batch-to-batch and within-batch %RSDs calculated over 18 IHLW MFPV batches for each of the 200 simulations of the 12 scenarios for each of the four HLW waste types. The total variation plus uncertainty %RSDs over the 18 IHLW MFPV batches for each of the 200 simulations of the 12 scenarios for each of the four HLW waste types are calculated using

$$\%RSD_{T,pq} = \sqrt{(\%RSD_{B,pq})^2 + (\%RSD_{W,pq})^2} \tag{6.1.17}$$

The %RSDs in Eqs. (6.1.16), 6.1.17), and (6.1.18) were calculated for each IHLW component (mass fraction) and property.

To summarize the $\%RSD_{T,pq}$ results for an IHLW component or property for each scenario associated with a given HLW waste type, the mean and a 90% ECI are calculated. The mean is calculated using the equation

$$\overline{\%RSD_{T,p}} = \frac{\sum_{q=1}^{200} \%RSD_{T,pq}}{200} \tag{6.1.18}$$

where

$\overline{\%RSD_{T,p}}$ = mean total %RSD (of an IHLW component or property) across the 200 simulations for the p^{th} scenario for a given HLW waste type

$\%RSD_{T,pq}$ = total %RSD (of an IHLW component or property) for the q^{th} simulation (q = 1, 2, … , 200) of the p^{th} scenario for a given HLW waste type.

To calculate the 90% ECI for a specific IHLW component (mass fraction) or property, the 5th percentile and 95th percentile are calculated from the simulation values for that specific component or property. This is represented in the following equations

$$\%RSD_{T,p}^{90\%\ ELCL} = 5^{th} \text{ percentile from all 200 simulated } \%RSD_{T,pq} \text{ values for the } p^{th} \text{ scenario and a given HLW waste type} \tag{6.1.19a}$$

$$\%RSD_{T,p}^{90\%\ EUCL} = 95^{\text{th}} \text{ percentile from all 200 simulated } \%RSD_{T,pq} \text{ values for the } p^{\text{th}} \text{ scenario and a given HLW waste type} \quad (6.1.19b)$$

where

$\%RSD_{T,p}^{90\%\ ELCL}$ = empirical lower confidence limit (ELCL) for a 90% ECI on the total %RSD (of an IHLW component or property) for the p^{th} scenario associated with a given HLW waste type

$\%RSD_{T,p}^{90\%\ EUCL}$ = empirical upper confidence limit (EUCL) for a 90% ECI on the total %RSD (of an IHLW component or property) for the p^{th} scenario associated with a given HLW waste type

and $\%RSD_{T,pq}$ is as previously defined.

To summarize the $\%RSD_{B,pq}$ results for an IHLW component or property for each scenario associated with a given HLW waste type, the mean and a 90% ECI are calculated. The mean is calculated using the equation

$$\overline{\%RSD_{B,p}} = \frac{\sum_{q=1}^{200} \%RSD_{B,pq}}{200} \quad (6.1.20)$$

where

$\overline{\%RSD_{B,p}}$ = mean batch-to-batch %RSD (of an IHLW component or property) across the 200 simulations for the p^{th} scenario associated with a given HLW waste type

$\%RSD_{B,pq}$ = batch-to-batch %RSD (of an IHLW component or property) for the q^{th} simulation (1 of 200 simulations) of the p^{th} scenario associated with a given HLW waste type.

The 90% ECI is given by

$$\%RSD_{B,p}^{90\%\ ELCL} = 5^{\text{th}} \text{ percentile from all 200 simulated } \%RSD_{B,pq} \text{ values for the } p^{\text{th}} \text{ scenario and a given HLW waste type} \quad (6.1.21a)$$

$$\%RSD_{B,p}^{90\%\ EUCL} = 95^{\text{th}} \text{ percentile from all 200 simulated } \%RSD_{B,pq} \text{ values for the } p^{\text{th}} \text{ scenario and a given HLW waste type} \quad (6.1.21b)$$

where

$\%RSD_{B,p}^{90\%\ ELCL}$ = ELCL for a 90% ECI on the batch-to-batch %RSD (of an IHLW component or property) for the p^{th} scenario associated with a given HLW waste type

$\%RSD_{B,p}^{90\%\ EUCL}$ = EUCL for a 90% ECI on the batch-to-batch %RSD (of an IHLW component or property) for the p^{th} scenario associated with a given HLW waste type

and $\%RSD_{B,pq}$ is as previously defined.

To summarize the $\%RSD_{W,pq}$ results for an IHLW component or property for each scenario associated with a given HLW waste type, the mean and an empirical confidence interval are calculated. The mean is calculated using the equation

$$\overline{\%RSD_{W,p}} = \frac{\sum_{q=1}^{200} \%RSD_{W,pq}}{200} \tag{6.1.22}$$

where

$\overline{\%RSD_{W,p}}$ = mean within-batch uncertainty %RSD (of an IHLW component or property) across the 200 simulations for the p^{th} scenario associated with given HLW waste type

$\%RSD_{W,pq}$ = within-batch uncertainty %RSD (of an IHLW component or property) for the q^{th} simulation (1 of 200 simulations) of the p^{th} scenario associated with a given HLW waste type.

The 90% ECI is given by

$$\%RSD_{W,p}^{90\%\ ELCL} = 5^{th} \text{ percentile from all 200 simulated } \%RSD_{W,pq} \text{ values for the } p^{th} \text{ scenario and a given HLW waste type} \tag{6.1.23a}$$

$$\%RSD_{W,p}^{90\%\ EUCL} = 95^{th} \text{ percentile from all 200 simulated } \%RSD_{W,pq} \text{ values for the } p^{th} \text{ scenario and a given HLW waste type} \tag{6.1.23b}$$

where

$\%RSD_{W,p}^{90\%\ ELCL}$ = ELCL for a 90% ECI on the within-batch uncertainty %RSD (of an IHLW component or property) for the p^{th} scenario associated with a given HLW waste type

$\%RSD_{W,p}^{90\%\ EUCL}$ = EUCL for a 90% ECI on the within-batch uncertainty %RSD (of an IHLW component or property) for the p^{th} scenario associated with a given HLW waste type

and $\%RSD_{W,pq}$ is as previously defined.

In summary, the equations in this section provide for calculating the means and 90% ECIs for values of total variation and uncertainty ($\%RSD_{T,pq}$), batch-to-batch variation ($\%RSD_{B,pq}$), and within-batch uncertainty ($\%RSD_{W,pq}$). These means and 90% ECIs were calculated for each IHLW component (mass fraction) and property. Section 7 presents and discusses the IHLW results where for simplicity of notation, $\%RSD_T = \%RSD_{T,pq}$, $\%RSD_B = \%RSD_{B,pq}$, and $\%RSD_W = \%RSD_{W,pq}$.

6.2 Equations Used to Assess the Effects of Variation and Uncertainties on ILAW Compositions and Properties

To assess the effects of variation and uncertainties on ILAW compositions and properties using the Monte Carlo simulation approach described in Section 5, equations are needed to calculate ILAW compositions (expressed in mass fractions of glass components) corresponding to MFPV batches. Then these mass fractions are used as inputs in calculating the ILAW properties of interest, which include PCT (B and Li releases), VHT, viscosity, and electrical conductivity. Section 6.2.1 discusses the mass-balance equations used to calculate the ILAW MFPV mass fractions of components (including radionuclides). Section 6.2.2 discusses how Monte Carlo simulation methods were applied with the mass-balance equations to simulate the variations and uncertainties associated with ILAW compositions of MFPV batches. Section 6.2.3 discusses the models used to calculate the ILAW properties relevant for process control and compliance. Section 6.2.4 discusses equations used to summarize the resulting variations and uncertainties in the ILAW MFPV compositions (mass fractions) and property values from the Monte Carlo simulations.

6.2.1 Mass-Balance Equations Used to Calculate ILAW MFPV Mass-Fraction Compositions

Piepel et al. (2005) present the mass-balance equations for calculating the mass-fraction compositions of ILAW (including radionuclides) corresponding to MFPV batches. Section B.1.2 of Appendix B in Piepel et al. (2005) provides equations and their derivations for balanced and unbalanced data. Data are considered balanced when the same number of samples (n_S^{CRV}) are taken from each LAW CRV batch, each sample is analyzed the same number (n_A^{CRV}) of times, and a consistent number of volume samples (n_V^{CRV} and n_V^{MFPV}) are taken. Balanced data are expected for WTP operations; therefore, this section only shows the final mass-balance equations for balanced data.

In the case of balanced data, the equation for calculating the mass fraction of the j^{th} component (oxide or halogen) of the ILAW composition (chemical or radionuclide) resulting from the i^{th} MFPV batch is given by

$$\bar{g}_{ij}^{MFPV} = \frac{\dfrac{1}{n_S^{CRV} n_A^{CRV}} \sum_{l=1}^{n_S^{CRV}} \sum_{m=1}^{n_A^{CRV}} c_{ijlm}^{CRV} f_j \bar{V}_i^{CRV to MFPV} u + \sum_{k=1}^{K} a_{ik}^{GFC} G_{ijk}^{GFC} + \bar{m}_{i-1,j}^{MFPV} \left(\dfrac{\dfrac{1}{n_V^{MFPV}} \sum_{h=1}^{n_V^{MFPV}} V_{i,h}^{MFPV\ Heel}}{\dfrac{1}{n_V^{MFPV}} \sum_{h=1}^{n_V^{MFPV}} V_{i-1,h}^{MFPV}} \right)}{\sum_{j=1}^{J} \left(\dfrac{1}{n_S^{CRV} n_A^{CRV}} \sum_{l=1}^{n_S^{CRV}} \sum_{m=1}^{n_A^{CRV}} c_{ijlm}^{CRV} f_j \bar{V}_i^{CRV to MFPV} u \right) + \sum_{j=1}^{J} \sum_{k=1}^{K} a_{ik}^{GFC} G_{ijk}^{GFC} + \sum_{j=1}^{J} \bar{m}_{i-1,j}^{MFPV} \left(\dfrac{\dfrac{1}{n_V^{MFPV}} \sum_{h=1}^{n_V^{MFPV}} V_{i,h}^{MFPV\ Heel}}{\dfrac{1}{n_V^{MFPV}} \sum_{h=1}^{n_V^{MFPV}} V_{i-1,h}^{MFPV}} \right)} \qquad (6.2.1)$$

where

$$\bar{m}_{i-1,j}^{MFPV} = \frac{1}{n_S^{CRV} n_A^{CRV}} \sum_{l=1}^{n_S^{CRV}} \sum_{m=1}^{n_A^{CRV}} c_{i-1,jlm}^{CRV} f_j \bar{V}_{i-1}^{CRV to MFPV} u + \sum_{k=1}^{K} a_{i-1,k}^{GFC} G_{i-1,jk}^{GFC} + \bar{m}_{i-2,j}^{MFPV} \left(\frac{\dfrac{1}{n_V^{MFPV}} \sum_{h=1}^{n_V^{MFPV}} V_{i-1,h}^{MFPV\ Heel}}{\dfrac{1}{n_V^{MFPV}} \sum_{h=1}^{n_V^{MFPV}} V_{i-2,h}^{MFPV}} \right) \qquad (6.2.2)$$

and

$$\bar{V}_i^{CRV to MFPV} = \frac{\hat{\sigma}^2_{\bar{V}_i^{MFPV\ after}} + \hat{\sigma}^2_{\bar{V}_i^{MFPV\ before}}}{\hat{\sigma}^2_{\bar{V}_i^{CRV\ before}} + \hat{\sigma}^2_{\bar{V}_i^{CRV\ after}} + \hat{\sigma}^2_{\bar{V}_i^{MFPV\ after}} + \hat{\sigma}^2_{\bar{V}_i^{MFPV\ before}}} \left(\frac{\sum_{h=1}^{n_V^{CRV}} V_{ih}^{CRV\ before}}{n_V^{CRV}} - \frac{\sum_{h=1}^{n_V^{CRV}} V_{ih}^{CRV\ after}}{n_V^{CRV}} \right)$$

$$+ \frac{\hat{\sigma}^2_{\bar{V}_i^{CRV\ before}} + \hat{\sigma}^2_{\bar{V}_i^{CRV\ after}}}{\hat{\sigma}^2_{\bar{V}_i^{CRV\ before}} + \hat{\sigma}^2_{\bar{V}_i^{CRV\ after}} + \hat{\sigma}^2_{\bar{V}_i^{MFPV\ after}} + \hat{\sigma}^2_{\bar{V}_i^{MFPV\ before}}} \left(\frac{\sum_{h=1}^{n_V^{MFPV}} V_{ih}^{MFPV\ after}}{n_V^{MFPV}} - \frac{\sum_{h=1}^{n_V^{MFPV}} V_{ih}^{MFPV\ before}}{n_V^{MFPV}} \right). \qquad (6.2.3)$$

The notation used in these equations is defined in Appendix B, where for clarity Eqs. (6.2.1) to (6.2.3) are represented as Eqs. (B.1) to (B.3). How radionuclide composition components *j* are handled is also addressed in Appendix B. These equations for calculating ILAW compositions $\bar{g}_{ij}^{MFPV}$ are more complicated than the corresponding equations in Section 6.1.1 for calculating IHLW compositions g_{ijl}^{MFPV} because of the different sampling plans and compliance strategies for IHLW and ILAW (see Sections 2.2 and 2.3, respectively). Specifically, the equations for calculating IHLW compositions are based on analyses of samples taken from the IHLW MFPV. Here, the equations for calculating ILAW compositions use analyses of LAW CRV samples, the volume transferred from the LAW CRV to MFPV, GFC compositon data, masses of GFCs added to the LAW MFPV, and volume determinations of the

MFPV before and after transfer to the LAW MFV. Thus, the equations for calculating ILAW composition are more complicated than those for IHLW.

Using the results from Piepel et al. (2005), it was decided for the work in this report to take three samples in the CRV ($n_S^{CRV} = 3$), one chemical and radiochemical analysis per sample ($n_A^{CRV} = 1$), and one volume determination in each of the CRV ($n_V^{CRV} = 1$) and MFPV ($n_V^{MFPV} = 1$).

6.2.2 Equations for Simulating Mass-Fraction Compositions of ILAW Associated with MFPV Batches

This section describes how ILAW compositions associated with each ILAW MFPV batch were simulated for the investigations discussed in this report. Equations (6.2.1) to (6.2.3) provide for calculating mass fractions of ILAW components given analyte concentrations c_{ijlm}^{CRV}, GFC compositions G_{ijk}^{GFC}, masses of GFCs added a_{ik}^{GFC}, and various volume determinations. During operation of the WTP ILAW facility, these quantities will be obtained by chemical and radiochemical analyses of ILAW CRV samples, vendor certification of GFC compositions, weighing of added GFCs, and volume determinations. In the Monte Carlo simulation work, these quantities are simulated as described in the balance of this section.

The general equation chosen to describe the relationship between the analyzed concentration of an analyte in an LAW CRV batch and the sources of variation and uncertainty mentioned in Section 4.1 is given by

$$c_{ijlm}^{CRV} = \mu_j^{CRV} + \varepsilon_{B,ij}^{CRV} + \varepsilon_{MS,ijl}^{CRV} + \varepsilon_{A,ijlm}^{CRV}, \qquad (6.2.4)$$

where

c_{ijlm}^{CRV} = simulated value of an analyzed concentration of the j^{th} analyte from the m^{th} analysis of the l^{th} sample from the CRV batch contributing to the i^{th} ILAW MFPV batch (μg/mL = mg/L)

μ_j^{CRV} = nominal concentration of the j^{th} analyte over the LAW CRV batches associated with an LAW waste type (μg/mL = mg/L)

$\varepsilon_{B,ij}^{CRV}$ = random effect caused by batch-to-batch variation on the concentration of the j^{th} analyte in the CRV batch contributing to the i^{th} ILAW MFPV batch (μg/mL = mg/L)

$\varepsilon_{MS,ijl}^{CRV}$ = random effect caused by mixing and sampling uncertainties on the concentration of the j^{th} analyte in the l^{th} sample from the CRV batch contributing to the i^{th} ILAW MFPV batch (μg/mL = mg/L)

$\varepsilon_{A,ijlm}^{CRV}$ = random effect caused by analytical uncertainty in the analyzed concentration of the j^{th} analyte from the m^{th} analysis of the l^{th} sample from the CRV batch contributing to the i^{th} ILAW MFPV batch (μg/mL = mg/L).

The preceding are given in general terms, although we note that the WTP plans to analyze each LAW CRV sample only once, so the "*m*" subscript is not needed in that case.

By starting with nominal analyte concentrations and simulating the various random effects according to statistical normal (Gaussian) distributions with zero means and specified standard deviations, Eq. (6.2.4) can be used to simulate analyte concentrations in an LAW CRV.

The GFC compositions G_{ijk}^{GFC} and GFC masses a_{ik}^{GFC} added to the ILAW MFPV, which occur in Eq. (6.2.1), were also simulated in the Monte Carlo simulation work. The general equation chosen to describe the relationship between the GFC compositions added to an LAW MFPV batch, and the source of uncertainty mentioned in Section 4.1 is given by

$$G_{ijk}^{GFC} = \mu_{G,jk}^{GFC} + \varepsilon_{G,ijk}^{GFC}, \tag{6.2.5}$$

where

G_{ijk}^{GFC} = simulated mass fraction of the j^{th} glass component in the k^{th} GFC added to the i^{th} ILAW MFPV batch ($g_{oxide\ j}/g_{GFC\ k}$)

$\mu_{G,jk}^{GFC}$ = nominal mass fraction of the j^{th} glass component in the k^{th} GFC used in the ILAW MFPV batches associated with an LAW waste type ($g_{oxide\ j}/g_{GFC\ k}$)

$\varepsilon_{G,ijk}^{GFC}$ = random uncertainty in the mass fraction of the j^{th} glass component in the k^{th} GFC added to the i^{th} ILAW MFPV batch (μg/mL = mg/L).

The random uncertainties $\varepsilon_{G,ijk}^{GFC}$ in mass fractions of glass components in GFCs were assumed to have triangular distributions defined by the component nominal values and ranges given in Table D.9 of Appendix D.

The general equation chosen to describe the relationship between the GFC masses added to an ILAW MFPV batch and the source of uncertainty mentioned in Section 4.1 is given by

$$a_{ik}^{GFC} = \mu_{a,ik}^{GFC} + \varepsilon_{a,ik}^{GFC}, \tag{6.2.6}$$

where

a_{ik}^{GFC} = simulated mass of the k^{th} GFC added to the i^{th} ILAW MFPV batch (g)

$\mu_{a,ik}^{GFC}$ = nominal mass of the k^{th} GFC added to the i^{th} ILAW MFPV batch (g)

$\varepsilon_{a,ik}^{GFC}$ = random uncertainty in the mass of the k^{th} GFC added to the i^{th} ILAW MFPV batch (g).

The random uncertainty in the mass of an added GFC includes all sources of uncertainty, including weighing, blending, and transfer to the ILAW MFPV. Such uncertainties were assumed to have a normal (Gaussian) distribution with mean zero and specified standard deviation.

In summary, simulated concentrations were generated using Eq. (6.2.4), simulated GFC compositions were generated using Eq. (6.2.5), and simulated GFC masses were generated using Eq. (6.2.6). Each simulated value was substituted in to Eq. (6.2.1) within the framework of the Monte Carlo approach described in Section 5.2. The resulting ILAW compositions were then used to assess the effects of the selected sources of variation and uncertainty on ILAW MFPV compositions and properties.

6.2.3 Glass Property-Composition Models Used to Calculate ILAW Properties

This section discusses and presents the glass property-composition models used to calculate the property values for estimated ILAW compositions corresponding to MFPV batches. These properties include PCT normalized B and Na releases ($r^{PCT\ h}$, h = B or Na in g/L), VHT alteration depth at 24 ± 2 days (D^{VHT} in μm), viscosity (η in poise), and electrical conductivity (ε in S/cm, where S denotes Siemens). As discussed in the following subsections, mathematical transformations of properties were modeled in some cases.

6.2.3.1 Property-Composition Models for PCT Normalized Releases of B and Na and VHT Alteration Depth of LAW Glasses

Reduced partial quadratic mixture (PQM) models were developed by PNWD and VSL (Muller et al. 2005) for predicting PCT normalized releases of B and Na, as well as VHT alteration depth, for ILAW compositions. These models, as applied in this work, are of the general form

$$\hat{\bar{y}}_i^{PCT\ h} = \hat{\ln}(\bar{r}_i^{PCT\ h}) = \sum_{k=1}^{n_{nmc}^{PCT\ h}} b_k^{PCT\ h}\,\bar{x}_{ik}^{MFPV} + Selected\left\{\sum_{k=1}^{n_{nmc}^{PCT\ h}} b_{kk}^{PCT\ h}\left(\bar{x}_{ik}^{MFPV}\right)^2 + \sum_{k=1}^{n_{nmc}^{PCT\ h}-1}\ \sum_{l>k}^{n_{nmc}^{PCT\ h}} b_{kl}^{PCT\ h}\,\bar{x}_{ik}^{MFPV}\,\bar{x}_{il}^{MFPV}\right\} \quad (6.2.7a)$$

$$\hat{\bar{y}}_i^{VHT\ D} = \hat{\ln}(\bar{D}_i^{VHT}) = \sum_{k=1}^{n_{nmc}^{VHT\ D}} b_k^{VHT\ D}\,\bar{x}_{ik}^{MFPV} + Selected\left\{\sum_{k=1}^{n_{nmc}^{VHT\ D}} b_{kk}^{VHT\ D}\left(\bar{x}_{ik}^{MFPV}\right)^2 + \sum_{k=1}^{n_{nmc}^{VHT\ D}-1}\ \sum_{l>k}^{n_{nmc}^{VHT\ D}} b_{kl}^{VHT\ D}\,\bar{x}_{ik}^{MFPV}\,\bar{x}_{il}^{MFPV}\right\} \quad (6.2.7b)$$

where

$\hat{\bar{y}}_i^{PCT\ h}$ = $\hat{\ln}(\bar{r}_i^{PCT\ h})$ = predicted natural logarithm of the PCT normalized release of h = B or Na for ILAW corresponding to the i^{th} MFPV batch, based on averages over multiple samples from a CRV batch, analyses per CRV sample, and CRV and MFPV volume determinations [ln(g/L)]

$\hat{\bar{y}}_i^{VHT\ D}$ = $\hat{\ln}(\overline{D}_i^{VHT})$ = predicted natural logarithm of the VHT alteration depth for ILAW corresponding to the i^{th} MFPV batch, based on averages over multiple samples from a CRV batch, analyses per CRV sample, and CRV and MFPV volume determinations [ln(μm)]

$n_{nmc}^{PCT\ h}$ = number of normalized ILAW components used in the model for PCT normalized release of h = B or Na

$n_{nmc}^{VHT\ D}$ = number of normalized ILAW components used in the model for VHT alteration depth

$b_k^{PCT\ h}$, $b_{kk}^{PCT\ h}$, $b_{kl}^{PCT\ h}$ = coefficients for the PQM model form involving normalized components (k and l) of ILAW in the model for PCT normalized release of h = B or Na. The coefficients are obtained by fitting the PQM model form to a property-composition data set using least squares regression.

$b_k^{VHT\ D}$, $b_{kk}^{VHT\ D}$, $b_{kl}^{VHT\ D}$ = coefficients for the PQM model form involving normalized components (k and l) of ILAW in the model for VHT alteration depth. The coefficients are obtained by fitting the PQM model form to a property-composition data set using least squares regression.

$\bar{x}_{ik}^{MFPV}$ = normalized mass fraction of the k^{th} ILAW component in the PQM model where the composition is for the i^{th} ILAW MFPV batch, such that $\sum_{k=1}^{n_{nmc}^{PCT\ h}} \bar{x}_{ik}^{MFPV} = 1$ for a PCT B or Na release model, and $\sum_{k=1}^{n_{nmc}^{VHT\ D}} \bar{x}_{ik}^{MFPV} = 1$ for the VHT model. The mass fractions are based on averages over multiple samples from a CRV batch, analyses per CRV sample, and CRV and MFPV volume determinations. Note that the same description applies for $\bar{x}_{ik}^{MFPV}$ with "l" substituted in place of "k."

In Eqs. (6.2.7a) and (6.2.7b), "Selected" means that only a subset of the squared and crossproduct terms in the curly brackets are included in the model. The subset is selected using standard stepwise regression or similar methods. See Piepel et al. (2002) for further discussion and illustrations of PQM models.

The normalized mass-fraction compositions of ILAW in Eqs. (6.2.7a) and (6.2.7b) are obtained from the ordinary (unnormalized) mass-fraction compositions by

$$\bar{x}_{ik}^{MFPV} = \frac{\bar{g}_{ik}^{MFPV}}{\sum_{j}^{n_{nmc}\ of\ J} \bar{g}_{ij}^{MFPV}} \quad k = 1,2,\cdots,n_{nmc} \tag{6.2.8}$$

where $\bar{g}_{ij}^{MFPV}$ is calculated using Eq. (6.2.1). Note that Eq. (6.2.8) uses the general notation n_{nmc} in place of the specific $n_{nmc}^{PCT\ h}$ because Eq. (6.2.8) is referred to subsequently for use with other property-composition models. Finally, note that $\bar{x}_{ik}^{MFPV}$ for the k^{th} ILAW component generally will not be the same for different ILAW property-composition models because the number of components in the model used to calculate the normalized composition can differ from property to property.

The "bars" in the $\bar{x}_{ik}^{MFPV}$ and $\bar{g}_{ij}^{MFPV}$ notations indicate averaging over multiple samples per LAW CRV batch. (The bars would also indicate averaging over multiple analyses per sample, multiple determinations per volume, multiple weights of GFCs, etc. if applicable, although current WTP plans call for only single analyses per sample, single volume determinations, single weighings of GFCs, etc.) These averages occur "inside" the mass-balance Eq. (6.2.1) so that there is only one estimate of ILAW composition per MFPV batch. The "bars" in the notations $\hat{\bar{y}}_i^{PCT\ h}$ and $\hat{\bar{y}}_i^{VHT\ D}$ represent this same "internal averaging" to obtain a single estimate of ILAW composition per MFPV batch, which is then used to calculate ILAW property values. Hence, the "bar" appears on *y* first, followed by the "hat" representing the model prediction. In Section 6.1.4 for IHLW properties, no "bar" notation is used. That is because it is possible to use Eq. (6.1.1) to estimate IHLW composition for each sample from each IHLW MFPV batch and obtain corresponding predictions of IHLW properties. This same discussion applies to all ILAW properties, but is given only once here to avoid duplication of discussion in subsequent subsections.

It is important to note that VHT is modeled in natural logarithm of alteration depth (in μm) at 24 ± 2 days, but the specification limit is in alteration rate (g/m^{2}day). An alteration depth from the model can be converted to alteration rate (in g/m^{2}day) using the following equation:

$$R^{VHT} = e^{\ln(D^{VHT})} \times \frac{2.65}{24} \tag{6.2.9}$$

where $\ln(D^{VHT})$ is the natural logarithm of the alteration depth as calculated from the VHT model, 2.65 represents the assumed glass density (g/cm^3), and 24 represents the number of test days.

Table 6.6 lists the PQM model terms and the coefficients for ILAW PCT B, PCT Na, and VHT used for the work in this report. These models and coefficients are documented in the report by Muller et al. (2005). It is important to note that the number of glass components used in the PCT B and Na models is different than the number of glass components used in the VHT model. Hence, the normalized compositions (calculated per Eq. (6.2.8)) substituted into the models will be different for the VHT model than for the PCT B and Na models.

Table 6.6. ILAW PCT and VHT Model Terms and Coefficients

PQM Model Term[(a)]	ln(PCT B)[(b)] Coefficient	ln(PCT Na)[(b)] Coefficient	ln(VHT)[(c)] Coefficient
Al_2O_3	-19.9158	-17.2629	49.8620
B_2O_3	1.6716	2.2622	8.5808
CaO	-1.5471	3.9240	-21.4725
Fe_2O_3	-0.8289	2.1598	18.3252
K_2O	4.9225	41.2770	137.6727
Li_2O	-6.9721	-5.4762	113.4367
MgO	-25.7905	-9.9926	-31.3959
Na_2O	15.2327	12.9487	35.2036
SO_3	(d)	(d)	-707.4950
SiO_2	-3.1991	-3.4173	-15.5899
TiO_2	-11.0586	-8.1687	-20.1469
ZnO	(d)	(d)	1.8503
ZrO_2	-18.0010	-19.8097	-73.6987
Others	(d)	(d)	-83.5317
Al_2O_3 * K_2O	(d)	(d)	-1206.9348
B_2O_3 * CaO	(d)	(d)	-731.6002
B_2O_3 * K_2O	(d)	-199.2665	(d)
B_2O_3 * MgO	493.3071	267.6811	(d)
B_2O_3 * SO_3	(d)	(d)	6505.9075
CaO * Fe_2O_3	(d)	(d)	-486.3382
CaO * SiO_2	(d)	(d)	304.4759
Fe_2O_3 * K_2O	(d)	-266.2859	(d)
Fe_2O_3 * Li_2O	349.7992	201.4967	(d)
K_2O * ZnO	(d)	(d)	-1288.2916
Li_2O * ZrO_2	541.9078	526.3173	(d)
MgO * Others	(d)	(d)	1733.1272
MgO * TiO_2	(d)	(d)	1430.2732

(a) Model terms use normalized mass-fraction values of the IHLW oxide components.
(b) PCT normalized elemental releases are modeled in ln(g/L).
(c) VHT alteration depth is modeled in ln(μm).
(d) A missing value indicates that the model term was not included for that particular property.

6.2.3.2 Property-Composition Model for Viscosity of LAW Glasses

The property-composition model form for viscosity used in this work was developed by VSL[(a)] for predicting the natural logarithm of viscosity (poise) as a function of the ILAW composition and melt temperature. This model, as applied in this work, is in the general form

(a) Z Feng, F Perez-Carenas, H Gan, and IL Pegg. 2004. *Summary and Recommendations on Viscosity and Electrical Conductivity Model Forms to Support LAW Vitrification*. Letter Report VSL-03L4480-2 Rev. 0, Vitreous State Laboratory, The Catholic University of America, Washington DC.

$$\hat{\bar{y}}_i^{\eta} = \hat{\ln}(\bar{\eta}_i) = b_0^{\eta 0} + \sum_{k=1}^{n_{umc}^{\eta 1}} b_k^{\eta 1}\, \bar{w}_{ik}^{MFPV} + \sum_{t=1}^{n_{umc}^{\eta 2}} b_s^{\eta 2}\, \frac{\bar{w}_{is}^{MFPV}}{T^2} \qquad (6.2.10)$$

where

$\hat{\bar{y}}_i^{\eta}$ = $\hat{\ln}(\bar{\eta}_i)$ = predicted natural logarithm of the viscosity for ILAW corresponding to the i^{th} MFPV batch, based on averages over multiple samples from a CRV batch, analyses per CRV sample, and CRV and MFPV volume determinations [$\hat{\ln}$(poise)]

$n_{umc}^{\eta 1}$ = number of unnormalized ILAW components used in the "linear component" terms of the viscosity model. Note that the number of unnormalized ILAW components used in the model may be less than the total number of unnormalized components varied in the data set used to develop the model.

$n_{umc}^{\eta 2}$ = number of unnormalized ILAW components used in the "linear component divided by temperature squared" terms of the viscosity model

$b_0^{\eta 0}$, $b_k^{\eta 1}$, $b_s^{\eta 2}$ = ILAW viscosity model coefficients, including the intercept ($b_0^{\eta 0}$), coefficients ($b_k^{\eta 1}$) for terms involving components of ILAW in the model, and coefficients ($b_s^{\eta 2}$) for terms involving components divided by temperature squared (T^2). The coefficients were obtained by fitting the model form to a property-composition data set using least squares regression.(a)

$\bar{w}_{ik}^{MFPV}$ = wt% of the k^{th} ILAW component in the "linear component" portion of a property-composition model, where the composition is for the i^{th} ILAW MFPV batch. The wt% values are based on averages over multiple samples from a CRV batch, analyses per CRV sample, and CRV and MFPV volume determinations. These wt% values are not normalized to sum to 100% over the components in the model. Note that $\bar{w}_{ikl}^{MFPV} = 100\ \bar{g}_{ikl}^{MFPV}$.

$\bar{w}_{isl}^{MFPV}$ = wt% of the s^{th} IHLW component in the "linear component divided by temperature squared" portion of a property-composition model, where the composition is for the l^{th} sample from the i^{th} IHLW MFPV batch. These wt% values are not normalized to sum to 100% over the components in the model. Note that $\bar{w}_{isl}^{MFPV} = 100\ \bar{g}_{isl}^{MFPV}$.

T = temperature measured in Kelvin.

Table 6.7 lists the ILAW viscosity model terms and the coefficients used for the work in this report. This model and its coefficients are documented in the report by Feng et al.[(a)] The model contains 10 individual component terms that have not been normalized to sum to 100%. Predictions were made at temperatures of 1373.15 K (1100ºC) and 1423.15 K (1150ºC) using the model information from Table 6.7.

Table 6.7. ILAW Viscosity Model Terms and Coefficients

Model Term[(a)]	Coefficient[(b)]
Intercept[(c)]	0.3432956
Al_2O_3	0.0105322
B_2O_3	-0.047249
CaO	-0.119366
Fe_2O_3	-0.053445
Li_2O	0.0603101
MgO	-0.158343
Na_2O	-0.003678
SiO_2	-0.020776
TiO_2	-0.122854
ZrO_2	-0.17393
Al_2O_3/T^2 [(d)]	224313.69
B_2O_3/T^2	-12764.09
CaO/T^2	129948.51
Fe_2O_3/T^2	134632.13
Li_2O/T^2	-762155.4
MgO/T^2	235209.39
Na_2O/T^2	-139576.9
SiO_2/T^2	265772.15
TiO_2/T^2	176165.82
ZrO_2/T^2	536962.61

(a) Model terms use unnormalized wt% values of the ILAW oxide components.
(b) Viscosity is modeled in ln(poise).
(c) An intercept term is present in this model.
(d) T^2 is temperature squared, with temperature measured in Kelvin.

(a) Z Feng, F Perez-Carenas, H Gan, and IL Pegg. 2004. *Summary and Recommendations on Viscosity and Electrical Conductivity Model Forms to Support LAW Vitrification*. Letter Report VSL-03L4480-2 Rev. 0, Vitreous State Laboratory, The Catholic University of America, Washington DC.

6.2.3.3 Property-Composition Model for Electrical Conductivity of LAW Glasses

VSL[(a)] developed the property-composition model form for electrical conductivity used in this work for predicting the natural logarithm of electrical conductivity (S/cm) as a function of the ILAW composition and melt temperature. This model, as applied in this work, is in the general form

$$\hat{\tilde{y}}_i^{\varepsilon} = \hat{\ln}(\bar{\varepsilon}_i) = \sum_{k=1}^{n_{umc}^{\varepsilon 0}} b_k^{\varepsilon 0}\, \overline{w}_{ik}^{MFPV} + \sum_{t=1}^{n_{umc}^{\varepsilon 1}} b_t^{\varepsilon 1}\, \frac{\overline{w}_{it}^{MFPV}}{T} + Selected\left\{ \sum_{k=1}^{n_{umc}^{\varepsilon 3}-1} \sum_{l>k}^{n_{umc}^{\varepsilon 3}} b_{kl}^{\varepsilon 3}\, \overline{w}_{ik}^{MFPV}\, \overline{w}_{il}^{MFPV} \right\} \quad (6.2.11)$$

where

$\hat{\tilde{y}}_i^{\varepsilon}$ = $\hat{\ln}(\bar{\varepsilon}_i)$ = predicted natural logarithm of the electrical conductivity for ILAW corresponding to the i^{th} MFPV batch, based on averages over multiple samples from a CRV batch, analyses per CRV sample, and CRV and MFPV volume determinations [$\hat{\ln}$(S/cm) , where S denotes Siemens]

$n_{umc}^{\varepsilon 0}$ = number of unnormalized ILAW components used in the "linear component" terms of the electrical conductivity model. Note that the number of unnormalized ILAW components used in the model is less than the total number of unnormalized components varied in the data set used to develop the model per Feng et al.[(a)]

$n_{umc}^{\varepsilon 1}$ = number of unnormalized ILAW components used in the "linear component divided by temperature" terms of the electrical conductivity model

$n_{umc}^{\varepsilon 3}$ = number of crossproduct terms involving unnormalized ILAW components in the electrical conductivity model

$b_k^{\varepsilon 0}$, $b_t^{\varepsilon 1}$, $b_{kl}^{\varepsilon 3}$ = ILAW electrical conductivity model coefficients for terms involving ILAW components (indexed by *k*), components divided by temperature (indexed by *t*), and the selected crossproduct terms (indexed by *kl*). The coefficients were obtained by fitting the model form to a property-composition data set using least squares regression.[(a)]

$\overline{w}_{ik}^{MFPV}$ = wt% of the k^{th} ILAW component in the "linear component" portion of a property-composition model, where the composition is for the i^{th} ILAW MFPV batch. The wt% values are based on averages over multiple samples from a CRV batch, analyses per CRV sample, and CRV and MFPV volume

(a) Feng Z, F Perez-Carenas, H Gan, and IL Pegg. 2004. *Summary and Recommendations on Viscosity and Electrical Conductivity Model Forms to Support LAW Vitrification*. Letter Report VSL-03L4480-2 Rev. 0, Vitreous State Laboratory, The Catholic University of America, Washington DC.

determinations. These wt% values are not normalized to sum to 100% over the components in the model.

T = temperature measured in Kelvin.

In the preceding notation, a superscript of "ε1" was used for model terms involving a linear component divided by temperature, the same as in Section 6.1.4.5 for IHLW electrical conductivity. A superscript of "ε3" was used for model terms involving products of two components (called crossproducts). The superscript of "ε2" was not used for the latter because it was previously used in Section 6.1.4.5 for model terms involving a linear component divided by temperature squared.

Table 6.8 lists the ILAW electrical conductivity model terms and the coefficients used for the work in this report. This model and its coefficients are documented in the report by Feng et al.[(a)] The model contains 13 individual component terms plus an "Others" term. The "Others" term is calculated by subtracting the total weight percent of the 13 component terms from 100%. Predictions were made at temperatures of 1373.15 K (1100ºC) and 1473.15 K (1200ºC) using the model information from Table 6.8.

6.2.4 Equations Used to Summarize ILAW Monte Carlo Simulation Results

Monte Carlo simulations for ILAW resulted in 64 scenarios (see Table 5.4) for each of the five data sets, with each scenario consisting of 10 ILAW MFPV batches being simulated 200 different times. It is necessary to summarize these results so that insight can be provided. Summaries are necessary for the resulting ILAW mass-fraction compositions as well as the property values. For each scenario, the batch-to-batch variation, within-batch uncertainty, and the total variation and uncertainty were summarized using means and 90% ECIs of %RSDs. Appendix G provides a description of a 90% ECI.

The equations presented in this section to summarize the ILAW Monte Carlo simulation results have some differences compared to the corresponding equations for IHLW given in Section 6.1.5. These differences are a result of the differences between the mass-balance equations used to estimate chemical and radionuclide compositions (mass fractions) for IHLW [Eq. (6.1.1)] and ILAW [Eq. (6.2.1)]. In the IHLW case, it is possible using Eq. (6.1.1) to obtain separate estimates of IHLW compositions corresponding to the n_S^{MFPV} samples per IHLW MFPV batch. However, it is not possible from Eq. (6.2.1) to get separate estimates of ILAW composition in an ILAW MFPV batch corresponding to the n_S^{CRV} samples per LAW CRV batch. Rather, only one estimate of ILAW composition is obtained for each ILAW MFPV batch. This necessitates a different approach to estimate and summarize the %RSD values for batch-to-batch variation, within-batch uncertainty, and total variation plus uncertainty.

Table 6.8. ILAW Electrical Conductivity Model Terms and Coefficients

Model Term[(a)]	Coefficient[(b)]
Al_2O_3	0.0705891
B_2O_3	0.0749012
CaO	-0.0070485
Fe_2O_3	0.0914271
K_2O	0.0539981
Li_2O	0.0816487
MgO	0.1411494
Na_2O	-0.0084818
SiO_2	0.0282614
SO_3	-0.0581097
TiO_2	-0.0008896
ZnO	0.1941581
ZrO_2	0.1245877
Others[(c)]	0.070433
Al_2O_3/T[(d)]	-147.74897
B_2O_3/T	-115.21734
CaO/T	-230.3538
Fe_2O_3/T	-158.754
K_2O/T	-70.53136
Li_2O/T	238.48164
MgO/T	-228.43201
Na_2O/T	103.51038
SiO_2/T	-86.76398
SO_3/T	-42.37753
TiO_2/T	-26.17098
ZnO/T	-293.74087
ZrO_2/T	-230.1823
Others/T	-134.22455
CaO * Li_2O	0.0135449
CaO * Na_2O	0.0083639
Li_2O * Na_2O	-0.0114408

(a) Model terms use unnormalized wt% values of the IHLW oxide components.
(b) Electrical conductivity is modeled in ln(S/cm) where S denotes Siemens.
(c) Others (wt%) equals 100% minus the sum of the wt% values for the 13 main components in the model (those having linear terms).
(d) T is temperature measured in Kelvin.

The total variation and uncertainty (of an ILAW component or property) was calculated for each of the 200 simulations of each of the scenarios associated with a given LAW data set (waste type) using the equation

$$\%RSD_{T,pq} = \frac{100\,\mathrm{SD(Calculated\ Values)}}{\mathrm{Mean(Calculated\ Values)}} = \frac{100\sqrt{\dfrac{\sum_{r=1}^{n} y_{pqr}^2 - \dfrac{\left(\sum_{r=1}^{n} y_{pqr}\right)^2}{n}}{n-1}}}{\dfrac{\sum_{r=1}^{n} y_{pqr}}{n}} \qquad (6.2.12)$$

where

$\%RSD_{T,pq}$ = total %RSD (of an ILAW component or property) for the q^{th} simulation (1 of 200 simulations) of the p^{th} scenario (from the 64 scenarios in Table 5.4) for each of the five LAW data sets

y_{pqr} = ILAW component or property value calculated for the p^{th} scenario, the q^{th} simulation, and the r^{th} ILAW MFPV batch associated with an LAW data set

n = the number of batches (10 batches are analyzed in the results).

Equation (6.2.12) results in the total %RSD values for 200 simulation realizations (of each of the 64 scenarios for each of the five LAW data sets) for the mass fraction of each ILAW component and each ILAW property.

To summarize the $\%RSD_{T,pq}$ results for an ILAW component or property for each scenario associated with a given LAW data set (waste type), the mean and a 90% ECI are calculated. The mean is calculated using the equation

$$\overline{\%RSD_{T,p}} = \frac{\sum_{q=1}^{200} \%RSD_{T,pq}}{200} \qquad (6.2.13)$$

where

$\overline{\%RSD_{T,p}}$ = mean total %RSD (of an ILAW component or property) across the 200 simulations for the p^{th} scenario (from the 64 scenarios in Table 5.4) for each of five LAW data sets

$\%RSD_{T,pq}$ = total %RSD (of an ILAW component or property) for the q^{th} simulation (1 of 200 simulations) of the p^{th} scenario (from the 64 scenarios in Table 5.4) for each of five LAW data sets.

To calculate the 90% ECI for a specific ILAW component (mass fraction) or property, the 5th percentile and 95th percentile are calculated from the simulation values for that specific component or property. This is represented in the following equations

$$\%RSD_{T,p}^{90\%\ ELCL} = 5^{th} \text{ percentile from all 200 simulated } \%RSD_{T,pq} \text{ values for the } p^{th} \text{ scenario and a given LAW waste type} \quad (6.2.14a)$$

$$\%RSD_{T,p}^{90\%\ EUCL} = 95^{th} \text{ percentile from all 200 simulated } \%RSD_{T,pq} \text{ values for the } p^{th} \text{ scenario and a given LAW waste type} \quad (6.2.14b)$$

where

$\%RSD_{T,p}^{90\%\ ELCL}$ = ELCL for a 90% ECI on the total %RSD (of an ILAW component or property) for the p^{th} scenario (from the 64 scenarios in Table 5.4) for each of five LAW data sets

$\%RSD_{T,p}^{90\%\ EUCL}$ = EUCL for a 90% ECI on the total %RSD (of an ILAW component or property) for the p^{th} scenario (from the 64 scenarios in Table 5.4) for each of five LAW data sets

and $\%RSD_{T,pq}$ is as previously defined.

To isolate the batch-to-batch variation, a different set of test scenarios (called control scenarios, as in Table 5.5) were performed. These control scenarios set to zero all uncertainties associated with CRV sampling, CRV chemical and radiochemical analyses of samples, vessel volumes, GFC compositions, and GFC additions. Thus, only the batch-to-batch variation in CRV analyte concentrations was allowed to vary. There are 10 control scenarios, with batch-to-batch variation at low or high values for each of the five LAW data sets (waste types). The batch-to-batch variation ($\%RSD_B$) is calculated for each of the 10 control scenarios (with each scenario having 200 simulations) using the equation

$$\%RSD_{B,cq} = \frac{100\ \text{SD(Calculated Values)}}{\text{Mean(Calculated Values)}} = \frac{100\sqrt{\dfrac{\sum_{r=1}^{n} y_{cqr}^2 - \dfrac{\left(\sum_{r=1}^{n} y_{cqr}\right)^2}{n}}{n-1}}}{\dfrac{\sum_{r=1}^{n} y_{cqr}}{n}} \quad (6.2.15)$$

where

$\%RSD_{B,cq}$ = batch-to-batch %RSD (of an ILAW component or property) for the q^{th} simulation (1 of 200 simulations) of the c^{th} control scenario (from the 10 control scenarios in Table 5.5)

y_{cqr} = ILAW component or property value calculated for the c^{th} control scenario, the q^{th} simulation, and the r^{th} ILAW MFPV batch

n = the number of batches (10 batches are analyzed in the results).

Equation (6.2.15) results in the batch-to-batch %RSD values for 200 simulation realizations of each of 10 control scenarios for the mass fraction of each ILAW component and each ILAW property.

To summarize the $\%RSD_{B,cq}$ results for an ILAW component or property for each control scenario, the mean and a 90% ECI are calculated. The mean is calculated using the equation

$$\overline{\%RSD_{B,c}} = \frac{\sum_{q=1}^{200} \%RSD_{B,cq}}{200} \tag{6.2.16}$$

where

$\overline{\%RSD_{B,c}}$ = mean batch-to-batch %RSD (of an ILAW component or property) across the 200 simulations for the c^{th} control scenario (from the 10 control scenarios in Table 5.5)

$\%RSD_{B,cq}$ = batch-to-batch %RSD (of an ILAW component or property) for the q^{th} simulation (1 of 200 simulations) of the c^{th} control scenario (from the 10 control scenarios in Table 5.5).

The 90% ECI is given by

$$\%RSD_{B,c}^{90\%\ ELCL} = 5^{th} \text{ percentile from all 200 simulated } \%RSD_{B,cq} \text{ values for the } c^{th} \text{ control scenario and a given LAW waste type} \tag{6.2.17a}$$

$$\%RSD_{B,c}^{90\%\ EUCL} = 95^{th} \text{ percentile from all 200 simulated } \%RSD_{B,cq} \text{ values for the } c^{th} \text{ control scenario and a given LAW waste type} \tag{6.2.17b}$$

where

$\%RSD_{B,c}^{90\%\ ELCL}$ = ELCL for a 90% ECI on the batch-to-batch %RSD (of an ILAW component or property) for the c^{th} control scenario (from the 10 control scenarios in Table 5.5)

$\%RSD_{B,c}^{90\%\ EUCL}$ = EUCL for a 90% ECI on the batch-to-batch %RSD (of an ILAW component or property) for the c^{th} scenario (from the 10 control scenarios in Table 5.5)

and $\%RSD_{B,cq}$ is as previously defined.

Although batch-to-batch variation was only calculated for 10 control scenarios, these 10 control scenarios can be mapped to the original 64 scenarios for each of the five data sets so that each scenario has a total variation estimate (the mean) and confidence interval and a batch-to-batch variation estimate (the mean) and confidence interval. The 10 control scenarios correspond to all five data sets (LAW waste types) with low- and high-case values for the random batch-to-batch variation component of the simulation. This means that the results from the first control scenario map to the first 32 scenarios for a first data set, the second control scenario results map to the next 32 scenarios for the first data set, the third control scenario results map to the first 32 scenarios for the second data set, and so forth.

This mapping is important to consider when calculating the within-batch uncertainty. Because the total variation is equal to the batch-to-batch variation plus the within-batch uncertainty, the within-batch uncertainty can be calculated by subtracting the batch-to-batch variation from the total variation. This can only be done when converting the variations into statistical variances or squared %RSDs. The following equation shows the proper way to calculate the within-batch uncertainty %RSD for each scenario associated with a given LAW data set (waste type).

$$\%RSD_{W,pq} = \sqrt{(\%RSD_{T,pq})^2 - (\%RSD_{B,pq})^2} \tag{6.2.18}$$

where

$\%RSD_{W,pq}$ = within-batch uncertainty %RSD (of an ILAW component or property) for the q^{th} simulation (1 of 200 simulations) for the p^{th} scenario (from the 64 scenarios in Table 5.4) for each of five LAW data sets

$\%RSD_{T,pq}$ = total variation plus uncertainty %RSD (of an ILAW component or property) for the q^{th} simulation (1 of 200 simulations) of the p^{th} scenario (from the 64 scenarios in Table 5.4) for each of five data sets

$\%RSD_{B,pq}$ = batch-to-batch variation %RSD (of an ILAW component or property) for the q^{th} simulation (1 of 200 simulations) of the p^{th} scenario (from the 64 scenarios in Table 5.4) for each of five data sets.

Note in all cases above that the p^{th} scenario is the one that correctly maps from the corresponding control scenario. Equation (6.2.18) results in the within-batch uncertainty %RSD values for 200 simulation realizations of 64 scenarios for each of five LAW data sets for the mass fraction of each ILAW component and each ILAW property.

To summarize the $\%RSD_{W,pq}$ results for an ILAW component or property for each scenario associated with an LAW data set (waste type), the mean and an empirical confidence interval are calculated for the within-batch uncertainty %RSD of each scenario. The mean is calculated using the equation

$$\overline{\%RSD_{W,p}} = \frac{\sum_{q=1}^{200} \%RSD_{W,pq}}{200} \tag{6.2.19}$$

where

$\overline{\%RSD_{W,p}}$ = mean within-batch uncertainty %RSD (of an ILAW component or property) across the 200 simulations for the p^{th} scenario (from the 64 scenarios in Table 5.4) for each of five LAW data sets

$\%RSD_{W,pq}$ = within-batch uncertainty %RSD (of an ILAW component or property) for the q^{th} simulation (1 of 200 simulations) of the p^{th} scenario (from the 64 scenarios in Table 5.4) for each of five LAW data sets.

The 90% ECI is given by

$$\%RSD_{W,p}^{90\%\ ELCL} = 5^{th} \text{ percentile from all 200 simulated } \%RSD_{W,pq} \text{ values for the } p^{th} \text{ scenario and a given LAW waste type} \tag{6.2.20a}$$

$$\%RSD_{W,p}^{90\%\ EUCL} = 95^{th} \text{ percentile from all 200 simulated } \%RSD_{W,pq} \text{ values for the } p^{th} \text{ scenario and a given LAW waste type} \tag{6.2.20b}$$

where

$\%RSD_{W,p}^{90\%\ ELCL}$ = ELCL for a 90% ECI on the within-batch uncertainty %RSD (of an ILAW component or property) for the p^{th} scenario (from the 64 scenarios in Table 5.4) for each of five LAW data sets

$\%RSD_{W,p}^{90\%\ EUCL}$ = EUCL for a 90% ECI on the within-batch uncertainty %RSD (of an ILAW component or property) for the p^{th} scenario (from the 64 scenarios in Table 5.4) for each of five LAW data sets

and $\%RSD_{W,pq}$ is as previously defined.

In summary, the equations in this section provide for calculating the means and 90% ECIs for values of total variation and uncertainty ($\%RSD_{T,pq}$), batch-to-batch variation ($\%RSD_{B,pq}$), and within-batch uncertainty ($\%RSD_{W,pq}$). These means and 90% ECIs were calculated for each ILAW component (mass fraction) and property. Section 8 presents and discusses the ILAW results where for simplicity of notation, $\%RSD_T = \%RSD_{T,pq}$, $\%RSD_B = \%RSD_{B,pq}$, and $\%RSD_W = \%RSD_{W,pq}$.

7.0 Results on the Variations and Uncertainties of IHLW Composition and Properties

This section describes the results of implementing the statistical methodology described in Section 6.1 to the Monte Carlo simulated data for 200 simulations of 12 scenarios with 18 IHLW MFPV batches for each of four HLW waste types. The 12 scenarios are combinations of low, medium, and high estimates of batch-to-batch variations as well as low and high estimates of within-batch uncertainties. This implementation includes calculating and summarizing the variations and uncertainties associated with IHLW chemical and radionuclide compositions (expressed in mass fractions of glass components) as well as IHLW properties of interest.

The uncertainties in IHLW compositions and properties reported in this section incorporate averages over the eight replicate samples (with one analysis each) per IHLW MFPV batch used in this work based on the current WTP sampling and analysis plan for the IHLW facility. The values of uncertainties (i.e., %RSDs) without the averaging over the eight samples would be $\sqrt{8} = 2.828$ times larger. Also, because of the number of scenarios (12) investigated for each of the HLW tanks (waste types), in this section, variation and uncertainty results are presented for the low-case (all variations and uncertainties at their low estimates) and the high-case (all variations and uncertainties at their high estimates) scenarios. Presenting the results in this way provides information on the lowest and highest possible variation and uncertainty in IHLW compositions and properties. Results for other IHLW scenarios (i.e., combinations of the variation and uncertainty factors) investigated are presented in Appendix E.

Section 7.1 discusses the results of calculating IHLW compositions corresponding to MFPV batches and calculating and summarizing the %RSDs for batch-to-batch variations, within-batch uncertainties, and total variations plus uncertainties for important IHLW chemical composition components. Section 7.1 also discusses the factors that most affect the total %RSD for each of the important IHLW chemical composition components. Section 7.2 discusses the results of calculating IHLW radionuclide compositions corresponding to MFPV batches and calculating and summarizing the %RSDs for batch-to-batch variations, within-batch uncertainties, and total variations plus uncertainties of important IHLW radionuclide composition components. Section 7.2 also discusses the factors that most affect the total %RSD for each of the important IHLW radionuclide composition components. Section 7.3 discusses the results of calculating and summarizing the %RSDs for batch-to-batch variations, within-batch uncertainties, and total variations plus uncertainties of the IHLW properties of interest, which include PCT (B, Li, and Na releases), TCLP Cd release, $T_{1\%}$, viscosity, and electrical conductivity.

7.1 Results on the Variations and Uncertainties of IHLW Chemical Composition

The variations and uncertainties affecting the IHLW vitrification process (see Table 5.1) were applied to the IHLW mass-balance equations using Monte Carlo simulation. Low, medium, and high cases were studied for MFPV random batch-to-batch %RSD ($\%RSD_B(c_j^{MFPV})$). Low and high cases were studied for each of the following uncertainties within the HLW vitrification process: MFPV mixing/sampling %RSD ($\%RSD_S(c_j^{MFPV})$) and MFPV analytical %RSD ($\%RSD_A(c_j^{MFPV})$). Data were simulated for

eight samples per IHLW MFPV batch with one analysis per sample. IHLW chemical compositions corresponding to MFPV batches were calculated for all glass components and for each of the four waste types using Eq. (6.1.1).

The %RSD values for batch-to-batch variations ($\%RSD_B$) within-batch uncertainties ($\%RSD_W$) were calculated by variance component analysis (see Section 6.1.5) for each of the IHLW chemical composition components across 18 MFPV batches and 8 samples per batch. Values of $\%RSD_B$ and $\%RSD_W$ were calculated for each of four HLW waste types (AY-102, AZ-102, C-104, and the AY-102 to AZ-102 transition) for each scenario in Table 5.2 and each of the 200 simulations within each scenario using Eqs. (6.1.15), and (6.1.16). Total variations plus uncertainties ($\%RSD_T$) were then calculated for each case using Eq. (6.1.17). The $\%RSD_T$, $\%RSD_B$, and $\%RSD_W$ values were then summarized for each of the 12 scenarios and each of the four HLW waste types (48 combinations) by calculating the mean and the lower and upper 90% ECIs from the 200 simulations for each combination. The $\%RSD_T$ summaries were calculated using Eqs. (6.1.18), (6.1.19a), and (6.1.19b). The $\%RSD_B$ summaries were calculated using Eqs. (6.1.20), (6.1.21a), and (6.1.21b). The $\%RSD_W$ summaries were calculated using Eqs. (6.1.21), (6.1.23a), and (6.1.23b).

Figure 7.1 summarizes the $\%RSD_T$ results for each of the important chemical composition components in IHLW corresponding to MFPV batches. The four different colors on the plot represent the four HLW waste types as defined in Table 5.1. The solid lines represent the 90% ECIs calculated using Eqs. (6.1.19a) and (6.1.19b) for the scenario with all uncertainties set to the low case (Scenario # 1 in Table 5.2). The dashed lines represent the 90% ECIs for the scenario with all uncertainties set to the high case (Scenario # 12 in Table 5.2). The solid square and the open circle represent the $\overline{\%RSD_T}$ values calculated using Eq. (6.1.18) for the scenario with all uncertainties at the low case and for the scenario with all uncertainties at the high case, respectively. Figure 7.2 through Figure 7.11 (discussed subsequently) use the same schema for identifying the four waste types, the low- and high-case 90% ECIs, and the mean %RSD values for the low and high case.

Figure 7.2 and Figure 7.3, respectively, summarize the $\%RSD_B$ and the $\%RSD_W$ results for each of the important chemical composition components in IHLW corresponding to MFPV batches. As expected, the high-case 90% ECIs (dashed lines) indicate a larger amount of variation than the low-case 90% ECIs (solid lines) for $\%RSD_T$ and $\%RSD_W$. The difference between the high-case 90% ECIs and low-case 90% ECIs is smaller for $\%RSD_B$ because the batch-to-batch variation does not include any of the MFPV mixing/sampling and analytical uncertainties. The batch-to-batch variation is generally larger for the transition waste type (from AY-102 to AZ-102), most notably for those IHLW chemical composition components with the most difference in values between AY-102 and AZ-102.

Figure 7.1 shows that most IHLW chemical compositions components (mass fractions) have $\%RSD_T$ values less than 5 to 10% for the low case, and less than 10 to 15% for the high case. Figure 7.2 and Figure 7.3 show that $\%RSD_B$ and $\%RSD_W$ values for most IHLW components are each less than 5% for the low case and less than 10% for the high case. Recall [per Eq. (6.1.14)] that the $\%RSD_W$ values, and hence the $\%RSD_T$ values, are reduced by averaging over the eight samples per IHLW MFPV batch.

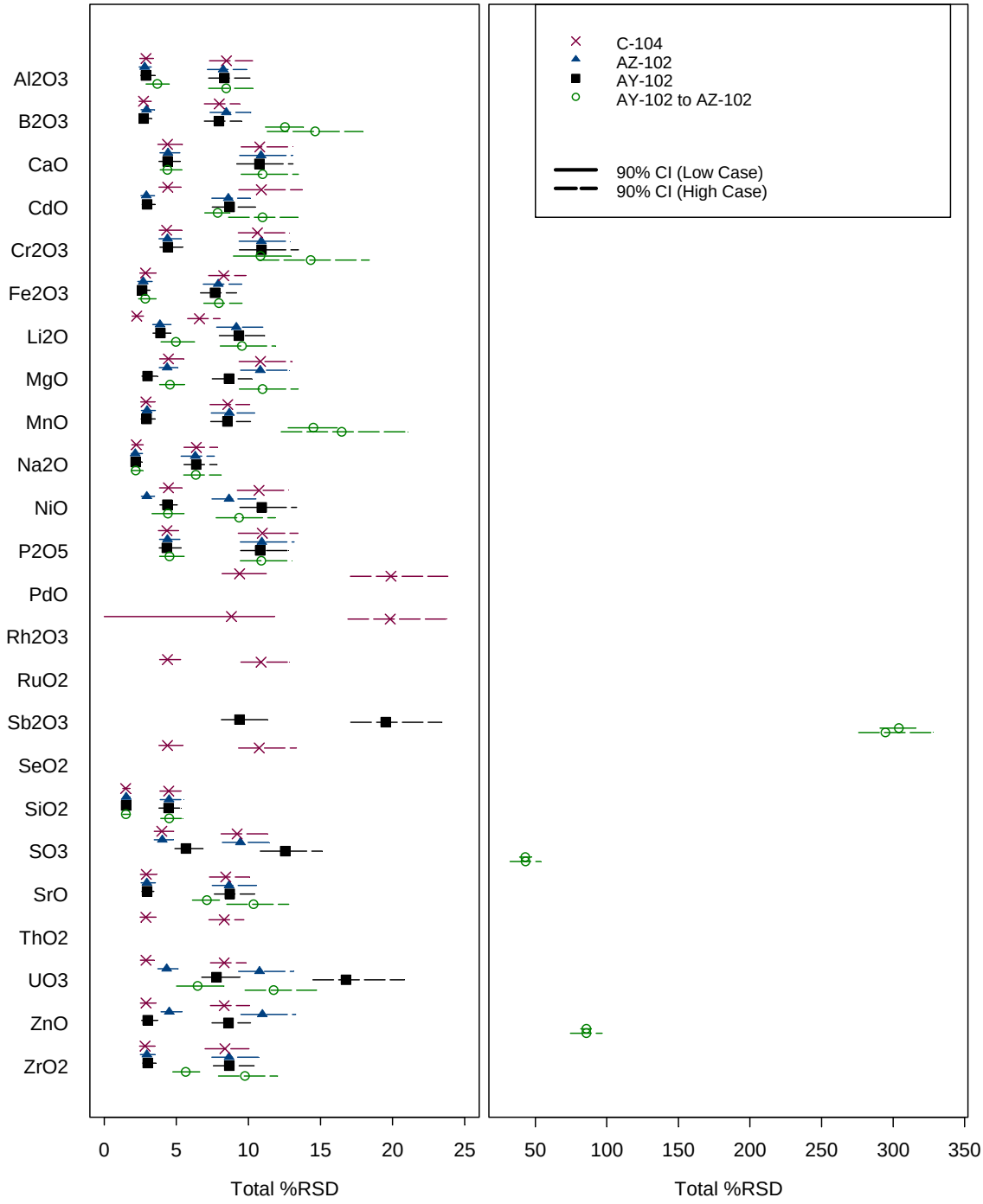

Figure 7.1. Means (the symbols) and 90% ECIs (lines) of Total %RSD Calculated from IHLW Simulations for Four Waste Types (differences in color) with All Uncertainties Set to the Low Cases (solid lines) and All Uncertainties Set to the High Cases (dashed lines) for Important IHLW Chemical Composition Components. Note that two different scales were used on the x-axis to better view the smaller %RSD values.

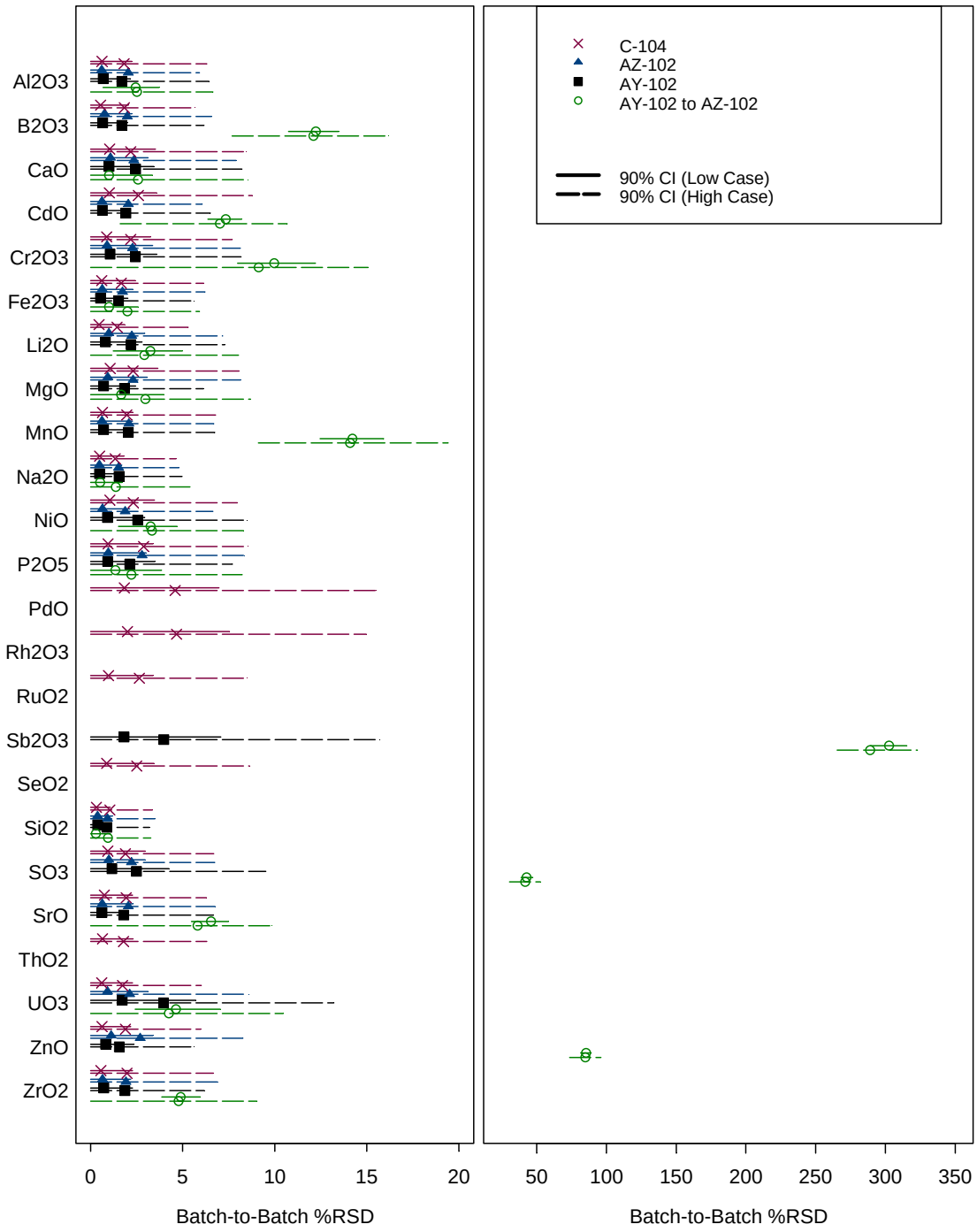

Figure 7.2. Means (the symbols) and 90% ECIs (lines) of Batch-to-Batch %RSDs Calculated from IHLW Simulations for Four Waste Types (differences in color) with All Uncertainties Set to the Low Cases (solid lines) and All Uncertainties Set to the High Cases (dashed lines) for Important IHLW Chemical Composition Components. Note that two different scales were used on the x-axis to better view the smaller %RSD values.

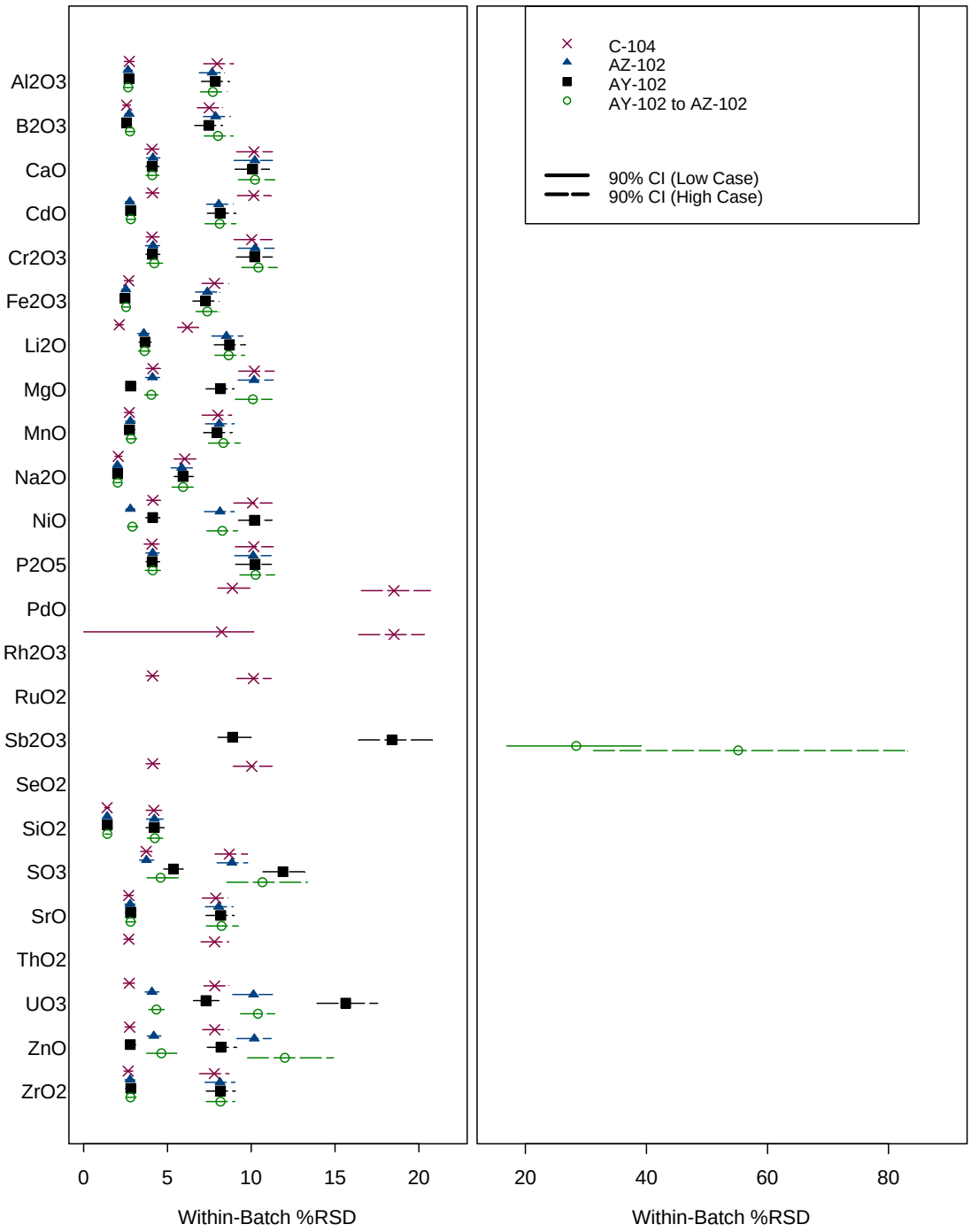

Figure 7.3. Means (the symbols) and 90% ECIs (lines) of Within-Batch %RSDs Calculated from IHLW Simulations for Four Waste Types (differences in color) with All Uncertainties Set to the Low Cases (solid lines) and All Uncertainties Set to the High Cases (dashed lines) for Important IHLW Chemical Composition Components. Note that two different scales were used on the x-axis to better view the smaller %RSD values.

Thus, the reduced $\%RSD_W$ values are roughly equal contributors with the $\%RSD_B$ values to the $\%RSD_T$ values. However, the variability in $\%RSD_W$ results is much less than the variability in $\%RSD_B$ results, as indicated by the widths of the 90% ECIs in Figure 7.3 and Figure 7.2, respectively.

It is interesting to note that for the transition waste type, Sb_2O_3 has the largest %RSDs for batch-to-batch variation (shown in Figure 7.2), within-batch uncertainty (shown in Figure 7.3), and total variation plus uncertainty (shown in Figure 7.1) of the chemical composition components shown. One reason for this is that Sb occurs at a relatively small concentration in AY-102 and does not occur at all in AZ-102. Another reason is that mass fractions of minor components can have large variation and uncertainty as a result of their own variation and uncertainty as well as that of major components. The components SO_3 and ZnO also have large %RSD values for batch-to-batch variation and total variation plus uncertainty for the transition waste type, although not as large as Sb_2O_5. The components SO_3 and ZnO each occur at relatively higher concentrations in AY-102 compared to AZ-102, thus leading to larger %RSD values of batch-to-batch variation. The rest of the chemical composition components shown in Figure 7.1 through Figure 7.3 have %RSDs values that are compatible with the variation and uncertainty levels used for the simulations.

The Monte Carlo simulation data were also analyzed using analysis of variance (ANOVA) to determine which factors, and two-factor interactions between the factors, had significant effects on the mean total variation plus uncertainties ($\overline{\%RSD_T}$) values obtained from the 12 scenarios for each of the four HLW waste types. The factors investigated in the ANOVA are HLW waste type, IHLW MFPV batch-to-batch %RSD ($\%RSD_B(c_j^{MFPV})$), IHLW MFPV mixing/sampling %RSD ($\%RSD_S(c_j^{MFPV})$), and IHLW MFPV analytical %RSD ($\%RSD_A(c_j^{MFPV})$). An ANOVA was performed for each of the important IHLW chemical composition components (see Table 2.2). Table 7.1 summarizes the results from the ANOVAs for IHLW chemical composition components. This table summarizes the percentage of chemical composition components (oxides or halogens) for which each factor and two-factor interaction was statistically significant. The factors and interactions are listed in the table in decreasing order of the percentage of components that were statistically significant.

From Table 7.1, it can be seen that the mixing/sampling and the analytical sources of uncertainty (and their interaction) significantly affect the %RSD results for high percentages of the important IHLW components. The "batch-to-batch variation" and "HLW waste type" factors also affected the results for a higher percentage of IHLW components. Thus, the main conclusion from these ANOVA results is that the values of total %RSD for IHLW chemical composition components can vary substantially, depending on the HLW waste type as well as the magnitudes of the batch-to-batch variation %RSD, mixing/sampling uncertainty %RSD, and analytical uncertainty %RSD for concentrations of analytes in the IHLW MFPV.

Table 7.1. Percentage of Important IHLW Chemical Composition Components for which the Factor or Interaction had a Statistically Significant Effect on Total %RSD in the ANOVAs ($\alpha = 0.05$)[(a)]

Factor / Interaction	% of Significant Components	Statistically Significant Important IHLW Chemical Composition Components
$\%RSD_A(c_j^{MFPV})$ [(b)]	100	All
$\%RSD_S(c_j^{MFPV})$ [(b)]	95.8	Al_2O_3, B_2O_3, CaO, CdO, Cr_2O_3, Fe_2O_3, Li_2O, MgO, MnO, Na_2O, NiO, P_2O_5, PdO, Rh_2O_3, RuO_2, SeO_2, SiO_2, SO_3, SrO, ThO_2, UO_3, ZnO, ZrO_2
$\%RSD_B(c_j^{MFPV})$ [(c)]	87.5	Al_2O_3, B_2O_3, CaO, CdO, Cr_2O_3, Fe_2O_3, Li_2O, MgO, MnO, Na_2O, NiO, P_2O_5, RuO_2, SeO_2, SiO_2, SO_3, SrO, ThO_2, UO_3, ZnO, ZrO_2
$\%RSD_S(c_j^{MFPV}) \times \%RSD_A(c_j^{MFPV})$	83.3	Al_2O_3, B_2O_3, CaO, CdO, Cr_2O_3, Fe_2O_3, Li_2O, MgO, MnO, Na_2O, NiO, P_2O_5, Rh_2O_3, RuO_2, SeO_2, SiO_2, SrO, ThO_2, UO_3, ZrO_2
Waste Type	75	Al_2O_3, B_2O_3, CdO, Cr_2O_3, Fe_2O_3, Li_2O, MgO, MnO, Na_2O, NiO, P_2O_5, Sb_2O_3, SiO_2, SO_3, SrO, UO_3, ZnO, ZrO_2
$\%RSD_B(c_j^{MFPV}) \times \%RSD_S(c_j^{MFPV})$	62.5	Al_2O_3, B_2O_3, CaO, CdO, Fe_2O_3, Li_2O, MgO, MnO, Na_2O, NiO, P_2O_5, SiO_2, SrO, ZnO, ZrO_2
Waste Type $\times$ $\%RSD_A(c_j^{MFPV})$	58.3	Al_2O_3, B_2O_3, CdO, Cr_2O_3, Li_2O, MgO, MnO, NiO, Sb_2O_3, SO_3, SrO, UO_3, ZnO, ZrO_2
Waste Type $\times$ $\%RSD_S(c_j^{MFPV})$	54.2	Al_2O_3, B_2O_3, CdO, Cr_2O_3, Fe_2O_3, Li_2O, MgO, MnO, NiO, SrO, UO_3, ZnO, ZrO_2
$\%RSD_B(c_j^{MFPV}) \times \%RSD_A(c_j^{MFPV})$	54.2	Al_2O_3, CaO, Cr_2O_3, Fe_2O_3, Li_2O, MgO, Na_2O, NiO, P_2O_5, SeO_2, SiO_2, SrO, UO_3, ZnO
Waste Type $\times$ $\%RSD_B(c_j^{MFPV})$	37.5	Al_2O_3, B_2O_3, CdO, Li_2O, MnO, SrO, UO_3, ZnO, ZrO_2

(a) Only two-factor interactions were included in the ANOVA model.
(b) This factor has a "low" case and a "high" case.
(c) This factor has a "low" case, "medium" case, and a "high" case.

7.2 Results on the Variations and Uncertainties of IHLW Radionuclide Composition

The %RSD values for batch-to-batch variations ($\%RSD_B$), within-batch uncertainties ($\%RSD_W$), and total variations plus uncertainties ($\%RSD_T$) were calculated for each of the IHLW radionuclide composition components across 18 MFPV batches for each of the four HLW waste types, for each scenario in Table 5.2, and for each of the 200 simulations within each scenario. The same process and equations used for IHLW chemical composition components (see the first two paragraphs of Section 7.1) were also used for IHLW radionuclide composition components.

Figure 7.4 summarizes the $\%RSD_T$ results for each of the important radionuclide composition components in IHLW corresponding to MFPV batches. Figure 7.5 and Figure 7.6, respectively, show the summary results of the $\%RSD_B$ and $\%RSD_W$ for each of the important radionuclide composition components in IHLW corresponding to MFPV batches. Because each of the four waste types did not contain every radionuclide (see tables in Appendix C), some radionuclides in the figures do not have four sets of plotting symbols (representing the means) and lines (representing the 90% ECIs). As expected, the high-case 90% ECIs (dashed lines) indicate a larger amount of variation and uncertainty than the low-case 90% ECIs (solid lines) for $\%RSD_T$ and $\%RSD_W$.

Figure 7.4 shows that most IHLW radionuclide composition components (mass fractions) have $\%RSD_T$ values less than 10% for the low case, and less than 20% for the high case. Figure 7.5 shows that $\%RSD_B$ values for most IHLW components are less than 10% for the low and high cases. Figure 7.6 shows that $\%RSD_W$ values are generally less than 10% for the low case and less than 20% for the high case. Recall [per Eq. (6.1.14)] that the $\%RSD_W$ values, and hence the $\%RSD_T$ values, are reduced by averaging over the 8 samples per IHLW MFPV batch. Thus, the reduced $\%RSD_W$ values contribute slightly more to the $\%RSD_T$ values than do the $\%RSD_B$ values, despite the reduction in $\%RSD_W$ resulting from averaging over 8 samples per IHLW MFPV batch. Finally, the variability in $\%RSD_W$ results is less than the variability in $\%RSD_B$ results, as indicated by the widths of the 90% ECIs in Figure 7.6 and Figure 7.5, respectively.

For the radionuclide oxides shown in Figure 7.4 through Figure 7.6, a few cases stand out as having %RSDs much larger than the rest. Although it is true that some radionuclides have nominal variation and uncertainty levels that are much higher than those for non-radionuclides (^{242}Cm for waste type C-104, for example, has a maximum 120% RSD nominal analytical uncertainty), this alone does not completely explain the large %RSD values for this and a few other radionuclide oxides shown in Figure 7.4 through Figure 7.6. The complete explanation lies in a combination of high nominal variation and uncertainty values and a nominal mean concentration very close to zero (the simulation code used in this work truncates simulated concentrations at zero when the added disturbance produces negative simulated concentration values). For the rest of the radionuclides, the %RSDs shown in Figure 7.4 through Figure 7.6 are well within the values that can be expected from the simulation model and the values chosen for the variation and uncertainty factors.

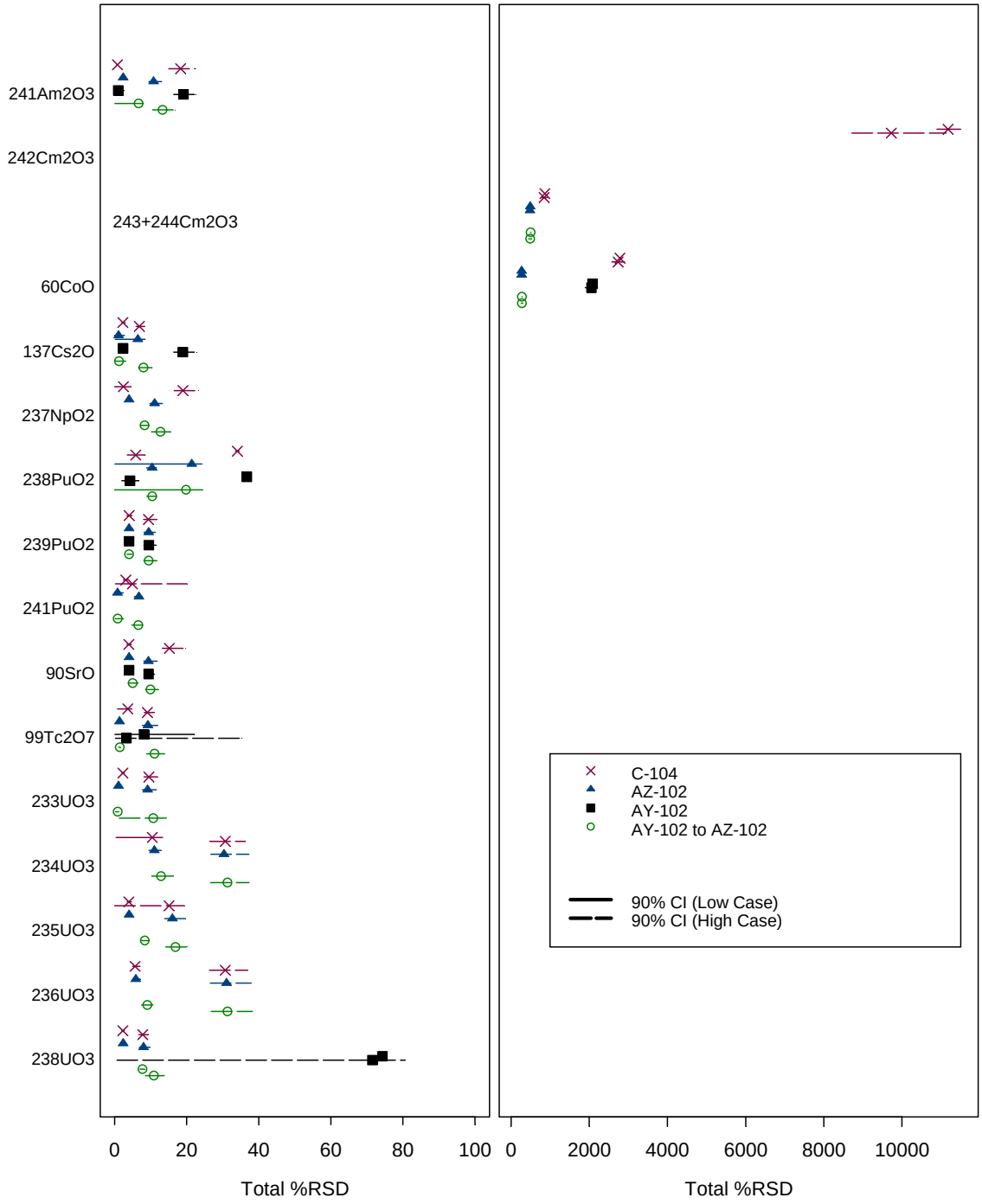

Figure 7.4. Means (the symbols) and 90% ECIs (lines) of Total %RSD Calculated from IHLW Simulations for Four Waste Types (differences in color) with All Uncertainties Set to the Low Cases (solid lines) and All Uncertainties Set to the High Cases (dashed lines) for Important IHLW Radionuclides. Note that two different scales were used on the x-axis to better view the smaller %RSD values.

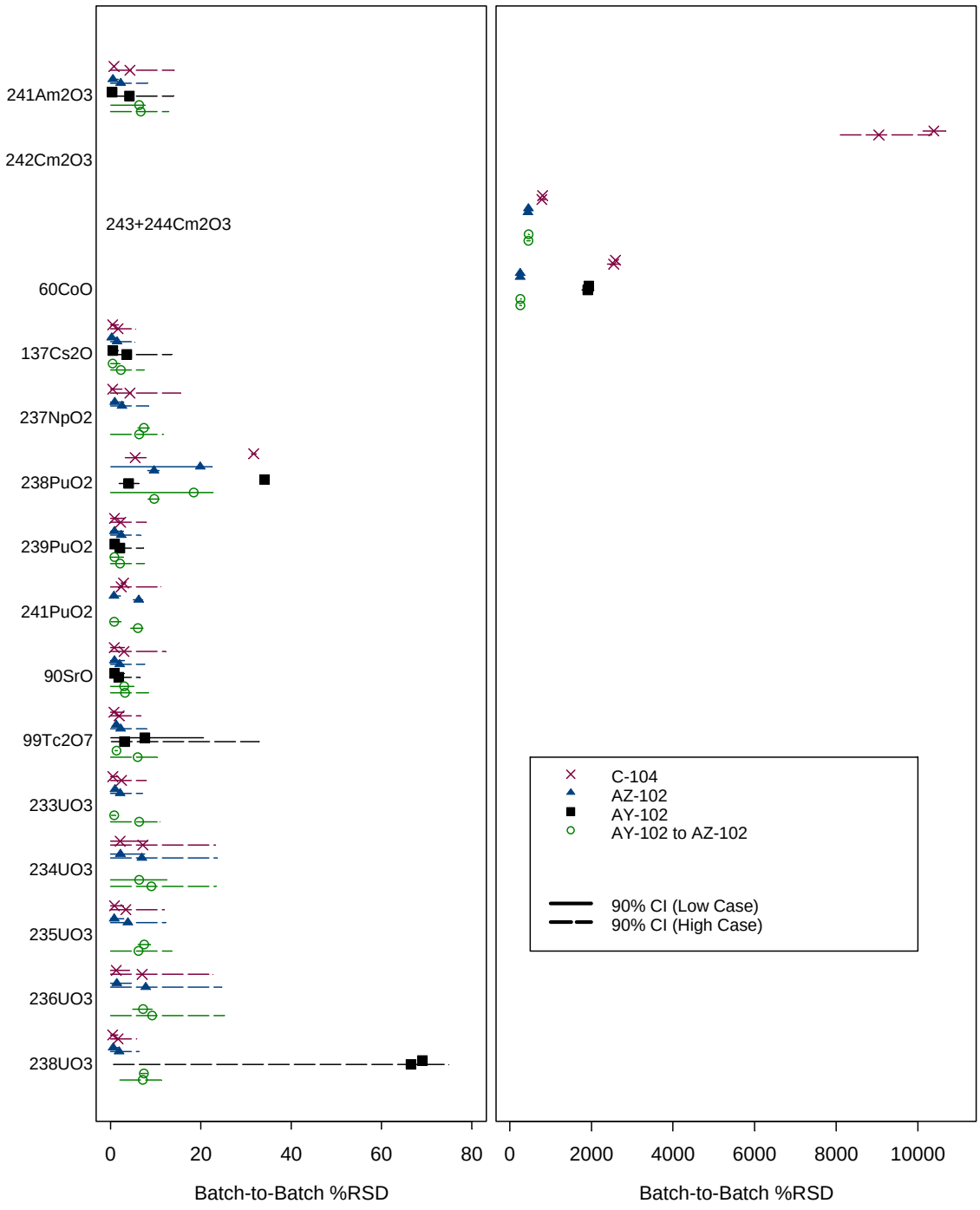

Figure 7.5. Means (the symbols) and 90% ECIs (lines) of Batch-to-Batch %RSDs Calculated from IHLW Simulations for Four Waste Types (differences in color) with All Uncertainties Set to the Low Cases (solid lines) and All Uncertainties Set to the High Cases (dashed lines) for Important IHLW Radionuclides. Note that two different scales were used on the x-axis to better view the smaller %RSD values.

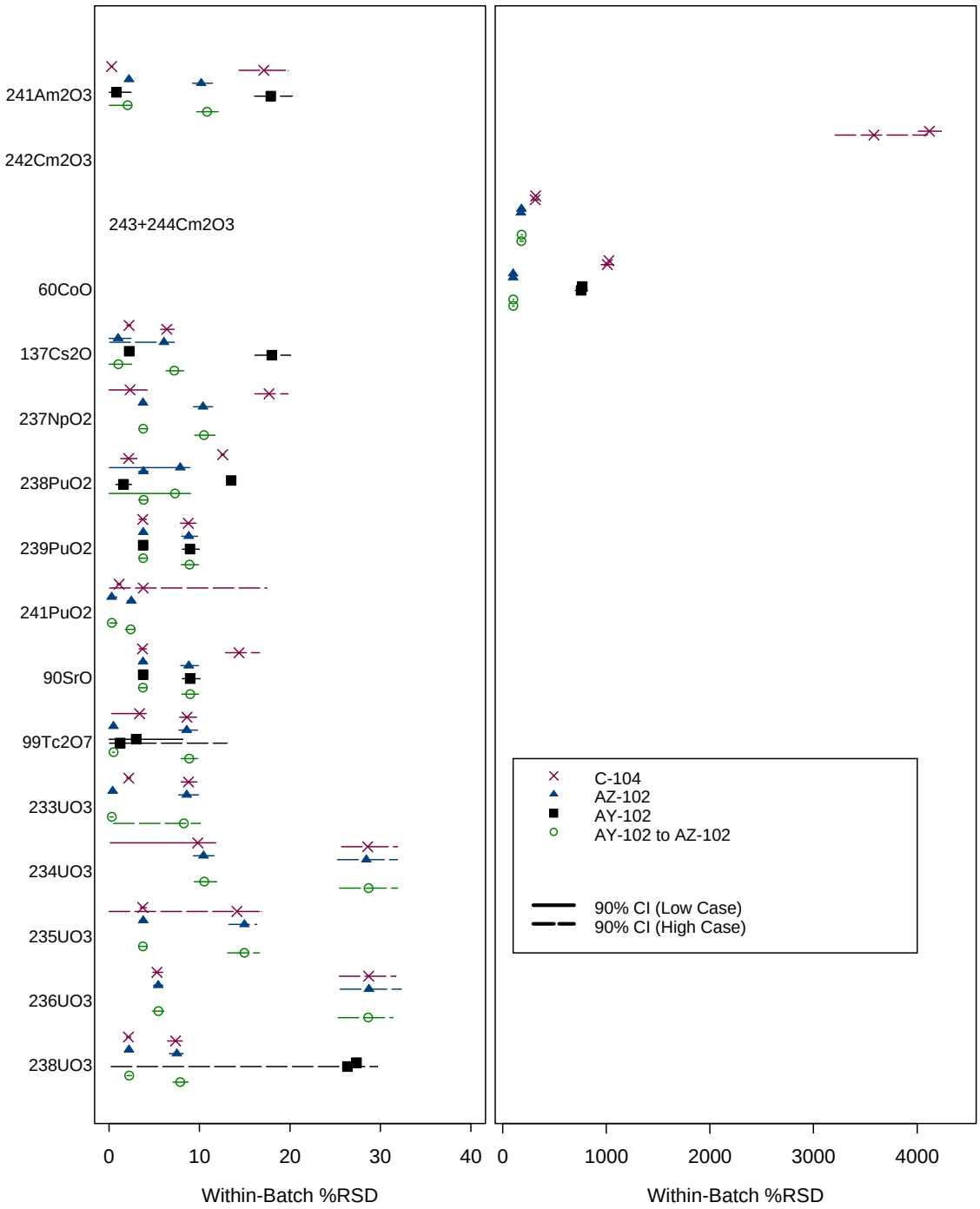

Figure 7.6. Means (the symbols) and 90% ECIs (lines) of Within-Batch %RSDs Calculated from IHLW Simulations for Four Waste Types (differences in color) with All Uncertainties Set to the Low Cases (solid lines) and All Uncertainties Set to the High Cases (dashed lines) for Important IHLW Radionuclides. Note that two different scales were used on the x-axis to better view the smaller %RSD values.

The Monte Carlo simulation data were also analyzed using ANOVA to determine which factors, and two-factor interactions between the factors, had significant effects on the mean total variation plus uncertainties ($\overline{\%RSD_T}$) obtained from the 12 scenarios for each of the four HLW waste types. The factors are the same as identified in Section 7.1. An ANOVA was performed for each of the important IHLW radionuclide composition components (Table 2.1) present in a given HLW waste type. Table 7.2 summarizes results from the ANOVAs for IHLW radionuclide composition components. This table summarizes the percentage of radionuclide composition components for which each factor and two-factor interaction was statistically significant. The factors and interactions are listed in the table in decreasing order of the percentage of radionuclides that were statistically significant.

From Table 7.2, it can be seen that four of the five effects with the highest percentage of radionuclide composition components significantly affected are main effects (analytical uncertainty, sampling uncertainty, waste type, and batch-to-batch variation) with the fifth one being the interaction between waste type and analytical uncertainty. Because analytical uncertainty is often the largest single source of

Table 7.2. Percentage of Important IHLW Radionuclide Composition Components for which the Factor or Interaction had a Statistically Significant Effect on Total %RSD in the ANOVAs ($\alpha = 0.05$)[a]

Factor / Interaction	% of Significant Components	Statistically Significant Important IHLW Radionuclide Composition Components
$\%RSD_A(c_j^{MFPV})$ [b]	100	All
$\%RSD_S(c_j^{MFPV})$ [b]	93.8	$^{241}Am_2O_3$, $^{242}Cm_2O_3$, $^{243+244}Cm_2O_3$, ^{60}CoO, $^{137}Cs_2O$, $^{237}NpO_2$, $^{238}PuO_2$, $^{239}PuO_2$, $^{241}PuO_2$, ^{90}SrO, $^{99}Tc_2O_7$, $^{233}UO_3$, $^{234}UO_3$, $^{235}UO_3$, $^{236}UO_3$
Waste Type	93.8	$^{241}Am_2O_3$, $^{243+244}Cm_2O_3$, ^{60}CoO, $^{137}Cs_2O$, $^{237}NpO_2$, $^{238}PuO_2$, $^{239}PuO_2$, $^{241}PuO_2$, ^{90}SrO, $^{99}Tc_2O_7$, $^{233}UO_3$, $^{234}UO_3$, $^{235}UO_3$, $^{236}UO_3$, $^{238}UO_3$
$\%RSD_B(c_j^{MFPV})$ [c]	87.5	$^{241}Am_2O_3$, $^{242}Cm_2O_3$, ^{60}CoO, $^{137}Cs_2O$, $^{237}NpO_2$, $^{238}PuO_2$, $^{239}PuO_2$, ^{90}SrO, $^{99}Tc_2O_7$, $^{233}UO_3$, $^{234}UO_3$, $^{235}UO_3$, $^{236}UO_3$, $^{238}UO_3$
Waste Type × $\%RSD_A(c_j^{MFPV})$	75	$^{241}Am_2O_3$, $^{243+244}Cm_2O_3$, ^{60}CoO, $^{137}Cs_2O$, $^{237}NpO_2$, $^{238}PuO_2$, ^{90}SrO, $^{233}UO_3$, $^{234}UO_3$, $^{235}UO_3$, $^{236}UO_3$, $^{238}UO_3$
$\%RSD_B(c_j^{MFPV})$ × $\%RSD_A(c_j^{MFPV})$	56.3	$^{241}Am_2O_3$, $^{242}Cm_2O_3$, $^{137}Cs_2O$, $^{237}NpO_2$, $^{238}PuO_2$, $^{239}PuO_2$, $^{241}PuO_2$, $^{234}UO_3$, $^{235}UO_3$
$\%RSD_S(c_j^{MFPV})$ × $\%RSD_A(c_j^{MFPV})$	56.3	$^{241}Am_2O_3$, $^{243+244}Cm_2O_3$, $^{137}Cs_2O$, $^{237}NpO_2$, $^{238}PuO_2$, $^{239}PuO_2$, $^{241}PuO_2$, $^{235}UO_3$, $^{236}UO_3$
Waste Type × $\%RSD_S(c_j^{MFPV})$	31.3	$^{243+244}Cm_2O_3$, ^{60}CoO, $^{239}PuO_2$, $^{241}PuO_2$, $^{238}UO_3$
$\%RSD_B(c_j^{MFPV})$ × $\%RSD_S(c_j^{MFPV})$	25.0	$^{137}Cs_2O$, $^{239}PuO_2$, $^{233}UO_3$, $^{236}UO_3$
Waste Type × $\%RSD_B(c_j^{MFPV})$	18.8	$^{241}PuO_2$, $^{235}UO_3$, $^{238}UO_3$

(a) Only two-factor interactions were included in the ANOVA model.
(b) This factor has a "low" case and a "high" case.
(c) This factor has a "low" case, "medium" case, and a "high" case.

uncertainty or variation, it is not surprising that this main effect significantly affects 100% of analyzed IHLW components. Because the ANOVA found several statistically significant effects, it is clear that the total %RSD results for IHLW radionuclide composition components are substantively different across the 12 scenarios investigated. This means that to accurately quantify the variation and uncertainty in IHLW radionuclide composition components (mass fractions), the batch-to-batch variation %RSDs, mixing/sampling uncertainty %RSDs, and analytical uncertainty %RSDs for concentrations of analytes in the IHLW MFPV must be well known. Also, because the "HLW waste type" factor had a statistically significant effect for nearly all radionuclide composition components, it can be concluded that magnitudes of total %RSDs for radionuclides depend on the waste type.

The ordering of significant factors and interactions in Table 7.2 is slightly different from the ordering in Table 7.1, with the first two and last three in each table having the same order. The main difference between the tables is that the "Waste Type" factor and interactions involving it are statistically significant for somewhat higher percentages of radionuclides compared to chemical composition components. However, these differences are not of practical concern, because the results in Table 7.2 agree with those in Table 7.1 that all of the factors have statistically significant effects on total %RSDs of chemical and radionuclide composition components.

7.3 Results on the Variations and Uncertainties of IHLW Glass Properties

This section discusses calculating and summarizing batch-to-batch variations, within-batch uncertainties, and total variation plus uncertainties of the IHLW properties of interest. Section 7.3.1 presents the variation and uncertainty results for PC T normalized releases of B, Li, and Na from HLW glasses. Section 7.3.2 presents the variation and uncertainty results for TCLP Cd release from HLW glasses. Section 7.3.3 presents the variation and uncertainty results for $T_{1\%}$ of HLW glasses using the Phase 1 and Phase 1a models. Section 7.3.4 presents the variation and uncertainty results for viscosity of HLW glasses at temperatures of 1373.15 K (1100ºC) and 1423.15 K (1150ºC). Section 7.3.5 presents the variation and uncertainty results for electrical conductivity of HLW glasses at temperatures of 1373.15 K (1100ºC) and 1473.15 K (1200ºC).

7.3.1 Results on the Variations and Uncertainties for PCT Normalized Releases of B, Li, and Na from HLW Glasses

Chemical compositions of IHLW MFPV batches were calculated for 18 MFPV batches (of each of the four waste types) and 200 Monte Carlo simulations for each of the 12 scenarios, as discussed in Section 7.1. These IHLW compositions corresponding to MFPV batches and the model coefficients from Table 6.1 were inserted into Eq. (6.1.7) to calculate the predicted natural logarithm of the PCT normalized release of B, Li, and Na for each of the 200 simulations within each of the 12 scenarios for each of the four HLW waste types.

The %RSD values for batch-to-batch variations ($\%RSD_B$), within-batch uncertainties ($\%RSD_W$), and total variations plus uncertainties ($\%RSD_T$) were calculated for PCT B, PCT Li, and PCT Na[(a)] across 18 batches for each of the four HLW waste types for each scenario in Table 5.2 and each of the 200 simulations within each scenario using Eqs. (6.1.15), (6.1.16), and (6.1.17), respectively. The $\%RSD_T$, $\%RSD_B$, and $\%RSD_W$ values were then summarized for each of the 12 scenarios for each of the four HLW waste types by calculating the mean, and the 90% ECIs from the 200 simulations. The $\%RSD_T$ summaries were calculated using Eqs. (6.1.18), (6.1.19a), and (6.1.19b). The $\%RSD_B$ summaries were calculated using Eqs. (6.1.20), (6.1.21a), and (6.1.21b). The $\%RSD_W$ summaries were calculated using Eqs. (6.1.22), (6.1.23a), and (6.1.23b).

Figure 7.7 summarizes the $\%RSD_T$, $\%RSD_B$, and $\%RSD_W$ results for PCT B, Li, and Na releases. As expected, the high-case 90% ECIs (dashed lines) indicate a larger amount of variation and uncertainty than the low-case 90% ECIs (solid lines) for each %RSD. Also, notice that the width of the 90% ECIs changes dramatically from the low case to the high case, meaning that PCT B, Li, and Na release values have more scatter when input variations and uncertainties are all at their highest values.

The top and bottom panels in Figure 7.7 show that PCT B, Li, and Na releases have mean values of $\%RSD_T$ and $\%RSD_W$ roughly from 5 to 10% for the low case, and from 18 to 40% for the high case. The second panel of Figure 7.7 shows that $\%RSD_B$ mean values for PCT B, Li, and Na releases are from 2 to 4% for the low case and from 3 to 8% for the high case. However, as noted previously, the 90% ECIs are much wider for all %RSDs at the high-case, yielding $\%RSD_T$ and $\%RSD_W$ values as large as 50 to 75%. The larger mean and 90% ECI values for total and within-batch %RSDs of PCT B, Li, and Na releases in the "high variation and uncertainty" case are a result of the nominal values of variation and uncertainties of the individual components that appear in the PCT release models and were used in the simulations. It is clear from Figure 7.7 that the within-batch uncertainties in PCT B, Li, and Na releases are much larger than the batch-to-batch variations and thus are the main contributor to total variation plus uncertainties. This is true even after the effective reduction of the within-batch uncertainty by averaging over the eight samples per IHLW MFPV batch [see Eq. (6.1.14)].

The Monte Carlo simulated glass property data were also analyzed using ANOVA in the same manner used on the chemical and radionuclide compositions in Sections 7.1 and 7.2, respectively. Table 7.3 summarizes the results from the ANOVAs for IHLW glass properties. Each of the four factors investigated (Waste Type, $\%RSD_B(c_j^{MFPV})$, $\%RSD_S(c_j^{MFPV})$, and $\%RSD_A(c_j^{MFPV})$) significantly affect the total %RSD values for PCT B, Li, and Na releases. The two-way interactions were also significant for at least one of the three PCT properties.

(a) Untransformed values of PCT B, Li, and Na releases (g/L) were obtained by taking the antilog of the values in natural logarithm units, and then %RSDs were calculated using the untransformed values.

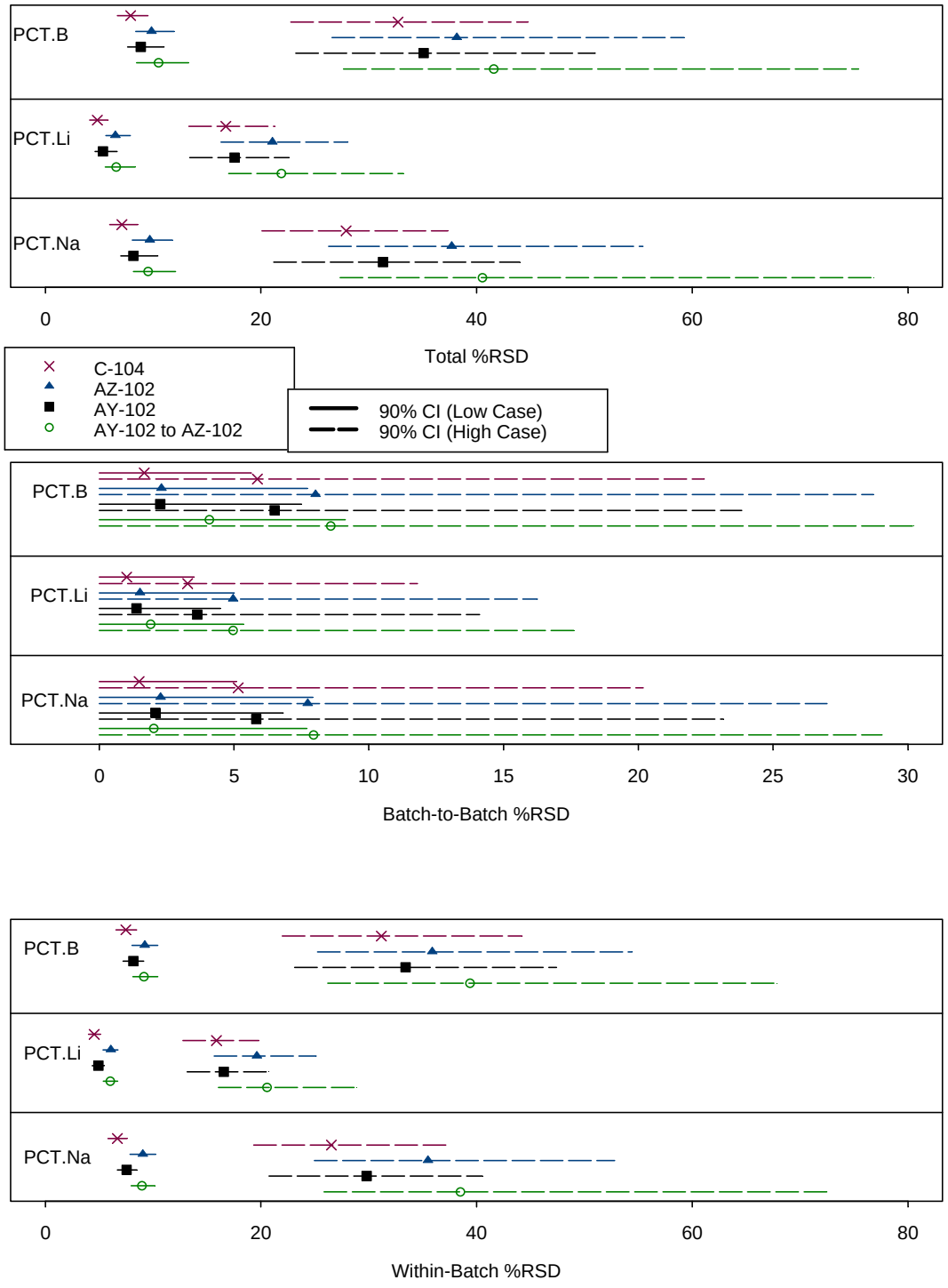

Figure 7.7. Means (the symbols) and 90% ECIs (lines) of Total, Batch-to-Batch, and Within-Batch %RSDs for PCT B, Li, and Na Releases Calculated from IHLW Simulations for Four Waste Types (differences in color) with All Uncertainties Set to the Low Cases (solid lines) and All Uncertainties Set to the High Cases (dashed lines)

Table 7.3. Factors or Interactions with Statistically Significant Effects on Total %RSD for All IHLW Glass Properties Using ANOVAs ($\alpha = 0.05$)[a]

Factor/Interaction	PCT B	PCT Li	PCT Na	TCLP Cd	$T_{1\%}$ (Phase 1)	$T_{1\%}$ (Phase 1A)	Viscosity 1100°C	Viscosity 1150 °C	Electrical Conductivity 1100 °C	Electrical Conductivity 1200 °C
Waste Type, $\%RSD_S(c_j^{MFPV})$ [b], $\%RSD_A(c_j^{MFPV})$ [b], $\%RSD_B(c_j^{MFPV})$ [c], Waste Type × $\%RSD_A(c_j^{MFPV})$	X[d]	X	X	X	X	X	X	X	X	X
Waste Type × $\%RSD_B(c_j^{MFPV})$	X	X	X	X	X	X			X	X
Waste Type × $\%RSD_S(c_j^{MFPV})$		X	X	X	X	X	X	X	X	X
$\%RSD_B(c_j^{MFPV})$ × $\%RSD_S(c_j^{MFPV})$	X		X		X	X	X	X	X	X
$\%RSD_B(c_j^{MFPV})$ × $\%RSD_A(c_j^{MFPV})$		X			X	X	X	X	X	X
$\%RSD_S(c_j^{MFPV})$ × $\%RSD_A(c_j^{MFPV})$		X		X	X	X	X	X	X	X

(a) Only two-factor interactions were included in the ANOVA model.
(b) This factor has a "low" case and a "high" case.
(c) This factor has a "low" case, "medium" case, and a "high" case.
(d) An "X" means that the factor or interactions are statistically significant for that particular glass property.

7.3.2 Results on the Variations and Uncertainties for TCLP Cd Release from HLW Glasses

Chemical compositions of IHLW MFPV batches were calculated for 18 MFPV batches (of each of the four HLW waste types) and 200 Monte Carlo simulations for each of the 12 scenarios, as discussed in Section 7.1. These IHLW compositions corresponding to MFPV batches and the TCLP Cd model coefficients from Table 6.2 were inserted into Eq. (6.1.9) to calculate the predicted natural logarithm of the TCLP normalized release of Cd for each of the 200 simulations within each of the 12 scenarios for each of the four HLW waste types.

The %RSD values for batch-to-batch variations ($\%RSD_B$), within-batch uncertainties ($\%RSD_W$), and total variations plus uncertainties ($\%RSD_T$) were calculated for TCLP Cd release[a] across 18 batches for each of the four HLW waste types for each scenario in Table 5.2 and each of the 200 simulations within each scenario. The same process and equations used to calculate and summarize %RSDs for PCT releases (see the second paragraph of Section 7.3.1) were also used for calculating TCLP Cd release %RSDs.

(a) Untransformed values of TCLP Cd releases (mg/L) were obtained by taking the antilog of the values in natural logarithm units, and then %RSDs were calculated using the untransformed values.

Figure 7.8 summarizes the $\%RSD_T$, $\%RSD_B$, and $\%RSD_W$ results for TCLP Cd release. As expected, the high-case 90% ECIs (dashed lines) indicate a larger amount of variation and uncertainty than the low-case 90% ECIs (solid lines) for each %RSD. All of the low-case 90% ECIs for total %RSD are within 5% and 10%. The low-case 90% ECIs for batch-to-batch %RSDs remain mostly under 5%. The low-case 90% ECIs for the within-batch %RSDs are similar to those for the total %RSD. The high-case 90% ECIs for the total %RSD are between 15% and 40%, with the batch-to-batch portion remaining under 20% and the within-batch portion between 15% and 35%. As expected, the high-case 90% ECIs are much wider than their low-case counterparts, reflecting the higher variability that occurs when the individual variation and uncertainty components are all simultaneously large.

The Monte Carlo simulated glass property data were also analyzed using ANOVA in the same manner used on the chemical and radionuclide compositions in Sections 7.1 and 7.2, respectively. Table 7.3 summarizes the results from the ANOVAs for IHLW glass properties. Each of the four factors investigated (Waste Type, $\%RSD_B(c_j^{MFPV})$, $\%RSD_S(c_j^{MFPV})$, and $\%RSD_A(c_j^{MFPV})$) significantly affect the total %RSD values for TCLP Cd release. The two-way interactions, including Waste Type and the $\%RSD_S(c_j^{MFPV}) \times \%RSD_A(c_j^{MFPV})$ interaction, also had significant effects.

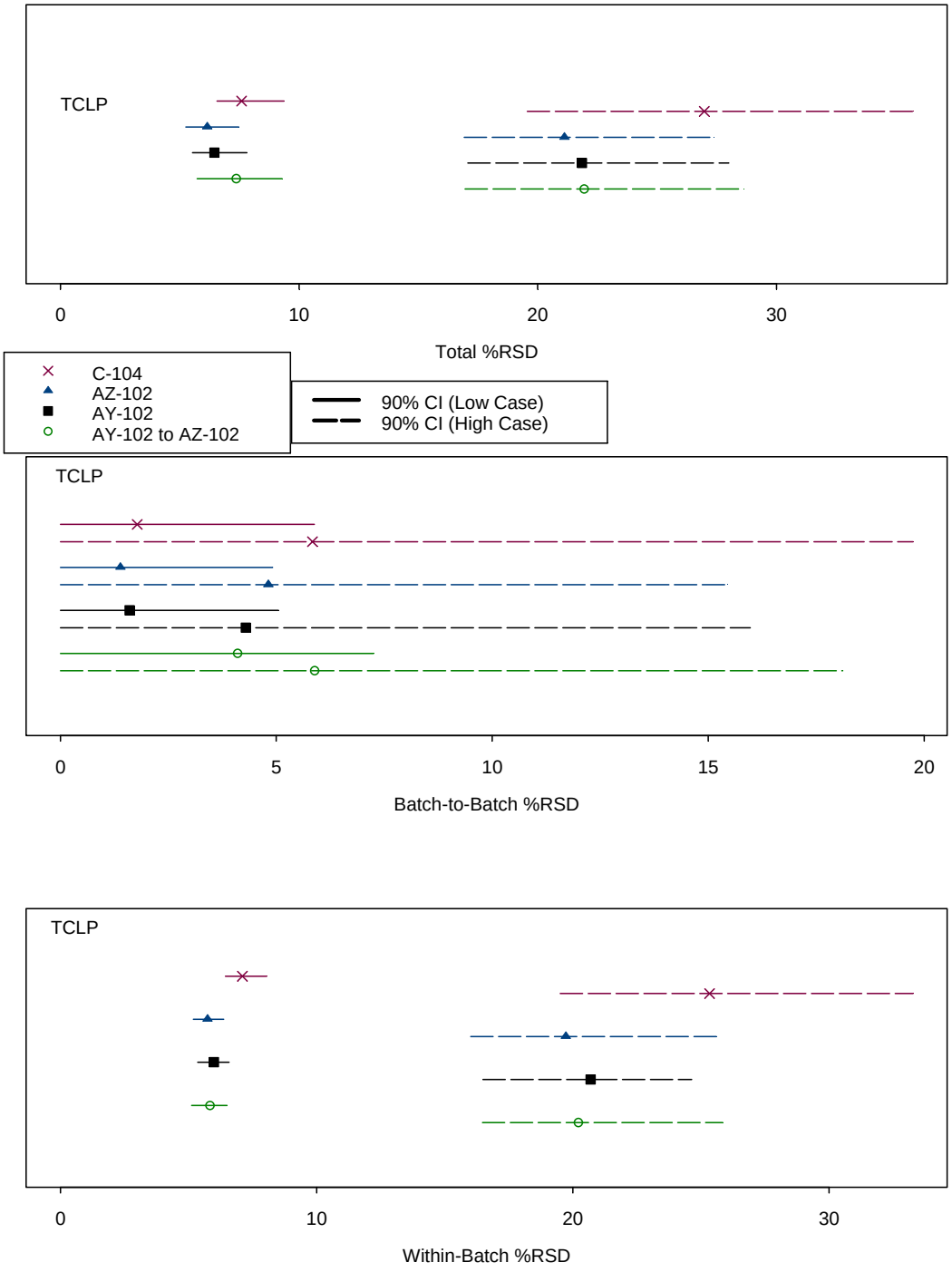

Figure 7.8. Means (the symbols) and 90% ECIs (lines) of Total, Batch-to-Batch, and Within-Batch %RSDs for TCLP Cd Releases Calculated from IHLW Simulations for Four Waste Types (differences in color) with All Uncertainties Set to the Low Cases (solid lines) and All Uncertainties Set to the High Cases (dashed lines)

7.3.3 Results on the Variations and Uncertainties for $T_{1\%}$ Spinel Crystallinity of HLW Glasses

Chemical compositions of IHLW MFPV batches were calculated for 18 MFPV batches (of each of the four HLW waste types) and 200 Monte Carlo simulations for each of the 12 scenarios, as discussed in Section 7.1. These IHLW compositions corresponding to MFPV batches and the $T_{1\%}$ spinel crystallinity model coefficients for Phase 1 and Phase 1a models from

Table 6.3 were inserted into Eq. (6.1.10) to calculate the predicted spinel $T_{1\%}$ for each of the 200 simulations within each of the 12 scenarios for each of the four HLW waste types.

The %RSD values for batch-to-batch variations ($\%RSD_B$), within-batch uncertainties ($\%RSD_W$), and total variations plus uncertainties ($\%RSD_T$) were calculated for spinel $T_{1\%}$ using the Phase 1 and Phase 1a models across 18 batches for each of the four HLW waste types for each scenario in Table 5.2 and each of the 200 simulations within each scenario. The same process and equations used to calculate and summarize %RSDs for PCT releases (see the second paragraph of Section 7.3.1) were also used for calculating spinel $T_{1\%}$ %RSDs.

Figure 7.9 summarizes the $\%RSD_T$, $\%RSD_B$, and $\%RSD_W$ results for spinel $T_{1\%}$. First, note that the results using the Phase 1 and Phase 1a property-composition models for $T_{1\%}$ are nearly identical. This is expected because the model form used was fairly robust. Fitting that model form to additional data over a somewhat larger IHLW composition region in Phase 1a had little impact compared to the model obtained in Phase 1. That is, there was little difference in model coefficients, predicted values, and model summary statistics (e.g., R^2) for the Phase 1 and 1a models.

The following additional observations are made regarding the %RSD results for spinel $T_{1\%}$ in Figure 7.9. As expected, the high-case 90% ECIs (dashed lines) indicate a larger amount of variation and uncertainty than the low-case 90% ECIs (solid lines) for each %RSD. Also, notice that the width of the 90% ECIs changes dramatically from the low case to the high case, meaning that spinel $T_{1\%}$ values have more scatter when input variations and uncertainties are all at their highest values.

It can also be seen in Figure 7.9 that the $T_{1\%}$ models (Phase 1 and Phase 1a) have the effect of drastically reducing the batch-to-batch variation, within-batch uncertainty, and total %RSDs of this property compared to the %RSDs of the components included in the model. None of the total %RSD values for $T_{1\%}$ exceeds 6%, although the 90% ECIs for the cases with high variation and uncertainties are still much wider than those for the cases with low variation and uncertainties.

The Monte Carlo simulated glass property data were also analyzed using ANOVA in the same manner used on the chemical and radionuclide compositions in Sections 7.1 and 7.2, respectively. Table 7.3 summarizes the results from the ANOVAs for IHLW glass properties. Each of the four factors investigated (Waste Type, $\%RSD_B(c_j^{MFPV})$, $\%RSD_S(c_j^{MFPV})$, and $\%RSD_A(c_j^{MFPV})$) significantly affect the total %RSD values for $T_{1\%}$ (using both the Phase 1 and Phase 1a models). All two-way interactions were also significant.

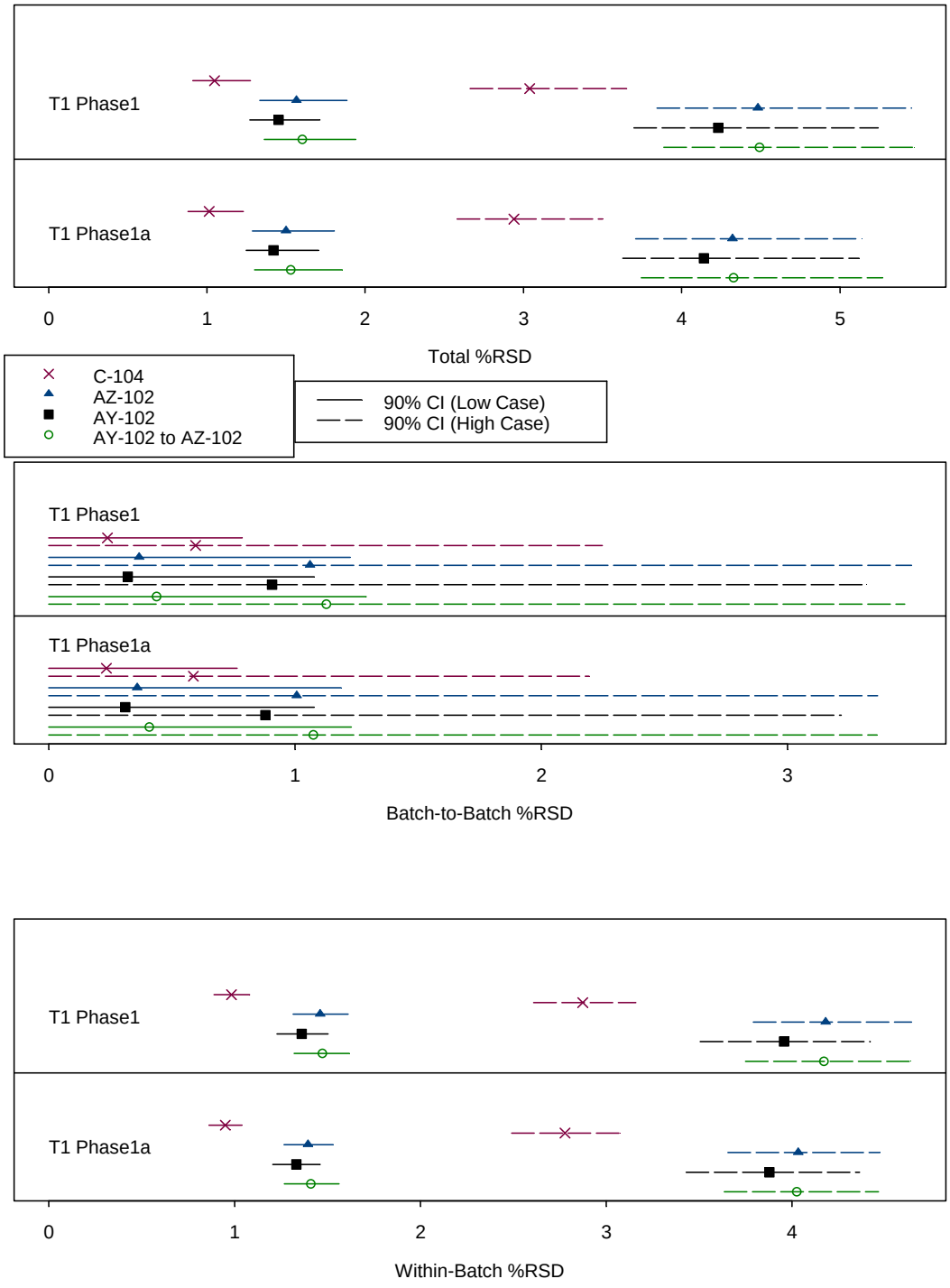

Figure 7.9. Means (the symbols) and 90% ECIs (lines) of Total, Batch-to-Batch, and Within-Batch %RSDs for $T_{1\%}$ Calculated Using Phase 1 and 1a Models with IHLW Simulations for Four Waste Types (differences in color) with All Uncertainties Set to the Low Cases (solid lines) and All Uncertainties Set to the High Cases (dashed lines)

7.3.4 Results on the Variations and Uncertainties for Viscosity of HLW Glasses

Chemical compositions of IHLW MFPV batches were calculated for 18 MFPV batches (of each of the four HLW waste types) and 200 Monte Carlo simulations for each of the 12 scenarios, as discussed in Section 7.1. These IHLW compositions corresponding to MFPV batches, the viscosity model coefficients from Table 6.4, and temperatures of 1373.15 K (1100ºC) and 1423.15 K (1150ºC) were inserted into Eq. (6.1.11) to calculate the predicted natural logarithm of viscosity at the given temperatures for each of the 200 simulations within each of the 12 scenarios for each of the four HLW waste types.

The %RSD values for batch-to-batch variations ($\%RSD_B$), within-batch uncertainties ($\%RSD_W$), and total variations plus uncertainties ($\%RSD_T$) were calculated for viscosity at 1373.15 K and 1423.15 K[(a)] across 18 MFPV batches for each of the four HLW waste types for each scenario in Table 5.2 and each of the 200 simulations within each scenario. The same process and equations used to calculate and summarize %RSDs for PCT releases (see the second paragraph of Section 7.3.1) were also used for calculating the viscosity %RSDs.

Figure 7.10 summarizes the $\%RSD_T$, $\%RSD_B$, and $\%RSD_W$ results for viscosity (poise) at temperatures of 1373.15 K (1100ºC) and 1423.15 K (1150ºC). As expected, the high-case 90% ECIs (dashed lines) indicate a larger amount of variation and uncertainty than the low-case 90% ECIs (solid lines) for each %RSD. Also, notice that the width of the 90% ECIs changes dramatically from the low case to the high case, meaning that viscosity values have more scatter when input variations and uncertainties are all at their highest values.

The top and bottom panels in Figure 7.10 show that the viscosity at the two temperatures has mean values of $\%RSD_T$ and $\%RSD_W$ roughly from 10 to 13% for the low case, and from 30 to 40% for the high case. The second panel of Figure 7.10 shows that $\%RSD_B$ mean viscosity values are roughly 3% for the low case and from 7 to 9% for the high case. However, as noted previously, the 90% ECIs are much wider for all %RSDs at the high-case, yielding values of $\%RSD_T$ and $\%RSD_W$ from 40 to over 50%. It is clear from Figure 7.10 that the within-batch uncertainties in viscosity values are much larger than the batch-to-batch variations and thus are the main contributor to total variation plus uncertainties. This is true even after the effective reduction of the within-batch uncertainty by averaging over the 8 samples per IHLW MFPV batch [see Eq. (6.1.14)].

The Monte Carlo simulated glass property data were also analyzed using ANOVA in the same manner used on the chemical and radionuclide compositions in Sections 7.1 and 7.2, respectively. Table 7.3 summarizes the results from the ANOVAs for IHLW glass properties. Each of the four factors investigated (Waste Type, $\%RSD_B(c_j^{MFPV})$, $\%RSD_S(c_j^{MFPV})$, and $\%RSD_A(c_j^{MFPV})$) significantly affect viscosity at 1373.15 K (1100ºC) and 1423.15 K (1150ºC). All two-way interactions were also significant, except for Waste Type × $\%RSD_B(c_j^{MFPV})$.

(a) Untransformed values of viscosity at the respective temperatures were obtained by taking the antilog of the values in natural logarithm units, and then %RSDs were calculated using the untransformed values.

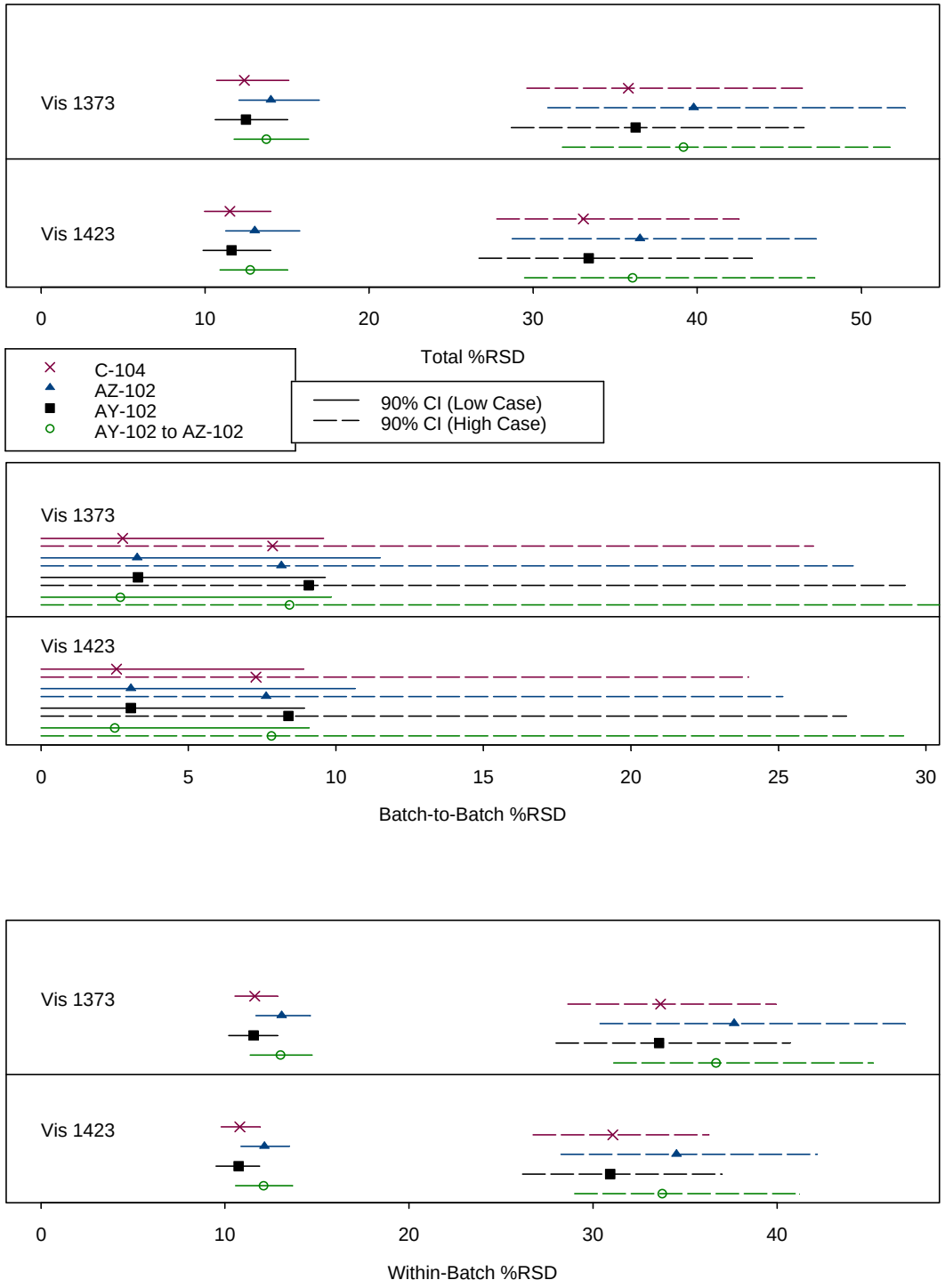

Figure 7.10. Means (the symbols) and 90% ECIs (lines) of Total, Batch-to-Batch, and Within-Batch %RSDs for Viscosity at 1373.15 K and 1423.15 K from IHLW Simulations for Four Waste Types (differences in color) with All Uncertainties Set to the Low Cases (solid lines) and All Uncertainties Set to the High Cases (dashed lines)

7.3.5 Results on the Variations and Uncertainties for Electrical Conductivity of HLW Glasses

Chemical compositions of IHLW MFPV batches were calculated for 18 MFPV batches (of each of the four HLW waste types) and 200 Monte Carlo simulations for each of the 12 scenarios, as discussed in Section 7.1. These IHLW compositions corresponding to MFPV batches, the electrical conductivity model coefficients from Table 6.5, and temperatures of 1373.15 K (1100ºC) and 1473.15 K (1200ºC) were inserted into Eq. (6.1.12) to calculate the predicted natural logarithm of electrical conductivity at the given temperatures for each of the 200 simulations within each of the 12 scenarios for each of the four HLW waste types.

The %RSD values for batch-to-batch variations ($\%RSD_B$), within-batch uncertainties ($\%RSD_W$), and total variations plus uncertainties ($\%RSD_T$) were calculated for electrical conductivity at 1373.15 K (1100ºC) and 1473.15 K (1200ºC)[(a)] across 18 MFPV batches for each of the four HLW waste types for each scenario in Table 5.2 and each of the 200 simulations within each scenario. The same process and equations used to calculate and summarize %RSDs for PCT releases (see the second paragraph of Section 7.3.1) were also used for calculating electrical conductivity %RSDs.

Figure 7.11 summarizes the $\%RSD_T$, $\%RSD_B$, and $\%RSD_W$ results for electrical conductivity at temperatures of 1373.15 K (1100ºC) and 1473.15 K (1200ºC). As expected, the high-case 90% ECIs (dashed lines) indicate a larger amount of variation and uncertainty than the low-case 90% ECIs (solid lines) for each %RSD. Also, notice that the width of the 90% ECIs changes dramatically from the low case to the high case, meaning that electrical conductivity values have more scatter when input variations and uncertainties are all at their highest values.

The top panel in Figure 7.11 shows that electrical conductivity at the two temperatures has mean values of $\%RSD_T$ from roughly 3 to 7% for the low case, and from 11 to 17% for the high case. The mean values of $\%RSD_W$ in the third panel of Figure 7.11 have slightly smaller ranges than for $\%RSD_T$. The second panel of Figure 7.11 shows that $\%RSD_B$ mean values for electrical conductivity are roughly 1% for the low case and from 3 to 5% for the high case. However, as noted previously, the 90% ECIs are much wider for all %RSDs at the high-case, yielding values of $\%RSD_T$ and $\%RSD_W$ as high as 18 to 20%. It is clear from Figure 7.11 that the within-batch uncertainties in electrical conductivity values are much larger than the batch-to-batch variations, and thus are the main contributor to total variation plus uncertainties. This is true even after the effective reduction of the within-batch uncertainty by averaging over the 8 samples per IHLW MFPV batch [see Eq. (6.1.14)].

(a) Untransformed values of electrical conductivity at the respective temperatures were obtained by taking the antilog of the values in natural logarithm units, and then %RSDs were calculated using the untransformed values.

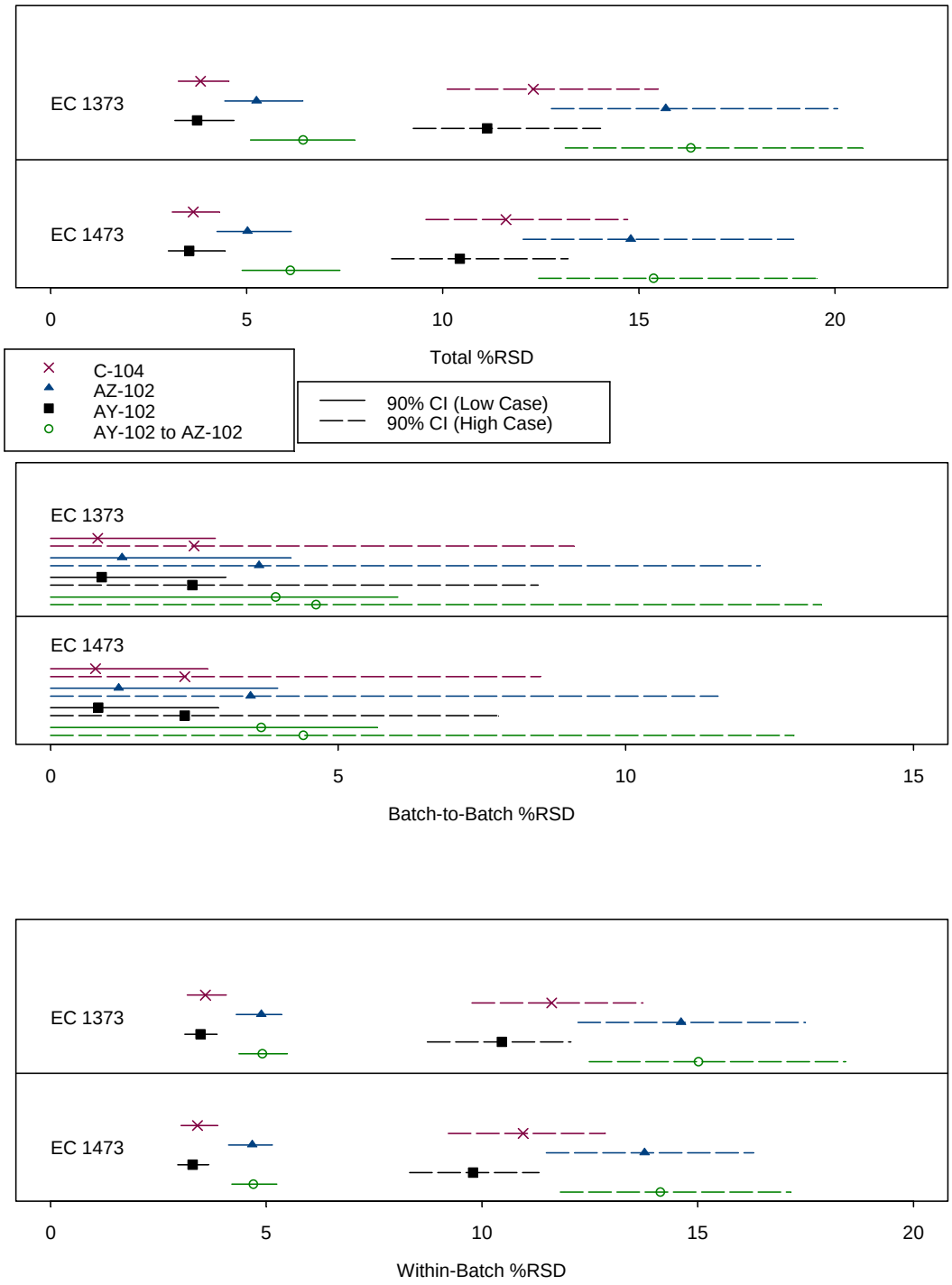

Figure 7.11. Means (the symbols) and 90% ECIs (lines) of Total, Batch-to-Batch, and Within-Batch %RSDs for Electrical Conductivity at 1373.15 K and 1473.15 K from IHLW Simulations for Four Waste Types (differences in color) with All Uncertainties Set to the Low Cases (solid lines) and All Uncertainties Set to the High Cases (dashed lines)

The Monte Carlo simulated glass property data were also analyzed using ANOVA in the same manner used on the chemical and radionuclide compositions in Sections 7.1 and 7.2, respectively. Table 7.3 summarizes the results from the ANOVAs for IHLW glass properties. Each of the four factors investigated (Waste Type, $\%RSD_B(c_j^{MFPV})$, $\%RSD_S(c_j^{MFPV})$, and $\%RSD_A(c_j^{MFPV})$) significantly affect electrical conductivity at 1373.15 K (1100ºC) and 1473.15 K (1200ºC). All two-way interactions were also significant.

8.0 Results on the Variations and Uncertainties of ILAW Composition and Properties

This section describes the results of implementing the statistical methodology described in Section 6.2 to the Monte Carlo simulated data for 200 simulations of 64 scenarios with 10 ILAW MFPV batches for each of five data sets (LAW waste types). The 64 scenarios are combinations of low and high estimates of variations and uncertainties. The implementation includes calculating and summarizing the variations and uncertainties associated with ILAW chemical and radionuclide compositions (expressed in mass fractions of glass components), as well as ILAW properties of interest.

The uncertainties in ILAW compositions and properties reported in this section incorporate averages over the three replicate LAW CRV samples (with one analysis each) used in this work based on the current WTP sampling and analysis plan for the ILAW facility. Also, because of the large number of scenarios (64) investigated for each of the five LAW data sets (waste types), in this section, variation and uncertainty results are presented for the low-case (all variations and uncertainties at their low estimates) and the high-case (all variations and uncertainties at their high estimates) scenarios. Presenting the results in this way provides information on the lowest and highest possible variation and uncertainty in ILAW compositions and properties. Appendix F presents results for other ILAW scenarios (i.e., combinations of the variation and uncertainty factors) investigated.

Section 8.1 discusses the results of calculating ILAW compositions corresponding to MFPV batches and calculating and summarizing the %RSDs for batch-to-batch variations, within-batch uncertainties, and total variations plus uncertainties for important ILAW chemical composition components. Section 8.1 also discusses the factors that most affect the total %RSD for each of the important ILAW chemical composition components. Section 8.2 discusses the results of calculating ILAW radionuclide compositions corresponding to MFPV batches and calculating and summarizing the %RSDs for batch-to-batch variations, within-batch uncertainties, and total variations plus uncertainties of important ILAW radionuclide composition components. Section 8.2 also discusses the factors that most affect the total %RSD for each of the important ILAW radionuclide composition components. Section 8.3 discusses the results of calculating and summarizing the %RSDs for batch-to-batch variations, within-batch uncertainties, and total variations plus uncertainties of the ILAW properties of interest, which include PCT (B and Na releases), VHT, viscosity, and electrical conductivity.

8.1 Results on the Variations and Uncertainties of ILAW Chemical Composition

The variations and uncertainties affecting the LAW vitrification process (see Table 5.3) were applied to the ILAW mass-balance equations using Monte Carlo simulation. Low and high cases were studied for each of the following variations and uncertainties within the LAW vitrification process: CRV random batch-to-batch %RSD ($\%RSD_B(c_j^{CRV})$), CRV mixing/sampling %RSD ($\%RSD_S(c_j^{CRV})$), CRV analytical %RSD ($\%RSD_A(c_j^{CRV})$), GFC composition uncertainty ($SD(G_{jk}^{GFC})$), GFC mass uncertainty ($SD(a_k^{GFC})$), and volume uncertainties in the CRV and MFPV (SD_V^{CRV} and SD_V^{MFPV}). Data were

simulated for three samples per LAW CRV batch with one analysis per sample and single volume determinations. ILAW chemical compositions corresponding to MFPV batches were calculated for all glass components and for each of the five data sets using Eqs. (6.2.1), (6.2.2), and (6.2.3).

The %RSD values for batch-to-batch variations ($\%RSD_B$), within-batch uncertainties ($\%RSD_W$), and total variations plus uncertainties ($\%RSD_T$) were calculated for each of the ILAW chemical composition components across 10 MFPV batches for each scenario in Table 5.4 and each of the 200 simulations within each scenario using Eqs. (6.2.12), (6.2.15), and (6.2.18), respectively. The $\%RSD_T$, $\%RSD_B$, and $\%RSD_W$ values were then summarized for each of the 64 scenarios for each of the five data sets by calculating the mean and the lower and upper 90% empirical confidence limits from the 200 simulations. The $\%RSD_T$ summaries were calculated using Eqs. (6.2.13), (6.2.14a), and (6.2.14b). The $\%RSD_B$ summaries were calculated using Eqs. (6.2.16), (6.2.17a), and (6.2.17b). The $\%RSD_W$ summaries were calculated using Eqs. (6.2.19), (6.2.20a), and (6.2.20b).

Figure 8.1 summarizes the $\%RSD_T$ results for each of the important chemical composition components in ILAW corresponding to MFPV batches. The five different colors on the plot represent the five data sets as defined in Sections 4.1, 5.3, and Tables D.1 to D.5. The solid lines represent the 90% empirical confidence interval (90% ECI) as calculated using Eqs. (6.2.14a) and (6.2.14b) for the scenario with all uncertainties set to the low case (Scenario # 1 in Table 5.4). The dashed lines represent the 90% ECI for the scenario with all uncertainties set to the high case (Scenario # 64 in Table 5.4). The solid square and the open circle represent the $\overline{\%RSD_T}$ values calculated using Eq. (6.2.13) for the scenario with all uncertainties at the low case and for the scenario with all uncertainties at the high case, respectively. Figure 8.2 through Figure 8.10 (discussed subsequently) use the same schema for identifying the five data sets, the low- and high-case 90% ECIs, and the mean %RSD values for the low and high case.

Figure 8.2 and Figure 8.3, respectively, show the summary results of the $\%RSD_B$ and the $\%RSD_W$ for each of the important chemical composition components in ILAW corresponding to MFPV batches. As expected, the high-case 90% ECIs (dashed lines) indicate a larger amount of variation than the low-case 90% ECIs (solid lines) for $\%RSD_T$ and $\%RSD_W$. The difference between the high-case 90% ECIs and low-case 90% ECIs is very small for $\%RSD_B$ because the batch-to-batch variation does not include any of the GFC uncertainties or the CRV mixing/sampling and analytical uncertainties. The batch-to-batch variation is much larger for the second data set, which is the transition from AP-101/AY-102 to AZ-101. The differences are most pronounced for those ILAW chemical composition components that vary substantially during this transition. In those cases where components did not vary substantially during the transition, the batch-to-batch variation was influenced mainly by the random batch-to-batch uncertainty factor. This resulted in very small $\%RSD_B$ values with small 90% ECIs.

Figure 8.1 shows that most ILAW components (mass fractions) have $\%RSD_T$ values less than 5 to 10% for the low case, and less than 15 to 20% for the high case. Figure 8.2 shows that $\%RSD_B$ values are below 1%, except for most of the Set 2 data (transition from AP-101/AY-102 to AZ-101), which range between just under 5% to about 23%. Figure 8.3 shows that $\%RSD_W$ values for most ILAW components are each less than 10% for the low case and less than 20% for the high case.

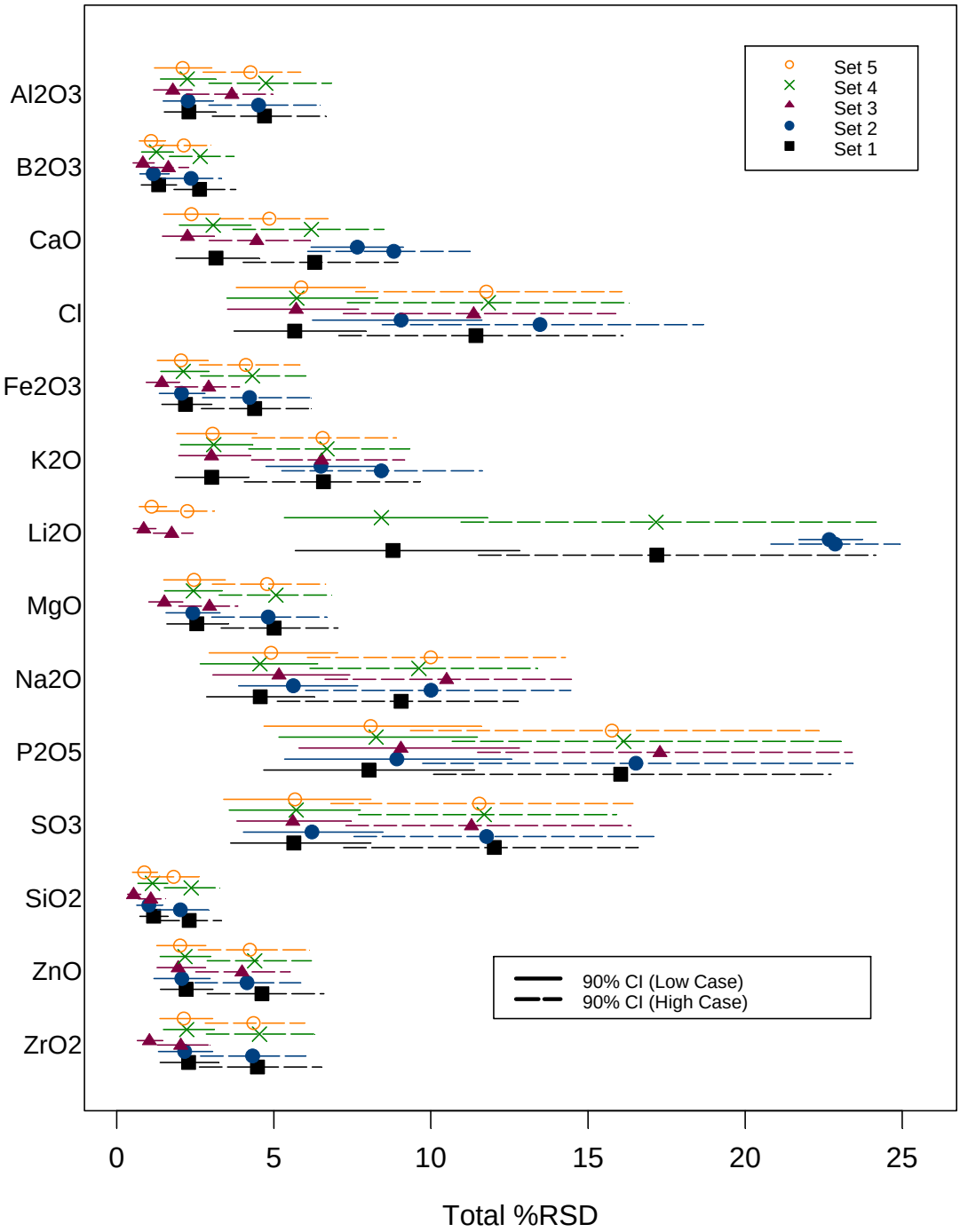

Figure 8.1. Means (the symbols) and 90% ECIs (lines) of Total %RSD Calculated from ILAW Simulations for All Five Data Sets (differences in color) with All Uncertainties Set to the Low Cases (solid lines) and All Uncertainties Set to the High Cases (dashed lines) for Important ILAW Chemical Composition Components

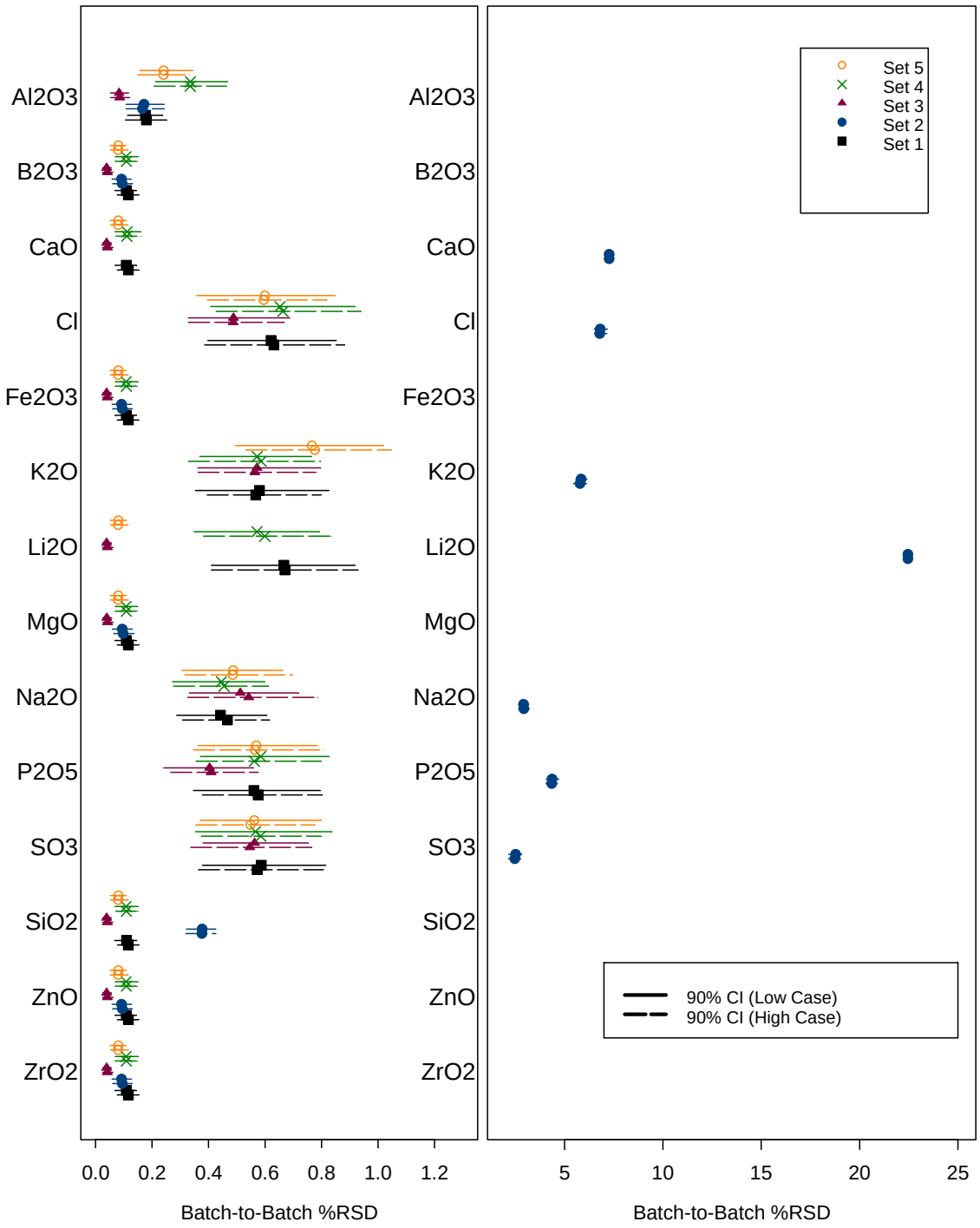

Figure 8.2. Means (the symbols) and 90% ECIs (lines) of Batch-to-Batch %RSDs Calculated from ILAW Simulations for All Five Data Sets (differences in color) with All Uncertainties Set to the Low Cases (solid lines) and All Uncertainties Set to the High Cases (dashed lines) for Important ILAW Chemical Composition Components. Note that two different scales were used on the x-axis to better view the smaller %RSD values.

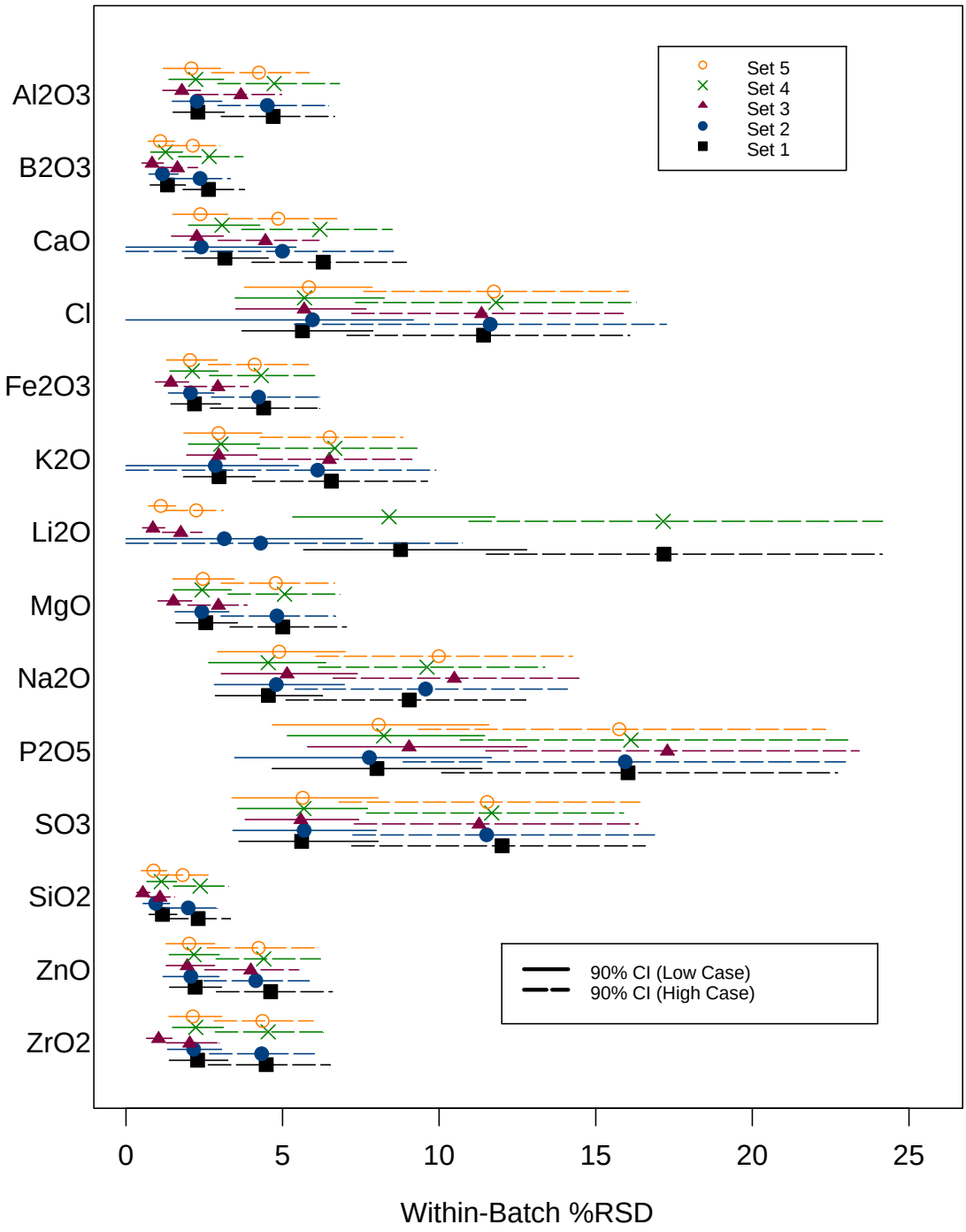

Figure 8.3. Means (the symbols) and 90% ECIs (lines) of Within-Batch %RSDs Calculated from ILAW Simulations for All Five Data Sets (differences in color) with All Uncertainties Set to the Low Cases (solid lines) and All Uncertainties Set to the High Cases (dashed lines) for Important ILAW Chemical Composition Components

It is also interesting to note that the ILAW chemical composition components included in the added GFCs have a smaller within-batch variation and total variation plus uncertainty ($\%RSD_W$ and $\%RSD_T$), than those that were only present in the CRV. This is because of the relatively small uncertainties expected in the GFC compositions and the batching of the GFCs, compared to the uncertainties in the mixing/sampling and, especially, the analysis of the samples. For example, Figure 8.1 shows that Li_2O has a large total variation plus uncertainties for data sets # 1, # 2, and # 4 whereas the total variation plus uncertainties is relatively small for data sets # 3 and # 5. Inspection of Table D.7 shows that Li_2CO_3 was added as a GFC to data sets # 3 and # 5, and a small amount to data set # 2. Figure 8.2 and Figure 8.3 show that total variation plus uncertainties in Li_2O for data set # 2 consists more of the batch-to-batch variation because of the transition, and a smaller portion of the within-batch uncertainty because of Li being added as a GFC.

The Monte Carlo simulation data were also analyzed using ANOVA to determine which factors, and two-factor interactions between the factors, had significant effects on the mean total variation plus uncertainties ($\overline{\%RSD_T}$) obtained from the 64 scenarios for each of the five LAW data sets. The factors investigated in the ANOVA are the LAW data set, the LAW CRV batch-to-batch %RSD ($\%RSD_B(c_j^{CRV})$), the LAW CRV mixing/sampling %RSD ($\%RSD_S(c_j^{CRV})$), the LAW CRV analytical %RSD ($\%RSD_A(c_j^{CRV})$), the SD of GFC composition ($SD(G_{jk}^{GFC})$), the SD of GFC amounts added to the ILAW MFPV ($SD(a_k^{GFC})$), and the SD of volume determinations (SD_V). An ANOVA was performed for each of the important ILAW chemical composition components (see Table 2.2). Table 8.1 summarizes results from the ANOVAs for ILAW chemical composition components. This table summarizes the percentage of chemical composition components (oxides or halogens) for which each factor and two-factor interaction was statistically significant. The factors and interactions are listed in the table in decreasing order of the percentage of components that were statistically significant.

From Table 8.1, it can be seen that changes in the %RSD of both CRV mixing/sampling ($\%RSD_S(c_j^{CRV})$) and CRV analytical ($\%RSD_A(c_j^{CRV})$) significantly affected the total variation plus uncertainty for all of the important ILAW components. Changes in the GFC composition uncertainties and GFC masses added significantly affected the total variation plus uncertainties for most of the studied chemical composition components. As expected, there were significant differences in total variation plus uncertainties across the five data sets. Changes in random batch-to-batch variation ($\%RSD_B(c_j^{CRV})$) and volume random uncertainty, as well as interactions containing either of these factors, had little effect on nearly all of the chemical composition components.

The main conclusion from these ANOVA results is that the values of total %RSD for ILAW chemical composition components (mass fractions) can vary substantially, depending on the data set (LAW waste type) as well as the mixing/sampling uncertainty %RSD and analytical uncertainty %RSD for concentrations of analytes in the ILAW MFPV. Uncertainties in GFC compositions and amounts of GFCs added to ILAW MFPV batches also had significant effects on the total %RSD for many components.

Table 8.1. Percentage of Important ILAW Chemical Composition Components for which the Factor or Interaction had a Statistically Significant Effect on Total %RSD in the ANOVAs (α = 0.05)[a]

Factor / Interaction	% of Significant Components	Statistically Significant Important ILAW Chemical Composition Components
Data Set, $\%RSD_S(c_j^{CRV})$ [b], $\%RSD_A(c_j^{CRV})$ [b], Data Set × $\%RSD_A(c_j^{CRV})$	100	All
$SD(a_k^{GFC})$ [b]	85.7	Al_2O_3, B_2O_3, CaO, Fe_2O_3, K_2O, Li_2O, MgO, Na_2O, SiO_2, SO_3, ZnO, ZrO_2
$SD(G_{jk}^{GFC})$ [b]	71.4	Al_2O_3, B_2O_3, CaO, Fe_2O_3, Li_2O, MgO, P_2O_5, SiO_2, ZnO, ZrO_2
$\%RSD_S(c_j^{CRV}) \times \%RSD_A(c_j^{CRV})$	71.4	Al_2O_3, B_2O_3, Cl, K_2O, Li_2O, MgO, Na_2O, P_2O_5, SO_3, SiO_2
Data Set × $\%RSD_S(c_j^{CRV})$	64.3	Al_2O_3, B_2O_3, Cl, Fe_2O_3, K_2O, Li_2O, Na_2O, P_2O_5, SiO_2
Data Set × $SD(G_{jk}^{GFC})$	57.1	Al_2O_3, B_2O_3, CaO, Fe_2O_3, MgO, P_2O_5, SiO_2, ZrO_2
Data Set × $SD(a_k^{GFC})$	57.1	Al_2O_3, B_2O_3, CaO, Fe_2O_3, Li_2O, MgO, ZnO, ZrO_2
$\%RSD_A(c_j^{CRV}) \times SD(G_{jk}^{GFC})$	57.1	Al_2O_3, B_2O_3, CaO, Fe_2O_3, MgO, P_2O_5, SiO_2, ZnO
$\%RSD_A(c_j^{CRV}) \times SD(a_k^{GFC})$	50.0	Al_2O_3, B_2O_3, Fe_2O_3, MgO, SiO_2, ZnO, ZrO_2
$SD(G_{jk}^{GFC}) \times SD(a_k^{GFC})$	35.7	Al_2O_3, CaO, Fe_2O_3, MgO, ZrO_2
$\%RSD_S(c_j^{CRV}) \times SD(a_k^{GFC})$	21.4	Al_2O_3, B_2O_3, MgO
Data Set × $\%RSD_B(c_j^{CRV})$	14.3	MgO, SO_3
$\%RSD_S(c_j^{CRV}) \times SD(G_{jk}^{GFC})$	14.3	B_2O_3, CaO
$\%RSD_B(c_j^{CRV})$ [b]	7.1	Na_2O
$\%RSD_B(c_j^{CRV}) \times \%RSD_S(c_j^{CRV})$	7.1	Cl
$\%RSD_B(c_j^{CRV}) \times SD_V$	7.1	P_2O_5
$\%RSD_S(c_j^{CRV}) \times SD_V$	7.1	Li_2O
$SD(a_k^{GFC}) \times SD_V$	7.1	K_2O
SD_V [c], Data Set × SD_V, $\%RSD_B(c_j^{CRV}) \times \%RSD_A(c_j^{CRV})$, $\%RSD_B(c_j^{CRV}) \times SD(G_{jk}^{GFC})$, $\%RSD_B(c_j^{CRV}) \times SD(G_{jk}^{GFC})$, $\%RSD_B(c_j^{CRV}) \times SD(a_k^{GFC})$, $\%RSD_A(c_j^{CRV}) \times SD_V$, $SD(G_{jk}^{GFC}) \times SD_V$	0	None

(a) Only two-factor interactions were included in the ANOVA model.

(b) This factor has a "low" case and a "high" case.

(c) The notation SD_V represents both SD_V^{CRV} and SD_V^{MFPV}. This factor has a "low" and "high" case where both SD_V^{CRV} and SD_V^{MFPV} are varied at the same time.

8.2 Results on the Variations and Uncertainties of ILAW Radionuclide Composition

The %RSD values for batch-to-batch variations ($\%RSD_B$), within-batch uncertainties ($\%RSD_W$), and total variations plus uncertainties ($\%RSD_T$) were calculated for each of the ILAW radionuclide composition components across 10 MFPV batches for each scenario in Table 5.4 and each of the 200 simulations within each scenario. The same process and equations used for ILAW chemical composition components (see the first two paragraphs of Section 8.1) were also used for ILAW radionuclide composition components.

Figure 8.4 summarizes the $\%RSD_T$ results for each of the important radionuclide composition components in ILAW corresponding to MFPV batches. Figure 8.5 and Figure 8.6, respectively, show the summary results of the $\%RSD_B$ and $\%RSD_W$ for each of the important radionuclide composition components in ILAW corresponding to MFPV batches. As expected, the high-case 90% ECIs (dashed lines) indicate a larger amount of variation and uncertainty than the low-case 90% ECIs (solid lines) for $\%RSD_T$ and $\%RSD_W$. The difference between the high-case 90% ECIs and low-case 90% ECIs is very small for $\%RSD_B$ because the batch-to-batch variation does not include any of the GFC uncertainties or the CRV mixing/sampling and analytical uncertainties. The batch-to-batch variation is larger for the second data set, which is the transition from AP-101/AY-102 to AZ-101. The differences are most pronounced for those ILAW radionuclides that vary substantially during this transition.

Figure 8.4 shows that most ILAW radionuclide composition components (mass fractions) have $\%RSD_T$ values less than 10 to 15% for the low case, and less than 20 to 25% for the high case. The exceptions for the high case were $^{125}Sb_2O_3$ and $^{151}Sm_2O_3$, with 90% ECI values ranging up to 40%. Figure 8.5 shows that $\%RSD_B$ values are generally below 1%, except for most of the Set 2 data (transition from AP-101/AY-102 to AZ-101), for which $\%RSD_B$ values range between 2% to about 14%. The $\%RSD_B$ values are larger in the transition case for those components that vary substantially during the transition. Figure 8.6 shows that $\%RSD_W$ values for most ILAW components are each less than 15% for the low case and less than 25% for the high case.

The Monte Carlo simulation data were also analyzed using ANOVA to determine which factors, and two-factor interactions between the factors, had significant effects on the mean total variation plus uncertainties ($\overline{\%RSD_T}$) obtained from the 64 scenarios for each of the five LAW data sets. The factors are the same as identified in Section 8.1. An ANOVA was performed for each of the important ILAW radionuclide composition components (Table 2.1). Table 8.2 summarizes results from the ANOVAs for ILAW radionuclide composition components. This table summarizes the percentage of radionuclide composition components for which each factor and two-factor interaction was statistically significant. The factors and interactions are listed in the table in decreasing order of the percentage of radionuclides that were statistically significant.

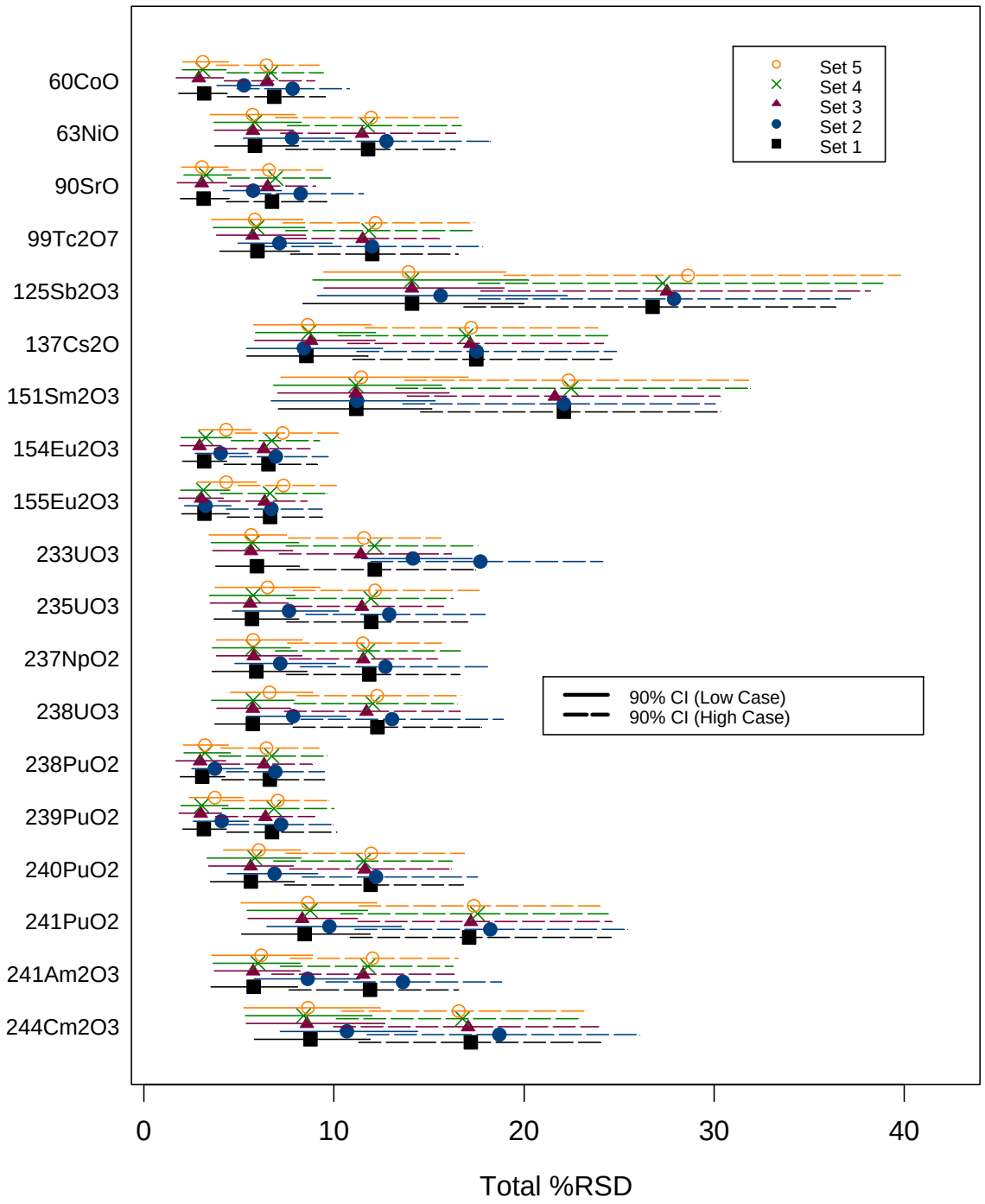

Figure 8.4. Means (the symbols) and 90% ECIs (lines) of Total %RSD Calculated from ILAW Simulations for All Five Data Sets (differences in color) with All Uncertainties Set to the Low Cases (solid lines) and All Uncertainties Set to the High Cases (dashed lines) for Important ILAW Radionuclides

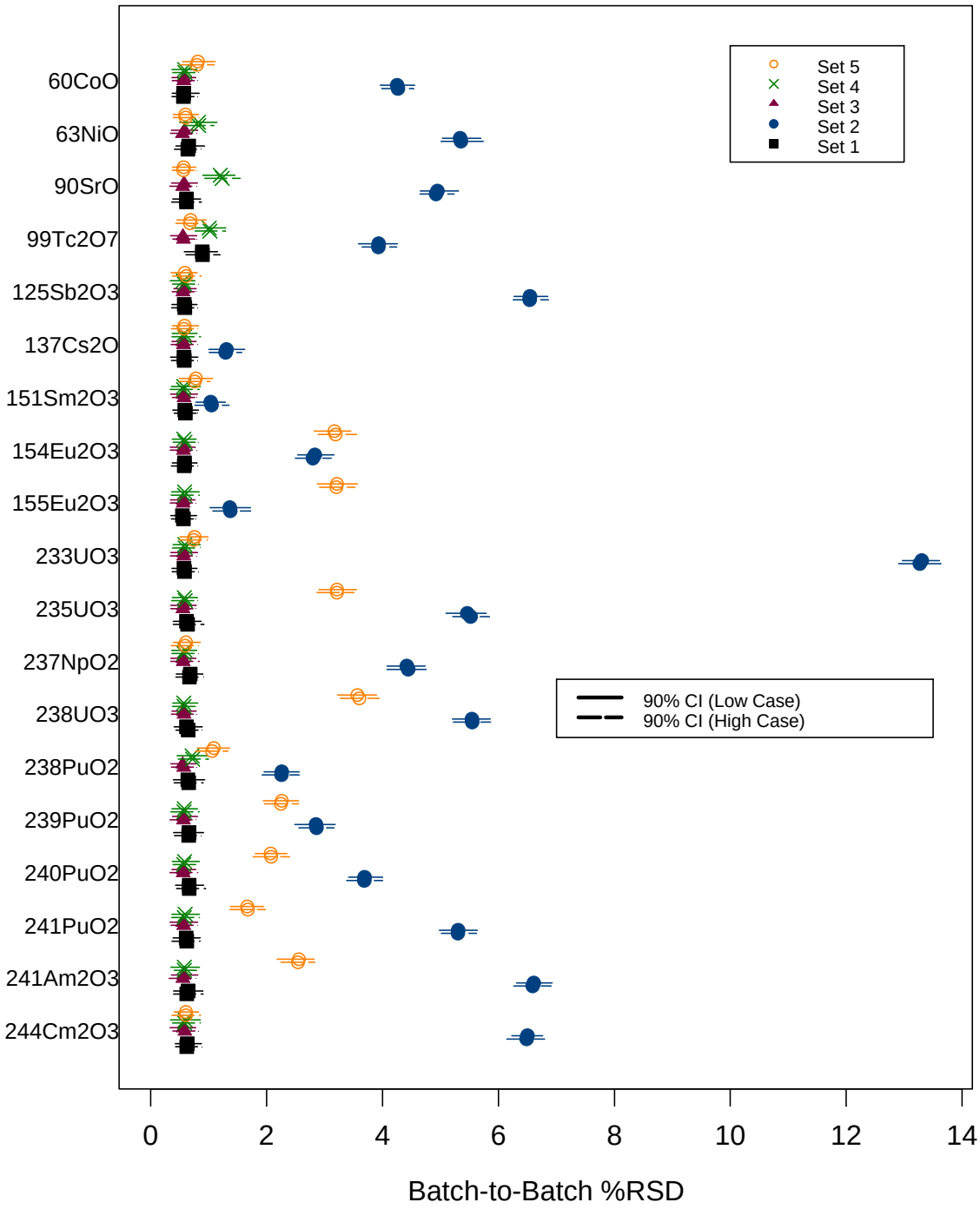

Figure 8.5. Means (the symbols) and 90% ECIs (lines) of Batch-to-Batch %RSD Calculated from ILAW Simulations for All Five Data Sets (differences in color) with All Uncertainties Set to the Low Cases (solid lines) and All Uncertainties Set to the High Cases (dashed lines) for Important ILAW Radionuclides

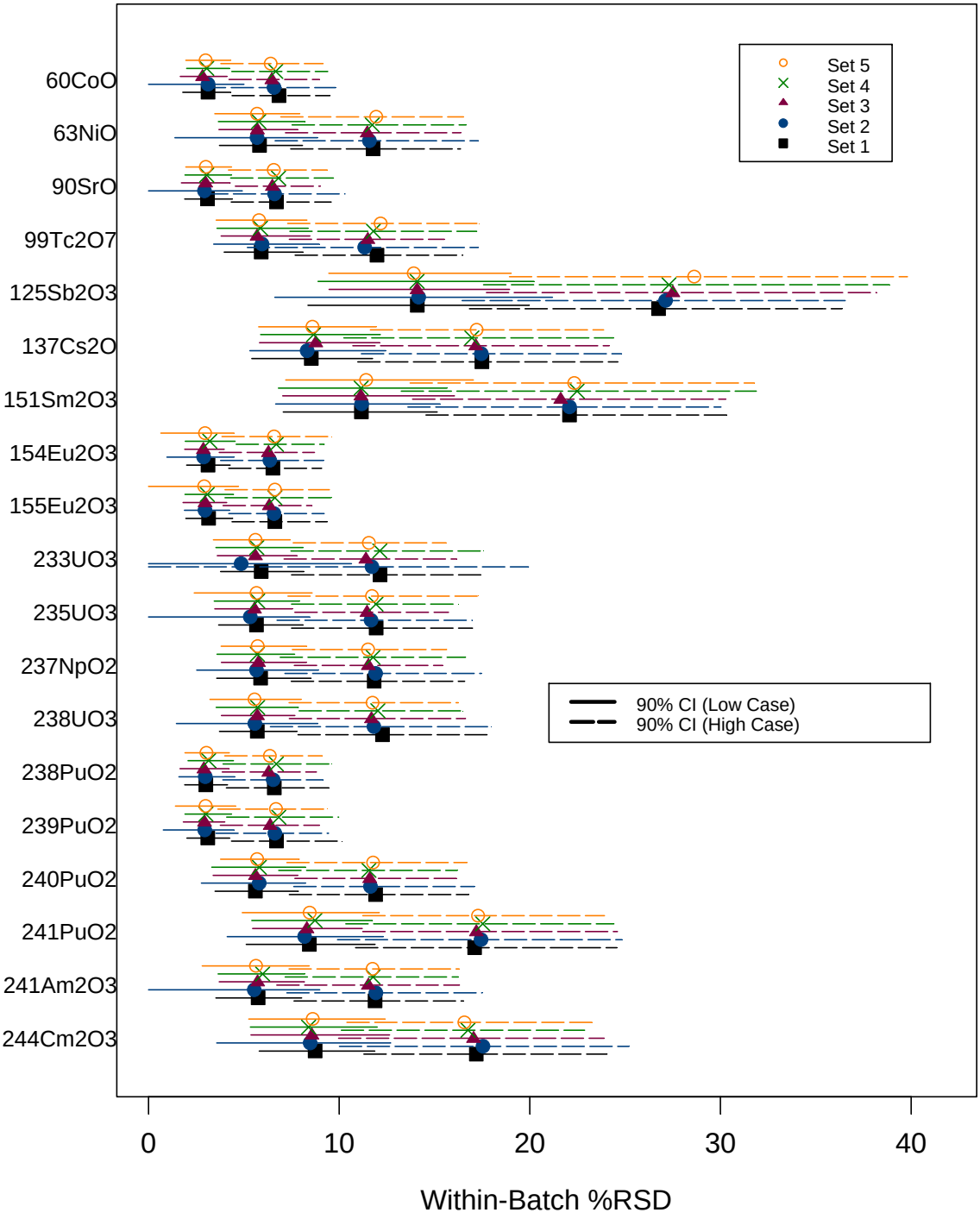

Figure 8.6. Means (the symbols) and 90% ECIs (lines) of Within-Batch %RSD Calculated from ILAW Simulations for All Five Data Sets (differences in color) with All Uncertainties Set to the Low Cases (solid lines) and All Uncertainties Set to the High Cases (dashed lines) for Important ILAW Radionuclides

Table 8.2. Percentage of Important ILAW Radionuclide Composition Components for which the Factor or Interaction had a Statistically Significant Effect on Total %RSD in the ANOVAs ($\alpha = 0.05$)[a]

Factor / Interaction	% of Significant Components	Statistically Significant Important Radionuclide Composition Components
$\%RSD_S(c_j^{CRV})$ [b], $\%RSD_A(c_j^{CRV})$ [b]	100	All
Data Set	94.7	^{60}CoO, ^{63}NiO, ^{90}SrO, $^{99}Tc_2O_7$, $^{137}Cs_2O$, $^{125}Sb_2O_3$, $^{154}Eu_2O_3$, $^{155}Eu_2O_3$, $^{233}UO_3$, $^{235}UO_3$, $^{237}NpO_2$, ^{60}CoO, $^{238}PuO_2$, $^{239}PuO_2$, $^{240}PuO_2$, $^{241}PuO_2$, $^{241}Am_2O_3$, $^{244}Cm_2O_3$
$\%RSD_S(c_j^{CRV}) \times \%RSD_A(c_j^{CRV})$	94.7	^{60}CoO, ^{63}NiO, ^{90}SrO, $^{99}Tc_2O_7$, $^{137}Csc_2O$, $^{151}Sm_2O_3$, $^{154}Eu_2O_3$, $^{155}Eu_2O_3$, $^{233}UO_3$, $^{235}UO_3$, $^{237}NpO_2$, $^{238}UO_3$, $^{238}PuO_2$, $^{239}PuO_2$, $^{240}PuO_2$, $^{241}PuO_2$, $^{241}Am_2O_3$, $^{244}Cm_2O_3$
Data Set × $\%RSD_A(c_j^{CRV})$	89.5	^{60}CoO, ^{63}NiO, ^{90}SrO, $^{99}Tc_2O_7$, $^{125}Sb_2O_3$, $^{154}Eu_2O_3$, $^{155}Eu_2O_3$, $^{233}UO_3$, $^{235}UO_3$, $^{237}NpO_2$, $^{238}UO_3$, $^{238}PuO_2$, $^{239}PuO_2$, $^{240}PuO_2$, $^{241}PuO_2$, $^{241}Am_2O_3$, $^{244}Cm_2O_3$
Data Set × $\%RSD_S(c_j^{CRV})$	57.9	^{60}CoO, ^{63}NiO, ^{90}SrO, $^{154}Eu_2O_3$, $^{155}Eu_2O_3$, $^{233}UO_3$, $^{238}UO_3$, $^{238}PuO_2$, $^{239}PuO_2$, $^{240}PuO_2$, $^{241}Am_2O_3$
$SD(a_k^{GFC})$ [b]	31.6	^{90}SrO, $^{154}Eu_2O_3$, $^{155}Eu_2O_3$, $^{238}UO_3$, $^{238}PuO_2$, $^{239}PuO_2$
$\%RSD_A(c_j^{CRV}) \times SD_V$	15.8	$^{151}Sm_2O_3$, $^{235}UO_3$, $^{238}UO_3$
$\%RSD_B(c_j^{CRV})$ [b]	10.5	$^{238}PuO_2$, $^{241}PuO_2$
$SD(G_{jk}^{GFC})$ [b]	10.5	^{60}CoO, $^{238}UO_3$
Data Set × $SD(G_{jk}^{GFC})$	10.5	$^{237}NpO_2$, $^{241}PuO_2$
$\%RSD_B(c_j^{CRV}) \times \%RSD_S(c_j^{CRV})$	10.5	$^{241}PuO_2$, $^{244}Cm_2O_3$
$\%RSD_A(c_j^{CRV}) \times SD(G_{jk}^{GFC})$	10.5	$^{238}PuO_2$, $^{240}PuO_2$
Data Set × $SD(a_k^{GFC})$, $SD(G_{jk}^{GFC}) \times SD(a_k^{GFC})$	5.3	$^{241}Am_2O_3$
$\%RSD_B(c_j^{CRV}) \times \%RSD_A(c_j^{CRV})$	5.3	$^{154}Eu_2O_3$
$\%RSD_B(c_j^{CRV}) \times SD(G_{jk}^{GFC})$, $\%RSD_B(c_j^{CRV}) \times SD_V$	5.3	$^{237}NpO_2$
$\%RSD_S(c_j^{CRV}) \times SD(G_{jk}^{GFC})$	5.3	$^{233}UO_3$
$\%RSD_S(c_j^{CRV}) \times SD_V$	5.3	$^{244}Cm_2O_3$
$\%RSD_A(c_j^{CRV}) \times SD(a_k^{GFC})$	5.3	$^{154}Eu_2O_3$
$SD(G_{jk}^{GFC}) \times SD_V$	5.3	$^{151}Sm_2O_3$
SD_V [c], Data Set × $\%RSD_B(c_j^{CRV})$, Data Set × SD_V, $\%RSD_B(c_j^{CRV}) \times SD(a_k^{GFC})$, $\%RSD_S(c_j^{CRV}) \times SD(a_k^{GFC})$, $SD(a_k^{GFC}) \times SD_V$	0	None

(a) Only two-factor interactions were included in the ANOVA model.
(b) This factor has a "low" case and a "high" case.
(c) The notation SD_V represents both SD_V^{CRV} and SD_V^{MFPV}. This factor has a "low" and "high" case, where both SD_V^{CRV} and SD_V^{MFPV} are varied at the same time.

From Table 8.2, it can be seen that changes in the %RSD of both CRV mixing/sampling ($\%RSD_S(c_j^{CRV})$) and CRV analytical ($\%RSD_A(c_j^{CRV})$) significantly affected the total variation plus uncertainties for all of the important ILAW radionuclide composition components. As expected, there were significant differences in total variation plus uncertainties across the five data sets. Changes in the "GFC uncertainties" and "GFC masses added" significantly affected the total variation plus uncertainty for a few of the studied radionuclide composition components. Changes in random batch-to-batch variation ($\%RSD_B(c_j^{CRV})$) and volume random uncertainty, as well as interactions containing either of these factors, had little affect on nearly all of the important ILAW radionuclide composition components.

The main conclusion from these ANOVA results is that the values of total %RSD for ILAW radionuclide composition components (mass fractions) can vary substantially, depending on the data set (LAW waste type) as well as the mixing/sampling uncertainty %RSD and the analytical uncertainty %RSD for concentrations of analytes in the ILAW MFPV. These same three factors also had statistically significant effects for most of the chemical composition components (see Section 8.1). However, the uncertainties in GFC compositions and amounts of GFCs added to ILAW MFPV batches had significant effects on the total %RSD for many chemical composition components, whereas they have significant effects for smaller percentages of radionuclide composition components.

8.3 Results on the Variations and Uncertainties of ILAW Glass Properties

This section discusses calculating and summarizing batch-to-batch variations, within-batch uncertainties, and total variation plus uncertainties of the ILAW properties of interest. Section 8.3.1 presents the variation and uncertainty results for PCT normalized releases of B and Na from LAW glasses. Section 8.3.2 presents the variation and uncertainty results for VHT alteration depth of LAW glasses. Section 8.3.3 presents the variation and uncertainty results for viscosity of LAW glasses at temperatures of 1373.15 K (1100ºC) and 1423.15 K (1150ºC). Section 8.3.4 presents the variation and uncertainty results for electrical conductivity of LAW glasses at temperatures of 1373.15 K (1100ºC) and 1473.15 K (1200ºC).

8.3.1 Results on the Variations and Uncertainties for PCT Normalized Releases of B and Na from LAW Glasses

Chemical compositions of ILAW MFPV batches were calculated for 10 MFPV batches per LAW data set (waste type) and 200 Monte Carlo simulations for each of 64 scenarios as discussed in Section 8.1. These ILAW compositions corresponding to MFPV batches and the model coefficients from Table 6.6 were inserted into Eqs. (6.2.8) and (6.2.7a) to calculate the predicted natural logarithm of the PCT normalized release of B and Na for each of the 200 simulations within each of the 64 scenarios.

The %RSD values for batch-to-batch variations ($\%RSD_B$), within-batch uncertainties ($\%RSD_W$), and total variations plus uncertainties ($\%RSD_T$) were calculated for PCT B and PCT Na[(a)] across

(a) Untransformed values of PCT B and Na releases (g/L) were obtained by taking the antilog of the values in natural logarithm units, and then %RSDs were calculated using the untransformed values.

10 batches for each scenario in Table 5.4 and each of the 200 simulations within each scenario using Eqs. (6.2.12), (6.2.15), and (6.2.18), respectively. The $\%RSD_T$, $\%RSD_B$, and $\%RSD_W$ values were then summarized for each of the 64 scenarios for each of the five data sets by calculating the mean, and the lower and upper 90% empirical confidence limits from the 200 simulations. The $\%RSD_T$ summaries were calculated using Eqs. (6.2.13), (6.2.14a), and (6.2.14b). The $\%RSD_B$ summaries were calculated using Eqs. (6.2.16), (6.2.17a), and (6.2.17b). The $\%RSD_W$ summaries were calculated using Eqs. (6.2.19), (6.2.20a), and (6.2.20b).

Figure 8.7 summarizes the $\%RSD_T$, $\%RSD_B$, and $\%RSD_W$ results for PCT B and PCT Na releases. The top and bottom panels in Figure 8.7 show that PCT B and Na releases have mean values of $\%RSD_T$ and $\%RSD_W$, roughly from 5% to 20% for the low case, and from 10% to 40% for the high case. As expected, the high-case 90% ECIs (dashed lines) indicate a larger amount of variation and uncertainty than the low-case 90% ECIs (solid lines) for $\%RSD_T$ and $\%RSD_W$. The second panel of Figure 8.7 shows that $\%RSD_B$ mean values for PCT B and Na releases are from 0.5% to 4%. The high-case 90% ECIs and low-case 90% ECIs are non-significantly different for $\%RSD_B$ because the batch-to-batch variation does not include any of the uncertainties caused by GFC compositions, GFCs added, or CRV mixing/sampling and analytical. The batch-to-batch variation is larger for the second data set, which is the transition from AP-101/AY-102 to AZ-101. The variation is larger because of the amount of change that occurs from batch to batch during the transition for the glass components in the PCT models. It is clear from Figure 8.7 that the within-batch uncertainties in PCT B and Na releases are much larger than the batch-to-batch variations and thus are the main contributor to total variation plus uncertainties.

The Monte Carlo simulated glass property data were also analyzed using ANOVA in the same manner used on the chemical and radionuclide compositions in Sections 8.1 and 8.2, respectively. Table 8.3 summarizes the results from the ANOVAs for ILAW glass properties. The factors [namely Data Set, $\%RSD_S(c_j^{MFPV})$, $\%RSD_A(c_j^{MFPV})$, $SD(G_{jk}^{GFC})$, and $SD(a_k^{GFC})$] significantly affect Total %RSD values for PCT B and Li releases. Most of the two-way interactions involving these factors were also significant. The factors SD_V and $\%RSD_B(c_j^{CRV})$ and the interactions involving these factors had no significant effects.

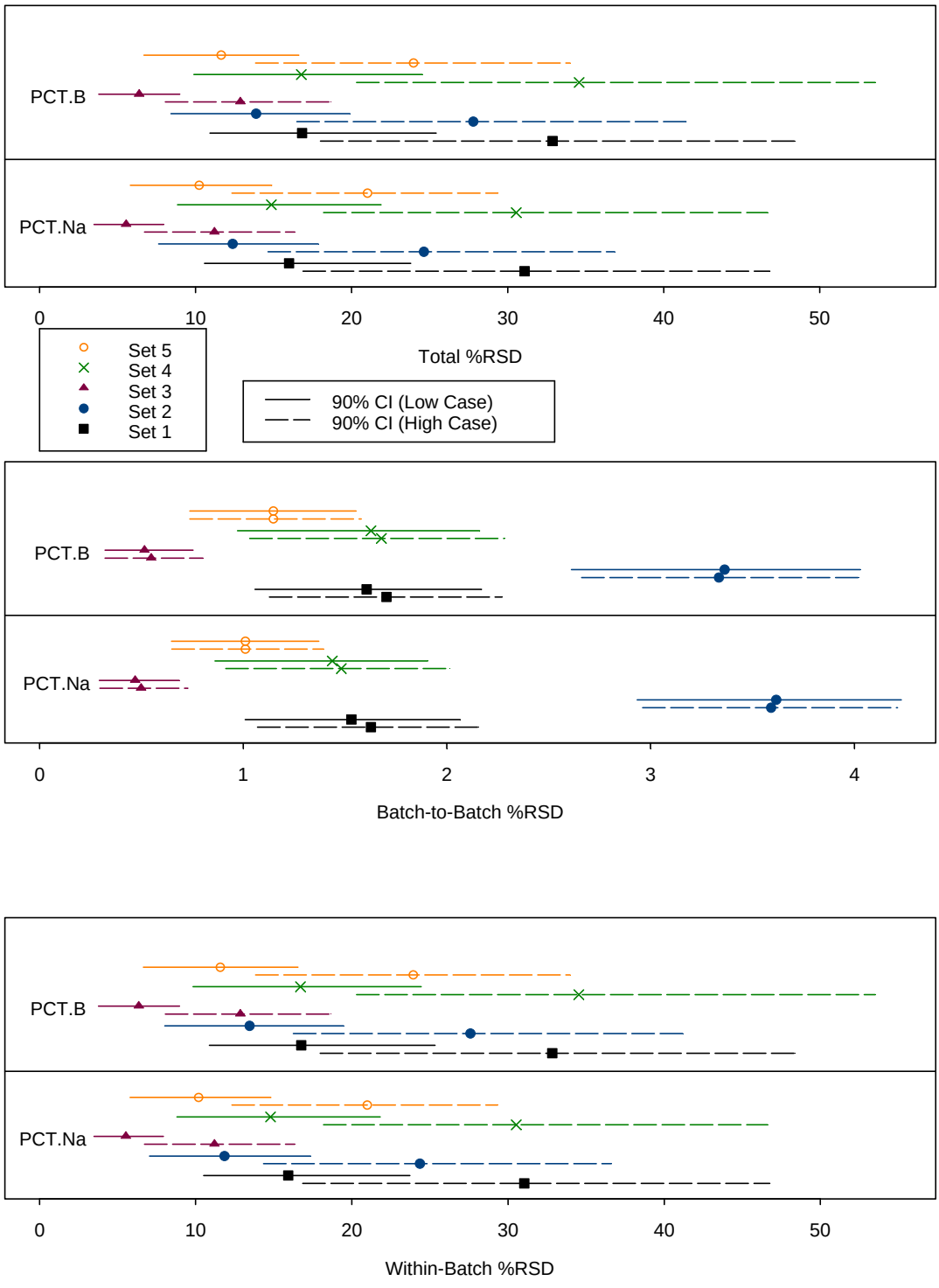

Figure 8.7. Means (the symbols) and 90% ECIs (lines) of Total, Batch-to-Batch, and Within-Batch %RSDs for PCT_B and PCT_{Na} Calculated from ILAW Simulations for All Five Data Sets (differences in color) with All Uncertainties Set to the Low Cases (solid lines) and All Uncertainties Set to the High Cases (dashed lines)

Table 8.3. Factors or Interactions with Statistically Significant Effects on Total %RSD for All ILAW Glass Properties Using ANOVAs ($\alpha = 0.05$)[a]

Factor/Interaction	PCT B	PCT Na	VHT	Viscosity 1100°C	Viscosity 1150 °C	Electrical Conductivity 1100 °C	Electrical Conductivity 1200 °C
Data Set, $\%RSD_S(c_j^{CRV})$[b], $\%RSD_A(c_j^{CRV})$[b], $SD(a_k^{GFC})$[b], Data Set × $\%RSD_S(c_j^{CRV})$, Data Set × $\%RSD_A(c_j^{CRV})$, Data Set × $SD(G_{jk}^{GFC})$, Data Set × $SD(a_k^{GFC})$, $\%RSD_S(c_j^{CRV})$ × $\%RSD_A(c_j^{CRV})$	X[d]	X	X	X	X	X	X
$SD(G_{jk}^{GFC})$[b], $\%RSD_A(c_j^{CRV})$ × $SD(a_k^{GFC})$	X	X	X	X	X		
$\%RSD_A(c_j^{CRV})$ × $SD(G_{jk}^{GFC})$	X	X	X				
$\%RSD_B(c_j^{CRV})$[b], SD_V[c], Data Set × $\%RSD_B(c_j^{CRV})$, Data Set × SD_V, $\%RSD_B(c_j^{CRV})$ × $\%RSD_S(c_j^{CRV})$, $\%RSD_B(c_j^{CRV})$ × $\%RSD_A(c_j^{CRV})$, $\%RSD_B(c_j^{CRV})$ × $SD(G_{jk}^{GFC})$, $\%RSD_B(c_j^{CRV})$ × $SD(a_k^{GFC})$, $\%RSD_B(c_j^{CRV})$ × SD_V, $\%RSD_S(c_j^{CRV})$ × $SD(G_{jk}^{GFC})$, $\%RSD_S(c_j^{CRV})$ × $SD(a_k^{GFC})$, $\%RSD_S(c_j^{CRV})$ × SD_V, $\%RSD_A(c_j^{CRV})$ × SD_V, $SD(G_{jk}^{GFC})$ × $SD(a_k^{GFC})$, $SD(G_{jk}^{GFC})$ × SD_V, $SD(a_k^{GFC})$ × SD_V							

(a) Only two-factor interactions were included in the ANOVA model.
(b) This factor has a "low" case and a "high" case.
(c) The notation SD_V represents both SD_V^{CRV} and SD_V^{MFPV}. This factor has a "low" and "high" case where both SD_V^{CRV} and SD_V^{MFPV} are varied at the same time.
(d) An "X" means that the factor or interactions are significant for that particular glass property.

8.3.2 Results on the Variations and Uncertainties for VHT Alteration Rate of LAW Glasses

Chemical compositions of ILAW MFPV batches were calculated for 10 MFPV batches per LAW data set (waste type) and 200 Monte Carlo simulations for each of 64 scenarios as discussed in Section 8.1. These ILAW compositions corresponding to MFPV batches and the VHT model coefficients from Table 6.6 were inserted into Eqs. (6.2.8) and (6.2.7a) to calculate the predicted natural logarithm of the VHT alteration depth for each of the 200 simulations within each of the 64 scenarios. The VHT alteration rate (μm) was then calculated from the natural logarithms of VHT alteration depths (g/m^2day) using Eq. (6.2.9).

The %RSD values for batch-to-batch variations ($\%RSD_B$), within-batch uncertainties ($\%RSD_W$), and total variations plus uncertainties ($\%RSD_T$) were calculated for VHT alteration rates[(a)] across 10 MFPV batches for each scenario in Table 5.4 and each of the 200 simulations within each scenario. The same process and equations used to calculate %RSDs for PCT releases (see the second paragraph of Section 8.3.1) were also used to calculate %RSDs for VHT alteration rates.

Figure 8.8 summarizes the $\%RSD_T$, $\%RSD_B$, and $\%RSD_W$ results for the VHT alteration rate (g/m^2day). The top and bottom panels in Figure 8.8 show mean values of $\%RSD_T$ and $\%RSD_W$, roughly from 5% to 22% for the low case, and from 10% to 50% for the high case. As expected, the high-case 90% ECIs (dashed lines) indicate a larger amount of variation and uncertainty than the low-case 90% ECIs (solid lines) for $\%RSD_T$ and $\%RSD_W$. The second panel of Figure 8.8 shows that $\%RSD_B$ mean values range from 0.5% to 2% for four of the data sets whereas the transition data set # 2 has $\%RSD_B$ values ranging from 9% to 10%. The variation is larger because of the magnitude of change that occurs from batch to batch during the transition for the glass components in the VHT model. The high-case 90% ECIs and low-case 90% ECIs are non-significantly different for $\%RSD_B$ because the batch-to-batch variation does not include any of the uncertainties caused by GFC composition, GFCs added, or CRV mixing/sampling and analytical uncertainties. It is clear from Figure 8.8 that the within-batch uncertainties in the VHT alteration rate are much larger than the batch-to-batch variations and thus are the main contributor to total variation plus uncertainties.

The Monte Carlo simulated glass property data were also analyzed using ANOVA in the same manner used on the chemical and radionuclide compositions in Sections 8.1 and 8.2, respectively. Table 8.3 summarizes the results from the ANOVAs for ILAW glass properties. The factors [namely Data Set, $\%RSD_S(c_j^{MFPV})$, $\%RSD_A(c_j^{MFPV})$, $SD(G_{jk}^{GFC})$, and $SD(a_k^{GFC})$] significantly affect Total %RSD values for VHT alteration. Most of the two-way interactions involving these factors were also significant. The factors SD_V and $\%RSD_B(c_j^{CRV})$ and the interactions involving these factors had no significant effects.

(a) Model predicted values of ln(VHT alteration depths) in units of ln(μm) for simulated ILAW compositions were converted to untransformed alteration depths by taking the antilog and were then transformed to the VHT alteration rate (g/m^2day) values. Those values were then used to calculate %RSDs for VHT alteration rates (g/m^2day).

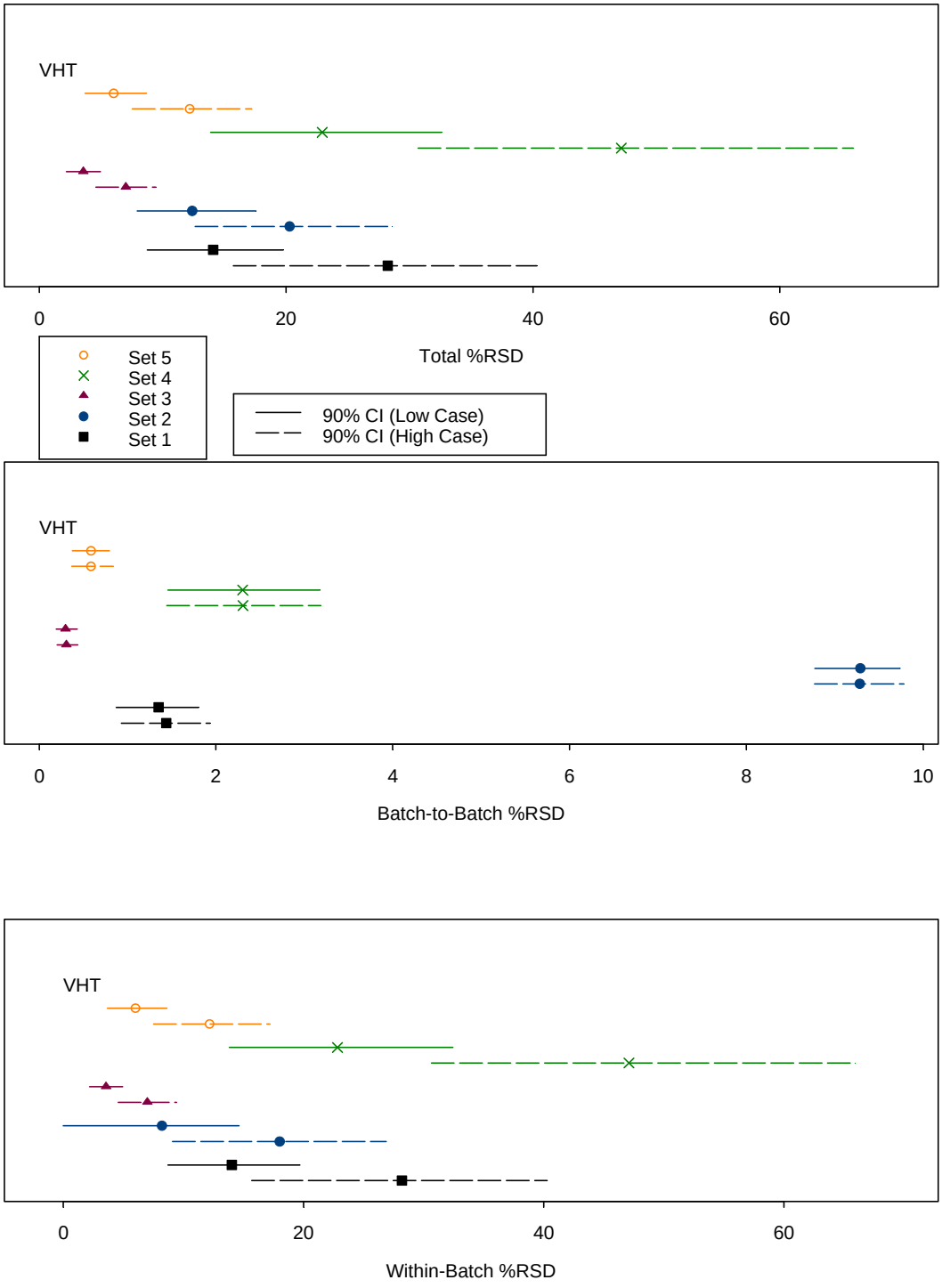

Figure 8.8. Means (the symbols) and 90% ECIs (lines) of Total, Batch-to-Batch, and Within-Batch %RSDs for VHT Alteration Rates Calculated from ILAW Simulations for All Five Data Sets (differences in color) with All Uncertainties Set to the Low Cases (solid lines) and All Uncertainties Set to the High Cases (dashed lines)

8.3.3 Results on the Variations and Uncertainties for Viscosity of LAW Glasses

Chemical compositions of ILAW MFPV batches were calculated for 10 MFPV batches per LAW data set (waste type) and 200 Monte Carlo simulations for each of 64 scenarios as discussed in Section 8.1. These ILAW compositions corresponding to MFPV batches, the viscosity model coefficients from Table 6.7, and temperatures of 1373.15 K (1100ºC) and 1423.15 K (1150ºC) were inserted into Eq. (6.2.10) to calculate the predicted natural logarithm of viscosity at the given temperatures for each of the 200 simulations within each of the 64 scenarios.

The %RSD values for batch-to-batch variations ($\%RSD_B$), within-batch uncertainties ($\%RSD_W$), and total variations plus uncertainties ($\%RSD_T$) were calculated for viscosity at 1373.15 K and 1423.15 K[(a)] across 10 MFPV batches for each waste type and scenario in Table 5.4 and each of the 200 simulations within each scenario. The same process and equations used to calculate %RSDs for PCT releases (see the second paragraph of Section 8.3.1) were also used for calculating viscosity %RSDs.

Figure 8.9 summarizes the $\%RSD_T$, $\%RSD_B$, and $\%RSD_W$ results for viscosity (poise) at each temperature. The top and bottom panels in Figure 8.9 show mean values of $\%RSD_T$ and $\%RSD_W$, roughly from 5% to 15% for the low case and from 10% to 30% for the high case. As expected, the high-case 90% ECIs (dashed lines) indicate a larger amount of variation and uncertainty than the low-case 90% ECIs (solid lines) for $\%RSD_T$ and $\%RSD_W$. The second panel of Figure 8.9 shows that $\%RSD_B$ mean values are around 1% for four of the data sets whereas the transition data set # 2 has $\%RSD_B$ values ranging from 11% to 13%. The variation for Set 2 is larger because of the magnitude of change that occurs from batch to batch during the transition for the glass components in the viscosity model. The high-case 90% ECIs and low-case 90% ECIs are non-significantly different for $\%RSD_B$ because the batch-to-batch variation does not include any of the uncertainties caused by GFC composition, GFCs added, or CRV mixing/sampling and analytical uncertainties. It is clear from Figure 8.9 that the within-batch uncertainties in viscosity are much larger than the batch-to-batch variations, and thus are the main contributor to total variation plus uncertainties.

The Monte Carlo simulated glass property data were also analyzed using ANOVA in the same manner used on the chemical and radionuclide compositions in Sections 8.1 and 8.2, respectively. Table 8.3 summarizes the results from the ANOVAs for ILAW glass properties. The factors [namely Data Set, $\%RSD_S(c_j^{MFPV})$, $\%RSD_A(c_j^{MFPV})$, $SD(G_{jk}^{GFC})$, and $SD(a_k^{GFC})$] significantly affect Total %RSD values for viscosity at 1373.15 K (1100ºC) and 1423.15 K (1150ºC). Most of the two-way interactions involving these factors were also significant. The factors SD_V and $\%RSD_B(c_j^{CRV})$ and the interactions involving these factors had no significant effects.

(a) Untransformed values of viscosity at the respective temperatures were obtained by taking the antilog of the values in natural logarithm units, and then %RSDs were calculated using the untransformed values.

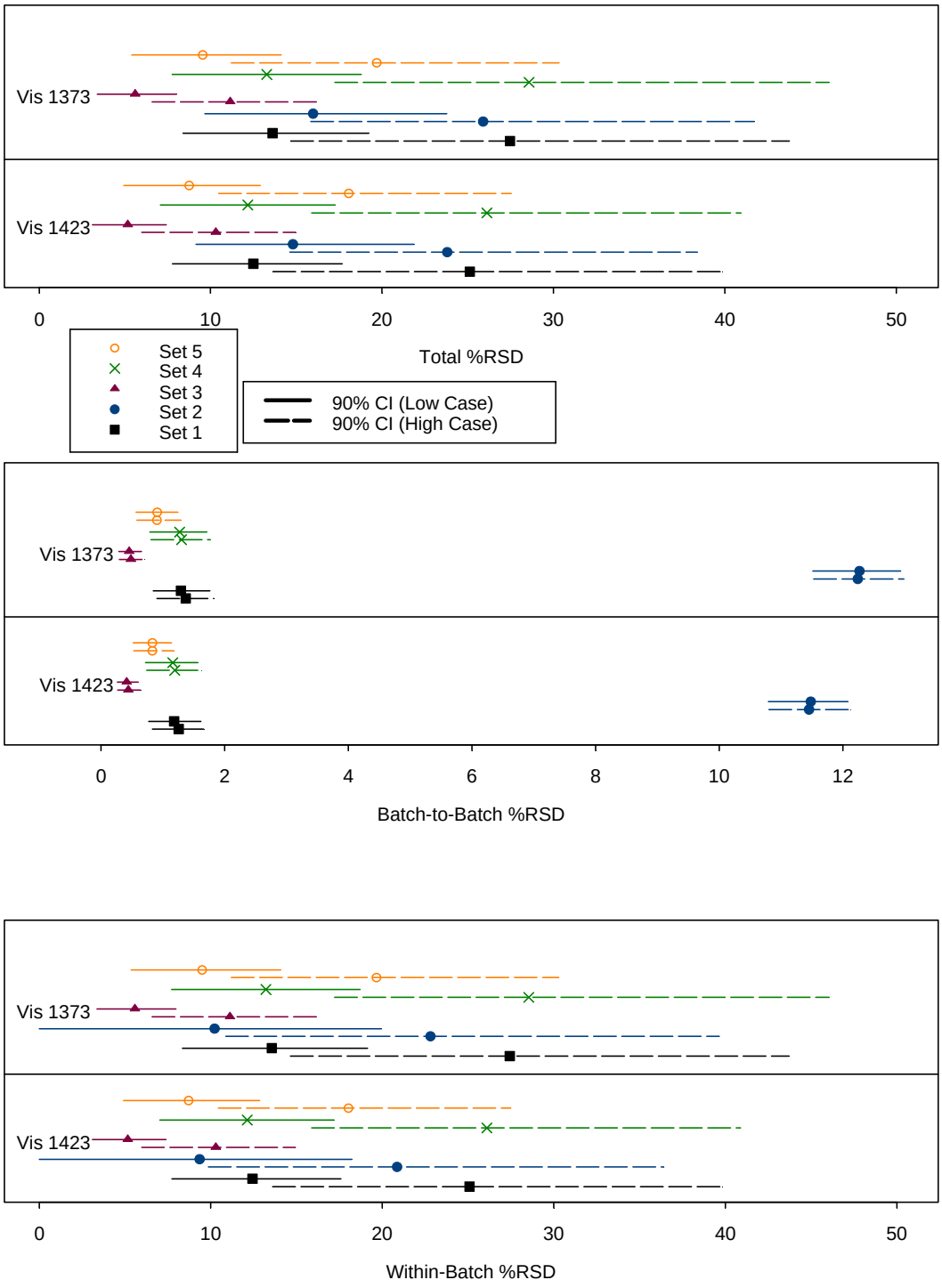

Figure 8.9. Means (the symbols) and 90% ECIs (lines) of Total, Batch-to-Batch, and Within-Batch %RSDs for Viscosity at 1373.15 K and 1423.15 K Calculated from ILAW Simulations for All Five Data Sets (differences in color) with All Uncertainties Set to the Low Cases (solid lines) and All Uncertainties Set to the High Cases (dashed lines)

8.3.4 Results on the Variations and Uncertainties for Electrical Conductivity of LAW Glasses

Chemical compositions of ILAW MFPV batches were calculated for 10 MFPV batches per LAW data set (waste type) and 200 Monte Carlo simulations for each of 64 scenarios as discussed in Section 8.1. These ILAW compositions corresponding to MFPV batches, the electrical conductivity model coefficients from Table 6.8, and temperatures of 1373.15 K (1100ºC) and 1473.15 K (1200ºC) were inserted into Eq. (6.2.11) to calculate the predicted natural logarithm of electrical conductivity at the given temperatures for each of the 200 simulations within each of the 64 scenarios for each of the five data sets.

The %RSD values for batch-to-batch variations ($\%RSD_B$), within-batch uncertainties ($\%RSD_W$), and total variations plus uncertainties ($\%RSD_T$) were calculated for electrical conductivity at 1373.15 K and 1473.15 K[(a)] across 10 MFPV batches for each scenario in Table 5.4 and each of the 200 simulations within each scenario. The same process and equations used to calculate %RSDs for PCT releases (see the second paragraph of Section 8.3.1) were also used for calculating electrical conductivity %RSDs.

Figure 8.10 summarizes the $\%RSD_T$, $\%RSD_B$, and $\%RSD_W$ results for electrical conductivity (S/cm) at each temperature. The top and bottom panels in Figure 8.10 show mean values of $\%RSD_T$ and $\%RSD_W$, roughly from 4% to 10% for the low case and from 7% to 22% for the high case. As expected, the high-case 90% ECIs (dashed lines) indicate a larger amount of variation and uncertainty than the low-case 90% ECIs (solid lines) for $\%RSD_T$ and $\%RSD_W$. The second panel of Figure 8.10 shows that the $\%RSD_B$ mean values are around 1%. It is interesting to note that the batch-to-batch variation is small for each of the five data sets, including the transition data set. This appears to result from the fact that many of the oxides with larger coefficients in the electrical conductivity model (Table 6.8) are oxides with smaller batch-to-batch variation for the transition data set (see Figure 8.2). It is clear from Figure 8.10 that the within-batch uncertainties in viscosity are much larger than the batch-to-batch variations, and thus are the main contributor to total variation plus uncertainties.

The Monte Carlo simulated glass property data were also analyzed using ANOVA in the same manner used on the chemical and radionuclide compositions in Sections 8.1 and 8.2, respectively. Table 8.3 summarizes the results from the ANOVAs for ILAW glass properties. The factors [namely Data Set, $\%RSD_S(c_j^{MFPV})$, $\%RSD_A(c_j^{MFPV})$, and $SD(a_k^{GFC})$] significantly affect Total %RSD values for electrical conductivity at 1373.15 K (1100ºC) and 1473.15 K (1200ºC). Most of the two-way interactions involving these factors were also significant. The factors $SD(G_{jk}^{GFC})$, SD_V , and $\%RSD_B(c_j^{CRV})$ and most of the interactions involving these factors had no significant effects on Total %RSD values for electrical conductivity.

(a) Untransformed values of electrical conductivity at the respective temperatures were obtained by taking the antilog of the values in natural logarithm units, and then %RSDs were calculated using the untransformed values.

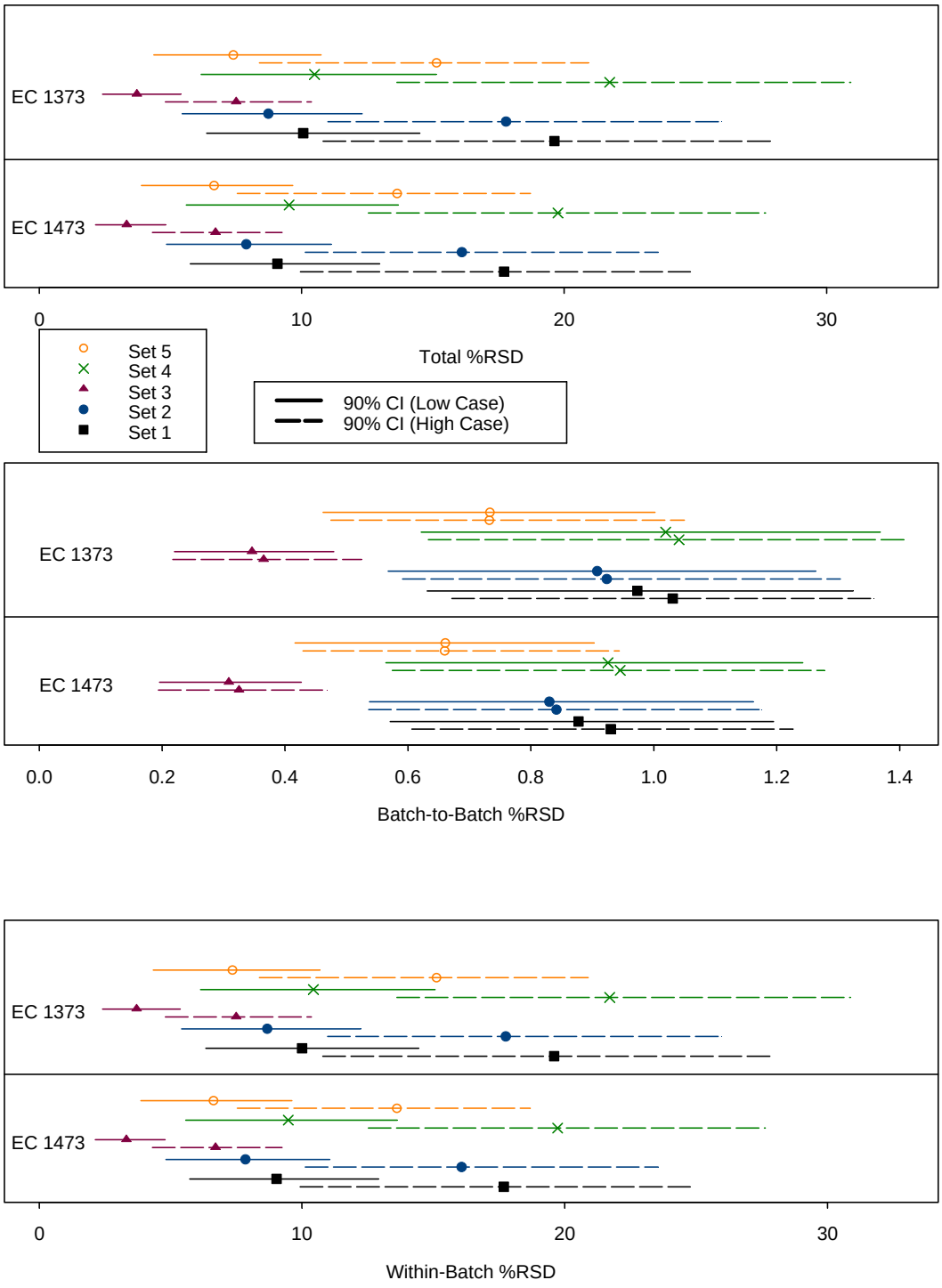

Figure 8.10. Means (the symbols) and 90% ECIs (lines) of Total, Batch-to-Batch, and Within-Batch %RSDs for Electrical Conductivity at 1373.15 K and 1473.15 K Calculated from ILAW Simulations for All Five Data Sets (differences in color) with All Uncertainties Set to the Low Cases (solid lines) and All Uncertainties Set to the High Cases (dashed lines)

9.0 Summary of IHLW and ILAW Variation and Uncertainty Estimates and Remaining Needs

Section 9.1 summarizes the current estimates of variations and uncertainties affecting various steps of the HLW and LAW vitrification processes. Section 9.2 summarizes the estimates of variations and uncertainties for IHLW and ILAW compositions (expressed as mass fractions of oxide and halogen components) and properties. Section 9.3 summarizes future work that is planned or is recommended to obtain data that will provide sufficient bases to quantify the variations and uncertainties that will affect the WTP HLW and LAW vitrification facilities. Such data will in turn provide for obtaining final estimates of variations and uncertainties of IHLW and ILAW compositions and properties.

9.1 Current Estimates of Variations and Uncertainties Affecting Steps of the WTP HLW and LAW Vitrification Processes

This section summarizes the results of using WTP Project data and information to develop current estimates of variations and uncertainties that will affect the WTP HLW and LAW vitrification processes. Included are the major sources of variation and uncertainty normally associated with a batch process (variation across batches over time, mixing, sampling, chemical analyses, volume, weight, and density measurements). Estimates of variations and uncertainties expected in the WTP HLW and LAW vitrification facilities were accumulated as discussed in the following bullets.

- IHLW MFPV and LAW CRV batch-to-batch variation. There were no WTP data for estimating both systematic and random batch-to-batch variations for analyte concentrations in the IHLW MFPV or the LAW CRV. In the work for this report, random batch-to-batch variation %RSDs for elemental concentrations were assumed to be (1) 1, 5, or 10% in the IHLW MFPV after GFC addition (see Sections 4.1 and 5.2) and (2) 1 or 5% in the LAW CRV (see Sections 4.1 and 5.3).

- IHLW MFPV and ILAW CRV mixing/sampling uncertainties. Experimental work to quantify mixing and sampling uncertainties in IHLW MFPVs and LAW CRVs is planned for the future (Sundar 2005a, 2005b). Based on DWPF, WVSP, and other experience, the WTP Project provided estimates of combined mixing/sampling uncertainties for use in the work described in this report. Sections 4.2.1 and 4.5.1 discuss mixing uncertainties whereas Sections 4.2.2 and 4.5.2 discuss sampling uncertainties. For the IHLW MFPV, low and high %RSD values of 1 and 5% were estimated as covering the likely range of combined mixing and sampling uncertainties for all soluble chemical composition analytes. The %RSD values of 5 and 15% were estimated for all insoluble chemical composition analytes. Low and high mixing/sampling %RSD values of 1 and 5% were estimated for all radionuclide analytes. For the LAW CRV, low and high mixing/sampling %RSD values of 1 and 5% were estimated for all chemical and radionuclide composition components.

- IHLW MFPV composition analytical uncertainties. Analytical uncertainties for elemental concentrations of chemical composition and radionuclide analytes in the IHLW MFPV were assessed by the WTP analytical group for HLW from tanks AY-102, AZ-102, and C-104. Random analytical uncertainty %RSDs are listed in Table C.1 for chemical composition analytes

and in Tables C.2 and C.3 for radionuclide analytes. Estimates of analytical uncertainty %RSDs for concentrations of chemical composition analytes in an IHLW MFPV range from 5 to 50%. However, the %RSD = 50 value occurs for only one analyte (V) in AY-102. Analytical %RSDs are below 25% for all other analytes. For radionuclides in an IHLW MFPV, the estimated %RSDs range from 5 to 60%, with most values below 25%. High estimates of analytical uncertainty are generally two times the nominal (denoted "low") estimates, with a few exceptions.

- LAW CRV composition analytical uncertainties. Analytical uncertainties for elemental concentrations of chemical and radionuclide composition components in the LAW CRV were assessed by the WTP analytical group. Table D.6 lists random analytical uncertainty %RSDs. Estimates of analytical uncertainties for elemental concentrations of chemical composition analytes in an LAW CRV range from 5 to 50 %RSD depending on the analyte and its concentration. However, the %RSD = 50 values occur infrequently and correspond to radionuclide analytes near detection or quantitation limits. Most %RSDs for elemental concentrations of chemical composition and radionuclide analytes are below 25%.

- LAW CRV density measurement uncertainties. Table 4.1 summarizes density measurement uncertainty estimates for LAW in the CRV. These estimates were based on measurements made by PNWD and SRTC on liquid phases from several different Hanford LAW tanks to be processed by WTP. Density measurement %RSDs (for LAW only) ranged from 0 to 0.5% whereas SDs ranged from 0 to 0.00625 g/mL. These uncertainty results are quite small. They may or may not be representative of uncertainties that will be experienced by the WTP for their laboratory and in-line methods of measuring density. These uncertainty estimates should be evaluated before operations. The current estimates are the best available at this time.

- IHLW MFPV, LAW CRV, and ILAW MFPV level and volume uncertainties. Uncertainties in IHLW and ILAW CRV and MFPV level measurements and corresponding volumes were quantified using vendor information and vessel design information. A level measurement SD of 0.5 inch was chosen as a compromise between a vendor accuracy estimates of 0.5 to 0.75 inches and total uncertainty estimates by knowledgeable personnel of 0.5 to 1.5 inches for measuring levels of vessels while being mixed.[(a)] The 0.5-inch level SD was translated to volume SDs using design information about CRVs and MFPVs in the WTP HLW and LAW vitrification facilities. For HLW, the volume SD was 112.05 liters for the MFPV (and MFV). For LAW, the volume SD was approximately 181.62 liters for the CRV and 112.12 liters for the MFPV (and MFV). For the work in this report, the preceding SD values were treated as low estimates of uncertainty. High estimates of uncertainty equal to two times the low estimates were used (see Table C.4 for IHLW and Table D.11 for ILAW).

- HLW MFPV and LAW CRV composition uncertainties for transfers. As discussed in Sections 4.2.5 and 4.5.5, no data were available to quantify composition uncertainties associated with transferring material from (1) the CSV to the CRV, the CRV to the MFPV, or the MFPV to the MFV for LAW or (2) the HBV to the MFPV or the MFPV to the MFV for HLW. However, only transfer uncertainties from the LAW CRV to the LAW MFPV are relevant to the work in

(a) Section 4.3 explains the rationale for this being a compromise.

this report. In that case, it was assumed there is no systematic uncertainty and that random uncertainty is negligible compared to random mixing uncertainties in the LAW CRV and MFPV. Hence, no estimates of composition uncertainties associated with vessel transfers are provided in this report.

- GFC composition uncertainties. Information consisting of nominal values and expected ranges was gathered from vendor information sheets where available. The ranges for the GFC components tended to be very tight (see Table D.9). Nominal values were occasionally outside the ranges given in information collected 2 to 3 years ago for previous work. Hence, there is some reason to question whether GFC compositions will actually vary as little as claimed in current vendor information. For GFCs where no vendor information was available, uncertainties were "interpolated" using uncertainties from other GFCs with components having comparable levels of a given oxide component.

- GFC batching, weighing, and transfer uncertainties. Section 4.4.2 discusses possible uncertainties associated with weighing GFCs using load cells on the GFC weigh hoppers. Information from four vendors (Cooper 2002; Sensotec 2003; Futek 2003; Amcells 2003) of precision (not ultra-precision) load cells indicates non-repeatability is ±0.02 to 0.05% of R.C., non-linearity is ±0.03 to 0.10% of R.C., and hysteresis is ±0.02 to 0.20% of R.C. WTP GFC weigh hoppers have been estimated to require load cells with R.C.s of 3,000 to 50,000 lb. Reproducibility uncertainties were not quantified by the load cell vendors, but would be expected to be somewhat larger than repeatability uncertainties. Therefore, the vendor non-repeatability uncertainty estimates underestimate the combined repeatability and reproducibility uncertainties in load cell determinations of weight.

  At the time of this work, WTP Project testing or other data on the magnitudes of GFC batching and transfer uncertainties were not available. However, the WTP Project has set design requirements for the GFC facility, as discussed in Section 4.4.3. These requirements include (1) the weight of any individual GFC shall not vary more than 0.5% from the weight required by the recipe, and (2) the total weight of any complete batch of GFCs shall not vary more than 2% from the required weight.

Section 9.3 summarizes the work/data needed to quantify each source of variation or uncertainty associated with the MFPV in the WTP HLW vitrification process and with the CRV and MFPV in the WTP LAW vitrification process.

The SD and %RSD estimates summarized in this section, as well as the more detailed information in Section 4, are the best currently available. All of the estimates are based on non-prototypic samples, non-prototypic preparation/analysis/measurement methods, vendor information sheets, and project design or equipment goals (which in some cases may eventually prove to be overly optimistic). The estimates in this report will need to be evaluated as additional research and technology (R&T) testing, vendor selection and certification, and cold and hot commissioning results become available. Section 9.3 discusses the additional data and work needed to quantify variations and uncertainties affecting the WTP HLW and LAW vitrification processes. This will then provide for quantifying the variations and uncertainties in IHLW and ILAW compositions and properties, which are important for IHLW and ILAW process control and compliance activities.

9.2 Current Estimates of Variations and Uncertainties in IHLW and ILAW Compositions and Properties

This section summarizes the results of applying Monte Carlo simulations to mass-balance equations for calculating IHLW and ILAW compositions and then using property-composition models to calculate glass property values. The estimates of variations and uncertainties affecting the HLW and LAW vitrification processes that served as inputs to the Monte Carlo simulations are preliminary at this time. Hence, combinations of low and high values of variations and uncertainties specified by computer experimental designs were used in the Monte Carlo simulations. The possible combinations of variations and uncertainties in the HLW and LAW vitrification processes were propagated through the applicable mass-balance equations as part of the Monte Carlo simulations. The resulting simulated data were used to calculate %RSD estimates of variation and uncertainty in IHLW and ILAW compositions (mass fractions of oxide or halogen components) and glass properties. Glass properties were calculated using the currently available property-composition models. Note that the WTP Project has work planned to update all property models. Section 9.2.1 summarizes the ranges of %RSD values for variation, uncertainty, and total variation plus uncertainty obtained for IHLW, and Section 9.2.2 summarizes the ranges for ILAW.

9.2.1 Summary of Variations and Uncertainties for IHLW Compositions and Properties

Table 9.1 contains the minimums and maximums of mean values of batch-to-batch, within-batch, and total %RSDs for the important IHLW chemical composition components. The mean %RSDs were calculated over the 200 simulations for each scenario and each HLW waste type. For each of the four HLW waste types (AY-102, AZ-102, C-104, and the transition between AY-102 and AZ-102), the minimums and maximums of mean %RSD values were determined over all variation and uncertainty scenarios (shown in Table 5.1). The mean values of batch-to-batch, within-batch, and total %RSDs for each of the important IHLW chemical composition components are listed in Tables E.1 to E.4 of Appendix E for 8 of the 12 IHLW scenarios and all four HLW waste types. The eight scenarios are the ones defined by all low-case and all high-case variation and uncertainty %RSD values. The mean %RSD values for all 12 IHLW variation/uncertainty scenarios were used to calculate the minimum and maximum mean %RSD values in Table 9.1.

Table 9.1 shows that the mean values of total %RSD for IHLW chemical composition components (mass fractions) vary from a minimum of 1.5% for SiO_2 (for all waste types) to a maximum (excluding Sb_2O_3, whose behavior was explained in Section 7.1) of 86.4% for ZnO in the transition waste type. Most mean values of total %RSD fall within the range of 5 to 10%. The mean values of batch-to-batch %RSD vary from 0.3% for SiO_2 to 85.8% for ZnO. The mean values of within-batch %RSD vary from a minimum of 1.4% for SiO_2 to a maximum of 18.5% for both PdO and RhO_3. In general, the mean values of total %RSD for the transition waste type (AY-102 to AZ-102) are the largest among the waste types investigated, reflecting the fact that the mean mass fractions of the IHLW components change during this period, unlike the other "pure" waste types considered. For all four HLW waste types, the mean values of total %RSD closely resemble the mean values of within-batch %RSD, indicating that analytical and mixing/sampling uncertainties (which together make up the within-batch uncertainty) are the dominant factors in determining overall variation plus uncertainty for IHLW chemical composition components.

Table 9.1. Minimums and Maximums of Mean Total, Batch-to-Batch, and Within-Batch %RSDs for all Important IHLW Chemical Composition Components for Each Waste Type[a]

Oxide Comp.	Waste Type	$\%RSD_T$[b]		$\%RSD_B$[b]		$\%RSD_W$[b]		Oxide Comp.	Waste Type	$\%RSD_T$[b]		$\%RSD_B$[b]		$\%RSD_W$[b]	
		Min	Max	Min	Max	Min	Max			Min	Max	Min	Max	Min	Max
Al_2O_3	AY-102	2.9	8.3	0.7	1.8	2.7	7.8	PdO	AY-102	-[d]	-	-	-	-	-
	AZ-102	2.8	8.2	0.6	2.0	2.6	7.7		AZ-102	-	-	-	-	-	-
	C-104	2.9	8.5	0.6	1.8	2.7	8.0		C-104	9.4	19.9	1.8	5.1	8.9	18.5
	Trans.[c]	3.7	8.5	2.0	2.6	2.7	7.7		Trans.	-	-	-	-	-	-
B_2O_3	AY-102	2.7	8.0	0.7	1.8	2.6	7.5	Rh_2O_3	AY-102	-	-	-	-	-	-
	AZ-102	2.9	8.5	0.8	2.0	2.7	7.9		AZ-102	-	-	-	-	-	-
	C-104	2.7	8.0	0.5	1.8	2.6	7.5		C-104	8.8	19.8	2.0	4.7	8.2	18.5
	Trans.	12.4	14.6	11.8	12.3	2.8	8.0		Trans.	-	-	-	-	-	-
CaO	AY-102	4.4	10.8	1.0	2.5	4.1	10.1	RuO_2	AY-102	-	-	-	-	-	-
	AZ-102	4.4	10.9	1.1	2.3	4.1	10.2		AZ-102	-	-	-	-	-	-
	C-104	4.4	10.8	0.9	2.2	4.1	10.2		C-104	4.4	10.9	1.0	2.6	4.1	10.1
	Trans.	4.4	11.0	1.0	2.6	4.1	10.2		Trans.	-	-	-	-	-	-
CdO	AY-102	3.0	8.7	0.6	1.9	2.8	8.2	Sb_2O_3	AY-102	9.4	19.8	1.8	5.2	8.9	18.4
	AZ-102	2.9	8.6	0.6	2.0	2.8	8.1		AZ-102	-	-	-	-	-	-
	C-104	4.4	10.9	1.0	2.6	4.1	10.1		C-104	-	-	-	-	-	-
	Trans.	7.9	11.0	7.0	7.4	2.8	8.1		Trans.	293.7	304.1	288.9	302.7	28.4	56.9
Cr_2O_3	AY-102	4.4	10.9	1.0	2.4	4.1	10.2	SeO_2	AY-102	-	-	-	-	-	-
	AZ-102	4.4	10.9	0.9	2.7	4.1	10.2		AZ-102	-	-	-	-	-	-
	C-104	4.3	10.6	0.9	2.2	4.1	10.0		C-104	4.4	10.7	0.9	2.5	4.1	10.0
	Trans.	10.8	14.3	8.9	10.0	4.2	10.4		Trans.	-	-	-	-	-	-
Fe_2O_3	AY-102	2.6	7.7	0.5	1.6	2.5	7.3	SiO_2	AY-102	1.5	4.5	0.4	1.1	1.4	4.2
	AZ-102	2.7	7.9	0.6	1.9	2.5	7.4		AZ-102	1.5	4.5	0.4	0.9	1.4	4.2
	C-104	2.9	8.3	0.6	1.7	2.7	7.8		C-104	1.5	4.5	0.3	1.1	1.4	4.2
	Trans.	2.9	8.0	1.0	2.0	2.5	7.4		Trans.	1.5	4.5	0.3	1.0	1.4	4.2
Li_2O	AY-102	3.9	9.3	0.8	2.2	3.7	8.7	SO_3	AY-102	5.7	12.6	1.2	3.0	5.4	11.9
	AZ-102	3.9	9.2	0.9	2.2	3.6	8.5		AZ-102	4.0	9.5	1.0	2.2	3.7	8.9
	C-104	2.3	6.6	0.5	1.4	2.1	6.2		C-104	4.0	9.2	0.9	2.1	3.7	8.7
	Trans.	5.0	9.6	2.7	3.4	3.6	8.7		Trans.	40.0	43.4	39.4	43.1	4.6	10.7
MgO	AY-102	3.0	8.7	0.7	1.9	2.8	8.2	SrO	AY-102	3.0	8.7	0.6	1.8	2.8	8.2
	AZ-102	4.4	10.8	0.9	2.3	4.1	10.2		AZ-102	3.0	8.7	0.6	2.0	2.8	8.1
	C-104	4.5	10.8	0.9	2.5	4.1	10.2		C-104	2.9	8.4	0.7	1.9	2.7	7.9
	Trans.	4.6	11.0	1.7	3.0	4.0	10.1		Trans.	7.1	10.4	5.8	6.5	2.8	8.2
MnO	AY-102	2.9	8.6	0.7	2.0	2.7	8.0	ThO_2	AY-102	-	-	-	-	-	-
	AZ-102	3.0	8.7	0.6	2.1	2.8	8.1		AZ-102	-	-	-	-	-	-
	C-104	2.9	8.6	0.6	2.0	2.7	8.0		C-104	2.9	8.3	0.6	1.9	2.7	7.8
	Trans.	14.5	16.5	14.0	14.4	2.8	8.3		Trans.	-	-	-	-	-	-
Na_2O	AY-102	2.2	6.4	0.5	1.5	2.0	5.9	UO_3	AY-102	7.8	16.8	1.7	4.1	7.3	15.6
	AZ-102	2.1	6.3	0.5	1.5	2.0	5.9		AZ-102	4.3	10.8	0.9	2.3	4.1	10.1
	C-104	2.2	6.4	0.5	1.4	2.1	6.0		C-104	2.9	8.3	0.6	1.7	2.7	7.8
	Trans.	2.2	6.3	0.5	1.4	2.0	5.9		Trans.	6.5	11.8	3.6	4.7	4.3	10.4
NiO	AY-102	4.4	10.9	0.9	2.6	4.1	10.2	ZnO	AY-102	3.0	8.6	0.8	1.9	2.8	8.2
	AZ-102	3.0	8.7	0.7	1.9	2.8	8.1		AZ-102	4.5	11.0	0.9	2.7	4.2	10.2
	C-104	4.4	10.7	1.0	2.3	4.1	10.1		C-104	2.9	8.3	0.6	2.0	2.7	7.8
	Trans.	4.4	9.4	2.6	3.3	2.9	8.3		Trans.	85.3	86.4	84.8	85.8	4.6	12.0
P_2O_5	AY-102	4.4	10.8	0.9	2.2	4.1	10.2	ZrO_2	AY-102	3.0	8.7	0.7	2.0	2.8	8.2
	AZ-102	4.4	10.9	1.0	2.8	4.1	10.1		AZ-102	3.0	8.7	0.6	1.9	2.8	8.1
	C-104	4.3	11.0	0.9	2.9	4.1	10.1		C-104	2.8	8.4	0.6	2.0	2.7	7.8
	Trans.	4.5	10.9	1.3	2.6	4.1	10.3		Trans.	5.7	9.8	4.1	5.0	2.8	8.2

(a) Means were calculated over the 200 simulations per scenario and waste type. Minimums and maximums were calculated over the means from the 12 scenarios for each waste type.

(b) $\%RSD_T$ = total batch-to-batch variation and within-batch uncertainty %RSD, $\%RSD_B$ = batch-to-batch variation %RSD, and $\%RSD_W$ = within-batch uncertainty %RSD.

(c) Transition waste type from AY-102 to AZ-102.

(d) A "–" denotes that the component is not contained in IHLW for that waste type.

Table 9.2 contains, for each of the four HLW waste types, the minimums and maximums of mean values of total, batch-to-batch and within-batch %RSDs for the IHLW radionuclide composition components. These minimums and maximums of mean %RSD values were calculated similarly to those for IHLW chemical composition components as described previously for the results in Table 9.1. The mean values of batch-to-batch, within-batch, and total %RSDs for each of the important IHLW radionuclide composition components are listed in Tables E.5 to E.8 of Appendix E for 8 of the 12 IHLW

Table 9.2. Minimums and Maximums of Mean Total, Batch-to-Batch, and Within-Batch %RSDs for all Important IHLW Radionuclide Composition Components for Each Waste Type[a]

Oxide Component	Waste Type	$\%RSD_T$[b]		$\%RSD_B$[b]		$\%RSD_W$[b]		Oxide Comp.	Waste Type	$\%RSD_T$[b]		$\%RSD_B$[b]		$\%RSD_W$[b]	
		Min	Max	Min	Max	Min	Max			Min	Max	Min	Max	Min	Max
$^{241}Am_2O_3$	AY-102	1.0	19.2	0.4	4.7	0.8	17.9	$^{241}PuO_2$	AY-102	NA	NA	NA	NA	NA	NA
	AZ-102	2.4	10.8	0.5	2.5	2.2	10.2		AZ-102	0.8	6.7	0.7	6.3	0.3	2.5
	C-104	0.8	18.3	0.5	4.3	0.3	17.1		C-104	1.2	8.8	1.1	3.5	0.4	7.4
	Trans.[c]	6.7	13.3	5.8	6.9	2.1	10.8		Trans.	0.9	6.6	0.8	6.1	0.3	2.4
$^{242}Cm_2O_3$	AY-102	-[d]	-	-	-	-	-	^{90}SrO	AY-102	4.0	9.4	0.9	2.3	3.8	9.0
	AZ-102	-	-	-	-	-	-		AZ-102	4.0	9.4	0.8	2.0	3.8	8.8
	C-104	9730.1	11180	9046.3	10395	3583.3	4117.6		C-104	2.4	15.2	0.5	4.0	2.2	14.4
	Trans.	-	-	-	-	-	-		Trans.	5.0	10.0	2.6	3.2	3.8	9.0
$^{243+244}Cm_2O_3$	AY-102	-	-	-	-	-	-	$^{99}Tc_2O_7$	AY-102	1.0	9.7	0.9	9.0	0.4	3.6
	AZ-102	480.2	488.9	446.5	454.5	176.9	180.0		AZ-102	1.3	9.3	1.0	2.3	0.5	8.6
	C-104	845.2	864.8	785.8	804.0	311.3	318.5		C-104	3.6	9.1	0.8	1.9	3.3	8.6
	Trans.	490.1	500.7	455.7	465.5	180.5	184.4		Trans.	1.4	11.1	1.3	6.7	0.5	8.9
^{60}CoO	AY-102	2059.5	2087.8	1914.8	1941.1	758.5	768.9	$^{233}UO_3$	AY-102	NA	NA	NA	NA	NA	NA
	AZ-102	272.4	275.6	253.3	256.2	100.3	101.5		AZ-102	1.1	9.2	0.4	2.1	0.4	8.6
	C-104	2740.6	2787.7	2548.0	2591.8	1009.3	1026.7		C-104	2.3	9.5	0.5	2.4	2.2	8.8
	Trans.	277.7	280.6	258.2	260.9	102.3	103.3		Trans.	0.9	10.7	0.8	6.3	0.3	8.3
$^{137}Cs_2O$	AY-102	2.3	19.0	0.5	4.3	2.2	18.0	$^{234}UO_3$	AY-102	NA	NA	NA	NA	NA	NA
	AZ-102	1.1	6.5	0.3	1.5	1.0	6.1		AZ-102	11.0	30.6	2.2	7.6	10.4	28.6
	C-104	2.3	6.9	0.5	1.7	2.2	6.4		C-104	10.4	30.7	2.1	7.5	9.8	28.6
	Trans.	1.2	8.0	0.5	2.3	1.0	7.2		Trans.	12.8	31.3	6.2	9.2	10.5	28.8
$^{237}NpO_2$	AY-102	-	-	-	-	-	-	$^{235}UO_3$	AY-102	NA	NA	NA	NA	NA	NA
	AZ-102	4.0	11.1	0.9	2.5	3.8	10.4		AZ-102	4.0	16.1	0.8	4.0	3.8	15.0
	C-104	2.5	19.3	0.5	5.5	2.3	17.7		C-104	3.9	15.1	0.8	3.5	3.7	14.1
	Trans.	8.3	12.7	6.4	7.4	3.8	10.5		Trans.	8.4	16.9	6.2	7.5	3.8	15.0
^{238}PuO	AY-102	3.5	37.3	3.3	34.7	1.3	13.7	$^{236}UO_3$	AY-102	NA	NA	NA	NA	NA	NA
	AZ-102	1.0	21.4	0.9	19.9	0.4	7.9		AZ-102	5.8	31.0	1.4	7.8	5.4	28.7
	C-104	4.9	34.5	4.6	32.0	1.8	12.7		C-104	5.7	30.7	1.3	7.0	5.3	28.7
	Trans.	0.9	19.8	0.9	18.4	0.3	7.3		Trans.	9.1	31.3	6.6	9.2	5.5	28.7
$^{239}PuO_2$	AY-102	4.0	9.5	0.9	2.2	3.8	9.0	$^{238}UO_3$	AY-102	71.6	77.0	66.5	71.6	26.4	28.4
	AZ-102	4.0	9.5	0.9	2.4	3.8	8.8		AZ-102	2.4	8.1	0.6	1.9	2.2	7.5
	C-104	4.0	9.4	0.9	2.2	3.7	8.8		C-104	2.3	7.8	0.4	1.7	2.1	7.4
	Trans.	4.0	9.5	0.9	2.1	3.8	8.9		Trans.	7.7	10.9	6.9	7.4	2.2	7.9

(a) Means were calculated over the 200 simulations per scenario and waste type. Minimums and maximums were calculated over the means from the 12 scenarios for each waste type.

(b) $\%RSD_T$ = total batch-to-batch variation and within-batch uncertainty %RSD, $\%RSD_B$ = batch-to-batch variation %RSD, and $\%RSD_W$ = within-batch uncertainty %RSD.

(c) Transition waste type from AY-102 to AZ-102.

(d) A "–" denotes that the component is not contained in IHLW for that waste type.

scenarios and all four HLW waste types. The eight scenarios are the ones defined by all low-case and all high-case variation and uncertainty %RSD values. As a way of showing the variability of the %RSD values across the 200 simulations, Figure 7.4 through Figure 7.6 display the mean and 90% ECI limits for the total, batch-to-batch, and within-batch %RSDs on the IHLW radionuclide composition components for the scenarios with all the factors at the low cases and all at the high cases.

Table 9.2 shows that for IHLW radionuclide composition components (mass fractions), the minimum value of the mean total %RSDs is 0.8% for $^{241}Am_2O_3$. The minimum value of the mean batch-to-batch %RSDs is 0.3% for $^{137}Cs_2O$. The minimum value of mean within-batch %RSDs is 0.3%, which occurs for $^{241}Am_2O_3$, $^{238}PuO_2$, and $^{241}PuO_2$. With the exception of $^{242}Cm_2O_3$, $^{243+244}Cm_2O_3$ and ^{60}CoO (which show mean %RSD values ranging from around 100% up to a little over 10000%), $^{238}UO_3$ has the maximum value of mean total %RSDs of 77% and also the maximum value of mean batch-to-batch %RSDs of 71.6%. The maximum value of mean within-batch %RSDs of 28.7% occurs for $^{236}UO_3$.

It is interesting to notice that the mean %RSD values shown in Table 9.2 are often much larger than what might be expected given the nominal batch-to-batch variation and uncertainty %RSD values that were applied to the activity-per-volume nominal values in each waste-type. This is the result of the non-linear transformation performed when converting activities per volume (which are the result of the simulations) into mass fractions. Because the mass fractions for radionuclides are generally much smaller than those for non-radionuclides, their values during the simulations are much more volatile.

Table 9.3 contains, for each of the four HLW waste types, the minimums and maximums of mean values of total, batch-to-batch and within-batch %RSDs for the IHLW properties. These minimums and maximums of mean %RSD values were calculated similarly to those for IHLW chemical composition components as described previously for the results in Table 9.1. The mean values of batch-to-batch, within-batch, and total %RSDs for each of the IHLW properties are listed in Tables E.9 to E.12 of Appendix E for 8 of the 12 IHLW scenarios and all four HLW waste types. The eight scenarios are the ones defined by all low-case and all high-case variation and uncertainty %RSD values. As a way of showing the variability of the %RSD values across the 200 simulations, Figure 7.7 through Figure 7.11 display the mean and 90% ECI limits for the total, batch-to-batch, and within-batch %RSDs on the IHLW properties for the scenarios with all the factors at the low cases and all at the high cases.

Table 9.3 shows that for IHLW properties, the smallest mean value of total %RSD is 1% (for T1% Phase 1a), and the largest is 41.6% (for PCT B). Similarly, the smallest and largest mean values of batch-to-batch %RSD are 0.2% (for viscosity at 1373 K) and 9.1% (for T1% Phase 1a). Mean values of within-batch %RSD vary from a minimum of 1% (for T1% with both Phase 1 and 1a models) to a maximum of 39.4% (for PCT B). In general, the within-batch %RSDs are larger than their batch-to-batch counterparts. This is a consequence of the relatively large analytical uncertainties present for most IHLW components and the fact that the within-batch variation is the sum of analytical plus mixing and sampling uncertainties.

Table 9.3. Minimums and Maximums of Mean Total, Batch-to-Batch, and Within-Batch %RSDs of IHLW Properties for Each Waste Type[a]

IHLW Glass Property	Waste Type	$\%RSD_T$[b]		$\%RSD_B$[b]		$\%RSD_W$[b]	
		Min	Max	Min	Max	Min	Max
PCT B	AY-102	8.9	35.1	2.3	6.6	8.2	33.4
	AZ-102	9.9	38.2	2.3	8.0	9.2	35.9
	C-104	7.9	32.7	1.7	6.0	7.5	31.2
	Trans.[c]	10.5	41.6	4.1	8.6	9.2	39.4
PCT Li	AY-102	5.4	17.5	1.4	3.6	4.9	16.6
	AZ-102	6.5	21.1	1.5	5.0	6.1	19.6
	C-104	4.8	16.8	1.0	3.4	4.5	15.9
	Trans.	6.6	21.9	1.9	5.0	6.0	20.6
PCT Na	AY-102	8.2	31.3	2.1	5.9	7.6	29.8
	AZ-102	9.7	37.7	2.3	7.7	9.1	35.5
	C-104	7.1	27.9	1.5	5.2	6.7	26.5
	Trans.	9.5	40.6	2.0	8.0	9.0	38.5
TCLP	AY-102	6.5	21.8	1.6	4.4	6.0	20.7
	AZ-102	6.2	21.1	1.4	4.8	5.8	19.7
	C-104	7.6	27.0	1.8	5.8	7.1	25.3
	Trans.	7.4	22.0	3.8	5.9	5.8	20.2
$T_{1\%}$ Phase 1	AY-102	1.5	4.2	0.3	0.9	1.4	4.0
	AZ-102	1.6	4.5	0.4	1.1	1.5	4.2
	C-104	1.0	3.0	0.2	0.7	1.0	2.9
	Trans.	1.6	4.5	0.4	1.1	1.5	4.2
$T_{1\%}$ Phase 1a	AY-102	1.4	4.1	0.3	0.9	1.3	3.9
	AZ-102	1.5	4.3	0.4	1.0	1.4	4.0
	C-104	1.0	2.9	0.2	0.7	1.0	2.8
	Trans.	1.5	4.3	0.4	1.1	1.4	4.0
Viscosity at 1373 K	AY-102	12.5	36.3	3.3	9.1	11.6	33.6
	AZ-102	14.0	39.8	3.3	8.2	13.1	37.7
	C-104	12.4	35.8	2.8	7.9	11.6	33.7
	Trans.	13.7	39.2	2.7	8.9	13.0	36.7
Viscosity at 1423 K	AY-102	11.6	33.4	3.1	8.4	10.7	30.9
	AZ-102	13.0	36.5	3.1	7.6	12.1	34.5
	C-104	11.5	33.1	2.6	7.3	10.8	31.1
	Trans.	12.8	36.1	2.5	8.2	12.1	33.8
Electrical Conductivity at 1373 K	AY-102	3.7	11.1	0.9	2.5	3.5	10.5
	AZ-102	5.3	15.7	1.2	3.6	4.9	14.6
	C-104	3.8	12.3	0.8	2.5	3.6	11.6
	Trans.	6.4	16.3	3.7	4.6	4.9	15.0
Electrical Conductivity at 1473 K	AY-102	3.5	10.4	0.8	2.3	3.3	9.8
	AZ-102	5.0	14.8	1.2	3.5	4.7	13.8
	C-104	3.6	11.6	0.8	2.3	3.4	11.0
	Trans.	6.1	15.4	3.5	4.4	4.7	14.1

(a) Means were calculated over the 200 simulations per scenario and waste type. Minimums and maximums were calculated over the mean values from the 12 scenarios for each waste type.

(b) $\%RSD_T$ = total batch-to-batch variation and within-batch uncertainty %RSD, $\%RSD_B$ = batch-to-batch variation %RSD, and $\%RSD_W$ = within-batch uncertainty %RSD.

(c) Transition waste type from AY-102 to AZ-102.

On first look, some ranges of %RSDs summarized in Table 9.1 to Table 9.3 seem smaller than would be expected given the magnitudes of input uncertainties. Two reasons for this are explained in the following paragraphs.

Each of the HLW simulations for each of the scenarios involved eight samples per IHLW MFPV batch with one analysis for each sample. Averaging over the eight samples causes a reduction in the random mixing/sampling and analytical uncertainties. Because analytical uncertainty is a major driver of total variation and uncertainty, averaging over eight samples to reduce mixing/sampling and analytical uncertainties is a substantial benefit. This explains why the resulting uncertainties found in Table 9.1 to Table 9.3 are generally smaller than would be expected given the magnitudes of process uncertainties used as inputs to the simulations.

The summarized %RSDs in Table 9.1 to Table 9.3 are ranges of mean %RSDs over all combinations of the input factors and the 200 simulations of each combination. These summaries do not reflect the range of variation and uncertainty that might happen for any particular instance of processing batches associated with a given waste type. As a way of showing the variability of the %RSD values across 200 simulations for a given scenario, Figure 7.1 through Figure 7.3 in Section 7 display the mean and 90% ECI limits for the total, batch-to-batch, and within-batch %RSDs on the IHLW chemical composition components, radionuclide composition components, and properties for the scenarios with all the factors at the low cases and all at the high cases.

9.2.2 Summary of Variations and Uncertainties for ILAW Composition and Properties

Table 9.4 contains the minimums and maximums of mean values of batch-to-batch, within-batch, and total %RSDs for the important ILAW chemical composition components. The mean %RSDs were calculated over the 200 simulations for each scenario and each of the five LAW data sets. For each of the five LAW data sets (AP-101/AY-102, transition from AP-101/AY-102 to AZ-101, AZ-102, AN-102, and an unknown tank), the minimums and maximums of mean %RSD values were determined over all variation and uncertainty scenarios (shown in Table 5.4). The mean values of batch-to-batch, within-batch, and total %RSDs for each of the important ILAW chemical composition components are listed in Tables F.1 to F.5 of Appendix F for the most statistically significant scenarios and all five data sets. The mean %RSD values for all 64 variation/uncertainty scenarios for each data set were used to calculate the minimum and maximum mean %RSD values in Table 9.4. As a way of showing the variability of the %RSD values across 200 simulations, Figure 8.1 through Figure 8.3 display the mean and 90% ECI limits for the total, batch-to-batch, and within-batch %RSDs on the ILAW chemical composition components for the scenarios with all the factors at the low cases and all at the high cases.

Table 9.4 shows that the mean values of total %RSD for ILAW chemical composition components (mass fractions) vary from a minimum of 0.5% for SO_3 (across all LAW data sets) to a maximum of 23% for Li_2O in the transition data set. Most mean values of total %RSD fall within 1 to 10%. The mean values of batch-to-batch %RSD vary from 0.04% (for multiple components) to 22.5% for Li_2O. The mean values of within-batch %RSD vary from a minimum of 0.5% for SO_3 to a maximum of 17.9% for Li_2O. Data set # 2 has significantly larger mean values of batch-to-batch %RSD because of being a transition between two LAW waste types. The other data sets have mean values of total %RSD that

Table 9.4. Minimums and Maximums of Mean Total, Batch-to-Batch, and Within-Batch %RSDs for all Important ILAW Chemical Composition Components for Each Waste Type[a]

Oxide Component	Data Set	$\%RSD_T$[b]		$\%RSD_B$[b]		$\%RSD_W$[b]		Oxide Component	Data Set	$\%RSD_T$[b]		$\%RSD_B$[b]		$\%RSD_W$[b]	
		Min	Max	Min	Max	Min	Max			Min	Max	Min	Max	Min	Max
Al_2O_3	Set 1	2.3	4.9	0.2	0.2	2.3	4.9	MgO	Set 1	2.5	5.2	0.1	0.1	2.5	5.2
	Set 2	2.2	4.8	0.2	0.2	2.2	4.8		Set 2	2.4	5.1	0.1	0.1	2.4	5.1
	Set 3	1.8	3.8	0.1	0.1	1.8	3.8		Set 3	1.4	3.0	0.04	0.04	1.4	3.0
	Set 4	2.2	4.8	0.3	0.3	2.2	4.8		Set 4	2.4	5.1	0.1	0.1	2.4	5.1
	Set 5	2.0	4.4	0.2	0.2	2.0	4.4		Set 5	2.4	4.9	0.1	0.1	2.4	4.9
B_2O_3	Set 1	1.3	2.8	0.1	0.1	1.3	2.8	Na_2O	Set 1	4.5	9.8	0.4	0.5	4.5	9.8
	Set 2	1.2	2.4	0.1	0.1	1.2	2.4		Set 2	5.4	10.4	2.9	2.9	4.6	10.0
	Set 3	0.8	1.7	0.04	0.04	0.8	1.7		Set 3	5.1	10.9	0.5	0.5	5.1	10.9
	Set 4	1.3	2.7	0.1	0.1	1.3	2.7		Set 4	4.5	9.8	0.5	0.5	4.4	9.8
	Set 5	1.1	2.2	0.1	0.1	1.1	2.2		Set 5	4.8	10.3	0.5	0.5	4.8	10.3
CaO	Set 1	3.1	6.3	0.1	0.1	3.1	6.3	P_2O_5	Set 1	7.9	16.5	0.6	0.6	7.9	16.5
	Set 2	7.6	8.9	7.3	7.3	2.3	5.2		Set 2	8.9	17.1	4.4	4.4	7.8	16.6
	Set 3	2.2	4.6	0.04	0.04	2.2	4.6		Set 3	9.0	17.6	0.4	0.4	9.0	17.5
	Set 4	3.0	6.3	0.1	0.1	3.0	6.3		Set 4	8.0	17.2	0.6	0.6	8.0	17.2
	Set 5	2.3	4.9	0.1	0.1	2.3	4.9		Set 5	7.8	16.7	0.6	0.6	7.8	16.7
Cl	Set 1	5.7	12.2	0.6	0.6	5.6	12.2	SiO_2	Set 1	5.6	12.0	0.6	0.6	5.6	12.0
	Set 2	8.8	14.1	6.8	6.8	5.6	12.4		Set 2	6.0	12.1	2.5	2.5	5.5	11.8
	Set 3	5.5	12.1	0.5	0.5	5.5	12.1		Set 3	5.6	11.8	0.6	0.6	5.6	11.8
	Set 4	5.6	12.2	0.7	0.7	5.6	12.2		Set 4	5.7	12.0	0.6	0.6	5.6	11.9
	Set 5	5.6	12.1	0.6	0.6	5.6	12.1		Set 5	5.6	11.7	0.6	0.6	5.6	11.7
Fe_2O_3	Set 1	2.1	4.5	0.1	0.1	2.1	4.5	SO_3	Set 1	1.2	2.5	0.1	0.1	1.2	2.5
	Set 2	2.0	4.4	0.1	0.1	2.0	4.4		Set 2	1.0	2.1	0.4	0.4	1.0	2.1
	Set 3	1.4	3.0	0.04	0.04	1.4	3.0		Set 3	0.5	1.2	0.04	0.04	0.5	1.2
	Set 4	2.1	4.5	0.1	0.1	2.1	4.5		Set 4	1.1	2.4	0.1	0.1	1.1	2.4
	Set 5	2.0	4.2	0.1	0.1	2.0	4.2		Set 5	0.9	1.8	0.1	0.1	0.9	1.8
K_2O	Set 1	3.0	6.7	0.6	0.6	3.0	6.7	ZnO	Set 1	2.2	4.6	0.1	0.1	2.2	4.6
	Set 2	6.4	9.0	5.8	5.8	2.8	6.8		Set 2	2.0	4.4	0.1	0.1	2.0	4.4
	Set 3	2.9	6.5	0.6	0.6	2.8	6.5		Set 3	1.9	4.0	0.04	0.04	1.9	4.0
	Set 4	3.0	6.8	0.6	0.6	3.0	6.8		Set 4	2.1	4.6	0.1	0.1	2.1	4.6
	Set 5	3.1	6.7	0.8	0.8	3.0	6.7		Set 5	2.0	4.3	0.1	0.1	2.0	4.3
Li_2O	Set 1	8.3	17.6	0.7	0.7	8.3	17.6	ZrO_2	Set 1	2.2	4.6	0.1	0.1	2.2	4.6
	Set 2	22.5	23.0	22.5	22.5	1.4	5.0		Set 2	2.2	4.6	0.1	0.1	2.2	4.6
	Set 3	0.9	1.8	0.04	0.04	0.9	1.8		Set 3	1.0	2.1	0.04	0.04	1.0	2.1
	Set 4	8.2	17.9	0.6	0.6	8.2	17.9		Set 4	2.2	4.6	0.1	0.1	2.2	4.6
	Set 5	1.1	2.3	0.1	0.1	1.1	2.3		Set 5	2.1	4.4	0.1	0.1	2.1	4.4

(a) Means were calculated over the 200 simulations per scenario and waste type. Minimums and maximums were calculated over the means from the 64 scenarios for each waste type.

(b) $\%RSD_T$ = total batch-to-batch variation and within-batch uncertainty %RSD, $\%RSD_B$ = batch-to-batch variation %RSD, and $\%RSD_W$ = within-batch uncertainty %RSD.

closely resemble the mean values of within-batch %RSD, indicating that analytical and mixing/sampling uncertainties, as well as GFC composition and weight uncertainties, are the dominant factors in determining overall variation plus uncertainty for ILAW chemical composition components.

Table 9.5 contains, for each of the five ILAW data sets, the minimums and maximums of mean values of total, batch-to-batch, and within-batch %RSDs for the ILAW radionuclide composition components. These minimums and maximums of mean %RSD values were calculated similarly to those for ILAW chemical composition components as described previously for the results in Table 9.4. The mean values of batch-to-batch, within-batch, and total %RSDs for each of the important ILAW radionuclide composition components are listed in Tables F.6 to F.10 of Appendix F for the most statistically significant scenarios and all five data sets. As a way of showing the variability of the %RSD values across 200 simulations, Figure 8.4 through Figure 8.6 display the mean and 90% ECI limits for the total, batch-to-batch, and within-batch %RSDs on the ILAW radionuclide composition components for the scenarios with all the factors at the low cases and all at the high cases.

Table 9.5 shows that the mean values of total %RSD for ILAW radionuclide composition components (mass fractions) vary from a minimum of 2.9% for $^{154}Eu_2O_3$ and ^{60}CoO (across all LAW data sets) to a maximum of 29.5% for $^{125}Sb_2O_3$. Most mean values of total %RSD fall within the range of 5 to 15%. The mean values of batch-to-batch %RSD vary from 0.6% for multiple components to 12.4% for $^{235}UO_3$. The mean values of within-batch %RSD vary from a minimum of 2.8% for $^{154}Eu_2O_3$ to a maximum of 28.8% for $^{125}Sb_2O_3$. Data set # 2 has significantly larger mean values of batch-to-batch %RSD because of being a transition between two LAW waste types. The other data sets have mean values of total %RSD that closely resemble the mean values of within-batch %RSD, indicating that analytical and mixing/sampling uncertainties, as well as GFC composition and weight uncertainties, are the dominant factors in determining overall variation plus uncertainty for ILAW radionuclide composition components.

Table 9.6 contains, for each of the five LAW data sets, the minimums and maximums of mean values of total, batch-to-batch, and within-batch %RSDs for the ILAW properties. These minimums and maximums of mean %RSD values were calculated similarly to those for ILAW chemical composition components as described previously for the results in Table 9.4. The mean values of batch-to-batch, within-batch, and total %RSDs for each of the ILAW glass properties are listed in Tables F.11 to F.15 of Appendix F for the most statistically significant scenarios and all five data sets. As a way of showing the variability of the %RSD values across 200 simulations, Figure 8.7 through Figure 8.10 display the mean and 90% ECI limits for the total, batch-to-batch, and within-batch %RSDs on the ILAW properties for the scenarios with all the factors at the low cases and all at the high cases.

Table 9.5. Minimums and Maximums of Mean Total, Batch-to-Batch, and Within-Batch %RSDs for all Important ILAW Radionuclide Composition Components for Each Waste Type[a]

Component	Data Set	$\%RSD_T$[b]		$\%RSD_B$[b]		$\%RSD_W$[b]		Component	Data Set	$\%RSD_T$[b]		$\%RSD_B$[b]		$\%RSD_W$[b]	
		Min	Max	Min	Max	Min	Max			Min	Max	Min	Max	Min	Max
^{60}CoO	Set 1	3.1	6.9	0.6	0.6	3.0	6.9	$^{155}Eu_2O_3$	Set 1	7.0	7.0	7.0	7.0	7.0	7.0
	Set 2	5.2	8.0	4.3	4.3	3.0	6.8		Set 2	6.8	6.8	6.8	6.8	6.8	6.8
	Set 3	2.9	6.6	0.6	0.6	2.8	6.6		Set 3	6.5	6.5	6.5	6.5	6.5	6.5
	Set 4	3.1	6.9	0.6	0.6	3.0	6.9		Set 4	7.0	7.0	7.0	7.0	7.0	7.0
	Set 5	3.0	6.7	0.8	0.8	2.9	6.7		Set 5	6.7	6.7	6.7	6.7	6.7	6.7
^{63}NiO	Set 1	5.7	12.0	0.6	0.7	5.7	12.0	$^{233}UO_3$	Set 1	12.2	12.2	12.2	12.2	12.2	12.2
	Set 2	7.6	13.5	5.3	5.4	5.4	12.4		Set 2	12.2	12.2	12.2	12.2	12.2	12.2
	Set 3	5.5	12.1	0.6	0.6	5.5	12.1		Set 3	12.2	12.2	12.2	12.2	12.2	12.2
	Set 4	5.7	12.1	0.8	0.8	5.6	12.1		Set 4	12.2	12.2	12.2	12.2	12.2	12.2
	Set 5	5.6	12.1	0.6	0.6	5.6	12.1		Set 5	12.0	12.0	12.0	12.0	12.0	12.0
^{90}SrO	Set 1	3.1	6.9	0.6	0.6	3.0	6.8	$^{235}UO_3$	Set 1	12.3	12.3	12.3	12.3	12.3	12.3
	Set 2	5.6	8.4	4.9	5.0	2.7	6.8		Set 2	12.0	12.0	12.0	12.0	12.0	12.0
	Set 3	2.8	6.6	0.6	0.6	2.8	6.6		Set 3	11.9	11.9	11.9	11.9	11.9	11.9
	Set 4	3.2	7.0	1.2	1.2	3.0	6.9		Set 4	12.1	12.1	12.1	12.1	12.1	12.1
	Set 5	3.0	6.9	0.6	0.6	2.9	6.8		Set 5	12.4	12.4	12.4	12.4	12.4	12.4
$^{99}Tc_2O_7$	Set 1	5.6	12.2	0.9	0.9	5.5	12.2	$^{237}NpO_2$	Set 1	12.2	12.2	12.2	12.2	12.2	12.2
	Set 2	6.8	12.8	3.9	3.9	5.6	12.2		Set 2	12.1	12.1	12.1	12.1	12.1	12.1
	Set 3	5.5	11.9	0.6	0.6	5.5	11.9		Set 3	11.9	11.9	11.9	11.9	11.9	11.9
	Set 4	5.8	12.1	1.0	1.0	5.7	12.1		Set 4	12.2	12.2	12.2	12.2	12.2	12.2
	Set 5	5.6	12.2	0.7	0.7	5.5	12.2		Set 5	11.9	11.9	11.9	11.9	11.9	11.9
$^{125}Sb_2O_3$	Set 1	13.6	28.6	0.6	0.6	13.6	28.6	$^{238}UO_3$	Set 1	12.3	12.3	12.3	12.3	12.3	12.3
	Set 2	15.1	29.5	6.5	6.5	13.7	28.8		Set 2	11.9	11.9	11.9	11.9	11.9	11.9
	Set 3	13.6	28.5	0.6	0.6	13.6	28.5		Set 3	12.1	12.1	12.1	12.1	12.1	12.1
	Set 4	13.7	28.8	0.6	0.6	13.7	28.8		Set 4	12.1	12.1	12.1	12.1	12.1	12.1
	Set 5	13.5	28.6	0.6	0.6	13.5	28.6		Set 5	12.0	12.0	12.0	12.0	12.0	12.0
$^{137}Cs_2O$	Set 1	8.2	17.8	0.6	0.6	8.2	17.8	$^{238}PuO_2$	Set 1	6.9	6.9	6.9	6.9	6.9	6.9
	Set 2	8.4	18.0	1.3	1.3	8.3	18.0		Set 2	6.8	6.8	6.8	6.8	6.8	6.8
	Set 3	8.3	18.0	0.6	0.6	8.3	18.0		Set 3	6.7	6.7	6.7	6.7	6.7	6.7
	Set 4	8.2	17.8	0.6	0.6	8.2	17.8		Set 4	6.9	6.9	6.9	6.9	6.9	6.9
	Set 5	8.2	17.9	0.6	0.6	8.2	17.9		Set 5	6.8	6.8	6.8	6.8	6.8	6.8
$^{151}Sm_2O_3$	Set 1	11.1	23.3	0.6	0.6	11.1	23.3	$^{239}PuO_2$	Set 1	6.9	6.9	6.9	6.9	6.9	6.9
	Set 2	10.9	23.4	1.0	1.1	10.8	23.3		Set 2	6.8	6.8	6.8	6.8	6.8	6.8
	Set 3	10.7	23.3	0.6	0.6	10.7	23.3		Set 3	6.5	6.5	6.5	6.5	6.5	6.5
	Set 4	11.2	23.4	0.6	0.6	11.1	23.4		Set 4	6.8	6.8	6.8	6.8	6.8	6.8
	Set 5	11.2	23.3	0.8	0.8	11.1	23.2		Set 5	6.7	6.7	6.7	6.7	6.7	6.7
$^{154}Eu_2O_3$	Set 1	3.1	7.0	0.6	0.6	3.0	7.0	$^{240}PuO_2$	Set 1	12.2	12.2	12.2	12.2	12.2	12.2
	Set 2	4.0	7.3	2.8	2.8	2.9	6.8		Set 2	12.1	12.1	12.1	12.1	12.1	12.1
	Set 3	2.9	6.5	0.6	0.6	2.9	6.4		Set 3	12.0	12.0	12.0	12.0	12.0	12.0
	Set 4	3.1	6.8	0.6	0.6	3.0	6.8		Set 4	12.1	12.1	12.1	12.1	12.1	12.1
	Set 5	4.3	7.4	3.2	3.2	2.9	6.6		Set 5	12.1	12.1	12.1	12.1	12.1	12.1

(a) Means were calculated over the 200 simulations per scenario and waste type. Minimums and maximums were calculated over the means from the 64 scenarios for each waste type.

(b) $\%RSD_T$ = total batch-to-batch variation and within-batch uncertainty %RSD, $\%RSD_B$ = batch-to-batch variation %RSD, and $\%RSD_W$ = within-batch uncertainty %RSD.

Table 9.5. Minimums and Maximums of Mean Total, Batch-to-Batch, and Within-Batch %RSDs for all Important ILAW Radionuclide Composition Components for Each Waste Type (cont'd)[a]

Component	Data Set	$\%RSD_T$[b]		$\%RSD_B$[b]		$\%RSD_W$[b]		Component	Data Set	$\%RSD_T$[b]		$\%RSD_B$[b]		$\%RSD_W$[b]	
		Min	Max	Min	Max	Min	Max			Min	Max	Min	Max	Min	Max
$^{241}PuO_2$	Set 1	8.3	17.8	0.6	0.6	8.3	17.8	$^{244}Cm_2O_3$	Set 1	8.4	17.7	0.6	0.6	8.3	17.7
	Set 2	9.7	18.5	5.3	5.3	8.1	17.7		Set 2	10.4	18.9	6.5	6.5	8.1	17.8
	Set 3	8.2	17.5	0.6	0.6	8.2	17.5		Set 3	8.3	17.7	0.6	0.6	8.2	17.7
	Set 4	8.4	17.6	0.6	0.6	8.3	17.6		Set 4	8.4	18.1	0.6	0.6	8.3	18.1
	Set 5	8.4	17.8	1.7	1.7	8.3	17.7		Set 5	8.3	17.5	0.6	0.6	8.2	17.5
$^{241}Am_2O_3$	Set 1	5.6	12.4	0.6	0.7	5.6	12.4								
	Set 2	8.3	13.8	6.6	6.6	5.1	12.1								
	Set 3	5.6	12.0	0.6	0.6	5.6	12.0								
	Set 4	5.6	12.1	0.6	0.6	5.6	12.1								
	Set 5	6.1	12.4	2.5	2.6	5.5	12.1								

(a) Means were calculated over the 200 simulations per scenario and waste type. Minimums and maximums were calculated over the means from the 64 scenarios for each waste type.

(b) $\%RSD_T$ = total batch-to-batch variation and within-batch uncertainty %RSD, $\%RSD_B$ = batch-to-batch variation %RSD, and $\%RSD_W$ = within-batch uncertainty %RSD.

Table 9.6 shows that mean values of total %RSDs for ILAW properties vary from a minimum of 3.3% for electrical conductivity at 1473 K (across all LAW data sets) to a maximum of 49.1% for VHT for data set # 4. Most mean values of total %RSD fall within the range of 5 to 20%. The mean values of batch-to-batch %RSD vary from 0.3% for multiple glass properties to 12.3% for viscosity at 1373 K. The mean values of within-batch %RSD vary from a minimum of 3.3% for electrical conductivity at 1473 K to a maximum of 49.0% for VHT for data set # 4.

The mean values of total %RSD for VHT with data set # 4 range from a minimum of 22.3 to a maximum of 49.1%. The mean values of within-batch %RSD range from a minimum of 22.1 to a maximum of 49.0%. These ranges for data set # 4 are the largest of the five data sets. This may be a result of limitations of the preliminary VHT model in the high-alkali region of glass composition space. Hence, there is a need to refine the estimates of VHT uncertainty for data set # 4 and the other data sets after the database for developing the VHT model is expanded, and a new VHT model is developed from that database.

Table 9.6 also shows that data set # 2 contains significantly larger mean values of batch-to-batch %RSD than the other data sets for all properties except electrical conductivity. This is because data set # 2 represents a transition between two waste types. The other data sets (i.e., # 1, # 3, # 4, and # 5) have mean values of total %RSD that closely resemble the mean values of within-batch %RSD for all properties, indicating that analytical and mixing/sampling uncertainties, as well as GFC composition and weight uncertainties, are the dominant factors in determining overall variation plus uncertainty for ILAW properties. These are still the dominant sources of total variation plus uncertainty for data set # 2, although batch-to-batch variation is a significant contributor.

Table 9.6. Minimums and Maximums of Mean Total, Batch-to-Batch, and Within-Batch %RSDs of ILAW Properties for Each Waste Type[a]

Glass Property	Data Set	$\%RSD_T$[b]		$\%RSD_B$[b]		$\%RSD_W$[b]	
		Min	Max	Min	Max	Min	Max
PCT B	Set 1	16.4	35.7	1.6	1.7	16.3	35.7
	Set 2	13.9	29.3	3.3	3.4	13.5	29.1
	Set 3	6.4	13.4	0.5	0.5	6.4	13.4
	Set 4	16.3	35.2	1.6	1.7	16.2	35.2
	Set 5	11.3	24.1	1.1	1.1	11.3	24.1
PCT Na	Set 1	15.5	33.8	1.5	1.6	15.5	33.8
	Set 2	12.4	26.0	3.6	3.6	11.9	25.8
	Set 3	5.6	11.7	0.5	0.5	5.5	11.7
	Set 4	14.4	31.1	1.4	1.5	14.3	31.1
	Set 5	10.0	21.2	1.0	1.0	10.0	21.2
VHT	Set 1	13.9	30.2	1.4	1.4	13.9	30.1
	Set 2	12.4	21.0	9.3	9.3	8.2	18.9
	Set 3	3.5	7.5	0.3	0.3	3.5	7.5
	Set 4	22.3	49.1	2.3	2.3	22.1	49.0
	Set 5	6.0	12.4	0.6	0.6	6.0	12.4
Viscosity 1373 K	Set 1	13.5	29.8	1.3	1.4	13.4	29.7
	Set 2	16.0	27.6	12.2	12.3	10.2	24.7
	Set 3	5.6	12.0	0.5	0.5	5.6	12.0
	Set 4	13.0	28.8	1.3	1.3	13.0	28.8
	Set 5	9.4	19.7	0.9	0.9	9.3	19.7
Viscosity 1423 K	Set 1	12.4	27.2	1.2	1.3	12.3	27.2
	Set 2	14.8	25.3	11.5	11.5	9.4	22.6
	Set 3	5.2	11.1	0.4	0.4	5.2	11.1
	Set 4	11.9	26.4	1.2	1.2	11.9	26.3
	Set 5	8.6	18.1	0.8	0.8	8.6	18.0
Electrical Conductivity 1373 K	Set 1	9.9	21.4	1.0	1.0	9.8	21.3
	Set 2	8.7	18.6	0.9	0.9	8.7	18.5
	Set 3	3.7	7.9	0.3	0.4	3.7	7.9
	Set 4	10.2	22.3	1.0	1.0	10.2	22.3
	Set 5	7.3	15.4	0.7	0.7	7.2	15.4
Electrical Conductivity 1473 K	Set 1	8.9	19.3	0.9	0.9	8.9	19.3
	Set 2	7.9	16.8	0.8	0.8	7.9	16.8
	Set 3	3.3	7.1	0.3	0.3	3.3	7.1
	Set 4	9.3	20.3	0.9	0.9	9.2	20.2
	Set 5	6.6	13.9	0.7	0.7	6.5	13.9

(a) Means were calculated over the 200 simulations per scenario and waste type. Minimums and maximums were calculated over the means from the 64 scenarios for each waste type.

(b) $\%RSD_T$ = total batch-to-batch variation and within-batch uncertainty %RSD, $\%RSD_B$ = batch-to-batch variation %RSD, and $\%RSD_W$ = within-batch uncertainty %RSD.

9.3 Additional Data Needed to Quantify Variations and Uncertainties

The following subsections discuss future WTP Project work that is planned or needed to quantify variations and uncertainties affecting the WTP HLW and LAW vitrification facilities. It is envisioned that the identified activities will be accomplished in one or more of the testing, WFQ, cold commissioning, or hot commissioning stages of the WTP Project.

9.3.1 Batch-to-Batch Variation of Incoming HLW and LAW

The Needs: The WTP Project should identify and implement an approach to quantify the expected variation in compositions of HLW and LAW corresponding to the range of HLW and LAW waste types to be processed.

Recommendation: Runs of the G2 software (Deng 2005) based on estimated "feed vectors" are a potential source for this data, although G2 currently assumes no variation in waste composition across a given waste type. Hence, G2 would have to be modified to track waste composition variations associated with HLW and LAW waste types.

Previously, batch-to-batch waste composition variations were quantified using DWPF and WVDP operating data.[(a)] However, those estimates of batch-to-batch variations for DWPF and WVDP were calculated over lengthy periods of production corresponding to a waste type. WTP batch-to-batch variations may be smaller than calculated for DWPF and WVDP because WTP waste types will correspond to much shorter periods of production. Because Hanford wastes, retrieval order, and pretreatment will be different than for DWPF and WVDP, at most the DWPF and WVDP estimates of batch-to-batch waste composition variation should be used for comparison to WTP estimates.

9.3.2 Systematic and Random Mixing Uncertainties for HLW MFPV and LAW CRV

The Needs: The WTP Project should demonstrate that HLW MFPVs (before and after addition of GFCs), LAW CRVs, and LAW MFPVs will be adequately mixed by MMs. From a statistical standpoint, a vessel would be considered adequately mixed and not have inhomogeneity (i.e., systematic uncertainty) if the difference in average composition (over time while mixing a given batch in that vessel) at any two points in a vessel is accounted for by the random uncertainty in composition at any particular point in the vessel. It is also necessary to quantify mixing random uncertainty and demonstrate that it does not vary significantly in magnitude at different points within a vessel.

Recommendation: Continue with the planned work as discussed in test specifications for HLW (Sundar 2005a) and LAW (Sundar 2005b).

(a) See Sections 3 and 4 of Heredia-Langner, A, GF Piepel, and SA Hartley. 2003. *Interim Report: Initial Assessment of Waste, Process, and Product Variations and Uncertainties for Waste Treatment Plant IHLW and ILAW*, WTP-RPT-073 Rev. 0, Battelle—Pacific Northwest Division, Richland, WA.

9.3.3 Systematic and Random Sampling Uncertainties

The Needs: According to WTP Project process control and compliance strategies, in the IHLW facility, MFPVs will be sampled before and after GFC addition whereas in the ILAW facility, only the CRVs will be sampled. However, the ILAW MFPV and MFVs for both HLW and LAW may be sampled during commissioning activities and possibly during production activities if required for sufficient cause. The compliance strategies for IHLW and ILAW also call for limited product sampling. As part of WFQ activities, the WTP Project should demonstrate that sampling systems for each vessel that will be sampled can draw representative samples. This is defined by the Engineering Specification for the Autosampling System (24590-WTP-3PS-MHSS-T0002, Section 3.3.1) as the source and sample results being within ± 1%. From a statistical perspective, this may be too restrictive a requirement if WFQ testing leads to an estimate of sampling systematic uncertainty (bias) greater than ± 1% that is not statistically significant relative to sampling random uncertainty. The initial sampling systems at the DWPF and WVDP HLW vitrification facilities drew non-representative samples during WFQ testing. Upon the discovery, the problems were corrected, and testing was performed again to demonstrate representative sampling. The WTP Project should also demonstrate that representative product samples can be taken. In addition, the WTP Project should quantify random sampling uncertainties (associated with slurry in vessels as well as product in canisters) for all components (including radionuclides) that will be used to make process control decisions, reported, or used in any of the methods to demonstrate compliance with WASRD (DOE-RW 2002) or Contract (DOE-ORP 2005) specifications.

Recommendation: Test specifications for HLW (Sundar 2005a) and LAW (Sundar 2005b) include plans for performing some of the work mentioned. Hence, the WTP Project should plan for how the other needs will be met.

9.3.4 Systematic and Random Analytical Uncertainties

The Needs: Samples collected from various vessels in the WTP HLW and LAW vitrification facilities (see Section 6.3.4) will be chemically analyzed for components of interest (including many radionuclides), depending on the vessel. The WTP Project should demonstrate during WFQ activities that the chemical analysis methods and results will yield unbiased results (i.e., results without systematic uncertainties). However, it is extremely difficult if not impossible for any chemical analysis procedure to always yield unbiased results. Therefore, it will be necessary for the WTP to have bias detection methods in place so that biased chemical analyses are detected and then either rejected or corrected. Weier and Piepel (2003) discuss methods for detecting and correcting biased chemical analysis results as well as methods to normalize analyzed chemical compositions so they sum to 100 wt% (which reduces uncertainties compared to not doing it). Also, the WTP Project should quantify random analytical uncertainties for all components (including radionuclides) that will be reported or used for process control decisions or in any of the methods to demonstrate compliance with WASRD (DOE-RW 2002) or Contract (DOE-ORP 2005) specifications.

Recommendation: The random analytical uncertainty estimates (1) discussed in Section 4.2.3 for IHLW and ILAW and (2) summarized in Tables C.1, C.2, and C.3 for IHLW and Table D.6 for ILAW are values based on experience of the WTP analytical group. To reflect the uncertainty in these uncertainty estimates, larger estimates were also investigated in the work of this report. Random analytical uncertainty was found to be a major contributor to the uncertainties of calculated IHLW and ILAW

compositions and properties. Therefore, the actual laboratory random uncertainties in chemical analysis results for components (including radionuclides) in an LAW CRV, an HLW MFPV (before GFC addition), and an IHLW MFPV (after GFC addition) will need to be reviewed, compared with those in this document, and revisions in overall uncertainties made as required. Also, because systematic uncertainties (biases) are likely to occur at times during WTP operations, the WTP Project should have procedures for detecting biased analyses when they occur and either correcting them (via bias correction methods, see Weier and Piepel 2003) or rejecting them and reanalyzing.

9.3.5 Systematic and Random Density Uncertainties

The Needs: The densities of the contents of HLW MFPVs (before and after GFCs addition) and LAW CRVs will be determined for compliance and/or process control purposes during operation of the WTP IHLW and ILAW facilities. Densities will be measured in-line as well as with laboratory methods for samples from some vessels. The WTP Project should demonstrate that both in-line and laboratory methods yield unbiased density values (i.e., values without systematic uncertainty). Work should also be performed to quantify the random uncertainties of density measurements made using both methods.

Recommendation: Continue with the work planned as discussed in test specifications by Sundar (2005a, 2005b), and consider including work to address needs that may not have been originally planned.

9.3.6 Systematic and Random Level and Volume Uncertainties

The Needs: Volumes of the contents of HLW MFPVs, LAW CRVs and MFPVs, and HLW and LAW MFVs will be determined for compliance and/or process control purposes during operation of the WTP IHLW and ILAW facilities. Volumes will not be measured directly, but indirectly by measuring the level of contents in a vessel. A radar level detection system is currently planned for this purpose. Then, a level-volume calibration equation for each vessel will be used to calculate the volume corresponding to the measured level of a vessel's contents. The WTP Project should develop and test the radar (or some other) level detection system and verify that it provides unbiased measures of the level of vessel contents. The random uncertainty in level measurements should also be quantified. Because current WTP plans are to continue mixing the contents of vessels while measuring their levels, the estimates of systematic and random uncertainties in vessel levels should take into account any bias and uncertainty in vessel levels caused by the operation of the mixing equipment. For example, mechanical mixers create a vortex in which the level at the center is lower than at the edges, such that measuring at an edge could provide a biased, over-estimate of vessel level.

The WTP Project should also collect volume-level calibration data for each vessel and use that data to develop volume-level calibration equations. It will be necessary to verify that the calibration equations yield unbiased estimates of volume given a measured level and also to quantify the uncertainty associated with volumes calculated using a given calibration equation. Assuming measured levels are unbiased and calibration equations are unbiased, the total random uncertainty in a calculated vessel volume should include both level measurement random uncertainty as well as volume-level calibration equation random uncertainty.

Recommendation: Continue the work planned to quantify systematic and random uncertainties associated with the radar level detection system in the HLW MFPV, LAW CRV, and LAW MFPV as discussed by

Sundar (2005a, 2005b). Collect volume versus level calibration data for WTP HLW and LAW CRVs, MFPVs, and MFVs, and develop volume-level calibration equations. Quantify the uncertainty in the calibration equations.

9.3.7 IHLW MFPV, LAW CRV, and ILAW MFPV Receipt and Transfer Uncertainties

The Needs: The process of transferring material out of an LAW CRV, and in or out of an HLW or LAW MFPV could be subject to uncertainties in composition. For example, there could be uncertainty caused by non-isokinetic flows at the transfer line suction or by solids segregation in vertical portions of the transfer line. The transfer processes that will be used in the IHLW and ILAW facilities should be studied to verify that there are no systematic uncertainties introduced and to quantify any random uncertainties inherent in the transfer process.

Recommendation: Continue the work discussed by Sundar (2005a, 2005b), and ascertain whether it will completely address these needs. If not, it is recommended that work to address the missing needs be incorporated in that or other appropriate testing.

9.3.8 GFC Composition and GFC Batching, Weighing, and Transfer Uncertainties

The Needs: The WTP Project will have to verify that the compositions of GFCs used for process control and compliance purposes are unbiased within applicable uncertainties. That is, the GFC compositions used for process control and compliance must represent the true average compositions over the period of time specific batches of GFCs are used. The WTP process control strategy and algorithms can account for different compositions of GFCs over different batches of GFCs, provided the estimated/nominal compositions are unbiased. It will also be necessary to quantify the random uncertainty in the compositions of GFCs about the nominal/estimated values that can occur over time (e.g., over a batch of GFCs). The WTP Project should also verify that weighing equipment associated with individual GFC weigh hoppers and GFC Blending Silos (in the GFC facility) and GFC Feed Hoppers (in the HLW and LAW vitrification facilities) yield unbiased weights. The uncertainties associated with measured weights in each of these hoppers should also be quantified. Finally, the WTP Project should verify that GFCs can be transferred from the GFC facilities to the MFPVs in the HLW and LAW vitrification facilities without significant loss (holdup) or gain (holdup breaking free). Such losses or gains would involve biases (systematic uncertainties) in either the makeup or mass of the GFCs to be added to an IHLW or ILAW MFPV. In addition, the random uncertainties in transfer of blended GFCs to an IHLW or ILAW MFPV should be quantified.

Recommendation: Section 4.4 discussed preliminary information about GFC compositions and uncertainties as well as GFC batching, weighing, and transfer uncertainties. Final estimates of GFC compositions and their uncertainties for each batch of GFCs are expected to come from vendor certifications when the GFCs are delivered. The remaining aspects to establish final bias and uncertainty estimates will also need to be addressed.

10.0 Results Relative to WTP Needs

The results in this report meet, or will contribute to meeting, several needs of the WTP Project. The following list identifies the WTP needs addressed by the results in this report.

1. Quantify the variations and uncertainties associated with individual steps of the HLW and LAW vitrification processes

   The WTP Project will use estimates of variations and uncertainties affecting the HLW and LAW vitrification processes in algorithms/software that will be used during plant operations to control the processes and demonstrate compliance with applicable specifications. Current estimates of these variations and uncertainties are presented and discussed in Section 4 (IHLW and ILAW), Appendix C (IHLW), and Appendix D (ILAW). While these estimates are not based on actual operational information, the values (or ranges) used are expected to be representative (or span the possible values) of what will occur during operations. As additional testing data and actual operating data become available in the future, they should be compared to the results in this report.

2. Quantify the variations and uncertainties in IHLW and ILAW compositions and properties

   The WTP Project must include in the IHLW and ILAW Product Qualification Reports information about the variation and uncertainty in IHLW and ILAW compositions and properties. Section 7 (IHLW) and Section 8 (ILAW) summarize estimates of %RSDs for batch-to-batch variation, within-batch uncertainty, and the total variation plus uncertainty in compositions and properties. These %RSD summaries are made for individual glass components (chemical and radionuclide) and glass properties for combinations of the factors studied. Table 10.1 summarizes the ranges of the total %RSD values displayed for (1) IHLW in Figure 7.1, Figure 7.4, Figure 7.7 through Figure 7.11 and (2) ILAW in Figure 8.1, Figure 8.4, Figure 8.7 through Figure 8.10, excluding extreme values. The ranges of total %RSD given in Table 10.1 for (1) IHLW are over the 8 combinations of the "all low" and "all high" scenarios for each of the four HLW waste types, and (2) ILAW are over the 10 combinations of the "all low" and "all high" scenarios for each of the five LAW data sets (waste types). However, the ranges in Table 10.1 over all (1) 48 combinations of 12 scenarios for each of the four HLW waste types and (2) 320 combinations of 64 scenarios for each of the five LAW data sets (waste types) would be expected to be very close to the ranges based only on the "all low" and "all high" scenarios.

   Ranges are given in Table 10.1 for means and 90% ECIs[(a)] of total %RSD values. The means and 90% ECIs for total %RSD were calculated over the 200 simulations of each scenario with each HLW or LAW waste type. Hence, the means of total %RSDs represent the average of total variation plus uncertainty that may be experienced by the WTP vitrification facilities for a particular waste type and variation/uncertainty scenario. The 90% ECIs of total %RSDs represent the intervals of total %RSD values that may be experienced by the WTP facilities for a given waste type and scenario. The ranges for means and 90% ECIs of total %RSDs in Table 10.1 can be used to make general conclusions about the total %RSD results depending on whether the variations and uncertainties in all factors are expected to be near the low case values or the high case values. Differentiating between the low and

(a) See the definitions in Sections 6.1.5 and 6.2.4 for IHLW and ILAW, respectively.

high case values is most important for those processing factors listed subsequently in Table 10.2 that are deemed highly influential. Recall that tables in Appendix E (IHLW) and Appendix F (ILAW) present summaries of mean %RSD values for batch-to-batch variation, within-batch uncertainty, and total variation plus uncertainty for additional scenarios compared to the ones with all factors at low levels and all at high levels. The effects of significant factors versus non-significant factors can be seen in those summaries.

Table 10.1. Ranges of Total %RSD (Variation plus Uncertainty) for Chemical Composition Components, Radionuclide Composition Components, and Glass Properties for IHLW and ILAW

Variables	Total %RSD Range with All Uncertainties at the Low Case		Total %RSD Range with All Uncertainties at the High Case	
	Mean[(a)]	90% ECI[(b)]	Mean[(a)]	90% ECI[(b)]
IHLW				
Chemical Composition Components	1% - 6%	1% - 11%	7% - 18%	5% - 23%
Radionuclide Composition Components	2% - 15%	1% - 18%	10% - 30%	7% - 39%
Glass Properties	1% - 13%	1% - 16%	5% - 40%	3% - 48%
ILAW				
Chemical Composition Components	2% - 8%	1% - 13%	3% - 17%	2% - 24%
Radionuclide Composition Components	3% - 14%	2% - 20%	7% - 28%	4% - 38%
Glass Properties	3% - 20%	2% - 24%	5% - 35%	3% - 49%

(a) The means and 90% EUCLs for total %RSD are over the 200 simulations for each scenario and each waste type (or data set) as defined in Table 5.2 for IHLW and Table 5.4 for ILAW.

(b) A 90% ECI is a 90% empirical confidence interval, defined in Section 6.1.5 for IHLW and in Section 6.2.4 for ILAW. The ranges given are the lower and upper limits on total %RSD that encompass most 90% ECIs (the exceptions being outlier 90% ECIs).

Note that the uncertainties of IHLW and ILAW properties summarized in Table 10.1 are only those uncertainties associated with composition variation and uncertainty. Properties will be predicted with property-composition models that are also subject to uncertainty. Methods for quantifying uncertainties in property-composition model predictions are discussed for the current IHLW models by Kot et al. (2004, 2005) and for the current ILAW models by Muller et al. (2005). Final versions of the Kot et al. (2005) and Muller et al. (2005) reports containing final property-composition models and uncertainties are planned for the future.

3. Understand which process factors influence the variations and uncertainties of WTP IHLW and ILAW compositions and properties

Table 10.2 summarizes the degree of influence that each factor had on total %RSD (variation and uncertainty) for IHLW and ILAW compositions (chemical and radionuclide) and properties. These results are only valid for factor values within the ranges defined in Table 5.1 (IHLW) and Table 5.3 (ILAW). Analytical uncertainty and mixing/sampling uncertainty have the most significant effects on total %RSD. Hence, they should be the first factors considered if decreasing total uncertainty is necessary. Recall that the results in Table 10.2 are after averaging results over single analyses of

multiple samples per LAW CRV or IHLW MFPV batch, which provides for effectively reducing mixing/sampling and analytical uncertainties.

Table 10.2. The Degree of Influence Each Factor[(a)] Had on Variation Plus Uncertainty (Total %RSD) for IHLW and ILAW

Highly Significant Influence[(b)]	Moderately Significant Influence	Slightly or No Significant Influence[(b)]
IHLW		
Analytical Uncertainty Mixing/Sampling Uncertainty Random Batch-to-Batch Variation Waste Type	None	None
ILAW		
Analytical Uncertainty Mixing/Sampling Uncertainty ILAW Data Set (Waste Type) GFC Batching & Transfer Uncertainty	GFC Composition Uncertainty	Random Batch-to-Batch Variation Volume Uncertainty

(a) The factors are listed in Table 5.1 for IHLW and Table 5.3 for ILAW.
(b) Factors are listed in the order of relative significance, with the most significant listed first.

As expected, the HLW or LAW waste type also significantly affects the total %RSD. Note that systematic batch-to-batch variations are contributors to differences in results for HLW or LAW waste types. Therefore, systematic batch-to-batch variation is not a factor directly varied in the simulations, only indirectly as nominal compositions for transition waste types change from batch to batch. That is why only random batch-to-batch variation is listed as a factor in Table 10.2. The "random batch-to-batch variation" factor was highly significant for IHLW, but not very significant for LAW. This difference is likely a result of systematic batch-to-batch variation existing in every LAW data set, whereas it was indistinguishable from random batch-to-batch variation for the HLW waste types except the AY-102 to AZ-102 transition waste type.

4. Determine the values of variations and uncertainties that would allow all processing and compliance requirements to be met

For design input, the WTP Project needs to know how much variation over a waste type, as well as various uncertainties (e.g., mixing uncertainty, sampling uncertainty, chemical and radionuclide analyses, volume and other measurements) affecting steps of the HLW and LAW vitrification processes can occur and still meet processing and compliance requirements. The results in this report do not address this need. The work of Piepel et al. (2005) addressed this need for compliance requirements, but not processing requirements. The algorithm development and testing work being conducted by the WTP Project (see Item 6, subsequently) is the other area of work where such needs could be addressed.

5. Determine the numbers of samples, analyses, and other process measurements needed to meet IHLW and ILAW processing and compliance requirements

Piepel et al. (2005) showed that the number of samples per batch (CRV for ILAW, MFPV for IHLW) and the number of analyses per sample significantly influence the magnitude of total uncertainty. All investigations in this report used three samples with one analysis each for ILAW and eight samples with one analysis each for IHLW. Single determinations of volume and density were also assumed. These values are the basis of current WTP planning and were shown by Piepel et al. (2005) to be sufficient for meeting all IHLW and ILAW compliance requirements, provided the variations and uncertainties in the vitrification processes fall within the ranges used in that work. A final iteration of this work is scheduled for the future and will use estimates of variations and uncertainties from this report or other sources that contain updated estimates compared to what was used in Piepel et al. (2005).

6. Develop glass formulation algorithms to be used in running the WTP HLW and LAW vitrification processes

The WTP Project is responsible for developing algorithms for the HLW and LAW vitrification facilities to develop glass formulations for each MFPV batch and to calculate volume transfers, GFC additions, and any other quantities associated with achieving the target glass composition. The algorithms will also calculate as-batched glass compositions and perform statistical and non-statistical verifications that each MFPV batch will meet applicable compliance specifications and processing requirements. The first iteration of this work has been completed for ILAW (Vienna 2005; Vienna et al. 2006) and is in progress for IHLW. The algorithms make significant use of statistical compliance methods presented by Piepel et al. (2005). They also make use of the variations and uncertainties and Monte Carlo simulation approach from this report to account for variations and uncertainties and thereby provide the desired protection against making melter feed batches that would not satisfy compliance or processing requirements.

11.0 References

Alcoa World Chemicals. 2003. *Normal Soda, Low Surface Area, Hard Burned Calcined Alumina*. USA/0101-R02/0101, Alcoa World Chemicals, Bauxite, AZ. (Previously available at the web site http://www.alumina.alcoa.com, although that web site is no longer available without permission.)

Amcells Corporation. 2003. Amcells Corporation, Carlsbad, CA. Available at: http://www.amcells.com.

Amidan BG, GF Piepel, DS Kim, and JD Vienna. 2004. *Statistical Assessment of Bias and Random Uncertainties in WTP HLW CRV Mixing and Sampling*. WTP-RPT-126 Rev. 0, Battelle—Pacific Northwest Division, Richland, WA.

Arakali A, D Blumenkranz, JL Meehan, LA Huffman, and J Yokel. 2004. *Regulatory Data Quality Objectives Optimization Report*. 24590-WTP-RPT-MGT-04-001, Rev. 0, River Protection Project, Waste Treatment Plant, Richland, WA.

Battelle—Pacific Northwest Division (PNWD). 2005a. *Bechtel National Inc. Support Program Quality Assurance Plan*. Rev. 0, Richland, WA.

Battelle—Pacific Northwest Division (PNWD). 2005b. *Waste Treatment Plant Support Project-Quality Assurance Requirements and Description*. Rev. 2, Richland, WA.

Brooks KP, PR Bredt, SK Cooley, GR Golcar, LK Jagoda, KG Rappe, and MW Urie. 2000. *Characterization, Washing, Leaching, and Filtration of AZ-102 Sludge*. PNWD-3045 (BNFL-RPT-038) Rev. 0, Battelle—Pacific Northwest Division, Richland, WA.

Cook J, and D Blumenkranz. 2003. *Data Quality Objectives Process in Support of LDR/Delisting at the RPP-WTP*. 24590-WTP-RPT-ENV-01-012 Rev. 2, River Protection Project, Waste Treatment Plant, Richland, WA.

Cooper Instruments and Systems. 2002. *LGP 312- Pancake Load Cell Specifications*. Cooper Instruments and Systems, Warrenton, VA.

Cross S. 2005. *HFP-VSL-00001 and HFP-VSL-00002 Vessel Sizing Calculation*. Calculation No. 24590-HLW-M6C-HFP-00001 Rev. D, River Protection Project, Waste Treatment Plant, Richland, WA.

Deng Y. 2005. *Dynamic (G2) Model Design Document.* 24590-WTP-MDD-PR-01-002 Rev. 8, River Protection Project, Waste Treatment Plant, Richland, WA.

DOE-ORP, see U.S. Department of Energy, Office of River Protection.

DOE-RW, see U.S. Department of Energy, Office of Civilian Radioactive Waste Management.

Fielding P. 2003. *Engineering Specification for Radar Level Measurement*. 24590-WTP-3PS-JL10-

T0002 Rev. 0, River Protection Project, Waste Treatment Plant, Richland, WA.

Futek. 2003. *L2920 Tension & Compression Load Cell*. Futek, Irvine, CA. Available at: http://www.futek.com.

Geeting JGH, RT Hallen, LK Jagoda, AP Poloski, RD Scheele, and DR Weier. 2002. *Filtration, Washing, and Caustic Leaching of Hanford Tank AZ-101 Sludge*. PNWD-3206 (WTP-RPT-043) Rev. 0, Battelle—Pacific Northwest Division, Richland, WA.

Goheen SC, PR Bredt, OT Farmer, SK Fiskum, KA Gaither, LR Greenwood, and LK Jagoda. 2002. *Chemical Analysis and Physical Property Testing of Diluted 241-AP-101 Tank Waste*. PNWD-3174 (WTP-RPT-022) Rev. 0, Battelle—Pacific Northwest Division, Richland, WA.

Hay MS, CJ Coleman, and KB Martin. 2003. *Characterization and Dilution of a River Protection Project Sample from Tank 241-AW-101*. WSRC-TR-2002-00509 (SRT-RPP-2002-00255) Rev. 0, Westinghouse Savannah River Company, Aikin, SC.

Heredia-Langner, A, GF Piepel, and SA Hartley. 2003. *Interim Report: Initial Assessment of Waste, Process, and Product Variations and Uncertainties for Waste Treatment Plant IHLW and ILAW*. WTP-RPT-073 Rev. 0, Battelle—Pacific Northwest Division, Richland, WA.

Holgado P. 2001. *LAW Concentrate Receipt Vessels LCP-VSL-00001/00002/00003 Sizing*. Calculation No. 24590-LAW-M6C-LCP-00001 Rev. 0, River Protection Project, Waste Treatment Plant, Richland, WA.

Holgado P. 2003. *LFP-VSL-00001, 00003, 00005 Sizing*. Calculation No. 24590-LAW-M6C-LFP-00001 Rev 0B, River Protection Project, Waste Treatment Plant, Richland, WA.

Insightful Corp. 2003. S-Plus®. Version 6.2 for Windows, Build 6713, Seattle, WA.

Kaiser B, S Rueff, S Bakhtiar, L Burchfield, D Dodd, B Kapoor, A Marcheson, and C Rueff. 2003. *Analytical Laboratory Design Requirements: WTP Sampling and Analysis Plan*. 24590-WTP-PL-PR-01-004 Rev. 3, River Protection Project, Waste Treatment Plant, Richland, WA.

Kaiser B, D Dodd, A Holland, and S Rueff. 2004. *Integrated Sampling and Analysis Requirements Document*. 24590-WTP-PL-PR-04-001 Rev. 0, River Protection Project, Waste Treatment Plant, Richland, WA.

Kot WK, K Klatt, H Gan, IL Pegg, SK Cooley, GF Piepel, and DJ Bates. 2004. *Regulatory Testing of RPP-WTP HLW Glasses to Support Delisting Compliance*. VSL-04R4780-1, Rev. 0, Vitreous State Laboratory, The Catholic University of America, Washington, DC.

Kot WK, H Gan, H Feng, F Perez-Cardenas, IL Pegg, SK Cooley, and GF Piepel. 2005. *Development of Phase 1 IHLW Models for PCT Response and One-Percent Crystal Fraction Temperature ($T_{1\%}$)*. VSL-05R5780-1, Rev. 0, Vitreous State Laboratory, The Catholic University of America, Washington, DC.

Kyanite Mining Corporation. 2001. *Characterization of HLW and LAW Glass Formers*. WSRC-TR-2002-00282 (SRT-RPP-2002-00146) Rev. 0, Westinghouse Savannah River Company, Aiken, SC.

Lee E. 2004. *Model Run Request: No Leach with Modified Oxalate Feed Vector Phase I Tanks*. 24590-WTP-MRQ-PO-03-128, Rev. 0, River Protection Project, Waste Treatment Plant, Richland, WA.

Martin KB, CJ Coleman, and MS Hay. 2003. *Compositing, Homogenization, and Characterization of Samples from Hanford Tank 241-AN-107 (U)*, WSRC-TR-2003-00210 Rev. 0, Westinghouse Savannah River Company, Aikin, SC.

The MathWorks, Inc. 2005. MATLAB®. Version 7.0.4.352, Release 14, Natick, MA.

Muller I, H Gan, IL Pegg, SK Cooley, and GF Piepel. 2005. *Phase 1 ILAW PCT and VHT Model Development*. VSL-04R4480-2 Rev. 0, Vitreous State Laboratory, The Catholic University of America, Washington, DC.

Nelson J. 2005. *IHLW Product Compliance Plan.* 24590-WTP-PL-RT-03-002 Rev. 2, River Protection Project, Waste Treatment Plant, Richland, WA.

NQA-1. 1989. *Quality Assurance Program Requirements for Nuclear Facilities*. American Society of Mechanical Engineers, New York, NY.

NQA-2a. 1990. *Quality Assurance Requirements for Nuclear Facility Applications*. American Society of Mechanical Engineers, New York, NY.

NYCO Minerals, Inc. 1998. Wollastonite data sheet. Willsboro, NY.

Patello GK, TL Almeida, JA Campbell, OT Farmer, EW Hoppe, CZ Soderquist, RG Swoboda, MW Urie, J Wagner, and D Blumenkranz. 2001. *Regulatory DQO Test Plan for Determining Method Detection Limits, Estimated Quantitation Limits, and Quality Assurance Criteria for Specified Analytes.* PNNL-13429, TP-41500-003 Rev.0, Pacific Northwest National Laboratory, Richland, WA.

Piepel GF, JM Szychowski, and JL Loeppky. 2002. "Augmenting Scheffé Linear Mixture Models with Squared and/or Crossproduct Terms." *Journal of Quality Technology* 34:297-314.

Piepel GF, and A Heredia-Langner. 2003. *Statistical Methods for Estimating Variations in HLW and LAW Waste Types.* Test Plan TP-RPP-WTP-193 Rev. 1, Battelle—Pacific Northwest Division, Richland, WA.

Piepel GF, BG Amidan, A Heredia-Langner, DR Weier, and SK Cooley. 2005. *Statistical Methods and Results for WTP IHLW and ILAW Compliance*. PNWD-3568 (WTP-RPT-072), Rev. 1, Battelle—Pacific Northwest Division, Richland, WA.

PNWD, see Battelle—Pacific Northwest Division.

Prince Manufacturing Company. 1999. *Analytical Data on Rouge (Iron Oxide) 5001*. Quincy, IL.

Reutell KP. 2005. *Engineering Specification for the Glass Former Storage Facility*. 24590-BOF-3PS-G000-T0007 Rev. 2, River Protection Project, Waste Treatment Plant, Richland, WA.

Schumacher RF. 2003. *Characterization of HLW and LAW Glass Formers*. WSRC-TR-2002-00282 (SRT-RPP-2002-00146) Rev. 1, Westinghouse Savannah River Company, Aiken, SC.

Sensotec (Honeywell). 2003. *Precision Pancake Load Cells, Models 41 and 43*. Sensotec, Columbus, OH. Available at: http://www.sensotec.com.

Sundar PS. 2005a. *Assess Blended HLW and Melter Feed Compositions Variability Due to Processing*. 24590-HLW-TSP-RT-01-015 Rev. 3, River Protection Project, Waste Treatment Plant, Richland, WA.

Sundar PS. 2005b. *Assess LAW Melter Feed Composition Variability Due to Processing*. 24590-LAW-TSP-RT-02-019 Rev. 1, River Protection Project, Waste Treatment Plant, Richland, WA.

Swanberg DJ. 2002. *Statistical Methods for Estimating Variations in HLW and LAW Waste Types.* Test Specification 24590-WTP-TSP-RT-02-007 Rev 0, River Protection Project, Waste Treatment Plant, Richland, WA.

Urie MW, JJ Wagner, LR Greenwood, OT Farmer, SK Fiskum, RT Ratner, CZ Soderquist. 1999. *Inorganic and Radiochemical Analysis of AW-101 and AN-107 "Diluted Feed" Materials.* PNWD-2463 (BNFL-RPT-003) Rev. 1, Battelle—Pacific Northwest Division, Richland, WA.

U.S. Borax Inc. 2001. *Borax Decahydrate Technical Granular, Product Specification B-0210-U*. Valencia, CA.

U.S. Department of Energy, Office of Civilian Radioactive Waste Management (DOE-RW). 2002. *Civilian Radioactive Waste Management System Waste Acceptance System Requirements Document*. DOE/RW-0351 Rev. 4, Washington, DC.

U.S. Department of Energy, Office of Civilian Radioactive Waste Management (DOE-RW). 2003. *Quality Assurance Requirements and Description*. DOE/RW-0333P Rev. 13, Washington DC.

U.S. Department of Energy Office of River Protection (DOE-ORP). 2005. *Design, Construction, and Commissioning of the Hanford Tank Waste Treatment and Immobilization Plant.* Contract No. DE-AC27-01RV14136, Modification No. M047 for Section C, Richland, WA.

U.S. Silica Company. 1997a. S*IL-CO-SIL 75 Ground Silica, Mill Creek, Oklahoma Plant, Product Data*. Berkeley Springs, WV.

U.S. Silica Company. 1997b. *SIL-CO-SIL 75 Ground Silica, Berkeley Springs, West Virginia Plant, Product Data*. Berkeley Springs, WV.

U.S. Silica Company. 1997c. *SIL-CO-SIL 75 Ground Silica, Pacific, Missouri Plant, Product Data*. Berkeley Springs, WV.

U.S. Silica Company. 1997d. *SIL-CO-SIL 75 Ground Silica, Columbia, South Carolina Plant, Product Data*. Berkeley Springs, WV.

Vienna JD. 2005. *Preliminary ILAW Formulation Algorithm Description*. 24590-LAW-RPT-RT-04-0003 Rev. 0, River Protection Project, Waste Treatment Plant, Richland, WA.

Vienna JD, GF Piepel, CA Musick, IS Muller, and IL Pegg. 2006. "Preliminary Control Strategy for Hanford Low-Activity Waste Glass Formulation," *Ceramic Transactions*, 176, 239-245, American Ceramic Society, Westerville, OH.

Vora V. 2004. *Dynamic (G2) Model Version 3.1 Verification and Validation Repor*t. 24590-WTP-VV-PO-04-0004 Rev. 0, River Protection Project, Waste Treatment Plant, Richland, WA.

Weier DR, and GF Piepel. 2003. *Methodology for Adjusting and Normalizing Analyzed Glass Compositions.* PNWD-3260 (WTP-RPT-049) Rev. 0, Battelle—Pacific Northwest Division, Richland, WA.

Westsik J, J Nelson, J Vienna, D Larson, and L Petkus. 2004. *ILAW Product Compliance Plan.* 24590-WTP-PL-RT-03-001 Rev. 1, River Protection Project, Waste Treatment Plant, Richland, WA.

Wilson DJ. 2002. *LFP-VSL-00002,00004,00006 Sizing.* Calculation No. 24590-LAW-M6C-LFP-00002 Rev. 0, River Protection Project, Waste Treatment Plant, Richland, WA.

Appendix A

Equations for Calculating the Chemical and Radionuclide Composition of IHLW Corresponding to an MFPV Batch

Appendix A: Equations for Calculating the Chemical and Radionuclide Composition of IHLW Corresponding to an MFPV Batch

This appendix presents the equations used to calculate the chemical and radionuclide composition of IHLW corresponding to an MFPV batch. The equations, notation, and terminology are taken from Sections A.1.2 and A.2.1 of Appendix A in Piepel et al. (2005). The derivations of the equations are included in that section of Appendix A.

For the m^{th} chemical and radionuclide analyses of the j^{th} analyte in the l^{th} sample from the i^{th} IHLW MFPV batch, the mass-balance equation to calculate IHLW composition is given by

$$g_{ijlm}^{MFPV} = \frac{c_{ijlm}^{MFPV} f_j}{\sum_{j=1}^{J} c_{ijlm}^{MFPV} f_j} \tag{A.1}$$

where

g_{ijlm}^{MFPV} = mass fraction of the j^{th} glass component (oxide or halogen) resulting from the m^{th} chemical and radionuclide analyses of the l^{th} sample from the i^{th} IHLW MFPV batch (g_{oxide}/g_{oxides})

c_{ijlm}^{MFPV} = analyzed concentration of the j^{th} analyte from the m^{th} analysis of the l^{th} sample from the i^{th} IHLW MFPV batch (μg/mL = mg/L)

f_j = $\frac{MW_j^{oxide}}{MW_j^{analyte}} R_j$ where MW_j^{oxide} and $MW_j^{analyte}$ are the molecular weights of oxide j and analyte j, respectively, and R_j is the ratio of moles of oxide per mole of analyte for oxide j. Hence, f_j is the factor for converting the concentration of analyte j (μg analyte j/mL = mg analyte j/L) to the concentration of oxide j (μg oxide j/mL = mg oxide/L). The quantity f_i is called the oxide factor for oxide j.

J = number of chemical and radionuclide composition components (oxides and halogens) for the IHLW composition.

A sample from the i^{th} IHLW MFPV batch is indexed by l = 1, 2, … , n_S^{MFPV} where x denotes the number of samples per MFPV batch. A chemical or radionuclide analysis is indexed by m = 1, 2, … , x where n_A^{MFPV} denotes the number of chemical or radionuclide analyses per MFPV sample. In the preceding notation, when n_A^{MFPV} = 1, the m subscript is not shown. The derivation of Eq. (A.1) is given in Section A.1.2 of Piepel et al. (2005).

Table A.1 lists the values of f_j for elements, radionuclides, and the expected prevalent oxide form for each in waste glass. Table A.1 applies to LAW glass as well as HLW glass.

During IHLW production, radiochemical analyses of MFPV samples will yield radionuclide concentrations in units of μCi/mL (= mCi/L). Such an activity-per-volume concentration of a radionuclide in the HLW MFPV can be converted to a mass-per-volume concentration by

$$c_{ijlm}^{MFPV} = \frac{r_{ijlm}^{MFPV}}{A_j} \tag{A.2}$$

where

c_{ijlm}^{MFPV} = mass-per-volume concentration of the j^{th} radionuclide for the m^{th} radiochemical analysis of the l^{th} sample from the i^{th} MFPV batch (μg/mL = mg/L)

r_{ijlm}^{MFPV} = activity-per-volume concentration of the j^{th} radionuclide for the m^{th} radiochemical analysis of the l^{th} sample from the i^{th} MFPV batch (μCi/mL = mCi/L)

A_j = specific activity of the j^{th} radionuclide (Ci/g = mCi/mg).

Table A.2 lists the values of A_j for a large number of radionuclides j. Table A.2 contains values for far more radionuclides than are reportable for IHLW (or immobilized low-activity waste [ILAW]), but the complete list is retained because the lists of reportable or otherwise important radionuclides are not yet finalized.

In summary, based on the WTP IHLW compliance strategy, Eqs. (A.1) and (A.2) provide for calculating the mass-fraction composition of IHLW corresponding to a single analysis of a single sample from a given IHLW MFPV batch.

Table A.1. Element and Radionuclide to Oxide Conversion Factors (f_j)

Element	Oxide	Oxide Factor
Ag	Ag_2O	1.074162
Al	Al_2O_3	1.889464
As	As_2O_5	1.533871
B	B_2O_3	3.219878
Ba	BaO	1.116506
Be	BeO	2.775308
Bi	Bi_2O_3	1.114839
Ca	CaO	1.399207
Cd	CdO	1.142329
Ce	Ce_2O_3	1.171281
Cl	Cl	1
Co	CoO	1.271484
Cr	Cr_2O_3	1.461556
Cs	Cs_2O	1.060191
Cu	CuO	1.251777
Dy	Dy_2O_3	1.147687
Eu	Eu_2O_3	1.157925
F	F	1
Fe	Fe_2O_3	1.429729
K	K_2O	1.204605
La	La_2O_3	1.172773
Li	Li_2O	2.152528
Mg	MgO	1.658276
Mn	MnO	1.291226
Mo	MoO_3	1.500294
Na	Na_2O	1.347968
Nd	Nd_2O_3	1.166383
Ni	NiO	1.272593
P	P_2O_5	2.291367
Pb	PbO	1.077217
Pd	PdO	1.150342
Pr	Pr_2O_3	1.170318
Rh	Rh_2O_3	1.233215
Ru	RuO_2	1.3166
S	SO_3	2.496856
Sb	Sb_2O_3	1.197107
Se	SeO_2	1.405253
Si	SiO_2	2.139335
Sn	SnO_2	1.269554

Element	Oxide	Oxide Factor
SO_4	SO_3	0.83345
Sr	SrO	1.1826
Th	ThO_2	1.137903
Ti	TiO_2	1.668312
Tl	Tl_2O	1.039141
U	UO_3	1.201649
V	V_2O_5	1.785185
W	WO_3	1.261073
Y	Y_2O_3	1.269938
Zn	ZnO	1.244677
Zr	ZrO_2	1.350772

Radionuclide	Oxide	Oxide Factor
^{241}Am	$^{241}Am_2O_3$	1.099581
^{243}Am	$^{243}Am_2O_3$	1.098762
^{144}Ce	$^{144}Ce_2O_3$	1.16666
^{242}Cm	$^{242}Cm_2O_3$	1.09917
$^{243+244}Cm$	$^{243+244}Cm_2O_3$	1.098559
^{60}Co	^{60}CoO	1.266657
^{51}Cr	$^{51}Cr_2O_3$	1.470571
^{134}Cs	$^{134}Cs_2O$	1.059699
^{135}Cs	$^{135}Cs_2O$	1.059257
^{137}Cs	$^{137}Cs_2O$	1.058392
^{152}Eu	$^{152}Eu_2O_3$	1.157889
^{154}Eu	$^{154}Eu_2O_3$	1.155838
^{155}Eu	$^{155}Eu_2O_3$	1.154833
^{59}Fe	$^{59}Fe_2O_3$	1.406764
^{93}Nb	$^{93}Nb_2O_5$	1.430091
^{95}Nb	$^{95}Nb_2O_5$	1.421037
^{59}Ni	^{59}NiO	1.271176
^{63}Ni	^{63}NiO	1.253959
^{237}Np	$^{237}NpO_2$	1.135021
^{236}Pu	$^{236}PuO_2$	1.135588
^{238}Pu	$^{238}PuO_2$	1.134449
^{239}Pu	$^{239}PuO_2$	1.133886
^{240}Pu	$^{240}PuO_2$	1.133328
^{241}Pu	$^{241}PuO_2$	1.132775
^{242}Pu	$^{242}PuO_2$	1.132226

Radionuclide	Oxide	Oxide Factor
^{106}Rh	$^{106}Rh_2O_3$	1.226407
^{103}Ru	$^{103}RuO_2$	1.310668
^{106}Ru	$^{106}RuO_2$	1.301875
^{125}Sb	$^{125}Sb_2O_3$	1.192
^{79}Se	$^{79}SeO_2$	1.405048
^{151}Sm	$^{151}Sm_2O_3$	1.158934
^{113}Sn	$^{113}SnO_2$	1.283175
^{126}Sn	$^{126}SnO_2$	1.253959
^{90}Sr	^{90}SrO	1.177771
^{99}Tc	$^{99}Tc_2O_7$	1.565657
^{232}Th	$^{232}ThO_2$	1.137926
^{233}U	$^{233}UO_3$	1.206009
^{234}U	$^{234}UO_3$	1.205128
^{235}U	$^{235}UO_3$	1.204255
^{236}U	$^{236}UO_3$	1.203390
^{238}U	$^{238}UO_3$	1.201681
^{88}Y	$^{88}Y_2O_3$	1.272717
^{93}Zr	$^{93}ZrO_2$	1.344073

Table A.2. List of Specific Activities A_j for Selected Isotopes j[(a)]

Isotope, j	A_j (Ci/g)	Isotope, j	A_j (Ci/g)	Isotope, j	A_j (Ci/g)	Isotope, j	A_j (Ci/g)	Isotope, j	A_j (Ci/g)
^{225}Ac	5.80E+04	^{139}Ce	8.00E+02	^{18}F	9.50E+07	^{87}Kr	2.80E+07	^{145}Pm	1.40E+02
^{227}Ac	7.20E+01	^{141}Ce	2.80E+04	^{52}Fe	7.30E+06	^{137}La	4.40E-02	^{147}Pm	9.30E+02
^{228}Ac	2.20E+06	^{143}Ce	6.60E+05	^{55}Fe	2.40E+03	^{140}La	5.60E+05	^{148m}P	2.10E+04
^{105}Ag	3.00E+04	^{144}Ce	3.20E+03	^{59}Fe	5.00E+04	^{172}Lu	1.10E+05	^{149}Pm	4.00E+05
^{108m}Ag	2.60E+01	^{248}Cf	1.60E+03	^{60}Fe	2.00E-02	^{173}Lu	1.50E+03	^{151}Pm	7.30E+05
^{110m}Ag	4.70E+03	^{249}Cf	4.10E+00	^{67}Ga	6.00E+05	^{174m}Lu	5.30E+03	^{208}Po	5.90E+02
^{111}Ag	1.60E+05	^{250}Cf	1.10E+02	^{68}Ga	4.10E+07	^{177}Lu	1.10E+05	^{209}Po	1.70E+01
^{26}Al	1.90E-02	^{251}Cf	1.60E+00	^{72}Ga	3.10E+06	^{74}Lu	6.20E+02	^{210}Po	4.50E+03
^{241}Am	3.40E+00	^{252}Cf	5.40E+02	^{146}Gd	1.90E+04	^{28}Mg	5.40E+06	^{143}Pr	1.20E+06
^{242m}Am	1.00E+01	^{253}Cf	2.90E+04	^{148}Gd	3.20E+01	^{52}Mn	4.40E+05	^{142}Pr	6.70E+04
^{243}Am	2.00E-01	^{254}Cf	8.50E+03	^{153}Gd	3.50E+03	^{53}Mn	1.80E-03	^{188}Pt	6.80E+04
^{37}Ar	9.90E+04	^{36}Cl	3.30E-02	^{159}Gd	1.10E+06	^{54}Mn	7.70E+03	^{191}Pt	2.40E+05
^{39}Ar	3.40E+01	^{38}Cl	1.30E+08	^{68}Ge	7.10E+03	^{56}Mn	2.20E+07	^{193}Pt	3.70E+01
^{41}Ar	4.20E+07	^{240}Cm	2.00E+04	^{71}Ge	1.60E+05	^{93}Mo	1.10E+00	^{193m}Pt	1.60E+05
^{42}Ar	2.60E+02	^{241}Cm	1.70E+04	^{77}Ge	3.60E+06	^{99}Mo	4.80E+05	^{195m}Pt	1.70E+05
^{72}As	1.70E+06	^{242}Cm	3.30E+03	^{3}H	9.70E+03	^{13}N	1.50E+09	^{197}Pt	8.70E+05
^{73}As	2.20E+04	^{243}Cm	5.20E+01	^{172}Hf	1.10E+03	^{22}Na	6.30E+03	^{197m}Pt	1.00E+07
^{74}As	9.90E+04	^{244}Cm	8.10E+01	^{175}Hf	1.10E+04	^{24}Na	8.70E+06	^{236}Pu	5.30E+02
^{76}As	1.60E+06	^{245}Cm	1.70E-01	^{181}Hf	1.70E+04	^{92m}Nb	1.40E+05	^{237}Pu	1.20E+04
^{77}As	1.00E+06	^{246}Cm	3.10E-01	^{182}Hf	2.20E-04	^{93m}Nb	2.40E+02	^{238}Pu	1.70E+01
^{211}At	2.10E+06	^{247}Cm	9.30E-05	^{194}Hg	3.50E+00	^{94}Nb	1.90E-01	^{239}Pu	6.20E-02
^{193}Au	9.20E+05	^{248}Cm	4.20E-03	^{195m}Hg	4.00E+05	^{95}Nb	3.90E+04	^{240}Pu	2.30E-01
^{194}Au	4.10E+05	^{55}Co	3.10E+06	^{197}Hg	2.50E+05	^{97}Nb	2.70E+07	^{241}Pu	1.00E+02
^{195}Au	3.70E+03	^{56}Co	3.00E+04	^{197m}Hg	6.70E+05	^{147}Nd	8.10E+04	^{242}Pu	3.90E-03
^{196}Au	1.10E+05	^{57}Co	8.40E+03	^{203}Hg	1.40E+04	^{149}Nd	1.20E+07	^{244}Pu	1.80E-05
^{198}Au	2.40E+05	^{58}Co	3.20E+04	^{163}Ho	7.60E+01	^{59}Ni	8.00E-02	^{223}Ra	5.10E+04
^{199}Au	2.10E+05	^{58m}Co	5.90E+06	^{166}Ho	7.00E+05	^{63}Ni	5.70E+01	^{224}Ra	1.60E+05
^{131}Ba	8.40E+04	^{60}Co	1.10E+03	^{166m}Ho	1.80E+00	^{65}Ni	1.90E+07	^{225}Ra	3.90E+04
^{133}Ba	2.60E+02	^{51}Cr	9.20E+04	^{123}I	1.90E+06	^{235}Np	1.40E+03	^{226}Ra	1.00E+00
^{133m}Ba	6.10E+05	^{129}Cs	7.60E+05	^{124}I	2.50E+05	^{236}Np	1.30E-02	^{228}Ra	2.70E+02
^{140}Ba	7.30E+04	^{131}Cs	1.00E+05	^{125}I	1.70E+04	^{237}Np	7.10E-04	^{nat}Rb	1.80E+08
^{10}Be	2.20E-02	^{132}Cs	1.50E+05	^{126}I	8.00E+04	^{239}Np	2.30E+05	^{81}Rb	8.40E+06
^{7}Be	3.50E+05	^{134}Cs	1.30E+03	^{129}I	1.80E-04	^{185}Os	7.50E+03	^{83}Rb	1.80E+04
^{205}Bi	4.20E+04	^{134m}Cs	8.00E+06	^{131}I	1.20E+05	^{191}Os	4.40E+04	^{84}Rb	4.70E+04
^{206}Bi	1.00E+05	^{135}Cs	1.20E-03	^{132}I	1.00E+07	^{191m}Os	1.30E+06	^{86}Rb	8.10E+04
^{207}Bi	5.20E+01	^{136}Cs	7.30E+04	^{133}I	1.10E+06	^{193}Os	5.30E+05	^{87}Rb	8.60E-08
^{210}Bi	1.20E+05	^{137}Cs	8.70E+01	^{134}I	2.70E+07	^{194}Os	3.10E+02	^{nat}Re	2.40E+08
^{210m}Bi	5.70E-04	^{64}Cu	3.90E+06	^{135}I	3.50E+06	^{32}P	2.90E+05	^{183}Re	1.00E+04
^{212}Bi	1.50E+07	^{67}Cu	7.60E+05	^{111}In	4.20E+05	^{33}P	1.60E+05	^{184}Re	1.90E+04
^{247}Bk	1.00E+00	^{159}Dy	5.70E+03	^{113m}In	1.70E+07	^{230}Pa	3.30E+04	^{184m}Re	4.30E+03
^{249}Bk	1.60E+03	^{165}Dy	8.20E+06	^{114m}In	2.30E+04	^{231}Pa	4.70E-02	^{186}Re	1.90E+05
^{76}Br	2.50E+06	^{166}Dy	2.30E+05	^{115m}In	6.10E+06	^{233}Pa	2.10E+04	^{187}Re	3.80E-08
^{77}Br	7.10E+05	^{169}Er	8.30E+04	^{189}Ir	5.20E+04	^{201}Pb	1.70E+06	^{188}Re	9.80E+05
^{82}Br	1.10E+06	^{171}Er	2.40E+06	^{190}Ir	6.20E+04	^{202}Pb	3.40E-03	^{189}Re	6.80E+05
^{11}C	8.40E+08	^{147}Eu	3.70E+04	^{192}Ir	9.20E+03	^{203}Pb	3.00E+05	^{101}Rh	1.10E+03
^{14}C	4.50E+00	^{148}Eu	1.60E+04	^{193m}Ir	6.40E+04	^{205}Pb	1.20E-04	^{102}Rh	1.20E+03
^{41}Ca	8.50E-02	^{149}Eu	9.40E+03	^{194}Ir	8.40E+05	^{210}Pb	7.60E+01	^{102m}Rh	6.20E+03
^{45}Ca	1.80E+04	^{150}Eu	1.60E+06	^{40}K	6.40E-06	^{212}Pb	1.40E+06	^{103m}Rh	3.30E+07
^{47}Ca	6.10E+05	^{152}Eu	1.80E+02	^{42}K	6.00E+06	^{103}Pd	7.50E+04	^{105}Rh	8.40E+05
^{109}Cd	2.60E+03	^{152m}Eu	2.20E+06	^{43}K	3.30E+06	^{107}Pd	5.10E-04	^{99}Rh	8.20E+04
^{113m}Cd	2.20E+02	^{154}Eu	2.60E+02	^{81}Kr	2.10E-02	^{109}Pd	2.10E+06	^{222}Rn	1.50E+05
^{115}Cd	5.10E+05	^{155}Eu	4.90E+02	^{85}Kr	3.90E+02	^{143}Pm	3.40E+03	^{103}Ru	3.20E+04
^{115m}Cd	2.50E+04	^{156}Eu	5.50E+04	^{85m}Kr	8.20E+06	^{144}Pm	2.50E+03	^{105}Ru	6.70E+06

(a) From 49CFR173.435, Rev. 10/1/2002.

Table A.2. List of Specific Activities A_j for Selected Isotopes j[(a)] (cont'd)

Isotope, j	A_j (Ci/g)	Isotope, j	A_j (Ci/g)	Isotope, j	A_j (Ci/g)	Isotope, j	A_j (Ci/g)	Isotope, j	A_j (Ci/g)
^{106}Ru	3.30E+03	^{123}Sn	8.20E+03	^{99}Tc	1.70E-02	^{201}Tl	2.10E+05	^{123}Xe	1.20E+07
^{97}Ru	4.60E+05	^{125}Sn	1.10E+05	^{99m}Tc	5.30E+06	^{202}Tl	5.30E+04	^{127}Xe	2.80E+04
^{35}S	4.30E+04	^{126}Sn	2.80E-02	^{118}Te	1.80E+05	^{204}Tl	4.60E+02	^{131m}Xe	8.40E+04
^{122}Sb	4.00E+05	^{82}Sr	6.20E+04	^{121}Te	6.40E+04	^{167}Tm	8.50E+04	^{133}Xe	1.90E+05
^{124}Sb	1.70E+04	^{85}Sr	2.40E+04	^{121m}Te	7.00E+03	^{168}Tm	8.30E+03	^{135}Xe	2.60E+06
^{125}Sb	1.00E+03	^{85m}Sr	3.30E+07	^{123m}Te	8.90E+03	^{170}Tm	6.00E+03	^{87}Y	4.50E+05
^{126}Sb	8.40E+04	^{87m}Sr	1.30E+07	^{125m}Te	1.80E+04	^{171}Tm	1.10E+03	^{88}Y	1.40E+04
^{44}Sc	1.80E+07	^{89}Sr	2.90E+04	^{127}Te	2.60E+06	^{nat}U	7.10E-07	^{90}Y	5.40E+05
^{46}Sc	3.40E+04	^{90}Sr	1.40E+02	^{127m}Te	9.40E+03	^{230}U	2.70E+04	^{91}Y	2.50E+04
^{47}Sc	8.30E+05	^{91}Sr	3.60E+06	^{129}Te	2.10E+07	^{232}U	2.20E+01	^{91m}Y	4.20E+07
^{48}Sc	1.50E+06	^{92}Sr	1.30E+07	^{129m}Te	3.00E+04	^{233}U	9.70E-03	^{92}Y	9.60E+06
^{75}Se	1.50E+04	^{178}Ta	1.10E+08	^{131m}Te	8.00E+05	^{234}U	6.20E-03	^{93}Y	3.30E+06
^{79}Se	7.00E-02	^{179}Ta	1.10E+03	^{132}Te	3.00E+05	^{235}U	2.20E-06	^{169}Yb	2.40E+04
^{31}Si	3.90E+07	^{182}Ta	6.20E+03	^{nat}Th	2.20E-07	^{236}U	6.50E-05	^{175}Yb	1.80E+05
^{32}Si	1.10E+02	^{157}Tb	1.50E+01	^{227}Th	3.10E+04	^{238}U	3.40E-07	^{65}Zn	8.20E+03
^{145}Sm	2.60E+03	^{158}Tb	1.50E+01	^{228}Th	8.20E+02	^{48}V	1.70E+05	^{69}Zn	4.90E+07
^{147}Sm	2.30E-08	^{160}Tb	1.10E+04	^{229}Th	2.10E-01	^{49}V	8.10E+03	^{69m}Zn	3.30E+06
^{151}Sm	2.60E+01	^{95m}Tc	2.20E+04	^{230}Th	2.10E-02	^{178}W	3.40E+04	^{88}Zr	1.80E+04
^{153}Sm	4.40E+05	^{96}Tc	3.20E+05	^{231}Th	5.30E+05	^{181}W	6.00E+03	^{93}Zr	2.50E-03
^{113}Sn	1.00E+04	^{96m}Tc	3.80E+07	^{232}Th	1.10E-07	^{185}W	9.40E+03	^{95}Zr	2.10E+04
^{117m}Sn	8.20E+04	^{97}Tc	1.40E-03	^{234}Th	2.30E+04	^{187}W	7.00E+05	^{97}Zr	1.90E+06
^{119m}Sn	3.70E+03	^{97m}Tc	1.50E+04	^{44}Ti	1.70E+02	^{188}W	1.00E+04		
^{121m}Sn	5.40E+01	^{98}Tc	8.70E-04	^{200}Tl	6.00E+05	^{122}Xe	1.30E+06		

(a) From 49CFR173.435, Rev. 10/1/2002.

Appendix B

Equations for Calculating the Chemical and Radionuclide Composition of ILAW Corresponding to an MFPV Batch

Appendix B: Equations for Calculating the Chemical and Radionuclide Composition of ILAW Corresponding to an MFPV Batch

This appendix presents the equations used to calculate the chemical and radionuclide composition of ILAW corresponding to an MFPV batch. The equations, notation, and terminology are taken from Sections B.1.2 and B.2.1 of Appendix B in Piepel et al. (2005). The derivations of the equations are included in those sections of Appendix B.

The equation for calculating from balanced data (described subsequently) the mass fraction of the j^{th} component (oxide or halogen) of the ILAW composition (chemical or radionuclide) resulting from the i^{th} MFPV batch is given by

$$\bar{g}_{ij}^{MFPV} = \frac{\dfrac{1}{n_S^{CRV} n_A^{CRV}} \sum_{l=1}^{n_S^{CRV}} \sum_{m=1}^{n_A^{CRV}} c_{ijlm}^{CRV} f_j \bar{V}_i^{CRV\,to\,MFPV} u + \sum_{k=1}^{K} a_{ik}^{GFC} G_{ijk}^{GFC} + \bar{m}_{i-1,j}^{MFPV} \left(\dfrac{\dfrac{1}{n_V^{MFPV}} \sum_{h=1}^{n_V^{MFPV}} V_{i,h}^{MFPV\,Heel}}{\dfrac{1}{n_V^{MFPV}} \sum_{h=1}^{n_V^{MFPV}} V_{i-1,h}^{MFPV}} \right)}{\sum_{j=1}^{J} \left(\dfrac{1}{n_S^{CRV} n_A^{CRV}} \sum_{l=1}^{n_S^{CRV}} \sum_{m=1}^{n_A^{CRV}} c_{ijlm}^{CRV} f_j \bar{V}_i^{CRV\,to\,MFPV} u \right) + \sum_{j=1}^{J} \sum_{k=1}^{K} a_{ik}^{GFC} G_{ijk}^{GFC} + \sum_{j=1}^{J} \bar{m}_{i-1,j}^{MFPV} \left(\dfrac{\dfrac{1}{n_V^{MFPV}} \sum_{h=1}^{n_V^{MFPV}} V_{i,h}^{MFPV\,Heel}}{\dfrac{1}{n_V^{MFPV}} \sum_{h=1}^{n_V^{MFPV}} V_{i-1,h}^{MFPV}} \right)} \qquad \text{(B.1)}$$

where

$$\bar{m}_{i-1,j}^{MFPV} = \frac{1}{n_S^{CRV} n_A^{CRV}} \sum_{l=1}^{n_S^{CRV}} \sum_{m=1}^{n_A^{CRV}} c_{i-1,jlm}^{CRV} f_j \bar{V}_{i-1}^{CRV\,to\,MFPV} u + \sum_{k=1}^{K} a_{i-1,k}^{GFC} G_{i-1,jk}^{GFC} + \bar{m}_{i-2,j}^{MFPV} \left(\frac{\dfrac{1}{n_V^{MFPV}} \sum_{h=1}^{n_V^{MFPV}} V_{i-1,h}^{MFPV\,Heel}}{\dfrac{1}{n_V^{MFPV}} \sum_{h=1}^{n_V^{MFPV}} V_{i-2,h}^{MFPV}} \right) \qquad \text{(B.2)}$$

and

$$\bar{V}_i^{CRV\,to\,MFPV} = \frac{\hat{\sigma}^2_{\bar{V}_i^{MFPV\,after}} + \hat{\sigma}^2_{\bar{V}_i^{MFPV\,before}}}{\hat{\sigma}^2_{\bar{V}_i^{CRV\,before}} + \hat{\sigma}^2_{\bar{V}_i^{CRV\,after}} + \hat{\sigma}^2_{\bar{V}_i^{MFPV\,after}} + \hat{\sigma}^2_{\bar{V}_i^{MFPV\,before}}} \left(\frac{\sum_{h=1}^{n_V^{CRV}} V_{ih}^{CRV\,before}}{n_V^{CRV}} - \frac{\sum_{h=1}^{n_V^{CRV}} V_{ih}^{CRV\,after}}{n_V^{CRV}} \right)$$

$$+ \frac{\hat{\sigma}^2_{\bar{V}_i^{CRV\,before}} + \hat{\sigma}^2_{\bar{V}_i^{CRV\,after}}}{\hat{\sigma}^2_{\bar{V}_i^{CRV\,before}} + \hat{\sigma}^2_{\bar{V}_i^{CRV\,after}} + \hat{\sigma}^2_{\bar{V}_i^{MFPV\,after}} + \hat{\sigma}^2_{\bar{V}_i^{MFPV\,before}}} \left(\frac{\sum_{h=1}^{n_V^{MFPV}} V_{ih}^{MFPV\,after}}{n_V^{MFPV}} - \frac{\sum_{h=1}^{n_V^{MFPV}} V_{ih}^{MFPV\,before}}{n_V^{MFPV}} \right). \qquad \text{(B.3)}$$

In Eqs. (B.1) to (B.3), the following notation is used

$\bar{g}_{ij}^{MFPV}$ = mass fraction of the j^{th} glass component (oxide or halogen) in the i^{th} MFPV batch, based on averages over n_S^{CRV} samples per CRV batch, n_A^{CRV} analyses per sample, and n_V^{CRV} and n_V^{MFPV} volume determinations per CRV and MFPV batches (g_{oxide}/g_{oxides})

n_S^{CRV} = number of samples per CRV batch

n_A^{CRV} = number of chemical analyses per CRV sample

c_{ijlm}^{CRV} = analyzed concentration of the j^{th} analyte from the m^{th} analysis of the l^{th} sample from the i^{th} CRV batch (μg/mL = mg/L)

J = number of glass components (oxides or halogens)

f_j = $\frac{MW_j^{oxide}}{MW_j^{analyte}} R_j$ where MW_j^{oxide} and $MW_j^{analyte}$ are the molecular weights of oxide j and analyte j, respectively, and R_j is the ratio of moles of oxide per mole of analyte for oxide j. Hence, f_j is the factor for converting the concentration of analyte j (μg analyte j/mL = mg analyte j/L) to the concentration of oxide j (μg oxide j/mL = mg oxide/L). The quantity f_i is called the oxide factor for oxide j.

u = $\frac{1(\text{g})}{1000(\text{mg})}$, a units conversion factor for converting mg to g

K = number of GFCs

a_{ik}^{GFC} = mass of the k^{th} GFC added to the i^{th} MFPV batch (g)

G_{ijk}^{GFC} = mass of the j^{th} glass component (oxide or halogen) per mass of the k^{th} GFC for the i^{th} MFPV batch ($g_{oxide\ j}/g_{GFC\ k}$). The mass fractions G_{ijk}^{GFC} $j = 1, 2, \ldots, J$ for the k^{th} GFC can sum to less than 1.0 to the extent the GFC contains interstitial water or other components that will not survive in the glass. The nominal G_{ijk}^{GFC} mass fractions of glass oxide components in the GFCs should not change frequently over MFPV batches. However, the i subscript was retained in case these mass fractions change (1) from one vendor to another for the same GFC or (2) for different lots of a given GFC from the same vendor.

$\overline{m}_{i-1,j}^{MFPV}$ = mass of the j^{th} glass oxide component in the $(i-1)^{st}$ MFPV batch, based on averages over multiple samples, analyses per sample, and volume determinations (g)

n_V^{MFPV} = number of volume determinations of the MFPV Heel ($V_{ih}^{MFPV\ before} = V_{ih}^{MFPV\ Heel}$), MFPV after transfer of CRV material ($V_{ih}^{MFPV\ after}$), and completed MFPV batch (V_{ih}^{MFPV}). The numbers of these three MFPV volume determinations are assumed to be the same and are given a single notation for simplicity in operation of the ILAW facility.

$V_{i,h}^{MFPV\ Heel}$ = h^{th} volume determination of the MFPV Heel included in the i^{th} MFPV batch (L)

$V_{i-1,h}^{MFPV}$ = h^{th} volume determination of the $(i-1)^{st}$ MFPV batch (L). This is the total volume of the $(i\text{-}1)^{st}$ MFPV batch, including the MFPV Heel, waste transferred from the CRV, GFCs added, and any water that may be added. Water will typically be added to Envelope B LAW in the MFPV to lower the sodium molarity. It is not anticipated that LAW from Envelopes A and C will require adding water in the MFPV.

n_V^{CRV} = number of volume determinations of the CRV batch before a transfer of material to the MFPV ($V_{ih}^{CRV\ before}$) and after a transfer of material to the MFPV ($V_{ih}^{CRV\ after}$). The numbers of these two CRV volume determinations are assumed to be the same and are given a single notation for simplicity in operation of the ILAW facility.

$\overline{V}_i^{CRV\ to\ MFPV}$ = estimate of the volume transferred from the CRV to the MFPV for the i^{th} MFPV batch, calculated as a weighted average of the estimates from the before and after volume determinations for each of the CRVs and MFPVs (L)

$V_{ih}^{CRV\ before}$ = h^{th} volume determination of the CRV before the transfer of material to the i^{th} MFPV batch (L)

$V_{ih}^{CRV\ after}$ = h^{th} volume determination of the CRV after the transfer of material to the i^{th} MFPV batch (L)

$V_{ih}^{MFPV\ before}$ = h^{th} volume determination of the MFPV before receipt of CRV material for the i^{th} MFPV batch

$V_{ih}^{MFPV\ Heel}$ = h^{th} volume determination of the MFPV Heel included in the i^{th} MFPV batch (L)

$V_i^{MFPV\ after}$ = volume of the MFPV after receipt of CRV material for the i^{th} MFPV batch but before receipt of GFCs or any added water (L)

$\hat{\sigma}^2_{\overline{V}_i^{CRV\ before}}$ = previously determined estimate of the variance (squared standard deviation [SD]) of an average volume determination in the LAW CRV before a transfer to the LAW MFPV

$\hat{\sigma}^2_{\overline{V}_i^{CRV\ after}}$ = previously determined estimate of the variance (squared SD) of an average volume determination in the LAW CRV after a transfer to the LAW MFPV

$\hat{\sigma}^2_{\overline{V}_i^{MFPV\ before}}$ = previously determined estimate of the variance (squared SD) of an average volume determination in the LAW MFPV before a transfer from the LAW CRV

$\hat{\sigma}^2_{\overline{V}_i^{MFPV\ after}}$ = previously determined estimate of the variance (squared SD) of an average volume determination in the LAW MFPV after a transfer from the LAW CRV.

The notations similar to $V_{i,h}^{MFPV}$, but with different superscripts and subscripts, have similar meanings where the (1) superscripts indicate the different vessel conditions for which volume determinations are made and (2) subscripts denote the MFPV batch (i.e., "*i*-1" or "*i*-2"). For other notations not defined, as well as derivations of the equations, see Sections B.1.1 and B.1.2 of Piepel et al. (2005).

Note that Eqs. (B.1) to (B.3) incorporate averages of replicate CRV samples, analyses per sample, and replicate CRV and MFPV volume determinations (if any). Such averaging effectively reduces the uncertainty inherent in single samples, analyses of samples, or volume determinations. The bars in certain notations (e.g., $\overline{V}_{i-1}^{CRV to MFPV}$) denote averages. The $\hat{\sigma}^2_{\overline{V}_i^{MFPV\ after}}$ notation in Eq. (B.3) represents the estimated variance of $\overline{V}_i^{MFPV\ after} = \frac{1}{n_V^{MFPV}} \sum_{h=1}^{n_V^{MFPV}} V_{i,h}^{MFPV\ After}$. The other variance notations in Eq. (B.3) have similar interpretations. Equation (B.1) and Eq. (B.2) assume uniform mixing of the ILAW MFPV.

When level-to-volume calibration equations are eventually developed for ILAW vessels and factored into the ILAW chemical-composition compliance equations, notations such as n_V^{CRV} and n_V^{MFPV} will be replaced with n_L^{CRV} and n_L^{MFPV}. The notation n_L^{CRV} will denote the number of level measurements of the CRV (before and after transfer of material to the MFPV). The notation n_L^{MFPV} will denote the number of level measurements of the MFPV (before a CRV transfer, after a CRV transfer, and after a complete MFPV batch is prepared).

In Eqs. (B.1) to (B.3), it is assumed that the amount of the k^{th} GFC (a_{ik}^{GFC}) to be added to the i^{th} MFPV batch can only be weighed once. This assumption is required because there is no way to relieve

the load cell on an individual GFC weigh hopper in the GFC facility and obtain additional weight measurements. Hence, averages over multiple weight determinations of the GFCs (a_{ik}^{GFC} , k = 1, 2, … , K) were not included in Eqs. (B.1) and (B.2). Also, it is assumed that the a_{ik}^{GFC} quantities will be well-determined average compositions of GFCs based on historical information from GFC vendors or WTP qualification and acceptance testing. Hence, averages of the a_{ik}^{GFC} quantities were not included in Eqs. (B.1) and (B.2).

During ILAW production, radiochemical analyses of MFPV samples will yield radionuclide concentrations in units of μCi/mL (= mCi/L). Such an activity-per-volume concentration of a radionuclide in the LAW CRV can be converted to a mass-per-volume concentration by

$$c_{ijlm}^{CRV} = \frac{r_{ijlm}^{CRV}}{A_j} \tag{B.4}$$

where

c_{ijlm}^{CRV} = mass-per-volume concentration of the j^{th} radionuclide for the m^{th} radiochemical analysis of the l^{th} sample from the i^{th} LAW CRV batch (μg/mL = mg/L)

r_{ijlm}^{CRV} = activity-per-volume concentration of the j^{th} radionuclide for the m^{th} radiochemical analysis of the l^{th} sample from the i^{th} LAW CRV batch (μCi/mL = mCi/L)

A_j = specific activity of the j^{th} radionuclide (Ci/g = mCi/mg).

Table A.2 lists values of A_j for a large number of radionuclides j. The ILAW simulations did not have to use Eq. (B.4) because the G2 run data were already in mass units, including the radionuclides.

In summary, the equations for calculating the mass-fraction composition of ILAW based on the WTP ILAW compliance strategy from balanced data are given by Eqs. (B.1) to (B.4). Balanced data refers to having the same number of samples per LAW CRV batch, analyses per LAW CRV sample, and volume determinations. See Section 5 and Appendix B of Piepel et al. (2005) for versions of the equations applicable to unbalanced data.

Appendix C

Nominal Concentrations and Estimates of Uncertainties Relevant to Quantifying IHLW Variations and Uncertainties for Three HLW Wastes

Appendix C: Nominal Concentrations and Estimates of Uncertainties Relevant to Quantifying IHLW Variations and Uncertainties for Three HLW Wastes

This appendix summarizes the immobilized high-level waste (IHLW) process composition and uncertainty inputs provided by the Waste Treatment and Immobilization Plant (WTP) Project that are relevant to quantifying variations and uncertainties in IHLW compositions and properties. The WTP process control and compliance strategies for IHLW are focused on estimating glass composition corresponding to each IHLW MFPV batch. Hence, the composition and uncertainty estimates provided by the WTP Project and presented in this appendix are associated with the IHLW MFPV. Composition and uncertainty information for HLW from three Hanford tanks was used to represent different possible realistic situations. Actual waste composition data from HLW tanks AY-102, AZ-102, and C-104 were used by the WTP Project to generate most of the inputs summarized in this appendix.

Table C.1 lists the nominal values and estimates of mixing/sampling uncertainty [$\%RSD_S(c_{ijlm}^{MFPV})$] and analytical uncertainty [$\%RSD_A(c_{ijlm}^{MFPV})$] for MFPV chemical-composition elemental concentrations in each of the three HLW waste tanks. The estimates of IHLW MFPV chemical-composition concentrations represent the completed state of an MFPV (i.e., after GFC addition) before transfer to an MFV. However, the WTP Project had to combine different sources of information to construct the inputs in Table C.1. They began with measured sludge concentrations and augmented them using target concentrations of the various GFCs. Hence, the estimates provided by the WTP Project in Table C.1 are not based on direct measurements of the MFPV after GFC addition because there was no representative testing to obtain such information.

Mixing/sampling uncertainty refers to combined random uncertainty caused by (1) random differences in composition resulting from mixing an MFPV and (2) random uncertainty in taking samples from the MFPV by the designated sampling method. Mixing and sampling uncertainties cannot be separately estimated during WTP IHLW production operations, so combined estimates of these uncertainties were used. Table C.1 lists the MFPV mixing/sampling uncertainty [$\%RSD_S(c_{ijlm}^{MFPV})$] values for the low and high cases of each of the low (L) and high (H) uncertainty categories of chemical composition analytes. Low and high cases represent the lower and upper expected values of the uncertainty for a given analyte whereas each analyte is classified into a low or high category for $\%RSD_S(c_{ijlm}^{MFPV})$.

Table C.2 lists the nominal concentrations of HLW radionuclides in the MFPV (after adding glass-forming chemicals [GFCs]) for each of three HLW tanks. Table C.2 also lists the low- and high-case mixing/sampling uncertainties [$\%RSD_S(c_{ijlm}^{MFPV})$] for HLW radionuclides in the MFPV (after GFC addition) for each of the three HLW tanks. Table C.3 provides HLW radionuclide analytical uncertainties [$\%RSD_A(c_{ijlm}^{MFPV})$], which are dependent on the concentration of HLW radionuclides in the MFPV (after GFC addition). Table C.2 lists the $\%RSD_S(c_{ijlm}^{MFPV})$ for HLW radionuclides in the MFPV (after GFC

addition) for each of three HLW tanks. These uncertainties were determined from Table C.3 based on the nominal concentrations in Table C.2.

The HLW analytical uncertainties listed in Tables C.1 to C.3 were originally provided informally (i.e., without any documentation) by the WTP Project for use in this work. Just before completing this report, current estimates of HLW analytical uncertainties were documented in a memorandum.[(a)] There are a few differences in the memorandum compared to the earlier values used in this work, but those differences would not be expected to have any significant impact on the results in this report. Also, for the work in this report the analytical uncertainties in Tables C.1 to C.3 were applied to chemical and radiochemical analyses of IHLW MFPV samples after GFC addition. The WTP analytical group expects that there could be differences in analytical uncertainties for samples taken from the HLW MFPV before GFC addition. However, the estimates in Tables C.1 to C.3 (or the updated values in the memorandum) are the best currently available, and could be applied for HLW MFPV samples before or after GFC addition.

Tables D.9 and D.10 of Appendix D summarize data on the GFC compositions (mass fractions of oxides) and corresponding low- and high-case uncertainties. The 12 GFCs listed in those tables are the ones that will be used by the WTP to produce both IHLW and ILAW. However, it is currently expected that only five of the GFCs (silica, zincite, borax, sodium carbonate, and lithium carbonate) will be used to produce IHLW.

Table C.4 lists the nominal levels and volumes as well as the corresponding low and high uncertainty estimates (standard deviations [SDs and %RSDs]) of the IHLW MFPV contents (1) before waste transfer from the HBV, (2) after the waste transfer from the HBV, and (3) after transfer of GFCs to the MFPV. Table C.5 lists the nominal compositions (in mass fractions) for glass made from the IHLW MFPV for each of three HLW tanks.

Tables C.6 through C.10 provide data concerning the waste type associated with the transition from AY-102 to AZ-102. Table C.6 presents nominal chemical composition for the first 10 to 18 batches of the transition period (the remaining eight have composition and other characteristics identical to the AZ-102 tank). Table C.7 shows radionuclide composition for the same 10 batches. Mixing/sampling %RSD values for chemical composition components can be found in Table C.8. A similar table for radionuclides is not included because their nominal mixing/sampling %RSD values do not change between AY-102 and AZ-102. The applicable mixing/sampling %RSDs for radionuclides are listed in Table C.2. Analytical %RSD values for chemical composition components are shown in Table C.9 and for radionuclides in Table C.10. Values in Tables C.6 through C.10 were used to generate the simulated data for the transition waste type.

It is important to note that Tables C.1 to C.3 use a slightly modified notation to better fit within the tables. The MFPV concentration mixing/sampling %RSD, usually denoted as $\%RSD_S(c_{ijlm}^{MFPV})$, is referred to as $\%RSD_S$. The MFPV concentration analytical relative standard deviation, usually denoted as $\%RSD_A(c_{ijlm}^{MFPV})$, is referred to as $\%RSD_A$.

(a) "Estimated Analytical Measurement Uncertainties of Selected HLW Analytes," CCN 132102, February 7, 2006, memorandum from David Dodd and Bruce Kaiser to John Vienna, Waste Treatment and Immobilization Plant, Richland, WA.

Finally, note that the MFPV nominal concentration data in Tables C.1 and C.2 were based on samples and analyses of actual waste tank samples. However, those analyses were not adjusted or normalized as described by Weier and Piepel (2003). Normalizing and adjusting compositions can be used to eliminate possible biases and reduce uncertainties in analyzed slurry and glass compositions. Applying the adjustment and normalization procedures discussed by Weier and Piepel (2003) to the WTP data provided by the WTP Project was beyond the scope of the present work. However, it remains an option to determine the extent to which the adjustments and normalization would affect the composition variations and uncertainties.

Table C.1. Nominal Chemical Composition Analyte Concentrations, Mixing/Sampling Uncertainties (%RSD$_S$), and Analytical Uncertainties (%RSD$_A$) in the IHLW MFPV (After GFC Addition) for Three HLW Tanks

Analyte	AY-102			AZ-102			C-104		
	MFPV Conc. (mg/L)	Mixing/ Sampling %RSD$_S$[(a)]	Analytical %RSD$_A$[(b)]	MFPV Conc. (mg/L)	Mixing/ Sampling %RSD$_S$[(a)]	Analytical %RSD$_A$[(b)]	MFPV Conc. (mg/L)	Mixing/ Sampling %RSD$_S$[(a)]	Analytical %RSD$_A$[(b)]
Ag	744.48	5 (15)	5 (10)	87.56	5 (15)	ND[(c)]	306.22	5 (15)	10 (20)
Al	11257.92	5 (15)	5 (10)	21009.76	5 (15)	5 (10)	6451.15	5 (15)	5 (10)
B	14516.64	5 (15)	5 (10)	6348.56	5 (15)	5 (10)	14107.44	5 (15)	5 (10)
Ba	290.88	5 (15)	10 (20)	171.55	5 (15)	15 (30)	85.06	5 (15)	15 (30)
Be	-[(d)]	-	-	5.55	1 (5)	ND	9.16	1 (5)	ND
Bi	-	-	-	-	-	-	11.40	5 (15)	ND
Ca	1548.00	5 (15)	10 (20)	1765.22	5 (15)	10 (20)	1658.53	5 (15)	10 (20)
Cd	47.52	5 (15)	ND	6257.73	5 (15)	5 (10)	268.21	5 (15)	ND
Ce	383.04	5 (15)	ND	245.03	5 (15)	ND	348.81	5 (15)	ND
Cl	-	-	-	274.48	1 (5)	10 (20)	7.38	1 (5)	ND
Co	-	-	-	24.21	5 (15)	ND	8.99	5 (15)	ND
Cr	656.64	5 (15)	10 (20)	328.48	5 (15)	10 (20)	480.51	5 (15)	10 (20)
Cs	2.88	1 (5)	ND	48.39	1 (5)	15 (30)	61.53	1 (5)	15 (30)
Cu	118.08	5 (15)	20 (40)	117.49	5 (15)	20 (40)	102.94	5 (15)	20 (40)
Dy	-	-	-	-	-	-	12.18	5 (15)	ND
Eu	-	-	-	-	-	-	5.49	5 (15)	ND
F	-	-	-	63.28	1 (5)	10 (20)	-	-	-
Fe	42037.92	5 (15)	5 (10)	43533.74	5 (15)	5 (10)	16628.44	5 (15)	5 (10)
K	37.44	1 (5)	ND	112.15	1 (5)	ND	250.64	1 (5)	15 (30)
La	279.36	5 (15)	15 (30)	1310.92	5 (15)	10 (20)	81.28	5 (15)	ND
Li	5237.28	1 (5)	10 (20)	11929.60	1 (5)	10 (20)	11721.60	1 (5)	5 (10)
Mg	411.84	5 (15)	ND	387.77	5 (15)	ND	196.88	5 (15)	ND
Mn	9370.08	5 (15)	5 (10)	3658.08	5 (15)	5 (10)	9927.65	5 (15)	5 (10)
Mo	92.16	5 (15)	15 (30)	-	-	-	7.55	5 (15)	ND
Na	40629.60	1 (5)	5 (10)	50564.26	1 (5)	5 (10)	32040.49	1 (5)	5 (10)
Nd	-	-	-	919.30	5 (15)	10 (20)	190.80	5 (15)	ND
Ni	1393.92	5 (15)	10 (20)	3084.07	5 (15)	5 (10)	933.82	5 (15)	10 (20)
P	1051.20	5 (15)	10 (20)	1038.16	5 (15)	10 (20)	725.13	5 (15)	10 (20)
Pb	2149.92	5 (15)	10 (20)	447.69	5 (15)	ND	716.97	5 (15)	15 (30)
Pd	-	-	-	-	-	-	48.24	5 (15)	25 (50)
Pr	-	-	-	-	-	-	19.98	5 (15)	25 (50)
Rh	-	-	-	-	-	-	131.86	5 (15)	25 (50)
Ru	-	-	-	-	-	-	62.72	5 (15)	ND
Sb	136.80	5 (15)	25 (50)	-	-	-	-	-	-
Se	-	-	-	-	-	-	12.66	5 (15)	ND
Si	95495.04	5 (15)	5 (10)	115275.34	5 (15)	5 (10)	112859.25	5 (15)	5 (10)
S	360.00	1 (5)	15 (30)	54.51	1 (5)	ND	7.72	1 (5)	ND
Sn	217.44	5 (15)	15 (30)	666.78	5 (15)	10 (20)	272.19	5 (15)	15 (30)
Sr	614.88	5 (15)	5 (10)	6458.22	5 (15)	5 (10)	14422.12	5 (15)	5 (10)

(a) MFPV mixing/sampling %RSD values are represented by %RSD$_S$ instead of $\%RSD_S(c_{ijlm}^{MFPV})$ for space reasons. The low value is listed first, followed by the high value in parentheses.

(b) MFPV analytical %RSD values are represented by %RSD$_A$ instead of $\%RSD_A(c_{ijlm}^{MFPV})$ for space reasons. The low value is listed first, followed by the high value in parentheses.

(c) %RSD$_A$ = 50 was used for non-detectable (ND) analytes for both low and high cases. Detection limits were used in place of concentration amounts for non-detects.

(d) A "-" means that no data were recorded for that analyte for that HLW tank, and hence mixing/sampling and analytical uncertainties were not estimated.

Table C.1. Nominal Chemical Composition Analyte Concentrations, Mixing/Sampling Uncertainties (%RSD$_S$), and Analytical Uncertainties (%RSD$_A$) in the IHLW MFPV (After GFC Addition) for Three HLW Tanks (cont'd)

Analyte	AY-102			AZ-102			C-104		
	MFPV Conc. (mg/L)	Mixing/ Sampling %RSD$_S$[(a)]	Analytical %RSD$_A$[(b)]	MFPV Conc. (mg/L)	Mixing/ Sampling %RSD$_S$[(a)]	Analytical %RSD$_A$[(b)]	MFPV Conc. (mg/L)	Mixing/ Sampling %RSD$_S$[(a)]	Analytical %RSD$_A$[(b)]
Th	-	-	-	-	-	-	18124.08	5 (15)	5 (10)
Ti	83.52	5 (15)	ND	43.33	5 (15)	ND	64.23	5 (15)	ND
U	1893.60	5 (15)	20 (40)	7333.91	5 (15)	10 (20)	16113.77	5 (15)	5 (10)
V	38.88	5 (15)	50 (50)	-	-	-	10.67	5 (15)	ND
Y	-	-	-	61.95	5 (15)	ND	12.00	5 (15)	ND
Zn	2473.92	5 (15)	5 (10)	170.37	5 (15)	10 (20)	8096.31	5 (15)	5 (10)
Zr	1467.36	5 (15)	5 (10)	5570.60	5 (15)	5 (10)	18033.49	5 (15)	5 (10)

(a) MFPV mixing/sampling %RSD values are represented by %RSD$_S$ instead of $\%RSD_S(c_{ijlm}^{MFPV})$ for space reasons. The low value is listed first, followed by the high value in parentheses.

(b) MFPV analytical %RSD values are represented by %RSD$_A$ instead of $\%RSD_A(c_{ijlm}^{MFPV})$ for space reasons. The low value is listed first, followed by the high value in parentheses.

(c) %RSD$_A$ = 50 was used for non-detectable (ND) analytes for both low and high cases. Detection limits were used in place of concentration amounts for non-detects.

(d) A "-" means that no data were recorded for that analyte for that HLW tank, and hence mixing/sampling and analytical uncertainties were not estimated.

Table C.2. Nominal Concentrations, Mixing/Sampling Uncertainties (%RSD$_S$), and Analytical Uncertainties (%RSD$_A$) for HLW Radionuclides in the MFPV (After GFC Addition) for Each of Three HLW Tanks

Isotope	AY-102			AZ-102			C-104		
	MFPV Conc. (µCi/mL)[a]	Mixing/ Sampling %RSD$_S$[b]	Analytical %RSD$_A$[c]	MFPV Conc. (µCi/mL)[a]	Mixing/ Sampling %RSD$_S$[b]	Analytical %RSD$_A$[c]	MFPV Conc. (µCi/mL)[a]	Mixing/ Sampling %RSD$_S$[b]	Analytical %RSD$_A$[c]
^{241}Am	2.016	1 (5)	25 (50)	35.18031	1 (5)	5 (10)	1.975684	1 (5)	25 (50)
^{242}Cm	-[d]	-	-	-	-	-	0.002744	1 (5)	60 (120)
$^{243+244}$Cm	-	-	-	0.051736	1 (5)	30 (60)	0.029129	1 (5)	30 (60)
^{60}Co	0.144	1 (5)	25 (50)	1.323573	1 (5)	25 (50)	0.129602	1 (5)	25 (50)
^{134}Cs	-	-	-	0.042251	1 (5)	30 (60)	0.067545	1 (5)	30 (60)
^{137}Cs	242.064	1 (5)	5 (10)	365.1682	1 (5)	5 (10)	540.3581	1 (5)	5 (10)
^{152}Eu	-	-	-	-	-	-	-	-	-
^{154}Eu	1.44	1 (5)	15 (30)	12.54592	1 (5)	15 (30)	0.527694	1 (5)	15 (30)
^{155}Eu	0.72	1 (5)	10 (20)	23.10864	1 (5)	10 (20)	0.308173	1 (5)	10 (20)
^{63}Ni	-	-	-	-	-	-	-	-	-
^{237}Np	-	-	-	0.014917	1 (5)	10 (20)	0.001689	1 (5)	25 (50)
^{238}Pu	0.144	1 (5)	25 (50)	0.275924	1 (5)	25 (50)	0.187015	1 (5)	25 (50)
^{239}Pu	1.296	1 (5)	10 (20)	1.70728	1 (5)	10 (20)	1.709727	1 (5)	10 (20)
^{240}Pu	-	-	-	-	-	-	-	-	-
^{241}Pu	-	-	-	6.941214	1 (5)	25 (50)	4.896996	1 (5)	25 (50)
^{106}Rh+^{106}Ru	-	-	-	-	-	-	-	-	-
^{125}Sb	-	-	-	6.941214	1 (5)	25 (50)	0.05488	1 (5)	25 (50)
^{79}Se	-	-	-	-	-	-	-	-	-
^{151}Sm	-	-	-	-	-	-	-	-	-
^{113}Sn	-	-	-	-	-	-	-	-	-
^{126}Sn	-	-	-	-	-	-	-	-	-
^{90}Sr	2334.528	1 (5)	10 (20)	5087.349	1 (5)	10 (20)	218.6762	1 (5)	20 (40)
^{99}Tc	0.000181	1 (5)	10 (20)	0.004048	1 (5)	10 (20)	0.00591	1 (5)	10 (20)
^{232}Th	-	-	-	-	-	-	-	-	-
^{233}U	-	-	-	0.002673	1 (5)	10 (20)	0.138467	1 (5)	10 (20)
^{234}U	-	-	-	0.002966	1 (5)	50 (100)	0.005784	1 (5)	50 (100)
^{235}U	-	-	-	0.00012	1 (5)	20 (40)	0.000198	1 (5)	20 (40)
^{236}U	-	-	-	0.000215	1 (5)	50 (100)	0.000265	1 (5)	50 (100)
^{238}U	1.32E-09	1 (5)	15 (30)	0.002182	1 (5)	5 (10)	0.004129	1 (5)	5 (10)

(a) The estimated concentrations are based on measurements of actual pretreated sludge samples and then scaled to account for GFC additions. The references for the sludge work are Hansen and Crawford (2005) for AY-102 and Smith et al. (2001) for AZ-102 and C-104.

(b) MFPV mixing/sampling %RSD values (low and high values) are represented by %RSD$_S$ instead of $\%RSD_S(r_{ijlm}^{MFPV})$ for space reasons. Low and high values were chosen by the WTP Project to span the range of expected mixing/sampling uncertainties (%RSD$_S$) for radionuclides. The WTP Project has no basis at this time to estimate different %RSD$_S$ for different radionuclides or different HLW tanks, so the range of 1 to 5 %RSD$_S$ was selected for all radionuclides and each of the three HLW tanks.

(c) MFPV analytical %RSD values are represented by %RSD$_A$ instead of $\%RSD_A(c_q^{MFPV})$ for space reasons. %RSD$_A$ values were determined from Table C.3 based on the nominal values in this table after applying a conversion factor of 1.48 to change the units from µCi/g to µCi/mL. Low and high %RSD$_A$ values were chosen by the WTP Project to span the range of expected analytical uncertainties for radionuclides.

(d) A "-" means no recorded data for that analyte.

Table C.3. HLW Radionuclide Analytical Uncertainties (%RSD_A) Dependent on the Concentration Range of the Radionuclide in the MFPV (After GFC Addition)[a]

Isotope	Concentration Range (µCi/g)[b]	%RSD_A[c]	Concentration Range (µCi/g)[b]	%RSD_A[c]	Comments
^{241}Am	1E-5 – 1E-3	25	1E-3 - 3E+3	5	
^{243}Am	5E-3 – 1E-1	40	1E-1 - 1E+2	25	
^{144}Ce[f]	No data	Assume 25	No data	Assume 25	284 day half-life
^{242}Cm	3E-6 – 1E-4	60	1E-4 - 1E+0	20	
$^{243+244}$Cm	1E-4 – 1E-1	30	1E-1 - 1E+1	10	
^{60}Co	1E-4 – 1E-2	25	1E-2 - 1E+2	5	
^{134}Cs[f]	1E-2 – 1E+0	30	1E+0 - 1E+3	20	High radiation from Cs-137
^{135}Cs	1E-3 – 1E+0	20	>1E+0	10	
^{137}Cs	1E-2 – 1E+2	5	1E+2 - 1E+5	10	(d)
^{152}Eu	2E-2 – 1E+0	10	1E+0 - 1E+3	5	
^{154}Eu	1E-4 – 1E-1	15	1E-1 - 1E+1	10	
^{155}Eu	1E-4 – 1E-2	10	1E-2 - 1E+0	5	
^{94}Nb	1E-1 - 1E+1	15	>1E+1	10	
^{59}Ni	1E-3 - 1E-1	20	1E-1 - 1E+1	10	
^{63}Ni	5E-3 - 1E+0	15	1E+0 - 1E+2	10	
^{237}Np	1E-4 - 1E-2	25	1E-2 - 1E+1	10	
^{238}Pu	1E-6 - 1E-2	25	1E-2 - 1E+0	10	
^{239}Pu	1E-4 - 1E-2	15	1E-2 - 1E+0	10	
^{240}Pu	1E-3 - 1E-1	50	1E-1 - 1E+1	20	
$^{239/240}$Pu	1E-6 - 1E-2	20	1E-2 - 1E+0	10	
^{241}Pu	5E-2 - 1E+0	25	1E+0 - 1E+3	15	
^{106}Ru[f]	1E-5 - 1E-2	15	1E-2 - 1E+2	10	368 day half-life
^{151}Sm	No data	Assume 50	No data	Assume 50	
^{113}Sn	No data	Assume 50	No data	Assume 50	
^{126}Sn	1E-4 - 1E-2	20	1E-2 - 1E+0	10	
^{90}Sr	1E-6 - 1E-2	20	1E-2 - 1E+4	10	
^{99}Tc	1E-5 - 1E-2	10	1E-2 - 1E+2	20	(e)
^{233}U	1E-4 - 1E+0	10	1E+0 - 1E+2	5	
^{234}U	1E-4 - 1E-2	50	1E-2 - 1E+1	30	
^{235}U	1E-2 - 1E+0	20	1E+0 - 1E+2	10	
^{236}U	3E-3 - 1E+0	50	1E+0 - 1E+3	15	
^{238}U	1E-2 - 1E+0	15	1E+0 - 1E+4	5	
^{93}Zr	No data	Assume 100	No data	Assume 100	

(a) The data in this table were gathered by the WTP analytical laboratory group from the following documents: Brooks et al. (2000), Hay et al. (2003a,b), and Martin et al. (2003).

(b) Concentrations within this range have the corresponding %RSD_A (next column) for analytical uncertainty.

(c) MFPV analytical %RSD values are represented by %RSD_A instead of $\%RSD_A(r_{ijlm}^{MFPV})$ for space reasons.

(d) The %RSD_A is estimated to be larger for higher concentrations because of additional requirements for dilution and handling in the hot cell.

(e) The %RSD_A is estimated to be larger for higher concentrations because of the higher probability of complexed species.

(f) These short-lived radionuclides are often not included and could have been deleted for this work. However, retaining them had no practical consequence on the results.

Table C.4. IHLW MFPV Level and Volume Uncertainties

Vessel Level or Volume	IHLW MFPV Status	Level	SD		%RSD[a]	
			Low	High[b]	Low	High[b]
Level	Heel	36 in.	0.5 in.	1.0 in.	1.39	2.78
Volume		1614.9 gal 6113.1 L	29.6 gal 112.05 L	59.2 gal 224.10 L	1.83	3.66
Level	After Waste Added	(c)	0.5 in.	1.0 in.	(d)	(d)
Volume		23,147.8 L	29.6 gal 112.05 L	59.2 gal 224.10 L	0.97	1.94
Level	Full[e]	128.9 in.	0.5 in.	1.0 in.	0.39	0.78
Volume		7114.9 gal 26932.8 L	29.6 gal 112.05 L	59.2 gal 224.10 L	0.42	0.84

(a) %RSD = 100 (SD/Level).
(b) The high SDs and %RSDs are two times the low SDs and %RSDs.
(c) Not available from the WTP Project at the time of this work.
(d) The %RSD values could not be calculated without the nominal value.
(e) "MFPV Full" denotes the MFPV after waste and GFCs are added.

Table C.5. Nominal Compositions for Glass Made from the HLW MFPV (in mass fractions) for Each of Three HLW Tanks[a]

Component	Mass Fractions			Component	Mass Fractions		
	AY-102	AZ-102	C-104		AY-102	AZ-102	C-104
Ag_2O	0.00185	0.00018	0.00065	V_2O_5	0.00016	0	3.77E-05
Al_2O_3	0.04915	0.07718	0.02412	Y_2O_3	0	0.00015	3.02E-05
B_2O_3	0.10800	0.03974	0.08987	ZnO	0.00711	0.00041	0.01994
BaO	0.00075	0.00037	0.00019	ZrO_2	0.00458	0.01463	0.04819
BeO	0	2.99E-05	5.03E-05	**Radionuclide Oxide**	**Mass Fractions**		
Bi_2O_3	0	0	2.51E-05		**AY-102[b]**	**AZ-102[b]**	**C-104[b]**
CaO	0.00500	0.00480	0.00459	$^{241}Am_2O_3$	1.51E-06	2.21E-05	1.26E-06
CdO	0.00013	0.01390	0.00061	$^{144}Ce_2O_3$[e]	0	0	0
Ce_2O_3	0.00104	0.00056	0.00081	$^{242}Cm_2O_3$	0	0	1.81E-12
Cl	0	0.00053	1.46E-05	$^{243+244}Cm_2O_3$	0	2.12E-09	1.22E-09
CoO	0	5.98E-05	2.26E-05	^{60}CoO	3.83E-10	2.96E-09	2.95E-10
Cr_2O_3	0.00222	0.00093	0.00139	$^{134}Cs_2O$	0	6.70E-11	1.09E-10
Cs_2O	7.06E-06	9.97E-05	0.00013	$^{137}Cs_2O$	6.80E-06	8.64E-06	1.30E-05
CuO	0.00034	0.00029	0.00025	$^{152}Eu_2O_3$	0	0	0
Dy_2O_3	0	0	2.76E-05	$^{154}Eu_2O_3$	1.48E-08	1.08E-07	4.64E-09
Eu_2O_3	0	0	1.26E-05	$^{155}Eu_2O_3$	3.92E-09	1.06E-07	1.44E-09
F	0	0.00012	0	$^{95}Nb_2O_5$	0	0	0
Fe_2O_3	0.13888	0.12101	0.04704	^{63}NiO	0	0	0
K_2O	0.00010	0.00026	0.00060	$^{237}NpO_2$	0	4.64E-05	5.34E-06
La_2O_3	0.00076	0.00299	0.00019	$^{238}PuO_2$	2.22E-08	3.58E-08	2.47E-08
Li_2O	0.02605	0.04992	0.04992	$^{239}PuO_2$	5.48E-05	6.07E-05	6.19E-05
MgO	0.00158	0.00125	0.00065	$^{240}PuO_2$	0	0	0
MnO	0.02796	0.00918	0.02536	$^{241}PuO_2$	0	1.53E-07	1.10E-07
MoO_3	0.00032	0	2.24E-05	$^{106}Rh_2O_3$[e]	0	0	0
Na_2O	0.12655	0.13251	0.08545	$^{103}RuO_2$[d]	0	0	0
Nd_2O_3	0	0.00208	0.00044	$^{106}RuO_2$	0	0	0
NiO	0.00410	0.00763	0.00235	$^{125}Sb_2O_3$	0	1.61E-08	1.29E-10
P_2O_5	0.00557	0.00462	0.00329	$^{79}SeO_2$	0	0	0
PbO	0.00535	0.00094	0.00153	$^{151}Sm_2O_3$	0	0	0
PdO	0	0	0.00011	$^{113}SnO_2$	0	0	0
Pr_2O_3	o	0	4.63E-05	$^{126}SnO_2$	0	0	0
Rh_2O_3	0	0	0.00032	^{90}SrO	4.54E-05	8.32E-05	3.64E-06
RuO_2	0	0	0.00016	$^{99}Tc_2O_7$	3.85E-08	7.25E-07	1.08E-06
Sb_2O_3	0.00038	0	0	$^{232}ThO_2$	0	0	0
SeO_2	0	0	3.52E-05	$^{233}UO_3$	0	6.46E-07	3.41E-05
SiO_2	0.47205	0.47945	0.47768	$^{234}UO_3$	0	1.12E-06	2.22E-06
SO_3	0.00208	0.00026	3.81E-05	$^{235}UO_3$	0	0.00013	0.00021
SnO_2	0.00064	0.00165	0.00068	$^{236}UO_3$	0	7.73E-06	9.70E-06
SrO	0.00168	0.01485	0.03374	$^{238}UO_3$	1.08E-08	0.01499	0.02887
ThO_2	0	0	0.04080	$^{88}Y_2O_3$[d]	0	0	0
TiO_2	0.00032	0.00014	0.00021	**Total[c]**	1.000	1.000	1.000
UO_3	0.00526	0.01713	0.03831				

(a) These nominal compositions were provided by the WTP Project. They are based on Kot et al. (2004a) for AY-102 and on Smith et al. (2001) for AZ-102 and C-104.

(b) Shaded cells denote radionuclide oxides that were considered to be already included in the chemical composition oxides (e.g., the isotopes of U were considered to be already included in UO_3). The mass fractions of these radionuclide oxides were not counted as part of the total. If the chemical composition was greater than zero, the associated radionuclides were not included. If the chemical composition was zero or not reported, the associated radionuclides were included.

(c) Total does not include the gray-shaded entries to avoid double counting some radioactive components. The table values may not sum to one exactly because of rounding, but the electronic data values to more decimal places sum to one.

(d) These short-lived radionuclide oxides will be deleted in future work.

(e) This radionuclide oxide is often combined with ^{106}Ru in work similar to this. Because there is no practical consequence to the results, these radionuclides were retained separately in this work.

Table C.6. Nominal Chemical Compositions (in mass fractions) for Each IHLW MFPV Batch of the AY-102 to AZ-102 Transition Waste Type[a]

Component	Batch 1	Batch 2	Batch 3	Batch 4	Batch 5	Batch 6	Batch 7	Batch 8	Batch 9	Batch 10
Ag_2O	0.00135	0.00100	0.00075	0.00058	0.00046	0.00038	0.00032	0.00028	0.00025	0.00023
Al_2O_3	0.05721	0.06285	0.06680	0.06957	0.07150	0.07286	0.07381	0.07447	0.07494	0.07526
B_2O_3	0.08734	0.07288	0.06276	0.05568	0.05072	0.04725	0.04482	0.04311	0.04192	0.04109
BaO	0.00064	0.00055	0.00050	0.00046	0.00043	0.00041	0.00040	0.00039	0.00038	0.00038
BeO	0.00001	0.00002	0.00002	0.00002	0.00002	0.00003	0.00003	0.00003	0.00003	0.00003
Bi_2O_3[b]	0.00000	0.00000	0.00000	0.00000	0.00000	0.00000	0.00000	0.00000	0.00000	0.00000
CaO	0.00492	0.00486	0.00482	0.00480	0.00478	0.00476	0.00475	0.00475	0.00474	0.00474
CdO	0.00420	0.00704	0.00904	0.01043	0.01141	0.01209	0.01257	0.01291	0.01314	0.01331
Ce_2O_3	0.00089	0.00079	0.00072	0.00067	0.00063	0.00061	0.00059	0.00058	0.00057	0.00056
Cl	0.00016	0.00027	0.00035	0.00040	0.00044	0.00046	0.00048	0.00050	0.00050	0.00051
CoO	0.00002	0.00003	0.00004	0.00004	0.00005	0.00005	0.00005	0.00006	0.00006	0.00006
Cr_2O_3	0.00183	0.00156	0.00136	0.00123	0.00114	0.00107	0.00103	0.00099	0.00097	0.00096
Cs_2O	0.00003	0.00005	0.00007	0.00008	0.00008	0.00009	0.00009	0.00009	0.00009	0.00010
CuO	0.00032	0.00031	0.00030	0.00030	0.00029	0.00029	0.00029	0.00029	0.00028	0.00028
Dy_2O_3[b]	0.00000	0.00000	0.00000	0.00000	0.00000	0.00000	0.00000	0.00000	0.00000	0.00000
Eu_2O_3[b]	0.00000	0.00000	0.00000	0.00000	0.00000	0.00000	0.00000	0.00000	0.00000	0.00000
F	0.00004	0.00006	0.00008	0.00009	0.00010	0.00011	0.00011	0.00011	0.00012	0.00012
Fe_2O_3	0.13297	0.12883	0.12594	0.12392	0.12250	0.12151	0.12081	0.12033	0.11999	0.11975
K_2O	0.00015	0.00018	0.00021	0.00022	0.00023	0.00024	0.00025	0.00025	0.00025	0.00025
La_2O_3	0.00141	0.00187	0.00219	0.00242	0.00258	0.00269	0.00276	0.00282	0.00286	0.00288
Li_2O	0.03299	0.03784	0.04124	0.04362	0.04529	0.04645	0.04727	0.04784	0.04824	0.04852
MgO	0.00147	0.00140	0.00135	0.00131	0.00129	0.00127	0.00126	0.00125	0.00125	0.00124
MnO	0.02228	0.01831	0.01553	0.01359	0.01222	0.01127	0.01060	0.01014	0.00981	0.00958
MoO_3	0.00022	0.00016	0.00011	0.00008	0.00005	0.00004	0.00003	0.00002	0.00001	0.00001
Na_2O	0.12774	0.12857	0.12916	0.12957	0.12985	0.13005	0.13020	0.13029	0.13036	0.13041
Nd_2O_3	0.00062	0.00105	0.00135	0.00156	0.00171	0.00181	0.00188	0.00193	0.00197	0.00200
NiO	0.00512	0.00584	0.00634	0.00670	0.00694	0.00711	0.00723	0.00732	0.00738	0.00742
P_2O_5	0.00526	0.00505	0.00490	0.00480	0.00473	0.00467	0.00464	0.00461	0.00460	0.00458
PbO	0.00402	0.00309	0.00244	0.00199	0.00167	0.00144	0.00129	0.00118	0.00110	0.00105
PdO[b]	0.00000	0.00000	0.00000	0.00000	0.00000	0.00000	0.00000	0.00000	0.00000	0.00000
Pr_2O_3[b]	0.00000	0.00000	0.00000	0.00000	0.00000	0.00000	0.00000	0.00000	0.00000	0.00000
Rh_2O_3[b]	0.00000	0.00000	0.00000	0.00000	0.00000	0.00000	0.00000	0.00000	0.00000	0.00000
RuO_2[b]	0.00000	0.00000	0.00000	0.00000	0.00000	0.00000	0.00000	0.00000	0.00000	0.00000
Sb_2O_3	0.00027	0.00019	0.00013	0.00009	0.00006	0.00004	0.00003	0.00002	0.00002	0.00001
SeO_2[b]	0.00000	0.00000	0.00000	0.00000	0.00000	0.00000	0.00000	0.00000	0.00000	0.00000
SiO_2	0.47210	0.47214	0.47218	0.47220	0.47222	0.47223	0.47224	0.47225	0.47225	0.47225
SO_3	0.00153	0.00115	0.00088	0.00070	0.00057	0.00047	0.00041	0.00037	0.00033	0.00031
SnO_2	0.00093	0.00114	0.00128	0.00138	0.00146	0.00151	0.00154	0.00156	0.00158	0.00159
SrO	0.00556	0.00828	0.01019	0.01152	0.01245	0.01310	0.01356	0.01388	0.01410	0.01426
ThO_2[b]	0.00000	0.00000	0.00000	0.00000	0.00000	0.00000	0.00000	0.00000	0.00000	0.00000
TiO_2	0.00027	0.00023	0.00020	0.00018	0.00017	0.00016	0.00015	0.00015	0.00015	0.00014
UO_3	0.00874	0.01118	0.01289	0.01409	0.01492	0.01551	0.01592	0.01621	0.01641	0.01655
V_2O_5	0.00011	0.00008	0.00006	0.00004	0.00003	0.00002	0.00001	0.00001	0.00001	0.00000
Y_2O_3	0.00005	0.00008	0.00010	0.00011	0.00013	0.00013	0.00014	0.00014	0.00014	0.00015
ZnO	0.00510	0.00369	0.00271	0.00202	0.00153	0.00120	0.00096	0.00079	0.00068	0.00060
ZrO_2	0.00753	0.00959	0.01104	0.01205	0.01276	0.01325	0.01360	0.01384	0.01401	0.01413

(a) Batches 11 to 18 of the AY-102 to AZ-102 transition waste type have the same nominal compositions as Batch 10.
(b) The nominal mass fraction for these components is zero in both AY-102 and AZ-102.

Table C.7. Nominal Radionuclide Oxide Compositions (in mass fractions) for Each Stage of the AY-102 to AZ-102 Transition Waste Type[a]

Component	Batch 1	Batch 2	Batch 3	Batch 4	Batch 5	Batch 6	Batch 7	Batch 8	Batch 9	Batch 10
$^{241}Am_2O_3$	7.59E-06	1.18E-05	1.48E-05	1.69E-05	1.84E-05	1.94E-05	2.01E-05	2.06E-05	2.10E-05	2.12E-05
$^{144}Ce_2O_3$[b]	0.00E+0	0.00E+0	0.00E+0	0.00E+0	0.00E+0	0.00E+0	0.00E+0	0.00E+0	0.00E+0	0.00E+0
$^{242}Cm_2O_3$[b]	0.00E+0	0.00E+0	0.00E+0	0.00E+0	0.00E+0	0.00E+0	0.00E+0	0.00E+0	0.00E+0	0.00E+0
$^{243+244}Cm_2O_3$	4.91E-10	8.35E-10	1.08E-09	1.24E-09	1.36E-09	1.44E-09	1.50E-09	1.54E-09	1.57E-09	1.59E-09
^{60}CoO	1.14E-09	1.68E-09	2.05E-09	2.31E-09	2.49E-09	2.62E-09	2.71E-09	2.77E-09	2.82E-09	2.85E-09
$^{134}Cs_2O$	1.98E-11	3.36E-11	4.33E-11	5.01E-11	5.49E-11	5.82E-11	6.05E-11	6.22E-11	6.33E-11	6.41E-11
$^{137}Cs_2O$	7.31E-06	7.67E-06	7.92E-06	8.10E-06	8.22E-06	8.31E-06	8.37E-06	8.41E-06	8.44E-06	8.46E-06
$^{152}Eu_2O_3$[b]	0.00E+0	0.00E+0	0.00E+0	0.00E+0	0.00E+0	0.00E+0	0.00E+0	0.00E+0	0.00E+0	0.00E+0
$^{154}Eu_2O_3$	4.24E-08	6.17E-08	7.52E-08	8.47E-08	9.13E-08	9.60E-08	9.92E-08	1.02E-07	1.03E-07	1.04E-07
$^{155}Eu_2O_3$	3.40E-08	5.51E-08	6.99E-08	8.02E-08	8.74E-08	9.25E-08	9.60E-08	9.85E-08	1.00E-07	1.01E-07
^{63}NiO[b]	0.00E+0	0.00E+0	0.00E+0	0.00E+0	0.00E+0	0.00E+0	0.00E+0	0.00E+0	0.00E+0	0.00E+0
$^{237}NpO_2$	1.37E-05	2.33E-05	3.00E-05	3.47E-05	3.80E-05	4.03E-05	4.19E-05	4.30E-05	4.38E-05	4.44E-05
$^{238}PuO_2$	2.61E-08	2.89E-08	3.08E-08	3.21E-08	3.31E-08	3.37E-08	3.42E-08	3.45E-08	3.47E-08	3.49E-08
$^{239}PuO_2$	5.63E-05	5.73E-05	5.81E-05	5.86E-05	5.89E-05	5.92E-05	5.94E-05	5.95E-05	5.96E-05	5.97E-05
$^{240}PuO_2$	0.00E+0	0.00E+0	0.00E+0	0.00E+0	0.00E+0	0.00E+0	0.00E+0	0.00E+0	0.00E+0	0.00E+0
$^{241}PuO_2$	4.52E-08	7.68E-08	9.89E-08	1.14E-07	1.25E-07	1.33E-07	1.38E-07	1.42E-07	1.44E-07	1.46E-07
$^{106}Rh_2O_3$[b]	0.00E+0	0.00E+0	0.00E+0	0.00E+0	0.00E+0	0.00E+0	0.00E+0	0.00E+0	0.00E+0	0.00E+0
$^{103}RuO_2$[b]	0.00E+0	0.00E+0	0.00E+0	0.00E+0	0.00E+0	0.00E+0	0.00E+0	0.00E+0	0.00E+0	0.00E+0
$^{106}RuO_2$[b]	0.00E+0	0.00E+0	0.00E+0	0.00E+0	0.00E+0	0.00E+0	0.00E+0	0.00E+0	0.00E+0	0.00E+0
$^{125}Sb_2O_3$	4.75E-09	8.08E-09	1.04E-08	1.20E-08	1.32E-08	1.40E-08	1.45E-08	1.49E-08	1.52E-08	1.54E-08
$^{79}SeO_2$[b]	0.00E+0	0.00E+0	0.00E+0	0.00E+0	0.00E+0	0.00E+0	0.00E+0	0.00E+0	0.00E+0	0.00E+0
$^{151}Sm_2O_3$[b]	0.00E+0	0.00E+0	0.00E+0	0.00E+0	0.00E+0	0.00E+0	0.00E+0	0.00E+0	0.00E+0	0.00E+0
$^{113}SnO_2$[b]	0.00E+0	0.00E+0	0.00E+0	0.00E+0	0.00E+0	0.00E+0	0.00E+0	0.00E+0	0.00E+0	0.00E+0
$^{126}SnO_2$[b]	0.00E+0	0.00E+0	0.00E+0	0.00E+0	0.00E+0	0.00E+0	0.00E+0	0.00E+0	0.00E+0	0.00E+0
^{90}SrO	5.64E-05	6.40E-05	6.94E-05	7.32E-05	7.58E-05	7.77E-05	7.89E-05	7.98E-05	8.05E-05	8.09E-05
$^{99}Tc_2O_7$	2.41E-07	3.83E-07	4.82E-07	5.52E-07	6.00E-07	6.34E-07	6.58E-07	6.75E-07	6.87E-07	6.95E-07
$^{232}ThO_2$[b]	0.00E+0	0.00E+0	0.00E+0	0.00E+0	0.00E+0	0.00E+0	0.00E+0	0.00E+0	0.00E+0	0.00E+0
$^{233}UO_3$	1.91E-07	3.25E-07	4.18E-07	4.84E-07	5.29E-07	5.62E-07	5.84E-07	6.00E-07	6.11E-07	6.18E-07
$^{234}UO_3$	3.31E-07	5.63E-07	7.25E-07	8.39E-07	9.18E-07	9.74E-07	1.01E-06	1.04E-06	1.06E-06	1.07E-06
$^{235}UO_3$	3.77E-05	6.42E-05	8.26E-05	9.56E-05	1.05E-04	1.11E-04	1.15E-04	1.19E-04	1.21E-04	1.22E-04
$^{236}UO_3$	2.29E-06	3.89E-06	5.01E-06	5.79E-06	6.34E-06	6.73E-06	6.99E-06	7.18E-06	7.31E-06	7.41E-06
$^{238}UO_3$	4.43E-03	7.53E-03	9.70E-03	1.12E-02	1.23E-02	1.30E-02	1.36E-02	1.39E-02	1.42E-02	1.44E-02
$^{88}Y_2O_3$[b]	0.00E+0	0.00E+0	0.00E+0	0.00E+0	0.00E+0	0.00E+0	0.00E+0	0.00E+0	0.00E+0	0.00E+0

(a) Batches 11 to 18 of the AY-102 to AZ-102 transition waste type have the same nominal compositions as Batch 10.
(b) The nominal mass fraction for these components is zero in both AY-102 and AZ-102.

Table C.8. Nominal Mixing/Sampling %RSDs for Chemical Compositions for Each Stage of the AY-102 to AZ-102 Transition Waste Type[a]

	Batch 1		Batch 2		Batch 3		Batch 4		Batch 5		Batch 6		Batch 7		Batch 8		Batch 9		Batch 10	
Component	Min	Max	Min	Max	Min	Max	Min	Max	Min	Max	Min	Max	Min	Max	Min	Max	Min	Max	Min	Max
Ag	5	15	5	15	5	15	5	15	5	15	5	15	5	15	5	15	5	15	5	15
Al	5	15	5	15	5	15	5	15	5	15	5	15	5	15	5	15	5	15	5	15
B	5	15	5	15	5	15	5	15	5	15	5	15	5	15	5	15	5	15	5	15
Ba	5	15	5	15	5	15	5	15	5	15	5	15	5	15	5	15	5	15	5	15
Be	1	5	1	5	1	5	1	5	1	5	1	5	1	5	1	5	1	5	1	5
Bi[b]	0	0	0	0	0	0	0	0	0	0	0	0	0	0	0	0	0	0	0	0
Ca	5	15	5	15	5	15	5	15	5	15	5	15	5	15	5	15	5	15	5	15
Cd	5	15	5	15	5	15	5	15	5	15	5	15	5	15	5	15	5	15	5	15
Ce	5	15	5	15	5	15	5	15	5	15	5	15	5	15	5	15	5	15	5	15
Cl	1	5	1	5	1	5	1	5	1	5	1	5	1	5	1	5	1	5	1	5
Co	5	15	5	15	5	15	5	15	5	15	5	15	5	15	5	15	5	15	5	15
Cr	5	15	5	15	5	15	5	15	5	15	5	15	5	15	5	15	5	15	5	15
Cs	1	5	1	5	1	5	1	5	1	5	1	5	1	5	1	5	1	5	1	5
Cu	5	15	5	15	5	15	5	15	5	15	5	15	5	15	5	15	5	15	5	15
Dy[b]	0	0	0	0	0	0	0	0	0	0	0	0	0	0	0	0	0	0	0	0
Eu[b]	0	0	0	0	0	0	0	0	0	0	0	0	0	0	0	0	0	0	0	0
F	1	5	1	5	1	5	1	5	1	5	1	5	1	5	1	5	1	5	1	5
Fe	5	15	5	15	5	15	5	15	5	15	5	15	5	15	5	15	5	15	5	15
K	1	5	1	5	1	5	1	5	1	5	1	5	1	5	1	5	1	5	1	5
La	5	15	5	15	5	15	5	15	5	15	5	15	5	15	5	15	5	15	5	15
Li	1	5	1	5	1	5	1	5	1	5	1	5	1	5	1	5	1	5	1	5
Mg	5	15	5	15	5	15	5	15	5	15	5	15	5	15	5	15	5	15	5	15
Mn	5	15	5	15	5	15	5	15	5	15	5	15	5	15	5	15	5	15	5	15
Mo	5	15	5	15	5	15	5	15	5	15	5	15	5	15	5	15	5	15	5	15
Na	1	5	1	5	1	5	1	5	1	5	1	5	1	5	1	5	1	5	1	5
Nd	5	15	5	15	5	15	5	15	5	15	5	15	5	15	5	15	5	15	5	15
Ni	5	15	5	15	5	15	5	15	5	15	5	15	5	15	5	15	5	15	5	15
P	5	15	5	15	5	15	5	15	5	15	5	15	5	15	5	15	5	15	5	15
Pb	5	15	5	15	5	15	5	15	5	15	5	15	5	15	5	15	5	15	5	15
Pd[b]	0	0	0	0	0	0	0	0	0	0	0	0	0	0	0	0	0	0	0	0
Pr[b]	0	0	0	0	0	0	0	0	0	0	0	0	0	0	0	0	0	0	0	0
Rh[b]	0	0	0	0	0	0	0	0	0	0	0	0	0	0	0	0	0	0	0	0
Ru[b]	0	0	0	0	0	0	0	0	0	0	0	0	0	0	0	0	0	0	0	0
Sb	5	15	5	15	5	15	5	15	5	15	5	15	5	15	5	15	5	15	5	15
Se[b]	0	0	0	0	0	0	0	0	0	0	0	0	0	0	0	0	0	0	0	0
Si	5	15	5	15	5	15	5	15	5	15	5	15	5	15	5	15	5	15	5	15
S	1	5	1	5	1	5	1	5	1	5	1	5	1	5	1	5	1	5	1	5
Sn	5	15	5	15	5	15	5	15	5	15	5	15	5	15	5	15	5	15	5	15
Sr	5	15	5	15	5	15	5	15	5	15	5	15	5	15	5	15	5	15	5	15
Th[b]	0	0	0	0	0	0	0	0	0	0	0	0	0	0	0	0	0	0	0	0
Ti	5	15	5	15	5	15	5	15	5	15	5	15	5	15	5	15	5	15	5	15
U	5	15	5	15	5	15	5	15	5	15	5	15	5	15	5	15	5	15	5	15
V	5	15	5	15	5	15	5	15	5	15	5	15	5	15	5	15	5	15	5	15
Y	5	15	5	15	5	15	5	15	5	15	5	15	5	15	5	15	5	15	5	15
Zn	5	15	5	15	5	15	5	15	5	15	5	15	5	15	5	15	5	15	5	15
Zr	5	15	5	15	5	15	5	15	5	15	5	15	5	15	5	15	5	15	5	15

(a) Batches 11 to 18 of the AY-102 to AZ-102 transition waste type have the same nominal compositions as Batch 10.
(b) The nominal mass fraction for these components is zero in both AY-102 and AZ-102.

Table C.9. Nominal Analytical %RSDs for Chemical Compositions for Batches 1 through 5 of the AY-102 to AZ-102 Transition Waste Type[a]

Component	Batch 1		Batch 2		Batch 3		Batch 4		Batch 5	
	Min	Max	Min	Max	Min	Max	Min	Max	Min	Max
Ag	5	10	5	10	5	10	5	10	5	10
Al	5	10	5	10	5	10	5	10	5	10
B	5	10	5	10	5	10	5	10	5	10
Ba	11.5	23	12.5	25.1	13.3	26.6	13.8	27.6	14.2	28.3
Be	10	20	10	20	10	20	10	20	10	20
Bi[b]	0	0	0	0	0	0	0	0	0	0
Ca	10	20	10	20	10	20	10	20	10	20
Cd	5	10	5	10	5	10	5	10	5	10
Ce	6.5	13	7.5	15.1	8.3	16.6	8.8	17.6	9.2	18.3
Cl	10	20	10	20	10	20	10	20	10	20
Co	10	20	10	20	10	20	10	20	10	20
Cr	10	20	10	20	10	20	10	20	10	20
Cs	8	16	10.1	20.2	11.6	23.1	12.6	25.2	13.3	26.6
Cu	20	40	20	40	20	40	20	40	20	40
Dy[b]	0	0	0	0	0	0	0	0	0	0
Eu[b]	0	0	0	0	0	0	0	0	0	0
F	10	20	10	20	10	20	10	20	10	20
Fe	5	10	5	10	5	10	5	10	5	10
K	6.5	13	7.5	15.1	8.3	16.6	8.8	17.6	9.2	18.3
La	13.5	27	12.4	24.9	11.7	23.4	11.2	22.4	10.8	21.7
Li	10	20	10	20	10	20	10	20	10	20
Mg	6.5	13	7.5	15.1	8.3	16.6	8.8	17.6	9.2	18.3
Mn	5	10	5	10	5	10	5	10	5	10
Mo	15	30	15	30	15	30	15	30	15	30
Na	5	10	5	10	5	10	5	10	5	10
Nd	10	20	10	20	10	20	10	20	10	20
Ni	8.5	17	7.45	14.9	6.7	13.4	6.2	12.4	5.8	11.7
P	10	20	10	20	10	20	10	20	10	20
Pb	10	20	10	20	10	20	10	20	10	20
Pd[b]	0	0	0	0	0	0	0	0	0	0
Pr[b]	0	0	0	0	0	0	0	0	0	0
Rh[b]	0	0	0	0	0	0	0	0	0	0
Ru[b]	0	0	0	0	0	0	0	0	0	0
Sb	25	50	25	50	25	50	25	50	25	50
Se[b]	0	0	0	0	0	0	0	0	0	0
Si	5	10	5	10	5	10	5	10	5	10
S	13.5	27	12.4	24.9	11.7	23.4	11.2	22.4	10.8	21.7
Sn	13.5	27	12.4	24.9	11.7	23.4	11.2	22.4	10.8	21.7
Sr	5	10	5	10	5	10	5	10	5	10
Th[b]	0	0	0	0	0	0	0	0	0	0
Ti	6.5	13	7.5	15.1	8.3	16.6	8.8	17.6	9.2	18.3
U	17	34	14.9	29.8	13.4	26.9	12.4	24.8	11.7	23.4
V	50	50	50	50	50	50	50	50	50	50
Y	10	20	10	20	10	20	10	20	10	20
Zn	6.5	13	7.5	15.1	8.3	16.6	8.8	17.6	9.2	18.3
Zr	5	10	5	10	5	10	5	10	5	10

(a) Batches 11 to 18 of the AY-102 to AZ-102 transition waste type have the same nominal compositions as Batch 10.
(b) The nominal mass fraction for these components is zero in both AY-102 and AZ-102.

Table C.9. Nominal Analytical %RSDs for Chemical Compositions for Batches 6 through 10 of the AY-102 to AZ-102 Transition Waste Type (cont'd)[a]

Component	Batch 6		Batch 7		Batch 8		Batch 9		Batch 10	
	Min	Max	Min	Max	Min	Max	Min	Max	Min	Max
Ag	5	10	5	10	5	10	5	10	5	10
Al	5	10	5	10	5	10	5	10	5	10
B	5	10	5	10	5	10	5	10	5	10
Ba	14.4	28.8	14.6	29.2	14.7	29.4	14.8	29.6	14.9	29.7
Be	10	20	10	20	10	20	10	20	10	20
Bi[b]	0	0	0	0	0	0	0	0	0	0
Ca	10	20	10	20	10	20	10	20	10	20
Cd	5	10	5	10	5	10	5	10	5	10
Ce	9.4	18.8	9.6	19.2	9.7	19.4	9.8	19.6	9.9	19.7
Cl	10	20	10	20	10	20	10	20	10	20
Co	10	20	10	20	10	20	10	20	10	20
Cr	10	20	10	20	10	20	10	20	10	20
Cs	13.8	27.6	14.2	28.3	14.4	28.8	14.6	29.2	14.7	29.4
Cu	20	40	20	40	20	40	20	40	20	40
Dy[b]	0	0	0	0	0	0	0	0	0	0
Eu[b]	0	0	0	0	0	0	0	0	0	0
F	10	20	10	20	10	20	10	20	10	20
Fe	5	10	5	10	5	10	5	10	5	10
K_2	9.4	18.8	9.6	19.2	9.7	19.4	9.8	19.6	9.9	19.7
La	10.6	21.2	10.4	20.8	10.3	20.6	10.2	20.4	10.1	20.3
Li	10	20	10	20	10	20	10	20	10	20
Mg	9.4	18.8	9.6	19.2	9.7	19.4	9.8	19.6	9.9	19.7
Mn	5	10	5	10	5	10	5	10	5	10
Mo	15	30	15	30	15	30	15	30	15	30
Na	5	10	5	10	5	10	5	10	5	10
Nd	10	20	10	20	10	20	10	20	10	20
Ni	5.6	11.2	5.4	10.8	5.3	10.6	5.2	10.4	5.1	10.3
P	10	20	10	20	10	20	10	20	10	20
Pb	10	20	10	20	10	20	10	20	10	20
Pd[b]	0	0	0	0	0	0	0	0	0	0
Pr[b]	0	0	0	0	0	0	0	0	0	0
Rh[b]	0	0	0	0	0	0	0	0	0	0
Ru[b]	0	0	0	0	0	0	0	0	0	0
Sb	25	50	25	50	25	50	25	50	25	50
Se[b]	0	0	0	0	0	0	0	0	0	0
Si	5	10	5	10	5	10	5	10	5	10
S	10.6	21.2	10.4	20.8	10.3	20.6	10.2	20.4	10.1	20.3
Sn	10.6	21.2	10.4	20.8	10.3	20.6	10.2	20.4	10.1	20.3
Sr	5	10	5	10	5	10	5	10	5	10
Th[b]	0	0	0	0	0	0	0	0	0	0
Ti	9.4	18.8	9.6	19.2	9.7	19.4	9.8	19.6	9.9	19.7
U	11.2	22.4	10.8	21.6	10.6	21.2	10.4	20.8	10.3	20.6
V	50	50	50	50	50	50	50	50	50	50
Y	10	20	10	20	10	20	10	20	10	20
Zn	9.4	18.8	9.6	19.2	9.7	19.4	9.8	19.6	9.9	19.7
Zr	5	10	5	10	5	10	5	10	5	10

(a) Batches 11 to 18 of the AY-102 to AZ-102 transition waste type have the same nominal compositions as Batch 10.
(b) The nominal mass fraction for these components is zero in both AY-102 and AZ-102.

Table C.10. Nominal Radionuclide Oxide Analytical %RSDs for the Batches 1 through 5 of the AY-102 to AZ-102 Transition Waste Type[a]

Component	Batch 1		Batch 2		Batch 3		Batch 4		Batch 5	
	Min	Max	Min	Max	Min	Max	Min	Max	Min	Max
^{241}Am	5	42.5	5	37.2	5	33.5	5	31	5	29.20
^{144}Ce[b]	0	0	0	0	0	0	0	0	0	0
^{242}Cm[b]	0	0	0	0	0	0	0	0	0	0
$^{243}Cm+^{244}Cm$	10	60	10	60	10	60	10	60	10	60
^{60}Co	5	50	5	50	5	50	5	50	5	50
^{134}Cs	20	60	20	60	20	60	20	60	20	60
^{137}Cs	5	38	5	29.6	5	23.7	5	19.6	5	16.72
^{152}Eu[b]	0	0	0	0	0	0	0	0	0	0
^{154}Eu	10	30	10	30	10	30	10	30	10	30
^{155}Eu	5	20	5	20	5	20	5	20	5	20
^{63}Ni[b]	0	0	0	0	0	0	0	0	0	0
^{237}Np	10	25	10	25	10	25	10	25	10	25
^{238}Pu	10	50	10	50	10	50	10	50	10	50
^{239}Pu	10	20	10	20	10	20	10	20	10	20
^{240}Pu	0	0	0	0	0	0	0	0	0	0
^{241}Pu	15	50	15	50	15	50	15	50	15	50
^{106}Rh[b]	0	0	0	0	0	0	0	0	0	0
^{103}Ru[b]	0	0	0	0	0	0	0	0	0	0
^{106}Ru[b]	0	0	0	0	0	0	0	0	0	0
^{125}Sb	25	50	25	50	25	50	25	50	25	50
^{79}Se[b]	0	0	0	0	0	0	0	0	0	0
^{151}Sm[b]	0	0	0	0	0	0	0	0	0	0
^{113}Sn[b]	0	0	0	0	0	0	0	0	0	0
^{126}Sn[b]	0	0	0	0	0	0	0	0	0	0
^{90}Sr	10	20	10	20	10	20	10	20	10	20
^{99}Tc	10	20	10	20	10	20	10	20	10	20
^{232}Th[b]	0	0	0	0	0	0	0	0	0	0
^{233}U	5	20	5	20	5	20	5	20	5	20
^{234}U	30	100	30	100	30	100	30	100	30	100
^{235}U	10	40	10	40	10	40	10	40	10	40
^{236}U	15	100	15	100	15	100	15	100	15	100
^{238}U	5	25.5	5	22.3	5	20.1	5	18.6	5	17.52
^{88}Y[b]	0	0	0	0	0	0	0	0	0	0

(a) Batches 11 to 18 of the AY-102 to AZ-102 transition waste type have the same nominal compositions as Batch 10.
(b) The nominal mass fraction for these components is zero in both AY-102 and AZ-102.

Table C.10. Nominal Radionuclide Oxide Analytical %RSDs for Batches 6 through 10 of the AY-102 to AZ-102 Transition Waste Type (cont'd)[a]

Component	Batch 6		Batch 7		Batch 8		Batch 9		Batch 10	
	Min	Max	Min	Max	Min	Max	Min	Max	Min	Max
^{241}Am	5	27.9	5	27.1	5	26.4	5	26	5	25.7
^{144}Ce[b]	0	0	0	0	0	0	0	0	0	0
^{242}Cm[b]	0	0	0	0	0	0	0	0	0	0
$^{243}Cm+^{244}Cm$	10	60	10	60	10	60	10	60	10	60
^{60}Co	5	50	5	50	5	50	5	50	5	50
^{134}Cs	20	60	20	60	20	60	20	60	20	60
^{137}Cs	5	14.7	5	13.3	5	12.3	5	11.6	5	11.1
^{152}Eu[b]	0	0	0	0	0	0	0	0	0	0
^{154}Eu	10	30	10	30	10	30	10	30	10	30
^{155}Eu	5	20	5	20	5	20	5	20	5	20
^{63}Ni[b]	0	0	0	0	0	0	0	0	0	0
^{237}Np	10	25	10	25	10	25	10	25	10	25
^{238}Pu	10	50	10	50	10	50	10	50	10	50
^{239}Pu	10	20	10	20	10	20	10	20	10	20
^{240}Pu	0	0	0	0	0	0	0	0	0	0
^{241}Pu	15	50	15	50	15	50	15	50	15	50
^{106}Rh[b]	0	0	0	0	0	0	0	0	0	0
^{103}Ru[b]	0	0	0	0	0	0	0	0	0	0
^{106}Ru[b]	0	0	0	0	0	0	0	0	0	0
^{125}Sb	25	50	25	50	25	50	25	50	25	50
^{79}Se[b]	0	0	0	0	0	0	0	0	0	0
^{151}Sm[b]	0	0	0	0	0	0	0	0	0	0
^{113}Sn[b]	0	0	0	0	0	0	0	0	0	0
^{126}Sn[b]	0	0	0	0	0	0	0	0	0	0
^{90}Sr	10	20	10	20	10	20	10	20	10	20
^{99}Tc	10	20	10	20	10	20	10	20	10	20
^{232}Th[b]	0	0	0	0	0	0	0	0	0	0
^{233}U	5	20	5	20	5	20	5	20	5	20
^{234}U	30	100	30	100	30	100	30	100	30	100
^{235}U	10	40	10	40	10	40	10	40	10	40
^{236}U	15	100	15	100	15	100	15	100	15	100
^{238}U	5	16.8	5	16.2	5	15.9	5	15.6	5	15.4
^{88}Y[b]	0	0	0	0	0	0	0	0	0	0

(a) Batches 11 to 18 of the AY-102 to AZ-102 transition waste type have the same nominal compositions as Batch 10.
(b) The nominal mass fraction for these components is zero in both AY-102 and AZ-102.

Appendix D

Nominal Concentrations and Estimates of Uncertainties Relevant to Quantifying ILAW Variations and Uncertainties

Appendix D: Nominal Concentrations and Estimates of Uncertainties Relevant to Quantifying ILAW Variations and Uncertainties

This appendix summarizes the immobilized low-activity waste (ILAW) process composition and uncertainty inputs provided by the WTP Project that are relevant to quantifying variations and uncertainties in ILAW compositions and properties. The WTP process control and compliance strategies for ILAW are focused on analyses of CRV samples, quantifying transfer volumes, weighing GFCs added to the MFPV, and ultimately on estimating the ILAW composition and properties corresponding to each MFPV batch. Hence, the composition and uncertainty estimates provided by the WTP Project are associated with the ILAW CRV, GFCs, and MFPV. The ILAW process composition and uncertainty information was provided for five selected sets of ILAW G2 runs. The WTP Project provided data on 1402 G2 runs corresponding to 701 events where each event consisted of two CRV batches labeled (a) and (b). The selected G2 runs (where each run is associated with an LAW CRV batch) consisted of tank waste from Envelopes A, B, and C, including transitions from one to another. These five sets of G2 batches represent LAW waste types corresponding to waste tanks AP-101/AY-102 (Envelope A), AZ-102 (Envelope B), AN-102 (Envelope C), an unknown tank with a Na/S ratio on the border between Envelopes B and C, and a transition from AP-101/AY-102 (Envelope A) to AZ-101 (Envelope B). Actual waste composition data from these envelopes were used by the WTP Project to generate the inputs summarized in this appendix.

Tables D.1 to D.5 list the nominal elemental concentrations of chemical and radionuclide composition components (mg/L) for pre-treated LAW in the CRV corresponding to the selected five sets of G2 runs (as discussed in the preceding paragraph). Each table lists the G2 event numbers used with each data set. Table D.1 lists composition data for AP-101/AY-102 (Envelope A). Table D.2 lists composition data for the transition period from AP-101/AY-102 (Envelope A) to AZ-101 (Envelope B). Table D.3 lists composition data for AZ-102 (Envelope B). Table D.4 lists composition data for AN-102 (Envelope C). Table D.5 lists composition data for an unknown tank with Na/S ratio on the border between Envelopes B and C. The data in these tables were provided by the WTP Project from the G2 run output files \\snapshots\LCP-1.cvs and \\snapshots\LCP-2.cvs. See Vora (2004) for a discussion of the G2 runs.

Table D.6 provides LAW element and radionuclide analytical uncertainties [$\%RSD_A(c_{ijlm}^{CRV})$] dependent on the concentrations of LAW for each element or radionuclide j in the CRV. The values in Table D.6 were provided by the WTP analytical group[(a)]. Although the %RSDs in Table D.6 are nominally for concentrations of elements or radionuclides, they also apply to the components (oxides or halogens) listed in Tables D.1 to D.5. That is the case because the element-to-oxide conversion factor f_j cancels out in the formula for %RSDs of the quantities in Tables D.1 to D.5. Finally, note that the %RSD values in Table D.6 correspond to the low-case uncertainty values as described in Table 5.4. The high-case values are two times the low-case values.

(a) "Estimated Analytical Measurement Uncertainties for Selected Analytes," CCN 111456, June 13, 2005, memorandum from David Dodd and Bruce Kaiser to John Vienna, Waste Treatment and Immobilization Plant, Richland, WA.

Table D.7 lists the nominal masses (g) of GFCs added per liter of LAW for each of the selected G2 runs (events). Note that sodium carbonate is also an ILAW GFC, but it was not used for these batches. Hence, it is not listed in Table D.7. Table D.8 lists the uncertainties for masses of GFCs [$\%RSD(a_{ik}^{GFC})$] added to the ILAW MFPV. These uncertainties include all uncertainties associated with batching, weighing, and transferring GFCs until they are added to the MFPV. Tables D.9 and D.10 summarize data on the GFC compositions (mass fractions of oxides) and corresponding low and high uncertainties. Table D.9 provides nominal values and low- and high-uncertainty ranges for each GFC component (oxide or halide). Table D.10 provides nominal values as well as low and high standard deviations [$SD(G_{jk}^{GFC})$] for each GFC component. The standard deviations were obtained using a formula assuming that GFC uncertainties follow triangular distributions, which are determined by the nominal values and ranges in Table D.9. This formula is given by

$$SD(G_{jk}^{GFC}) = \sqrt{\frac{\Delta_l^2 + \Delta_u^2 + \Delta_n^2 - \Delta_l * \Delta_u - \Delta_l * \Delta_n - \Delta_u * \Delta_n}{18}} \quad \text{(D.1)}$$

where

Δ_l = lower limit value specified for the triangular distribution

Δ_u = upper limit value specified for the triangular distribution

Δ_n = nominal value specified for the triangular distribution.

The 12 GFCs listed in Tables D.9 and D.10 will be used by the WTP to produce ILAW and/or IHLW.

Table D.11 lists the nominal volumes as well as low- and high-uncertainty estimates (SDs) of (1) the LAW CRV contents with varying fractions of waste being present, (2) the MFPV contents after a transfer from the CRV with GFCs added, and (3) the MFPV contents when only the heel is present.

Table D.12 lists the nominal volume information broken down into its varying components for each of the selected G2 events. These volume components include the volume transferred from CRV to MFPV, the MFPV heel volume, the flush volume, the volume of GFCs added, the dust volume, the sugar volume, the dilute volume, and the total volume in the MFPV. This table also lists the nominal number of MFPV batches that are made from each individual CRV batch. The data in Table D.12 were taken from the G2 run output files mentioned earlier. See Vora (2004) for discussion of the G2 runs.

Table D.1. Nominal Chemical Composition and Radionuclide Concentrations (mg/L) of Components in the LAW CRV for Set 1 (AP-101/AY-102) from the Selected G2 Runs

Component[(a)]	G2 Event Number									
	25(a)	25(b)	26(a)	26(b)	27(a)	27(b)	28(a)	28(b)	29(a)	29(b)
$^{227}Ac_2O_3$	7.24E-09	7.24E-09	7.24E-09	7.27E-09	7.27E-09	7.24E-09	7.20E-09	7.20E-09	7.20E-09	7.22E-09
Ag_2O	1.2702	1.2899	1.296	1.2995	1.2946	1.2887	1.2751	1.2621	1.2518	1.248
Al_2O_3	20188.581	20015.742	19932.687	19929.217	19964.548	20066.066	20299.858	20464.17	20492.238	20444.553
$^{241}Am_2O_3$	8.98E-05	9.07E-05	9.12E-05	9.16E-05	9.14E-05	9.09E-05	9.01E-05	8.94E-05	8.90E-05	8.87E-05
$^{243}Am_2O_3$	8.41E-08	8.52E-08	8.54E-08	8.58E-08	8.54E-08	8.52E-08	8.43E-08	8.36E-08	8.30E-08	8.27E-08
As_2O_5	4.6413	4.7238	4.7455	4.7657	4.7422	4.7158	4.6594	4.6128	4.5674	4.5496
B_2O_3	60.7637	61.0769	61.2121	61.3769	61.3119	61.1433	60.6786	60.454	60.2796	60.2777
BaO	0.4921	0.4958	0.4971	0.4986	0.4977	0.4961	0.4919	0.4895	0.4874	0.4871
BeO	3.9446	3.957	3.9643	3.9739	3.9723	3.9632	3.936	3.9252	3.9183	3.9205
Bi_2O_3	2.3717	2.3767	2.3803	2.3863	2.3859	2.381	2.3658	2.3613	2.3581	2.36
P_2O_5	2731.044	2773.1396	2781.9187	2792.29	2779.1656	2768.209	2747.208	2726.5674	2700.9343	2687.8366
Cl	2146.9537	2150.6446	2160.7026	2147.3437	2153.5102	2154.6597	2148.1238	2124.8738	2127.4224	2130.0766
CaO	21.1553	21.4504	21.5323	21.6172	21.5341	21.4314	21.2016	21.0332	20.8693	20.8124
CdO	2.4617	2.4715	2.4774	2.4811	2.4803	2.475	2.4583	2.448	2.4433	2.4442
Ce_2O_3	0.1096	0.1105	0.1108	0.1112	0.1109	0.1105	0.1096	0.109	0.1085	0.474
$^{242}Cm_2O_3$	0	0	0	0	0	0	0	0	0	0
$^{244}Cm_2O_3$	7.70E-08	7.88E-08	7.92E-08	7.94E-08	7.88E-08	7.81E-08	7.70E-08	7.59E-08	7.48E-08	7.44E-08
^{60}CoO	2.36E-06	2.38E-06	2.38E-06	2.38E-06	2.37E-06	2.36E-06	2.33E-06	2.32E-06	2.30E-06	2.30E-06
Cr_2O_3	369.5497	371.9066	372.4198	373.3603	372.7152	372.2148	371.0256	370.0318	368.3613	367.4385
Cs_2O	2.88E-03	2.88E-03	2.88E-03	2.88E-03	2.87E-03	2.86E-03	2.84E-03	2.83E-03	2.84E-03	2.85E-03
$^{134}Cs_2O$	2.16E-09	2.16E-09	2.16E-09	2.16E-09	2.16E-09	2.14E-09	2.12E-09	2.12E-09	2.14E-09	2.14E-09
$^{137}Cs_2O$	8.22E-04	8.22E-04	8.22E-04	8.22E-04	8.20E-04	8.14E-04	8.10E-04	8.08E-04	8.10E-04	8.12E-04
$^{152}Eu_2O_3$	1.16E-05	1.17E-05	1.17E-05	1.17E-05	1.17E-05	1.16E-05	1.15E-05	1.15E-05	1.15E-05	1.15E-05
$^{154}Eu_2O_3$	1.09E-04	1.11E-04	1.12E-04	1.12E-04	1.11E-04	1.09E-04	1.08E-04	1.06E-04	1.04E-04	1.03E-04
$^{155}Eu_2O_3$	3.04E-05	3.09E-05	3.09E-05	3.09E-05	3.04E-05	3.02E-05	2.95E-05	2.91E-05	2.86E-05	2.81E-05
F	3091.8781	3096.229	3110.078	3092.0105	3100.8029	3102.3255	3092.7449	3061.0318	3064.8381	3068.8586
Fe_2O_3	7.555	7.6695	7.7005	7.7321	7.6995	7.6607	7.5753	7.5106	7.447	7.424
^{129}I	0.6243	0.6311	0.6461	0.6193	0.6307	0.6399	0.6487	0.615	0.623	0.626
K_2O	36540.337	36553.661	36602.956	36674.803	36693.17	36633.726	36418.687	36366.857	36358.789	36410.017
Li_2O	25.1437	25.8068	25.9654	26.1054	25.9081	25.7145	25.3306	24.9708	24.6048	24.4429
^{113m}CdO	1.05E-04	1.05E-04	1.05E-04	1.05E-04	1.05E-04	1.05E-04	1.04E-04	1.04E-04	1.04E-04	1.04E-04
MgO	12.7953	13.0359	13.0974	13.1568	13.0868	13.0104	12.8493	12.716	12.5828	12.5297
MnO	1.4927	1.493	1.4949	1.4978	1.4986	1.4962	1.4876	1.4856	1.4854	1.4876
$^{93m}Nb_2O_5$	3.68E-05	3.71E-05	3.71E-05	3.74E-05	3.71E-05	3.71E-05	3.68E-05	3.66E-05	3.66E-05	3.66E-05
MoO_6	31.4167	31.5143	31.5822	31.6319	31.6286	31.565	31.359	31.2466	31.1988	31.2179
Na_2O	246006.92	246110.1	246141.73	246121.93	246134.34	246190.21	246347.36	246304.06	246224.24	246124.46
Nd_2O_3	8.6832	8.8444	8.8869	8.9247	8.8789	8.8284	8.7209	8.6291	8.5406	8.5054
NiO	46.3939	47.3935	47.6429	47.8721	47.5795	47.2742	46.6458	46.0951	45.5428	45.3117
^{59}NiO	0.0289	0.0296	0.0297	0.0299	0.0297	0.0295	0.0291	0.0287	0.0283	0.0282
^{63}NiO	3.84E-03	3.92E-03	3.94E-03	3.96E-03	3.94E-03	3.91E-03	3.85E-03	3.80E-03	3.76E-03	3.73E-03
$^{237}NpO_2$	0.2449	0.2513	0.2528	0.2542	0.2523	0.2504	0.2467	0.2432	0.2397	0.2381
$^{231}Pa_2O_5$	4.15E-05	4.15E-05	4.17E-05	4.17E-05	4.17E-05	4.17E-05	4.12E-05	4.12E-05	4.10E-05	4.10E-05

(a) According to the mass-balance equation given in Eq. (B.1), the chemical and radiochemical analyses of samples from the LAW CRV will yield concentrations of elements and radionuclides, not oxide and halogen components. However, the G2 run data were in terms of masses of oxide and halogen components, so it was easier to work with concentrations on that basis. Note that such concentrations are just $c_{ijlm}^{CRV} f_j$ in the notation of Eq. (B.1).

Table D.1. Nominal Chemical Composition and Radionuclide Concentrations (mg/L) of Components in the LAW CRV for Set 1 (AP-101/AY-102) from the Selected G2 Runs (cont'd)

Component[(a)]	G2 Event Number									
	25(a)	25(b)	26(a)	26(b)	27(a)	27(b)	28(a)	28(b)	29(a)	29(b)
PbO	44.6963	45.5	45.7165	45.9004	45.6764	45.4253	44.8849	44.4183	43.9801	43.8076
PdO	0.323	0.3318	0.3339	0.3357	0.3331	0.3306	0.3255	0.3208	0.316	0.3138
Pr_2O_3	0.0514	0.0522	0.0525	0.0527	0.0524	0.0521	0.0515	0.051	0.0506	0.0504
$^{238}PuO_2$	9.13E-06	9.36E-06	9.40E-06	9.45E-06	9.38E-06	9.31E-06	9.18E-06	9.04E-06	8.93E-06	8.86E-06
$^{239}PuO_2$	0.0172	0.0176	0.0177	0.0178	0.0177	0.0176	0.0173	0.0171	0.0169	0.0168
$^{240}PuO_2$	9.85E-04	1.01E-03	1.01E-03	1.02E-03	1.01E-03	1.01E-03	9.92E-04	9.78E-04	9.64E-04	9.58E-04
$^{241}PuO_2$	1.95E-05	1.99E-05	2.00E-05	2.01E-05	1.99E-05	1.97E-05	1.94E-05	1.91E-05	1.89E-05	1.87E-05
$^{242}PuO_2$	6.56E-06	6.72E-06	6.76E-06	6.79E-06	6.74E-06	6.69E-06	6.60E-06	6.51E-06	6.42E-06	6.38E-06
^{226}RaO	1.23E-07	1.25E-07	1.28E-07	1.24E-07	1.26E-07	1.28E-07	1.30E-07	1.24E-07	1.26E-07	1.28E-07
^{228}RaO	4.10E-07	4.15E-07	4.23E-07	4.08E-07	4.17E-07	4.23E-07	4.30E-07	4.10E-07	4.17E-07	4.19E-07
Rb_2O	4.4796	4.4891	4.4967	4.5066	4.5063	4.4973	4.4681	4.4578	4.4525	4.4564
Rh_2O_3	1.1198	1.1502	1.1576	1.1636	1.1547	1.1461	1.1288	1.1121	1.0955	1.0881
RuO_2	23.1824	23.8176	24.0821	23.9939	23.9252	23.8468	23.6141	23.0513	22.8134	22.7047
Sb_2O_3	0.0987	0.1004	0.1009	0.1013	0.1008	0.1003	0.099	0.0981	0.0971	0.0967
$^{125}Sb_2O_3$	1.29E-05	1.29E-05	1.29E-05	1.29E-05	1.29E-05	1.29E-05	1.28E-05	1.28E-05	1.28E-05	1.28E-05
SeO_2	17.9325	18.3412	18.6577	18.3218	18.434	18.5169	18.5178	17.867	17.8605	17.8596
$^{79}SeO_2$	0.017	0.0172	0.0172	0.0173	0.0172	0.0172	0.017	0.0169	0.0168	0.0168
SiO_2	520.0584	526.4774	528.3064	530.2903	528.5063	526.1994	520.9289	517.2462	513.6569	512.4732
$^{151}Sm_2O_3$	0.2138	0.2152	0.2157	0.2163	0.216	0.2153	0.2135	0.2126	0.2118	0.2117
SO_3	4199.0955	4223.4893	4233.4386	4242.2263	4236.2646	4223.5512	4190.6545	4170.5587	4156.282	4154.4035
SrO	18.9823	19.4903	19.6118	19.7179	19.5668	19.4192	19.1269	18.8511	18.5708	18.4464
^{90}SrO	0.0066	0.0068	0.0068	0.0069	0.0068	0.0068	0.0067	0.0066	0.0065	0.0064
Ta_2O_5	0.1693	0.1711	0.1717	0.1723	0.1718	0.1711	0.1695	0.1684	0.1674	0.1671
$^{99}Tc_2O_7$	5.5832	5.6112	5.6672	5.5714	5.6067	5.6275	5.6326	5.4973	5.5142	5.5202
TeO_2	0.5889	0.605	0.6102	0.6107	0.6074	0.6041	0.5966	0.5851	0.5776	0.5742
$^{229}ThO_2$	1.31E-05	1.31E-05	1.32E-05	1.32E-05	1.32E-05	1.32E-05	1.31E-05	1.31E-05	1.31E-05	1.31E-05
$^{232}ThO_2$	137.4096	137.4676	137.6358	137.9547	138.0037	137.7629	136.9316	136.7837	136.7375	136.9275
TiO_2	1.6324	1.6516	1.6572	1.6633	1.658	1.6509	1.6345	1.6233	1.6127	1.6094
Tl_2O	0.204	0.2093	0.213	0.2094	0.2106	0.2115	0.2114	0.2038	0.2035	0.2034
$^{232}UO_3$	7.06E-07	7.06E-07	7.09E-07	7.09E-07	7.09E-07	7.09E-07	7.04E-07	7.04E-07	7.04E-07	7.04E-07
$^{233}UO_3$	7.10E-03	7.10E-03	7.11E-03	7.13E-03	7.13E-03	7.12E-03	7.08E-03	7.07E-03	7.07E-03	7.08E-03
$^{234}UO_3$	1.05E-02	1.06E-02	1.07E-02	1.07E-02	1.07E-02	1.06E-02	1.05E-02	1.04E-02	1.03E-02	1.03E-02
$^{235}UO_3$	1.2075	1.2278	1.2332	1.2384	1.2326	1.226	1.2116	1.2003	1.189	1.1847
$^{236}UO_3$	0.0598	0.0611	0.0614	0.0617	0.0613	0.0609	0.0601	0.0594	0.0587	0.0584
$^{238}UO_3$	158.7954	161.3929	162.0823	162.7678	162.0234	161.1645	159.3041	157.8449	156.4053	155.8629
UO_3	0.0488	0.0501	0.0504	0.0507	0.0503	0.0499	0.0492	0.0484	0.0477	0.0474
V_2O_5	2.0757	2.0976	2.1044	2.1114	2.1057	2.0974	2.0776	2.0642	2.0521	2.0487
WO_3	34.6413	34.6457	34.6897	34.7601	34.7792	34.7238	34.5216	34.4801	34.4762	34.5272
Y_2O_3	2.9842	3.0651	3.0846	3.1011	3.0772	3.0539	3.0077	2.9635	2.919	2.8992
ZnO	8.0572	8.0967	8.1136	8.1369	8.1283	8.1059	8.0443	8.0173	7.9948	7.9951
ZrO_2	2.4781	2.4989	2.5057	2.514	2.5086	2.4997	2.4777	2.4651	2.4535	2.451
$^{93}ZrO_2$	4.0738	4.0979	4.1072	4.1196	4.1139	4.1016	4.0689	4.0532	4.0396	4.0384

(a) According to the mass-balance equation given in Eq. (B.1), the chemical and radiochemical analyses of samples from the LAW CRV will yield concentrations of elements and radionuclides, not oxide and halogen components. However, the G2 run data were in terms of masses of oxide and halogen components, so it was easier to work with concentrations on that basis. Note that such concentrations are just $c_{ijlm}^{CRV} f_j$ in the notation of Eq. (B.1).

Table D.2. Nominal Chemical Composition and Radionuclide Concentrations (mg/L) of Components in the LAW CRV for Set 2 (transition from AP-101/AY-102 to AZ-101) from the Selected G2 Runs

Component[(a)]	G2 Event Number									
	42(a)	42(b)	43(a)	43(b)	44(a)	44(b)	45(a)	45(b)	46(a)	46(b)
$^{227}Ac_2O_3$	8.13E-10	6.01E-10	4.97E-10	4.11E-10	3.40E-10	2.85E-10	2.52E-10	2.21E-10	2.06E-10	1.91E-10
Ag_2O	2.6382	2.895	3.0878	3.204	3.3675	3.4611	3.5558	3.6656	3.6995	3.7444
Al_2O_3	20231.86	19537.482	19158.314	18874.59	18598.605	18446.757	18320.274	18249.726	18158.359	18081.085
$^{241}Am_2O_3$	0.0103	0.0137	0.0162	0.0177	0.0199	0.0213	0.0225	0.024	0.0244	0.0249
$^{243}Am_2O_3$	3.75E-05	5.03E-05	5.93E-05	6.50E-05	7.31E-05	7.81E-05	8.25E-05	8.78E-05	8.93E-05	9.13E-05
As_2O_5	7.9329	8.0037	8.0891	8.1246	8.1676	8.1356	8.1705	8.2124	8.2081	8.2079
B_2O_3	38.0362	38.1903	38.6899	38.8343	39.3041	39.3212	39.6664	40.0977	40.1461	40.2476
BaO	0.3149	0.2859	0.2682	0.2557	0.2397	0.2263	0.2181	0.2087	0.2051	0.2008
BeO	1.3239	1.1708	1.0843	1.0205	0.9513	0.8934	0.8596	0.8216	0.8075	0.7906
Bi_2O_3	2.2319	2.6699	3.0055	3.2086	3.5346	3.788	3.982	4.2398	4.3027	4.4001
P_2O_5	4180.531	3852.8	3635.7535	3490.2998	3279.0958	3107.0086	2995.2381	2865.6483	2816.9809	2755.9268
Cl	575.7921	504.5506	454.602	423.0889	386.9605	366.5908	351.5454	330.2035	333.3425	334.7361
CaO	31.0264	31.925	32.9236	33.496	35.6971	39.6169	41.4025	45.0521	45.6107	47.0161
CdO	1.353	1.3772	1.4085	1.4222	1.4532	1.4651	1.4859	1.5107	1.518	1.5282
Ce_2O_3	491.5293	456.065	429.0573	412.9637	388.9954	374.5052	361.9261	349.4612	343.9029	337.7909
$^{242}Cm_2O_3$	4.26E-08	5.66E-08	6.70E-08	7.36E-08	8.26E-08	8.83E-08	9.33E-08	9.95E-08	1.01E-07	1.03E-07
$^{244}Cm_2O_3$	4.85E-06	6.41E-06	7.55E-06	8.25E-06	9.24E-06	9.87E-06	1.04E-05	1.11E-05	1.13E-05	1.15E-05
^{60}CoO	5.41E-06	6.48E-06	7.26E-06	7.74E-06	8.43E-06	8.83E-06	9.24E-06	9.67E-06	9.79E-06	9.97E-06
Cr_2O_3	538.1749	564.1282	585.484	597.6491	616.4927	627.9272	639.4332	654.3875	657.3394	662.179
Cs_2O	8.01E-04	7.24E-04	6.97E-04	6.67E-04	6.54E-04	6.40E-04	6.37E-04	6.37E-04	6.37E-04	6.37E-04
$^{134}Cs_2O$	1.20E-09	1.42E-09	1.60E-09	1.70E-09	1.85E-09	1.95E-09	2.04E-09	2.16E-09	2.18E-09	2.22E-09
$^{137}Cs_2O$	2.79E-04	2.75E-04	2.79E-04	2.77E-04	2.83E-04	2.88E-04	2.92E-04	3.00E-04	3.00E-04	3.04E-04
$^{152}Eu_2O_3$	2.96E-05	3.68E-05	4.21E-05	4.53E-05	5.00E-05	5.30E-05	5.55E-05	5.85E-05	5.94E-05	6.06E-05
$^{154}Eu_2O_3$	2.19E-04	2.10E-04	2.05E-04	2.01E-04	1.96E-04	1.90E-04	1.87E-04	1.84E-04	1.82E-04	1.81E-04
$^{155}Eu_2O_3$	6.55E-05	6.53E-05	6.55E-05	6.55E-05	6.53E-05	6.46E-05	6.46E-05	6.46E-05	6.44E-05	6.44E-05
F	1063.9854	1068.136	1074.7801	1077.7996	1095.8885	1111.9857	1129.2405	1144.4192	1164.8349	1187.7074
Fe_2O_3	13.5988	14.4897	15.1906	15.5987	16.1728	16.4564	16.7939	17.1948	17.2808	17.407
^{129}I	0.7542	0.7831	0.7559	0.7574	0.7463	0.7808	0.7882	0.7661	0.8365	0.9049
K_2O	5779.1484	4997.4044	4648.8582	4348.0146	4163.428	3986.8615	3919.6558	3858.7786	3828.687	3801.5272
Li_2O	46.7754	42.4205	39.4729	37.5253	34.6356	32.3061	30.7683	28.9672	28.3221	27.5008
^{113m}CdO	6.11E-05	6.43E-05	6.75E-05	6.91E-05	7.18E-05	7.32E-05	7.50E-05	7.71E-05	7.75E-05	7.82E-05
MgO	28.2326	30.2087	31.7393	32.6394	33.8856	34.5115	35.2387	36.0989	36.2862	36.5569
MnO	0.906	1.1065	1.2606	1.3529	1.4934	1.5817	1.6616	1.7561	1.7826	1.8186
$^{93m}Nb_2O_5$	3.11E-05	3.26E-05	3.40E-05	3.48E-05	3.60E-05	3.66E-05	3.74E-05	3.83E-05	3.83E-05	3.86E-05
MoO_6	42.1488	51.5269	58.4992	62.759	68.9486	72.8505	76.3496	80.4612	81.6666	83.2822
Na_2O	207400.35	197987.11	192751.03	188849.47	185005.14	182022.23	180152.69	178122.68	177404.08	176563.53
Nd_2O_3	19.1551	20.5362	21.5993	22.2272	23.0976	23.5438	24.0508	24.6469	24.7875	24.9858
NiO	72.489	66.0775	61.7973	58.9427	54.7601	51.349	49.138	46.5538	45.6177	44.4316
^{59}NiO	0.0477	0.0432	0.0402	0.0382	0.0353	0.033	0.0314	0.0296	0.0289	0.0281
^{63}NiO	6.30E-03	5.71E-03	5.32E-03	5.06E-03	4.67E-03	4.36E-03	4.15E-03	3.91E-03	3.82E-03	3.72E-03
$^{237}NpO_2$	0.4744	0.439	0.4152	0.3994	0.3757	0.3558	0.3433	0.3286	0.3231	0.3161
$^{231}Pa_2O_5$	1.87E-05	1.63E-05	1.48E-05	1.38E-05	1.26E-05	1.15E-05	1.09E-05	1.02E-05	9.89E-06	9.56E-06

(a) According to the mass-balance equation given in Eq. (B.1), the chemical and radiochemical analyses of samples from the LAW CRV will yield concentrations of elements and radionuclides, not oxide and halogen components. However, the G2 run data were in terms of masses of oxide and halogen components, so it was easier to work with concentrations on that basis. Note that such concentrations are just $c_{ijlm}^{CRV} f_j$ in the notation of Eq. (B.1).

Table D.2. Nominal Chemical Composition and Radionuclide Concentrations (mg/L) of Components in the LAW CRV for Set 2 (transition from AP-101/AY-102 to AZ-101) from the Selected G2 Runs (cont'd)

Component[(a)]	G2 Event Number									
	42(a)	42(b)	43(a)	43(b)	44(a)	44(b)	45(a)	45(b)	46(a)	46(b)
PbO	59.6059	54.4157	50.9666	48.6596	45.3233	42.6121	40.8602	38.7988	38.0913	37.1856
PdO	0.6149	0.557	0.5177	0.4917	0.4532	0.4222	0.4016	0.3776	0.369	0.358
Pr_2O_3	0.0755	0.0734	0.0723	0.0714	0.07	0.0686	0.0679	0.0672	0.0668	0.0664
$^{238}PuO_2$	2.92E-05	3.22E-05	3.47E-05	3.60E-05	3.78E-05	3.90E-05	3.99E-05	4.12E-05	4.15E-05	4.19E-05
$^{239}PuO_2$	0.0633	0.0718	0.0781	0.082	0.0874	0.0905	0.0936	0.0972	0.0981	0.0993
$^{240}PuO_2$	4.52E-03	5.30E-03	5.87E-03	6.22E-03	6.71E-03	7.01E-03	7.28E-03	7.61E-03	7.69E-03	7.81E-03
$^{241}PuO_2$	1.71E-04	2.14E-04	2.44E-04	2.65E-04	2.92E-04	3.08E-04	3.24E-04	3.42E-04	3.46E-04	3.53E-04
$^{242}PuO_2$	3.69E-05	4.41E-05	4.95E-05	5.27E-05	5.74E-05	6.02E-05	6.29E-05	6.58E-05	6.67E-05	6.79E-05
^{226}RaO	8.88E-07	8.77E-07	8.43E-07	8.32E-07	8.13E-07	8.32E-07	8.28E-07	8.13E-07	8.64E-07	9.18E-07
^{228}RaO	3.87E-07	3.89E-07	3.61E-07	3.55E-07	3.38E-07	3.55E-07	3.55E-07	3.36E-07	3.83E-07	4.30E-07
Rb_2O	1.7478	1.7823	1.8345	1.8559	1.9121	1.9363	1.9727	2.0175	2.0275	2.0429
Rh_2O_3	2.5815	2.5303	2.5016	2.4789	2.4401	2.3945	2.3763	2.3545	2.3436	2.3304
RuO_2	44.4433	40.998	38.1956	36.5295	33.9237	32.2939	31.0321	29.2132	29.4547	29.5229
Sb_2O_3	0.1398	0.1315	0.1262	0.1226	0.1172	0.1125	0.1098	0.1066	0.1053	0.1037
$^{125}Sb_2O_3$	7.36E-05	9.71E-05	1.15E-04	1.25E-04	1.40E-04	1.50E-04	1.59E-04	1.68E-04	1.71E-04	1.75E-04
SeO_2	35.2374	35.6649	35.1864	35.1619	34.908	35.4095	35.5554	35.0758	36.6891	38.2863
$^{79}SeO_2$	0.0503	0.0617	0.0701	0.0752	0.0825	0.0871	0.0912	0.0961	0.0974	0.0992
SiO_2	550.483	520.3557	502.266	489.25	471.5749	455.5981	446.7853	436.8773	432.5251	427.3313
$^{151}Sm_2O_3$	0.1582	0.1589	0.1608	0.1614	0.163	0.1628	0.164	0.1655	0.1656	0.1658
SO_3	4522.6296	5042.031	5446.6034	5685.99	6045.8784	6261.9523	6470.1786	6718.7466	6803.4924	6917.1181
SrO	36.2695	33.1169	30.9907	29.5811	27.4824	25.7727	24.6602	23.3578	22.887	22.2893
^{90}SrO	0.0477	0.0588	0.0669	0.0719	0.0789	0.0833	0.0873	0.0919	0.0932	0.0949
Ta_2O_5	0.1508	0.1404	0.1339	0.1294	0.1233	0.1179	0.1148	0.1112	0.1099	0.1082
$^{99}Tc_2O_7$	8.7459	10.4637	11.6351	12.3913	13.4849	14.2837	14.9355	15.6231	16.1485	16.7641
TeO_2	1.1383	1.0467	0.979	0.9365	0.8714	0.8244	0.7913	0.7484	0.7442	0.7359
$^{229}ThO_2$	1.48E-06	1.10E-06	9.02E-07	7.49E-07	6.22E-07	5.19E-07	4.60E-07	3.98E-07	3.76E-07	3.51E-07
$^{232}ThO_2$	21.1299	17.7994	16.2289	14.9256	13.9935	13.1555	12.765	12.3813	12.2055	12.0256
TiO_2	2.5459	2.7616	2.9292	3.028	3.1696	3.2459	3.3278	3.4247	3.4475	3.4797
Tl_2O	0.3844	0.3696	0.3492	0.3398	0.3232	0.3202	0.3143	0.2997	0.3144	0.3278
$^{232}UO_3$	7.98E-08	5.93E-08	4.87E-08	4.05E-08	3.35E-08	2.80E-08	2.48E-08	2.15E-08	2.03E-08	1.89E-08
$^{233}UO_3$	8.09E-04	6.05E-04	4.99E-04	4.17E-04	3.49E-04	2.96E-04	2.65E-04	2.33E-04	2.20E-04	2.07E-04
$^{234}UO_3$	1.33E-02	1.20E-02	1.11E-02	1.06E-02	9.74E-03	9.08E-03	8.65E-03	8.14E-03	7.96E-03	7.73E-03
$^{235}UO_3$	1.4818	1.3375	1.2419	1.178	1.0864	1.0124	0.964	0.9075	0.8872	0.8614
$^{236}UO_3$	0.092	0.0835	0.0777	0.0739	0.0683	0.0638	0.0609	0.0574	0.0562	0.0546
$^{238}UO_3$	189.3392	170.5583	158.1405	149.8253	137.9509	128.3772	122.1044	114.7956	112.1687	108.8445
UO_3	0.093	0.0843	0.0784	0.0745	0.0688	0.0641	0.061	0.0574	0.0561	0.0545
V_2O_5	2.6254	2.7618	2.8743	2.9378	3.0312	3.0746	3.1303	3.1963	3.2108	3.2319
WO_3	3.9741	2.9622	2.4367	2.0302	1.6887	1.4183	1.2605	1.093	1.0334	0.9661
Y_2O_3	5.6851	5.1517	4.7892	4.5503	4.1952	3.9103	3.7213	3.4993	3.4216	3.3221
ZnO	4.3357	4.1725	4.1063	4.043	3.9899	3.9182	3.8987	3.8796	3.8631	3.846
ZrO_2	2.481	2.5779	2.6649	2.7114	2.7842	2.8139	2.8585	2.912	2.9218	2.937
$^{93}ZrO_2$	2.4589	2.3518	2.301	2.2578	2.2133	2.1629	2.1437	2.1231	2.1107	2.0971

(a) According to the mass-balance equation given in Eq. (B.1), the chemical and radiochemical analyses of samples from the LAW CRV will yield concentrations of elements and radionuclides, not oxide and halogen components. However, the G2 run data were in terms of masses of oxide and halogen components, so it was easier to work with concentrations on that basis. Note that such concentrations are just $c_{ijlm}^{CRV} f_j$ in the notation of Eq. (B.1).

Table D.3. Nominal Chemical Composition and Radionuclide Concentrations (mg/L) of Components in the LAW CRV for Set 3 (AZ-102) from the Selected G2 Runs

Component[(a)]	G2 Event Number									
	90(a)	90(b)	91(a)	91(b)	92(a)	92(b)	93(a)	93(b)	94(a)	94(b)
$^{227}Ac_2O_3$	0.00E+00	0.00E+00	0.00E+00	0.00E+00	0.00E+00	0.00E+00	0.00E+00	0.00E+00	0.00E+00	0.00E+00
Ag_2O	6.0483	6.0341	6.0217	6.0188	5.9996	6.0024	5.9853	5.9481	5.9106	5.9001
Al_2O_3	19480.183	19532.824	19554.414	19653.791	19566.326	19664.381	19567.887	19610.085	19576.664	19862.37
$^{241}Am_2O_3$	0.0497	0.0494	0.0492	0.0491	0.0487	0.0488	0.0485	0.0486	0.0486	0.0496
$^{243}Am_2O_3$	1.83E-04	1.82E-04	1.81E-04	1.80E-04	1.79E-04	1.79E-04	1.78E-04	1.78E-04	1.78E-04	1.82E-04
As_2O_5	9.7555	9.7322	9.7049	9.7136	9.6525	9.6784	9.6243	9.5835	9.5225	9.4955
B_2O_3	52.7838	52.5503	52.2712	52.1955	51.7981	51.7697	51.4056	51.0408	50.6214	50.3319
BaO	0.0767	0.0764	0.0759	0.0758	0.0752	0.0751	0.0746	0.0741	0.0735	0.0731
BeO	0.4272	0.4261	0.4248	0.4251	0.4224	0.4234	0.421	0.4189	0.4161	0.4144
Bi_2O_3	8.6574	8.6505	8.637	8.6572	8.6069	8.6417	8.5962	8.5986	8.5725	8.6438
P_2O_5	841.7535	837.8702	833.0828	831.855	825.0379	826.3101	820.8603	826.3569	828.2946	851.5123
Cl	152.9064	152.2215	152.0493	150.5231	152.1815	154.2914	157.6431	180.8565	199.901	264.2899
CaO	88.3975	88.9092	89.2174	89.8913	89.6111	90.0229	89.5681	89.2361	88.6709	88.8512
CdO	2.1709	2.1601	2.1482	2.1413	2.1291	2.1224	2.111	2.0916	2.0738	2.0632
Ce_2O_3	380.9154	399.5957	420.2499	440.4141	449.7276	473.731	482.1577	496.0881	502.8097	512.9425
$^{242}Cm_2O_3$	2.06E-07	2.05E-07	2.04E-07	2.03E-07	2.02E-07	2.02E-07	2.00E-07	1.99E-07	1.97E-07	1.96E-07
$^{244}Cm_2O_3$	2.28E-05	2.26E-05	2.26E-05	2.26E-05	2.24E-05	2.24E-05	2.22E-05	2.19E-05	2.19E-05	2.18E-05
^{60}CoO	1.80E-05	1.79E-05	1.78E-05	1.78E-05	1.77E-05	1.77E-05	1.75E-05	1.74E-05	1.73E-05	1.73E-05
Cr_2O_3	927.6382	924.2071	919.9017	919.1676	912.502	913.0973	907.1862	905.4284	901.6103	907.9179
Cs_2O	1.00E-03	9.95E-04	9.93E-04	9.93E-04	9.89E-04	9.87E-04	9.83E-04	9.76E-04	9.68E-04	1.03E-03
$^{134}Cs_2O$	4.47E-09	4.45E-09	4.45E-09	4.45E-09	4.42E-09	4.40E-09	4.38E-09	4.36E-09	4.32E-09	4.57E-09
$^{137}Cs_2O$	5.26E-04	5.24E-04	5.22E-04	5.22E-04	5.18E-04	5.16E-04	5.14E-04	5.07E-04	5.03E-04	5.33E-04
$^{152}Eu_2O_3$	1.15E-04	1.14E-04	1.13E-04	1.13E-04	1.12E-04	1.12E-04	1.12E-04	1.11E-04	1.10E-04	1.10E-04
$^{154}Eu_2O_3$	1.40E-04	1.40E-04	1.39E-04	1.39E-04	1.38E-04	1.38E-04	1.37E-04	1.37E-04	1.36E-04	1.37E-04
$^{155}Eu_2O_3$	6.90E-05	6.87E-05	6.83E-05	6.83E-05	6.76E-05	6.76E-05	6.71E-05	6.71E-05	6.67E-05	6.69E-05
F	1955.391	1948.1114	1947.2582	1930.2041	1950.5348	1930.5878	1949.8324	1939.9657	1944.7985	2006.6353
Fe_2O_3	26.3413	26.2087	26.0466	25.9964	25.7747	25.7798	25.5917	25.6113	25.5547	25.9131
^{129}I	2.2137	2.2177	2.277	2.1812	2.4187	2.2691	2.4825	2.3412	2.3507	2.473
K_2O	4859.9598	4838.968	4814.2271	4807.0626	4772.3385	4781.2973	4754.9545	4794.7222	4813.6476	4969.8372
Li_2O	0.8481	0.8404	0.8316	0.8269	0.818	0.8137	0.8057	0.7974	0.7892	0.7827
^{113m}CdO	1.21E-04	1.21E-04	1.20E-04	1.20E-04	1.19E-04	1.19E-04	1.18E-04	1.19E-04	1.18E-04	1.20E-04
MgO	53.5375	53.3041	53.0191	52.9576	52.5312	52.5273	52.1386	51.7986	51.3827	51.1079
MnO	3.6218	3.6134	3.6039	3.6067	3.5858	3.6002	3.5843	3.6031	3.6076	3.6841
$^{93m}Nb_2O_5$	5.68E-05	5.66E-05	5.63E-05	5.60E-05	5.57E-05	5.57E-05	5.54E-05	5.54E-05	5.51E-05	5.57E-05
MoO_6	159.104	158.3918	157.6092	157.2279	156.3286	156.0105	155.1765	153.9117	152.6811	152.0146
Na_2O	157342.72	157256.61	157220.02	157095.71	157148.7	156961.72	156984.01	156663.06	156451.14	159051.35
Nd_2O_3	36.5141	36.3532	36.1617	36.1078	35.8377	35.8168	35.5697	35.3231	35.0397	34.8615
NiO	7.7263	7.7001	7.6691	7.6692	7.6143	7.6516	7.6141	7.7281	7.7932	8.1396
^{59}NiO	0.0014	0.0014	0.0014	0.0014	0.0013	0.0014	0.0014	0.0015	0.0015	0.0018
^{63}NiO	1.85E-04	1.83E-04	1.81E-04	1.80E-04	1.78E-04	1.80E-04	1.79E-04	1.91E-04	1.99E-04	2.31E-04
$^{237}NpO_2$	0.0927	0.0922	0.0917	0.0915	0.0907	0.092	0.092	0.0997	0.1055	0.1256
$^{231}Pa_2O_5$	2.91E-08	2.72E-08	2.51E-08	2.32E-08	2.19E-08	9.28E-08	1.25E-07	5.72E-07	9.19E-07	2.02E-06

(a) According to the mass-balance equation given in Eq. (B.1), the chemical and radiochemical analyses of samples from the LAW CRV will yield concentrations of elements and radionuclides, not oxide and halogen components. However, the G2 run data were in terms of masses of oxide and halogen components, so it was easier to work with concentrations on that basis. Note that such concentrations are just $c_{ijlm}^{CRV} f_j$ in the notation of Eq. (B.1).

Table D.3. Nominal Chemical Composition and Radionuclide Concentrations (mg/L) of Components in the LAW CRV for Set 3 (AZ-102) from the Selected G2 Runs (cont'd)

Component[(a)]	G2 Event Number									
	90(a)	90(b)	91(a)	91(b)	92(a)	92(b)	93(a)	93(b)	94(a)	94(b)
PbO	7.7325	7.7074	7.6793	7.6774	7.6299	7.68	7.6564	7.8674	8.0109	8.6077
PdO	0.0012	0.0011	0.001	0.0009	0.0009	0.0014	0.0017	0.0054	0.0084	0.0178
Pr_2O_3	0.0608	0.0605	0.0602	0.0601	0.0597	0.0596	0.0592	0.0588	0.0583	0.058
$^{238}PuO_2$	6.55E-05	6.53E-05	6.48E-05	6.48E-05	6.41E-05	6.41E-05	6.37E-05	6.32E-05	6.28E-05	6.25E-05
$^{239}PuO_2$	0.164	0.1632	0.1623	0.1621	0.1608	0.1608	0.1596	0.1586	0.1574	0.1568
$^{240}PuO_2$	1.36E-02	1.35E-02	1.34E-02	1.34E-02	1.33E-02	1.33E-02	1.32E-02	1.31E-02	1.30E-02	1.30E-02
$^{241}PuO_2$	6.65E-04	6.61E-04	6.58E-04	6.56E-04	6.52E-04	6.52E-04	6.47E-04	6.43E-04	6.38E-04	6.34E-04
$^{242}PuO_2$	1.22E-04	1.21E-04	1.21E-04	1.20E-04	1.19E-04	1.19E-04	1.18E-04	1.18E-04	1.17E-04	1.16E-04
^{226}RaO	3.59E-06	3.62E-06	3.74E-06	3.62E-06	4.00E-06	3.79E-06	4.15E-06	3.89E-06	3.91E-06	4.09E-06
^{228}RaO	5.52E-07	5.49E-07	5.62E-07	5.34E-07	5.94E-07	5.49E-07	6.05E-07	5.62E-07	5.62E-07	5.88E-07
Rb_2O	3.1861	3.1787	3.1702	3.1726	3.1541	3.1621	3.1458	3.1337	3.1154	3.1119
Rh_2O_3	2.1664	2.1611	2.1551	2.1565	2.1438	2.1496	2.1387	2.1343	2.1248	2.1321
RuO_2	0.4483	0.4288	0.4089	0.3842	0.3821	0.3509	0.3473	0.3231	0.3119	0.3062
Sb_2O_3	0.062	0.0618	0.0614	0.0613	0.0608	0.0608	0.0604	0.06	0.0595	0.0592
$^{125}Sb_2O_3$	3.48E-04	3.45E-04	3.45E-04	3.45E-04	3.41E-04	3.41E-04	3.38E-04	3.36E-04	3.33E-04	3.33E-04
SeO_2	54.2382	54.0527	54.5684	53.057	55.9661	53.6576	56.1969	53.766	53.4328	54.2808
$^{79}SeO_2$	0.1877	0.1873	0.1867	0.187	0.1857	0.1863	0.1853	0.1848	0.1839	0.184
SiO_2	325.0939	324.201	322.9364	323.0202	320.6854	321.186	319.0654	318.7113	317.4753	320.0049
$^{151}Sm_2O_3$	0.21	0.2091	0.2079	0.2077	0.206	0.2063	0.2049	0.2053	0.205	0.2083
SO_3	15318.729	15278.482	15330.537	15127.471	15485.254	15183.407	15494.864	15155.462	15086.288	15277.461
SrO	3.6729	3.6602	3.6452	3.645	3.6187	3.6259	3.6032	3.5941	3.576	3.5849
^{90}SrO	0.1794	0.179	0.1785	0.1787	0.1775	0.1781	0.177	0.1763	0.1752	0.1748
Ta_2O_5	0.0636	0.0633	0.0629	0.0628	0.0624	0.0623	0.0619	0.0614	0.0609	0.0606
$^{99}Tc_2O_7$	43.5939	43.4355	43.682	42.7723	44.3879	43.0238	44.4379	42.9769	42.7273	43.2916
TeO_2	0.0768	0.0763	0.0758	0.0751	0.0752	0.0743	0.0744	0.0731	0.0724	0.0722
$^{229}ThO_2$	2.91E-10	2.71E-10	2.46E-10	2.30E-10	2.14E-10	2.62E-08	3.80E-08	1.98E-07	3.21E-07	7.15E-07
$^{232}ThO_2$	12.297	12.15	11.9698	11.8519	11.6909	11.6134	11.4881	11.6889	11.8264	12.6234
TiO_2	5.0743	5.0267	4.9684	4.9342	4.8768	4.8385	4.7843	4.7244	4.6684	4.6219
Tl_2O	0.13	0.129	0.1295	0.1251	0.1318	0.1253	0.131	0.1244	0.1232	0.1246
$^{232}UO_3$	1.68E-11	1.68E-11	1.12E-11	1.12E-11	1.12E-11	2.13E-10	3.01E-10	1.53E-09	2.48E-09	5.50E-09
$^{233}UO_3$	3.42E-05	3.40E-05	3.37E-05	3.37E-05	3.35E-05	3.61E-05	3.73E-05	5.42E-05	6.75E-05	1.10E-04
$^{234}UO_3$	3.92E-04	3.90E-04	3.85E-04	3.83E-04	3.80E-04	3.83E-04	3.83E-04	4.16E-04	4.41E-04	5.32E-04
$^{235}UO_3$	0.0443	0.044	0.0435	0.0433	0.0429	0.0431	0.0429	0.0455	0.0473	0.0542
$^{236}UO_3$	0.004	0.004	0.0039	0.0039	0.0039	0.0039	0.0039	0.0042	0.0044	0.0051
$^{238}UO_3$	5.0582	5.0118	4.9572	4.9273	4.8725	4.9203	4.9055	5.3289	5.6461	6.7779
UO_3	0.0011	0.0011	0.0011	0.0011	0.0011	0.0011	0.0011	0.0011	0.001	0.001
V_2O_5	4.2606	4.2099	4.1482	4.1064	4.0531	4.0032	3.9522	3.8883	3.8339	3.7859
WO_3	0.0012	0.0012	0.0011	0.001	0.001	0.0009	0.0009	0.0008	0.0008	0.0008
Y_2O_3	0.0112	0.0105	0.0097	0.009	0.0085	0.0077	0.0072	0.0066	0.0062	0.0058
ZnO	3.7918	3.7463	3.6906	3.6541	3.6042	3.5611	3.5136	3.458	3.4094	3.3658
ZrO_2	4.1697	4.1599	4.148	4.1525	4.125	4.1432	4.1215	4.1412	4.1431	4.22
$^{93}ZrO_2$	2.1147	2.1096	2.1034	2.1056	2.0916	2.1038	2.0942	2.1237	2.1397	2.2268

(a) According to the mass-balance equation given in Eq. (B.1), the chemical and radiochemical analyses of samples from the LAW CRV will yield concentrations of elements and radionuclides, not oxide and halogen components. However, the G2 run data were in terms of masses of oxide and halogen components, so it was easier to work with concentrations on that basis. Note that such concentrations are just $c_{ijlm}^{CRV} f_j$ in the notation of Eq. (B.1).

Table D.4. Nominal Chemical Composition and Radionuclide Concentrations (mg/L) of Components in the LAW CRV for Set 4 (AN-102) from the Selected G2 Runs

Component[(a)]	G2 Event Number									
	225(a)	225(b)	226(a)	226(b)	227(a)	227(b)	228(a)	228(b)	229(a)	229(b)
$^{227}Ac_2O_3$	5.52E-11	5.52E-11	5.52E-11	5.52E-11	5.52E-11	5.52E-11	5.52E-11	5.52E-11	5.52E-11	5.52E-11
Ag_2O	7.1996	7.2691	7.2705	7.2872	7.2681	7.3395	7.3354	7.3837	7.3774	7.3881
Al_2O_3	48285.307	48090.799	47951.791	48017.849	47994.089	47563.207	47522.735	47507.729	47449.731	47615.139
$^{241}Am_2O_3$	0.0635	0.0643	0.0641	0.0643	0.0647	0.0659	0.0659	0.0659	0.0658	0.0641
$^{243}Am_2O_3$	6.72E-05	6.78E-05	6.76E-05	6.78E-05	6.80E-05	6.91E-05	6.91E-05	6.91E-05	6.89E-05	6.74E-05
As_2O_5	35.1453	35.558	35.5148	35.639	35.5816	35.889	35.8877	36.1847	36.0883	36.1554
B_2O_3	100.383	101.548	101.4285	101.7733	101.6026	102.48	102.4723	103.3129	103.0441	103.2376
BaO	13.2854	13.4417	13.4248	13.4718	13.4502	13.5656	13.5655	13.6792	13.6422	13.6692
BeO	3.3945	3.4338	3.43	3.4416	3.4357	3.4657	3.4654	3.4936	3.4849	3.4913
Bi_2O_3	104.6568	103.2912	103.8854	106.7438	107.9543	104.9501	105.4795	104.4852	105.3265	106.7437
P_2O_5	6079.1646	6110.1002	6102.712	6147.1711	6175.6856	6200.193	6212.2287	6212.9949	6213.6139	6152.9243
Cl	4577.946	4589.0945	4627.1011	4623.5125	4592.6108	4673.0315	4661.4637	4654.9553	4694.5196	4690.3405
CaO	60.7741	61.0146	60.8932	61.048	60.9807	60.9305	60.866	61.0645	60.9121	61.0535
CdO	2.1256	2.118	2.1081	2.0865	2.0748	2.0819	2.0765	2.0838	2.0791	2.0774
Ce_2O_3	133.36	150.8075	165.972	181.9289	181.4859	174.8926	181.7449	186.4211	198.5967	204.2633
$^{242}Cm_2O_3$	7.03E-10	7.07E-10	7.07E-10	7.11E-10	7.11E-10	7.18E-10	7.18E-10	7.29E-10	7.29E-10	7.29E-10
$^{244}Cm_2O_3$	6.12E-07	6.17E-07	6.14E-07	6.14E-07	6.17E-07	6.21E-07	6.21E-07	6.25E-07	6.23E-07	6.19E-07
^{60}CoO	1.69E-06	1.70E-06	1.70E-06	1.70E-06	1.69E-06	1.71E-06	1.71E-06	1.72E-06	1.71E-06	1.72E-06
Cr_2O_3	903.5268	906.0251	903.2757	902.603	901.2636	901.8021	900.1892	901.6928	899.0301	896.6878
Cs_2O	1.05E-03	1.06E-03	1.06E-03	1.06E-03	1.06E-03	1.08E-03	1.08E-03	1.08E-03	1.08E-03	1.08E-03
$^{134}Cs_2O$	2.84E-12	2.84E-12	2.84E-12	2.84E-12	2.84E-12	2.84E-12	2.84E-12	2.84E-12	2.84E-12	2.84E-12
$^{137}Cs_2O$	3.53E-04	3.55E-04	3.55E-04	3.55E-04	3.57E-04	3.62E-04	3.62E-04	3.64E-04	3.64E-04	3.62E-04
$^{152}Eu_2O_3$	5.23E-05	5.30E-05	5.30E-05	5.32E-05	5.37E-05	5.46E-05	5.46E-05	5.46E-05	5.46E-05	5.32E-05
$^{154}Eu_2O_3$	5.13E-04	5.20E-04	5.20E-04	5.22E-04	5.24E-04	5.33E-04	5.33E-04	5.33E-04	5.33E-04	5.22E-04
$^{155}Eu_2O_3$	9.87E-05	0.0001001	9.99E-05	0.0001003	0.000101	0.0001026	0.0001029	0.0001029	0.0001026	0.0001006
F	6781.7617	6771.6616	6816.549	6786.6445	6743.5342	6853.9376	6836.1656	6812.7787	6870.0307	6830.3413
Fe_2O_3	24.238	24.0233	23.8638	23.5755	23.4642	23.4074	23.3446	23.4174	23.3246	23.3382
^{129}I	2.5282	2.4145	2.5684	2.5137	2.4256	2.5677	2.5294	2.4015	2.57	2.5419
K_2O	4652.4346	4705.4714	4700.5917	4715.9815	4707.6838	4748.7817	4747.8636	4785.22	4773.3967	4780.861
Li_2O	14.1627	14.3323	14.3126	14.365	14.348	14.4757	14.4767	14.5932	14.5529	14.5629
^{113m}CdO	5.34E-05	5.40E-05	5.38E-05	5.40E-05	5.38E-05	5.43E-05	5.43E-05	5.47E-05	5.45E-05	5.47E-05
MgO	41.8861	42.3796	42.3186	42.465	42.4006	42.7589	42.7595	43.1202	42.9966	43.0762
MnO	6.144	6.2098	6.2025	6.2195	6.2078	6.2609	6.26	6.3101	6.2948	6.3068
$^{93m}Nb_2O_5$	2.33E-05	2.33E-05	2.32E-05	2.30E-05	2.29E-05	2.30E-05	2.29E-05	2.31E-05	2.30E-05	2.29E-05
MoO_6	78.2848	79.1225	79.1094	79.3478	79.1711	79.927	79.901	80.4812	80.3659	80.5035
Na_2O	247017.33	246764.68	246760.96	247067.2	247001.5	246829.55	246789.27	246689.21	246827.61	246952.38
Nd_2O_3	27.1737	27.4842	27.4527	27.5427	27.4958	27.7348	27.7323	27.9569	27.8869	27.9354
NiO	32.068	32.2506	32.1368	32.0682	31.9818	32.1779	32.1502	32.3703	32.2662	32.2755
^{59}NiO	0.0041	0.0041	0.0041	0.004	0.004	0.004	0.004	0.004	0.004	0.004
^{63}NiO	5.44E-04	5.41E-04	5.36E-04	5.31E-04	5.29E-04	5.29E-04	5.29E-04	5.29E-04	5.26E-04	5.24E-04
$^{237}NpO_2$	0.9974	1.0092	1.0078	1.0114	1.0099	1.0186	1.0186	1.0271	1.0242	1.0258
$^{231}Pa_2O_5$	3.23E-05	3.16E-05	3.14E-05	3.05E-05	3.02E-05	3.00E-05	3.00E-05	3.00E-05	2.98E-05	2.95E-05

(a) According to the mass-balance equation given in Eq. (B.1), the chemical and radiochemical analyses of samples from the LAW CRV will yield concentrations of elements and radionuclides, not oxide and halogen components. However, the G2 run data were in terms of masses of oxide and halogen components, so it was easier to work with concentrations on that basis. Note that such concentrations are just $c_{ijlm}^{CRV} f_j$ in the notation of Eq. (B.1).

Table D.4. Nominal Chemical Composition and Radionuclide Concentrations (mg/L) of Components in the LAW CRV for Set 4 (AN-102) from the Selected G2 Runs (cont'd)

Component[(a)]	G2 Event Number									
	225(a)	225(b)	226(a)	226(b)	227(a)	227(b)	228(a)	228(b)	229(a)	229(b)
PbO	81.4199	82.1165	81.9159	81.9849	82.0658	83.0048	83.0095	83.2675	83.1058	82.1659
PdO	0.009	0.0092	0.0091	0.0092	0.0093	0.0094	0.0094	0.0094	0.0094	0.0092
Pr_2O_3	0.0099	0.01	0.01	0.01	0.01	0.0101	0.0101	0.0102	0.0102	0.0102
$^{238}PuO_2$	1.79E-05	1.79E-05	1.78E-05	1.77E-05	1.76E-05	1.77E-05	1.77E-05	1.77E-05	1.77E-05	1.75E-05
$^{239}PuO_2$	0.0916	0.0927	0.0925	0.0928	0.0931	0.0943	0.0944	0.0947	0.0945	0.0932
$^{240}PuO_2$	5.01E-03	5.06E-03	5.05E-03	5.07E-03	5.07E-03	5.13E-03	5.14E-03	5.16E-03	5.15E-03	5.09E-03
$^{241}PuO_2$	6.29E-05	6.36E-05	6.34E-05	6.34E-05	6.34E-05	6.40E-05	6.43E-05	6.45E-05	6.43E-05	6.36E-05
$^{242}PuO_2$	3.10E-05	3.12E-05	3.12E-05	3.12E-05	3.12E-05	3.17E-05	3.17E-05	3.17E-05	3.17E-05	3.14E-05
^{226}RaO	1.62E-06	1.52E-06	1.71E-06	1.68E-06	1.58E-06	1.63E-06	1.65E-06	1.57E-06	1.81E-06	1.83E-06
^{228}RaO	3.96E-06	3.66E-06	4.08E-06	3.93E-06	3.68E-06	3.76E-06	3.72E-06	3.42E-06	3.85E-06	3.83E-06
Rb_2O	0.0112	0.0111	0.011	0.0109	0.0109	0.0109	0.0109	0.0108	0.0107	0.0104
Rh_2O_3	0.0658	0.0663	0.0661	0.0662	0.0663	0.0672	0.0672	0.0673	0.0672	0.066
RuO_2	0.6851	0.6887	0.6961	0.6983	0.6983	0.7189	0.7184	0.7115	0.7208	0.7038
Sb_2O_3	15.8398	16.0287	16.0076	16.0654	16.0402	16.1765	16.1763	16.313	16.2672	16.2997
$^{125}Sb_2O_3$	1.35E-06	1.36E-06	1.36E-06	1.37E-06	1.36E-06	1.38E-06	1.37E-06	1.39E-06	1.38E-06	1.38E-06
SeO_2	39.5456	38.801	40.0083	39.6007	38.8496	40.2894	39.9498	39.0298	40.3722	40.1592
$^{79}SeO_2$	0.41	0.4118	0.4096	0.4083	0.4099	0.4152	0.4152	0.4144	0.4134	0.4028
SiO_2	1046.2877	1036.5961	1035.5103	1043.4574	1048.5948	1034.02	1034.6814	1027.6974	1029.2637	1027.5905
$^{151}Sm_2O_3$	0.1152	0.1166	0.1164	0.1168	0.1166	0.1176	0.1176	0.1186	0.1183	0.1184
SO_3	5144.8727	5168.51	5168.7792	5178.0403	5173.0981	5209.8066	5209.3925	5222.6504	5226.7116	5209.7008
SrO	7.2879	7.337	7.3153	7.3085	7.2941	7.3454	7.3407	7.3888	7.3658	7.3581
^{90}SrO	0.0375	0.0369	0.0365	0.0356	0.0354	0.0354	0.0352	0.0352	0.035	0.0346
Ta_2O_5	0.0021	0.0022	0.0022	0.0022	0.0022	0.0022	0.0022	0.0022	0.0022	0.0022
$^{99}Tc_2O_7$	17.6647	17.4843	17.8692	17.7548	17.5048	18.0283	17.9214	17.6611	18.0883	18.0222
TeO_2	0.017	0.0172	0.0173	0.0174	0.0174	0.0178	0.0179	0.0178	0.0179	0.0174
$^{229}ThO_2$	8.22E-06	8.31E-06	8.29E-06	8.33E-06	8.31E-06	8.38E-06	8.38E-06	8.45E-06	8.42E-06	8.42E-06
$^{232}ThO_2$	68.1076	68.8268	68.6987	68.8579	68.7312	69.2703	69.2533	69.8132	69.6035	69.7199
TiO_2	3.8871	3.9326	3.927	3.9404	3.9344	3.9678	3.9678	4.001	3.9897	3.9969
Tl_2O	18.398	18.0869	18.6537	18.4955	18.1556	18.8414	18.6915	18.2786	18.9091	18.8227
$^{232}UO_3$	1.41E-06	1.42E-06	1.42E-06	1.43E-06	1.42E-06	1.43E-06	1.43E-06	1.44E-06	1.44E-06	1.44E-06
$^{233}UO_3$	1.51E-02	1.52E-02	1.52E-02	1.52E-02	1.51E-02	1.52E-02	1.52E-02	1.53E-02	1.53E-02	1.53E-02
$^{234}UO_3$	2.87E-02	2.90E-02	2.90E-02	2.91E-02	2.92E-02	2.97E-02	2.97E-02	2.98E-02	2.97E-02	2.93E-02
$^{235}UO_3$	2.8809	2.9178	2.9128	2.9261	2.9345	2.9742	2.977	2.9878	2.9816	2.9419
$^{236}UO_3$	0.1432	0.1451	0.1448	0.1455	0.1459	0.1479	0.148	0.1486	0.1483	0.1463
$^{238}UO_3$	443.9561	449.7777	448.9966	451.2153	452.9674	459.6154	460.1585	461.347	460.4874	452.8407
UO_3	0.7463	0.7371	0.7294	0.7148	0.7106	0.7026	0.6965	0.6892	0.6835	0.6715
V_2O_5	20.2389	20.4734	20.4509	20.5208	20.4858	20.6646	20.6632	20.8324	20.7803	20.8198
WO_3	0.2907	0.2939	0.2935	0.2943	0.2936	0.2956	0.2952	0.2971	0.296	0.2962
Y_2O_3	0.2033	0.206	0.2057	0.2068	0.2075	0.2105	0.2107	0.2113	0.211	0.2078
ZnO	4.0136	4.0533	4.0446	4.0515	4.0438	4.0746	4.0733	4.1054	4.0928	4.0982
ZrO_2	82.916	83.8637	83.7318	83.9932	83.8551	84.5446	84.5383	85.2459	84.9963	85.1585
$^{93}ZrO_2$	1.6749	1.6838	1.6774	1.673	1.6681	1.6774	1.6755	1.6867	1.6808	1.6813

(a) According to the mass-balance equation given in Eq. (B.1), the chemical and radiochemical analyses of samples from the LAW CRV will yield concentrations of elements and radionuclides, not oxide and halogen components. However, the G2 run data was in terms of masses of oxide and halogen components, so it was easier to work with concentrations on that basis. Note that such concentrations are just $c_{ijlm}^{CRV} f_j$ in the notation of Eq. (B.1).

Table D.5. Nominal Chemical Composition and Radionuclide Concentrations (mg/L) of Components in the LAW CRV for Set 5 (unknown tank) from the Selected G2 Runs

Component[(a)]	G2 Event Number									
	255(a)	255(b)	256(a)	256(b)	257(a)	257(b)	258(a)	258(b)	259(a)	259(b)
$^{227}Ac_2O_3$	2.32E-09	2.30E-09	2.25E-09	2.23E-09	2.23E-09	2.23E-09	2.21E-09	2.19E-09	2.13E-09	2.09E-09
Ag_2O	2.8648	2.8481	2.7997	2.7858	2.7831	2.764	2.754	2.7154	2.6492	2.5992
Al_2O_3	42847.611	42647.368	43370.587	43692.265	43578.81	43979.598	44356.367	45392.062	46863.899	47411.769
$^{241}Am_2O_3$	0.0172	0.0166	0.0158	0.0152	0.0147	0.0143	0.0139	0.0135	0.0131	0.0129
$^{243}Am_2O_3$	2.30E-05	2.28E-05	2.20E-05	2.15E-05	2.12E-05	2.08E-05	2.05E-05	2.02E-05	1.96E-05	1.95E-05
As_2O_5	15.8599	15.76	15.4728	15.4121	15.4124	15.2887	15.2412	15.0341	14.6416	14.3736
B_2O_3	32.6835	32.4888	31.9083	31.7867	31.7964	31.5486	31.4537	31.0318	30.2322	29.6934
BaO	4.9924	4.9614	4.8713	4.8527	4.8535	4.8146	4.8	4.7351	4.6115	4.5277
BeO	1.2662	1.2586	1.236	1.2312	1.2314	1.2218	1.2181	1.2016	1.1707	1.1496
Bi_2O_3	20.7315	20.1083	19.24	18.7226	18.2326	17.8358	17.5316	17.1611	16.6576	16.2988
P_2O_5	5315.8602	5303.4536	5269.2539	5258.0801	5266.1517	5257.3539	5257.4933	5254.9963	5235.2471	5243.8192
Cl	3833.9737	3839.3746	3817.5979	3793.5098	3795.8656	3804.7058	3792.0938	3743.7588	3697.2591	3641.0553
CaO	134.7271	135.6926	136.4975	137.4405	139.0407	139.7799	140.7278	141.6626	142.0703	143.104
CdO	2.508	2.5277	2.5176	2.5244	2.5573	2.5592	2.5642	2.5472	2.5085	2.5053
Ce_2O_3	264.0239	263.591	265.1555	256.637	237.6716	231.188	216.8456	212.3977	217.3846	214.7459
$^{242}Cm_2O_3$	1.98E-09	1.96E-09	1.92E-09	1.92E-09	1.91E-09	1.90E-09	1.89E-09	1.87E-09	1.82E-09	1.78E-09
$^{244}Cm_2O_3$	9.43E-07	9.50E-07	9.43E-07	9.46E-07	9.59E-07	9.59E-07	9.59E-07	9.52E-07	9.37E-07	9.39E-07
^{60}CoO	7.06E-07	7.06E-07	6.96E-07	6.93E-07	6.98E-07	6.93E-07	6.93E-07	6.86E-07	6.71E-07	6.63E-07
Cr_2O_3	1507.2774	1506.0913	1524.3444	1534.0703	1538.8961	1552.6109	1565.0191	1593.8974	1632.5536	1654.8691
Cs_2O	9.42E-04	9.42E-04	9.38E-04	9.38E-04	9.40E-04	9.34E-04	9.30E-04	9.17E-04	9.00E-04	8.96E-04
$^{134}Cs_2O$	1.98E-11	1.98E-11	1.98E-11	1.98E-11	1.98E-11	1.98E-11	1.98E-11	1.98E-11	1.98E-11	1.98E-11
$^{137}Cs_2O$	3.57E-04	3.57E-04	3.55E-04	3.55E-04	3.57E-04	3.55E-04	3.53E-04	3.49E-04	3.43E-04	3.40E-04
$^{152}Eu_2O_3$	6.82E-06	6.31E-06	5.64E-06	5.13E-06	4.60E-06	4.26E-06	3.96E-06	3.68E-06	3.42E-06	3.24E-06
$^{154}Eu_2O_3$	9.90E-05	9.51E-05	8.91E-05	8.52E-05	8.13E-05	7.85E-05	7.60E-05	7.34E-05	7.07E-05	6.88E-05
$^{155}Eu_2O_3$	1.97E-05	1.88E-05	1.76E-05	1.68E-05	1.60E-05	1.54E-05	1.49E-05	1.43E-05	1.37E-05	1.34E-05
F	1144.9713	1138.0119	1121.3693	1101.5617	1087.4604	1083.2307	1070.1759	1052.0276	1039.4855	1024.8503
Fe_2O_3	86.3424	85.7265	89.2319	90.2377	89.1443	90.9657	92.6539	97.644	104.7094	107.564
^{129}I	1.0391	1.0491	1.0803	1.0442	1.0146	1.0519	1.0336	1.0077	1.0447	1.0031
K_2O	2500.9472	2498.5671	2466.0633	2462.7007	2475.2315	2463.3008	2460.4629	2433.8424	2380.2742	2353.4302
Li_2O	4.2321	4.2046	4.1255	4.1066	4.1056	4.0715	4.0575	4.0026	3.8991	3.8326
^{113m}CdO	4.10E-05	4.13E-05	4.08E-05	4.10E-05	4.13E-05	4.13E-05	4.13E-05	4.10E-05	4.01E-05	3.99E-05
MgO	15.1073	15.0091	14.7308	14.6728	14.6722	14.551	14.5053	14.308	13.9308	13.6756
MnO	3.5785	3.5939	3.5654	3.5707	3.6071	3.6004	3.6035	3.5742	3.5085	3.4918
$^{93m}Nb_2O_5$	7.66E-05	7.74E-05	7.68E-05	7.74E-05	7.83E-05	7.86E-05	7.86E-05	7.83E-05	7.68E-05	7.68E-05
MoO_6	25.9867	25.844	25.4055	25.2938	25.2913	25.116	25.0342	24.695	24.0887	23.6587
Na_2O	233757.99	233528.41	232914.66	232528.69	232280.39	232053.39	231794.96	231356.11	230749.48	230359
Nd_2O_3	10.9779	10.9131	10.7187	10.6774	10.6807	10.5983	10.5664	10.4248	10.1572	9.9768
NiO	8.6949	8.7313	8.6576	8.6675	8.7562	8.737	8.7434	8.6736	8.514	8.4828
^{59}NiO	0.0028	0.0028	0.0027	0.0027	0.0027	0.0027	0.0027	0.0027	0.0027	0.0026
^{63}NiO	3.51E-04	3.51E-04	3.48E-04	3.48E-04	3.48E-04	3.48E-04	3.48E-04	3.46E-04	3.38E-04	3.36E-04
$^{237}NpO_2$	0.1355	0.1364	0.1355	0.1358	0.1374	0.1373	0.1375	0.1365	0.1342	0.1341
$^{231}Pa_2O_5$	2.44E-05	2.44E-05	2.41E-05	2.41E-05	2.44E-05	2.44E-05	2.44E-05	2.41E-05	2.37E-05	2.37E-05

(a) According to the mass-balance equation given in Eq. (B.1), the chemical and radiochemical analyses of samples from the LAW CRV will yield concentrations of elements and radionuclides, not oxide and halogen components. However, the G2 run data were in terms of masses of oxide and halogen components, so it was easier to work with concentrations on that basis. Note that such concentrations are just $c_{ijlm}^{CRV} f_j$ in the notation of Eq. (B.1).

Table D.5. Nominal Chemical Composition and Radionuclide Concentrations (mg/L) of Components in the LAW CRV for Set 5 (unknown tank) from the Selected G2 Runs (cont'd)

Component[(a)]	G2 Event Number									
	255(a)	255(b)	256(a)	256(b)	257(a)	257(b)	258(a)	258(b)	259(a)	259(b)
PbO	36.1333	35.9162	35.2021	34.8917	34.8417	34.5519	34.3629	33.9189	33.1762	32.8952
PdO	0.0153	0.0153	0.0152	0.0151	0.0153	0.0152	0.0152	0.0151	0.0148	0.0149
Pr_2O_3	0.0003	0.0003	0.0003	0.0002	0.0002	0.0002	0.0002	0.0002	0.0002	0.0002
$^{238}PuO_2$	3.31E-06	3.29E-06	3.22E-06	3.20E-06	3.17E-06	3.15E-06	3.13E-06	3.08E-06	3.01E-06	3.01E-06
$^{239}PuO_2$	0.0158	0.0154	0.0147	0.0143	0.0139	0.0135	0.0133	0.0129	0.0126	0.0124
$^{240}PuO_2$	7.77E-04	7.58E-04	7.27E-04	7.06E-04	6.93E-04	6.77E-04	6.66E-04	6.52E-04	6.32E-04	6.25E-04
$^{241}PuO_2$	1.17E-05	1.15E-05	1.11E-05	1.08E-05	1.07E-05	1.05E-05	1.03E-05	1.01E-05	9.89E-06	9.78E-06
$^{242}PuO_2$	4.18E-06	4.12E-06	3.98E-06	3.89E-06	3.85E-06	3.78E-06	3.73E-06	3.66E-06	3.57E-06	3.55E-06
^{226}RaO	2.85E-06	2.87E-06	2.99E-06	2.85E-06	2.63E-06	2.70E-06	2.57E-06	2.48E-06	2.67E-06	2.57E-06
^{228}RaO	1.14E-06	1.14E-06	1.16E-06	1.07E-06	9.60E-07	9.85E-07	9.19E-07	8.59E-07	9.09E-07	8.29E-07
Rb_2O	0.0174	0.0175	0.0174	0.0174	0.0176	0.0175	0.0175	0.0174	0.0171	0.0171
Rh_2O_3	0.0337	0.0336	0.0329	0.0326	0.0326	0.0324	0.0322	0.0318	0.0312	0.0311
RuO_2	0.0964	0.0893	0.0803	0.0712	0.0612	0.0567	0.051	0.0459	0.0428	0.0385
Sb_2O_3	6.6298	6.5911	6.4736	6.4508	6.4548	6.4044	6.3862	6.3015	6.1384	6.0302
$^{125}Sb_2O_3$	3.60E-06	3.62E-06	3.60E-06	3.62E-06	3.67E-06	3.67E-06	3.69E-06	3.67E-06	3.60E-06	3.62E-06
SeO_2	26.2243	26.3412	26.5882	26.0893	25.764	26.2123	25.9654	25.4804	25.6918	24.975
$^{79}SeO_2$	0.163	0.1602	0.1549	0.1518	0.1496	0.1472	0.1453	0.1427	0.1389	0.1373
SiO_2	2553.9852	2541.8894	2556.5237	2555.9873	2542.8414	2551.2976	2560.1543	2597.468	2648.9019	2675.3422
$^{151}Sm_2O_3$	0.0473	0.0473	0.0467	0.0466	0.0469	0.0467	0.0466	0.0462	0.0451	0.0447
SO_3	8619.9673	8667.7303	8644.7736	8633.6653	8702.9122	8732.7283	8734.0782	8662.9196	8573.2201	8517.6021
SrO	14.8369	14.9688	14.91	14.9657	15.1849	15.1899	15.2277	15.1399	14.9046	14.9246
^{90}SrO	3.4111	3.4475	3.4401	3.4567	3.5131	3.5176	3.5289	3.5114	3.4602	3.4705
Ta_2O_5	0.0003	0.0003	0.0002	0.0002	0.0002	0.0002	0.0002	0.0002	0.0002	0.0002
$^{99}Tc_2O_7$	10.784	10.8393	10.8971	10.7632	10.7154	10.8557	10.7949	10.6347	10.6502	10.4344
TeO_2	0.0019	0.0017	0.0015	0.0013	0.0011	0.0009	0.0008	0.0007	0.0006	0.0006
$^{229}ThO_2$	4.64E-06	4.62E-06	4.55E-06	4.55E-06	4.55E-06	4.53E-06	4.53E-06	4.46E-06	4.37E-06	4.30E-06
$^{232}ThO_2$	14.4855	14.5304	14.3949	14.4092	14.5434	14.503	14.5103	14.3858	14.1058	14.025
TiO_2	1.5298	1.5204	1.4928	1.4872	1.4876	1.4757	1.4713	1.4515	1.4137	1.3885
Tl_2O	23.1744	23.1164	23.156	22.5503	21.9958	22.2695	21.9251	21.3667	21.4303	20.5858
$^{232}UO_3$	8.15E-08	8.08E-08	7.93E-08	7.88E-08	7.88E-08	7.81E-08	7.79E-08	7.67E-08	7.47E-08	7.33E-08
$^{233}UO_3$	1.54E-03	1.54E-03	1.52E-03	1.52E-03	1.53E-03	1.52E-03	1.52E-03	1.50E-03	1.47E-03	1.46E-03
$^{234}UO_3$	4.01E-03	3.84E-03	3.59E-03	3.42E-03	3.26E-03	3.14E-03	3.03E-03	2.92E-03	2.81E-03	2.74E-03
$^{235}UO_3$	0.4526	0.4337	0.406	0.3865	0.3681	0.3546	0.3427	0.3309	0.3181	0.3103
$^{236}UO_3$	0.0171	0.0163	0.0152	0.0145	0.0138	0.0132	0.0128	0.0123	0.0118	0.0115
$^{238}UO_3$	59.5251	56.7069	52.6888	49.8225	47.0388	45.0682	43.3256	41.6452	39.8793	38.7518
UO_3	0.0607	0.0578	0.0562	0.0542	0.051	0.0503	0.0496	0.0508	0.0531	0.0536
V_2O_5	8.1513	8.1011	7.9549	7.9236	7.9242	7.862	7.8377	7.7316	7.5313	7.3941
WO_3	0.0029	0.0029	0.0028	0.0028	0.0028	0.0028	0.0027	0.0027	0.0026	0.0026
Y_2O_3	0.0103	0.0092	0.0078	0.0067	0.0055	0.0048	0.0041	0.0036	0.0031	0.0027
ZnO	2.6274	2.6107	2.5626	2.5527	2.553	2.5321	2.5242	2.4901	2.4247	2.3806
ZrO_2	12.4962	12.581	12.5076	12.5438	12.7048	12.6949	12.7185	12.6328	12.4179	12.4023
$^{93}ZrO_2$	1.8158	1.8241	1.8096	1.8128	1.8322	1.8285	1.8304	1.816	1.7823	1.7751

(a) According to the mass-balance equation given in Eq. (B.1), the chemical and radiochemical analyses of samples from the LAW CRV will yield concentrations of elements and radionuclides, not oxide and halogen components. However, the G2 run data was in terms of masses of oxide and halogen components, so it was easier to work with concentrations on that basis. Note that such concentrations are just $c_{ijlm}^{CRV} f_j$ in the notation of Eq. (B.1).

Table D.6. LAW Analyte and Radionuclide Concentration Boundaries for Determining CRV Analytical Uncertainties ($\%RSD_A(c_{ijlm}^{CRV})$)

Element / Radionuclide	Decision Point (mg/L)	CRV Analytical Uncertainty[a]	
		Hi %RSD	Low %RSD
^{227}Ac	2.23E-08	50	10
Ag	16.89157	20	5
Al	6.18E+04	5	5
^{241}Am	0.13485	10	10
^{243}Am	4.54E-04	15	15
As	53.72426	25	10
B	68.61189	25	10
Ba	26.33368	15	5
Be	3.33269	25	5
Bi	200.7145	15	10
PO_4	8.16E+04	15	10
Cl	1.10E+04	10	10
Ca	899.4333	15	5
Cd	59.00702	10	5
Ce	1090.696	25	10
^{242}Cm	3.61E-07	10	10
^{244}Cm	4.01E-05	15	15
^{60}Co	2.79E-05	5	5
CrTOTAL[b]	3489.229	5	5
Cs	0.056399	15	10
^{134}Cs	1.70E-08	25	10
^{137}Cs	0.001849	15	5
Cu	27.3338	25	10
^{152}Eu	1.91E-04	5	5
^{154}Eu	0.001074	5	5
^{155}Eu	1.84E-04	5	5
F	1.97E+04	10	10
Fe	614.8948	5	5
^{129}I	11.21935	15	10
K	7.90E+04	5	5
La	31.38793	10	5
Li	53.24516	15	5
^{113m}Cd	2.70E-04	25	10
Mg	66.72149	25	10
Mn	570.9798	15	5
^{93m}Nb	1.12E-04	15	10
^{6}MO	154.7449	10	5
Na	3.76E+05	10	10
Nd	89.48267	15	5
Ni	586.9718	10	5
^{59}Ni	0.092518	10	10
^{63}Ni	0.012898	10	10
^{237}Np	2.157695	10	5

Element/ Radionuclide	Decision Point (mg/L)	CRV Analytical Uncertainty[a]	
		Hi %RSD	Low %RSD
^{231}Pa	0.001908	50	50
Pb	173.6545	15	15
Pd	1.807387	15	15
Pr	0.638416	15	10
^{238}Pu	1.11E-04	5	5
^{239}Pu	0.284675	5	5
^{240}Pu	0.023092	10	10
^{241}Pu	0.00113	15	15
^{242}Pu	2.07E-04	10	10
^{226}Ra	1.74E-05	25	10
^{228}Ra	4.59E-05	50	25
Rb	14.96336	25	15
Rh	4.234247	20	5
Ru	85.53627	25	5
Sb	49.82821	25	10
^{125}Sb	5.63E-04	25	5
Se	337.1882	25	10
^{79}Se	1.342833	15	10
Si	7696.5	15	5
^{151}Sm	0.468296	20	10
^{4}SO	3.55E+04	10	5
Sr	1281.673	5	5
^{90}Sr	6.532331	5	5
Ta	27.84957	15	5
^{99}Tc	54.30884	10	10
Te	2.734446	25	10
^{229}Th	0.001539	50	50
^{232}Th	314.3238	25	10
Ti	6.167837	25	5
Tl	143.6609	25	10
^{232}U	2.84E-06	25	5
^{233}U	0.030154	10	5
^{234}U	0.048534	5	5
^{235}U	4.848993	10	5
^{236}U	0.239392	10	5
^{238}U	749.4125	10	10
V	26.23482	15	5
W	184.4871	15	5
Y	11.24589	25	5
Zn	30.83324	25	5
Zr	122.8395	15	5
^{93}Zr	8.065117	10	10

(a) If a concentration is larger than the decision point, then the low %RSD applies; if the concentration is smaller than the decision point, then the high %RSD applies. The %RSD values in this table correspond to the low-case estimates of analytical uncertainty. The high-case estimates are often two times the low-case estimates, although there are some exceptions as provided by the WTP Project.

(b) CrTOTAL denotes all isotopes of Cr.

Table D.7. Masses (g) of GFCs (a_{ik}^{GFC}) per Liter of LAW for Each Selected G2 Batch

Event (a)	Kyanite Al_2SiO_5	Boric Acid H_3BO_3	Wollastonite $CaSiO_3$	Hematite Fe_2O_3	Olivine Mg_2SiO_4	Lithium Carb. Li_2CO_3	Silica SiO_2	Rutile TiO_2	Zincite ZnO	Zircon $ZrSiO_4$
25(a)	95.41	222.18	53.28	66.94	38.34	0.00	445.07	17.94	44.01	56.59
25(b)	95.77	222.28	53.30	66.97	38.36	0.00	445.04	17.95	44.03	56.61
26(a)	95.95	222.33	53.31	66.98	38.37	0.00	445.03	17.95	44.04	56.63
26(b)	95.97	222.35	53.31	66.99	38.37	0.00	445.05	17.95	44.04	56.63
27(a)	95.92	222.37	53.32	66.99	38.37	0.00	445.12	17.95	44.05	56.64
27(b)	95.75	222.38	53.32	67.00	38.38	0.00	445.27	17.96	44.05	56.64
28(a)	95.34	222.40	53.33	67.01	38.38	0.00	445.62	17.96	44.05	56.64
28(b)	95.02	222.33	53.31	66.99	38.37	0.00	445.73	17.96	44.04	56.63
29(a)	94.93	222.26	53.30	66.97	38.36	0.00	445.65	17.95	44.03	56.61
29(b)	94.98	222.21	53.28	66.95	38.35	0.00	445.49	17.95	44.01	56.59
42(a)	80.37	196.99	70.08	59.28	33.91	0.00	410.73	15.93	39.02	50.16
42(b)	85.22	203.23	94.01	61.05	34.93	23.91	409.02	16.42	40.25	51.75
43(a)	89.33	209.12	113.02	62.75	35.92	45.65	407.42	16.88	41.42	53.25
43(b)	91.63	212.22	124.47	63.63	36.45	56.68	406.50	17.11	42.03	54.04
44(a)	95.41	217.86	139.41	65.26	37.43	69.81	410.01	17.56	43.15	55.48
44(b)	97.46	220.92	147.89	66.14	37.98	77.33	412.35	17.80	43.76	56.26
45(a)	99.69	224.36	155.12	67.14	38.62	83.59	416.50	18.07	44.44	57.13
45(b)	102.27	228.56	163.05	68.37	39.42	90.57	422.50	18.40	45.27	58.20
46(a)	103.26	229.99	165.63	68.78	39.71	92.88	424.61	18.51	45.55	58.57
46(b)	104.55	231.95	168.94	69.35	40.11	95.85	427.73	18.66	45.94	59.07
90(a)	199.66	398.52	329.53	114.09	128.79	237.89	754.27	31.88	78.93	101.48
90(b)	199.05	397.63	328.79	113.84	128.41	237.32	752.51	31.81	78.75	101.26
91(a)	199.64	398.70	329.69	114.13	128.93	238.03	754.81	31.90	78.96	101.53
91(b)	196.94	394.39	326.06	112.95	126.95	235.20	745.92	31.56	78.11	100.43
92(a)	201.50	401.91	332.40	115.01	130.45	240.17	761.61	32.15	79.60	102.35
92(b)	197.57	395.49	327.00	113.25	127.53	235.96	748.31	31.65	78.33	100.71
93(a)	201.57	402.03	332.51	115.04	130.57	240.27	761.94	32.16	79.62	102.38
93(b)	197.23	394.76	326.39	113.04	127.29	235.52	746.84	31.59	78.18	100.53
94(a)	196.38	393.21	325.09	112.61	126.63	234.52	743.64	31.46	77.88	100.13
94(b)	198.99	398.50	329.44	114.14	128.13	237.58	753.23	31.89	78.92	101.48
225(a)	50.33	229.48	77.26	69.44	39.51	0.00	486.31	18.94	45.47	58.33
225(b)	50.89	229.85	78.05	69.54	39.57	0.00	486.82	18.96	45.55	58.42
226(a)	51.13	229.86	78.07	69.54	39.57	0.00	486.64	18.96	45.55	58.43
226(b)	51.22	230.20	78.25	69.65	39.63	0.00	487.35	18.99	45.62	58.51
227(a)	51.18	230.07	78.12	69.61	39.61	0.00	487.11	18.98	45.59	58.48
227(b)	52.34	230.75	79.32	69.80	39.73	0.00	487.91	19.03	45.72	58.65
228(a)	52.39	230.72	79.32	69.79	39.72	0.00	487.83	19.02	45.72	58.64
228(b)	52.55	230.95	79.75	69.86	39.76	0.00	488.27	19.04	45.76	58.70
229(a)	52.75	231.10	79.84	69.91	39.78	0.00	488.44	19.05	45.79	58.74
229(b)	52.28	230.81	79.25	69.82	39.73	0.00	488.10	19.03	45.74	58.67
255(a)	98.65	295.90	209.55	88.71	51.08	115.82	555.16	24.10	58.60	75.32
255(b)	99.52	296.79	211.00	88.96	51.25	117.06	556.40	24.17	58.78	75.55
256(a)	97.79	296.01	210.46	88.74	51.11	116.77	555.54	24.12	58.62	75.35
256(b)	96.97	295.59	210.20	88.61	51.04	116.65	555.04	24.09	58.54	75.24
257(a)	97.95	296.91	212.25	89.00	51.29	118.40	557.07	24.19	58.80	75.58
257(b)	97.55	297.43	213.15	89.16	51.40	119.20	558.13	24.24	58.90	75.71
258(a)	96.83	297.33	213.23	89.13	51.38	119.33	558.20	24.24	58.88	75.68
258(b)	94.01	295.62	211.26	88.63	51.07	117.82	556.07	24.12	58.55	75.25
259(a)	90.15	293.44	208.78	88.00	50.67	115.94	553.44	23.97	58.12	74.69
259(b)	88.39	292.09	207.23	87.61	50.43	114.76	551.58	23.87	57.85	74.35

(a) The (a) and (b) following an event number from the G2 runs denote material going from one of two LAW CRVs to each of the two LAW MFPVs planned for the LAW vitrification facility.

Table D.8. Uncertainties for Masses of Individual GFCs [$\%RSD(a_{ik}^{GFC})$] Added to the ILAW MFPV

Uncertainty Category	$\%RSD(a_k^{GFC})$ Low[(a)]	$\%RSD(a_k^{GFC})$ High[(b)]
Low (>100 g/L of LAW)	0.67	1.34
High (<100 g/L of LAW)	2.0	4.0

(a) The low $\%RSD(a_{ik}^{GFC})$ for the low uncertainty category is based on a WTP estimate of 2% total precision, which was assumed to represent three times the $\%RSD(a_{ik}^{GFC})$, thus yielding 2/3 = 0.67 %RSD. The low $\%RSD(a_{ik}^{GFC})$ for the high-uncertainty category was based on the assumption that GFCs added in smaller quantities will be subject to a higher %RSD. All GFCs with greater than 100 g added per liter of LAW were considered to be in the low-uncertainty category. All others were considered to be in the high-uncertainty category.

(b) The high uncertainty values are two times the low uncertainty values.

Table D.9. GFC Compositions (G_{ijk}^{GFC}) and Uncertainty Case Ranges Expressed as Mass Fractions.[a] These GFCs are the total set used in ILAW and IHLW.

Oxide	Kyanite		Boric Acid		Wollastonite		Hematite	
	Nominal	Case Ranges[b]	Nominal	Case Ranges	Nominal	Case Ranges	Nominal	Case Ranges
Al_2O_3	0.5703	0.5400 – 0.6000 0.5097 – 0.6297	0	(e)	0.0020	0.0013 – 0.0027 0.0006 – 0.0034	0.0150	0.0099 – 0.0201 0.0048 – 0.0252
B_2O_3	0	(e)	0.5652	0.5625 – 0.5680 0.5598 – 0.5708	0	(e)	0	(e)
CaO	0.0003	0 – 0.0004 0 – 0.0005	0	(e)	0.4750	0.4477 – 0.5023 0.4204 – 0.5296	0.0004	0 – 0.0008 0 – 0.0011
CdO	0	(e)	0	(e)	0	(e)	0	(e)
Cl	0	(e)	0	(e)	0	(e)	0	(e)
Cr_2O_3	0	(e)	0	(e)	0	(e)	0	(e)
Fe_2O_3	0.0078	0.0042 – 0.0100 0.0006 – 0.0122	0	(e)	0.0040	0.0029 – 0.0051 0.0018 – 0.0062	0.9700	0.9615 – 0.9785 0.9530 – 0.9870
K_2O	0	0 – 0.0007 0 – 0.0014	0	(e)	0	(e)	0	(e)
Li_2O	0	(e)	0	(e)	0	(e)	0	(e)
MgO	0.0001	0 – 0.0004 0 – 0.0007	0	(e)	0.0010	0 – 0.0010 0 – 0.0010	0.0010	0.0001 – 0.0037 0 – 0.0054
MnO	0	(e)	0	(e)	0.0010	0.0009 – 0.0011 0.0008 – 0.0012	0.0012	0.0003 – 0.0039 0 – 0.0066
Na_2O	0.0042	0 – 0.0042 0 – 0.0042	0	(e)	0	(e)	0	(e)
NiO	0	(e)	0	(e)	0	(e)	0	(e)
P_2O_5	0	(e)	0	(e)	0	(e)	0.0027	0.0018 – 0.0054 0.0009 – 0.0081
PbO	0	(e)	0	(e)	0	(e)	0	
SiO_2	0.4067	0.3900 – 0.4200 0.3733 – 0.4333	0	(e)	0.5100	0.4800 – 0.5300 0.4500 – 0.5500	0.0135	0.0084 – 0.0186 0.0033 – 0.0237
SO_3	0	(e)	0	0 – 0.0003 0 – 0.0006	0	(e)	0.0007	0.0006 – 0.0009 0.0005 – 0.0011
TiO_2	0.0079	0.0050 – 0.0160 0.0021 – 0.0241	0	(e)	0.0002	0.0001 – 0.0003 0 – 0.0004	0	(e)
UO_2	0	(e)	0	(e)	0	(e)	0	(e)
V_2O_5	0	(e)	0	(e)	0	(e)	0	(e)
ZnO	0	(e)	0	(e)	0	(e)	0	(e)
ZrO_2	0	(e)	0	(e)	0	(e)	0	(e)
Total[c]	0.9973	0.9392 – 1.0517 0.8857 – 1.1061	0.5652	0.5625 – 0.5683 0.5598 – 0.5714	0.9932	0.9329 – 1.0425 0.8736 – 1.0918	1.0045[d]	0.9826 – 1.0319 0.9625 – 1.0582

(a) This table is the same as Table D.7 of Piepel et al. (2005).

(b) The top range is the low case, and the bottom range is the high case. The high case generally doubles the range about the nominal value compared to the low case.

(c) Total mass fractions less than one indicate GFCs containing water or other volatile components that will not be present in the glass. Ranges shown for the total were obtained by summing the lower values and summing the upper values of the ranges for the individual oxide components. Obviously, a total mass-fraction value greater than 1 is not possible and must be dealt with appropriately in the use of the information in this table.

(d) This was the result of converting minor components from element to oxide bases. The mass fractions of Hematite will need to be corrected based on updated/corrected vendor information.

(e) Uncertainty ranges were not available from vendor information on this oxide with zero nominal value.

Table D.9. GFC Compositions (G_{ijk}^{GFC}) and Uncertainty Case Ranges Expressed as Mass Fractions of Oxides. These GFCs are the total set used in ILAW and IHLW (cont'd)

Oxide	Olivine		Silica		Rutile		Zincite	
	Nominal	Case Ranges[(b)]	Nominal	Case Ranges	Nominal	Case Ranges	Nominal	Case Ranges
Al_2O_3	0.0019	0.0003 – 0.0078 0 – 0.0137	0.0014	0.0004 – 0.0040 0 – 0.0067	0.0050	0 – 0.0075 0 – 0.0100	0	(e)
B_2O_3	0	(e)	0	(e)	0	(e)	0	(e)
CaO	0.0002	0 – 0.0003 0 – 0.0004	0.0001	0 – 0.0002 0 – 0.0003	0	(e)	0	(e)
CdO	0	(e)	0	(e)	0	(e)	0.0001	0 – 0.0002 0 – 0.0003
Cl	0	(e)	0	(e)	0	(e)	0	(e)
Cr_2O_3	0.0013	0 – 0.0078 0 – 0.0143	0	(e)	0.0016	0 – 0.0075 0 – 0.0134	0	(e)
Fe_2O_3	0.0768	0.0468 – 0.1068 0.0168 – 0.1368	0.0002	0.0001 – 0.0004 0 – 0.0005	0.0070	0 – 0.0250 0 – 0.0430	0	0 – 0.0001 0 – 0.0001
K_2O	0	(e)	0	0 – 0.0002 0 – 0.0004	0	(e)	0	(e)
Li_2O	0	(e)	0	(e)	0	(e)	0	(e)
MgO	0.4801	0.4634 – 0.4934 0.4467 – 0.5067	0.0001	0 – 0.0001 0 – 0.0001	0	(e)	0	(e)
MnO	0	(e)	0	(e)	0	(e)	0	0 – 0.0001 0 – 0.0001
Na_2O	0.0003	0 – 0.0004 0 – 0.0005	0.0002	0 – 0.0002 0 – 0.0002	0	(e)	0	(e)
NiO	0.0037	0.0022 – 0.0052 0.0007 – 0.0067	0	(e)	0	(e)	0	(e)
P_2O_5	0	(e)	0	(e)	0	0 – 0.0007 0 – 0.0014	0	(e)
PbO	0	(e)	0	(e)	0	(e)	0	0 – 0.0001 0 – 0.0001
SiO_2	0.4252	0.4085 – 0.4385 0.3918 – 0.4518	0.9970	0.9920 – 0.9990 0.9870 – 1.0000	0.0220	0 – 0.0250 0 – 0.0280	0	(e)
SO_3	0	(e)	0	(e)	0	0 – 0.0007 0 – 0.0014	0	(e)
TiO_2	0	(e)	0.0001	0 – 0.0005 0 – 0.0009	0.9320	0.9280 – 0.9360 0.9240 – 0.9400	0	(e)
UO_2	0	(e)	0	(e)	0	(e)	0	(e)
V_2O_5	0	(e)	0	(e)	0.0045	0 – 0.0075 0 – 0.0105	0	(e)
ZnO	0	(e)	0	(e)	0	(e)	0.9990	0.9930 – 0.9999 0.9870 – 1.0000
ZrO_2	0	(e)	0	(e)	0.0190	0 – 0.0250 0 – 0.0310	0	(e)
Total[(c)]	0.9895	0.9217 – 1.0602 0.8560 – 1.1309	0.9987	0.9925 – 1.0046 0.9870 – 1.0091	0.9911	0.9320 – 1.0349 0.9240 – 1.0787	0.9991	0.9931 – 1.0004 0.9870 – 1.0006

(b) The top range is the low case, and the bottom range is the high case. The high case generally doubles the range about the nominal value compared to the low case.

(c) Total mass fractions less than one indicate GFCs containing water or other volatile components that will not be present in the glass. Ranges shown for the total were obtained by summing the lower values and summing the upper values of the ranges for the individual oxide components. Obviously, a total mass-fraction value greater than 1 is not possible and must be dealt with appropriately in the use of the information in this table.

(e) Uncertainty ranges were not available from vendor information on this oxide with zero nominal value.

Table D.9. GFC Compositions (G_{ijk}^{GFC}) and Uncertainty Case Ranges Expressed as Mass Fractions of Oxides. These GFCs are the total set used in ILAW and IHLW (cont'd)

Oxide	Zircon		Borax		Sodium Carbonate		Lithium Carbonate	
	Nominal	Case Ranges[(b)]	Nominal	Case Ranges	Nominal	Case Ranges	Nominal	Case Ranges
Al_2O_3	0.0025	0.0010 – 0.0040 0 – 0.0055	0	(e)	0	(e)	0	(e)
B_2O_3	0	(e)	0.3750	0.3690 – 0.3820 0.3630 – 0.3890	0	(e)	0	(e)
CaO	0	(e)	0	(e)	0	0 – 0.0001 0 – 0.0002	0	0 – 0.0220 0 – 0.0439
CdO	0	(e)	0	(e)	0	(e)	0	(e)
Cl	0	(e)	0	0 – 0.0007 0 – 0.0014	0.0002	0 – 0.0002 0 – 0.0002	0.0001	0 – 0.0001 0 – 0.0001
Cr_2O_3	0	(e)	0	(e)	0	0 – 0.0006 0 – 0.0010	0.0001	0 – 0.0002 0 – 0.0002
Fe_2O_3	0.0008	0.0006 – 0.0009 0.0004 – 0.0010	0	0 – 0.0001 0 – 0.0001	0	0 – 0.0001 0 – 0.0001	0	0 – 0.0001 0 – 0.0001
K_2O	0	(e)	0	(e)	0	(e)	0	0 – 0.0001 0 – 0.0001
Li_2O	0	(e)	0	(e)	0	(e)	0.4020	0.4000 – 0.4044 0.3980 – 0.4068
MgO	0	(e)	0	(e)	0	0 – 0.0001 0 – 0.0002	0.0001	0 – 0.0002 0 – 0.0002
MnO	0	(e)	0	(e)	0	(e)	0	(e)
Na_2O	0	(e)	0.1670	0.1640 – 0.1700 0.1610 – 0.1730	0.5837	0.5831 – 0.5848 0.5825 – 0.5859	0.0008	0 – 0.0011 0 – 0.0014
NiO	0	(e)	0	(e)	0	(e)	0	(e)
P_2O_5	0	(e)	0	(e)	0	(e)	0	(e)
PbO	0	(e)	0	(e)	0	(e)	0	(e)
SiO_2	0.3225	0.3200 – 0.3250 0.3175 – 0.3275	0	(e)	0	(e)	0	(e)
SO_3	0	(e)	0	0 – 0.0005 0 – 0.0010	0.0001	0 – 0.0002 0 – 0.0003	0.0003	0 – 0.0004 0 – 0.0005
TiO_2	0.0010	0.0007 – 0.0014 0.0004 – 0.0018	0	(e)	0	(e)	0	(e)
UO_2	0.0004	0.0003 – 0.0008 0.0002 – 0.0012	0	(e)	0	(e)	0	(e)
V_2O_5	0	(e)	0	(e)	0	(e)	0	(e)
ZnO	0	(e)	0	(e)	0	(e)	0	(e)
ZrO_2	0.6600	0.6500 – 0.6700 0.6400 – 0.6800	0	(e)	0	(e)	0	(e)
Total[(c)]	0.9908	0.9726 – 1.0021 0.9583 – 1.0170	0.5420	0.5330 – 0.5533 0.5240 – 0.5645	0.5842	0.5831 – 0.5861 0.5825 – 0.5879	0.4027	0.4000 – 0.4542 0.3980 – 0.4533

(b) The top range is the low case, and the bottom range is the high case. The high case generally doubles the range about the nominal value compared to the low case.

(c) Total mass fractions less than one indicate GFCs containing water or other volatile components that will not be present in the glass. Ranges shown for the total were obtained by summing the lower values and summing the upper values of the ranges for the individual oxide components. Obviously, a total mass-fraction value greater than 1 is not possible and must be dealt with appropriately in the use of the information in this table.

(e) Uncertainty ranges were not available from vendor information on this oxide with zero nominal value.

Table D.10. GFC Nominal Compositions (G_{ijk}^{GFC}) and SDs Expressed as Mass Fractions of Oxides

Oxide	Value Type	Kyanite	Boric Acid	Wollastonite	Hematite	Olivine	Silica
Al_2O_3	Nominal	0.5703	(b)	0.0020	0.0150	0.0019	0.0014
	Low SD[(a)]	0.0122	(b)	0.0003	0.0021	0.0016	0.0008
	High SD[(a)]	0.0245	(b)	0.0006	0.0042	0.0030	0.0014
B_2O_3	Nominal	(b)	0.5652	(b)	(b)	(b)	(b)
	Low SD	(b)	0.0011	(b)	(b)	(b)	(b)
	High SD	(b)	0.0022	(b)	(b)	(b)	(b)
CaO	Nominal	0.0003	(b)	0.4750	0.0004	0.0002	0.0001
	Low SD	0.00008	(b)	0.0111	0.0002	0.00006	0.00004
	High SD	0.00010	(b)	0.0223	0.0002	0.00008	0.00006
Cr_2O_3	Nominal	(b)	(b)	(b)	(b)	0.0013	(b)
	Low SD	(b)	(b)	(b)	(b)	0.0016	(b)
	High SD	(b)	(b)	(b)	(b)	0.0032	(b)
Fe_2O_3	Nominal	0.0078	(b)	0.0040	0.9700	0.0768	0.0002
	Low SD	0.0012	(b)	0.0004	0.0035	0.0122	0.00006
	High SD	0.0024	(b)	0.0009	0.0069	0.0250	0.00010
K_2O	Nominal	0	(b)	(b)	(b)	(b)	0
	Low SD	0.0002	(b)	(b)	(b)	(b)	0.00005
	High SD	0.0003	(b)	(b)	(b)	(b)	0.00009
MgO	Nominal	0.0001	(b)	0.0010	0.0010	0.4801	0.0001
	Low SD	0.00008	(b)	0.0002	0.0008	0.0061	0.00002
	High SD	0.00015	(b)	0.0002	0.0012	0.0123	0.00002
MnO	Nominal	(b)	(b)	0.0010	0.0012	(b)	(b)
	Low SD	(b)	(b)	0.00004	0.0008	(b)	(b)
	High SD	(b)	(b)	0.00008	0.0014	(b)	(b)
Na_2O	Nominal	0.0042	(b)	(b)	(b)	0.0003	0.0002
	Low SD	0.0011	(b)	(b)	(b)	0.00008	0.00005
	High SD	0.0012	(b)	(b)	(b)	0.00010	0.00005
NiO	Nominal	(b)	(b)	(b)	(b)	0.0037	(b)
	Low SD	(b)	(b)	(b)	(b)	0.0006	(b)
	High SD	(b)	(b)	(b)	(b)	0.0012	(b)
P_2O_5	Nominal	(b)	(b)	(b)	0.0027	(b)	(b)
	Low SD	(b)	(b)	(b)	0.0008	(b)	(b)
	High SD	(b)	(b)	(b)	0.0015	(b)	(b)
SO_3	Nominal	(b)	0	(b)	0.0007	(b)	(b)
	Low SD	(b)	0.00007	(b)	0.00006	(b)	(b)
	High SD	(b)	0.00014	(b)	0.00012	(b)	(b)
SiO_2	Nominal	0.4067	(b)	0.5100	0.0135	0.4252	0.9970
	Low SD	0.0061	(b)	0.0103	0.0021	0.0061	0.0015
	High SD	0.0123	(b)	0.0205	0.0042	0.0123	0.0028
TiO_2[(c)]	Nominal	0.0079	(b)	0.0002	(b)	(b)	0.0001
	Low SD	0.0023	(b)	0.00004	(b)	(b)	0.0001
	High SD	0.0047	(b)	0.00008	(b)	(b)	0.0002

(a) The low and high SDs were obtained using Eq. (D.1) with inputs to the equation given by the nominal values and the low- and high-range values in Table D.9.

(b) An empty cell means that the GFC does not contain the given oxide in measurable quantities.

(c) The GFCs on this page of Table D.10 do not contain UO_3, V_2O_5, ZnO, or ZrO_2, so those components are not included as they are in the continuation of this table on a subsequent page.

Table D.10. GFC Nominal Compositions (G_{ijk}^{GFC}) and SDs Expressed as Mass Fractions of Oxides (cont'd)

Oxide	Value Type	Rutile	Zincite	Zircon	Borax	Sodium Carbonate	Lithium Carbonate
Al_2O_3	Nominal	0.0050(a)	(b)	0.0025	(b)	(b)	(b)
	Low SD[(a)]	0.0016	(b)	0.0006	(b)	(b)	(b)
	High SD[(a)]	0.0020	(b)	0.0011	(b)	(b)	(b)
B_2O_3	Nominal	(b)	(b)	(b)	0.3750	(b)	(b)
	Low SD	(b)	(b)	(b)	0.0027	(b)	(b)
	High SD	(b)	(b)	(b)	0.0053	(b)	(b)
CaO	Nominal	(b)	(b)	(b)	(b)	0	0
	Low SD	(b)	(b)	(b)	(b)	0.00002	0.0052
	High SD	(b)	(b)	(b)	(b)	0.00005	0.0103
CdO	Nominal	(b)	0.0001	(b)	(b)	(b)	(b)
	Low SD	(b)	0.00002	(b)	(b)	(b)	(b)
	High SD	(b)	0.00006	(b)	(b)	(b)	(b)
Cl	Nominal	(b)	(b)	(b)	0	0.0002	0.0001
	Low SD	(b)	(b)	(b)	0.0002	0.00004	0.00002
	High SD	(b)	(b)	(b)	0.0003	0.00005	0.00002
Cr_2O_3	Nominal	0.0016	(b)	(b)	(b)	0	0.0001
	Low SD	0.0015	(b)	(b)	(b)	0.0001	0.00004
	High SD	0.0030	(b)	(b)	(b)	0.0002	0.00004
Fe_2O_3	Nominal	0.0070	0	0.0008	0	0	0
	Low SD	0.0053	0.00002	0.00006	0.00002	0.00002	0.00002
	High SD	0.0094	0.00002	0.00012	0.00002	0.00002	0.00002
K_2O	Nominal	(b)	(b)	(b)	(b)	(b)	0
	Low SD	(b)	(b)	(b)	(b)	(b)	0.00002
	High SD	(b)	(b)	(b)	(b)	(b)	0.00002
Li_2O	Nominal	(b)	(b)	(b)	(b)	(b)	0.4020
	Low SD	(b)	(b)	(b)	(b)	(b)	0.0009
	High SD	(b)	(b)	(b)	(b)	(b)	0.0018
MgO	Nominal	(b)	(b)	(b)	(b)	0	0.0001
	Low SD	(b)	(b)	(b)	(b)	0.00002	0.00004
	High SD	(b)	(b)	(b)	(b)	0.00005	0.00004
MnO	Nominal	(b)	0	(b)	(b)	(b)	(b)
	Low SD	(b)	0.00002	(b)	(b)	(b)	(b)
	High SD	(b)	0.00002	(b)	(b)	(b)	(b)
Na_2O	Nominal	(b)	(b)	(b)	0.1670	0.5837	0.0008
	Low SD	(b)	(b)	(b)	0.0012	0.0004	0.0002
	High SD	(b)	(b)	(b)	0.0024	0.0007	0.0003
P_2O_5	Nominal	0	(b)	(b)	(b)	(b)	(b)
	Low SD	0.0002	(b)	(b)	(b)	(b)	(b)
	High SD	0.0003	(b)	(b)	(b)	(b)	(b)
PbO	Nominal	(b)	0	(b)	(b)	(b)	(b)
	Low SD	(b)	0.00002	(b)	(b)	(b)	(b)
	High SD	(b)	0.00002	(b)	(b)	(b)	(b)
SO_3	Nominal	0	(b)	(b)	0	0.0001	0.0003
	Low SD	0.0002	(b)	(b)	0.0001	0.00004	0.00008
	High SD	0.0003	(b)	(b)	0.0002	0.00006	0.00010
SiO_2	Nominal	0.0220	(b)	0.3225	(b)	(b)	(b)
	Low SD	0.0053	(b)	0.0010	(b)	(b)	(b)
	High SD	0.0060	(b)	0.0020	(b)	(b)	(b)
TiO_2	Nominal	0.9320	(b)	0.0010	(b)	(b)	(b)
	Low SD	0.0016	(b)	0.0001	(b)	(b)	(b)
	High SD	0.0033	(b)	0.0003	(b)	(b)	(b)

(a) The low and high SDs were obtained using Eq. (D.1) with inputs to the equation given by the nominal values and the low- and high-range values in Table D.9.

(b) An empty cell means that the GFC does not contain the given oxide in measurable quantities.

Table D.10. GFC Nominal Compositions (G_{ijk}^{GFC}) and SDs Expressed as Mass Fractions of Oxides (cont'd)

Oxide	Value Type	Rutile	Zincite	Zircon	Borax	Sodium Carbonate	Lithium Carbonate
UO_3	Nominal	(b)	(b)	0.0004	(b)	(b)	(b)
	Low SD	(b)	(b)	0.00006	(b)	(b)	(b)
	High SD	(b)	(b)	0.00022	(b)	(b)	(b)
V_2O_5	Nominal	0.0045	(b)	(b)	(b)	(b)	(b)
	Low SD	0.0009	(b)	(b)	(b)	(b)	(b)
	High SD	0.0022	(b)	(b)	(b)	(b)	(b)
ZnO	Nominal	(b)	0.9990	(b)	(b)	(b)	(b)
	Low SD	(b)	0.0015	(b)	(b)	(b)	(b)
	High SD	(b)	0.0030	(b)	(b)	(b)	(b)
ZrO_2	Nominal	0.0190	(b)	0.6600	(b)	(b)	(b)
	Low SD	0.0053	(b)	0.0041	(b)	(b)	(b)
	High SD	0.0064	(b)	0.0082	(b)	(b)	(b)

(a) The low and high SDs were obtained via a formula for the SD of a triangular distribution whereas the low and high distributions are specified by the nominal and range values in Table D.9.
(b) An empty cell means that the GFC does not contain the given oxide in measurable quantities.

Table D.11. Nominal ILAW Vessel Levels, Volumes, and Uncertainties

Vessel Level or Volume	ILAW CRV Status	Nominal Value[(a)]	SD[(b)]	%RSD	ILAW MFPV Status	Nominal Value[(c)]	SD[(b)]	%RSD
Level	Full	147 in	0.5 in	0.34	Full	105.96 in	0.5 in	0.47
Volume		13230 gal 50421.69 L	47.98 gal 181.62 L	0.36		5860 gal 22182.5 L	29.62 gal 112.12 L	0.51
Level	¾	123.24 in	0.5 in	0.41	After LAW, Before GFCs	(d)	0.5 in	(e)
Volume		10952.25 gal 41458.8 L	47.98 gal 181.62 L	0.44		4808.75 gal 18203.1 L	29.62 gal 112.12 L	0.62
Level	½	99.48 in	0.5 in	0.50	Heel	49.8 in	0.5 in	1.00
Volume		8673.5 gal 32832.8 L	47.98 gal 181.62 L	0.55		2530 gal 9577.1 L	29.62 gal 112.12 L	1.17
Level	¼	75.72 in	0.5 in	0.66				
Volume		6394.75 gal 24206.8 L	47.98 gal 181.62 L	0.75				
Level	Heel	51.96 in	0.5 in	0.96				
Volume		4116 gal 15580.8 L	47.98 gal 181.62 L	1.17				

(a) The Full and Heel values were determined from information in Holgado (2002). The ¾, ½, and ¼ values were provided by the WTP Project.
(b) The SDs and %RSDs listed are low uncertainties. High uncertainties are twice the low values.
(c) The Full and Hell values were determined from information in Holgado (2003). The information for the MFPV after LAW addition was previously determined and provided by Joe Westsik of the WTP Project.
(d) Not available from the WTP Project at the time of this work.
(e) The %RSD value could not be calculated without the nominal value.

Table D.12. Nominal Volume Information for Each Selected G2 ILAW MFPV Batch

Event[a]	Number of MFPV Batches[b]	Volume Transferred CRV to MFPV (L)	Volume MFPV Heel (L)	Volume Flush (L)	Volume GFC (L)	Volume Dust (L)	Volume Sugar (L)	Volume Dilute (L)	MFPV Volume Total (L)
25(a)	6.045	8282.32	9577	167	3416.67	344.47	395.55	0.00	22183
25(b)	6.045	8282.25	9577	167	3418.15	344.64	393.95	0.00	22183
26(a)	6.045	8281.98	9577	167	3418.84	344.72	393.46	0.00	22183
26(b)	6.045	8282.16	9577	167	3419.23	344.76	392.85	0.00	22183
27(a)	6.045	8281.76	9577	167	3419.33	344.76	393.15	0.00	22183
27(b)	6.045	8281.41	9577	167	3419.35	344.75	393.49	0.00	22183
28(a)	6.046	8280.68	9577	167	3419.27	344.72	394.33	0.00	22183
28(b)	6.046	8280.85	9577	167	3418.39	344.61	395.16	0.00	22183
29(a)	6.046	8280.87	9577	167	3417.36	344.50	396.27	0.00	22183
29(b)	6.046	8281.06	9577	167	3416.65	344.43	396.86	0.00	22183
42(a)	5.827	8592.07	9577	167	3251.52	328.72	266.68	0.00	22183
42(b)	5.940	8428.85	9577	167	3407.99	343.83	258.33	0.00	22183
43(a)	6.041	8289.14	9577	167	3539.58	356.35	253.93	0.00	22183
43(b)	6.094	8216.11	9577	167	3609.02	363.07	250.81	0.00	22183
44(a)	6.179	8104.03	9577	167	3712.39	373.23	249.34	0.00	22183
44(b)	6.227	8041.36	9577	167	3769.74	378.87	249.03	0.00	22183
45(a)	6.275	7979.43	9577	167	3826.54	384.50	248.52	0.00	22183
45(b)	6.333	7906.65	9577	167	3893.11	391.10	248.14	0.00	22183
46(a)	6.353	7882.22	9577	167	3915.35	393.32	248.12	0.00	22183
46(b)	6.379	7849.38	9577	167	3945.17	396.29	248.16	0.00	22183
90(a)	10.398	4815.64	9577	167	4546.91	457.49	182.59	2436.36	22183
90(b)	10.376	4825.71	9577	167	4545.66	457.36	183.00	2427.27	22183
91(a)	10.402	4813.79	9577	167	4547.70	457.57	182.56	2437.38	22183
91(b)	10.298	4862.63	9577	167	4540.39	456.80	184.63	2394.56	22183
92(a)	10.479	4778.49	9577	167	4553.66	458.19	181.16	2467.50	22183
92(b)	10.324	4850.29	9577	167	4542.84	457.05	184.27	2404.55	22183
93(a)	10.481	4777.46	9577	167	4554.45	458.27	181.27	2467.55	22183
93(b)	10.305	4859.13	9577	167	4542.59	457.03	184.84	2395.42	22183
94(a)	10.267	4877.26	9577	167	4540.56	456.81	185.67	2378.70	22183
94(b)	10.408	4811.12	9577	167	4537.87	456.54	187.12	2446.36	22183
225(a)	6.143	8149.15	9577	167	3501.75	350.44	437.66	0.00	22183
225(b)	6.148	8142.94	9577	167	3506.86	351.02	438.18	0.00	22183
226(a)	6.148	8142.68	9577	167	3506.85	351.03	438.43	0.00	22183
226(b)	6.152	8138.29	9577	167	3510.36	351.39	438.97	0.00	22183
227(a)	6.151	8139.70	9577	167	3508.77	351.22	439.30	0.00	22183
227(b)	6.159	8128.94	9577	167	3517.63	352.23	440.20	0.00	22183
228(a)	6.159	8129.01	9577	167	3517.35	352.20	440.44	0.00	22183
228(b)	6.161	8125.62	9577	167	3520.48	352.54	440.36	0.00	22183
229(a)	6.163	8123.99	9577	167	3522.10	352.71	440.20	0.00	22183
229(b)	6.159	8128.49	9577	167	3518.12	352.27	440.12	0.00	22183

(a) The (a) and (b) following an event number from the G2 runs denote material going from one of two LAW CRVs to each of the two LAW MFPVs planned for the LAW vitrification facility.

(b) The number of batches shown is the exact number of whole and fractional MFPV batches that result from the CRV batch. The next CRV batch is added to the process so that only complete MFPV batches are used.

Table D.12. Nominal Volume Information for Each Selected G2 ILAW MFPV Batch (cont'd)

Event[a]	Number of MFPV Batches[b]	Volume Transferred CRV to MFPV (L)	Volume MFPV Heel (L)	Volume Flush (L)	Volume GFC (L)	Volume Dust (L)	Volume Sugar (L)	Volume Dilute (L)	MFPV Volume Total (L)
255(a)	7.894	6342.25	9577	167	3992.47	399.03	310.89	1394.36	22183
255(b)	7.918	6322.64	9577	167	3996.62	399.46	310.16	1410.12	22183
256(a)	7.897	6339.64	9577	167	3995.60	399.27	310.84	1393.65	22183
256(b)	7.886	6348.88	9577	167	3995.43	399.21	310.94	1384.54	22183
257(a)	7.921	6320.19	9577	167	4001.26	399.81	309.09	1408.66	22183
257(b)	7.935	6309.63	9577	167	4003.65	400.00	308.01	1417.71	22183
258(a)	7.931	6312.16	9577	167	4004.10	400.00	307.51	1415.23	22183
258(b)	7.884	6349.90	9577	167	3999.15	399.38	308.27	1382.30	22183
259(a)	7.824	6398.59	9577	167	3992.60	398.56	309.71	1339.54	22183
259(b)	7.787	6428.88	9577	167	3988.86	398.11	310.84	1312.30	22183

(a) The (a) and (b) following an event number from the G2 runs denote material going from one of two LAW CRVs to each of the two LAW MFPVs planned for the LAW vitrification facility.

(b) The number of batches shown is the exact number of whole and fractional MFPV batches that result from the CRV batch. The next CRV batch is added to the process so that only complete MFPV batches are used.

Appendix E

Detailed Results on the Variations and Uncertainties of IHLW Composition and Properties

Appendix E: Detailed Results on the Variations and Uncertainties of IHLW Composition and Properties

This appendix presents additional details on the variation and uncertainty results of IHLW compositions and properties presented in Section 7.

E.1 Detailed Results on the Variations and Uncertainties of IHLW Chemical Composition

Figure 7.1 through Figure 7.3 graphically show the mean and 90% empirical confidence interval (90% ECI) summaries of %RSDs for batch-to-batch variation, within-batch uncertainty, and total variation plus uncertainty for each of the important IHLW chemical composition components for only the scenarios with all the factors at the low case and with all the factors at the high case. To show the %RSD results for other combinations of the factors, Tables E.1 to E.4 give the mean %RSD results for all low-case and high-case combinations from the three %RSD factors in Table 5.1 for each of the four HLW waste types. Note that results from the medium case from the "random batch-to-batch variation" factor were not included in these tables. Each table lists the mean %RSD results for each of the important IHLW chemical composition components where each cell within the table displays the total variation plus uncertainty ($\overline{\%RSD_T}$) as the top number, the batch-to-batch variation ($\overline{\%RSD_B}$) as the middle number, and the within-batch uncertainty ($\overline{\%RSD_W}$) as the bottom number. The mean %RSD values were calculated using the individual %RSD values from the 200 simulations for each scenario represented by a column in the tables.

Table E.1. %RSD Means of the Total, Batch-to-Batch Variations, and Within-Batch Uncertainties for Important IHLW Chemical Composition Components of AY-102 for All Combinations of the Factors at the Low and High Cases

Component	%RSD Mean[a]	All Low Case	$\%RSD_S$[b]	$\%RSD_A$[b]	$\%RSD_B$[b]	$\%RSD_S$ $\%RSD_A$[b]	$\%RSD_S$ $\%RSD_B$[b]	$\%RSD_A$ $\%RSD_B$[b]	All High Case
Al_2O_3	$\%RSD_T$	2.9	6.4	4.5	4.9	7.4	7.6	6.1	8.3
	$\%RSD_B$	0.7	1.5	0.9	1.0	1.7	1.8	1.5	1.7
	$\%RSD_W$	2.7	6.0	4.3	4.6	6.9	7.1	5.7	7.8
B_2O_3	$\%RSD_T$	2.7	6.0	4.3	4.7	7.0	7.3	5.8	8.0
	$\%RSD_B$	0.7	1.3	0.9	1.0	1.6	1.8	1.3	1.7
	$\%RSD_W$	2.6	5.7	4.1	4.4	6.5	6.8	5.4	7.5
CaO	$\%RSD_T$	4.4	7.4	7.9	6.1	9.9	8.5	9.1	10.8
	$\%RSD_B$	1.0	1.5	1.4	1.3	2.2	1.6	2.1	2.5
	$\%RSD_W$	4.1	6.9	7.5	5.7	9.3	8.0	8.5	10.1
CdO	$\%RSD_T$	3.0	6.6	4.8	5.2	7.6	7.9	6.2	8.7
	$\%RSD_B$	0.6	1.5	1.2	1.0	1.7	1.7	1.3	1.9
	$\%RSD_W$	2.8	6.2	4.4	4.9	7.1	7.4	5.9	8.2
Cr_2O_3	$\%RSD_T$	4.4	7.4	8.0	6.1	10.1	8.6	9.0	10.9
	$\%RSD_B$	1.1	1.6	2.0	1.3	2.4	2.0	1.9	2.4
	$\%RSD_W$	4.1	7.0	7.5	5.7	9.4	8.0	8.5	10.2
Fe_2O_3	$\%RSD_T$	2.6	5.9	4.2	4.6	6.7	7.0	5.6	7.7
	$\%RSD_B$	0.5	1.2	1.1	1.0	1.5	1.5	1.3	1.5
	$\%RSD_W$	2.5	5.6	3.9	4.3	6.3	6.6	5.3	7.3
Li_2O	$\%RSD_T$	3.9	5.1	7.6	5.6	8.4	6.7	8.8	9.3
	$\%RSD_B$	0.8	1.2	1.6	1.4	1.9	1.6	2.1	2.2
	$\%RSD_W$	3.7	4.8	7.2	5.2	7.8	6.2	8.2	8.7
MgO	$\%RSD_T$	3.0	6.6	4.7	5.3	7.7	7.9	6.2	8.7
	$\%RSD_B$	0.7	1.4	0.9	1.3	1.9	1.9	1.2	1.8
	$\%RSD_W$	2.8	6.2	4.4	4.9	7.1	7.4	5.9	8.2
MnO	$\%RSD_T$	2.9	6.5	4.6	5.0	7.4	7.7	6.2	8.6
	$\%RSD_B$	0.7	1.6	0.9	1.2	1.7	1.8	1.5	2.0
	$\%RSD_W$	2.7	6.1	4.4	4.7	6.9	7.2	5.8	8.0
Na_2O	$\%RSD_T$	2.2	3.9	4.0	4.3	5.1	5.4	5.5	6.4
	$\%RSD_B$	0.5	0.9	0.8	0.9	1.3	1.2	1.1	1.5
	$\%RSD_W$	2.0	3.6	3.7	4.0	4.7	5.1	5.1	5.9
NiO	$\%RSD_T$	4.4	7.3	7.9	6.0	9.9	8.6	9.1	10.9
	$\%RSD_B$	0.9	1.5	1.6	1.0	2.0	1.9	2.1	2.6
	$\%RSD_W$	4.1	6.9	7.5	5.7	9.3	8.0	8.5	10.2
P_2O_5	$\%RSD_T$	4.4	7.4	8.0	6.0	10.0	8.4	9.0	10.8
	$\%RSD_B$	0.9	1.6	1.6	1.1	2.2	1.8	1.9	2.1
	$\%RSD_W$	4.1	7.0	7.5	5.7	9.3	8.0	8.5	10.2
PdO	$\%RSD_T$								
	$\%RSD_B$	NA[c]	NA	NA	NA	NA	NA	NA	NA
	$\%RSD_W$								
Rh_2O_3	$\%RSD_T$								
	$\%RSD_B$	NA	NA	NA	NA	NA	NA	NA	NA
	$\%RSD_W$								

(a) In the main body of the report bars were used over the %RSDs to denote means, but these tables have no room for the bars. Here, $\%RSD_T$ = mean total batch-to-batch variation and within-batch uncertainty %RSD, $\%RSD_B$ = mean batch-to-batch variation %RSD, and $\%RSD_W$ = mean within-batch uncertainty %RSD.

(b) All factors listed are at the high case whereas all others not listed are at the low case. The factor notation has been abbreviated from the notation used in the report to better fit in the table.

(c) NA is used to represent no recorded data for that particular component.

Table E.1. %RSD Means of the Total, Batch-to-Batch Variations, and Within-Batch Uncertainties for Important IHLW Chemical Composition Components of AY-102 for All Combinations of the Factors at the Low and High Cases (cont'd)

Component	%RSD Mean[a]	All Low Case	$\%RSD_S$[b]	$\%RSD_A$[b]	$\%RSD_B$[b]	$\%RSD_S$ $\%RSD_A$[b]	$\%RSD_S$ $\%RSD_B$[b]	$\%RSD_A$ $\%RSD_B$[b]	All High Case
RuO_2	$\%RSD_T$ $\%RSD_B$ $\%RSD_W$	NA[c]	NA	NA	NA	NA	NA	NA	NA
Sb_2O_3	$\%RSD_T$ $\%RSD_B$ $\%RSD_W$	9.4 1.8 8.9	11.4 2.4 10.7	18.6 4.5 17.4	10.5 2.0 9.9	19.2 4.0 18.1	12.2 2.5 11.4	18.9 4.1 17.8	19.5 4.0 18.4
SeO_2	$\%RSD_T$ $\%RSD_B$ $\%RSD_W$	NA	NA	NA	NA	NA	NA	NA	NA
SiO_2	$\%RSD_T$ $\%RSD_B$ $\%RSD_W$	1.5 0.4 1.4	3.4 0.7 3.2	2.5 0.6 2.3	2.6 0.5 2.5	4.0 1.0 3.7	4.2 1.1 3.8	3.3 0.7 3.1	4.5 0.9 4.2
SO_3	$\%RSD_T$ $\%RSD_B$ $\%RSD_W$	5.7 1.2 5.4	6.7 1.5 6.3	11.4 2.4 10.7	7.3 1.8 6.7	11.9 3.0 11.0	8.0 2.1 7.4	12.1 2.3 11.5	12.6 2.5 11.9
SrO	$\%RSD_T$ $\%RSD_B$ $\%RSD_W$	3.0 0.6 2.8	6.6 1.3 6.3	4.7 1.1 4.4	5.2 1.3 4.8	7.6 1.5 7.1	7.8 1.6 7.4	6.3 1.4 5.9	8.7 1.8 8.2
ThO_2	$\%RSD_T$ $\%RSD_B$ $\%RSD_W$	NA	NA	NA	NA	NA	NA	NA	NA
UO_3	$\%RSD_T$ $\%RSD_B$ $\%RSD_W$	7.8 1.7 7.3	9.9 2.3 9.2	15.1 3.5 14.1	8.9 2.0 8.3	16.0 3.6 15.0	10.6 2.0 10.0	15.5 3.0 14.7	16.8 4.0 15.6
ZnO	$\%RSD_T$ $\%RSD_B$ $\%RSD_W$	3.0 0.8 2.8	6.6 1.3 6.2	4.7 1.1 4.4	5.1 1.2 4.8	7.6 1.6 7.2	7.9 1.6 7.4	6.3 1.3 5.9	8.6 1.6 8.2
ZrO_2	$\%RSD_T$ $\%RSD_B$ $\%RSD_W$	3.0 0.7 2.8	6.6 1.4 6.2	4.7 1.0 4.4	5.2 1.2 4.8	7.6 1.7 7.1	8.0 2.0 7.4	6.3 1.4 5.9	8.7 1.9 8.2

(a) In the main body of the report bars were used over the %RSDs to denote means, but these tables have no room for the bars. Here, $\%RSD_T$ = mean total batch-to-batch variation and within-batch uncertainty %RSD, $\%RSD_B$ = mean batch-to-batch variation %RSD, and $\%RSD_W$ = mean within-batch uncertainty %RSD.

(b) All factors listed are at the high case whereas all others not listed are at the low case. The factor notation has been abbreviated from the notation used in the report to better fit in the table.

(c) NA is used to represent no recorded data for that particular component.

Table E.2. %RSD Means of the Total, Batch-to-Batch Variations, and Within-Batch Uncertainties for Important IHLW Chemical Composition Components of AZ-102 for All Combinations of the Factors at the Low and High Cases

Component	%RSD Mean[a]	All Low Case	$\%RSD_S$[b]	$\%RSD_A$[b]	$\%RSD_B$[b]	$\%RSD_S$ $\%RSD_A$[b]	$\%RSD_S$ $\%RSD_B$[b]	$\%RSD_A$ $\%RSD_B$[b]	All High Case
Al_2O_3	$\%RSD_T$	2.8	6.3	4.4	4.9	7.2	7.5	5.9	8.2
	$\%RSD_B$	0.6	1.5	1.2	1.1	1.6	1.8	1.2	2.0
	$\%RSD_W$	2.6	5.9	4.1	4.5	6.7	6.9	5.6	7.7
B_2O_3	$\%RSD_T$	.2.9	6.4	4.5	5.0	7.4	7.6	6.2	8.5
	$\%RSD_B$	0.8	1.5	0.9	1.2	1.5	1.7	1.6	2.0
	$\%RSD_W$	2.7	6.0	4.3	4.7	7.0	7.1	5.8	7.9
CaO	$\%RSD_T$	4.4	7.5	8.0	6.1	10.0	8.6	9.0	10.9
	$\%RSD_B$	1.1	1.9	1.7	1.4	2.3	1.9	1.8	2.3
	$\%RSD_W$	4.1	7.0	7.5	5.7	9.4	8.0	8.5	10.2
CdO	$\%RSD_T$	2.9	6.5	4.7	5.1	7.6	7.7	6.3	8.6
	$\%RSD_B$	0.6	1.5	1.0	1.0	1.7	1.5	1.6	2.0
	$\%RSD_W$	2.8	6.1	4.4	4.8	7.1	7.3	5.9	8.1
Cr_2O_3	$\%RSD_T$	4.4	7.4	8.1	6.2	10.1	8.6	9.0	10.9
	$\%RSD_B$	0.9	1.4	1.9	1.5	2.6	1.9	2.1	2.3
	$\%RSD_W$	4.1	7.0	7.5	5.7	9.4	8.0	8.4	10.2
Fe_2O_3	$\%RSD_T$	2.7	6.0	4.2	4.6	6.8	7.1	5.7	7.9
	$\%RSD_B$	0.6	1.3	1.0	1.0	1.4	1.6	1.2	1.7
	$\%RSD_W$	2.5	5.6	4.0	4.4	6.4	6.6	5.4	7.4
Li_2O	$\%RSD_T$	3.9	5.0	7.4	5.6	8.1	6.5	8.5	9.2
	$\%RSD_B$	1.0	1.1	1.6	1.4	1.7	1.7	1.8	2.2
	$\%RSD_W$	3.6	4.7	7.0	5.2	7.7	6.0	8.0	8.5
MgO	$\%RSD_T$	4.4	7.4	8.0	6.1	9.9	8.7	9.0	10.8
	$\%RSD_B$	0.9	1.6	1.7	1.5	2.1	2.3	1.9	2.3
	$\%RSD_W$	4.1	6.9	7.5	5.7	9.3	8.0	8.5	10.2
MnO	$\%RSD_T$	3.0	6.6	4.7	5.1	7.5	7.8	6.2	8.7
	$\%RSD_B$	0.6	1.5	1.2	1.0	1.5	1.7	1.3	2.1
	$\%RSD_W$	2.8	6.2	4.4	4.8	7.1	7.3	5.9	8.1
Na_2O	$\%RSD_T$	2.1	3.8	3.9	4.3	5.0	5.3	5.4	6.3
	$\%RSD_B$	0.5	0.8	0.9	0.9	1.1	1.2	1.1	1.5
	$\%RSD_W$	2.0	3.6	3.7	4.0	4.7	5.0	5.1	5.9
NiO	$\%RSD_T$	3.0	6.6	4.7	5.1	7.6	7.8	6.3	8.7
	$\%RSD_B$	0.7	1.3	1.0	1.1	1.7	1.5	1.4	1.9
	$\%RSD_W$	2.8	6.2	4.4	4.8	7.1	7.4	5.9	8.1
P_2O_5	$\%RSD_T$	4.4	7.3	8.0	6.1	9.9	8.5	9.1	10.9
	$\%RSD_B$	1.0	1.4	1.8	1.4	2.1	1.7	1.9	2.8
	$\%RSD_W$	4.1	6.9	7.4	5.7	9.4	8.0	8.5	10.1
PdO	$\%RSD_T$								
	$\%RSD_B$	NA[c]	NA	NA	NA	NA	NA	NA	NA
	$\%RSD_W$								
Rh_2O_3	$\%RSD_T$								
	$\%RSD_B$	NA	NA	NA	NA	NA	NA	NA	NA
	$\%RSD_W$								

(a) In the main body of the report bars were used over the %RSDs to denote means, but these tables have no room for the bars. Here, $\%RSD_T$ = mean total batch-to-batch variation and within-batch uncertainty %RSD, $\%RSD_B$ = mean batch-to-batch variation %RSD, and $\%RSD_W$ = mean within-batch uncertainty %RSD.

(b) All factors listed are at the high case whereas all others not listed are at the low case. The factor notation has been abbreviated from the notation used in the report to better fit in the table.

(c) NA is used to represent no recorded data for that particular component.

Table E.2. %RSD Means of the Total, Batch-to-Batch Variations, and Within-Batch Uncertainties for Important IHLW Chemical Composition Components of AZ-102 for All Combinations of the Factors at the Low and High Cases (cont'd)

Component	%RSD Mean[a]	All Low Case	$\%RSD_S$[b]	$\%RSD_A$[b]	$\%RSD_B$[b]	$\%RSD_S$ $\%RSD_A$[b]	$\%RSD_S$ $\%RSD_B$[b]	$\%RSD_A$ $\%RSD_B$[b]	All High Case
RuO_2	$\%RSD_T$ $\%RSD_B$ $\%RSD_W$	NA[c]	NA	NA	NA	NA	NA	NA	NA
Sb_2O_3	$\%RSD_T$ $\%RSD_B$ $\%RSD_W$	NA	NA	NA	NA	NA	NA	NA	NA
SeO_2	$\%RSD_T$ $\%RSD_B$ $\%RSD_W$	NA	NA	NA	NA	NA	NA	NA	NA
SiO_2	$\%RSD_T$ $\%RSD_B$ $\%RSD_W$	1.5 0.4 1.4	3.4 0.7 3.2	2.4 0.4 2.3	2.6 0.5 2.5	3.9 0.8 3.7	4.0 0.9 3.8	3.2 0.6 3.1	4.5 0.9 4.2
SO_3	$\%RSD_T$ $\%RSD_B$ $\%RSD_W$	4.0 1.0 3.7	5.2 1.2 4.9	7.8 1.7 7.3	5.8 1.3 5.5	8.5 1.9 8.0	6.7 1.5 6.3	8.9 1.9 8.3	9.5 2.2 8.9
SrO	$\%RSD_T$ $\%RSD_B$ $\%RSD_W$	3.0 0.6 2.8	6.6 1.4 6.2	4.7 1.0 4.4	5.1 1.3 4.8	7.5 1.7 7.0	7.8 1.6 7.3	6.3 1.3 5.9	8.7 2.0 8.1
ThO_2	$\%RSD_T$ $\%RSD_B$ $\%RSD_W$	NA	NA	NA	NA	NA	NA	NA	NA
UO_3	$\%RSD_T$ $\%RSD_B$ $\%RSD_W$	4.3 0.9 4.1	7.3 1.6 6.9	7.9 1.8 7.4	6.0 1.3 5.6	9.6 2.1 9.0	8.4 1.8 7.9	8.7 2.0 8.2	10.8 2.1 10.1
ZnO	$\%RSD_T$ $\%RSD_B$ $\%RSD_W$	4.5 1.1 4.2	6.7 1.6 6.3	7.0 1.5 6.6	6.1 1.4 5.7	10.2 2.5 9.4	8.2 1.8 7.7	9.0 2.0 8.4	11.0 2.7 10.2
ZrO_2	$\%RSD_T$ $\%RSD_B$ $\%RSD_W$	3.0 0.6 2.8	6.6 1.6 6.2	4.6 0.9 4.4	5.0 1.0 4.8	7.5 1.6 7.0	7.7 1.6 7.3	6.3 1.3 5.9	8.7 1.9 8.1

(a) In the main body of the report bars were used over the %RSDs to denote means, but these tables have no room for the bars. Here, $\%RSD_T$ = mean total batch-to-batch variation and within-batch uncertainty %RSD, $\%RSD_B$ = mean batch-to-batch variation %RSD, and $\%RSD_W$ = mean within-batch uncertainty %RSD.

(b) All factors listed are at the high case whereas all others not listed are at the low case. The factor notation has been abbreviated from the notation used in the report to better fit in the table.

(c) NA is used to represent no recorded data for that particular component.

Table E.3. %RSD Means of the Total, Batch-to-Batch Variations, and Within-Batch Uncertainties for Important IHLW Chemical Composition Components of C-104 for All Combinations of the Factors at the Low and High Cases

Component	%RSD Mean[a]	All Low Case	$\%RSD_S$[b]	$\%RSD_A$[b]	$\%RSD_B$[b]	$\%RSD_S$ $\%RSD_A$[b]	$\%RSD_S$ $\%RSD_B$[b]	$\%RSD_A$ $\%RSD_B$[b]	All High Case
Al_2O_3	$\%RSD_T$	2.9	6.3	4.6	5.0	7.4	7.7	6.1	8.5
	$\%RSD_B$	0.6	1.3	0.9	1.0	1.6	1.7	1.5	1.8
	$\%RSD_W$	2.7	6.0	4.3	4.7	7.0	7.2	5.7	8.0
B_2O_3	$\%RSD_T$	2.7	6.2	4.3	4.7	7.1	7.2	5.7	8.0
	$\%RSD_B$	0.5	1.5	1.0	1.0	1.7	1.4	1.1	1.8
	$\%RSD_W$	2.6	5.8	4.1	4.4	6.6	6.8	5.5	7.5
CaO	$\%RSD_T$	4.4	7.3	8.1	6.1	9.9	8.5	9.0	10.8
	$\%RSD_B$	1.0	1.6	2.0	1.5	2.0	2.2	2.1	2.2
	$\%RSD_W$	4.1	6.9	7.5	5.6	9.3	7.9	8.4	10.2
CdO	$\%RSD_T$	4.4	7.3	8.0	5.8	10.0	8.6	9.1	10.9
	$\%RSD_B$	1.0	1.5	1.7	1.2	2.3	2.2	2.2	2.6
	$\%RSD_W$	4.1	6.9	7.5	5.5	9.3	8.0	8.4	10.1
Cr_2O_3	$\%RSD_T$	4.3	7.4	8.0	6.0	9.8	8.4	9.0	10.6
	$\%RSD_B$	0.9	1.8	2.0	1.5	1.9	1.7	1.8	2.2
	$\%RSD_W$	4.1	6.9	7.4	5.6	9.3	7.9	8.5	10.0
Fe_2O_3	$\%RSD_T$	2.9	6.3	4.5	4.9	7.3	7.5	6.0	8.3
	$\%RSD_B$	0.6	1.4	1.0	1.1	1.7	1.7	1.2	1.7
	$\%RSD_W$	2.7	6.0	4.2	4.6	6.8	7.0	5.7	7.8
Li_2O	$\%RSD_T$	2.3	3.9	4.2	4.6	5.2	5.6	5.8	6.6
	$\%RSD_B$	0.5	0.9	0.9	1.0	1.1	1.4	1.2	1.4
	$\%RSD_W$	2.1	3.6	3.9	4.3	4.9	5.2	5.4	6.2
MgO	$\%RSD_T$	4.5	7.4	8.0	6.0	9.9	8.5	9.0	10.8
	$\%RSD_B$	1.1	1.8	1.9	1.4	2.0	2.0	2.0	2.3
	$\%RSD_W$	4.1	6.9	7.5	5.6	9.4	7.9	8.5	10.2
MnO	$\%RSD_T$	2.9	6.5	4.6	5.0	7.4	7.7	6.1	8.6
	$\%RSD_B$	0.6	1.5	0.9	1.0	1.5	1.8	1.4	2.0
	$\%RSD_W$	2.7	6.0	4.3	4.7	7.0	7.1	5.7	8.0
Na_2O	$\%RSD_T$	2.2	3.8	4.0	4.5	5.0	5.4	5.7	6.4
	$\%RSD_B$	0.5	0.8	1.0	1.1	0.9	1.1	1.4	1.3
	$\%RSD_W$	2.1	3.6	3.8	4.2	4.8	5.1	5.2	6.0
NiO	$\%RSD_T$	4.4	7.3	8.0	6.0	10.0	8.5	9.0	10.7
	$\%RSD_B$	1.0	1.5	1.7	1.3	2.2	2.0	2.1	2.3
	$\%RSD_W$	4.1	6.9	7.5	5.7	9.4	7.9	8.4	10.1
P_2O_5	$\%RSD_T$	4.3	7.4	8.0	6.1	10.0	8.4	9.0	11.0
	$\%RSD_B$	0.9	1.7	1.7	1.5	2.4	1.9	1.9	2.9
	$\%RSD_W$	4.1	6.9	7.5	5.7	9.3	7.9	8.5	10.1
PdO	$\%RSD_T$	9.4	11.3	18.4	10.6	19.5	12.1	18.9	19.9
	$\%RSD_B$	1.8	2.6	3.8	2.5	5.1	2.7	4.4	4.6
	$\%RSD_W$	8.9	10.6	17.4	9.8	18.1	11.3	17.6	18.5
Rh_2O_3	$\%RSD_T$	8.8	11.2	18.7	9.2	19.0	12.0	19.1	19.8
	$\%RSD_B$	2.0	2.3	4.4	2.1	4.1	2.5	4.7	4.7
	$\%RSD_W$	8.2	10.6	17.5	8.6	17.9	11.3	17.7	18.5

(a) In the main body of the report bars were used over the %RSDs to denote means, but these tables have no room for the bars. Here, $\%RSD_T$ = mean total batch-to-batch variation and within-batch uncertainty %RSD, $\%RSD_B$ = mean batch-to-batch variation %RSD, and $\%RSD_W$ = mean within-batch uncertainty %RSD.

(b) All factors listed are at the high case whereas all others not listed are at the low case. The factor notation has been abbreviated from the notation used in the report to better fit in the table.

(c) NA is used to represent no recorded data for that particular component.

Table E.3. %RSD Means of the Total, Batch-to-Batch Variations, and Within-Batch Uncertainties for Important IHLW Chemical Composition Components of C-104 for All Combinations of the Factors at the Low and High Cases (cont'd)

Component	%RSD Mean[a]	All Low Case	$\%RSD_S$[b]	$\%RSD_A$[b]	$\%RSD_B$[b]	$\%RSD_S$ $\%RSD_A$[b]	$\%RSD_S$ $\%RSD_B$[b]	$\%RSD_A$ $\%RSD_B$[b]	All High Case
RuO_2	$\%RSD_T$	4.4	7.5	8.0	6.1	10.0	8.6	9.0	10.9
	$\%RSD_B$	1.0	2.0	1.7	1.4	2.2	2.0	2.1	2.6
	$\%RSD_W$	4.1	6.9	7.6	5.7	9.4	8.0	8.4	10.1
Sb_2O_3	$\%RSD_T$ $\%RSD_B$ $\%RSD_W$	NA[c]	NA	NA	NA	NA	NA	NA	NA
SeO_2	$\%RSD_T$	4.4	7.4	8.0	5.9	10.0	8.5	8.9	10.7
	$\%RSD_B$	0.9	1.7	1.6	1.3	2.3	2.1	1.8	2.5
	$\%RSD_W$	4.1	6.9	7.5	5.6	9.3	7.9	8.5	10.0
SiO_2	$\%RSD_T$	1.5	3.4	2.4	2.6	3.9	4.0	3.2	4.5
	$\%RSD_B$	0.3	0.8	0.5	0.6	0.9	0.9	0.7	1.1
	$\%RSD_W$	1.4	3.2	2.2	2.4	3.6	3.8	3.0	4.2
SO_3	$\%RSD_T$	4.0	5.1	7.7	5.7	8.3	6.6	8.8	9.2
	$\%RSD_B$	0.9	1.1	1.5	1.3	2.0	1.5	1.9	1.9
	$\%RSD_W$	3.7	4.8	7.2	5.4	7.8	6.2	8.2	8.7
SrO	$\%RSD_T$	2.9	6.4	4.6	4.9	7.4	7.7	6.2	8.4
	$\%RSD_B$	0.7	1.2	1.0	1.2	1.6	1.7	1.3	1.9
	$\%RSD_W$	2.7	6.0	4.3	4.6	6.9	7.2	5.8	7.9
ThO_2	$\%RSD_T$	2.9	6.3	4.6	5.0	7.2	7.7	6.1	8.3
	$\%RSD_B$	0.6	1.3	1.1	1.1	1.5	1.9	1.6	1.8
	$\%RSD_W$	2.7	6.0	4.2	4.6	6.8	7.1	5.7	7.8
UO_3	$\%RSD_T$	2.9	6.4	4.6	5.0	7.3	7.6	6.0	8.3
	$\%RSD_B$	0.6	1.3	1.1	1.2	1.6	1.7	1.2	1.7
	$\%RSD_W$	2.7	6.0	4.3	4.7	6.8	7.1	5.7	7.8
ZnO	$\%RSD_T$	2.9	6.5	4.7	5.0	7.3	7.6	6.3	8.3
	$\%RSD_B$	0.6	1.5	1.1	1.1	1.6	1.6	1.6	1.9
	$\%RSD_W$	2.7	6.1	4.3	4.7	6.8	7.2	5.8	7.8
ZrO_2	$\%RSD_T$	2.8	6.3	4.5	4.9	7.3	7.5	6.0	8.4
	$\%RSD_B$	0.6	1.3	0.9	1.1	1.7	1.5	1.2	2.0
	$\%RSD_W$	2.7	6.0	4.2	4.6	6.8	7.1	5.7	7.8

(a) In the main body of the report bars were used over the %RSDs to denote means, but these tables have no room for the bars. Here, $\%RSD_T$ = mean total batch-to-batch variation and within-batch uncertainty %RSD, $\%RSD_B$ = mean batch-to-batch variation %RSD, and $\%RSD_W$ = mean within-batch uncertainty %RSD.

(b) All factors listed are at the high case whereas all others not listed are at the low case. The factor notation has been abbreviated from the notation used in the report to better fit in the table.

(c) NA is used to represent no recorded data for that particular component.

Table E.4. %RSD Means of the Total, Batch-to-Batch Variations, and Within-Batch Uncertainties for Important IHLW Chemical Composition Components of the AY-102 to AZ-102 Transition for All Combinations of the Factors at the Low and High Cases

Component	%RSD Mean[a]	All Low Case	$\%RSD_S$[b]	$\%RSD_A$[b]	$\%RSD_B$[b]	$\%RSD_S$ $\%RSD_A$[b]	$\%RSD_S$ $\%RSD_B$[b]	$\%RSD_A$ $\%RSD_B$[b]	All High Case
Al_2O_3	$\%RSD_T$	3.7	6.6	5.0	5.3	7.5	7.7	6.3	8.5
	$\%RSD_B$	2.4	2.4	2.3	2.2	2.6	2.5	2.0	2.5
	$\%RSD_W$	2.7	5.9	4.2	4.6	6.7	7.0	5.6	7.7
B_2O_3	$\%RSD_T$	12.5	13.4	12.9	13.2	13.8	14.3	13.4	14.6
	$\%RSD_B$	12.2	11.8	12.1	12.3	11.8	12.1	12.0	12.1
	$\%RSD_W$	2.8	6.1	4.3	4.8	7.0	7.3	5.8	8.0
CaO	$\%RSD_T$	4.4	7.5	8.0	6.0	10.0	8.4	9.0	11.0
	$\%RSD_B$	1.0	1.9	1.8	1.3	2.4	1.7	1.8	2.6
	$\%RSD_W$	4.1	6.9	7.5	5.7	9.3	8.0	8.5	10.2
CdO	$\%RSD_T$	7.9	9.6	8.5	8.8	10.2	10.4	9.4	11.0
	$\%RSD_B$	7.3	7.2	7.2	7.4	7.0	7.0	7.1	7.0
	$\%RSD_W$	2.8	6.2	4.4	4.8	7.2	7.4	6.0	8.1
Cr_2O_3	$\%RSD_T$	10.8	11.9	12.4	11.3	13.4	12.8	12.6	14.3
	$\%RSD_B$	10.0	9.4	9.6	9.6	9.0	9.7	8.9	9.1
	$\%RSD_W$	4.2	7.1	7.6	5.7	9.5	8.1	8.6	10.4
Fe_2O_3	$\%RSD_T$	2.9	6.1	4.3	4.7	6.9	7.1	5.8	8.0
	$\%RSD_B$	1.0	1.5	1.1	1.2	1.6	1.6	1.4	2.0
	$\%RSD_W$	2.5	5.6	4.0	4.3	6.4	6.6	5.4	7.4
Li_2O	$\%RSD_T$	5.0	5.9	8.0	6.5	8.6	7.1	8.9	9.6
	$\%RSD_B$	3.3	3.1	3.0	3.4	3.0	2.9	2.7	2.9
	$\%RSD_W$	3.6	4.7	7.1	5.3	7.7	6.1	8.1	8.7
MgO	$\%RSD_T$	4.6	7.5	8.0	6.2	10.0	8.6	9.0	11.0
	$\%RSD_B$	1.7	2.1	2.6	1.9	2.5	2.1	2.6	3.0
	$\%RSD_W$	4.0	6.9	7.3	5.7	9.2	8.0	8.2	10.1
MnO	$\%RSD_T$	14.5	15.7	14.9	15.2	16.1	16.1	15.4	16.5
	$\%RSD_B$	14.2	14.3	14.2	14.4	14.3	14.2	14.1	14.1
	$\%RSD_W$	2.8	6.3	4.5	4.9	7.2	7.5	6.0	8.3
Na_2O	$\%RSD_T$	2.2	3.8	3.9	4.3	5.0	5.3	5.4	6.3
	$\%RSD_B$	0.5	0.9	0.8	1.0	1.1	1.2	1.1	1.4
	$\%RSD_W$	2.0	3.6	3.7	4.0	4.7	5.0	5.1	5.9
NiO	$\%RSD_T$	4.4	7.2	5.7	5.9	8.1	8.2	7.0	9.4
	$\%RSD_B$	3.3	2.8	2.8	2.9	2.8	2.6	2.8	3.3
	$\%RSD_W$	2.9	6.3	4.7	4.9	7.2	7.4	6.1	8.3
P_2O_5	$\%RSD_T$	4.5	7.5	8.2	6.2	10.1	8.5	9.1	10.9
	$\%RSD_B$	1.3	2.1	2.3	1.8	2.4	2.0	1.9	2.2
	$\%RSD_W$	4.1	6.9	7.5	5.7	9.4	8.0	8.5	10.3
PdO	$\%RSD_T$ $\%RSD_B$ $\%RSD_W$	NA[c]	NA	NA	NA	NA	NA	NA	NA
Rh_2O_3	$\%RSD_T$ $\%RSD_B$ $\%RSD_W$	NA	NA	NA	NA	NA	NA	NA	NA

(a) In the main body of the report bars were used over the %RSDs to denote means, but these tables have no room for the bars. Here, $\%RSD_T$ = mean total batch-to-batch variation and within-batch uncertainty %RSD, $\%RSD_B$ = mean batch-to-batch variation %RSD, and $\%RSD_W$ = mean within-batch uncertainty %RSD.

(b) All factors listed are at the high case whereas all others not listed are at the low case. The factor notation has been abbreviated from the notation used in the report to better fit in the table.

(c) NA is used to represent no recorded data for that particular component.

Table E.4. %RSD Means of the Total, Batch-to-Batch Variations, and Within-Batch Uncertainties for Important IHLW Chemical Composition Components of the AY-102 to AZ-102 Transition for All Combinations of the Factors at the Low and High Cases (cont'd)

Component	%RSD Mean[a]	All Low Case	$\%RSD_S$[b]	$\%RSD_A$[b]	$\%RSD_B$[b]	$\%RSD_S$ $\%RSD_A$[b]	$\%RSD_S$ $\%RSD_B$[b]	$\%RSD_A$ $\%RSD_B$[b]	All High Case
RuO_2	$\%RSD_T$ $\%RSD_B$ $\%RSD_W$	NA[c]	NA	NA	NA	NA	NA	NA	NA
Sb_2O_3	$\%RSD_T$ $\%RSD_B$ $\%RSD_W$	304.1 302.7 28.4	303.4 301.4 33.2	299.2 294.0 53.5	303.0 301.3 31.7	301.4 296.1 54.1	302.9 300.7 35.5	298.1 292.7 54.7	294.7 289.1 55.1
SeO_2	$\%RSD_T$ $\%RSD_B$ $\%RSD_W$	NA	NA	NA	NA	NA	NA	NA	NA
SiO_2	$\%RSD_T$ $\%RSD_B$ $\%RSD_W$	1.5 0.3 1.4	3.4 0.8 3.2	2.4 0.5 2.3	2.6 0.7 2.4	3.9 0.8 3.6	4.0 0.8 3.8	3.2 0.6 3.0	4.5 1.0 4.2
SO_3	$\%RSD_T$ $\%RSD_B$ $\%RSD_W$	43.1 42.9 4.6	43.2 42.8 5.7	41.1 40.2 8.4	41.6 41.1 6.0	42.0 41.0 9.0	40.0 39.4 6.5	43.2 42.0 10.0	43.2 41.8 10.7
SrO	$\%RSD_T$ $\%RSD_B$ $\%RSD_W$	7.1 6.5 2.8	9.1 6.5 6.2	7.9 6.5 4.5	8.1 6.4 4.8	9.5 5.9 7.1	9.8 6.1 7.4	8.8 6.3 5.9	10.4 5.8 8.2
ThO_2	$\%RSD_T$ $\%RSD_B$ $\%RSD_W$	NA	NA	NA	NA	NA	NA	NA	NA
UO_3	$\%RSD_T$ $\%RSD_B$ $\%RSD_W$	6.5 4.6 4.3	8.6 4.4 7.0	9.6 4.7 7.8	7.6 4.5 5.8	10.8 3.6 9.7	9.5 4.1 8.1	10.3 4.6 8.7	11.8 4.2 10.4
ZnO	$\%RSD_T$ $\%RSD_B$ $\%RSD_W$	85.6 85.5 4.6	85.9 85.5 8.5	86.0 85.6 8.0	85.7 85.4 6.9	86.3 85.6 10.7	86.4 85.8 10.0	85.8 85.2 9.6	85.7 84.9 12.0
ZrO_2	$\%RSD_T$ $\%RSD_B$ $\%RSD_W$	5.7 4.9 2.8	8.0 4.7 6.2	6.7 5.0 4.4	6.8 4.7 4.8	8.7 4.4 7.1	8.8 4.1 7.4	7.7 4.7 5.9	9.8 4.8 8.2

(a) In the main body of the report bars were used over the %RSDs to denote means, but these tables have no room for the bars. Here, $\%RSD_T$ = mean total batch-to-batch variation and within-batch uncertainty %RSD, $\%RSD_B$ = mean batch-to-batch variation %RSD, and $\%RSD_W$ = mean within-batch uncertainty %RSD.

(b) All factors listed are at the high case whereas all others not listed are at the low case. The factor notation has been abbreviated from the notation used in the report to better fit in the table.

(c) NA is used to represent no recorded data for that particular component.

E.2 Detailed Results on the Variations and Uncertainties of IHLW Radionuclide Composition

Figure 7.4 through Figure 7.6 graphically show the mean and 90% ECI summaries of %RSDs for batch-to-batch variation, within-batch uncertainty, and total variation plus uncertainty for each of the important IHLW radionuclide composition components for only the scenarios with all the factors at the low case and with all the factors at the high case. To show the %RSD results for other combinations of the factors, Tables E.5 to E.8 give the mean %RSD results for all low-case and high-case combinations from the three %RSD factors in Table 5.1 for each of the four HLW waste types. Note that results from the medium case from the "random batch-to-batch variation" factor were not included in these tables. Each table lists the mean %RSD results for each of the important IHLW radionuclide composition components where each cell within the table displays the total variation plus uncertainty ($\overline{\%RSD_T}$) as the top number, the batch-to-batch variation ($\overline{\%RSD_B}$) as the middle number, and the within-batch uncertainty ($\overline{\%RSD_W}$) as the bottom number. The mean %RSD values were calculated using the individual %RSD values from the 200 simulations for each scenario represented by a column in the tables.

Table E.5. %RSD Means of the Total, Batch-to-Batch Variations, and Within-Batch Uncertainties for Important IHLW Radionuclide Composition Components of AY-102 for All Combinations of the Factors at the Low and High Cases

Component	%RSD Mean[a]	All Low Case	$\%RSD_S$[b]	$\%RSD_A$[b]	$\%RSD_B$[b]	$\%RSD_S$ $\%RSD_A$[b]	$\%RSD_S$ $\%RSD_B$[b]	$\%RSD_A$ $\%RSD_B$[b]	All High Case
$^{241}Am_2O_3$	$\%RSD_T$	1.0	3.8	18.3	4.3	18.6	5.6	18.5	19.1
	$\%RSD_B$	0.4	0.8	4.3	1.0	4.5	1.2	4.1	4.2
	$\%RSD_W$	0.8	3.6	17.0	4.0	17.3	5.3	17.4	17.9
$^{242}Cm_2O_3$	NA[c]	NA	NA	NA	NA	NA	NA	NA	NA
$^{243+244}Cm_2O_3$	NA	NA	NA	NA	NA	NA	NA	NA	NA
^{60}CoO	$\%RSD_T$	2087.4	2076.5	2077.1	2082.8	2069.7	2070.2	2075.4	2059.5
	$\%RSD_B$	1940.7	1930.6	1931.1	1936.4	1924.2	1924.7	1929.5	1914.8
	$\%RSD_W$	768.7	764.7	764.9	767.0	762.2	762.4	764.3	758.5
$^{127}Cs_2O$	$\%RSD_T$	2.4	4.0	18.2	4.8	18.8	5.9	18.6	19.0
	$\%RSD_B$	0.5	0.7	3.3	1.0	4.3	1.4	3.7	3.6
	$\%RSD_W$	2.2	3.8	17.3	4.6	17.6	5.5	17.5	18.0
$^{237}NpO_2$	NA	NA	NA	NA	NA	NA	NA	NA	NA
$^{238}PuO_2$	$\%RSD_T$	36.7	37.1	3.5	37.3	3.9	19.6	4.1	4.3
	$\%RSD_B$	34.1	34.5	3.3	34.7	3.6	18.2	3.8	4.0
	$\%RSD_W$	13.5	13.6	1.3	13.7	1.4	7.2	1.5	1.6
$^{239}PuO_2$	$\%RSD_T$	4.0	5.3	7.7	5.9	8.5	6.8	8.9	9.5
	$\%RSD_B$	0.9	1.2	1.7	1.3	1.8	1.5	1.9	2.0
	$\%RSD_W$	3.8	4.9	7.3	5.5	8.0	6.3	8.3	9.0
$^{241}PuO_2$	NA	NA	NA	NA	NA	NA	NA	NA	NA
^{90}SrO	$\%RSD_T$	4.0	5.2	7.8	5.8	8.4	6.7	9.0	9.4
	$\%RSD_B$	0.9	1.1	1.8	1.3	1.7	1.6	2.3	1.8
	$\%RSD_W$	3.8	4.9	7.3	5.5	8.0	6.3	8.4	9.0
$^{99}Tc_2O_7$	$\%RSD_T$	8.2	1.4	5.8	2.2	9.7	3.3	8.2	3.3
	$\%RSD_B$	7.6	1.3	5.4	2.0	9.0	3.0	7.6	3.1
	$\%RSD_W$	3.0	0.5	2.1	0.8	3.6	1.2	3.0	1.2
$^{233}UO_3$	NA	NA	NA	NA	NA	NA	NA	NA	NA
$^{234}UO_3$	NA	NA	NA	NA	NA	NA	NA	NA	NA
$^{235}UO_3$	NA	NA	NA	NA	NA	NA	NA	NA	NA
$^{236}UO_3$	NA	NA	NA	NA	NA	NA	NA	NA	NA
$^{238}UO_3$	$\%RSD_T$	74.3	74.2	77.0	74.5	76.3	74.3	76.4	71.6
	$\%RSD_B$	69.1	69.0	71.6	69.3	70.9	69.0	71.0	66.5
	$\%RSD_W$	27.4	27.3	28.4	27.4	28.1	27.3	28.1	26.4

(a) In the main body of the report bars were used over the %RSDs to denote means, but these tables have no room for the bars. Here, $\%RSD_T$ = mean total batch-to-batch variation and within-batch uncertainty %RSD, $\%RSD_B$ = mean batch-to-batch variation %RSD, and $\%RSD_W$ = mean within-batch uncertainty %RSD.

(b) All factors listed are at the high case whereas all others not listed are at the low case. The factor notation has been abbreviated from the notation used in the report to better fit in the table.

(c) NA is used to represent no recorded data for that particular component.

Table E.6. %RSD Means of the Total, Batch-to-Batch Variations, and Within-Batch Uncertainties for Important IHLW Radionuclide Composition Components of AZ-102 for All Combinations of the Factors at the Low and High Cases

Component	%RSD Mean[a]	All Low Case	$\%RSD_S$[b]	$\%RSD_A$[b]	$\%RSD_B$[b]	$\%RSD_S$ $\%RSD_A$[b]	$\%RSD_S$ $\%RSD_B$[b]	$\%RSD_A$ $\%RSD_B$[b]	All High Case
$^{241}Am_2O_3$	$\%RSD_T$	2.4	4.1	9.5	4.8	10.0	5.8	10.4	10.8
	$\%RSD_B$	0.5	1.0	2.3	1.1	2.3	1.4	2.1	2.2
	$\%RSD_W$	2.2	3.8	8.9	4.5	9.4	5.4	9.8	10.2
$^{242}Cm_2O_3$	NA[c]	NA	NA	NA	NA	NA	NA	NA	NA
$^{243+244}Cm_2O_3$	$\%RSD_T$	488.9	485.9	486.6	487.1	480.2	485.1	481.6	480.3
	$\%RSD_B$	454.5	451.8	452.4	452.9	446.5	451.0	447.8	446.6
	$\%RSD_W$	180.0	179.0	179.2	179.4	176.9	178.7	177.4	176.9
^{60}CoO	$\%RSD_T$	274.1	272.8	274.9	273.2	273.2	272.4	273.6	273.6
	$\%RSD_B$	254.9	253.6	255.5	254.0	254.0	253.3	254.4	254.3
	$\%RSD_W$	101.0	100.5	101.2	100.6	100.6	100.3	100.8	100.7
$^{127}Cs_2O$	$\%RSD_T$	1.1	4.0	4.4	4.8	5.4	5.8	6.0	6.5
	$\%RSD_B$	0.3	0.8	1.1	1.1	1.1	1.2	1.4	1.5
	$\%RSD_W$	1.0	3.8	4.1	4.5	5.1	5.5	5.6	6.1
$^{237}NpO_2$	$\%RSD_T$	4.0	5.2	9.7	5.8	10.2	6.7	10.4	11.1
	$\%RSD_B$	0.9	1.3	2.1	1.5	2.2	1.5	2.2	2.5
	$\%RSD_W$	3.8	4.9	9.1	5.4	9.6	6.3	9.8	10.4
$^{238}PuO_2$	$\%RSD_T$	21.4	1.0	10.1	1.7	10.3	2.8	10.4	10.4
	$\%RSD_B$	19.9	0.9	9.4	1.6	9.6	2.6	9.7	9.6
	$\%RSD_W$	7.9	0.4	3.7	0.6	3.8	1.0	3.8	3.8
$^{239}PuO_2$	$\%RSD_T$	4.0	5.2	7.9	5.9	8.5	6.7	9.0	9.5
	$\%RSD_B$	0.9	1.2	1.8	1.5	1.9	1.4	1.9	2.4
	$\%RSD_W$	3.8	4.8	7.3	5.4	8.0	6.3	8.4	8.8
$^{241}PuO_2$	$\%RSD_T$	0.8	1.7	6.2	2.3	6.4	3.3	6.5	6.7
	$\%RSD_B$	0.7	1.6	5.8	2.1	6.0	3.0	6.0	6.3
	$\%RSD_W$	0.3	0.6	2.3	0.8	2.4	1.2	2.4	2.5
^{90}SrO	$\%RSD_T$	4.0	5.2	7.7	5.8	8.4	6.7	8.8	9.4
	$\%RSD_B$	0.8	1.1	1.7	1.4	1.9	1.4	1.9	2.0
	$\%RSD_W$	3.8	4.9	7.3	5.4	7.9	6.3	8.3	8.8
$^{99}Tc_2O_7$	$\%RSD_T$	1.4	3.5	5.4	5.5	7.9	5.6	8.8	9.3
	$\%RSD_B$	1.3	1.0	1.3	1.3	1.8	1.3	1.9	2.3
	$\%RSD_W$	0.5	3.1	4.9	5.1	7.4	5.1	8.2	8.6
$^{233}UO_3$	$\%RSD_T$	1.1	1.1	6.6	1.6	6.5	4.0	6.6	9.2
	$\%RSD_B$	1.0	1.1	1.6	1.5	1.7	0.9	1.4	2.1
	$\%RSD_W$	0.4	0.4	6.0	0.6	5.9	3.6	6.1	8.6
$^{234}UO_3$	$\%RSD_T$	11.0	11.6	30.5	11.8	30.0	12.3	30.1	30.4
	$\%RSD_B$	2.2	2.7	7.6	2.9	6.1	2.6	7.0	7.0
	$\%RSD_W$	10.4	10.8	28.2	11.0	28.4	11.6	28.1	28.5
$^{235}UO_3$	$\%RSD_T$	4.0	5.1	15.0	5.7	15.4	6.6	15.7	16.1
	$\%RSD_B$	0.8	1.2	2.7	1.2	3.5	1.4	4.0	3.8
	$\%RSD_W$	3.8	4.8	14.2	5.4	14.4	6.2	14.6	15.0
$^{236}UO_3$	$\%RSD_T$	5.8	6.7	30.4	6.9	30.0	7.3	30.1	31.0
	$\%RSD_B$	1.4	1.5	7.4	1.6	6.1	1.6	5.7	7.8
	$\%RSD_W$	5.4	6.2	28.2	6.5	28.4	6.8	28.5	28.7
$^{238}UO_3$	$\%RSD_T$	2.4	4.0	6.0	4.8	6.8	5.8	7.3	8.1
	$\%RSD_B$	0.6	1.0	1.3	1.2	1.4	1.3	1.5	1.9
	$\%RSD_W$	2.2	3.7	5.6	4.5	6.4	5.4	6.8	7.5

(a) In the main body of the report bars were used over the %RSDs to denote means, but these tables have no room for the bars. Here, $\%RSD_T$ = mean total batch-to-batch variation and within-batch uncertainty %RSD, $\%RSD_B$ = mean batch-to-batch variation %RSD, and $\%RSD_W$ = mean within-batch uncertainty %RSD.

(b) All factors listed are at the high case whereas all others not listed are at the low case. The factor notation has been abbreviated from the notation used in the report to better fit in the table.

(c) NA is used to represent no recorded data for that particular component.

Table E.7. %RSD Means of the Total, Batch-to-Batch Variations, and Within-Batch Uncertainties for Important IHLW Radionuclide Composition Components of C-104 for All Combinations of the Factors at the Low and High Cases

Component	%RSD Mean[a]	All Low Case	$\%RSD_S$[b]	$\%RSD_A$[b]	$\%RSD_B$[b]	$\%RSD_S$ $\%RSD_A$[b]	$\%RSD_S$ $\%RSD_B$[b]	$\%RSD_A$ $\%RSD_B$[b]	All High Case
$^{241}Am_2O_3$	$\%RSD_T$	0.8	3.4	16.9	4.3	16.9	5.3	17.9	18.3
	$\%RSD_B$	0.7	0.9	3.3	1.0	3.1	1.4	4.1	4.3
	$\%RSD_W$	0.3	3.1	16.0	4.0	16.0	4.9	16.8	17.1
$^{242}Cm_2O_3$	$\%RSD_T$	11180.9	11127.0	9899.6	11164.8	9803.9	11088.9	9799.1	9730.1
	$\%RSD_B$	10395.1	10345.0	9203.8	10380.1	9114.9	10309.6	9110.4	9046.3
	$\%RSD_W$	4117.6	4097.8	3645.7	4111.7	3610.5	4083.7	3608.7	3583.3
$^{243+244}Cm_2O_3$	$\%RSD_T$	864.8	860.7	853.9	861.8	845.2	857.4	853.9	847.8
	$\%RSD_B$	804.0	800.2	793.9	801.2	785.8	797.2	793.9	788.2
	$\%RSD_W$	318.5	317.0	314.5	317.4	311.3	315.8	314.5	312.2
^{60}CoO	$\%RSD_T$	2786.2	2772.6	2770.1	2785.7	2763.6	2766.2	2772.9	2740.6
	$\%RSD_B$	2590.4	2577.7	2575.4	2589.9	2569.4	2571.8	2578.1	2548.0
	$\%RSD_W$	1026.1	1021.1	1020.2	1025.9	1017.8	1018.7	1021.2	1009.3
$^{127}Cs_2O$	$\%RSD_T$	2.3	3.9	4.3	4.5	5.3	5.7	6.0	6.9
	$\%RSD_B$	0.5	0.8	0.9	1.1	1.1	1.3	1.2	1.7
	$\%RSD_W$	2.2	3.7	4.0	4.2	5.0	5.3	5.7	6.4
$^{237}NpO_2$	$\%RSD_T$	2.5	5.0	18.2	5.7	19.3	6.6	18.8	18.9
	$\%RSD_B$	0.5	1.0	3.5	1.2	5.5	1.3	4.3	4.3
	$\%RSD_W$	2.3	4.8	17.2	5.4	17.6	6.2	17.5	17.7
$^{238}PuO_2$	$\%RSD_T$	34.1	34.5	4.9	32.8	5.3	8.8	5.6	5.9
	$\%RSD_B$	31.7	32.0	4.6	30.5	4.9	8.2	5.2	5.5
	$\%RSD_W$	12.6	12.7	1.8	12.1	2.0	3.3	2.1	2.2
$^{239}PuO_2$	$\%RSD_T$	4.0	5.1	7.7	5.7	8.4	6.7	8.8	9.4
	$\%RSD_B$	0.9	1.4	1.5	1.2	1.8	1.8	1.7	2.2
	$\%RSD_W$	3.7	4.7	7.3	5.4	7.9	6.2	8.3	8.8
$^{241}PuO_2$	$\%RSD_T$	3.1	3.4	8.8	2.6	8.2	1.2	6.5	5.0
	$\%RSD_B$	2.9	3.1	3.2	2.4	3.5	1.1	2.7	2.4
	$\%RSD_W$	1.1	1.2	7.4	1.0	6.5	0.4	5.3	3.8
^{90}SrO	$\%RSD_T$	3.9	3.7	15.0	2.8	14.8	6.1	15.0	15.2
	$\%RSD_B$	0.8	1.0	3.3	0.5	4.0	1.3	3.4	3.0
	$\%RSD_W$	3.7	3.4	14.0	2.6	13.6	5.7	14.1	14.4
$^{99}Tc_2O_7$	$\%RSD_T$	3.6	3.6	6.1	5.2	7.8	6.3	8.0	9.1
	$\%RSD_B$	0.8	0.9	1.5	1.3	1.8	1.6	1.6	1.9
	$\%RSD_W$	3.4	3.3	5.7	4.8	7.2	5.9	7.6	8.6
$^{233}UO_3$	$\%RSD_T$	2.3	4.0	7.8	4.8	8.5	5.8	8.7	9.5
	$\%RSD_B$	0.5	0.9	1.7	1.1	1.8	1.2	1.8	2.4
	$\%RSD_W$	2.2	3.7	7.3	4.5	8.0	5.4	8.2	8.8
$^{234}UO_3$	$\%RSD_T$	10.4	11.0	29.9	11.7	30.1	12.2	29.7	30.7
	$\%RSD_B$	2.1	2.4	5.9	2.4	6.6	2.7	5.7	7.2
	$\%RSD_W$	9.8	10.3	28.2	11.0	28.4	11.5	28.2	28.6
$^{235}UO_3$	$\%RSD_T$	3.9	5.1	13.5	5.8	13.1	6.7	14.1	15.1
	$\%RSD_B$	0.9	1.1	2.8	1.3	2.6	1.5	3.4	3.4
	$\%RSD_W$	3.7	4.8	12.8	5.4	12.3	6.2	13.2	14.1
$^{236}UO_3$	$\%RSD_T$	5.7	6.1	29.8	6.9	29.4	7.8	30.0	30.7
	$\%RSD_B$	1.3	1.3	6.5	1.6	6.4	1.6	6.9	7.0
	$\%RSD_W$	5.3	5.7	28.1	6.5	27.6	7.4	28.1	28.7
$^{238}UO_3$	$\%RSD_T$	2.3	3.9	5.8	4.7	6.6	5.4	7.1	7.8
	$\%RSD_B$	0.4	0.9	1.4	1.1	1.4	1.0	1.6	1.7
	$\%RSD_W$	2.1	3.6	5.4	4.4	6.2	5.1	6.7	7.4

(a) In the main body of the report bars were used over the %RSDs to denote means, but these tables have no room for the bars. Here, $\%RSD_T$ = mean total batch-to-batch variation and within-batch uncertainty %RSD, $\%RSD_B$ = mean batch-to-batch variation %RSD, and $\%RSD_W$ = mean within-batch uncertainty %RSD.

(b) All factors listed are at the high case whereas all others not listed are at the low case. The factor notation has been abbreviated from the notation used in the report to better fit in the table.

Table E.8. %RSD Means of the Total, Batch-to-Batch Variations, and Within-Batch Uncertainties for Important IHLW Radionuclide Composition Components of the AY-102 to AZ-102 Transition for All Combinations of the Factors at the Low and High Cases

Component	%RSD Mean[a]	All Low Case	$\%RSD_S$[b]	$\%RSD_A$[b]	$\%RSD_B$[b]	$\%RSD_S$ $\%RSD_A$[b]	$\%RSD_S$ $\%RSD_B$[b]	$\%RSD_A$ $\%RSD_B$[b]	All High Case
$^{241}Am_2O_3$	$\%RSD_T$	6.7	7.9	11.9	8.2	12.3	8.6	12.7	13.3
	$\%RSD_B$	6.4	6.9	6.1	6.8	5.8	6.5	6.4	6.7
	$\%RSD_W$	2.1	3.8	9.6	4.5	10.2	5.5	10.4	10.8
$^{242}Cm_2O_3$	NA[c]	NA	NA	NA	NA	NA	NA	NA	NA
$^{243+244}Cm_2O_3$	$\%RSD_T$	500.7	498.9	497.3	499.2	494.2	497.3	499.7	491.1
	$\%RSD_B$	465.5	463.8	462.4	464.1	459.4	462.3	464.6	456.6
	$\%RSD_W$	184.4	183.7	183.2	183.8	182.0	183.1	184.0	180.9
^{60}CoO	$\%RSD_T$	279.7	278.5	279.8	278.9	279.5	277.7	280.6	278.9
	$\%RSD_B$	260.0	258.9	260.2	259.3	259.8	258.2	260.9	259.3
	$\%RSD_W$	103.0	102.6	103.1	102.7	102.9	102.3	103.3	102.7
$^{127}Cs_2O$	$\%RSD_T$	1.2	4.3	5.7	5.0	6.6	6.0	6.9	8.0
	$\%RSD_B$	0.5	1.5	1.4	1.5	1.7	1.8	1.9	2.3
	$\%RSD_W$	1.0	3.8	5.2	4.5	6.1	5.4	6.3	7.2
$^{237}NpO_2$	$\%RSD_T$	8.3	8.9	11.7	9.2	12.2	9.6	12.3	12.7
	$\%RSD_B$	7.4	7.4	6.9	7.3	6.9	7.0	6.5	6.4
	$\%RSD_W$	3.8	4.9	9.1	5.5	9.6	6.4	10.0	10.5
$^{238}PuO_2$	$\%RSD_T$	19.8	0.9	10.0	1.7	10.2	2.7	10.4	10.4
	$\%RSD_B$	18.4	0.9	9.3	1.6	9.5	2.5	9.7	9.7
	$\%RSD_W$	7.3	0.3	3.7	0.6	3.8	1.0	3.8	3.8
$^{239}PuO_2$	$\%RSD_T$	4.0	5.2	7.7	5.8	8.5	6.7	8.9	9.5
	$\%RSD_B$	0.9	1.4	1.5	1.5	1.9	1.6	2.0	2.1
	$\%RSD_W$	3.8	4.8	7.3	5.3	8.0	6.3	8.3	8.9
$^{241}PuO_2$	$\%RSD_T$	0.9	1.6	5.9	2.3	6.4	3.3	6.4	6.6
	$\%RSD_B$	0.8	1.5	5.5	2.1	5.9	3.0	5.9	6.1
	$\%RSD_W$	0.3	0.6	2.2	0.8	2.4	1.2	2.3	2.4
^{90}SrO	$\%RSD_T$	5.0	5.9	8.2	6.5	8.8	7.2	9.1	10.0
	$\%RSD_B$	3.1	2.9	2.6	3.0	3.0	2.7	2.9	3.2
	$\%RSD_W$	3.8	4.9	7.4	5.5	7.9	6.3	8.3	9.0
$^{99}Tc_2O_7$	$\%RSD_T$	1.4	5.2	7.3	8.2	9.5	8.5	10.8	11.1
	$\%RSD_B$	1.3	4.2	4.9	6.3	5.9	6.3	6.7	6.0
	$\%RSD_W$	0.5	3.0	5.3	5.1	7.2	5.7	8.2	8.9
$^{233}UO_3$	$\%RSD_T$	0.9	1.2	8.7	1.7	7.6	5.6	8.0	10.7
	$\%RSD_B$	0.8	1.1	6.0	1.6	4.9	4.5	4.8	6.3
	$\%RSD_W$	0.3	0.4	6.1	0.6	5.5	3.4	6.1	8.3
$^{234}UO_3$	$\%RSD_T$	12.9	13.2	30.5	13.2	30.8	13.7	31.1	31.3
	$\%RSD_B$	6.4	6.6	7.5	6.5	8.0	6.2	9.2	9.1
	$\%RSD_W$	10.5	10.9	28.2	10.9	28.6	11.7	28.4	28.7
$^{235}UO_3$	$\%RSD_T$	8.4	8.8	16.3	9.0	16.7	9.7	16.7	16.9
	$\%RSD_B$	7.5	7.3	6.5	7.2	6.2	7.3	6.2	6.2
	$\%RSD_W$	3.8	4.9	14.2	5.4	14.6	6.2	14.7	15.0
$^{236}UO_3$	$\%RSD_T$	9.1	9.6	31.2	9.7	30.7	9.9	30.8	31.3
	$\%RSD_B$	7.2	7.2	8.9	6.9	7.2	6.6	7.6	9.2
	$\%RSD_W$	5.5	6.2	28.5	6.6	28.5	7.1	28.7	28.6
$^{238}UO_3$	$\%RSD_T$	7.7	8.3	9.6	8.6	9.9	9.0	10.4	10.9
	$\%RSD_B$	7.4	7.4	7.4	7.3	7.1	7.0	7.2	7.1
	$\%RSD_W$	2.2	3.8	6.0	4.5	6.7	5.5	7.2	7.9

(a) In the main body of the report bars were used over the %RSDs to denote means, but these tables have no room for the bars. Here, $\%RSD_T$ = mean total batch-to-batch variation and within-batch uncertainty %RSD, $\%RSD_B$ = mean batch-to-batch variation %RSD, and $\%RSD_W$ = mean within-batch uncertainty %RSD.

(b) All factors listed are at the high case whereas all others not listed are at the low case. The factor notation has been abbreviated from the notation used in the report to better fit in the table.

(c) NA is used to represent no recorded data for that particular component.

E.3 Detailed Results on the Variations and Uncertainties of IHLW Glass Properties

Figure 7.7 through Figure 7.11 graphically show the mean and 90% ECI summaries of %RSDs for batch-to-batch variation, within-batch uncertainty, and total variation plus uncertainty for each of the IHLW glass properties (PCT, TCLP, spinel $T_{1\%}$, viscosity, and electrical conductivity) for only the scenarios with all the factors at the low case and with all the factors at the high case. To show the %RSD results for other combinations of the factors, Tables E.9 to E.12 give the mean %RSD results for all low-case and high-case combinations from the three %RSD factors in Table 5.1 or each of the four waste types. Note that results from the medium case from the "random batch-to-batch variation" factor were not included in these tables. Each table lists the mean %RSD results for each of the IHLW properties where each cell within the table displays the total variation plus uncertainty ($\overline{\%RSD_T}$) as the top number, the batch-to-batch variation ($\overline{\%RSD_B}$) as the middle number, and the within-batch uncertainty ($\overline{\%RSD_W}$) as the bottom number. The mean %RSD values were calculated using the individual %RSD values from the 200 simulations for each scenario represented by a column in the tables.

Table E.9. %RSD Means of the Total, Batch-to-Batch Variations, and Within-Batch Uncertainties for IHLW Glass Properties of AY-102 for All Combinations of the Factors at the Low and High Cases

Glass Property	%RSD Mean[a]	All Low Case	$\%RSD_S$[b]	$\%RSD_A$[b]	$\%RSD_B$[b]	$\%RSD_S$ $\%RSD_A$[b]	$\%RSD_S$ $\%RSD_B$[b]	$\%RSD_A$ $\%RSD_B$[b]	All High Case
PCT B	$\%RSD_T$	8.9	21.1	15.8	16.5	27.9	29.7	22.6	35.1
	$\%RSD_B$	2.3	4.0	4.0	3.2	6.4	6.6	4.8	6.5
	$\%RSD_W$	8.2	20.1	14.6	15.6	26.0	27.9	21.2	33.4
PCT Li	$\%RSD_T$	5.4	11.3	9.4	9.5	14.7	15.2	12.7	17.5
	$\%RSD_B$	1.4	2.1	2.4	1.9	3.5	3.5	2.9	3.6
	$\%RSD_W$	4.9	10.8	8.7	9.0	13.6	14.2	11.9	16.6
PCT Na	$\%RSD_T$	8.2	18.5	14.9	15.4	24.8	26.3	21.1	31.3
	$\%RSD_B$	2.1	3.5	3.7	3.0	5.8	5.9	4.7	5.8
	$\%RSD_W$	7.6	17.6	13.8	14.6	23.0	24.7	19.8	29.8
TCLP	$\%RSD_T$	6.5	15.2	10.7	11.4	18.5	19.5	14.8	21.8
	$\%RSD_B$	1.6	3.1	2.6	2.3	4.4	4.3	3.3	4.3
	$\%RSD_W$	6.0	14.4	10.0	10.8	17.2	18.3	13.8	20.7
$T_{1\%}$ (Phase 1)	$\%RSD_T$	1.5	3.0	2.4	2.6	3.6	3.7	3.3	4.2
	$\%RSD_B$	0.3	0.6	0.5	0.6	0.8	0.8	0.8	0.9
	$\%RSD_W$	1.4	2.8	2.3	2.4	3.4	3.5	3.0	4.0
$T_{1\%}$ (Phase 1a)	$\%RSD_T$	1.4	3.0	2.4	2.5	3.5	3.7	3.2	4.1
	$\%RSD_B$	0.3	0.6	0.6	0.6	0.8	0.8	0.7	0.9
	$\%RSD_W$	1.3	2.8	2.2	2.4	3.3	3.4	3.0	3.9
Viscosity 1373 K	$\%RSD_T$	12.5	25.4	21.3	21.2	30.8	31.6	27.5	36.3
	$\%RSD_B$	3.3	4.8	5.2	4.2	7.3	8.1	6.9	9.1
	$\%RSD_W$	11.6	24.1	19.7	20.1	28.6	29.4	25.5	33.6
Viscosity 1423 K	$\%RSD_T$	11.6	23.6	19.7	19.6	28.5	29.2	25.4	33.4
	$\%RSD_B$	3.1	4.5	4.8	3.9	6.8	7.6	6.4	8.4
	$\%RSD_W$	10.7	22.4	18.2	18.6	26.5	27.2	23.6	30.9
E.C.[c] 1373 K	$\%RSD_T$	3.7	7.2	6.8	6.5	9.5	9.5	8.9	11.1
	$\%RSD_B$	0.9	1.5	1.8	1.3	2.3	2.3	2.3	2.5
	$\%RSD_W$	3.5	6.7	6.3	6.1	8.8	8.8	8.3	10.5
E.C. 1473 K	$\%RSD_T$	3.5	6.7	6.5	6.1	8.9	8.9	8.5	10.4
	$\%RSD_B$	0.8	1.4	1.7	1.2	2.2	2.1	2.2	2.3
	$\%RSD_W$	3.3	6.3	6.0	5.8	8.2	8.2	7.8	9.8

(a) In the main body of the report bars were used over the %RSDs to denote means, but these tables have no room for the bars. Here, $\%RSD_T$ = mean total batch-to-batch variation and within-batch uncertainty %RSD, $\%RSD_B$ = mean batch-to-batch variation %RSD, and $\%RSD_W$ = mean within-batch uncertainty %RSD.

(b) All factors listed are at the high case whereas all others not listed are at the low case. The factor notation has been abbreviated from the notation used in the report to better fit in the table.

(c) E.C. represents electrical conductivity of HLW glasses.

Table E.10. %RSD Means of the Total, Batch-to-Batch Variations, and Within-Batch Uncertainties for IHLW Glass Properties of AZ-102 for All Combinations of the Factors at the Low and High Cases

Glass Property	%RSD Mean[a]	All Low Case	$\%RSD_S$[b]	$\%RSD_A$[b]	$\%RSD_B$[b]	$\%RSD_S$ $\%RSD_A$[b]	$\%RSD_S$ $\%RSD_B$[b]	$\%RSD_A$ $\%RSD_B$[b]	All High Case
PCT B	$\%RSD_T$	9.9	21.5	18.4	18.6	29.1	30.1	25.4	38.2
	$\%RSD_B$	2.3	4.9	3.5	4.2	5.9	6.3	4.8	8.0
	$\%RSD_W$	9.2	20.2	17.4	17.4	27.5	28.5	24	35.9
PCT Li	$\%RSD_T$	6.5	12.8	11.9	11.5	17.1	17.0	15.5	21.1
	$\%RSD_B$	1.5	2.9	2.5	2.6	3.6	4.0	2.9	5.0
	$\%RSD_W$	6.1	12.0	11.2	10.7	16.0	15.9	14.7	19.6
PCT Na	$\%RSD_T$	9.7	21.0	18.1	18.4	28.6	29.8	25.1	37.7
	$\%RSD_B$	2.3	4.6	3.4	4.1	5.8	6.2	4.7	7.7
	$\%RSD_W$	9.1	19.8	17.2	17.2	27.0	28.2	23.8	35.5
TCLP	$\%RSD_T$	6.2	14.2	10.3	11.0	17.2	17.8	14.2	21.1
	$\%RSD_B$	1.4	3.2	2.0	2.1	3.3	3.9	2.7	4.8
	$\%RSD_W$	5.8	13.4	9.7	10.4	16.2	16.8	13.4	19.7
$T_{1\%}$ (Phase 1)	$\%RSD_T$	1.6	3.1	2.7	2.8	3.8	3.9	3.5	4.5
	$\%RSD_B$	0.4	0.7	0.7	0.6	0.9	0.8	0.6	1.1
	$\%RSD_W$	1.5	2.9	2.5	2.6	3.6	3.6	3.3	4.2
$T_{1\%}$ (Phase 1a)	$\%RSD_T$	1.5	3.0	2.5	2.7	3.7	3.8	3.3	4.3
	$\%RSD_B$	0.4	0.6	0.6	0.6	0.9	0.8	0.6	1.0
	$\%RSD_W$	1.4	2.9	2.4	2.5	3.5	3.5	3.2	4.0
Viscosity 1373 K	$\%RSD_T$	14.0	27.0	25.1	23.5	34.2	32.6	31.7	39.8
	$\%RSD_B$	3.3	5.8	5.6	4.6	6.7	7.0	6.2	8.2
	$\%RSD_W$	13.1	25.3	23.5	22.2	32.4	30.7	30.0	37.7
Viscosity 1423 K	$\%RSD_T$	13.0	24.9	23.1	21.7	31.5	30.1	29.1	36.5
	$\%RSD_B$	3.1	5.4	5.1	4.3	6.2	6.6	5.7	7.6
	$\%RSD_W$	12.1	23.4	21.6	20.5	29.9	28.4	27.6	34.5
E.C.[c] 1373 K	$\%RSD_T$	5.3	9.7	9.6	8.8	13.0	12.6	12.1	15.7
	$\%RSD_B$	1.2	2.0	1.9	2.0	2.6	2.9	2.2	3.6
	$\%RSD_W$	4.9	9.1	9.1	8.2	12.3	11.8	11.5	14.6
E.C. 1473 K	$\%RSD_T$	5.0	9.1	9.2	8.4	12.3	11.9	11.6	14.8
	$\%RSD_B$	1.2	1.9	1.9	1.9	2.5	2.7	2.1	3.5
	$\%RSD_W$	4.7	8.6	8.7	7.8	11.6	11.1	11.0	13.8

(a) In the main body of the report bars were used over the %RSDs to denote means, but these tables have no room for the bars. Here, $\%RSD_T$ = mean total batch-to-batch variation and within-batch uncertainty %RSD, $\%RSD_B$ = mean batch-to-batch variation %RSD, and $\%RSD_W$ = mean within-batch uncertainty %RSD.

(b) All factors listed are at the high case whereas all others not listed are at the low case. The factor notation has been abbreviated from the notation used in the report to better fit in the table.

(c) E.C. represents electrical conductivity of HLW glasses.

Table E.11. %RSD Means of the Total, Batch-to-Batch Variations, and Within-Batch Uncertainties for IHLW Glass Properties of C-104 for All Combinations of the Factors at the Low and High Cases

Glass Property	%RSD Mean[a]	All Low Case	$\%RSD_S$[b]	$\%RSD_A$[b]	$\%RSD_B$[b]	$\%RSD_S$ $\%RSD_A$[b]	$\%RSD_S$ $\%RSD_B$[b]	$\%RSD_A$ $\%RSD_B$[b]	All High Case
PCT B	$\%RSD_T$	7.9	19.6	13.8	15.2	24.3	26.4	20.3	32.7
	$\%RSD_B$	1.7	4.4	3.1	3.3	4.6	6.0	4.3	5.9
	$\%RSD_W$	7.5	18.3	13.0	14.4	23.0	24.6	19.2	31.2
PCT Li	$\%RSD_T$	4.8	10.9	8.3	9.1	13.3	14.3	11.7	16.8
	$\%RSD_B$	1.0	2.5	1.8	2.0	2.7	3.4	2.5	3.3
	$\%RSD_W$	4.5	10.2	7.8	8.6	12.6	13.3	11.0	15.9
PCT Na	$\%RSD_T$	7.1	16.6	12.5	13.7	20.8	22.6	18.2	27.9
	$\%RSD_B$	1.5	3.6	2.7	3.0	3.8	5.2	4.1	5.2
	$\%RSD_W$	6.7	15.6	11.7	12.9	19.7	21.1	17.1	26.5
TCLP	$\%RSD_T$	7.6	17.4	13.2	13.1	21.7	22.1	17.8	27.0
	$\%RSD_B$	1.8	4.1	2.6	3.1	4.5	5.3	4.0	5.8
	$\%RSD_W$	7.1	16.3	12.5	12.3	20.5	20.6	16.7	25.3
$T_{1\%}$ (Phase 1)	$\%RSD_T$	1.0	2.0	1.8	2.0	2.5	2.7	2.5	3.0
	$\%RSD_B$	0.2	0.4	0.4	0.4	0.5	0.6	0.6	0.6
	$\%RSD_W$	1.0	1.9	1.7	1.8	2.4	2.5	2.3	2.9
$T_{1\%}$ (Phase 1a)	$\%RSD_T$	1.0	2.0	1.7	1.9	2.5	2.6	2.3	2.9
	$\%RSD_B$	0.2	0.4	0.4	0.4	0.5	0.6	0.5	0.6
	$\%RSD_W$	1.0	1.9	1.6	1.7	2.3	2.4	2.2	2.8
Viscosity 1373 K	$\%RSD_T$	12.4	26.4	20.2	22.1	31.1	32.1	27.2	35.8
	$\%RSD_B$	2.8	5.7	4.5	4.8	7.7	6.8	5.3	7.9
	$\%RSD_W$	11.6	24.8	19.0	20.7	29.0	30.1	25.6	33.7
Viscosity 1423 K	$\%RSD_T$	11.5	24.4	18.8	20.4	28.8	29.7	25.2	33.1
	$\%RSD_B$	2.6	5.3	4.1	4.5	7.1	6.4	5.0	7.3
	$\%RSD_W$	10.8	23.0	17.6	19.2	26.8	27.9	23.7	31.1
E.C.[c] 1373 K	$\%RSD_T$	3.8	8.1	6.6	7.2	10.0	10.6	9.2	12.3
	$\%RSD_B$	0.8	1.8	1.4	1.6	2.0	2.5	2.1	2.5
	$\%RSD_W$	3.6	7.6	6.2	6.8	9.4	9.8	8.6	11.6
E.C. 1473 K	$\%RSD_T$	3.6	7.6	6.3	6.9	9.4	10.0	8.7	11.6
	$\%RSD_B$	0.8	1.7	1.4	1.5	1.9	2.3	2.0	2.3
	$\%RSD_W$	3.4	7.1	5.9	6.5	8.9	9.3	8.2	11.0

(a) In the main body of the report bars were used over the %RSDs to denote means, but these tables have no room for the bars. Here, $\%RSD_T$ = mean total batch-to-batch variation and within-batch uncertainty %RSD, $\%RSD_B$ = mean batch-to-batch variation %RSD, and $\%RSD_W$ = mean within-batch uncertainty %RSD.

(b) All factors listed are at the high case whereas all others not listed are at the low case. The factor notation has been abbreviated from the notation used in the report to better fit in the table.

(c) E.C. represents electrical conductivity of HLW glasses.

Table E.12. %RSD Means of the Total, Batch-to-Batch Variations, and Within-Batch Uncertainties for IHLW Glass Properties of the AY-102 to AZ-102 Transition for All Combinations of the Factors at the Low and High Cases

Glass Property	%RSD Mean[a]	All Low Case	$\%RSD_S$[b]	$\%RSD_A$[b]	$\%RSD_B$[b]	$\%RSD_S$ $\%RSD_A$[b]	$\%RSD_S$ $\%RSD_B$[b]	$\%RSD_A$ $\%RSD_B$[b]	All High Case
PCT B	$\%RSD_T$	10.5	22.1	18.7	19.0	30.4	31.1	25.7	41.6
	$\%RSD_B$	4.1	5.6	5.4	5.4	6.3	7.5	6.0	8.6
	$\%RSD_W$	9.2	20.4	17.1	17.3	28.7	28.9	24	39.4
PCT Li	$\%RSD_T$	6.6	12.9	12.0	11.5	17.4	17.3	15.7	21.9
	$\%RSD_B$	1.9	3.1	3.0	2.9	3.7	4.1	3.5	5.0
	$\%RSD_W$	6.0	12.0	11.1	10.7	16.3	16.1	14.7	20.6
PCT Na	$\%RSD_T$	9.5	21.2	18.1	18.4	29.5	30.2	25.2	40.6
	$\%RSD_B$	2.0	4.8	4.3	4.4	5.6	6.4	5.7	8.0
	$\%RSD_W$	9.0	19.9	16.8	17.1	28.0	28.4	23.6	38.5
TCLP	$\%RSD_T$	7.4	14.8	10.9	11.9	17.7	18.4	14.7	22.0
	$\%RSD_B$	4.1	4.6	3.8	4.5	4.3	4.6	4.1	5.9
	$\%RSD_W$	5.8	13.4	9.7	10.4	16.4	17.1	13.5	20.2
T1 (Phase 1)	$\%RSD_T$	1.6	3.1	2.7	2.8	3.8	3.8	3.6	4.5
	$\%RSD_B$	0.4	0.7	0.6	0.6	0.8	0.8	0.8	1.1
	$\%RSD_W$	1.5	2.9	2.5	2.6	3.6	3.6	3.3	4.2
T1 (Phase 1a)	$\%RSD_T$	1.5	3.0	2.5	2.7	3.7	3.7	3.4	4.3
	$\%RSD_B$	0.4	0.7	0.5	0.6	0.8	0.8	0.8	1.1
	$\%RSD_W$	1.4	2.9	2.4	2.5	3.4	3.5	3.2	4.0
Viscosity 1373 K	$\%RSD_T$	13.7	26.8	24.7	23.7	33.9	32.6	31.6	39.2
	$\%RSD_B$	2.7	6.3	4.9	6.3	7.2	6.3	6.2	8.4
	$\%RSD_W$	13.0	25.0	23.3	21.9	31.9	30.9	29.9	36.7
Viscosity 1423 K	$\%RSD_T$	12.8	24.8	22.8	21.9	31.3	30.1	29.1	36.1
	$\%RSD_B$	2.5	5.9	4.6	5.8	6.7	5.8	5.7	7.8
	$\%RSD_W$	12.1	23.1	21.5	20.3	29.4	28.5	27.5	33.8
E.C.[c] 1373 K	$\%RSD_T$	6.4	10.4	10.3	9.6	13.6	13.0	12.6	16.3
	$\%RSD_B$	3.9	4.1	3.7	4.0	3.9	3.7	3.9	4.6
	$\%RSD_W$	4.9	9.1	9.1	8.2	12.4	11.9	11.4	15.0
E.C. 1473 K	$\%RSD_T$	6.1	9.7	9.8	9.1	12.9	12.2	12.0	15.4
	$\%RSD_B$	3.7	3.8	3.5	3.8	3.7	3.5	3.7	4.4
	$\%RSD_W$	4.7	8.5	8.7	7.8	11.7	11.1	10.9	14.1

(a) In the main body of the report bars were used over the %RSDs to denote means, but these tables have no room for the bars. Here, $\%RSD_T$ = mean total batch-to-batch variation and within-batch uncertainty %RSD, $\%RSD_B$ = mean batch-to-batch variation %RSD, and $\%RSD_W$ = mean within-batch uncertainty %RSD.

(b) All factors listed are at the high case whereas all others not listed are at the low case. The factor notation has been abbreviated from the notation used in the report to better fit in the table.

(c) E.C. represents electrical conductivity of HLW glasses.

Appendix F

Detailed Results on the Variations and Uncertainties of ILAW Composition and Properties

Appendix F: Detailed Results on the Variations and Uncertainties of ILAW Composition and Properties

This appendix presents additional details on the variation and uncertainty results of ILAW compositions and properties presented in Section 8.

F.1 Detailed Results on the Variations and Uncertainties of ILAW Chemical Composition

Figure 8.1 through Figure 8.3 graphically show the mean and 90% empirical confidence interval (90% ECI) summaries of %RSDs for batch-to-batch variation, within-batch uncertainty, and total variation plus uncertainty for each of the important ILAW chemical composition components for only the scenarios with all the factors at the low case and with all the factors at the high case. To show the %RSD results for other combinations of the factors, Tables F.1 to F.5 give the mean %RSD results for the nine most significant combinations from the scenarios listed in Table 5.4 for each of the five LAW data sets. The nine most significant scenarios include the "all low case" and the "all high case", as well as others determined by the factors having significant effects for a large percentage of the components. Tables F.1 to F.5 each list the mean %RSD results for each of the important ILAW chemical composition components. Each cell within a table displays the total variation plus uncertainty ($\overline{\%RSD_T}$) as the top number, the batch-to-batch variation ($\overline{\%RSD_B}$) as the middle number, and the within-batch uncertainty ($\overline{\%RSD_W}$) as the bottom number. The mean %RSD values were calculated using the individual %RSD values from the 200 simulations for each scenario represented by a column in the tables.

Table F.1. %RSD Means of the Total, Batch-to-Batch Variations, and Within-Batch Uncertainties for Important ILAW Chemical Composition Components of Set 1 (AP-101/AY-102) for the Statistically Significant Combinations of Factors

Component	%RSD Mean[a]	All Low Case	$\%RSD_S$[b]	$\%RSD_A$[b]	$SD(a^{GFC})$ $SD(G^{GFC})$[b]	$\%RSD_S$ $\%RSD_A$[b]	$\%RSD_S$ $SD(a^{GFC})$ $SD(G^{GFC})$[b]	$\%RSD_A$ $SD(a^{GFC})$ $SD(G^{GFC})$[b]	$\%RSD_S$ $\%RSD_A$ $SD(a^{GFC})$ $SD(G^{GFC})$[b]	All High Case
Al_2O_3	$\%RSD_T$	2.3	2.5	3.3	4.1	3.4	4.2	4.6	4.7	4.7
	$\%RSD_B$	0.2	0.2	0.2	0.2	0.2	0.2	0.2	0.2	0.2
	$\%RSD_W$	2.3	2.5	3.3	4.1	3.4	4.2	4.6	4.7	4.7
B_2O_3	$\%RSD_T$	1.3	1.4	2.3	1.8	2.4	1.9	2.7	2.6	2.6
	$\%RSD_B$	0.1	0.1	0.1	0.1	0.1	0.1	0.1	0.1	0.1
	$\%RSD_W$	1.3	1.4	2.3	1.8	2.4	1.9	2.7	2.6	2.6
CaO	$\%RSD_T$	3.2	3.1	3.6	5.9	3.8	5.9	6.3	6.3	6.3
	$\%RSD_B$	0.1	0.1	0.1	0.1	0.1	0.1	0.1	0.1	0.1
	$\%RSD_W$	3.2	3.1	3.6	5.9	3.8	5.9	6.3	6.3	6.3
Cl	$\%RSD_T$	5.7	6.5	11.5	5.8	12.1	6.5	11.4	11.7	11.4
	$\%RSD_B$	0.6	0.6	0.6	0.6	0.6	0.6	0.6	0.6	0.6
	$\%RSD_W$	5.6	6.4	11.5	5.8	12.1	6.5	11.4	11.7	11.4
Fe_2O_3	$\%RSD_T$	2.2	2.3	2.8	3.9	3.0	4.0	4.5	4.4	4.4
	$\%RSD_B$	0.1	0.1	0.1	0.1	0.1	0.1	0.1	0.1	0.1
	$\%RSD_W$	2.2	2.3	2.8	3.9	3.0	4.0	4.5	4.4	4.4
K_2O	$\%RSD_T$	3.0	4.0	5.9	3.1	6.5	4.1	6.2	6.5	6.6
	$\%RSD_B$	0.6	0.6	0.6	0.6	0.6	0.6	0.6	0.6	0.6
	$\%RSD_W$	3.0	3.9	5.9	3.1	6.4	4.0	6.1	6.5	6.6
Li_2O	$\%RSD_T$	8.8	9.5	17.0	8.4	16.8	8.9	17.2	17.1	17.2
	$\%RSD_B$	0.7	0.7	0.7	0.7	0.7	0.7	0.7	0.7	0.7
	$\%RSD_W$	8.8	9.5	17.0	8.3	16.7	8.8	17.2	17.1	17.2
MgO	$\%RSD_T$	2.5	2.6	3.2	4.6	3.2	4.7	5.1	5.0	5.0
	$\%RSD_B$	0.1	0.1	0.1	0.1	0.1	0.1	0.1	0.1	0.1
	$\%RSD_W$	2.5	2.6	3.2	4.6	3.2	4.7	5.1	5.0	5.0
Na_2O	$\%RSD_T$	4.6	5.1	8.9	4.5	9.3	5.2	9.4	9.2	9.1
	$\%RSD_B$	0.4	0.4	0.4	0.4	0.4	0.4	0.4	0.4	0.5
	$\%RSD_W$	4.6	5.1	8.9	4.5	9.3	5.2	9.4	9.2	9.0
P_2O_5	$\%RSD_T$	8.0	8.5	15.4	8.3	15.8	8.9	15.6	15.7	16.0
	$\%RSD_B$	0.6	0.6	0.6	0.6	0.6	0.6	0.6	0.6	0.6
	$\%RSD_W$	8.0	8.5	15.4	8.2	15.8	8.9	15.6	15.7	16.0
SiO_2	$\%RSD_T$	1.2	1.3	2.2	1.3	2.3	1.4	2.4	2.4	2.3
	$\%RSD_B$	0.1	0.1	0.1	0.1	0.1	0.1	0.1	0.1	0.1
	$\%RSD_W$	1.2	1.3	2.2	1.3	2.3	1.4	2.4	2.4	2.3
SO_3	$\%RSD_T$	5.6	6.4	11.2	5.8	11.5	6.4	11.5	11.7	12.0
	$\%RSD_B$	0.6	0.6	0.6	0.6	0.6	0.6	0.6	0.6	0.6
	$\%RSD_W$	5.6	6.4	11.1	5.7	11.4	6.3	11.5	11.7	12.0
ZnO	$\%RSD_T$	2.2	2.3	2.9	4.1	3.0	4.1	4.4	4.4	4.6
	$\%RSD_B$	0.1	0.1	0.1	0.1	0.1	0.1	0.1	0.1	0.1
	$\%RSD_W$	2.2	2.3	2.9	4.1	3.0	4.1	4.4	4.4	4.6
ZrO_2	$\%RSD_T$	2.3	2.3	3.0	4.2	3.1	4.2	4.4	4.5	4.5
	$\%RSD_B$	0.1	0.1	0.1	0.1	0.1	0.1	0.1	0.1	0.1
	$\%RSD_W$	2.3	2.3	3.0	4.2	3.1	4.2	4.4	4.5	4.5

(a) In the main body of the report bars were used over the %RSDs to denote means, but these tables have no room for the bars. Here, $\%RSD_T$ = mean total batch-to-batch variation and within-batch uncertainty %RSD, $\%RSD_B$ = mean batch-to-batch variation %RSD, and $\%RSD_W$ = mean within-batch uncertainty %RSD.

(b) All factors listed are at the high case whereas all others not listed are at the low case. All factors that are not included within any of these columns were not significant according to the ANOVA. Hence, they were held constant at the low (nominal) uncertainty case. The factor notation has been abbreviated from the notation used in the report to better fit in the table.

Table F.2. %RSD Means of the Total, Batch-to-Batch Variations, and Within-Batch Uncertainties for Important ILAW Chemical Composition Components of Set 2 (transition from AP-101/AY-102 to AZ-101) for the Statistically Significant Combinations of Factors

Component	%RSD Mean[a]	All Low Case	$\%RSD_S$[b]	$\%RSD_A$[b]	$SD(a^{GFC})$ $SD(G^{GFC})$[b]	$\%RSD_S$ $\%RSD_A$[b]	$\%RSD_S$ $SD(a^{GFC})$ $SD(G^{GFC})$[b]	$\%RSD_A$ $SD(a^{GFC})$ $SD(G^{GFC})$[b]	$\%RSD_S$ $\%RSD_A$ $SD(a^{GFC})$ $SD(G^{GFC})$[b]	All High Case
Al_2O_3	$\%RSD_T$	2.3	2.4	3.0	4.0	3.0	4.2	4.6	4.6	4.5
	$\%RSD_B$	0.2	0.2	0.2	0.2	0.2	0.2	0.2	0.2	0.2
	$\%RSD_W$	2.3	2.4	3.0	4.0	3.0	4.2	4.5	4.6	4.5
B_2O_3	$\%RSD_T$	1.2	1.3	1.9	1.7	2.0	1.7	2.3	2.4	2.4
	$\%RSD_B$	0.1	0.1	0.1	0.1	0.1	0.1	0.1	0.1	0.1
	$\%RSD_W$	1.2	1.3	1.9	1.7	2.0	1.7	2.3	2.4	2.4
CaO	$\%RSD_T$	7.7	7.7	7.8	8.5	7.9	8.5	8.8	8.9	8.8
	$\%RSD_B$	7.3	7.3	7.3	7.3	7.3	7.3	7.3	7.3	7.3
	$\%RSD_W$	2.4	2.6	2.9	4.4	3.1	4.4	4.9	5.1	5.0
Cl	$\%RSD_T$	9.1	9.5	13.2	9.1	13.2	9.4	13.4	13.3	13.5
	$\%RSD_B$	6.8	6.8	6.8	6.8	6.8	6.8	6.8	6.8	6.8
	$\%RSD_W$	6.0	6.6	11.3	6.1	11.3	6.5	11.5	11.5	11.6
Fe_2O_3	$\%RSD_T$	2.1	2.2	2.6	3.9	2.7	3.8	4.1	4.2	4.2
	$\%RSD_B$	0.1	0.1	0.1	0.1	0.1	0.1	0.1	0.1	0.1
	$\%RSD_W$	2.1	2.2	2.6	3.9	2.7	3.8	4.1	4.2	4.2
K_2O	$\%RSD_T$	6.5	7.1	8.2	6.6	8.7	7.0	8.2	8.6	8.4
	$\%RSD_B$	5.8	5.8	5.8	5.8	5.8	5.8	5.8	5.8	5.8
	$\%RSD_W$	2.9	4.0	5.8	3.0	6.5	3.9	5.8	6.3	6.1
Li_2O	$\%RSD_T$	22.7	22.6	22.6	22.6	22.6	22.8	22.9	22.9	22.9
	$\%RSD_B$	22.5	22.5	22.5	22.5	22.5	22.5	22.5	22.5	22.5
	$\%RSD_W$	3.1	2.1	2.6	2.9	2.6	4.1	4.3	4.6	4.3
MgO	$\%RSD_T$	2.4	2.5	2.8	4.7	3.0	4.7	4.9	5.1	4.8
	$\%RSD_B$	0.1	0.1	0.1	0.1	0.1	0.1	0.1	0.1	0.1
	$\%RSD_W$	2.4	2.5	2.8	4.7	3.0	4.7	4.9	5.1	4.8
Na_2O	$\%RSD_T$	5.6	5.9	9.5	5.6	10.0	6.0	9.8	10.0	10.0
	$\%RSD_B$	2.9	2.9	2.9	2.9	2.9	2.9	2.9	2.9	2.9
	$\%RSD_W$	4.8	5.1	9.0	4.7	9.6	5.2	9.4	9.6	9.6
P_2O_5	$\%RSD_T$	8.9	9.8	16.1	9.2	17.0	9.5	16.5	17.0	16.5
	$\%RSD_B$	4.4	4.4	4.4	4.4	4.4	4.4	4.4	4.4	4.3
	$\%RSD_W$	7.8	8.7	15.5	8.1	16.4	8.4	15.9	16.4	15.9
SiO_2	$\%RSD_T$	1.0	1.2	1.9	1.2	2.0	1.3	2.0	2.0	2.0
	$\%RSD_B$	0.4	0.4	0.4	0.4	0.4	0.4	0.4	0.4	0.4
	$\%RSD_W$	1.0	1.1	1.8	1.2	1.9	1.3	2.0	2.0	2.0
SO_3	$\%RSD_T$	6.2	6.6	11.6	6.1	11.9	6.9	11.5	11.7	11.8
	$\%RSD_B$	2.5	2.5	2.5	2.5	2.5	2.5	2.5	2.5	2.5
	$\%RSD_W$	5.7	6.1	11.3	5.6	11.7	6.4	11.2	11.4	11.5
ZnO	$\%RSD_T$	2.1	2.2	2.6	3.9	2.7	3.9	4.3	4.3	4.1
	$\%RSD_B$	0.1	0.1	0.1	0.1	0.1	0.1	0.1	0.1	0.1
	$\%RSD_W$	2.1	2.2	2.6	3.9	2.7	3.9	4.3	4.3	4.1
ZrO_2	$\%RSD_T$	2.2	2.2	2.7	4.0	2.7	4.1	4.3	4.4	4.3
	$\%RSD_B$	0.1	0.1	0.1	0.1	0.1	0.1	0.1	0.1	0.1
	$\%RSD_W$	2.2	2.2	2.7	4.0	2.7	4.1	4.3	4.4	4.3

(a) In the main body of the report bars were used over the %RSDs to denote means, but these tables have no room for the bars. Here, $\%RSD_T$ = mean total batch-to-batch variation and within-batch uncertainty %RSD, $\%RSD_B$ = mean batch-to-batch variation %RSD, and $\%RSD_W$ = mean within-batch uncertainty %RSD.

(b) All factors listed are at the high case whereas all others not listed are at the low case. All factors that are not included within any of these columns were not significant according to the ANOVA. Hence, they were held constant at the low (nominal) uncertainty case. The factor notation has been abbreviated from the notation used in the report to better fit in the table.

Table F.3. %RSD Means of the Total, Batch-to-Batch Variations, and Within-Batch Uncertainties for Important ILAW Chemical Composition Components of Set 3 (AZ-102) for the Statistically Significant Combinations of Factors

Component	%RSD Mean[a]	All Low Case	$\%RSD_S$[b]	$\%RSD_A$[b]	$SD(a^{GFC})$ $SD(G^{GFC})$[b]	$\%RSD_S$ $\%RSD_A$[b]	$\%RSD_S$ $SD(a^{GFC})$ $SD(G^{GFC})$[b]	$\%RSD_A$ $SD(a^{GFC})$ $SD(G^{GFC})$[b]	$\%RSD_S$ $\%RSD_A$ $SD(a^{GFC})$ $SD(G^{GFC})$[b]	All High Case
Al_2O_3	$\%RSD_T$	1.8	1.9	2.1	3.6	2.1	3.6	3.6	3.6	3.7
	$\%RSD_B$	0.08	0.08	0.08	0.08	0.08	0.08	0.08	0.08	0.09
	$\%RSD_W$	1.8	1.9	2.1	3.6	2.1	3.6	3.6	3.6	3.7
B_2O_3	$\%RSD_T$	0.8	0.8	1.1	1.5	1.1	1.5	1.6	1.7	1.6
	$\%RSD_B$	0.04	0.04	0.04	0.04	0.04	0.04	0.04	0.04	0.04
	$\%RSD_W$	0.8	0.8	1.1	1.5	1.1	1.5	1.6	1.7	1.6
CaO	$\%RSD_T$	2.3	2.3	2.4	4.6	2.4	4.5	4.6	4.5	4.5
	$\%RSD_B$	0.04	0.04	0.04	0.04	0.04	0.04	0.04	0.04	0.04
	$\%RSD_W$	2.3	2.3	2.4	4.6	2.4	4.5	4.6	4.5	4.5
Cl	$\%RSD_T$	5.7	6.4	11.0	5.6	11.7	6.4	11.5	11.3	11.4
	$\%RSD_B$	0.5	0.5	0.5	0.5	0.5	0.5	0.5	0.5	0.5
	$\%RSD_W$	5.7	6.4	11.0	5.6	11.7	6.4	11.5	11.3	11.4
Fe_2O_3	$\%RSD_T$	1.4	1.5	1.6	2.8	1.6	2.8	2.9	2.9	2.9
	$\%RSD_B$	0.04	0.04	0.04	0.04	0.04	0.04	0.04	0.04	0.04
	$\%RSD_W$	1.4	1.5	1.6	2.8	1.6	2.8	2.9	2.9	2.9
K_2O	$\%RSD_T$	3.0	4.0	5.6	3.0	6.5	4.2	5.8	6.5	6.5
	$\%RSD_B$	0.6	0.6	0.6	0.6	0.6	0.6	0.6	0.6	0.6
	$\%RSD_W$	3.0	3.9	5.6	2.9	6.5	4.2	5.7	6.5	6.5
Li_2O	$\%RSD_T$	0.9	0.9	1.1	1.6	1.1	1.5	1.7	1.8	1.8
	$\%RSD_B$	0.04	0.04	0.04	0.04	0.04	0.04	0.04	0.04	0.04
	$\%RSD_W$	0.9	0.9	1.1	1.6	1.1	1.5	1.7	1.8	1.8
MgO	$\%RSD_T$	1.5	1.5	1.6	2.9	1.6	2.9	3.0	2.9	3.0
	$\%RSD_B$	0.04	0.04	0.04	0.04	0.04	0.04	0.04	0.04	0.04
	$\%RSD_W$	1.5	1.5	1.6	2.9	1.6	2.9	3.0	2.9	3.0
Na_2O	$\%RSD_T$	5.2	5.6	10.5	5.2	10.7	5.8	10.3	10.7	10.5
	$\%RSD_B$	0.5	0.5	0.5	0.5	0.5	0.5	0.5	0.5	0.5
	$\%RSD_W$	5.1	5.6	10.5	5.1	10.7	5.8	10.3	10.7	10.5
P_2O_5	$\%RSD_T$	9.0	9.3	13.8	14.8	13.8	14.5	17.1	17.6	17.3
	$\%RSD_B$	0.4	0.4	0.4	0.4	0.4	0.4	0.4	0.4	0.4
	$\%RSD_W$	9.0	9.2	13.8	14.8	13.8	14.5	17.1	17.5	17.3
SiO_2	$\%RSD_T$	0.5	0.6	0.9	0.9	0.9	0.9	1.1	1.1	1.1
	$\%RSD_B$	0.04	0.04	0.04	0.04	0.04	0.04	0.04	0.04	0.04
	$\%RSD_W$	0.5	0.6	0.9	0.9	0.9	0.9	1.1	1.1	1.1
SO_3	$\%RSD_T$	5.6	6.2	10.9	5.6	11.3	6.3	10.9	11.5	11.3
	$\%RSD_B$	0.6	0.6	0.6	0.6	0.6	0.6	0.6	0.6	0.6
	$\%RSD_W$	5.6	6.2	10.9	5.6	11.3	6.2	10.9	11.5	11.3
ZnO	$\%RSD_T$	2.0	2.0	2.1	3.9	2.0	3.9	3.9	3.9	4.0
	$\%RSD_B$	0.04	0.04	0.04	0.04	0.04	0.04	0.04	0.04	0.04
	$\%RSD_W$	2.0	2.0	2.1	3.9	2.0	3.9	3.9	3.9	4.0
ZrO_2	$\%RSD_T$	1.0	1.1	1.3	1.9	1.3	1.9	2.0	2.1	2.0
	$\%RSD_B$	0.04	0.04	0.04	0.04	0.04	0.04	0.04	0.04	0.04
	$\%RSD_W$	1.0	1.1	1.3	1.9	1.3	1.9	2.0	2.1	2.0

(a) In the main body of the report bars were used over the %RSDs to denote means, but these tables have no room for the bars. Here, $\%RSD_T$ = mean total batch-to-batch variation and within-batch uncertainty %RSD, $\%RSD_B$ = mean batch-to-batch variation %RSD, and $\%RSD_W$ = mean within-batch uncertainty %RSD.

(b) All factors listed are at the high case whereas all others not listed are at the low case. All factors that are not included within any of these columns were not significant according to the ANOVA. Hence, they were held constant at the low (nominal) uncertainty case. The factor notation has been abbreviated from the notation used in the report to better fit in the table.

Table F.4. %RSD Means of the Total, Batch-to-Batch Variations, and Within-Batch Uncertainties for Important ILAW Chemical Composition Components of Set 4 (AN-102) for the Statistically Significant Combinations of Factors

Component	%RSD Mean[a]	All Low Case	$\%RSD_S$[b]	$\%RSD_A$[b]	$SD(a^{GFC})$ $SD(G^{GFC})$[b]	$\%RSD_S$ $\%RSD_A$[b]	$\%RSD_S$ $SD(a^{GFC})$ $SD(G^{GFC})$[b]	$\%RSD_A$ $SD(a^{GFC})$ $SD(G^{GFC})$[b]	$\%RSD_S$ $\%RSD_A$ $SD(a^{GFC})$ $SD(G^{GFC})$[b]	All High Case
Al_2O_3	$\%RSD_T$	2.3	2.8	4.1	2.8	4.4	3.4	4.5	4.8	4.7
	$\%RSD_B$	0.3	0.3	0.3	0.3	0.3	0.3	0.3	0.3	0.3
	$\%RSD_W$	2.2	2.7	4.0	2.8	4.4	3.4	4.5	4.8	4.7
B_2O_3	$\%RSD_T$	1.3	1.4	2.2	1.8	2.4	1.8	2.6	2.5	2.7
	$\%RSD_B$	0.1	0.1	0.1	0.1	0.1	0.1	0.1	0.1	0.1
	$\%RSD_W$	1.3	1.4	2.2	1.8	2.4	1.8	2.6	2.5	2.7
CaO	$\%RSD_T$	3.1	3.1	3.5	5.9	3.7	6.0	6.3	6.3	6.2
	$\%RSD_B$	0.1	0.1	0.1	0.1	0.1	0.1	0.1	0.1	0.1
	$\%RSD_W$	3.1	3.1	3.5	5.9	3.7	6.0	6.3	6.3	6.2
Cl	$\%RSD_T$	5.7	6.4	11.2	5.7	12.0	6.6	11.6	11.5	11.8
	$\%RSD_B$	0.7	0.7	0.7	0.7	0.7	0.7	0.7	0.7	0.7
	$\%RSD_W$	5.7	6.4	11.2	5.7	12.0	6.5	11.6	11.5	11.8
Fe_2O_3	$\%RSD_T$	2.1	2.2	2.9	4.0	3.0	4.0	4.3	4.4	4.3
	$\%RSD_B$	0.1	0.1	0.1	0.1	0.1	0.1	0.1	0.1	0.1
	$\%RSD_W$	2.1	2.2	2.9	4.0	3.0	4.0	4.3	4.4	4.3
K_2O	$\%RSD_T$	3.1	4.1	6.1	3.2	6.7	4.2	6.2	6.6	6.7
	$\%RSD_B$	0.6	0.6	0.6	0.6	0.6	0.6	0.6	0.6	0.6
	$\%RSD_W$	3.0	4.0	6.0	3.1	6.7	4.1	6.2	6.6	6.7
Li_2O	$\%RSD_T$	8.4	8.8	16.6	8.7	17.3	8.9	17.4	17.3	17.2
	$\%RSD_B$	0.6	0.6	0.6	0.6	0.6	0.6	0.6	0.6	0.6
	$\%RSD_W$	8.4	8.8	16.6	8.7	17.3	8.9	17.4	17.3	17.2
MgO	$\%RSD_T$	2.4	2.5	3.1	4.7	3.2	4.6	4.9	5.0	5.1
	$\%RSD_B$	0.1	0.1	0.1	0.1	0.1	0.1	0.1	0.1	0.1
	$\%RSD_W$	2.4	2.5	3.1	4.7	3.2	4.6	4.9	4.9	5.1
Na_2O	$\%RSD_T$	4.6	5.1	8.8	4.7	9.8	5.0	9.3	9.3	9.6
	$\%RSD_B$	0.5	0.5	0.5	0.5	0.5	0.5	0.5	0.5	0.5
	$\%RSD_W$	4.5	5.1	8.8	4.7	9.8	5.0	9.3	9.3	9.6
P_2O_5	$\%RSD_T$	8.3	8.4	16.4	8.3	16.4	8.5	16.1	16.2	16.1
	$\%RSD_B$	0.6	0.6	0.6	0.6	0.6	0.6	0.6	0.6	0.6
	$\%RSD_W$	8.2	8.4	16.4	8.3	16.4	8.5	16.1	16.2	16.1
SiO_2	$\%RSD_T$	1.1	1.3	2.1	1.3	2.3	1.4	2.3	2.3	2.4
	$\%RSD_B$	0.1	0.1	0.1	0.1	0.1	0.1	0.1	0.1	0.1
	$\%RSD_W$	1.1	1.3	2.1	1.3	2.3	1.4	2.3	2.3	2.4
SO_3	$\%RSD_T$	5.7	6.2	11.8	5.7	11.9	6.3	11.4	11.8	11.7
	$\%RSD_B$	0.6	0.6	0.6	0.6	0.6	0.6	0.6	0.6	0.6
	$\%RSD_W$	5.7	6.1	11.7	5.6	11.9	6.2	11.4	11.7	11.7
ZnO	$\%RSD_T$	2.2	2.2	2.8	4.1	3.0	4.0	4.4	4.5	4.4
	$\%RSD_B$	0.1	0.1	0.1	0.1	0.1	0.1	0.1	0.1	0.1
	$\%RSD_W$	2.2	2.2	2.8	4.1	3.0	4.0	4.4	4.5	4.4
ZrO_2	$\%RSD_T$	2.2	2.3	2.9	4.0	3.0	4.1	4.4	4.5	4.5
	$\%RSD_B$	0.1	0.1	0.1	0.1	0.1	0.1	0.1	0.1	0.1
	$\%RSD_W$	2.2	2.3	2.9	4.0	3.0	4.1	4.4	4.5	4.5

(a) In the main body of the report bars were used over the %RSDs to denote means, but these tables have no room for the bars. Here, $\%RSD_T$ = mean total batch-to-batch variation and within-batch uncertainty %RSD, $\%RSD_B$ = mean batch-to-batch variation %RSD, and $\%RSD_W$ = mean within-batch uncertainty %RSD.

(b) All factors listed are at the high case whereas all others not listed are at the low case. All factors that are not included within any of these columns were not significant according to the ANOVA. Hence, they were held constant at the low (nominal) uncertainty case. The factor notation has been abbreviated from the notation used in the report to better fit in the table.

Table F.5. %RSD Means of the Total, Batch-to-Batch Variations, and Within-Batch Uncertainties for Important ILAW Chemical Composition Components of Set 5 (unknown tank) for the Statistically Significant Combinations of Factors

Component	%RSD Mean[a]	All Low Case	$\%RSD_S$[b]	$\%RSD_A$[b]	$SD(a^{GFC})$ $SD(G^{GFC})$[b]	$\%RSD_S$ $\%RSD_A$[b]	$\%RSD_S$ $SD(a^{GFC})$ $SD(G^{GFC})$[b]	$\%RSD_A$ $SD(a^{GFC})$ $SD(G^{GFC})$[b]	$\%RSD_S$ $\%RSD_A$ $SD(a^{GFC})$ $SD(G^{GFC})$[b]	All High Case
Al_2O_3	$\%RSD_T$	2.1	2.5	3.1	3.4	3.4	3.5	3.9	4.4	4.3
	$\%RSD_B$	0.2	0.2	0.2	0.2	0.2	0.2	0.2	0.2	0.2
	$\%RSD_W$	2.1	2.5	3.1	3.4	3.4	3.5	3.9	4.4	4.3
B_2O_3	$\%RSD_T$	1.1	1.1	1.7	1.7	1.8	1.7	2.2	2.2	2.1
	$\%RSD_B$	0.1	0.1	0.1	0.1	0.1	0.1	0.1	0.1	0.1
	$\%RSD_W$	1.1	1.1	1.7	1.7	1.8	1.7	2.2	2.2	2.1
CaO	$\%RSD_T$	2.4	2.4	2.8	4.6	2.8	4.7	4.8	4.7	4.9
	$\%RSD_B$	0.1	0.1	0.1	0.1	0.1	0.1	0.1	0.1	0.1
	$\%RSD_W$	2.4	2.4	2.8	4.6	2.8	4.7	4.8	4.7	4.9
Cl	$\%RSD_T$	5.9	6.4	11.2	5.8	12.1	6.5	11.3	11.7	11.8
	$\%RSD_B$	0.6	0.6	0.6	0.6	0.6	0.6	0.6	0.6	0.6
	$\%RSD_W$	5.9	6.4	11.2	5.8	12.1	6.4	11.3	11.7	11.8
Fe_2O_3	$\%RSD_T$	2.1	2.1	2.4	3.8	2.6	4.0	4.1	4.1	4.1
	$\%RSD_B$	0.1	0.1	0.1	0.1	0.1	0.1	0.1	0.1	0.1
	$\%RSD_W$	2.1	2.1	2.4	3.8	2.6	4.0	4.1	4.1	4.1
K_2O	$\%RSD_T$	3.1	4.1	5.9	3.2	6.5	4.1	6.0	6.5	6.6
	$\%RSD_B$	0.8	0.8	0.8	0.8	0.8	0.8	0.8	0.8	0.8
	$\%RSD_W$	3.0	4.1	5.9	3.1	6.4	4.0	6.0	6.4	6.5
Li_2O	$\%RSD_T$	1.1	1.2	1.8	1.7	1.8	1.8	2.3	2.2	2.2
	$\%RSD_B$	0.1	0.1	0.1	0.1	0.1	0.1	0.1	0.1	0.1
	$\%RSD_W$	1.1	1.1	1.8	1.7	1.8	1.8	2.3	2.2	2.2
MgO	$\%RSD_T$	2.5	2.4	2.7	4.6	2.8	4.6	4.8	4.6	4.8
	$\%RSD_B$	0.1	0.1	0.1	0.1	0.1	0.1	0.1	0.1	0.1
	$\%RSD_W$	2.5	2.4	2.7	4.6	2.8	4.6	4.8	4.6	4.8
Na_2O	$\%RSD_T$	4.9	5.4	9.6	4.9	10.0	5.4	9.8	9.9	10.0
	$\%RSD_B$	0.5	0.5	0.5	0.5	0.5	0.5	0.5	0.5	0.5
	$\%RSD_W$	4.9	5.3	9.6	4.9	10.0	5.4	9.8	9.9	10.0
P_2O_5	$\%RSD_T$	8.1	8.8	16.1	8.2	16.0	8.9	15.6	16.2	15.8
	$\%RSD_B$	0.6	0.6	0.6	0.6	0.6	0.6	0.6	0.6	0.6
	$\%RSD_W$	8.1	8.8	16.1	8.2	15.9	8.8	15.6	16.1	15.8
SiO_2	$\%RSD_T$	0.9	1.0	1.6	1.1	1.7	1.2	1.8	1.8	1.8
	$\%RSD_B$	0.1	0.1	0.1	0.1	0.1	0.1	0.1	0.1	0.1
	$\%RSD_W$	0.9	1.0	1.6	1.1	1.7	1.2	1.8	1.8	1.8
SO_3	$\%RSD_T$	5.7	6.2	11.1	5.6	11.6	6.3	11.4	11.5	11.6
	$\%RSD_B$	0.6	0.6	0.6	0.6	0.6	0.6	0.6	0.6	0.6
	$\%RSD_W$	5.7	6.2	11.1	5.6	11.5	6.3	11.3	11.5	11.5
ZnO	$\%RSD_T$	2.0	2.1	2.5	4.0	2.5	4.1	4.2	4.1	4.2
	$\%RSD_B$	0.1	0.1	0.1	0.1	0.1	0.1	0.1	0.1	0.1
	$\%RSD_W$	2.0	2.1	2.5	4.0	2.5	4.1	4.2	4.1	4.2
ZrO_2	$\%RSD_T$	2.1	2.2	2.5	4.1	2.6	4.1	4.4	4.2	4.4
	$\%RSD_B$	0.1	0.1	0.1	0.1	0.1	0.1	0.1	0.1	0.1
	$\%RSD_W$	2.1	2.2	2.5	4.1	2.6	4.1	4.4	4.2	4.4

(a) In the main body of the report bars were used over the %RSDs to denote means, but these tables have no room for the bars. Here, $\%RSD_T$ = mean total batch-to-batch variation and within-batch uncertainty %RSD, $\%RSD_B$ = mean batch-to-batch variation %RSD, and $\%RSD_W$ = mean within-batch uncertainty %RSD.

(b) All factors listed are at the high case whereas all others not listed are at the low case. All factors that are not included within any of these columns were not significant according to the ANOVA. Hence, they were held constant at the low (nominal) uncertainty case. The factor notation has been abbreviated from the notation used in the report to better fit in the table.

F.2 Detailed Results on the Variations and Uncertainties of ILAW Radionuclide Composition

Figure 8.4 through Figure 8.6 graphically show the mean and 90% ECI summaries of %RSDs for batch-to-batch variation, within-batch uncertainty, and total variation plus uncertainty for each of the important ILAW radionuclide composition components for only the scenarios with all the factors at the low case and with all the factors at the high case. To show the %RSD results for other combinations of the factors, Tables F.6 to F.10 give the mean %RSD results for the nine most significant combinations from the scenarios listed in Table 5.4 for each of the five LAW data sets. The nine most significant scenarios include the "all low case" and the "all high case," as well as others determined by the factors having significant effects for a large percentage of the components. Tables F.6 to F.10 each list the mean %RSD results for each of the important ILAW radionuclide composition components. Each cell within a table displays the total variation plus uncertainty ($\overline{\%RSD_T}$) as the top number, the batch-to-batch variation ($\overline{\%RSD_B}$) as the middle number, and the within-batch uncertainty ($\overline{\%RSD_W}$) as the bottom number. The mean %RSD values were calculated using the individual %RSD values from the 200 simulations for each scenario represented by a column in the tables.

Table F.6. %RSD Means of the Total, Batch-to-Batch Variations, and Within-Batch Uncertainties for Important ILAW Radionuclide Composition Components of Set 1 (AP-101/AY-102) for the Statistically Significant Combinations of Factors

Component	%RSD Mean[a]	All Low Case	$\%RSD_S$[b]	$\%RSD_A$[b]	$SD(a^{GFC})$ $SD(G^{GFC})$[b]	$\%RSD_S$ $\%RSD_A$[b]	$\%RSD_S$ $SD(a^{GFC})$ $SD(G^{GFC})$[b]	$\%RSD_A$ $SD(a^{GFC})$ $SD(G^{GFC})$[b]	$\%RSD_S$ $\%RSD_A$ $SD(a^{GFC})$ $SD(G^{GFC})$[b]	All High Case
^{60}CoO	$\%RSD_T$	3.2	4.1	6.1	3.2	6.7	4.2	6.1	6.7	6.9
	$\%RSD_B$	0.6	0.6	0.6	0.6	0.6	0.6	0.6	0.6	0.6
	$\%RSD_W$	3.1	4.1	6.0	3.1	6.7	4.2	6.0	6.6	6.8
^{63}NiO	$\%RSD_T$	5.9	6.5	11.5	5.8	11.7	6.7	11.3	12.0	11.8
	$\%RSD_B$	0.7	0.7	0.7	0.7	0.7	0.7	0.7	0.7	0.6
	$\%RSD_W$	5.8	6.4	11.5	5.8	11.7	6.6	11.2	12.0	11.8
^{90}SrO	$\%RSD_T$	3.2	4.2	6.3	3.2	6.8	4.3	6.1	6.9	6.8
	$\%RSD_B$	0.6	0.6	0.6	0.6	0.6	0.6	0.6	0.6	0.6
	$\%RSD_W$	3.1	4.1	6.3	3.2	6.8	4.3	6.1	6.8	6.7
$^{99}Tc_2O_7$	$\%RSD_T$	6.0	6.4	11.5	5.8	11.9	6.4	11.7	11.9	12.0
	$\%RSD_B$	0.9	0.9	0.9	0.9	0.9	0.9	0.9	0.9	0.9
	$\%RSD_W$	5.9	6.4	11.5	5.7	11.9	6.3	11.6	11.8	12.0
$^{125}Sb_2O_3$	$\%RSD_T$	14.1	15.2	27.5	13.6	27.3	15.0	27.6	27.6	26.8
	$\%RSD_B$	0.6	0.6	0.6	0.6	0.6	0.6	0.6	0.6	0.6
	$\%RSD_W$	14.1	15.2	27.5	13.6	27.3	15.0	27.6	27.6	26.8
$^{137}Cs_2O$	$\%RSD_T$	8.6	9.0	17.0	8.5	17.2	9.0	16.8	17.2	17.5
	$\%RSD_B$	0.6	0.6	0.6	0.6	0.6	0.6	0.6	0.6	0.6
	$\%RSD_W$	8.5	8.9	17.0	8.5	17.1	9.0	16.7	17.2	17.5
$^{151}Sm_2O_3$	$\%RSD_T$	11.2	11.9	22.3	11.3	23.0	11.4	22.5	22.3	22.1
	$\%RSD_B$	0.6	0.6	0.6	0.6	0.6	0.6	0.6	0.6	0.6
	$\%RSD_W$	11.2	11.9	22.3	11.3	23.0	11.4	22.5	22.3	22.1
$^{154}Eu_2O_3$	$\%RSD_T$	3.2	4.3	6.1	3.3	6.8	4.3	6.2	6.7	6.6
	$\%RSD_B$	0.6	0.6	0.6	0.6	0.6	0.6	0.6	0.6	0.6
	$\%RSD_W$	3.1	4.3	6.0	3.2	6.8	4.2	6.2	6.7	6.5
$^{155}Eu_2O_3$	$\%RSD_T$	3.2	4.2	6.0	3.2	6.8	4.2	6.3	6.9	6.7
	$\%RSD_B$	0.6	0.6	0.6	0.6	0.6	0.6	0.6	0.6	0.6
	$\%RSD_W$	3.2	4.2	6.0	3.1	6.8	4.2	6.3	6.8	6.6
$^{233}UO_3$	$\%RSD_T$	6.0	6.4	12.1	5.8	11.8	6.7	11.6	11.8	12.2
	$\%RSD_B$	0.6	0.6	0.6	0.6	0.6	0.6	0.6	0.6	0.6
	$\%RSD_W$	5.9	6.4	12.1	5.8	11.8	6.6	11.6	11.8	12.1
$^{235}UO_3$	$\%RSD_T$	5.7	6.2	11.5	5.8	11.8	6.6	11.5	12.2	12.0
	$\%RSD_B$	0.6	0.6	0.6	0.6	0.6	0.6	0.6	0.6	0.6
	$\%RSD_W$	5.7	6.2	11.4	5.8	11.8	6.6	11.5	12.2	11.9
$^{237}NpO_2$	$\%RSD_T$	5.9	6.5	11.8	5.8	11.8	6.6	11.4	12.3	11.9
	$\%RSD_B$	0.7	0.7	0.7	0.7	0.7	0.7	0.7	0.7	0.7
	$\%RSD_W$	5.9	6.5	11.8	5.7	11.8	6.6	11.4	12.2	11.8
$^{238}UO_3$	$\%RSD_T$	5.7	6.4	11.3	5.8	11.8	6.6	11.6	11.8	12.3
	$\%RSD_B$	0.6	0.6	0.6	0.6	0.6	0.6	0.6	0.6	0.7
	$\%RSD_W$	5.7	6.4	11.3	5.8	11.7	6.5	11.5	11.7	12.3
$^{238}PuO_2$	$\%RSD_T$	3.1	4.2	6.4	3.2	6.8	4.3	6.2	6.7	6.6
	$\%RSD_B$	0.7	0.7	0.7	0.7	0.7	0.7	0.7	0.7	0.7
	$\%RSD_W$	3.0	4.1	6.3	3.2	6.8	4.3	6.2	6.6	6.6

(a) In the main body of the report bars were used over the %RSDs to denote means, but these tables have no room for the bars. Here, $\%RSD_T$ = mean total batch-to-batch variation and within-batch uncertainty %RSD, $\%RSD_B$ = mean batch-to-batch variation %RSD, and $\%RSD_W$ = mean within-batch uncertainty %RSD.

(b) All factors listed are at the high case whereas all others not listed are at the low case. All factors that are not included within any of these columns were not significant according to the ANOVA. Hence, they were held constant at the low (nominal) uncertainty case. The factor notation has been abbreviated from the notation used in the report to better fit in the table.

Table F.6. %RSD Means of the Total, Batch-to-Batch Variations, and Within-Batch Uncertainties for Important ILAW Radionuclide Composition Components of Set 1 (AP-101/AY-102) for the Statistically Significant Combinations of Factors (cont'd)

Component	%RSD Mean[a]	All Low Case	$\%RSD_S$[b]	$\%RSD_A$[b]	$SD(a^{GFC})$ $SD(G^{GFC})$[b]	$\%RSD_S$ $\%RSD_A$[b]	$\%RSD_S$ $SD(a^{GFC})$ $SD(G^{GFC})$[b]	$\%RSD_A$ $SD(a^{GFC})$ $SD(G^{GFC})$[b]	$\%RSD_S$ $\%RSD_A$ $SD(a^{GFC})$ $SD(G^{GFC})$[b]	All High Case
$^{239}PuO_2$	$\%RSD_T$	3.2	4.2	6.1	3.2	6.6	4.3	6.3	6.7	6.8
	$\%RSD_B$	0.7	0.7	0.7	0.7	0.7	0.7	0.7	0.7	0.7
	$\%RSD_W$	3.1	4.2	6.0	3.2	6.6	4.2	6.3	6.7	6.7
$^{240}PuO_2$	$\%RSD_T$	5.6	6.5	11.6	5.8	12.2	6.4	11.2	11.8	11.9
	$\%RSD_B$	0.7	0.7	0.7	0.7	0.7	0.7	0.7	0.7	0.7
	$\%RSD_W$	5.6	6.5	11.6	5.8	12.2	6.3	11.2	11.8	11.9
$^{241}PuO_2$	$\%RSD_T$	8.5	9.0	16.8	8.7	17.4	9.1	17.0	17.3	17.1
	$\%RSD_B$	0.6	0.6	0.6	0.6	0.6	0.6	0.6	0.6	0.6
	$\%RSD_W$	8.4	9.0	16.8	8.7	17.4	9.1	17.0	17.2	17.1
$^{241}Am_2O_3$	$\%RSD_T$	5.8	6.5	11.4	5.9	11.7	6.5	11.6	12.4	11.9
	$\%RSD_B$	0.7	0.7	0.7	0.7	0.7	0.7	0.7	0.7	0.6
	$\%RSD_W$	5.8	6.5	11.4	5.9	11.7	6.5	11.6	12.4	11.9
$^{244}Cm_2O_3$	$\%RSD_T$	8.8	8.7	17.0	8.6	17.2	9.0	17.3	17.4	17.2
	$\%RSD_B$	0.6	0.6	0.6	0.6	0.6	0.6	0.6	0.6	0.6
	$\%RSD_W$	8.7	8.7	17.0	8.6	17.2	9.0	17.3	17.4	17.2

(a) In the main body of the report bars were used over the %RSDs to denote means, but these tables have no room for the bars. Here, $\%RSD_T$ = mean total batch-to-batch variation and within-batch uncertainty %RSD, $\%RSD_B$ = mean batch-to-batch variation %RSD, and $\%RSD_W$ = mean within-batch uncertainty %RSD.

(b) All factors listed are at the high case whereas all others not listed are at the low case. All factors that are not included within any of these columns were not significant according to the ANOVA. Hence, they were held constant at the low (nominal) uncertainty case. The factor notation has been abbreviated from the notation used in the report to better fit in the table.

Table F.7. %RSD Means of the Total, Batch-to-Batch Variations, and Within-Batch Uncertainties for Important ILAW Radionuclide Composition Components of Set 2 (transition from AP-101/AY-102 to AZ-101) for the Statistically Significant Combinations of Factors

Component	%RSD Mean[a]	All Low Case	$\%RSD_S$[b]	$\%RSD_A$[b]	$SD(a^{GFC})$ $SD(G^{GFC})$[b]	$\%RSD_S$ $\%RSD_A$[b]	$\%RSD_S$ $SD(a^{GFC})$ $SD(G^{GFC})$[b]	$\%RSD_A$ $SD(a^{GFC})$ $SD(G^{GFC})$[b]	$\%RSD_S$ $\%RSD_A$ $SD(a^{GFC})$ $SD(G^{GFC})$[b]	All High Case
^{60}CoO	$\%RSD_T$	5.3	5.9	7.3	5.3	7.8	5.9	7.4	8.0	7.8
	$\%RSD_B$	4.3	4.3	4.3	4.3	4.3	4.3	4.3	4.3	4.3
	$\%RSD_W$	3.1	4.0	5.9	3.1	6.6	4.1	6.0	6.8	6.6
^{63}NiO	$\%RSD_T$	7.8	8.3	12.4	7.8	12.8	8.2	12.3	12.7	12.8
	$\%RSD_B$	5.3	5.3	5.3	5.3	5.3	5.3	5.3	5.3	5.4
	$\%RSD_W$	5.7	6.4	11.2	5.7	11.6	6.2	11.1	11.5	11.6
^{90}SrO	$\%RSD_T$	5.8	6.3	7.5	5.8	8.1	6.3	7.8	8.3	8.3
	$\%RSD_B$	5.0	5.0	5.0	5.0	5.0	5.0	5.0	5.0	4.9
	$\%RSD_W$	2.9	3.9	5.7	3.1	6.4	3.9	6.1	6.7	6.6
$^{99}Tc_2O_7$	$\%RSD_T$	7.1	7.6	11.8	7.0	12.4	7.6	12.0	12.5	12.0
	$\%RSD_B$	3.9	3.9	3.9	3.9	3.9	3.9	3.9	3.9	3.9
	$\%RSD_W$	6.0	6.5	11.1	5.8	11.7	6.4	11.4	11.9	11.3
$^{125}Sb_2O_3$	$\%RSD_T$	15.6	15.5	28.5	15.5	28.2	15.9	28.4	29.3	27.9
	$\%RSD_B$	6.5	6.5	6.5	6.5	6.5	6.5	6.5	6.5	6.5
	$\%RSD_W$	14.2	14.1	27.7	14.0	27.5	14.5	27.6	28.6	27.1
$^{137}Cs_2O$	$\%RSD_T$	8.4	9.2	17.0	8.7	17.1	9.1	17.4	17.2	17.5
	$\%RSD_B$	1.3	1.3	1.3	1.3	1.3	1.3	1.3	1.3	1.3
	$\%RSD_W$	8.3	9.1	17.0	8.6	17.1	9.0	17.4	17.2	17.5
$^{151}Sm_2O_3$	$\%RSD_T$	11.2	12.0	22.4	10.9	22.4	11.6	22.5	21.8	22.1
	$\%RSD_B$	1.0	1.0	1.0	1.0	1.0	1.0	1.0	1.0	1.1
	$\%RSD_W$	11.2	12.0	22.3	10.8	22.3	11.6	22.5	21.8	22.1
$^{154}Eu_2O_3$	$\%RSD_T$	4.1	5.0	6.7	4.1	7.2	5.0	6.4	7.0	7.0
	$\%RSD_B$	2.8	2.8	2.8	2.8	2.8	2.8	2.8	2.8	2.8
	$\%RSD_W$	2.9	4.1	6.0	3.0	6.6	4.1	5.7	6.4	6.4
$^{155}Eu_2O_3$	$\%RSD_T$	3.3	4.4	6.3	3.4	6.6	4.5	6.2	6.6	6.7
	$\%RSD_B$	1.4	1.4	1.4	1.4	1.4	1.4	1.4	1.4	1.4
	$\%RSD_W$	3.0	4.2	6.2	3.1	6.5	4.3	6.0	6.5	6.6
$^{233}UO_3$	$\%RSD_T$	14.2	14.6	17.6	14.5	17.4	14.6	17.7	17.6	17.7
	$\%RSD_B$	13.3	13.3	13.3	13.3	13.3	13.3	13.3	13.3	13.3
	$\%RSD_W$	4.9	6.0	11.4	5.8	11.3	6.1	11.7	11.5	11.7
$^{235}UO_3$	$\%RSD_T$	7.6	8.2	12.5	7.9	12.9	8.5	13.1	13.2	12.9
	$\%RSD_B$	5.5	5.5	5.5	5.5	5.5	5.5	5.5	5.5	5.5
	$\%RSD_W$	5.3	6.1	11.3	5.7	11.7	6.5	11.9	12.0	11.7
$^{237}NpO_2$	$\%RSD_T$	7.2	7.5	12.1	7.0	12.6	8.0	12.5	12.6	12.7
	$\%RSD_B$	4.4	4.4	4.4	4.4	4.4	4.4	4.4	4.4	4.4
	$\%RSD_W$	5.7	6.1	11.3	5.5	11.8	6.7	11.7	11.8	11.9
$^{238}UO_3$	$\%RSD_T$	7.9	8.4	12.8	8.0	12.9	8.6	12.7	12.7	13.1
	$\%RSD_B$	5.5	5.5	5.5	5.5	5.5	5.5	5.5	5.5	5.6
	$\%RSD_W$	5.6	6.3	11.5	5.8	11.6	6.6	11.4	11.4	11.8
$^{238}PuO_2$	$\%RSD_T$	3.7	4.6	6.3	3.7	6.8	4.7	6.4	6.9	6.9
	$\%RSD_B$	2.3	2.3	2.3	2.3	2.3	2.3	2.3	2.3	2.3
	$\%RSD_W$	3.0	4.1	5.9	3.0	6.4	4.1	6.0	6.6	6.5

(a) In the main body of the report bars were used over the %RSDs to denote means, but these tables have no room for the bars. Here, $\%RSD_T$ = mean total batch-to-batch variation and within-batch uncertainty %RSD, $\%RSD_B$ = mean batch-to-batch variation %RSD, and $\%RSD_W$ = mean within-batch uncertainty %RSD.

(b) All factors listed are at the high case whereas all others not listed are at the low case. All factors that are not included within any of these columns were not significant according to the ANOVA. Hence, they were held constant at the low (nominal) uncertainty case. The factor notation has been abbreviated from the notation used in the report to better fit in the table.

Table F.7. %RSD Means of the Total, Batch-to-Batch Variations, and Within-Batch Uncertainties for Important ILAW Radionuclide Composition Components of Set 2 (transition from AP-101/AY-102 to AZ-101) for the Statistically Significant Combinations of Factors (cont'd)

Component	%RSD Mean[a]	All Low Case	$\%RSD_S$[b]	$\%RSD_A$[b]	$SD(a^{GFC})$ $SD(G^{GFC})$[b]	$\%RSD_S$ $\%RSD_A$[b]	$\%RSD_S$ $SD(a^{GFC})$ $SD(G^{GFC})$[b]	$\%RSD_A$ $SD(a^{GFC})$ $SD(G^{GFC})$[b]	$\%RSD_S$ $\%RSD_A$ $SD(a^{GFC})$ $SD(G^{GFC})$[b]	All High Case
$^{239}PuO_2$	$\%RSD_T$	4.1	4.9	6.5	4.2	7.2	5.1	6.6	7.1	7.2
	$\%RSD_B$	2.9	2.9	2.9	2.9	2.9	2.9	2.9	2.9	2.9
	$\%RSD_W$	2.9	4.0	5.9	3.1	6.6	4.2	5.9	6.5	6.6
$^{240}PuO_2$	$\%RSD_T$	6.9	7.3	12.1	7.0	12.6	7.4	11.7	12.6	12.2
	$\%RSD_B$	3.7	3.7	3.7	3.7	3.7	3.7	3.7	3.7	3.7
	$\%RSD_W$	5.8	6.2	11.5	5.9	12.0	6.4	11.1	12.1	11.7
$^{241}PuO_2$	$\%RSD_T$	9.8	10.4	17.1	9.7	18.0	10.6	17.6	17.7	18.2
	$\%RSD_B$	5.3	5.3	5.3	5.3	5.3	5.3	5.3	5.3	5.3
	$\%RSD_W$	8.2	8.9	16.2	8.1	17.2	9.2	16.8	16.8	17.4
$^{241}Am_2O_3$	$\%RSD_T$	8.6	8.9	13.3	8.9	13.3	9.2	13.0	13.3	13.6
	$\%RSD_B$	6.6	6.6	6.6	6.6	6.6	6.6	6.6	6.6	6.6
	$\%RSD_W$	5.6	5.9	11.6	6.0	11.6	6.4	11.2	11.6	11.9
$^{244}Cm_2O_3$	$\%RSD_T$	10.7	11.1	17.8	10.5	18.2	11.2	18.5	18.5	18.7
	$\%RSD_B$	6.5	6.5	6.5	6.5	6.5	6.5	6.5	6.5	6.5
	$\%RSD_W$	8.5	9.0	16.6	8.3	17.0	9.1	17.4	17.3	17.6

(a) In the main body of the report bars were used over the %RSDs to denote means, but these tables have no room for the bars. Here, $\%RSD_T$ = mean total batch-to-batch variation and within-batch uncertainty %RSD, $\%RSD_B$ = mean batch-to-batch variation %RSD, and $\%RSD_W$ = mean within-batch uncertainty %RSD.

(b) All factors listed are at the high case whereas all others not listed are at the low case. All factors that are not included within any of these columns were not significant according to the ANOVA. Hence, they were held constant at the low (nominal) uncertainty case. The factor notation has been abbreviated from the notation used in the report to better fit in the table.

Table F.8. %RSD Means of the Total, Batch-to-Batch Variations, and Within-Batch Uncertainties for Important ILAW Radionuclide Composition Components of Set 3 (AZ-102) for the Statistically Significant Combinations of Factors

Component	%RSD Mean[(a)]	All Low Case	$\%RSD_S$[(b)]	$\%RSD_A$[(b)]	$SD(a^{GFC})$ $SD(G^{GFC})$[(b)]	$\%RSD_S$ $\%RSD_A$[(b)]	$\%RSD_S$ $SD(a^{GFC})$ $SD(G^{GFC})$[(b)]	$\%RSD_A$ $SD(a^{GFC})$ $SD(G^{GFC})$[(b)]	$\%RSD_S$ $\%RSD_A$ $SD(a^{GFC})$ $SD(G^{GFC})$[(b)]	All High Case
^{60}CoO	$\%RSD_T$	2.9	4.1	5.6	3.1	6.3	4.1	5.5	6.4	6.5
	$\%RSD_B$	0.6	0.6	0.6	0.6	0.6	0.6	0.6	0.6	0.6
	$\%RSD_W$	2.8	4.0	5.6	3.0	6.3	4.1	5.5	6.4	6.5
^{63}NiO	$\%RSD_T$	5.7	6.3	11.0	5.7	11.9	6.4	11.2	11.5	11.5
	$\%RSD_B$	0.6	0.6	0.6	0.6	0.6	0.6	0.6	0.6	0.6
	$\%RSD_W$	5.7	6.3	11.0	5.7	11.9	6.3	11.2	11.5	11.5
^{90}SrO	$\%RSD_T$	3.1	4.0	5.7	3.1	6.5	4.2	6.0	6.2	6.5
	$\%RSD_B$	0.6	0.6	0.6	0.6	0.6	0.6	0.6	0.6	0.6
	$\%RSD_W$	3.0	3.9	5.6	3.0	6.5	4.1	5.9	6.2	6.5
$^{99}Tc_2O_7$	$\%RSD_T$	5.7	6.3	11.3	5.6	11.7	6.4	11.1	11.6	11.5
	$\%RSD_B$	0.6	0.6	0.6	0.6	0.6	0.6	0.6	0.6	0.6
	$\%RSD_W$	5.7	6.3	11.3	5.6	11.7	6.4	11.0	11.6	11.5
$^{125}Sb_2O_3$	$\%RSD_T$	14.1	14.6	27.2	14.2	28.0	14.0	27.1	27.6	27.5
	$\%RSD_B$	0.6	0.6	0.6	0.6	0.6	0.6	0.6	0.6	0.6
	$\%RSD_W$	14.1	14.6	27.2	14.2	28.0	14.0	27.1	27.6	27.5
$^{137}Cs_2O$	$\%RSD_T$	8.8	8.9	16.9	8.5	17.0	9.0	17.0	17.7	17.2
	$\%RSD_B$	0.6	0.6	0.6	0.6	0.6	0.6	0.6	0.6	0.6
	$\%RSD_W$	8.8	8.9	16.9	8.5	17.0	9.0	17.0	17.7	17.2
$^{151}Sm_2O_3$	$\%RSD_T$	11.2	11.9	22.4	11.1	22.6	12.0	22.1	23.1	21.6
	$\%RSD_B$	0.6	0.6	0.6	0.6	0.6	0.6	0.6	0.6	0.6
	$\%RSD_W$	11.1	11.9	22.4	11.1	22.6	12.0	22.1	23.1	21.6
$^{154}Eu_2O_3$	$\%RSD_T$	2.9	4.0	6.0	3.1	6.4	4.1	5.7	6.4	6.3
	$\%RSD_B$	0.6	0.6	0.6	0.6	0.6	0.6	0.6	0.6	0.6
	$\%RSD_W$	2.9	4.0	5.9	3.0	6.4	4.1	5.7	6.3	6.3
$^{155}Eu_2O_3$	$\%RSD_T$	3.0	4.0	5.7	3.0	6.2	4.0	5.8	6.5	6.4
	$\%RSD_B$	0.6	0.6	0.6	0.6	0.6	0.6	0.6	0.6	0.6
	$\%RSD_W$	3.0	4.0	5.7	2.9	6.2	3.9	5.8	6.5	6.3
$^{233}UO_3$	$\%RSD_T$	5.6	6.2	11.3	5.6	11.5	6.3	11.3	12.2	11.4
	$\%RSD_B$	0.6	0.6	0.6	0.6	0.6	0.6	0.6	0.6	0.6
	$\%RSD_W$	5.6	6.2	11.3	5.5	11.5	6.3	11.3	12.2	11.4
$^{235}UO_3$	$\%RSD_T$	5.6	6.3	11.6	5.7	11.8	6.4	11.4	11.5	11.5
	$\%RSD_B$	0.6	0.6	0.6	0.6	0.6	0.6	0.6	0.6	0.6
	$\%RSD_W$	5.6	6.3	11.6	5.7	11.8	6.4	11.4	11.5	11.5
$^{237}NpO_2$	$\%RSD_T$	5.8	6.4	11.3	5.8	11.8	6.5	11.4	11.9	11.6
	$\%RSD_B$	0.6	0.6	0.6	0.6	0.6	0.6	0.6	0.6	0.6
	$\%RSD_W$	5.8	6.3	11.3	5.8	11.8	6.5	11.4	11.9	11.5
$^{238}UO_3$	$\%RSD_T$	5.7	6.4	11.0	5.6	11.6	6.5	11.3	11.6	11.7
	$\%RSD_B$	0.6	0.6	0.6	0.6	0.6	0.6	0.6	0.6	0.6
	$\%RSD_W$	5.7	6.4	11.0	5.6	11.6	6.4	11.3	11.6	11.7
$^{238}PuO_2$	$\%RSD_T$	3.0	3.9	5.9	3.1	6.6	4.2	5.9	6.4	6.3
	$\%RSD_B$	0.6	0.6	0.6	0.6	0.6	0.6	0.6	0.6	0.6
	$\%RSD_W$	2.9	3.9	5.9	3.0	6.6	4.2	5.9	6.4	6.3

(a) In the main body of the report bars were used over the %RSDs to denote means, but these tables have no room for the bars. Here, $\%RSD_T$ = mean total batch-to-batch variation and within-batch uncertainty %RSD, $\%RSD_B$ = mean batch-to-batch variation %RSD, and $\%RSD_W$ = mean within-batch uncertainty %RSD.

(b) All factors listed are at the high case whereas all others not listed are at the low case. All factors that are not included within any of these columns were not significant according to the ANOVA. Hence, they were held constant at the low (nominal) uncertainty case. The factor notation has been abbreviated from the notation used in the report to better fit in the table.

Table F.8. %RSD Means of the Total, Batch-to-Batch Variations, and Within-Batch Uncertainties for Important ILAW Radionuclide Composition Components of Set 3 (AZ-102) for the Statistically Significant Combinations of Factors (cont'd)

Component	%RSD Mean[a]	All Low Case	$\%RSD_S$[b]	$\%RSD_A$[b]	$SD(a^{GFC})$ $SD(G^{GFC})$[b]	$\%RSD_S$ $\%RSD_A$[b]	$\%RSD_S$ $SD(a^{GFC})$ $SD(G^{GFC})$[b]	$\%RSD_A$ $SD(a^{GFC})$ $SD(G^{GFC})$[b]	$\%RSD_S$ $\%RSD_A$ $SD(a^{GFC})$ $SD(G^{GFC})$[b]	All High Case
$^{239}PuO_2$	$\%RSD_T$	3.0	4.1	5.7	3.0	6.3	4.1	5.7	6.5	6.4
	$\%RSD_B$	0.6	0.6	0.6	0.6	0.6	0.6	0.6	0.6	0.6
	$\%RSD_W$	2.9	4.1	5.7	2.9	6.3	4.1	5.7	6.4	6.4
$^{240}PuO_2$	$\%RSD_T$	5.6	6.4	11.5	5.6	11.6	6.3	11.5	11.5	11.6
	$\%RSD_B$	0.6	0.6	0.6	0.6	0.6	0.6	0.6	0.6	0.6
	$\%RSD_W$	5.6	6.4	11.4	5.6	11.6	6.2	11.5	11.5	11.6
$^{241}PuO_2$	$\%RSD_T$	8.3	8.8	16.2	8.7	17.1	8.6	17.0	17.3	17.2
	$\%RSD_B$	0.6	0.6	0.6	0.6	0.6	0.6	0.6	0.6	0.6
	$\%RSD_W$	8.3	8.8	16.2	8.7	17.1	8.5	17.0	17.3	17.2
$^{241}Am_2O_3$	$\%RSD_T$	5.8	6.4	11.2	5.7	11.7	6.6	11.2	11.6	11.5
	$\%RSD_B$	0.6	0.6	0.6	0.6	0.6	0.6	0.6	0.6	0.6
	$\%RSD_W$	5.7	6.4	11.2	5.6	11.7	6.6	11.2	11.6	11.5
$^{244}Cm_2O_3$	$\%RSD_T$	8.6	9.1	16.9	8.3	17.0	9.2	16.7	16.9	17.1
	$\%RSD_B$	0.6	0.6	0.6	0.6	0.6	0.6	0.6	0.6	0.6
	$\%RSD_W$	8.6	9.1	16.9	8.2	17.0	9.2	16.7	16.9	17.1

(a) In the main body of the report bars were used over the %RSDs to denote means, but these tables have no room for the bars. Here, $\%RSD_T$ = mean total batch-to-batch variation and within-batch uncertainty %RSD, $\%RSD_B$ = mean batch-to-batch variation %RSD, and $\%RSD_W$ = mean within-batch uncertainty %RSD.

(b) All factors listed are at the high case whereas all others not listed are at the low case. All factors that are not included within any of these columns were not significant according to the ANOVA. Hence, they were held constant at the low (nominal) uncertainty case. The factor notation has been abbreviated from the notation used in the report to better fit in the table.

Table F.9. %RSD Means of the Total, Batch-to-Batch Variations, and Within-Batch Uncertainties for Important ILAW Radionuclide Composition Components of Set 4 (AN-102) for the Statistically Significant Combinations of Factors

Component	%RSD Mean[(a)]	All Low Case	$\%RSD_S$[(b)]	$\%RSD_A$[(b)]	$SD(a^{GFC})$ $SD(G^{GFC})$[(b)]	$\%RSD_S$ $\%RSD_A$[(b)]	$\%RSD_S$ $SD(a^{GFC})$ $SD(G^{GFC})$[(b)]	$\%RSD_A$ $SD(a^{GFC})$ $SD(G^{GFC})$[(b)]	$\%RSD_S$ $\%RSD_A$ $SD(a^{GFC})$ $SD(G^{GFC})$[(b)]	All High Case
^{60}CoO	$\%RSD_T$	3.1	4.2	6.0	3.2	6.6	4.2	6.4	6.9	6.7
	$\%RSD_B$	0.6	0.6	0.6	0.6	0.6	0.6	0.6	0.6	0.6
	$\%RSD_W$	3.1	4.1	6.0	3.1	6.6	4.2	6.4	6.9	6.7
^{63}NiO	$\%RSD_T$	5.8	6.4	11.4	5.9	12.0	6.4	11.6	11.9	11.8
	$\%RSD_B$	0.8	0.8	0.8	0.8	0.8	0.8	0.8	0.8	0.8
	$\%RSD_W$	5.8	6.4	11.4	5.9	12.0	6.4	11.6	11.9	11.7
^{90}SrO	$\%RSD_T$	3.3	4.3	6.1	3.4	6.8	4.3	6.2	7.0	6.9
	$\%RSD_B$	1.2	1.2	1.2	1.2	1.2	1.2	1.2	1.2	1.2
	$\%RSD_W$	3.1	4.1	6.0	3.2	6.7	4.1	6.1	6.9	6.8
$^{99}Tc_2O_7$	$\%RSD_T$	6.0	6.7	11.6	5.9	11.7	6.6	11.7	11.6	11.8
	$\%RSD_B$	1.0	1.0	1.0	1.0	1.0	1.0	1.0	1.0	1.0
	$\%RSD_W$	5.9	6.7	11.5	5.8	11.6	6.5	11.7	11.6	11.8
$^{125}Sb_2O_3$	$\%RSD_T$	14.1	14.3	27.6	14.0	28.0	14.6	26.3	27.7	27.3
	$\%RSD_B$	0.6	0.6	0.6	0.6	0.6	0.6	0.6	0.6	0.6
	$\%RSD_W$	14.1	14.3	27.6	14.0	28.0	14.6	26.3	27.7	27.3
$^{137}Cs_2O$	$\%RSD_T$	8.7	9.0	17.1	8.6	17.5	8.8	17.0	17.8	17.0
	$\%RSD_B$	0.6	0.6	0.6	0.6	0.6	0.6	0.6	0.6	0.6
	$\%RSD_W$	8.7	9.0	17.0	8.5	17.5	8.8	17.0	17.8	17.0
$^{151}Sm_2O_3$	$\%RSD_T$	11.2	11.7	22.8	11.2	22.3	11.7	23.1	23.1	22.5
	$\%RSD_B$	0.6	0.6	0.6	0.6	0.6	0.6	0.6	0.6	0.6
	$\%RSD_W$	11.1	11.7	22.8	11.2	22.2	11.7	23.1	23.1	22.5
$^{154}Eu_2O_3$	$\%RSD_T$	3.3	4.3	6.0	3.2	6.7	4.3	6.1	6.7	6.7
	$\%RSD_B$	0.6	0.6	0.6	0.6	0.6	0.6	0.6	0.6	0.6
	$\%RSD_W$	3.2	4.2	6.0	3.2	6.7	4.3	6.1	6.7	6.7
$^{155}Eu_2O_3$	$\%RSD_T$	3.1	4.2	6.2	3.2	7.0	4.3	6.1	6.6	6.7
	$\%RSD_B$	0.6	0.6	0.6	0.6	0.6	0.6	0.6	0.6	0.6
	$\%RSD_W$	3.1	4.2	6.2	3.2	7.0	4.3	6.1	6.6	6.6
$^{233}UO_3$	$\%RSD_T$	5.7	6.3	11.8	5.9	11.9	6.5	11.6	11.9	12.1
	$\%RSD_B$	0.6	0.6	0.6	0.6	0.6	0.6	0.6	0.6	0.6
	$\%RSD_W$	5.7	6.3	11.8	5.8	11.9	6.5	11.6	11.9	12.1
$^{235}UO_3$	$\%RSD_T$	5.8	6.4	11.4	5.7	11.7	6.3	11.1	11.6	11.9
	$\%RSD_B$	0.6	0.6	0.6	0.6	0.6	0.6	0.6	0.6	0.6
	$\%RSD_W$	5.7	6.4	11.4	5.7	11.7	6.3	11.1	11.6	11.9
$^{237}NpO_2$	$\%RSD_T$	5.7	6.5	11.9	5.9	11.8	6.4	11.5	11.9	11.8
	$\%RSD_B$	0.6	0.6	0.6	0.6	0.6	0.6	0.6	0.6	0.6
	$\%RSD_W$	5.7	6.4	11.9	5.8	11.8	6.3	11.5	11.9	11.8
$^{238}UO_3$	$\%RSD_T$	5.8	6.4	11.3	5.9	11.8	6.5	11.2	11.7	12.0
	$\%RSD_B$	0.6	0.6	0.6	0.6	0.6	0.6	0.6	0.6	0.6
	$\%RSD_W$	5.7	6.3	11.3	5.9	11.8	6.4	11.2	11.7	12.0
$^{238}PuO_2$	$\%RSD_T$	3.2	4.2	6.1	3.2	6.9	4.2	6.4	6.7	6.7
	$\%RSD_B$	0.7	0.7	0.7	0.7	0.7	0.7	0.7	0.7	0.7
	$\%RSD_W$	3.2	4.1	6.1	3.1	6.8	4.1	6.3	6.7	6.7

(a) In the main body of the report bars were used over the %RSDs to denote means, but these tables have no room for the bars. Here, $\%RSD_T$ = mean total batch-to-batch variation and within-batch uncertainty %RSD, $\%RSD_B$ = mean batch-to-batch variation %RSD, and $\%RSD_W$ = mean within-batch uncertainty %RSD.

(b) All factors listed are at the high case whereas all others not listed are at the low case. All factors that are not included within any of these columns were not significant according to the ANOVA. Hence, they were held constant at the low (nominal) uncertainty case. The factor notation has been abbreviated from the notation used in the report to better fit in the table.

Table F.9. %RSD Means of the Total, Batch-to-Batch Variations, and Within-Batch Uncertainties for Important ILAW Radionuclide Composition Components of Set 4 (AN-102) for the Statistically Significant Combinations of Factors (cont'd)

Component	%RSD Mean[(a)]	All Low Case	$\%RSD_S$[(b)]	$\%RSD_A$[(b)]	$SD(a^{GFC})$ $SD(G^{GFC})$[(b)]	$\%RSD_S$ $\%RSD_A$[(b)]	$\%RSD_S$ $SD(a^{GFC})$ $SD(G^{GFC})$[(b)]	$\%RSD_A$ $SD(a^{GFC})$ $SD(G^{GFC})$[(b)]	$\%RSD_S$ $\%RSD_A$ $SD(a^{GFC})$ $SD(G^{GFC})$[(b)]	All High Case
$^{239}PuO_2$	$\%RSD_T$	3.1	4.3	6.2	3.2	6.7	4.2	5.9	6.6	6.9
	$\%RSD_B$	0.6	0.6	0.6	0.6	0.6	0.6	0.6	0.6	0.6
	$\%RSD_W$	3.0	4.2	6.1	3.1	6.6	4.2	5.9	6.6	6.8
$^{240}PuO_2$	$\%RSD_T$	5.8	6.4	11.3	5.9	12.2	6.4	11.5	11.4	11.6
	$\%RSD_B$	0.6	0.6	0.6	0.6	0.6	0.6	0.6	0.6	0.6
	$\%RSD_W$	5.8	6.3	11.2	5.8	12.1	6.4	11.5	11.4	11.6
$^{241}PuO_2$	$\%RSD_T$	8.8	9.0	16.5	8.7	17.5	9.1	17.0	17.6	17.6
	$\%RSD_B$	0.6	0.6	0.6	0.6	0.6	0.6	0.6	0.6	0.6
	$\%RSD_W$	8.7	9.0	16.5	8.7	17.5	9.1	17.0	17.6	17.5
$^{241}Am_2O_3$	$\%RSD_T$	6.0	6.4	11.6	5.8	11.7	6.4	11.4	11.8	11.8
	$\%RSD_B$	0.6	0.6	0.6	0.6	0.6	0.6	0.6	0.6	0.6
	$\%RSD_W$	6.0	6.4	11.6	5.8	11.7	6.4	11.4	11.8	11.8
$^{244}Cm_2O_3$	$\%RSD_T$	8.4	9.1	16.6	8.8	17.0	9.2	17.3	17.5	16.8
	$\%RSD_B$	0.6	0.6	0.6	0.6	0.6	0.6	0.6	0.6	0.6
	$\%RSD_W$	8.4	9.1	16.6	8.7	17.0	9.2	17.3	17.4	16.8

(a) In the main body of the report bars were used over the %RSDs to denote means, but these tables have no room for the bars. Here, $\%RSD_T$ = mean total batch-to-batch variation and within-batch uncertainty %RSD, $\%RSD_B$ = mean batch-to-batch variation %RSD, and $\%RSD_W$ = mean within-batch uncertainty %RSD.

(b) All factors listed are at the high case whereas all others not listed are at the low case. All factors that are not included within any of these columns were not significant according to the ANOVA. Hence, they were held constant at the low (nominal) uncertainty case. The factor notation has been abbreviated from the notation used in the report to better fit in the table.

Table F.10. %RSD Means of the Total, Batch-to-Batch Variations, and Within-Batch Uncertainties for Important ILAW Radionuclide Composition Components of Set 5 (unknown tank) for the Statistically Significant Combinations of Factors

Component	%RSD Mean[a]	All Low Case	$\%RSD_S$[b]	$\%RSD_A$[b]	$SD(a^{GFC})$ $SD(G^{GFC})$[b]	$\%RSD_S$ $\%RSD_A$[b]	$\%RSD_S$ $SD(a^{GFC})$ $SD(G^{GFC})$[b]	$\%RSD_A$ $SD(a^{GFC})$ $SD(G^{GFC})$[b]	$\%RSD_S$ $\%RSD_A$ $SD(a^{GFC})$ $SD(G^{GFC})$[b]	All High Case
^{60}CoO	$\%RSD_T$	3.1	4.2	5.9	3.2	6.4	4.3	6.0	6.5	6.5
	$\%RSD_B$	0.8	0.8	0.8	0.8	0.8	0.8	0.8	0.8	0.8
	$\%RSD_W$	3.0	4.1	5.8	3.1	6.3	4.2	5.9	6.4	6.4
^{63}NiO	$\%RSD_T$	5.7	6.3	11.4	5.6	11.8	6.5	11.6	11.5	12.0
	$\%RSD_B$	0.6	0.6	0.6	0.6	0.6	0.6	0.6	0.6	0.6
	$\%RSD_W$	5.7	6.3	11.4	5.6	11.8	6.4	11.6	11.5	11.9
^{90}SrO	$\%RSD_T$	3.1	4.1	6.1	3.1	6.5	4.2	6.0	6.6	6.6
	$\%RSD_B$	0.6	0.6	0.6	0.6	0.6	0.6	0.6	0.6	0.6
	$\%RSD_W$	3.0	4.0	6.1	3.0	6.4	4.2	6.0	6.6	6.6
$^{99}Tc_2O_7$	$\%RSD_T$	5.8	6.5	11.4	5.8	11.6	6.5	11.1	11.9	12.2
	$\%RSD_B$	0.7	0.7	0.7	0.7	0.7	0.7	0.7	0.7	0.7
	$\%RSD_W$	5.8	6.5	11.4	5.8	11.6	6.5	11.1	11.8	12.2
$^{125}Sb_2O_3$	$\%RSD_T$	13.9	14.5	28.3	14.5	28.0	14.6	28.5	28.0	28.6
	$\%RSD_B$	0.6	0.6	0.6	0.6	0.6	0.6	0.6	0.6	0.6
	$\%RSD_W$	13.9	14.5	28.3	14.5	28.0	14.6	28.5	28.0	28.6
$^{137}Cs_2O$	$\%RSD_T$	8.6	8.9	17.0	8.7	16.6	9.0	17.3	17.1	17.2
	$\%RSD_B$	0.6	0.6	0.6	0.6	0.6	0.6	0.6	0.6	0.6
	$\%RSD_W$	8.6	8.9	17.0	8.6	16.6	8.9	17.3	17.1	17.2
$^{151}Sm_2O_3$	$\%RSD_T$	11.4	11.5	22.5	11.2	22.7	11.5	22.4	22.5	22.3
	$\%RSD_B$	0.8	0.8	0.8	0.8	0.8	0.8	0.8	0.8	0.8
	$\%RSD_W$	11.4	11.5	22.5	11.2	22.7	11.5	22.4	22.5	22.3
$^{154}Eu_2O_3$	$\%RSD_T$	4.3	5.2	6.4	4.3	7.2	5.2	6.7	7.3	7.3
	$\%RSD_B$	3.2	3.2	3.2	3.2	3.2	3.2	3.2	3.2	3.2
	$\%RSD_W$	3.0	4.1	5.6	3.0	6.5	4.1	5.9	6.6	6.6
$^{155}Eu_2O_3$	$\%RSD_T$	4.3	5.2	6.6	4.5	7.3	5.2	6.8	7.3	7.4
	$\%RSD_B$	3.2	3.2	3.2	3.2	3.2	3.2	3.2	3.2	3.2
	$\%RSD_W$	2.9	4.0	5.7	3.1	6.5	4.0	6.0	6.5	6.6
$^{233}UO_3$	$\%RSD_T$	5.7	6.3	11.5	5.7	11.9	6.5	11.4	11.6	11.6
	$\%RSD_B$	0.8	0.8	0.8	0.8	0.8	0.8	0.8	0.8	0.7
	$\%RSD_W$	5.6	6.2	11.5	5.7	11.9	6.5	11.3	11.6	11.6
$^{235}UO_3$	$\%RSD_T$	6.5	7.1	11.8	6.5	12.2	7.1	12.0	12.8	12.2
	$\%RSD_B$	3.2	3.2	3.2	3.2	3.2	3.2	3.2	3.2	3.2
	$\%RSD_W$	5.7	6.3	11.4	5.6	11.8	6.4	11.5	12.4	11.7
$^{237}NpO_2$	$\%RSD_T$	5.8	6.3	11.7	5.6	11.9	6.5	11.6	11.6	11.5
	$\%RSD_B$	0.6	0.6	0.6	0.6	0.6	0.6	0.6	0.6	0.6
	$\%RSD_W$	5.7	6.3	11.7	5.5	11.9	6.4	11.6	11.6	11.5
$^{238}UO_3$	$\%RSD_T$	6.6	7.3	11.7	6.7	12.1	7.3	11.8	12.1	12.3
	$\%RSD_B$	3.6	3.6	3.6	3.6	3.6	3.6	3.6	3.6	3.6
	$\%RSD_W$	5.6	6.4	11.2	5.7	11.6	6.4	11.2	11.6	11.7
$^{238}PuO_2$	$\%RSD_T$	3.2	4.2	6.1	3.3	6.7	4.3	6.1	6.8	6.5
	$\%RSD_B$	1.1	1.1	1.1	1.1	1.1	1.1	1.1	1.1	1.1
	$\%RSD_W$	3.0	4.1	6.0	3.1	6.6	4.1	6.0	6.7	6.4

(a) In the main body of the report bars were used over the %RSDs to denote means, but these tables have no room for the bars. Here, $\%RSD_T$ = mean total batch-to-batch variation and within-batch uncertainty %RSD, $\%RSD_B$ = mean batch-to-batch variation %RSD, and $\%RSD_W$ = mean within-batch uncertainty %RSD.

(b) All factors listed are at the high case whereas all others not listed are at the low case. All factors that are not included within any of these columns were not significant according to the ANOVA. Hence, they were held constant at the low (nominal) uncertainty case. The factor notation has been abbreviated from the notation used in the report to better fit in the table.

Table F.10. %RSD Means of the Total, Batch-to-Batch Variations, and Within-Batch Uncertainties for Important ILAW Radionuclide Composition Components of Set 5 (unknown tank) for the Statistically Significant Combinations of Factors (cont'd)

Component	%RSD Mean[a]	All Low Case	$\%RSD_S$[b]	$\%RSD_A$[b]	$SD(a^{GFC})$ $SD(G^{GFC})$[b]	$\%RSD_S$ $\%RSD_A$[b]	$\%RSD_S$ $SD(a^{GFC})$ $SD(G^{GFC})$[b]	$\%RSD_A$ $SD(a^{GFC})$ $SD(G^{GFC})$[b]	$\%RSD_S$ $\%RSD_A$ $SD(a^{GFC})$ $SD(G^{GFC})$[b]	All High Case
$^{239}PuO_2$	$\%RSD_T$	3.8	4.5	6.4	3.7	6.8	4.8	6.2	7.1	7.1
	$\%RSD_B$	2.3	2.3	2.3	2.3	2.3	2.3	2.3	2.3	2.3
	$\%RSD_W$	3.0	3.9	6.0	2.9	6.4	4.2	5.8	6.7	6.7
$^{240}PuO_2$	$\%RSD_T$	6.1	6.8	11.7	6.0	12.0	6.6	11.7	12.0	12.0
	$\%RSD_B$	2.1	2.1	2.1	2.1	2.1	2.1	2.1	2.1	2.1
	$\%RSD_W$	5.7	6.4	11.5	5.6	11.8	6.3	11.6	11.8	11.8
$^{241}PuO_2$	$\%RSD_T$	8.6	9.2	17.2	8.6	17.5	9.2	17.5	17.3	17.4
	$\%RSD_B$	1.7	1.7	1.7	1.7	1.7	1.7	1.7	1.7	1.7
	$\%RSD_W$	8.5	9.0	17.1	8.5	17.4	9.1	17.4	17.2	17.3
$^{241}Am_2O_3$	$\%RSD_T$	6.2	6.7	11.6	6.2	12.1	6.7	11.4	12.1	12.0
	$\%RSD_B$	2.6	2.6	2.6	2.6	2.6	2.6	2.6	2.6	2.5
	$\%RSD_W$	5.6	6.2	11.3	5.7	11.8	6.1	11.1	11.9	11.8
$^{244}Cm_2O_3$	$\%RSD_T$	8.6	8.9	17.0	8.7	16.8	9.1	16.9	17.5	16.6
	$\%RSD_B$	0.6	0.6	0.6	0.6	0.6	0.6	0.6	0.6	0.6
	$\%RSD_W$	8.6	8.9	17.0	8.7	16.8	9.1	16.9	17.5	16.6

(a) In the main body of the report bars were used over the %RSDs to denote means, but these tables have no room for the bars. Here, $\%RSD_T$ = mean total batch-to-batch variation and within-batch uncertainty %RSD, $\%RSD_B$ = mean batch-to-batch variation %RSD, and $\%RSD_W$ = mean within-batch uncertainty %RSD.

(b) All factors listed are at the high case whereas all others not listed are at the low case. All factors that are not included within any of these columns were not significant according to the ANOVA. Hence, they were held constant at the low (nominal) uncertainty case. The factor notation has been abbreviated from the notation used in the report to better fit in the table.

F.3 Detailed Results on the Variations and Uncertainties of ILAW Glass Properties

Figure 8.7 through Figure 8.10 graphically show the mean and 90% ECI summaries of %RSDs for batch-to-batch variation, within-batch uncertainty, and total variation plus uncertainty for each of the ILAW glass properties (PCT, VHT, viscosity, and electrical conductivity) for only the scenarios with all the factors at the low case and with all the factors at the high case. To show the %RSD results for other combinations of the factors, Tables F.11 to F.15 give the mean %RSD results for the nine most significant combinations from the scenarios listed in Table 5.4 for each of the five LAW data sets. The nine most significant scenarios include the "all low case" and the "all high case," as well as others determined by the factors having significant effects for a large percentage of the components. Tables F.11 to F.15 each list the mean %RSD results for each of the ILAW properties. Each cell within a table displays the total variation plus uncertainty ($\overline{\%RSD_T}$) as the top number, the batch-to-batch variation ($\overline{\%RSD_B}$) as the middle number, and the within-batch uncertainty ($\overline{\%RSD_W}$) as the bottom number. The mean %RSD values were calculated using the individual %RSD values from the 200 simulations for each scenario represented by a column in the tables.

Tables F.16 to F.19 summarize the values used to make the plots in Figure 8.7 through Figure 8.10 for each of the glass properties. These tables were not included for the chemical and radionuclide composition components (Figure 8.1 through Figure 8.6) because of the large number of tables that would be needed to summarize each component individually in the same manner.

Table F.11. %RSD Means of the Total, Batch-to-Batch Variations, and Within-Batch Uncertainties for ILAW Glass Properties of Set 1 (AP-101/AY-102) for the Statistically Significant Combinations of Factors

Glass Property	%RSD Mean[a]	All Low Case	$\%RSD_S$[b]	$\%RSD_A$[b]	$SD(a^{GFC})$ $SD(G^{GFC})$[b]	$\%RSD_S$ $\%RSD_A$[b]	$\%RSD_S$ $SD(a^{GFC})$ $SD(G^{GFC})$[b]	$\%RSD_A$ $SD(a^{GFC})$ $SD(G^{GFC})$[b]	$\%RSD_S$ $\%RSD_A$ $SD(a^{GFC})$ $SD(G^{GFC})$[b]	All High Case
PCT B	$\%RSD_T$	16.8	19.1	32.3	17.8	34.0	20.1	34.3	33.6	32.9
	$\%RSD_B$	1.6	1.6	1.6	1.6	1.6	1.6	1.6	1.6	1.7
	$\%RSD_W$	16.8	19.0	32.2	17.7	34.0	20.0	34.2	33.5	32.8
PCT Na	$\%RSD_T$	16.0	18.1	30.7	16.6	32.4	18.8	32.3	31.8	31.1
	$\%RSD_B$	1.5	1.5	1.5	1.5	1.5	1.5	1.5	1.5	1.6
	$\%RSD_W$	15.9	18.1	30.6	16.6	32.3	18.7	32.3	31.8	31.1
VHT	$\%RSD_T$	14.1	15.8	27.4	14.7	28.6	16.2	28.9	28.5	28.3
	$\%RSD_B$	1.4	1.4	1.4	1.4	1.4	1.4	1.4	1.4	1.4
	$\%RSD_W$	14.0	15.7	27.3	14.6	28.6	16.2	28.9	28.5	28.2
Viscosity 1373 K	$\%RSD_T$	13.6	15.0	26.7	14.2	27.9	15.9	28.6	27.9	27.5
	$\%RSD_B$	1.3	1.3	1.3	1.3	1.3	1.3	1.3	1.3	1.4
	$\%RSD_W$	13.6	15.0	26.6	14.2	27.9	15.8	28.6	27.9	27.4
Viscosity 1423 K	$\%RSD_T$	12.5	13.8	24.4	13.1	25.5	14.6	26.2	25.5	25.1
	$\%RSD_B$	1.2	1.2	1.2	1.2	1.2	1.2	1.2	1.2	1.3
	$\%RSD_W$	12.4	13.8	24.4	13.0	25.5	14.5	26.2	25.5	25.1
E.C.[c] 1373 K	$\%RSD_T$	10.1	11.4	19.4	10.0	20.5	11.4	20.5	20.0	19.6
	$\%RSD_B$	1.0	1.0	1.0	1.0	1.0	1.0	1.0	1.0	1.0
	$\%RSD_W$	10.0	11.3	19.4	10.0	20.5	11.4	20.5	20.0	19.6
E.C. 1473 K	$\%RSD_T$	9.1	10.2	17.6	9.0	18.5	10.3	18.5	18.1	17.7
	$\%RSD_B$	0.9	0.9	0.9	0.9	0.9	0.9	0.9	0.9	0.9
	$\%RSD_W$	9.0	10.2	17.5	9.0	18.4	10.3	18.5	18.0	17.7

(a) In the main body of the report bars were used over the %RSDs to denote means, but these tables have no room for the bars. Here, $\%RSD_T$ = mean total batch-to-batch variation and within-batch uncertainty %RSD, $\%RSD_B$ = mean batch-to-batch variation %RSD, and $\%RSD_W$ = mean within-batch uncertainty %RSD.

(b) All factors listed are at the high case whereas all others not listed are at the low case. All factors that are not included within any of these columns were not significant according to the ANOVA. Hence, they were held constant at the low (nominal) uncertainty case. The factor notation has been abbreviated from the notation used in the report to better fit in the table.

(c) E.C. represents electrical conductivity of LAW glasses.

Table F.12. %RSD Means of the Total, Batch-to-Batch Variations, and Within-Batch Uncertainties for ILAW Glass Properties of Set 2 (transition from AP-101/AY-102 to AZ-101) for the Statistically Significant Combinations of Factors

Glass Property	%RSD Mean[a]	All Low Case	$\%RSD_S$[b]	$\%RSD_A$[b]	$SD(a^{GFC})$ $SD(G^{GFC})$[b]	$\%RSD_S$ $\%RSD_A$[b]	$\%RSD_S$ $SD(a^{GFC})$ $SD(G^{GFC})$[b]	$\%RSD_A$ $SD(a^{GFC})$ $SD(G^{GFC})$[b]	$\%RSD_S$ $\%RSD_A$ $SD(a^{GFC})$ $SD(G^{GFC})$[b]	All High Case
PCT B	$\%RSD_T$	13.9	15.7	26.1	16.0	27.7	17.1	27.0	27.9	27.8
	$\%RSD_B$	3.4	3.4	3.4	3.4	3.4	3.4	3.4	3.4	3.3
	$\%RSD_W$	13.5	15.3	25.9	15.7	27.5	16.8	26.7	27.7	27.6
PCT Na	$\%RSD_T$	12.4	14.0	23.2	14.1	24.6	15.2	24.0	24.9	24.6
	$\%RSD_B$	3.6	3.6	3.6	3.6	3.6	3.6	3.6	3.6	3.6
	$\%RSD_W$	11.9	13.6	22.9	13.7	24.3	14.7	23.7	24.6	24.4
VHT	$\%RSD_T$	12.4	13.7	19.3	13.4	20.3	14.3	19.7	20.3	20.3
	$\%RSD_B$	9.3	9.3	9.3	9.3	9.3	9.3	9.3	9.3	9.3
	$\%RSD_W$	8.2	10.1	16.9	9.6	18.0	10.9	17.4	18.1	18.0
Viscosity 1373 K	$\%RSD_T$	16.0	17.7	25.0	17.4	26.3	18.3	25.5	26.2	25.9
	$\%RSD_B$	12.3	12.3	12.3	12.3	12.3	12.3	12.3	12.3	12.2
	$\%RSD_W$	10.2	12.8	21.8	12.3	23.2	13.5	22.4	23.1	22.8
Viscosity 1423 K	$\%RSD_T$	14.8	16.4	23.0	16.1	24.1	16.9	23.5	24.1	23.8
	$\%RSD_B$	11.5	11.5	11.5	11.5	11.5	11.5	11.5	11.5	11.5
	$\%RSD_W$	9.4	11.7	19.9	11.3	21.2	12.5	20.5	21.2	20.9
E.C.[c] 1373 K	$\%RSD_T$	8.7	9.9	16.9	9.2	18.0	10.0	17.2	18.0	17.8
	$\%RSD_B$	0.9	0.9	0.9	0.9	0.9	0.9	0.9	0.9	0.9
	$\%RSD_W$	8.7	9.8	16.9	9.1	18.0	10.0	17.2	17.9	17.8
E.C. 1473 K	$\%RSD_T$	7.9	9.0	15.3	8.3	16.3	9.1	15.6	16.2	16.1
	$\%RSD_B$	0.8	0.8	0.8	0.8	0.8	0.8	0.8	0.8	0.8
	$\%RSD_W$	7.9	8.9	15.3	8.2	16.3	9.0	15.6	16.2	16.1

(a) In the main body of the report bars were used over the %RSDs to denote means, but these tables have no room for the bars. Here, $\%RSD_T$ = mean total batch-to-batch variation and within-batch uncertainty %RSD, $\%RSD_B$ = mean batch-to-batch variation %RSD, and $\%RSD_W$ = mean within-batch uncertainty %RSD.

(b) All factors listed are at the high case whereas all others not listed are at the low case. All factors that are not included within any of these columns were not significant according to the ANOVA. Hence, they were held constant at the low (nominal) uncertainty case. The factor notation has been abbreviated from the notation used in the report to better fit in the table.

(c) E.C. represents electrical conductivity of LAW glasses.

Table F.13. %RSD Means of the Total, Batch-to-Batch Variations, and Within-Batch Uncertainties for ILAW Glass Properties of Set 3 (AZ-102) for the Statistically Significant Combinations of Factors

Glass Property	%RSD Mean[a]	All Low Case	$\%RSD_S$[b]	$\%RSD_A$[b]	$SD(a^{GFC})$ $SD(G^{GFC})$[b]	$\%RSD_S$ $\%RSD_A$[b]	$\%RSD_S$ $SD(a^{GFC})$ $SD(G^{GFC})$[b]	$\%RSD_A$ $SD(a^{GFC})$ $SD(G^{GFC})$[b]	$\%RSD_S$ $\%RSD_A$ $SD(a^{GFC})$ $SD(G^{GFC})$[b]	All High Case
PCT B	$\%RSD_T$	6.4	6.8	11.1	9.2	11.3	9.6	12.6	13.2	12.9
	$\%RSD_B$	0.5	0.5	0.5	0.5	0.5	0.5	0.5	0.5	0.5
	$\%RSD_W$	6.4	6.8	11.1	9.1	11.3	9.6	12.5	13.1	12.9
PCT Na	$\%RSD_T$	5.6	6.0	10.0	7.6	10.1	8.0	10.8	11.4	11.2
	$\%RSD_B$	0.5	0.5	0.5	0.5	0.5	0.5	0.5	0.5	0.5
	$\%RSD_W$	5.5	6.0	9.9	7.5	10.1	8.0	10.8	11.4	11.2
VHT	$\%RSD_T$	3.6	3.8	6.2	5.0	6.3	5.2	7.2	7.2	7.0
	$\%RSD_B$	0.3	0.3	0.3	0.3	0.3	0.3	0.3	0.3	0.3
	$\%RSD_W$	3.6	3.7	6.2	4.9	6.3	5.2	7.2	7.2	7.0
Viscosity 1373 K	$\%RSD_T$	5.6	5.9	9.9	7.7	10.0	8.1	10.9	11.3	11.1
	$\%RSD_B$	0.5	0.5	0.5	0.5	0.5	0.5	0.5	0.5	0.5
	$\%RSD_W$	5.6	5.9	9.9	7.7	10.0	8.1	10.9	11.3	11.1
Viscosity 1423 K	$\%RSD_T$	5.2	5.5	9.1	7.3	9.2	7.6	10.1	10.4	10.3
	$\%RSD_B$	0.4	0.4	0.4	0.4	0.4	0.4	0.4	0.4	0.4
	$\%RSD_W$	5.2	5.4	9.1	7.2	9.2	7.6	10.1	10.4	10.3
E.C.[c] 1373 K	$\%RSD_T$	3.7	4.0	7.2	4.4	7.3	4.7	7.5	7.7	7.5
	$\%RSD_B$	0.3	0.3	0.3	0.3	0.3	0.3	0.3	0.3	0.4
	$\%RSD_W$	3.7	4.0	7.2	4.4	7.3	4.7	7.5	7.7	7.5
E.C. 1473 K	$\%RSD_T$	3.3	3.6	6.4	4.0	6.5	4.2	6.7	6.9	6.7
	$\%RSD_B$	0.3	0.3	0.3	0.3	0.3	0.3	0.3	0.3	0.3
	$\%RSD_W$	3.3	3.6	6.4	4.0	6.5	4.2	6.7	6.9	6.7

(a) In the main body of the report bars were used over the %RSDs to denote means, but these tables have no room for the bars. Here, $\%RSD_T$ = mean total batch-to-batch variation and within-batch uncertainty %RSD, $\%RSD_B$ = mean batch-to-batch variation %RSD, and $\%RSD_W$ = mean within-batch uncertainty %RSD.

(b) All factors listed are at the high case whereas all others not listed are at the low case. All factors that are not included within any of these columns were not significant according to the ANOVA. Hence, they were held constant at the low (nominal) uncertainty case. The factor notation has been abbreviated from the notation used in the report to better fit in the table.

(c) E.C. represents electrical conductivity of LAW glasses.

Table F.14. %RSD Means of the Total, Batch-to-Batch Variations, and Within-Batch Uncertainties for ILAW Glass Properties of Set 4 (AN-102) for the Statistically Significant Combinations of Factors

Glass Property	%RSD Mean[a]	All Low Case	$\%RSD_S$[b]	$\%RSD_A$[b]	$SD(a^{GFC})$ $SD(G^{GFC})$[b]	$\%RSD_S$ $\%RSD_A$[b]	$\%RSD_S$ $SD(a^{GFC})$ $SD(G^{GFC})$[b]	$\%RSD_A$ $SD(a^{GFC})$ $SD(G^{GFC})$[b]	$\%RSD_S$ $\%RSD_A$ $SD(a^{GFC})$ $SD(G^{GFC})$[b]	All High Case
PCT B	$\%RSD_T$	16.8	18.4	31.7	17.2	35.2	18.8	33.2	34.0	34.6
	$\%RSD_B$	1.6	1.6	1.6	1.6	1.6	1.6	1.6	1.6	1.7
	$\%RSD_W$	16.7	18.3	31.6	17.2	35.2	18.8	33.1	33.9	34.5
PCT Na	$\%RSD_T$	14.9	16.3	28.0	15.2	31.1	16.7	29.4	30.0	30.6
	$\%RSD_B$	1.4	1.4	1.4	1.4	1.4	1.4	1.4	1.4	1.5
	$\%RSD_W$	14.8	16.2	27.9	15.2	31.1	16.6	29.3	29.9	30.5
VHT	$\%RSD_T$	22.9	25.2	43.3	24.3	49.1	26.1	46.0	45.7	47.2
	$\%RSD_B$	2.3	2.3	2.3	2.3	2.3	2.3	2.3	2.3	2.3
	$\%RSD_W$	22.8	25.1	43.2	24.2	49.0	26.0	45.9	45.6	47.1
Viscosity 1373 K	$\%RSD_T$	13.3	14.8	25.4	14.1	28.7	15.2	27.6	27.1	28.6
	$\%RSD_B$	1.3	1.3	1.3	1.3	1.3	1.3	1.3	1.3	1.3
	$\%RSD_W$	13.2	14.7	25.4	14.0	28.6	15.1	27.6	27.1	28.5
Viscosity 1423 K	$\%RSD_T$	12.2	13.5	23.3	12.9	26.2	14.0	25.2	24.8	26.1
	$\%RSD_B$	1.2	1.2	1.2	1.2	1.2	1.2	1.2	1.2	1.2
	$\%RSD_W$	12.1	13.5	23.2	12.9	26.2	13.9	25.2	24.8	26.1
E.C.[c] 1373 K	$\%RSD_T$	10.5	11.6	20.0	10.7	22.2	11.5	21.0	21.2	21.7
	$\%RSD_B$	1.0	1.0	1.0	1.0	1.0	1.0	1.0	1.0	1.0
	$\%RSD_W$	10.4	11.5	20.0	10.6	22.2	11.5	21.0	21.2	21.7
E.C. 1473 K	$\%RSD_T$	9.5	10.5	18.2	9.7	20.2	10.5	19.1	19.2	19.8
	$\%RSD_B$	0.9	0.9	0.9	0.9	0.9	0.9	0.9	0.9	0.9
	$\%RSD_W$	9.5	10.5	18.1	9.7	20.2	10.4	19.0	19.2	19.7

(a) In the main body of the report bars were used over the %RSDs to denote means, but these tables have no room for the bars. Here, $\%RSD_T$ = mean total batch-to-batch variation and within-batch uncertainty %RSD, $\%RSD_B$ = mean batch-to-batch variation %RSD, and $\%RSD_W$ = mean within-batch uncertainty %RSD.

(b) All factors listed are at the high case whereas all others not listed are at the low case. All factors that are not included within any of these columns were not significant according to the ANOVA. Hence, they were held constant at the low (nominal) uncertainty case. The factor notation has been abbreviated from the notation used in the report to better fit in the table.

(c) E.C. represents electrical conductivity of LAW glasses.

Table F.15. %RSD Means of the Total, Batch-to-Batch Variations, and Within-Batch Uncertainties for ILAW Glass Properties of Set 5 (unknown tank) for the Statistically Significant Combinations of Factors

Glass Property	%RSD Mean[a]	All Low Case	$\%RSD_S$[b]	$\%RSD_A$[b]	$SD(a^{GFC})$ $SD(G^{GFC})$[b]	$\%RSD_S$ $\%RSD_A$[b]	$\%RSD_S$ $SD(a^{GFC})$ $SD(G^{GFC})$[b]	$\%RSD_A$ $SD(a^{GFC})$ $SD(G^{GFC})$[b]	$\%RSD_S$ $\%RSD_A$ $SD(a^{GFC})$ $SD(G^{GFC})$[b]	All High Case
PCT B	$\%RSD_T$	11.6	12.8	21.8	13.0	22.9	13.9	22.8	23.4	24.0
	$\%RSD_B$	1.1	1.1	1.1	1.1	1.1	1.1	1.1	1.1	1.1
	$\%RSD_W$	11.6	12.7	21.8	12.9	22.9	13.8	22.8	23.4	23.9
PCT Na	$\%RSD_T$	10.2	11.3	19.2	11.3	20.2	12.1	20.1	20.5	21.0
	$\%RSD_B$	1.0	1.0	1.0	1.0	1.0	1.0	1.0	1.0	1.0
	$\%RSD_W$	10.2	11.2	19.2	11.3	20.2	12.1	20.1	20.5	21.0
VHT	$\%RSD_T$	6.0	6.7	11.3	7.0	11.8	7.5	12.1	12.1	12.2
	$\%RSD_B$	0.6	0.6	0.6	0.6	0.6	0.6	0.6	0.6	0.6
	$\%RSD_W$	6.0	6.6	11.3	7.0	11.8	7.5	12.1	12.1	12.2
Viscosity 1373 K	$\%RSD_T$	9.6	10.5	18.2	10.9	19.0	11.7	19.1	19.2	19.7
	$\%RSD_B$	0.9	0.9	0.9	0.9	0.9	0.9	0.9	0.9	0.9
	$\%RSD_W$	9.5	10.5	18.2	10.8	19.0	11.6	19.1	19.1	19.7
Viscosity 1423 K	$\%RSD_T$	8.8	9.7	16.6	10.0	17.3	10.8	17.5	17.6	18.1
	$\%RSD_B$	0.8	0.8	0.8	0.8	0.8	0.8	0.8	0.8	0.8
	$\%RSD_W$	8.7	9.6	16.6	10.0	17.3	10.7	17.5	17.6	18.0
E.C.[c] 1373 K	$\%RSD_T$	7.4	8.1	14.2	7.6	14.9	8.3	14.7	14.8	15.1
	$\%RSD_B$	0.7	0.7	0.7	0.7	0.7	0.7	0.7	0.7	0.7
	$\%RSD_W$	7.4	8.1	14.2	7.6	14.9	8.2	14.7	14.8	15.1
E.C. 1473 K	$\%RSD_T$	6.7	7.3	12.8	6.8	13.4	7.5	13.2	13.3	13.6
	$\%RSD_B$	0.7	0.7	0.7	0.7	0.7	0.7	0.7	0.7	0.7
	$\%RSD_W$	6.6	7.3	12.8	6.8	13.4	7.4	13.2	13.3	13.6

(a) In the main body of the report bars were used over the %RSDs to denote means, but these tables have no room for the bars. Here, $\%RSD_T$ = mean total batch-to-batch variation and within-batch uncertainty %RSD, $\%RSD_B$ = mean batch-to-batch variation %RSD, and $\%RSD_W$ = mean within-batch uncertainty %RSD.

(b) All factors listed are at the high case whereas all others not listed are at the low case. All factors that are not included within any of these columns were not significant according to the ANOVA. Hence, they were held constant at the low (nominal) uncertainty case. The factor notation has been abbreviated from the notation used in the report to better fit in the table.

(c) E.C. represents electrical conductivity of LAW glasses.

Table F.16. %RSD Means and Empirical Confidence Limits for the Total, Batch-to-Batch Variations, and Within-Batch Uncertainties of ILAW PCT_B and PCT_{Na} for All Five Data Sets and Low and High Uncertainty Values for All Factors

Set[a]	Factor Uncertainty Levels[b]	%RSD Type	PCT_B[c]			PCT_{Na}[d]		
			90% ELCL[e]	Mean %RSD	90% EUCL[f]	90% ELCL[e]	Mean %RSD	90% EUCL[f]
1	Low	Total	10.93	16.84	25.43	10.57	16.00	23.80
		Batch-to-Batch	1.06	1.61	2.17	1.01	1.53	2.06
		Within-Batch	10.88	16.76	25.33	10.52	15.93	23.71
	High	Total	18.01	32.88	48.42	16.89	31.09	46.81
		Batch-to-Batch	1.13	1.70	2.27	1.07	1.63	2.16
		Within-Batch	17.97	32.83	48.36	16.85	31.05	46.76
2	Low	Total	8.43	13.88	19.89	7.64	12.39	17.87
		Batch-to-Batch	2.61	3.36	4.03	2.93	3.62	4.23
		Within-Batch	8.02	13.47	19.47	7.05	11.85	17.36
	High	Total	16.48	27.81	41.43	14.65	24.64	36.86
		Batch-to-Batch	2.66	3.34	4.02	2.96	3.59	4.21
		Within-Batch	16.27	27.61	41.23	14.35	24.38	36.62
3	Low	Total	3.80	6.39	8.99	3.50	5.55	7.96
		Batch-to-Batch	0.32	0.52	0.75	0.29	0.47	0.69
		Within-Batch	3.79	6.37	8.96	3.49	5.53	7.93
	High	Total	8.07	12.88	18.70	6.72	11.21	16.36
		Batch-to-Batch	0.32	0.55	0.80	0.30	0.50	0.73
		Within-Batch	8.06	12.87	18.68	6.72	11.20	16.34
4	Low	Total	9.89	16.79	24.54	8.84	14.87	21.90
		Batch-to-Batch	0.97	1.63	2.16	0.86	1.44	1.91
		Within-Batch	9.84	16.71	24.44	8.80	14.80	21.81
	High	Total	20.32	34.58	53.56	18.21	30.55	46.66
		Batch-to-Batch	1.03	1.68	2.28	0.91	1.48	2.02
		Within-Batch	20.30	34.54	53.51	18.18	30.52	46.62
5	Low	Total	6.70	11.64	16.63	5.83	10.24	14.88
		Batch-to-Batch	0.74	1.15	1.55	0.65	1.01	1.37
		Within-Batch	6.66	11.58	16.55	5.80	10.19	14.82
	High	Total	13.86	23.97	34.01	12.34	21.02	29.37
		Batch-to-Batch	0.74	1.15	1.58	0.65	1.01	1.39
		Within-Batch	13.84	23.94	33.97	12.32	21.00	29.33

(a) Set of data representing an LAW waste type, as discussed in Sections 4.1 and 5.3.
(b) This represents all factors in Table 5.3 at their low or high values, thus giving the ranges of variations, uncertainties, and totals. These factors are random CRV batch-to-batch %RSD, CRV mixing/sampling %RSD, CRV analytical %RSD, GFC composition uncertainty, GFC batching uncertainty, and volume uncertainty.
(c) PCT normalized releases of B.
(d) PCT normalized releases of Na.
(e) 90% ELCL is the empirical lower confidence limit for a 90% empirical confidence interval.
(f) 90% EUCL is the empirical upper confidence limit for a 90% empirical confidence interval.

Table F.17. %RSD Means and Empirical Confidence Limits for the Total, Batch-to-Batch Variations, and Within-Batch Uncertainties of ILAW VHT for All Five Data Sets and Low and High Uncertainty Values for All Factors

Set[a]	Factor Uncertainty Levels[b]	%RSD Type	VHT[c]		
			90% ELCL[d]	Mean %RSD	90% EUCL[e]
1	Low	Total	8.77	14.11	19.77
		Batch-to-Batch	0.87	1.35	1.80
		Within-Batch	8.72	14.05	19.69
	High	Total	15.74	28.25	40.33
		Batch-to-Batch	0.93	1.44	1.93
		Within-Batch	15.71	28.21	40.28
2	Low	Total	7.95	12.41	17.57
		Batch-to-Batch	8.77	9.29	9.74
		Within-Batch	0.00	8.23	14.63
	High	Total	12.64	20.29	28.61
		Batch-to-Batch	8.77	9.28	9.78
		Within-Batch	9.10	18.04	26.89
3	Low	Total	2.22	3.59	4.96
		Batch-to-Batch	0.19	0.30	0.43
		Within-Batch	2.21	3.58	4.95
	High	Total	4.59	7.02	9.45
		Batch-to-Batch	0.20	0.31	0.44
		Within-Batch	4.58	7.02	9.44
4	Low	Total	13.90	22.94	32.60
		Batch-to-Batch	1.46	2.30	3.18
		Within-Batch	13.83	22.82	32.44
	High	Total	30.70	47.16	65.96
		Batch-to-Batch	1.45	2.30	3.19
		Within-Batch	30.66	47.10	65.88
5	Low	Total	3.71	6.04	8.68
		Batch-to-Batch	0.38	0.59	0.79
		Within-Batch	3.69	6.01	8.64
	High	Total	7.54	12.21	17.23
		Batch-to-Batch	0.37	0.59	0.84
		Within-Batch	7.53	12.20	17.20

(a) Set of data representing an LAW waste type, as discussed in Sections 4.1 and 5.3.
(b) This represents all factors in Table 5.3 at their low or high values, thus giving the ranges of variations, uncertainties, and totals. These factors are random CRV batch-to-batch %RSD, CRV mixing/sampling %RSD, CRV analytical %RSD, GFC composition uncertainty, GFC batching uncertainty, and volume uncertainty.
(c) VHT alteration depth.
(d) 90% ELCL is the empirical lower confidence limit for a 90% empirical confidence interval.
(e) 90% EUCL is the empirical upper confidence limit for a 90% empirical confidence interval.

Table F.18. %RSD Means and Empirical Confidence Limits for the Total, Batch-to-Batch Variations, and Within-Batch Uncertainties of ILAW Viscosity at 1373.15 K and 1423.15 K for All Five Data Sets and Low and High Uncertainty Values for All Factors

Set[a]	Factor Uncertainty Levels[b]	%RSD Type	Viscosity (1373.15 K)[c]			Viscosity (1423.15 K)[d]		
			90% ELCL[e]	Mean %RSD	90% EUCL[f]	90% ELCL[e]	Mean %RSD	90% EUCL[f]
1	Low	Total	8.39	13.63	19.22	7.78	12.49	17.66
		Batch-to-Batch	0.01	0.01	0.02	0.01	0.01	0.02
		Within-Batch	8.39	13.63	19.22	7.78	12.49	17.66
	High	Total	14.68	27.47	43.76	13.64	25.12	39.88
		Batch-to-Batch	0.01	0.01	0.02	0.01	0.01	0.02
		Within-Batch	14.68	27.47	43.76	13.64	25.12	39.88
2	Low	Total	9.66	15.98	23.77	9.14	14.81	21.88
		Batch-to-Batch	0.11	0.12	0.12	0.10	0.11	0.11
		Within-Batch	9.66	15.98	23.77	9.14	14.81	21.88
	High	Total	15.85	25.90	41.72	14.64	23.80	38.38
		Batch-to-Batch	0.11	0.12	0.12	0.10	0.11	0.11
		Within-Batch	15.85	25.90	41.72	14.64	23.80	38.38
3	Low	Total	3.38	5.59	8.00	3.11	5.18	7.43
		Batch-to-Batch	0.00	0.00	0.01	0.00	0.00	0.01
		Within-Batch	3.38	5.59	8.00	3.11	5.18	7.43
	High	Total	6.59	11.14	16.19	5.99	10.31	14.95
		Batch-to-Batch	0.00	0.00	0.01	0.00	0.00	0.01
		Within-Batch	6.59	11.14	16.19	5.99	10.31	14.95
4	Low	Total	7.76	13.27	18.79	7.07	12.18	17.26
		Batch-to-Batch	0.01	0.01	0.02	0.01	0.01	0.02
		Within-Batch	7.76	13.27	18.79	7.07	12.18	17.26
	High	Total	17.25	28.58	46.07	15.90	26.12	40.92
		Batch-to-Batch	0.01	0.01	0.02	0.01	0.01	0.02
		Within-Batch	17.25	28.58	46.07	15.90	26.12	40.92
5	Low	Total	5.40	9.55	14.12	4.95	8.76	12.90
		Batch-to-Batch	0.01	0.01	0.01	0.01	0.01	0.01
		Within-Batch	5.40	9.55	14.12	4.95	8.76	12.90
	High	Total	11.22	19.69	30.33	10.46	18.06	27.51
		Batch-to-Batch	0.01	0.01	0.01	0.01	0.01	0.01
		Within-Batch	11.22	19.69	30.33	10.46	18.06	27.51

(a) Set of data representing an LAW waste type, as discussed in Sections 4.1 and 5.3.
(b) This represents all factors in Table 5.3 at their low or high values, thus giving the ranges of variations, uncertainties, and totals. These factors are random CRV batch-to-batch %RSD, CRV mixing/sampling %RSD, CRV analytical %RSD, GFC composition uncertainty, GFC batching uncertainty, and volume uncertainty.
(c) Viscosity with temperature at 1373.15 K (1100ºC).
(d) Viscosity with temperature at 1423.15 K (1150ºC).
(e) 90% ELCL is the empirical lower confidence limit for a 90% empirical confidence interval.
(f) 90% EUCL is the empirical upper confidence limit for a 90% empirical confidence interval.

Table F.19. %RSD Means and Empirical Confidence Limits for the Total, Batch-to-Batch Variations, and Within-Batch Uncertainties of ILAW Electrical Conductivity at 1373.15 K and 1473.15 K for All Five Data Sets and Low and High Uncertainty Values for All Factors

Set[a]	Factor Uncertainty Levels[b]	%RSD Type	EC (1373.15 K)[c]			EC (1473.15 K)[d]		
			90% ELCL[e]	Mean %RSD	90% EUCL[f]	90% ELCL[e]	Mean %RSD	90% EUCL[f]
1	Low	Total	6.38	9.08	14.50	5.76	10.06	12.97
		Batch-to-Batch	0.63	0.88	1.32	0.57	0.97	1.19
		Within-Batch	6.35	9.04	14.44	5.73	10.01	12.91
	High	Total	10.81	17.71	27.84	9.95	19.63	24.80
		Batch-to-Batch	0.67	0.93	1.36	0.61	1.03	1.23
		Within-Batch	10.79	17.69	27.81	9.93	19.60	24.77
2	Low	Total	5.45	7.90	12.30	4.86	8.73	11.13
		Batch-to-Batch	0.57	0.83	1.26	0.54	0.91	1.16
		Within-Batch	5.42	7.85	12.24	4.83	8.68	11.07
	High	Total	10.99	16.11	26.01	10.14	17.79	23.58
		Batch-to-Batch	0.59	0.84	1.30	0.54	0.92	1.18
		Within-Batch	10.98	16.08	25.98	10.12	17.76	23.55
3	Low	Total	2.42	3.34	5.39	2.15	3.73	4.82
		Batch-to-Batch	0.22	0.31	0.48	0.20	0.35	0.43
		Within-Batch	2.41	3.32	5.37	2.14	3.71	4.80
	High	Total	4.81	6.72	10.37	4.32	7.51	9.25
		Batch-to-Batch	0.22	0.33	0.52	0.19	0.37	0.47
		Within-Batch	4.81	6.71	10.36	4.31	7.50	9.24
4	Low	Total	6.17	9.52	15.13	5.61	10.49	13.68
		Batch-to-Batch	0.62	0.93	1.37	0.56	1.02	1.24
		Within-Batch	6.14	9.48	15.07	5.58	10.44	13.62
	High	Total	13.63	19.76	30.91	12.54	21.74	27.67
		Batch-to-Batch	0.63	0.95	1.41	0.57	1.04	1.28
		Within-Batch	13.62	19.73	30.88	12.53	21.71	27.64
5	Low	Total	4.37	6.67	10.74	3.89	7.40	9.67
		Batch-to-Batch	0.46	0.66	1.00	0.42	0.73	0.90
		Within-Batch	4.34	6.64	10.69	3.87	7.36	9.62
	High	Total	8.40	13.63	20.92	7.55	15.14	18.72
		Batch-to-Batch	0.48	0.66	1.05	0.43	0.73	0.94
		Within-Batch	8.38	13.62	20.90	7.54	15.12	18.69

(a) Set of data representing an LAW waste type, as discussed in Sections 4.1 and 5.3.
(b) This represents all factors in Table 5.3 at their low or high values, thus giving the range of variations and uncertainties. These factors are random CRV batch-to-batch %RSD, CRV mixing/sampling %RSD, CRV analytical %RSD, GFC composition uncertainty, GFC batching uncertainty, and volume uncertainty.
(c) Electrical conductivity with temperature at 1373.15 K (1100ºC).
(d) Electrical conductivity with temperature at 1473.15 K (1200ºC).
(e) 90% ELCL is the empirical lower confidence limit for a 90% empirical confidence interval.
(f) 90% EUCL is the empirical upper confidence limit for a 90% empirical confidence interval.

Appendix G

Acronyms, Terms, and Abbreviations

Appendix G: Acronyms, Terms, and Abbreviations

ANOVA	analysis of variance
ASX	automated sampling system
Batch-to-batch variation	Real changes in a variable from batch-to-batch in the IHLW or ILAW vitrification facilities over an HLW or LAW waste type. The variable could be an IHLW or ILAW composition component (e.g., Na_2O) or a property of IHLW or ILAW (e.g., the release of boron from the Product Consistency Test). Also see "Variation."
BNI	Bechtel National, Inc.
BNI-SP	Bechtel National, Inc Support Program (replacing the WTPSP)
CAD	computer aided design
Chemical composition	The composition of IHLW or ILAW that can be determined by chemical analyses, not including radiochemical analyses. Chemical composition is expressed as weight percents or mass fractions of oxide or halogen components of the IHLW or ILAW.
Ci	Curies
CRV	Concentrate Receipt Vessel (in the WTP ILAW facility)
CSV	Concentrate Storage Vessel (holds LAW in the WTP Pretreatment facility)
DOE	U.S. Department of Energy
DOE-ORP	U.S. DOE-Office of River Protection
DOE-RW	U.S. DOE-Office of Civilian Radioactive Waste Management
DQO	data quality objectives
DWPF	Defense Waste Processing Facility
ECI	empirical confidence interval
90% ECI	A 90% ECI is expected to cover (on average) 90% of possible values of the random variable for which the interval is calculated.
EQL	estimated quantitation limit
ELCL	empirical lower confidence limit, the lower limit of an empirical confidence interval

EUCL	empirical upper confidence limit, the upper limit of an empirical confidence interval
g	grams
gal	gallons
GFC	glass forming chemical
g/L	grams per liter
g/mL	grams per milliliter
g/m^2	grams per square meter
g/m^2day	grams per square meter per day
HBV	HLW Blend Vessel (holds blended HLW in the WTP pretreatment facility)
HLW	high-level waste
Hysteresis	The maximum difference between load cell readings for the same applied load, with one reading obtained by increasing the load from zero and the other reading obtained by decreasing the load from the Rated Capacity. Usually measured at one-half the Rated Capacity and expressed as a percentage of the Rated Capacity.
ICP	inductively coupled plasma
ICP-AES	inductively coupled plasma-atomic emission spectrometry
ICP-MS	inductively coupled plasma-mass spectrometry
IHLW	immobilized high-level waste
IHLW PCP	IHLW Product Compliance Plan
ILAW	immobilized low-activity waste
ILAW PCP	ILAW Product Compliance Plan
L	liters
LAW	low-activity waste
lb	pounds
LDR	land disposal restriction
MDL	minimum detection limit
MF	mass fraction (g_{oxide}/g_{oxides})
MFPV	Melter Feed Preparation Vessel (in the WTP IHLW or ILAW facility)

MFV	Melter Feed Vessel (in the WTP IHLW or ILAW facility)
mg/L	milligrams per liter
Mixing/sampling uncertainty	Samples from the IHLW MFPV and ILAW CRV will be subject to uncertainties from random uncertainty related to the inability to perfectly mix the vessel contents as well as random uncertainties in the sampling system. Multiple samples taken from an IHLW MFPV or an ILAW CRV will be subject to both mixing and sampling uncertainties, and it is not possible to separately estimate these two sources of uncertainty from data on multiple samples. Hence, the combined uncertainties are referred to as mixing/sampling uncertainty.
MM	mechanical mixing (agitation)
MRQ	minimum reportable quantity
Non-Linearity	The maximum deviation of a load cell calibration curve from a straight line drawn between the outputs for no-load and the Rated Capacity, expressed as a percentage of the Rated Capacity and measured on increasing load only.
Non-repeatability	The ability of a load cell transducer to reproduce output readings when the same load is applied to it consecutively, under the same conditions and in the same direction. Non-repeatability is expressed as the maximum difference between output readings as a percentage of the Rated Capacity.
NQA	nuclear quality assurance
ORP	Office of River Protection
PCP	Product Compliance Plan
PCT	Product Consistency Test
PNWD	Battelle—Pacific Northwest Division
PQM	partial quadratic mixture
QA	quality assurance
QARD	Quality Assurance Requirements and Description
Radionuclide composition	The composition of IHLW or ILAW that can be determined by radiochemical analyses. Radionuclide composition is expressed as weight percents or mass fractions of radionuclide oxide components of the IHLW or ILAW.
Rated Capacity (R.C.)	The maximum capacity (load) that a load-cell is designed to measure within its specification.
R&T	research and technology

Repeatability	A measure of uncertainty that quantifies the variability between test or measurement results obtained within a single laboratory in a short period of time by a single operator with a specific test/measurement method and/or instrument using specimens taken at random from a single sample of material.
Reproducibility	A measure of uncertainty that quantifies the variability between single test results obtained in different laboratories (or at different times by different operators at a single laboratory) using test specimens taken at random from a single sample of material.
RPP-WTP	River Protection Project-Waste Treatment and Immobilization Plant
RSD	relative standard deviation
%RSD	percent relative standard deviation (that is, the relative standard deviation multiplied by 100%)
S	Siemens
S/cm	Siemens per centimeter (units for electrical conductivity)
SD	standard deviation
SD_V	standard deviation of a volume determination (L)
SRNL	Savannah River National Laboratory
SRTC	Savannah River Technology Center
TCLP	Toxicity Characteristic Leach Procedure
T	temperature measured in Kelvin
$T_{1\%}$	temperature at which one volume percent of waste glass is crystalline (°C)
TSS	test scoping statement
Uncertainty	Lack of knowledge about a true, fixed state of affairs (e.g., analytical *uncertainty* in chemical analyses of a glass sample).
Variation	Real changes in a variable over time or space (for example, *variation* in glass composition within a waste type).
VHT	Vapor Hydration Test
VSL	Vitreous State Laboratory
WASRD	Waste Acceptance System Requirements Document
Waste type	A quantity of waste feed to a vitrification facility that is relatively constant in composition

WFQ	waste form qualification
Within-batch uncertainty	Lack of knowledge about the true value of a variable for a given IHLW or ILAW MFPV batch. The variable could be an IHLW or ILAW composition component (e.g., Na_2O) or a property of IHLW or ILAW (e.g., the release of boron from the Product Consistency Test). The lack of knowledge could be as a result of mixing/sampling uncertainty or analytical uncertainty, for example. Also see "Uncertainty".
WSRC	Westinghouse Savannah River Company
WTP	Waste Treatment and Immobilization Plant
WTPSP	Waste Treatment Plant Support Project
wt%	weight percent
WVDP	West Valley Demonstration Project

Appendix H

Notation

Appendix H: Notations

A_j	specific activity of the j^{th} analyte, which is a radionuclide (Ci/g)
a_{ik}^{GFC}	mass of the k^{th} GFC added to the i^{th} MFPV batch (g)
$b_k^{PCT\ h}$	coefficient of a linear mixture model term for the k^{th} normalized component of IHLW for PCT normalized release of h = B, Li, or Na, or of ILAW for PCT normalized release of h = B or Na
$b_{kk}^{PCT\ h}$	coefficient of a squared mixture model term in a PQM model, corresponding to the k^{th} normalized component of ILAW in the model for VHT alteration depth or PCT normalized release of h = B or Na
$b_{kl}^{PCT\ h}$	coefficient of a crossproduct mixture model term in a PQM model, corresponding to the k^{th} normalized component of ILAW in the model for VHT alteration depth or PCT normalized release of h = B or Na
$b_k^{TCLP\ Cd}$	coefficients for the linear mixture portion of the model form for TCLP Cd release, which involves normalized components (k) of IHLW
$b_{CdO}^{TCLP\ Cd}$	coefficient for the term of the TCLP Cd release model involving the unnormalized mass fraction of CdO
$b_k^{T1\%\ h}$	coefficients for the $T_{1\%}$ model form involving normalized components (k) of IHLW, where h = 1 denotes the IHLW Phase 1 model and h = 1a denotes the updated IHLW Phase 1a model
$b_0^{\eta 0}$, $b_s^{\eta 2}$	IHLW viscosity model coefficients, including the intercept ($b_0^{\eta 0}$) and the coefficients ($b_s^{\eta 2}$) corresponding to the IHLW components divided by temperature squared (T^2)
$b_0^{\eta 0}$, $b_k^{\eta 0}$, $b_s^{\eta 2}$	ILAW viscosity model coefficients, including the intercept ($b_0^{\eta 0}$), coefficients ($b_k^{\eta 0}$) for terms involving components of ILAW in the model, and coefficients ($b_s^{\eta 2}$) for terms involving components divided by temperature squared (T^2)
$b_k^{\varepsilon 0}$, $b_t^{\varepsilon 1}$, $b_s^{\varepsilon 2}$	IHLW electrical conductivity model coefficients for terms involving IHLW components (indexed by k), components divided by temperature (indexed by t), and components divided by temperature squared (indexed by s)
$b_k^{VHT\ D}$	coefficient of a linear mixture model term for the k^{th} normalized component of ILAW in the model for VHT alteration depth

$b_{kk}^{VHT\ D}$	coefficient of a squared mixture model term in a PQM model, corresponding to the k^{th} normalized component of ILAW in the model for VHT alteration depth
$b_{kl}^{VHT\ D}$	coefficient of a crossproduct mixture model term in a PQM model, corresponding to the k^{th} normalized component of ILAW in the model for VHT alteration depth
$b_k^{\varepsilon 0}$, $b_t^{\varepsilon 1}$, $b_{kl}^{\varepsilon 3}$	ILAW electrical conductivity model coefficients for terms involving ILAW components (indexed by *k*), components divided by temperature (indexed by *t*), and the selected crossproduct terms (indexed by *kl*)
c_{ij}^{CRV}	concentration of the j^{th} element in the LAW CRV batch, a portion of which is transferred to the i^{th} MFPV batch (μg/mL = mg/L)
$\bar{c}_{ij}^{CRV}$	average concentration of the j^{th} analyte over n_A^{CRV} analyses each of n_S^{MCRV} samples from the LAW CRV batch, a portion of which is transferred to the i^{th} ILAW MFPV batch (μg/mL = mg/L)
c_{ijlm}^{CRV}	analyzed concentration of the j^{th} analyte from the m^{th} analysis of the l^{th} sample from the CRV batch contributing to the i^{th} ILAW MFPV batch (μg/mL = mg/L)
c_{ij}^{MFPV}	analyzed concentration of analyte *j* in the i^{th} IHLW MFPV batch (μg/mL = mg/L)
$\bar{c}_{ij}^{MFPV}$	average concentration of the j^{th} analyte over n_A^{MFPV} analyses each of n_S^{MFPV} samples from the i^{th} IHLW MFPV batch (μg/mL = mg/L)
c_{ijlm}^{MFPV}	analyzed concentration of the j^{th} analyte from the m^{th} analysis of the l^{th} sample from the i^{th} IHLW MFPV batch (μg/mL = mg/L)
c_{ijl}^{MFPV}	analyzed concentration of the j^{th} analyte from a single analysis of the l^{th} sample from the i^{th} IHLW MFPV batch (μg/mL = mg/L)
$c^{TCLP\ Cd}$	concentration of Cd released from a TCLP test of HLW glass (mg/L)
D^{VHT}	alteration depth on a test coupon from running the VHT (μm)
ε	symbol denoting electrical conductivity (S/cm)
$\varepsilon_{B,ij}^{CRV}$	random effect caused by batch-to-batch variation on the concentration of the j^{th} analyte in the CRV batch contributing to the i^{th} ILAW MFPV batch (μg/mL = mg/L)

$\varepsilon_{MS,ijl}^{CRV}$	random effect caused by mixing and sampling uncertainties on the concentration of the j^{th} analyte in the l^{th} sample from the CRV batch contributing to the i^{th} ILAW MFPV batch (μg/mL = mg/L)
$\varepsilon_{A,ijlm}^{CRV}$	random effect caused by analytical uncertainty in the analyzed concentration of the j^{th} analyte from the m^{th} analysis of the l^{th} sample from the CRV batch contributing to the i^{th} ILAW MFPV batch (μg/mL = mg/L)
$\varepsilon_{G,ijk}^{GFC}$	random uncertainty in the mass fraction of the j^{th} glass component in the k^{th} GFC added to the i^{th} ILAW MFPV batch (μg/mL = mg/L)
$\varepsilon_{a,ik}^{GFC}$	random uncertainty in the mass of the k^{th} GFC added to the i^{th} ILAW MFPV batch (g)
$\varepsilon_{B,pq}$	effect on an IHLW component or property value because of batch-to-batch variation over the r = 1, 2, … , 18 batches for the q^{th} simulation of the p^{th} scenario for a given HLW waste type, where the effect has mean 0 and standard deviation $\sigma_{B,pq}$
$\varepsilon_{W,pq}$	effect on an IHLW component or property value because of within-batch uncertainty over the r = 1, 2, … , 18 batches for the q^{th} simulation of the p^{th} scenario for a given HLW waste type, where the effect has mean 0 and standard deviation $\sigma_{W,pq}$
η	symbol denoting viscosity (poise)
f_j	factor for converting the concentration of analyte j to the concentration of oxide j ($g_{oxide}/g_{analyte}$)
g_{ij}^{MFPV}	mass fraction of the j^{th} glass component (oxide or halogen) in the i^{th} IHLW or ILAW MFPV batch (g_{oxide}/g_{oxides})
$\overline{g}_{ij}^{MFPV}$	mean mass fraction of the j^{th} component (chemical composition or radionuclide composition) in ILAW that would be made from the i^{th} ILAW MFPV batch. The "mean" mass fraction is based on separate averages of (1) multiple samples per CRV batch and one or more chemical analyses per CRV sample and (2) multiple volume determinations per CRV and MFPV volume if more than one determination per volume is made. (g_{oxide}/g_{oxides})
g_{ijlm}^{MFPV}	mass fraction of the j^{th} glass-oxide component corresponding to the m^{th} analysis of the l^{th} sample from the i^{th} IHLW MFPV batch (g_{oxide}/g_{oxides})

g_{ijl}^{MFPV}	mass fraction of the j^{th} glass-oxide component corresponding to a single analysis of the l^{th} sample from the i^{th} IHLW MFPV batch (g_{oxide}/g_{oxides})
$g_{il,CdO}^{MFPV}$	original, unnormalized mass fraction of CdO for the l^{th} sample from the i^{th} IHLW MFPV batch
G_{ijk}^{GFC}	mass of the j^{th} glass oxide component per mass of the k^{th} GFC for the i^{th} IHLW MFPV batch ($g_{oxide\ j}/g_{GFC\ k}$)
J	number of IHLW or ILAW chemical and radionuclide composition components (oxides and halogens) for the IHLW or ILAW composition corresponding to each MFPV batch
$\overline{m}_{i-1,j}^{MFPV}$	mass of the j^{th} glass oxide component in the $(i-1)^{st}$ MFPV batch, based on averages over multiple samples, analyses per sample, and volume determinations (g)
m_{Aj}^{MFPV}	mass of the j^{th} IHLW component in an IHLW MFPV batch containing only Material *A* (kg)
M^{MFPV}	total mass of IHLW that would be made from an MFPV batch (kg)
MW_j^{oxide}	molecular weight of oxide *j* (g/mole)
$MW_j^{analyte}$	molecular weights of analyte *j* (g/mole)
μ_j^{CRV}	nominal concentration of the j^{th} analyte over the LAW CRV batches associated with an LAW waste type (μg/mL = mg/L)
$\mu_{G,jk}^{GFC}$	nominal mass fraction of the j^{th} glass component in the k^{th} GFC used in the ILAW MFPV batches associated with an LAW waste type ($g_{oxide\ j}/g_{GFC\ k}$)
$\mu_{a,ik}^{GFC}$	nominal mass of the k^{th} GFC added to the i^{th} ILAW MFPV batch (g)
μ_{pq}	nominal value of the IHLW component or property for the q^{th} simulation of the p^{th} scenario over the IHLW MFPV batches associated with an HLW waste type
n_A^{CRV}	number of analyses per LAW CRV sample
n_S^{CRV}	number of samples per LAW CRV batch
n_V^{CRV}	number of volume determinations of the LAW CRV before and after transfers

n_A^{MFPV}	number of chemical analyses per IHLW MFPV sample
n_S^{MFPV}	number of samples per IHLW MFPV batch
n_V^{MFPV}	number of volume determinations of the IHLW MFPV or ILAW MFPV before and after transfers
n_{nmc}	number of normalized IHLW or ILAW components in a property-composition model
$n_{nmc}^{PCT\ h}$	number of normalized IHLW components in the model for PCT normalized release of h = B, Li, or Na; or the number of normalized ILAW components in the model for PCT normalized release of h = B or Na
$n_{nmc}^{TCLP\ Cd}$	number of normalized IHLW components used in the model for TCLP Cd release
$n_{nmc}^{T1\%\ h}$	number of normalized IHLW components used in the spinel $T_{1\%}$ model, where h = 1 denotes the IHLW Phase 1 model and h = 1a denotes the updated IHLW Phase 1a model
$n_{umc}^{\eta 2}$	number of unnormalized IHLW or ILAW components used in the "linear component divided by temperature squared" terms of the IHLW or ILAW viscosity model
$n_{nmc}^{VHT\ D}$	number of normalized ILAW components in the model for VHT alteration depth
$n_{umc}^{\eta 1}$	number of unnormalized ILAW components used in the "linear component" terms of the viscosity model
$n_{umc}^{\varepsilon 0}$	number of unnormalized IHLW or ILAW components used in the "linear component" terms of the electrical conductivity model
$n_{umc}^{\varepsilon 1}$	number of unnormalized IHLW or ILAW components used in the "linear component divided by temperature" terms of the electrical conductivity model
$n_{umc}^{\varepsilon 2}$	number of unnormalized IHLW components used in the "linear component divided by temperature squared" terms of the electrical conductivity model
$n_{umc}^{\varepsilon 3}$	number of crossproduct terms involving unnormalized ILAW components in the electrical conductivity model
R_j	ratio of moles of oxide per mole of analyte for oxide j ($moles_{oxide}/moles_{analyte}$)

r_{ij}^{CRV}	activity-per-volume concentration of the j^{th} radionuclide in the LAW CRV batch contributing to the i^{th} ILAW MFPV batch (μCi/mL = mCi/L)
$\bar{r}_{ij}^{CRV}$	activity-per-volume concentration of the j^{th} radionuclide in the LAW CRV batch contributing to the i^{th} ILAW MFPV batch, based on averages over multiple samples, analyses per sample, and volume determinations (μCi/mL = mCi/L)
r_{ij}^{MFPV}	activity-per-volume concentration of the j^{th} radionuclide in the i^{th} IHLW MFPV batch (Ci/m^3)
$\bar{r}_{ij}^{MFPV}$	mean activity-per-volume concentration of the j^{th} radionuclide in the i^{th} IHLW and ILAW MFPV batch (μCi/mL = mCi/L)
r_{ijlm}^{CRV}	activity-per-volume concentration of the j^{th} radionuclide in the i^{th} LAW CRV batch, based on the m^{th} radionuclide analysis of the l^{th} LAW CRV sample (μCi/mL = mCi/L)
r_{ijlm}^{MFPV}	analyzed concentration of the j^{th} radionuclide from the m^{th} analysis of the l^{th} sample from the i^{th} IHLW MFPV batch (μCi/mL = mCi/L)
$r_i^{PCT\ h}$	normalized PCT release of h = B, Li, or Na for IHLW, or h = B and Na for ILAW (g/L) from IHLW or ILAW corresponding to the i^{th} MFPV batch
R^{VHT}	VHT alteration rate (g/m^2day)
$\%RSD_A$	%RSD of random analytical uncertainty
$\%RSD_B$	%RSD of batch-to-batch variation over an HLW or LAW waste type
$\%RSD_S$	%RSD of random mixing/sampling uncertainty
$\%RSD_W$	%RSD of within-batch variation
$\%RSD_A(c_j^{CRV})$	analytical %RSD for the concentration of the j^{th} element in an LAW CRV batch
$\%RSD_A(c_j^{MFPV})$	analytical %RSD for the concentration of the j^{th} element in an IHLW MFPV batch
$\%RSD_B(c_j^{CRV})$	%RSD representing the random batch-to-batch variation in the concentration of the j^{th} element over LAW CRV batches corresponding to an LAW waste type
$\%RSD_B(c_j^{MFPV})$	%RSD representing the random batch-to-batch variation in the concentration of the j^{th} element over IHLW MFPV batches corresponding to an HLW waste type

$\%RSD_S(c_j^{CRV})$ mixing/sampling %RSD in the concentration of the j^{th} element in an LAW CRV batch

$\%RSD_S(c_j^{MFPV})$ mixing/sampling %RSD in the concentration of the j^{th} element in an IHLW MFPV batch

$\%RSD_{B,pq}$ batch-to-batch variation %RSD (for an IHLW or ILAW component or property) associated with the q^{th} simulation of the p^{th} scenario for a given HLW or LAW waste type

$\%RSD_{W,pq}$ within-batch uncertainty %RSD (for an IHLW or ILAW component or property) associated with the q^{th} simulation of the p^{th} scenario when averaging results over the 8 samples per IHLW MFPV batch for a given HLW or LAW waste type

$\%RSD_{T,pq}$ total variation plus uncertainties %RSD (for an IHLW or ILAW component or property) associated with the q^{th} simulation of the p^{th} scenario for a given HLW or LAW waste type

$\overline{\%RSD_{T,p}}$ mean total %RSD (of an IHLW or ILAW component or property) across the 200 simulations for the p^{th} scenario for a given HLW or LAW waste type

$\%RSD_{T,p}^{90\%\ ELCL}$ empirical lower confidence limit (ELCL) for a 90% ECI on the total %RSD (of an IHLW or ILAW component or property) for the p^{th} scenario associated with a given HLW or LAW waste type, equal to the 5th percentile from all 200 simulated $\%RSD_{T,pq}$ values

$\%RSD_{T,p}^{90\%\ EUCL}$ empirical upper confidence limit (EUCL) for a 90% ECI on the total %RSD (of an IHLW or ILAW component or property) for the p^{th} scenario associated with a given HLW or LAW waste type, equal to the 95th percentile from all 200 simulated $\%RSD_{T,pq}$ values

$\overline{\%RSD_{B,p}}$ mean batch-to-batch %RSD (of an IHLW or ILAW component or property) across the 200 simulations for the p^{th} scenario associated with a given HLW or LAW waste type

$\%RSD_{B,p}^{90\%\ ELCL}$ empirical lower confidence limit for a 90% ECI on the batch-to-batch %RSD (of an IHLW or ILAW component or property) for the p^{th} scenario associated with a given HLW or LAW waste type, equal to the 5th percentile from all 200 simulated $\%RSD_{B,pq}$ values

$\%RSD_{B,p}^{90\%\ EUCL}$ empirical upper confidence limit for a 90% ECI on the batch-to-batch %RSD (of an IHLW or ILAW component or property) for the p^{th} scenario associated with a

	given HLW or LAW waste type, equal to the 95th percentile from all 200 simulated $\%RSD_{B,pq}$ values
$\overline{\%RSD_{W,p}}$	mean within-batch %RSD (of an IHLW or ILAW component or property) across the 200 simulations for the p^{th} scenario associated with a given HLW or LAW waste type
$\%RSD_{W,p}^{90\%\ ELCL}$	empirical lower confidence limit for a 90% ECI on the within-batch %RSD (of an IHLW or ILAW component or property) for the p^{th} scenario associated with a given HLW or LAW waste type, equal to the 5th percentile from all 200 simulated $\%RSD_{W,pq}$ values
$\%RSD_{W,p}^{90\%\ EUCL}$	empirical upper confidence limit for a 90% ECI on the within-batch %RSD (of an IHLW or ILAW component or property) for the p^{th} scenario associated with a given HLW or LAW waste type, equal to the 95th percentile from all 200 simulated $\%RSD_{W,pq}$ values
$\%RSD_{B,cq}$	batch-to-batch %RSD (of an ILAW component or property) for the q^{th} simulation (1 of 200 simulations) of the c^{th} control scenario (from the 10 control scenarios in Table 5.5)
$\overline{\%RSD_{B,c}}$	mean batch-to-batch %RSD (of an IHLW or ILAW component or property) across the 200 simulations for the c^{th} control scenario (from the 10 control scenarios in Table 5.5)
$\%RSD_{B,c}^{90\%\ ELCL}$	empirical lower confidence limit for a 90% ECI on the batch-to-batch %RSD (of an ILAW component or property) for the c^{th} control scenario (from the 10 control scenarios in Table 5.5), equal to the 5th percentile from all 200 simulated $\%RSD_{B,cq}$ values
$\%RSD_{B,c}^{90\%\ EUCL}$	empirical upper confidence limit for a 90% ECI on the batch-to-batch %RSD (of an ILAW component or property) for the c^{th} control scenario, equal to the 95th percentile from all 200 simulated $\%RSD_{B,cq}$ values
SD_V^{CRV}	standard deviation of a volume determination on the LAW CRV (L)
SD_V^{MFPV}	standard deviation of a volume determination on the IHLW MFPV or ILAW MFPV (L)
$SD(G_{jk}^{GFC})$	GFC composition uncertainty, represented by the standard deviation in the mass fraction of the j^{th} component (oxide or halogen) in the k^{th} GFC ($g_{oxide\ j}/g_{GFC\ k}$)

$SD(a_k^{GFC})$	uncertainty in the mass of the k^{th} GFC added to an ILAW MFPV batch, expressed as a standard deviation (g)
$SD_{B,pq}$	batch-to-batch standard deviation for an IHLW or ILAW component or property, representing variation over MFPV batches associated with an HLW or LAW waste type for the q^{th} simulation of the p^{th} scenario
$SD_{W,pq}$	within-batch standard deviation for an IHLW or ILAW component or property, representing the uncertainty in that quantity for each MFPV batch for the q^{th} simulation of the p^{th} scenario
$\overline{SD}_{W,pq}$	within-batch standard deviation for an IHLW component or property based on averaging the results from the 8 samples per IHLW MFPV batch for the q^{th} simulation of the p^{th} scenario
$\hat{\sigma}^2_{\bar{V}_i^{CRV\ before}}$	estimate of the variance (squared standard deviation) of an average volume determination in the LAW CRV before a transfer to the LAW MFPV
$\hat{\sigma}^2_{\bar{V}_i^{CRV\ after}}$	estimate of the variance (squared standard deviation) of an average volume determination in the LAW CRV after a transfer to the LAW MFPV
$\hat{\sigma}^2_{\bar{V}_i^{MFPV\ before}}$	estimate of the variance (squared standard deviation) of an average volume determination in the LAW MFPV before a transfer from the LAW CRV
$\hat{\sigma}^2_{\bar{V}_i^{MFPV\ after}}$	estimate of the variance (squared standard deviation) of an average volume determination in the LAW MFPV after a transfer from the LAW CRV.
u	units conversion factor for converting mg to g
$\overline{V}_i^{CRV to MFPV}$	estimate of the volume transferred from the CRV to the MFPV for the i^{th} MFPV batch, calculated as a weighted average of the estimates from the before and after volume determinations for each of the CRV and MFPV (L)
$V_{ih}^{CRV\ before}$	h^{th} volume determination of the LAW CRV before the transfer of material to the i^{th} ILAW MFPV batch (L)
$\overline{V}_i^{CRV\ before}$	volume of the LAW CRV before the transfer of material to the i^{th} ILAW MFPV batch, averaged over n_V^{CRV} volume determinations (L)
$V_{ih}^{CRV\ after}$	h^{th} volume determination of the LAW CRV after the transfer of material to the i^{th} ILAW MFPV batch (L)

$\overline{V}_i^{CRV\ after}$ volume of the LAW CRV after the transfer of material to the i^{th} ILAW MFPV batch, averaged over n_V^{CRV} volume determinations (L)

$V_{i,h}^{MFPV\ Heel}$ h^{th} volume determination of the MFPV Heel included in the i^{th} ILAW MFPV batch (L)

$V_{ih}^{MFPV\ before}$ h^{th} volume determination of the ILAW MFPV before receipt of LAW CRV material for the i^{th} ILAW MFPV batch (L)

$\overline{V}_i^{MFPV\ before}$ volume of the ILAW MFPV before receipt of LAW CRV material for the i^{th} ILAW MFPV batch, averaged over n_V^{MFPV} volume determinations (L)

$V_{ih}^{MFPV\ after}$ h^{th} volume determination of the ILAW MFPV after receipt of LAW CRV material for the i^{th} ILAW MFPV batch but before receipt of GFCs or any added water (L)

$\overline{V}_i^{MFPV\ after}$ volume of the ILAW MFPV after receipt of LAW CRV material for the i^{th} ILAW MFPV batch but before receipt of GFCs or any added water, averaged over n_V^{MFPV} volume determinations (L)

$V_{i-1,h}^{MFPV}$ h^{th} volume determination of the $(i\text{-}1)^{st}$ ILAW MFPV batch (L)

w_{ikl}^{MFPV} weight percent (wt%) of the k^{th} IHLW component in the "linear component" portion of a property-composition model, where the composition is for the l^{th} sample from the i^{th} IHLW MFPV batch. These wt% values are not normalized to sum to 100% over the components in the model. Note that $w_{ikl}^{MFPV} = 100\ g_{ikl}^{MFPV}$.

w_{itl}^{MFPV} wt% of the t^{th} IHLW component in the "linear component divided by temperature" portion of a property-composition model where the composition is for the l^{th} sample from the i^{th} IHLW MFPV batch. These wt% values are not normalized to sum to 100% over the components in the model. Note that $w_{itl}^{MFPV} = 100\ g_{itl}^{MFPV}$.

w_{isl}^{MFPV} wt% of the s^{th} IHLW component in the "linear component divided by temperature squared" portion of a property-composition model, where the composition is for the l^{th} sample from the i^{th} IHLW MFPV batch. These wt% values are not normalized to sum to 100% over the components in the model. Note that $w_{isl}^{MFPV} = 100\ g_{isl}^{MFPV}$.

$\overline{w}_{ik}^{MFPV}$ wt% of the k^{th} ILAW component in the "linear component" portion of a property-composition model, where the composition is for the i^{th} ILAW MFPV batch. The wt% values are based on averages over multiple samples from a CRV batch,

analyses per CRV sample, and CRV and MFPV volume determinations. These wt% values are not normalized to sum to 100% over the components in the model. Note that $\overline{w}_{ikl}^{MFPV} = 100\ \overline{g}_{ikl}^{MFPV}$.

$\overline{w}_{isl}^{MFPV}$ wt% of the s^{th} IHLW component in the "linear component divided by temperature squared" portion of a property-composition model, where the composition is for the l^{th} sample from the i^{th} IHLW MFPV batch. These wt% values are not normalized to sum to 100% over the components in the model. Note that $\overline{w}_{isl}^{MFPV} = 100\ \overline{g}_{isl}^{MFPV}$.

$\overline{x}_{ik}^{MFPV}$ normalized mass fraction of the k^{th} ILAW component in a property-composition model where the composition is for the i^{th} ILAW MFPV batch, such that $\sum_{k=1}^{n_{nmc}} \overline{x}_{ik}^{MFPV} = 1$, where n_{nmc} is the number of normalized model components in a given glass property-composition model. The mass fractions are based on averages over multiple samples from a CRV batch, analyses per CRV sample, and CRV and MFPV volume determinations (g_{oxide}/g_{oxides})

x_{ikl}^{MFPV} normalized mass fraction of the k^{th} IHLW component from a single analysis of the l^{th} sample from the i^{th} MFPV batch, where k is one of the n_{nmc} IHLW components in a property-composition model, such that $\sum_{k=1}^{n_{nmc}} x_{ikl}^{MFPV} = 1$ (g_{oxide}/g_{oxides})

x_{Aj}^{MFPV} mass fraction of the j^{th} IHLW component in an IHLW MFPV batch containing only Material A ($kg_{component\ i}$/kg IHLW)

x_{Bj}^{MFPV} mass fraction of the j^{th} IHLW component in an IHLW MFPV batch containing only Material B ($kg_{component\ i}$/kg IHLW)

x_{pj}^{MFPV} mass fraction of the j^{th} IHLW component in the p^{th} IHLW MFPV transition batch from one waste type to another ($kg_{component\ i}$/kg IHLW)

$\hat{y}_{il}^{PCT\ h}$ $\hat{\ln}(r_{il}^{PCT\ h})$ = predicted natural logarithm of the PCT normalized release of h = B, Li, or Na [$\hat{\ln}(r_i^{PCT\ h})$] for IHLW corresponding to the l^{th} sample from the i^{th} MFPV batch [ln(g/L)]

$\hat{\overline{y}}_i^{PCT\ h}$ $\hat{\ln}(\overline{r}_i^{PCT\ h})$ = predicted natural logarithm of the PCT normalized release of h = B or Na for ILAW corresponding to the i^{th} MFPV batch, based on averages over multiple samples from a CRV batch, analyses per CRV sample, and CRV and MFPV volume determinations [ln(g/L)]

$\hat{\bar{y}}_i^{VHT\ D}$ $\hat{\ln}(\overline{D}_i^{VHT})$ = predicted natural logarithm of the VHT alteration depth for ILAW corresponding to the i^{th} MFPV batch, based on averages over multiple samples from a CRV batch, analyses per CRV sample, and CRV and MFPV volume determinations [ln(μm)]

$\hat{y}_{il}^{T1\%\ h}$ predicted spinel $T_{1\%}$ for IHLW corresponding to the l^{th} sample from the i^{th} MFPV batch, where h = 1 denotes the IHLW Phase 1 model and h = 1a denotes the updated IHLW Phase 1a model (^oC)

$\hat{y}_{il}^{TCLP\ Cd}$ $\hat{\ln}(c_{il}^{TCLP\ Cd})$ = predicted natural logarithm of TCLP Cd release, for IHLW corresponding to the l^{th} sample from the i^{th} MFPV batch [ln(mg/L)]

$\hat{y}_{il}^{T1\%\ h}$ predicted spinel $T_{1\%}$ for IHLW corresponding to the l^{th} sample from the i^{th} MFPV batch, where h = 1 denotes the IHLW Phase 1 model and h = 1a denotes the updated IHLW Phase 1a model (^oC)

$\hat{y}_{il}^{\eta}$ $\hat{\ln}(\eta_{il})$ = predicted natural logarithm of the viscosity [$\hat{\ln}$(poise)] for IHLW corresponding to the l^{th} sample from the i^{th} MFPV batch

$\hat{y}_{il}^{\varepsilon}$ $\hat{\ln}(\varepsilon_{il})$ = predicted natural logarithm of the electrical conductivity for IHLW corresponding to the l^{th} sample from the i^{th} MFPV batch [$\hat{\ln}$(S/cm), where S denotes Siemens]

$\hat{\bar{y}}_i^{\varepsilon}$ $\hat{\ln}(\bar{\varepsilon}_i)$ = predicted natural logarithm of the electrical conductivity for ILAW corresponding to the i^{th} MFPV batch, based on averages over multiple samples from a CRV batch, analyses per CRV sample, and CRV and MFPV volume determinations [$\hat{\ln}$(S/cm), where S denotes Siemens]

y_{pqr} IHLW or ILAW component (mass fraction) or property value calculated for the p^{th} scenario, the q^{th} simulation, and the r^{th} IHLW or ILAW MFPV batch associated with an HLW or LAW waste type

y_{cqr} ILAW component or property value calculated for the c^{th} control scenario, the q^{th} simulation, and the r^{th} ILAW MFPV batch associated with an LAW waste type

Distribution

No. of Copies

OFFSITE

1 Savannah River National Laboratory
Richard Edwards
Savannah River National Laboratory
Westinghouse SA
Aiken, SC 29808-0001

No. of Copies

ONSITE

17 Battelle−Pacific Northwest Division

B. G. Amidan (2)	K6-08
S. K. Cooley	K6-08
A. Heredia-Langner (2)	K6-08
P. Hrma	K6-24
D.-S. Kim	K6-24
D. E. Kurath	P7-28
G. F. Piepel (3)	K6-08
G. L. Smith	H4-02
J. D. Vienna	K6-24
Project File (2)	P7-28
Information Release (2)	K1-06

13 Bechtel National, Inc.

K. H. Abel (2)	H4-02
S. M. Barnes	H4-02
D. B. Blumenkranz	H4-02
L. O. Bostic	H4-02
D. Dodd	H4-02
R. F. Gimpel	H4-02
B. Kaiser	H4-02
J. L. Nelson	H4-02
I. G. Papp	H4-02
J. G. Reynolds	H4-02
J. Talbott (2)	H4-02